Institute For
Information
Storage
Technology

The Head-Disk Interface

A Short Course
December 12-14, 1989

SANTA CLARA UNIVERSITY

THE HEAD-DISK INTERFACE

III. THE HEAD

Paul W. Smith
Applied Magnetics Corporation

Institute for Information Storage Technology
Santa Clara University
December 12-14, 1989

THE HEAD. . .

- What does it do?
- How has it evolved?
- How does it work?
- What will it look like in the future?

THE HEAD...What Does It Do?

- Meet the design constraints of magnetic recording
  - High BPI (bits/inch) => Flying Height -> 0

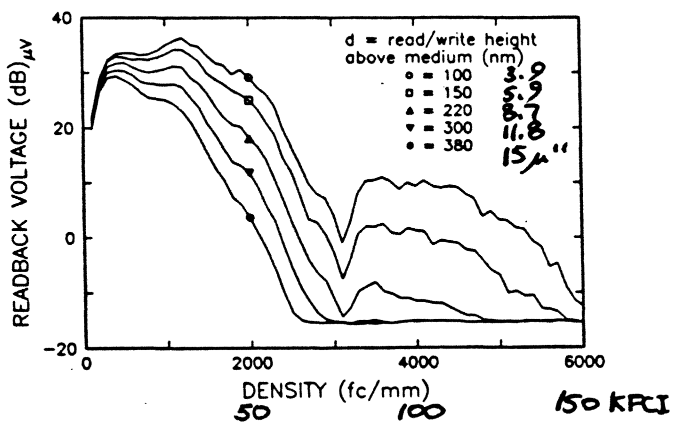

Figure 3: Spectral amplitude rolloff curve made using the Head Spacing Controller. An IBM 3380 thin film head and CoCr thin film disk (Hc= 760 Oe., Mr= 577 emu/cc, and t= 0.035 microns) were used. The rotational speed was 2700 RPM and the head/disk velocity was 14.4 m/sec. A 0.025 micron overcoat is included in the tabulated spacings.

used servo position + laser method of positioning head

* Jefferson, C. M., "A Variable Head-to-Disk Spacing Controller for Magnetic Recording on Rigid Disks", IEEE Trans. Mag. VOL 24, No. 6, November, 1988, p. 2736.

THE HEAD...What Does It Do? (cont.)

- Minimum Wear => Flying Height -> high

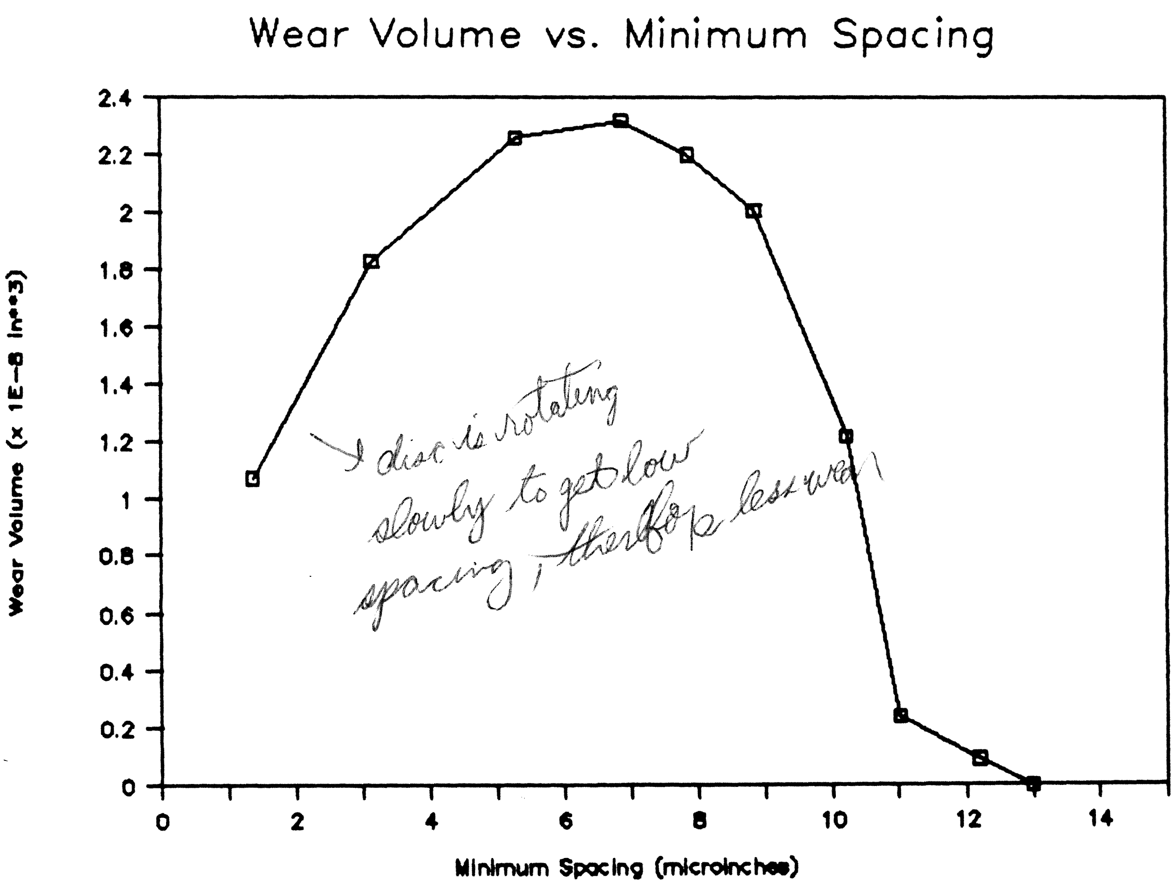

Wear volume

Run head on disc for 30 min

- Minimum signal modulation => delta Flying Height -> 0

Wallace Formula *

$$A = A_o e^{-2\pi h/\lambda}$$

where

A = readback signal amplitude

A_o = constant which depends on recording parameters

h = spacing (core/media)

λ = recorded wavelength

Flying Height Increase vs. Density

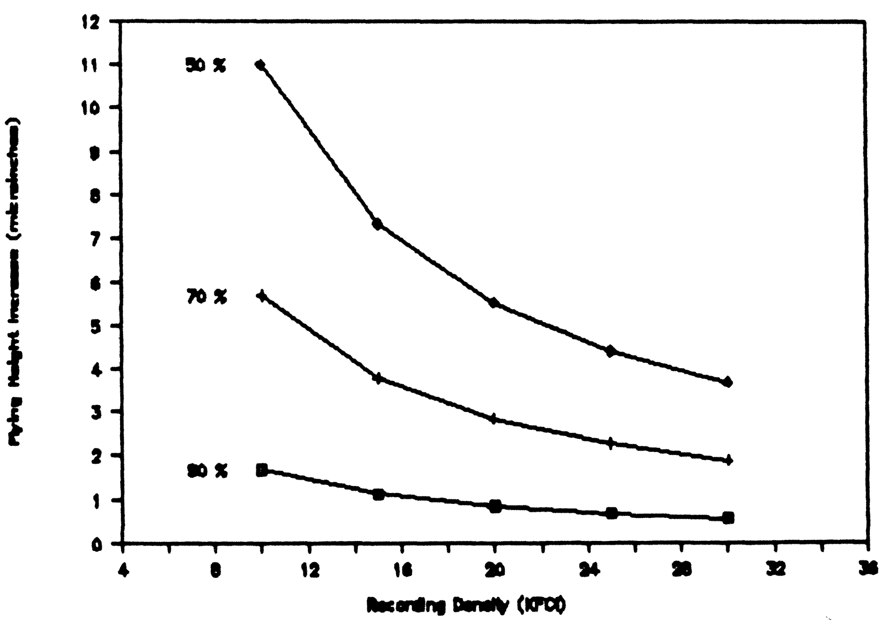

---

* Wallace, R. L., "The Reproduction of Magnetically Recorded Signals", Bell System Tech. Journ., October, 1951, pp. 1145-1173.

Resonances
disc 100hz
flex 1000hz
air bear 10000
slider 100000

THE HEAD...What Does It Do? (cont.)

- High TPI (tracks/inch) ⇒ Support Stiffness → infinity

  In the Disk Plane, K → infinity

Ideal Closed-Loop Mechanical Transfer

Function with No Resonances

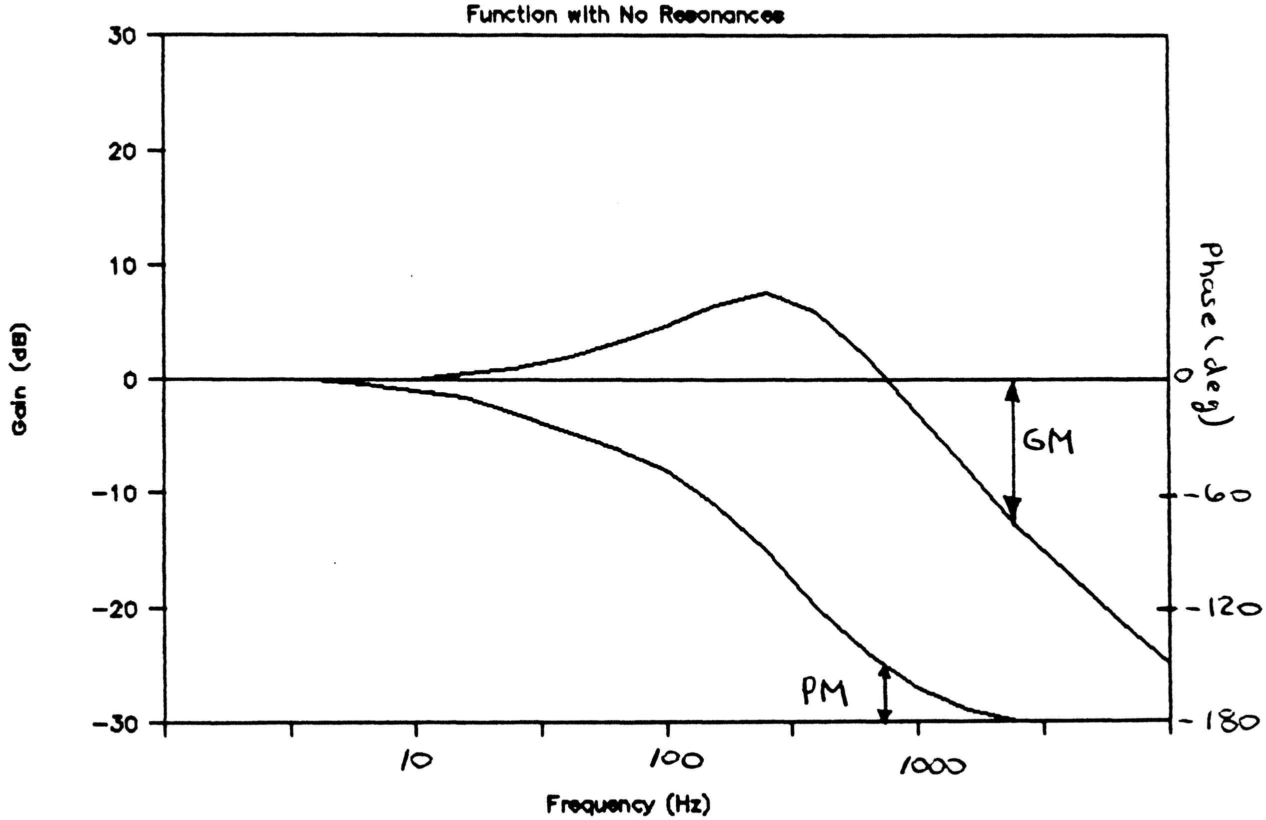

Phase Margin 40° - 70° ⇒ well damped system

Cross-Over Point Higher ⇒ High Bandwidth for Servo Speed

Mechanical Resonances 2 Octaves Above Cross-Over

THE HEAD... What Does It Do? (cont.)

- Pitch, Roll ... K -> 0
- Heave (Vert)... resist air bearing load

Air bearing should dominate for proper disk-following

Typical values

	Stiffness	Flexure	Air Bearing
vertical	K_h	50 gms/in	3.8×10^6 gms/in
roll	K_r	3 in-gms/rad	9.5×10^3 in-gms/rad
pitch	K_p	1.3 in-gms/rad	7.8×10^3 in-gms/rad

Flying Height vs. Flexure Pitch → caused by "bent" head

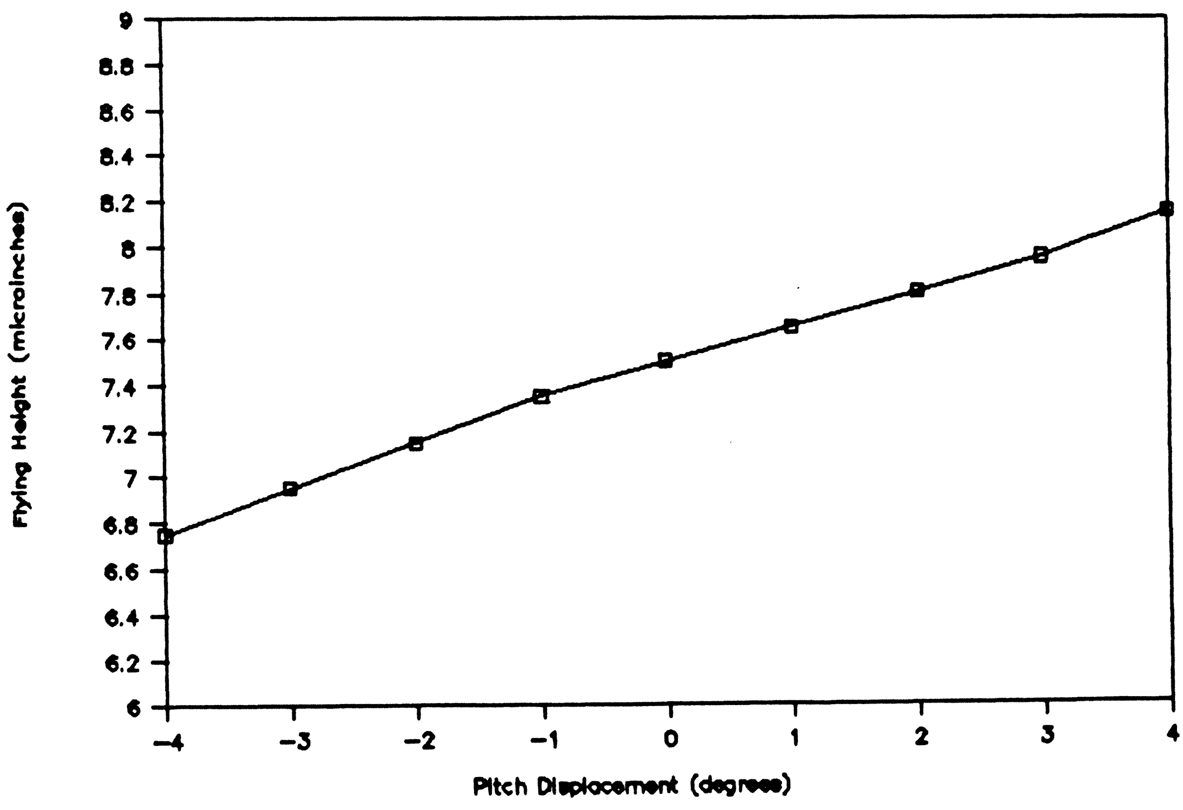

Flying Height vs. Flexure Roll

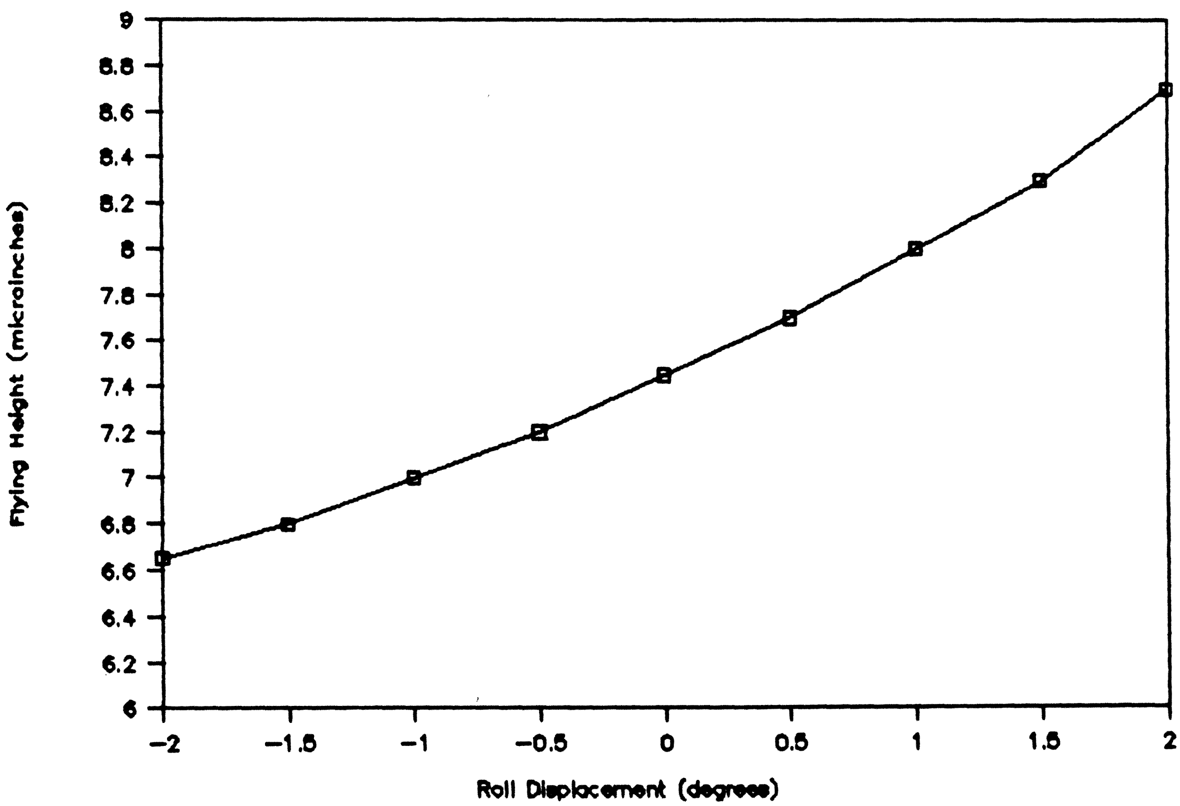

THE HEAD... What Does It Do? (cont.)

- Minimal Tolerance Sensitivity

  - There is a flying height "budget"

$$\sigma_h = \sqrt{\sum_{i=1}^{n} \left\{ \frac{\partial h}{\partial x_i} \sigma_i \right\}^2}$$

where

σ_h = flying height standard deviation

$\partial h / \partial x_i$ = sensitivity of flying height to x_i (load, for ex.)

σ_i = standard deviation of x_i

Important parameters:

Load

ABS Width

Pivot Location

- General Rule:

Nominal Flying Height $- 4\sigma_h \geq$ Glide Height of Disk

~~Nominal~~

THE HEAD... What Does It Do? (cont.)

- Flexure Tolerances Effect Modal Coupling

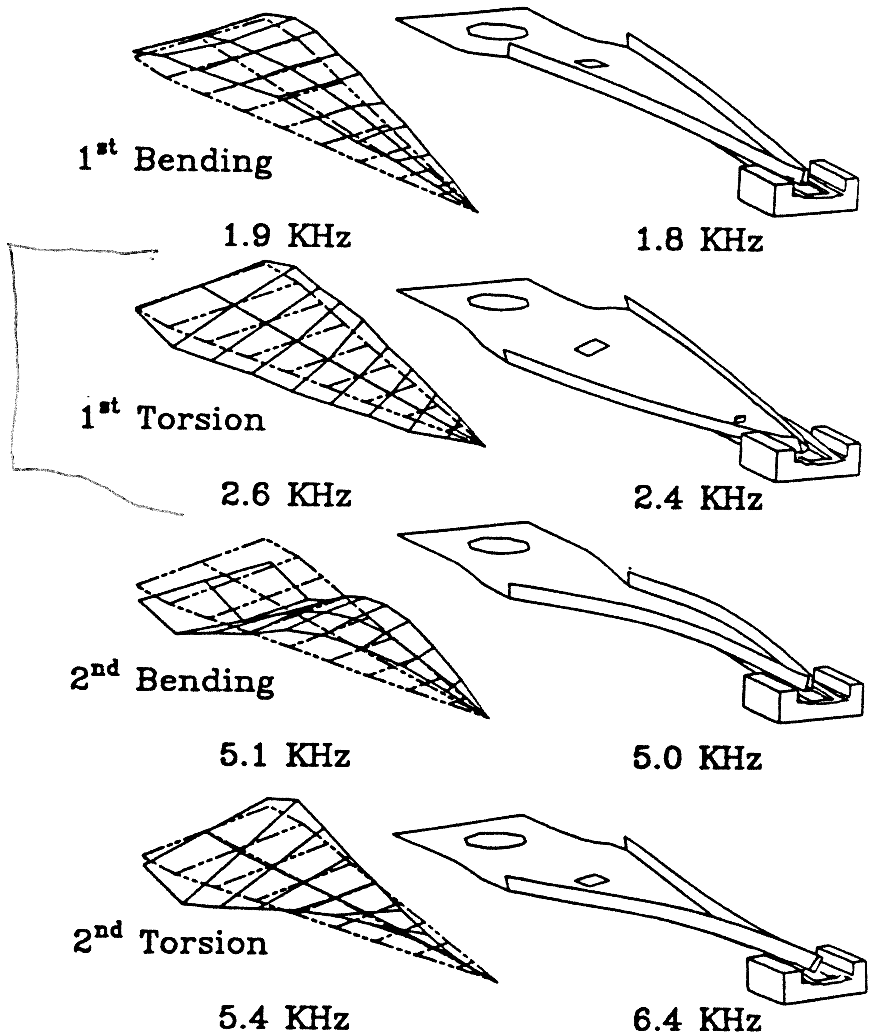

Miu, D. K., Frees, G. M., and Gompertz, R. S., "Tracking Dynamics of Read/Write Head Suspensions in High-Performance Small Form-Factor Rigid Disk Drives," UCLA Res. Lab. for Comp. Machinery, TR# 88-03.

THE HEAD... What Does It Do? (cont.)

- Lowest Possible Cost

Example: 8 disk, 5 1/4" drive

8 disks x $15 each = $120

16 heads x $10 each = $160

Typical drive cost = $1000

THE HEAD... What Does It Do? (cont.)

- High Long-Term Confidence Level

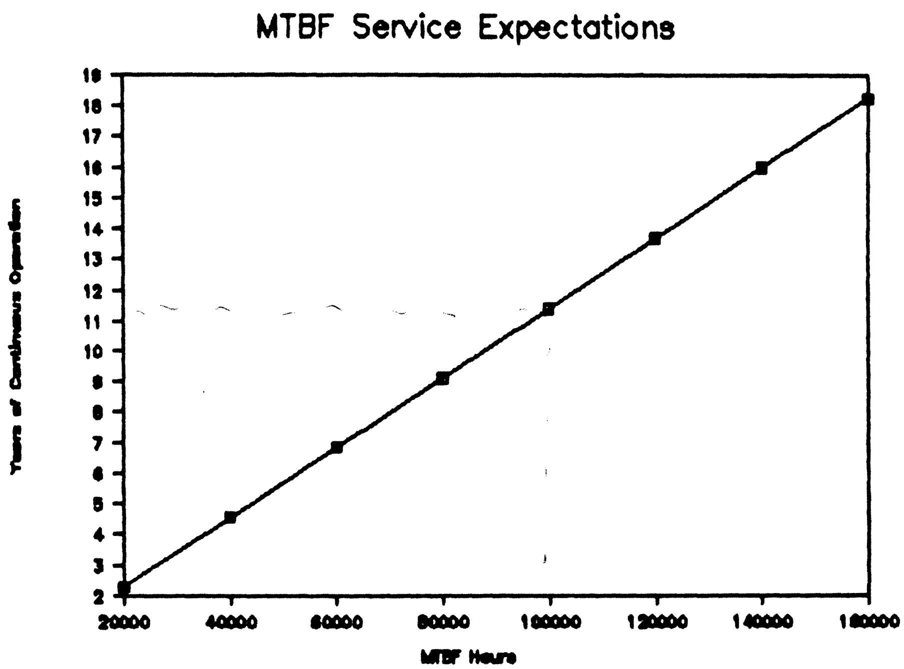

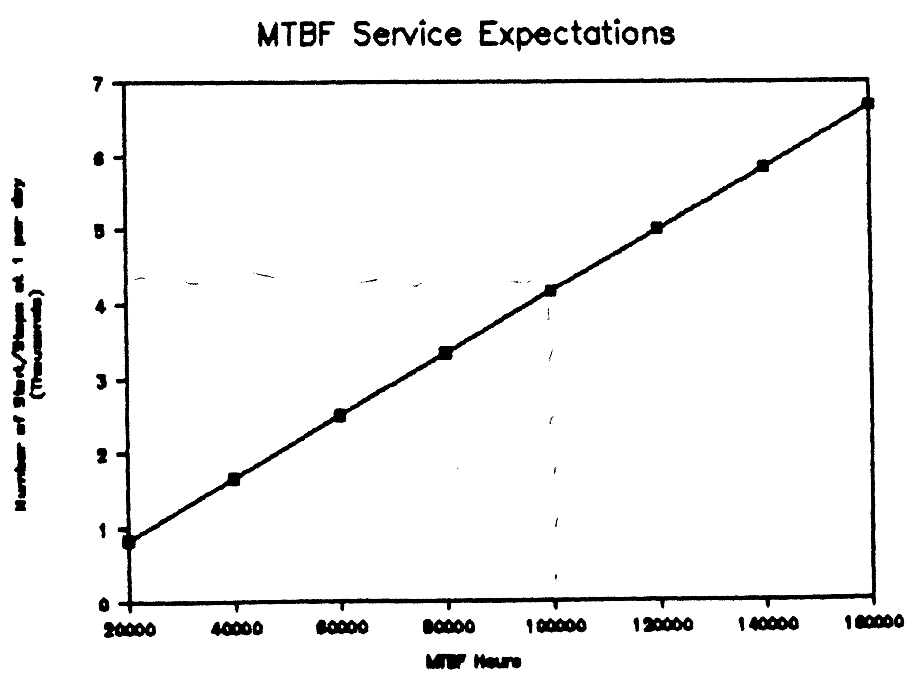

THE HEAD... How Has It Evolved?

- Slider
  - Geometry
    - "Footprint"
      - Friction

        Dynamic Load (early and recent)

        1973 - IBM 3340 "Winchester" first CSS head

        Smooth surfaces; friction force proportional to apparent -> real area of contact

$$F = s * A_r$$

F = total friction force

s = bulk shear strength of weaker material

A_r = real area of contact

Friction vs. Humidity / Lube

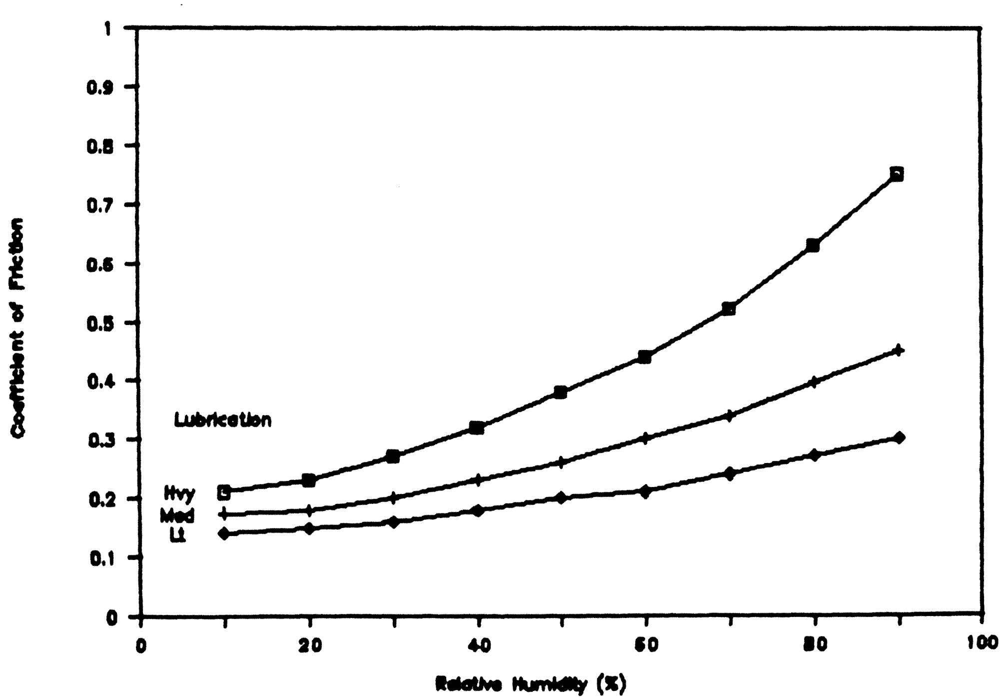

THE HEAD... How Has It Evolved? (cont.)

- Friction...

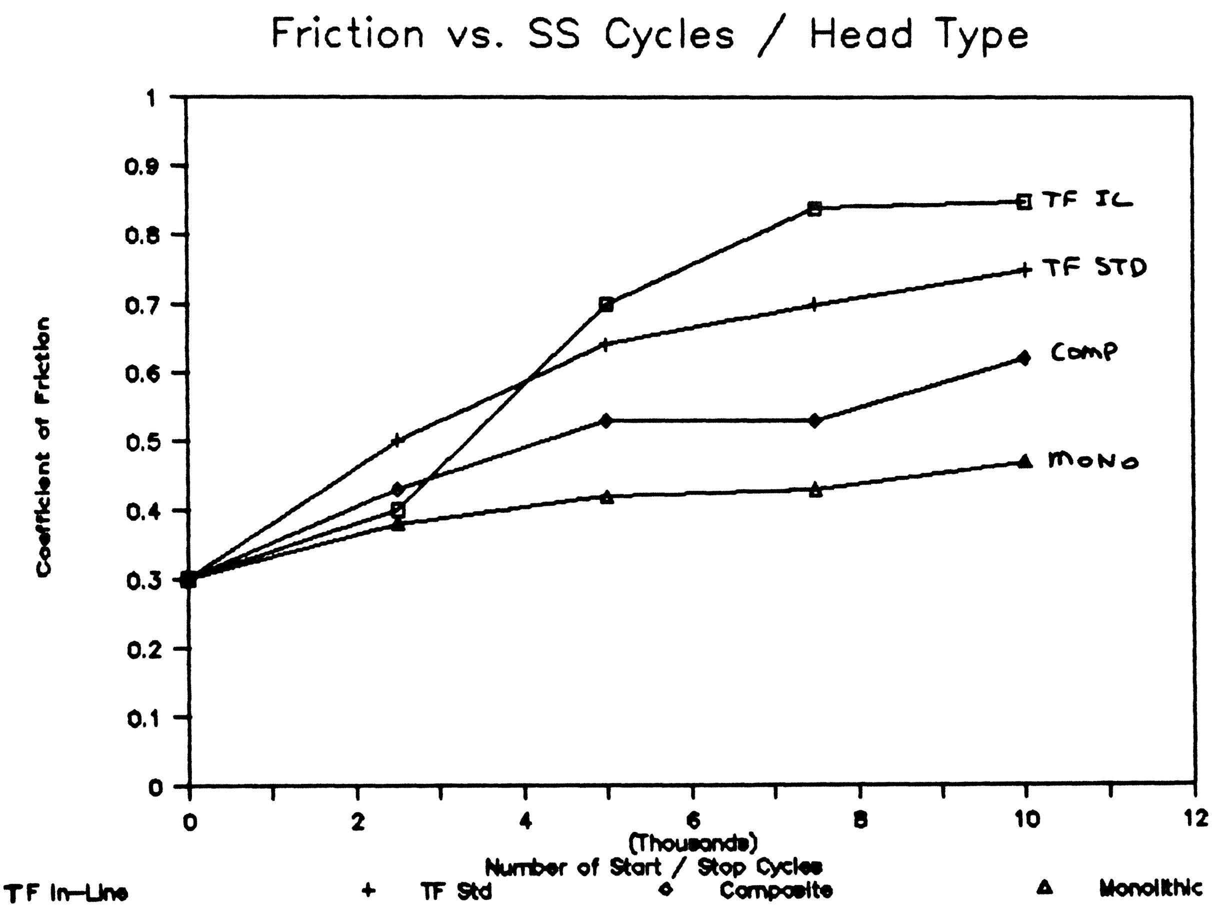

THE HEAD... How Has It Evolved? (cont.)

- Stiction

  Smaller footprint heads have lower loads and thus less stiction force

  Smaller footprint heads have less contact area and thus less stiction force

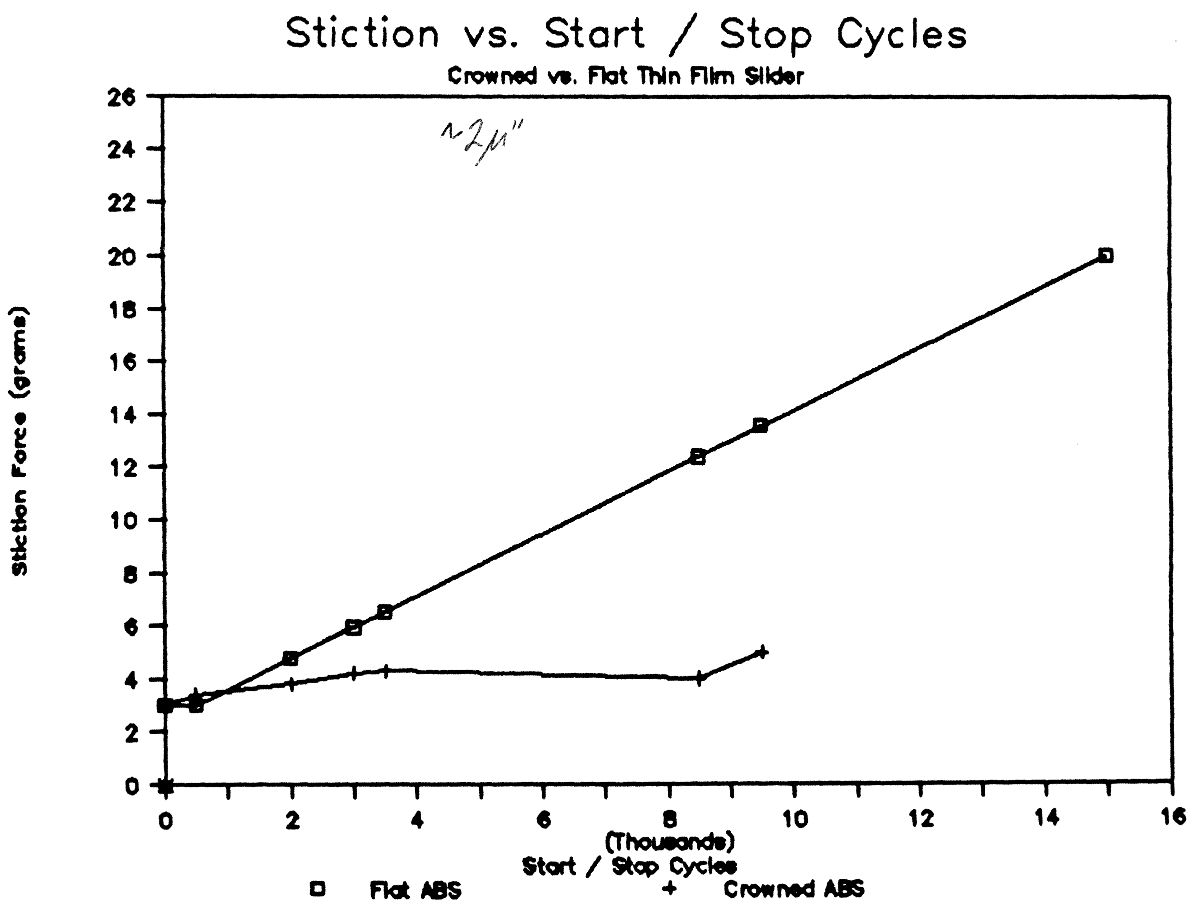

THE HEAD... How Has It Evolved? (cont.)

- Height (the "other dimension")

  Closer disk spacing allows more MBytes/Box

  Less seek (or crash stop) -induced moment

- Volume (i.e., mass)
  - Higher Natural Frequencies

    Better disk following

    Better operating shock / vibration
  - Modified air bearing stiffness

Air Bearing Stiffness vs. Frequency

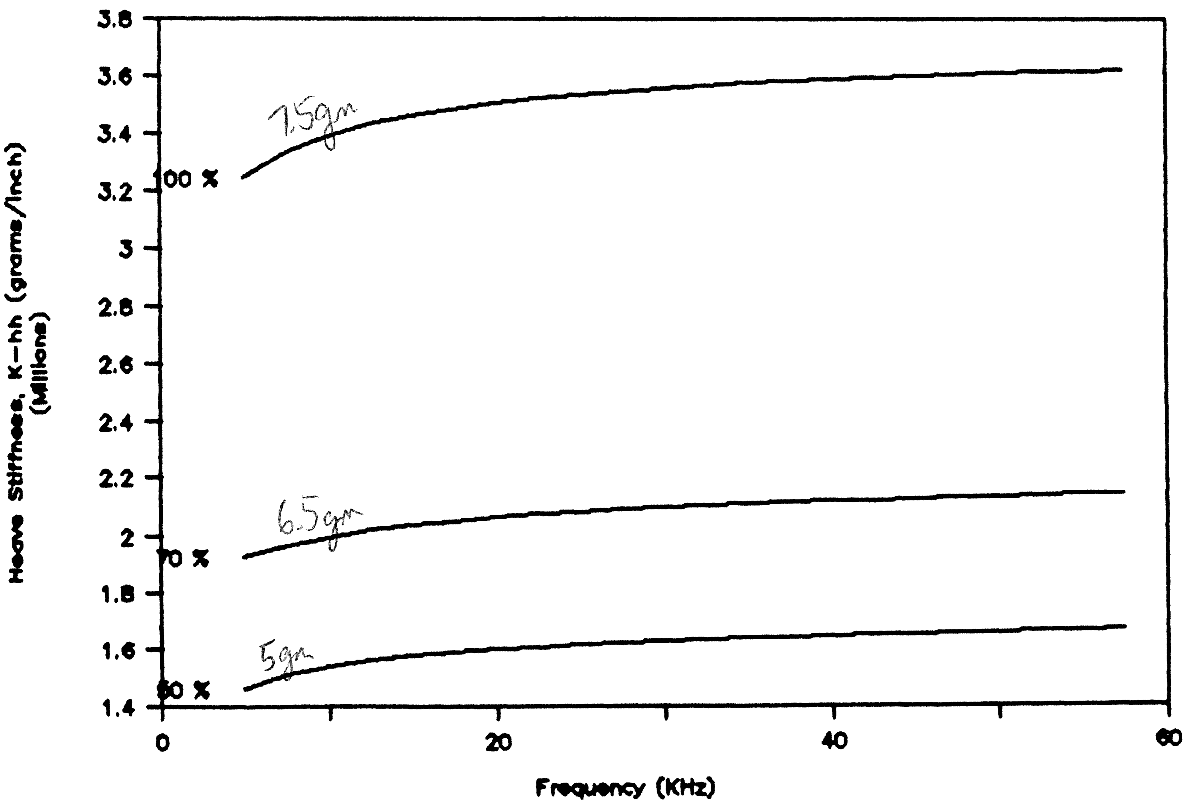

- Modified air bearing damping

Air Bearing Damping vs. Frequency

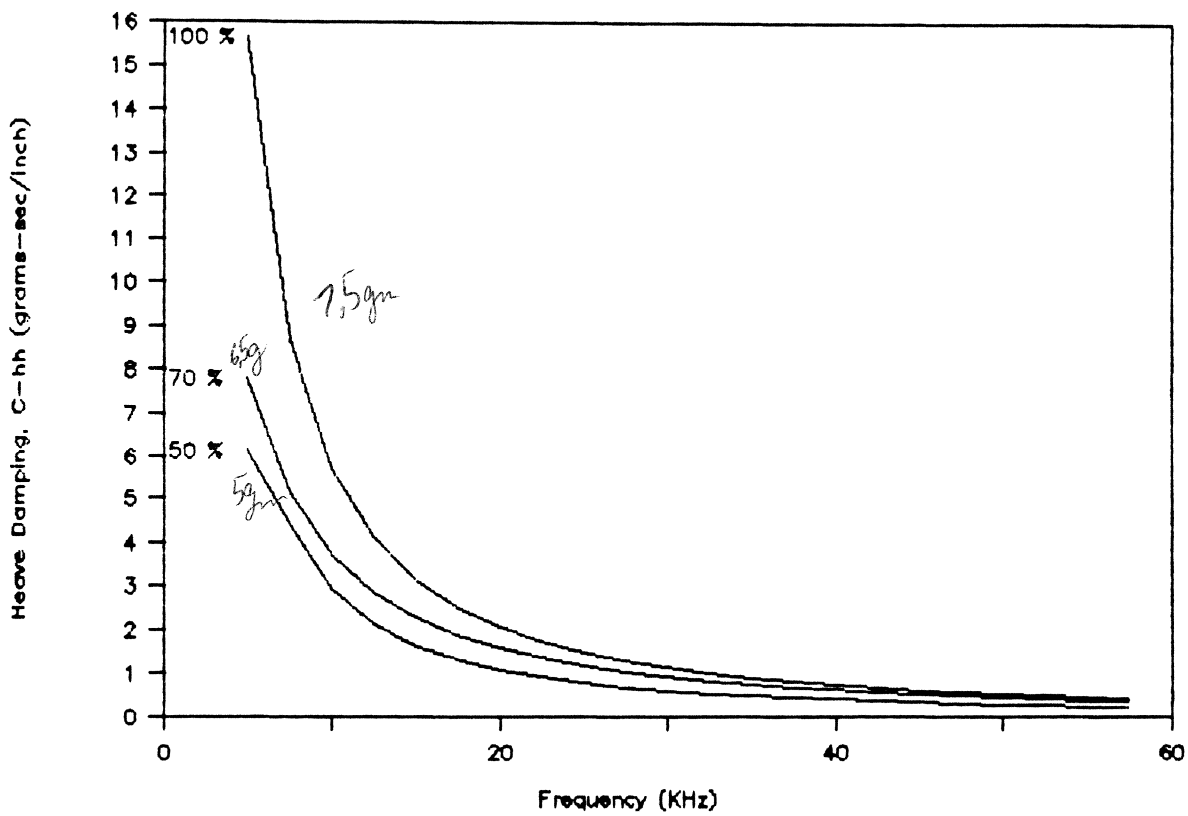

THE HEAD... How Has It Evolved? (cont.)

- Faster Seeks

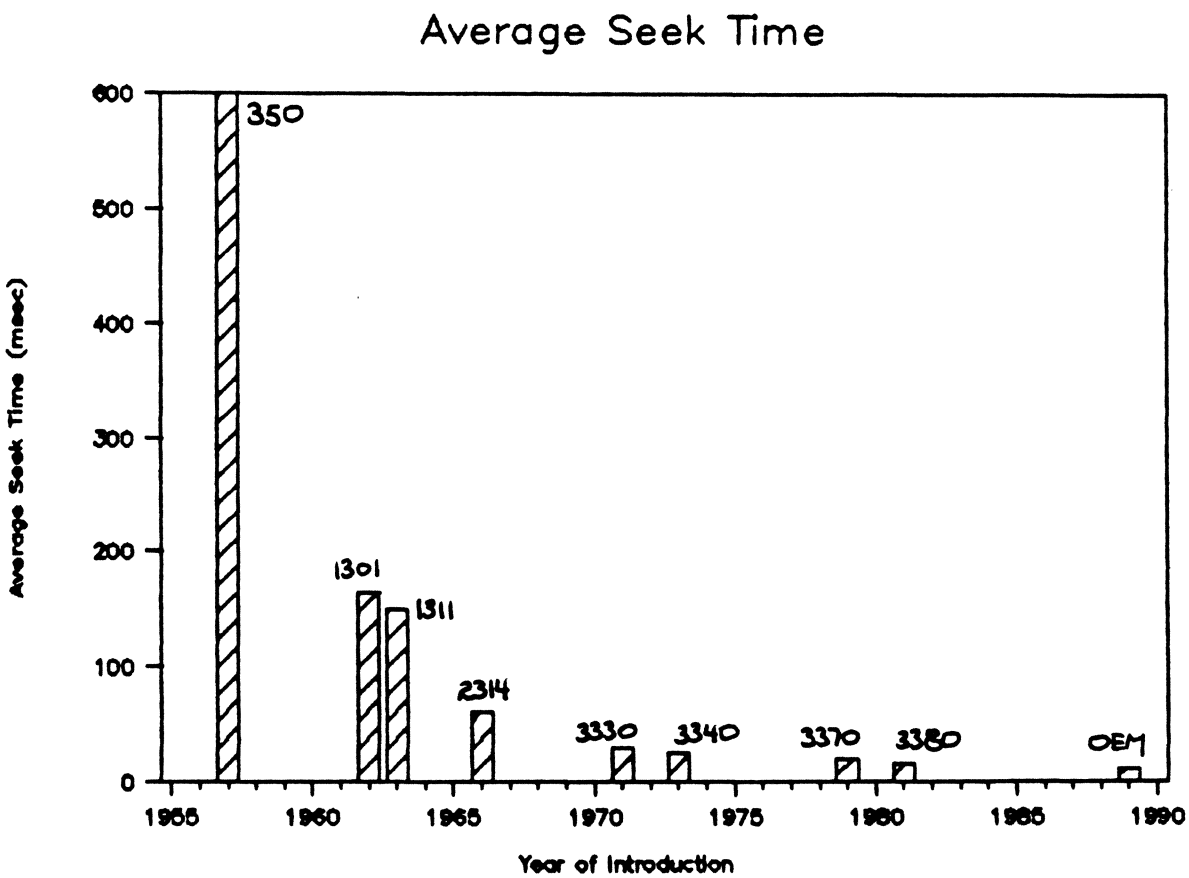

IBM Journal of Research and Development, VOL. 25, No. 5, September, 1981. (25th Anniversary Issue)

THE HEAD... How Has It Evolved? (cont.)

- Material
  - Aluminum
  - Steel
  - Ceramics
  - Ferrite
  - Hard Ceramics
- Important Properties
  - Surface Finish
  - Density
  - Porosity
  - Hardness
  - Corrosion Resistance
  - Thermal Expansion Coefficient

THE HEAD... How Has It Evolved? (cont.)

- Flexure

1953...IBM Ramac...massive positioning system

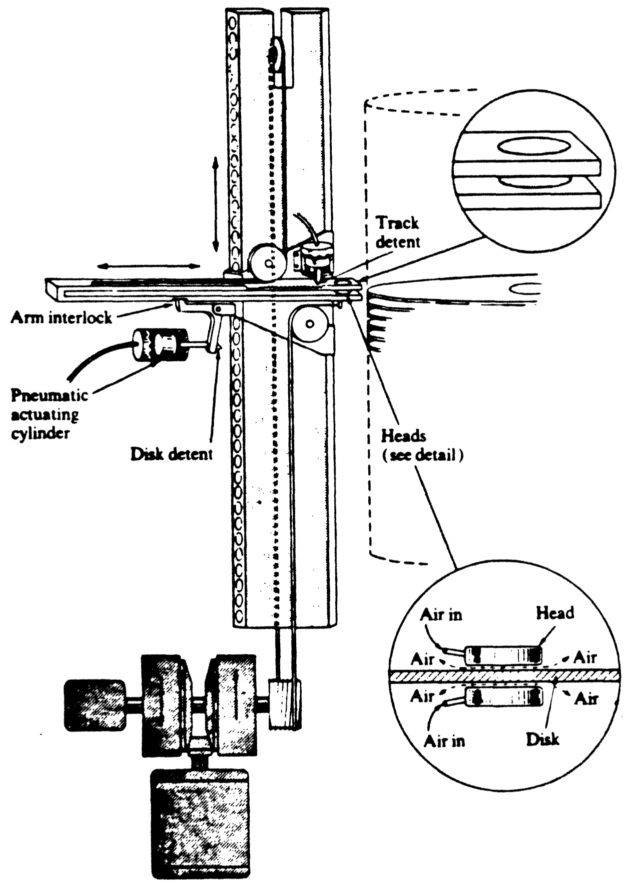

1962...IBM 1301...1 slider/disk surface to reduce total mechanisms required

---

IBM Journal of Research and Development, VOL. 25, No. 5, September, 1981. (25th Anniversary Issue)

THE HEAD... How Has It Evolved? (cont.)

1973...IBM 3340...

Low load (< 20 grams)...eliminates mechanism for 300-400 gram load

Contact stop/start...eliminates load/unload mechanism

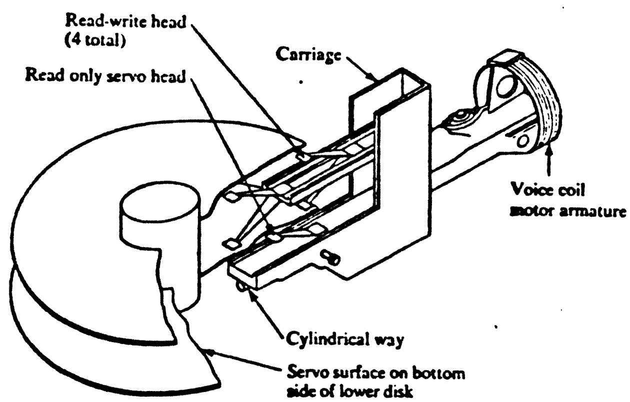

Shorter access times => higher servo bandwidth which require higher mechanical resonances from flexure/suspension assembly

---

Oswald, R. K., "Design of a Disk File Head Positioning Servo", IBM Journ. of Res. and Dev., Vol. 18, No. 6, November, 1974, p. 506.

THE HEAD... How Has It Evolved? (cont.)

- Air Bearings (made disk drives possible!)
  - Contours

    Flat (hydro-static)

    Spherical (with holes)

    Cylindrical (with holes or slots)

    Taper-Flat

    Taper-Flat Rails (1973 - Present)

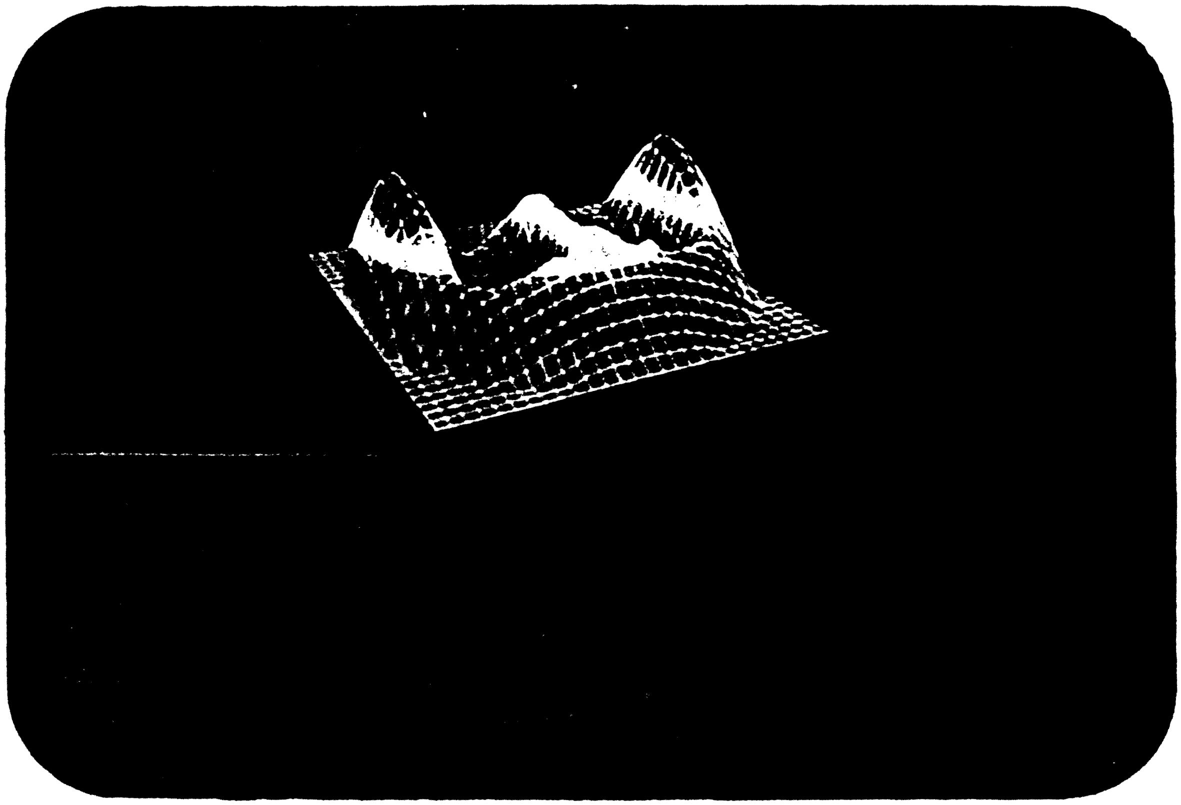

"Sperical bearing" head

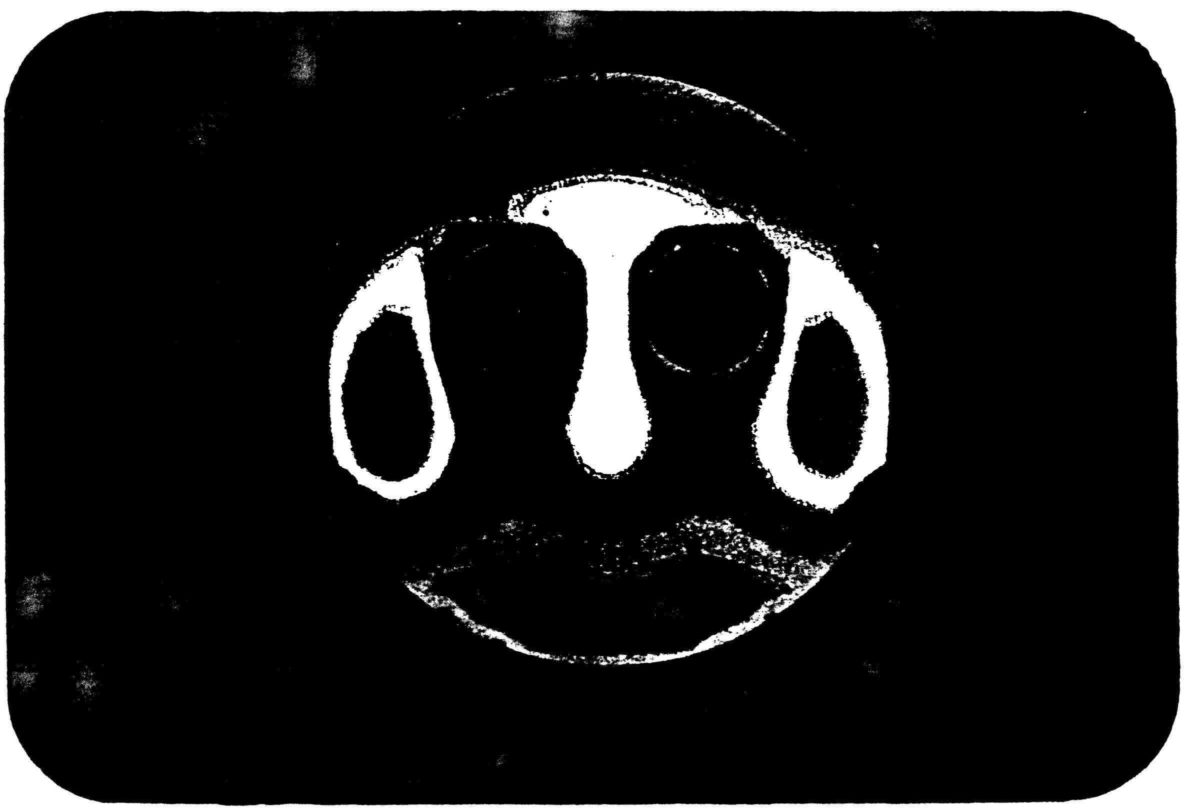

Pressure contours

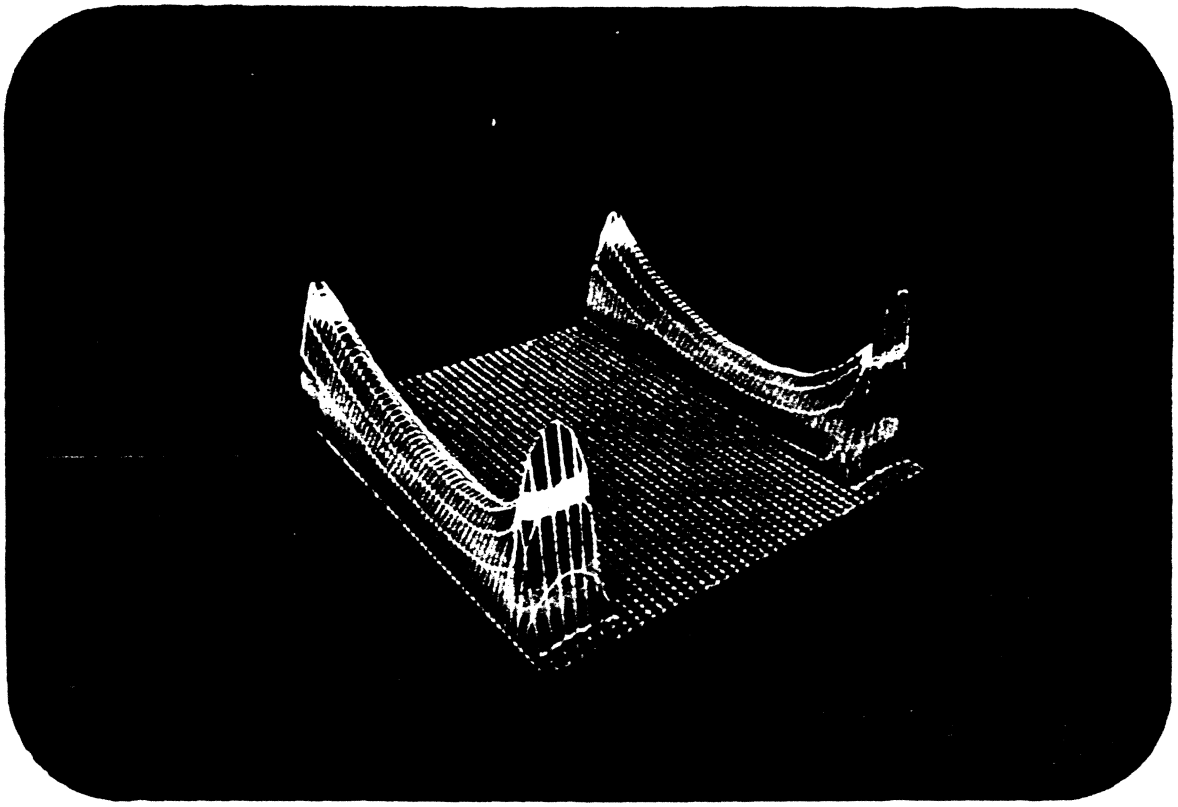

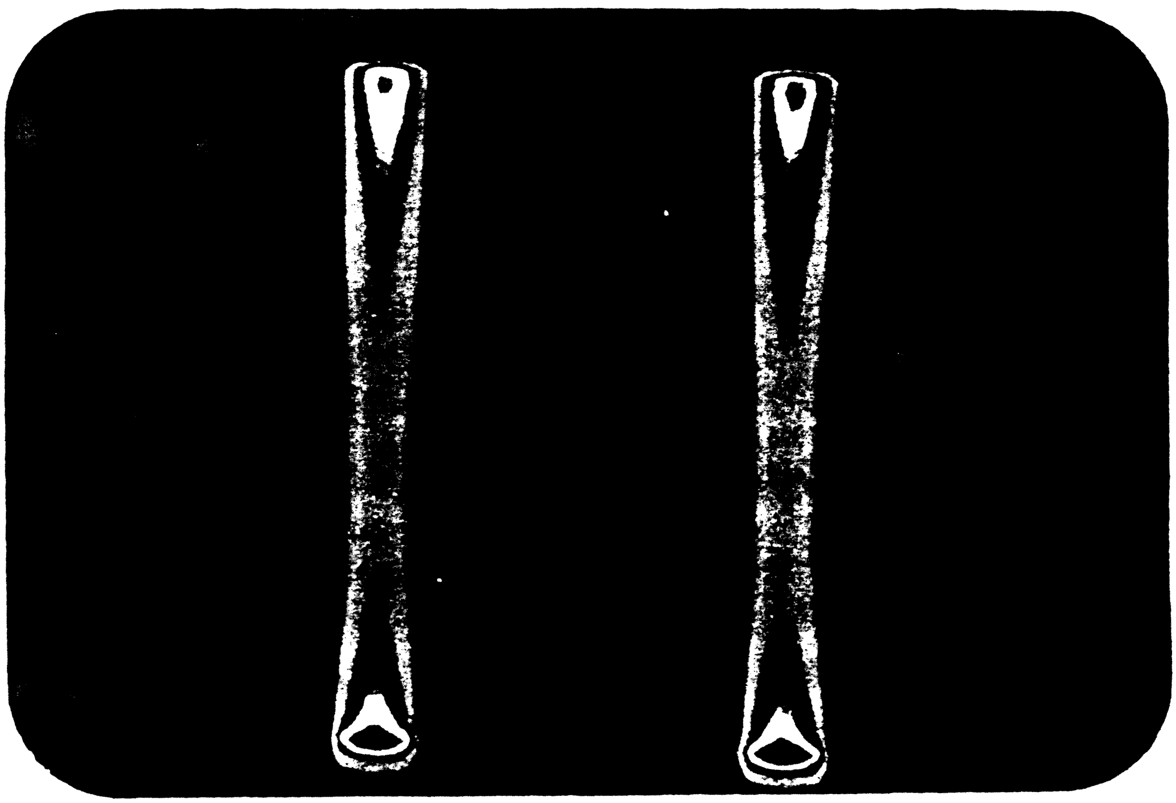

THE HEAD... How Has It Evolved? (cont.)

- Flying Height

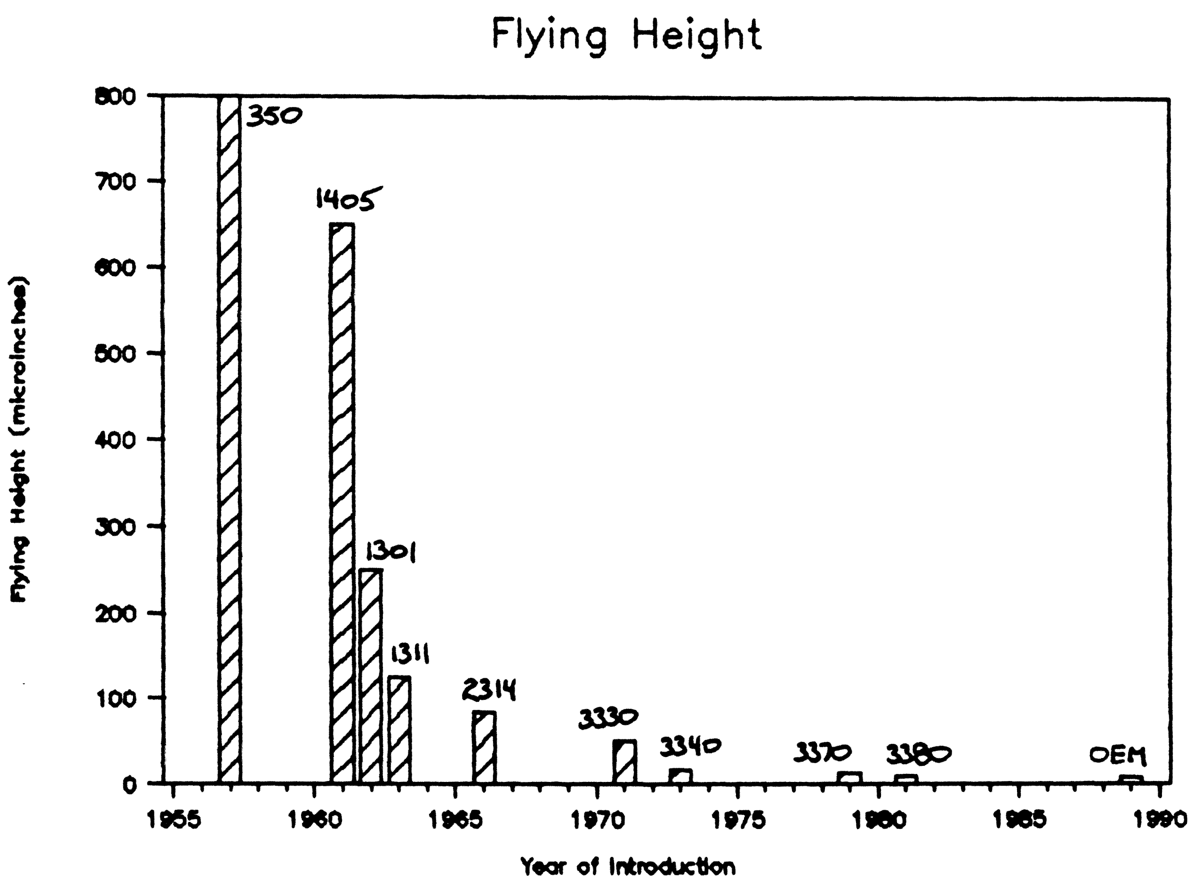

IBM Journal of Research and Development, VOL. 25, No. 5, September, 1981. (25th Anniversary Issue)

THE HEAD... How Has It Evolved? (cont.)

- Flying Height Decrease ⇒ Higher Stiffness

Minimum K–hh vs. Flying Height

(by Load and ABS Width)

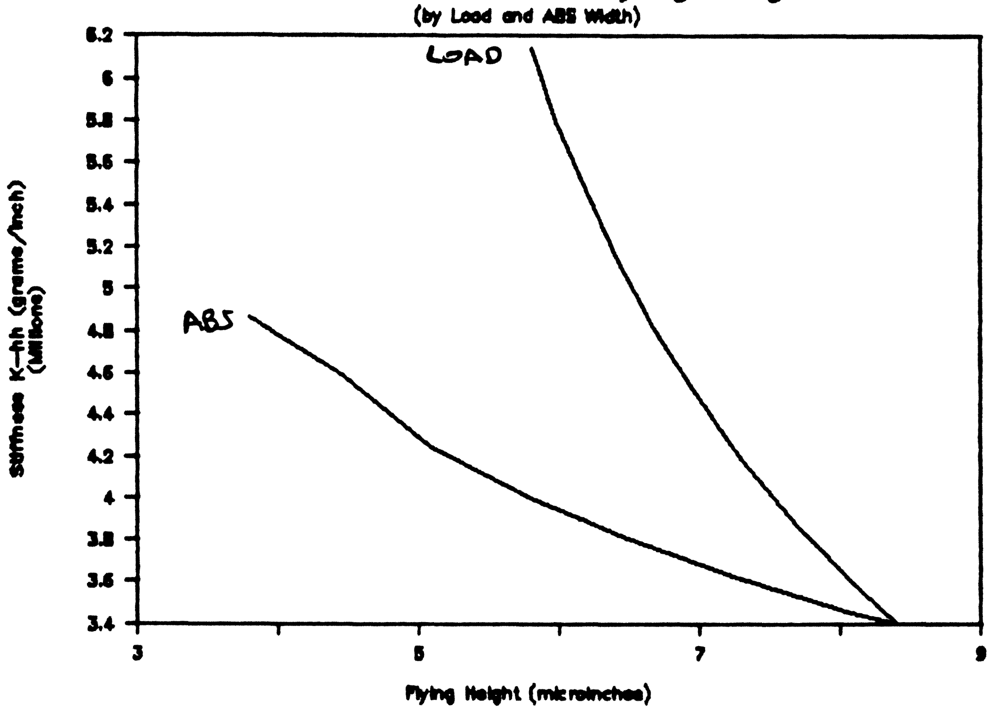

- Flying Height Decrease ⇒ Lower Damping

Minimum C–hh vs. Flying Height

(by Load and ABS Width)

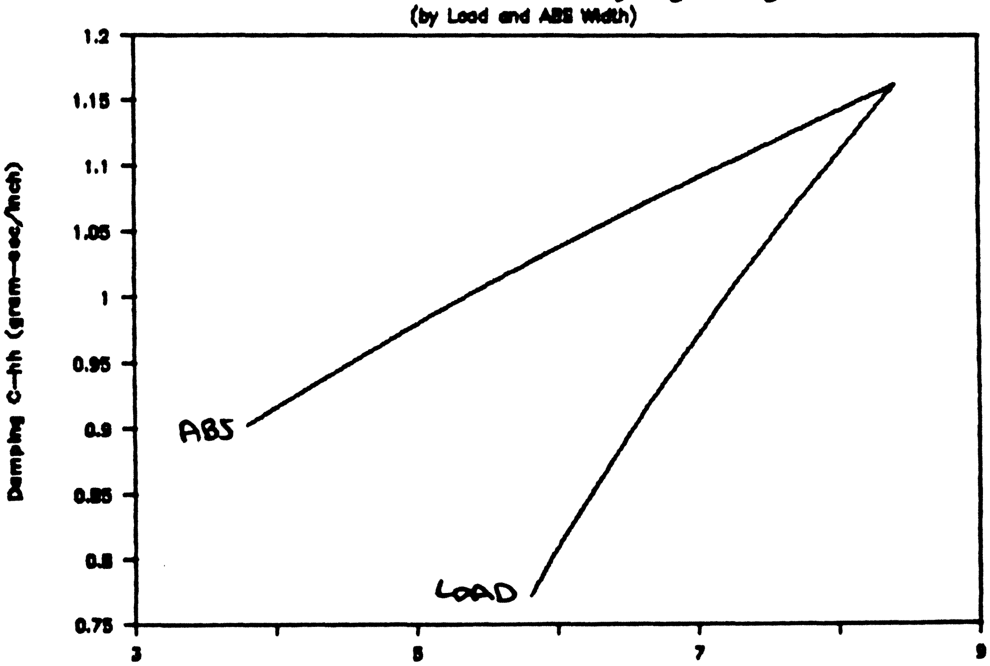

THE HEAD... What Will It Look Like in the Future?

- Lower Flying Heights
  - New Air Bearing Computer Models
    - Slip Flow?
    - Kinetic Theory?
    - Mostly Disk Limited
  - Must Consider Damping
  - Skew Sensitivity
    - Skew-Bias Optimization

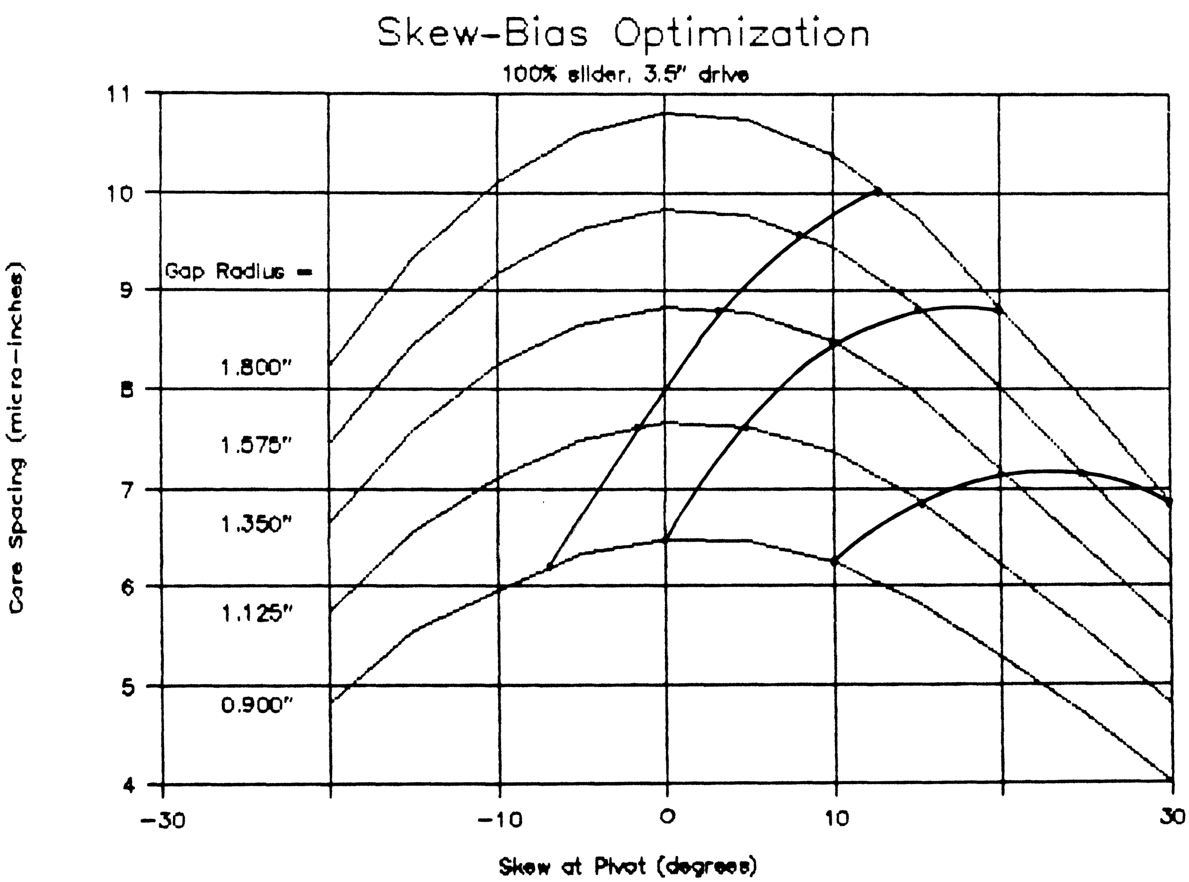

THE HEAD... What Will It Look Like in the Future? (cont.)

- Skew Sensitivity
  - Heavy-Blend...Transverse Pressure Contour
  - Transverse Slot
- Smaller Sliders
  - 100% since 1979
  - 70% becoming popular
  - 50% under development
- Techniques for Reducing Stiction / Friction
  - Texture (mechanical or chemical)
  - Slider Crown
  - Lower Load
  - Smaller Footprint
  - Dynamic Load
- Materials
- Flexure
  - Thinner Profile
  - New Mounting Techniques
    - Screw Mount
    - Swage Mount
    - Glue, etc.
  - New Designs
    - Higher Natural Frequencies
    - Better Damping
    - Less Off-Track Coupling of Modes

THE HEAD... What Will It Look Like in the Future? (cont.)

- Some Examples...
  - Evolution of Current Product Types
  - LETI "IC" Integrated Head Design
  - Springer Technology
  - Miscellaneous Future Concepts (things we can't even talk about!)

FLYING HEIGHT AND CONTROL

S. Scott Murray
Read-Rite Corporation

AIR BEARING CONSEQUENCES OF TRENDS IN DISK DRIVE DESIGNS

THE NUMBER OF FLUX TRANSITIONS PER INCH IS INCREASING

- Greater lineal density means:
  - Heads must fly lower over smoother media. (This is a big subject, and will be covered in detail as this session continues.)
  - Control of flying height must become tighter.

ACTUATOR PERFORMANCE AND TRACKS PER INCH ARE BOTH INCREASING

- Stiffer track-access requirements mean:
  - Dampeners are frequently required.
  - Suspensions are getting smaller and/or stiffer.
  - Access velocity combined with rotational velocity has an effect on flying which is similar to skew. At radii associated with pre-existing (actuator induced) skew, the head crash risk due to seeking may thus depend on seek direction.
  - Head and suspension mass are becoming more important issues.

DRIVES ARE GETTING SMALLER

- Reduced inner radius means:
  - The load point (dimple) offset in width on the slider needs to increase for zero nominal roll at the inner tracks.
  - Circumferential (curvilinear) disk velocity components mean that heads need to be tested at the same rpm, radius, and skew as the application. Matching speed by flying at a greater radius and reduced rpm no longer produces an accurate representation of head performance.

CONSEQUENCES IN DISK DRIVE DESIGN TRENDS, CONTINUED....

DISKS ARE BEING PLACED CLOSER TOGETHER

- Reduced spacing means:
  - Heads are getting smaller.
  - Low profile suspensions are frequently required.
  - Less torque per surface for starting may be available, which means reduced suspension load.
  - More attention is required for testing to such critical (but often mundane) items such as the design of the head lifters on the test equipment.

SOME UNSEALED DRIVES ARE SPECIFIED FOR USE AT VERY HIGH ALTITUDES

- High altitude specifications mean:
  - Flight height will be greatly affected at high skew angles.
  - The head/disk interface may not compete well with drives designed for lower altitude use when used at lower altitudes.

  Opinion:

  Very few disk drives are used at altitudes above 3,000 meters mean sea level. If your marketing department insists that they can not sell a drive unless it meets reliability specifications to 15,000 feet, then you need a sealed drive and/or a more astute sales & marketing organization.

power $\propto$ RPM^3

DRIVES ARE CONSUMING LESS POWER

- Reduced power means:
  - Some drives (particularly for battery-powered computers) are being designed with rpm values less than 3,600. This means wider air bearing surfaces for a given preload.
  - Smaller head geometries with lower loads are being designed into drives. Reducing the preload reduces the required starting torque.

CONSEQUENCES OF TRENDS IN DISK DRIVE DESIGN, CONTINUED...

MULTIPLE-ZONE RECORDING ABILITY IS BEING DESIGNED INTO DRIVES

- Zone-bit-recording means:
  - Flying height must be controlled as a function of radius. This can be accomplished by either wise actuator design, novel head design, or both.
  - More must be known about the drive early in design. This increases the need for accurate modeling and simulation.

SOME DRIVES ARE EXCEEDING 3,600 RPM (CHIEFLY FOR WORKSTATIONS)

acc $\propto$ RPM^2

- High rotational rates mean:
  - Heads must handle higher axial disk accelerations. Axial acceleration for a fixed flatness value increases with the square of rpm.

SEALED DRIVES ARE BEING DESIGNED WITH NOVEL ATMOSPHERES

- Positive gauge pressure oxygen free use means:
  - The rail width to achieve a given flying height will probably be different than for conventional use.
  - Extreme care must be taken to interpret how test results will relate to customer drive performance.
  - Mean free path will remain constant over the designed temperature range, but viscosity and pressure will increase with absolute temperature, making flying height more temperature sensitive. (An increase in flying height with an increase in temperature has recording performance consequences.)

Static
H_2O
O_2
CH_4
} Reasons to purge

Note that η changes with temperature, so purging does not eliminate FHT variation

EFFECT OF CUSTOMER ALTITUDE

If a drive is not sealed, then ambiant pressure drops as altitude increases. The standard pressure as a function of altitude to 10,000 feet can be approximated as:

Ambiant pressure (psia) = 14.696 * EXP(-3.58526*10^(-5) * A)

where A is the altitude in feet.

The mean free path of an air molecule increases with decreasing pressure at a specific temperature. It also approximately increases with increasing absolute temperature (Kelvin or Rankine). This is because it has a 1/n relationship to the old chemistry formula:

$$PV = nRT$$

Because $\lambda \propto 1/n$,

$$\lambda \propto T/P$$

where λ = mean free path.

When mean free path increases, flying height becomes more sensitive to skew. With some actuator geometries which have a small skew magnitude at the inner track and a large skew at the outermost, heads will fly lowest at the inner radius when the drive is at sea level. Taking the drive up to the maximum specified altitude will sometimes change the flying height vs radius curve such that the heads will fly lowest at the outermost disk radius.

2.67 μ" is mean free path

STANDARD ATMOSPHERIC PRESSURE VS ALTITUDE

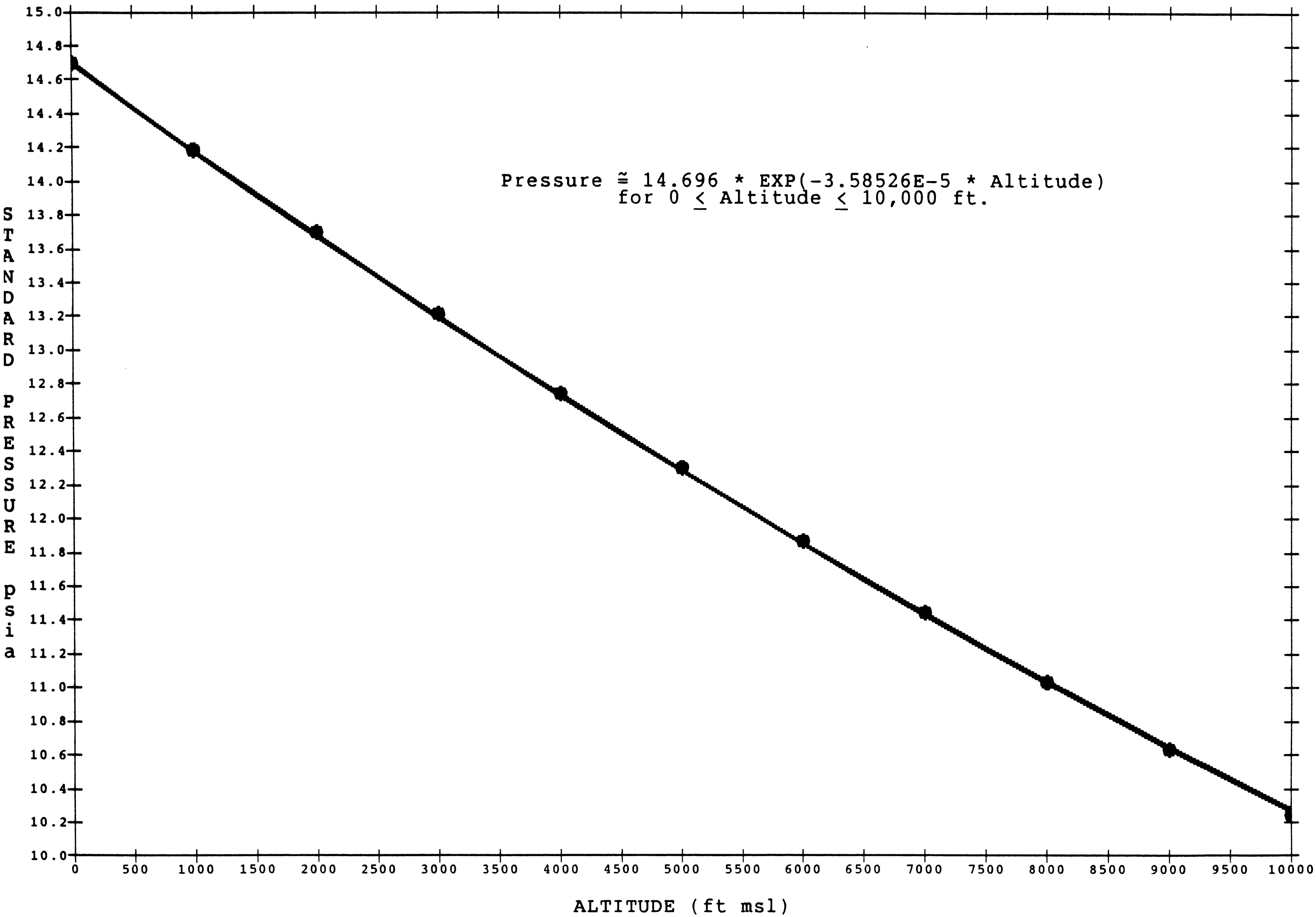

TAPER LENGTH AND ANGLE

The variable most sensitive to taper length is pitch. The attached curves demonstrate this, showing flying height and attitude for a full sized (160 mil) slider under the following conditions:

RPM:	3600
Radius:	1.25 inches @ trailing edge center
Rails:	19 mils
Skew:	0 degrees along trailing edge
Load:	9.5 grams, 5 mils behind length center, 2 mils od of width center.
Taper angle:	50 minutes

As the curves indicate, there is a taper length associated with maximum pitch. The concavity of pitch as a function of taper length is negative, while that of flying height vs pitch may be either positive or negative. A distribution of taper lengths will generally produce an average pitch which is less then the pitch associated with the mean taper length due to this concavity.

Taper angle also affects flying attitude and height. One can show that for many cases, a more shallow angle will produce more pitch, and the head will depart the disk sooner. When taper angle is changed, the nominal taper length may also change.

A drawback to reducing taper angle is that if all else is the same, the standard deviation of taper length is approximately proportional to 1/SIN(taper angle). Because the taper angles are small (<1.2 degrees) this may be approximated as 1/taper angle. For Monte-Carlo analysis in predicting flying height distributions, a 30 minute taper should thus be given twice the standard deviation in length as a 60 minute taper.

Reducing taper angles may thus result in improved optimum performance, with a broader distribution in performance.

Mfg taper length variation ↑ as taper ∠ decr

SLIDER PITCH AS A FUNCTION OF TAPER LENGTH

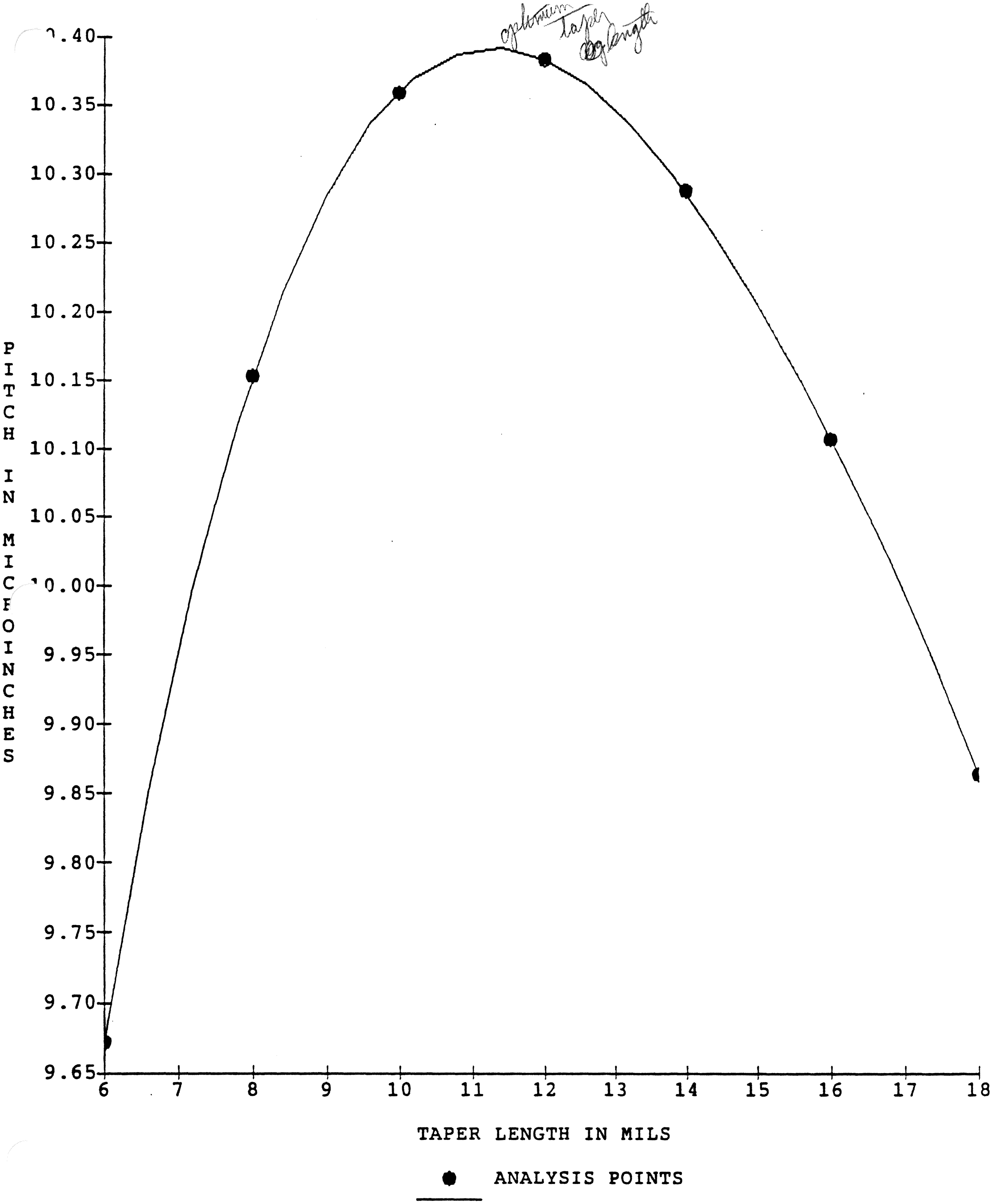

TRAILING EDGE RAIL CLEARANCE AS A FUNCTION OF TAPER LENGTH

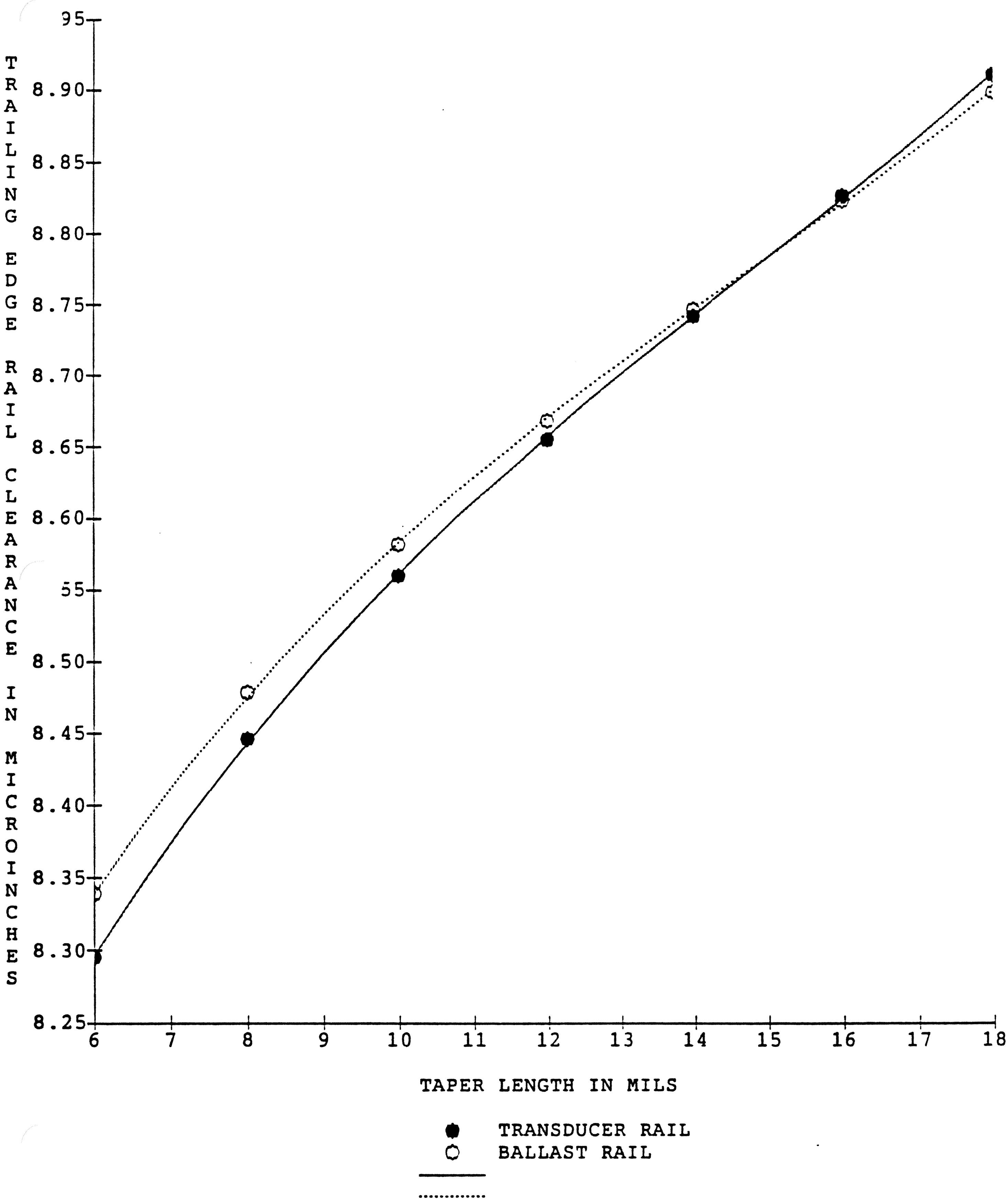

SLIDER SKEW

Skew greatly affects slider clearance and pitch. A slider will fly highest when the load point skew is approximately zero. Pitch has a local minimum very close to a trailing edge center skew of zero.

The two graphs which follow show the effect of skew on flight height and pitch. Skew here is called positive when a line can be drawn from the trailing edge slider center to the center of rotation of the disk without intersecting the slider body.

Sliders with more narrow rails tend to be more skew sensitive. Attitude becomes more skew sensitive at higher altitudes in non-sealed disk drives as well.

Later in this discussion we will discuss this in more detail, along with how to use the effect of skew on flight height to our advantage.

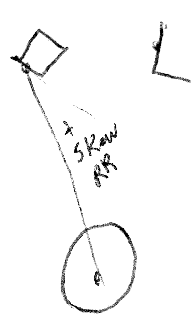

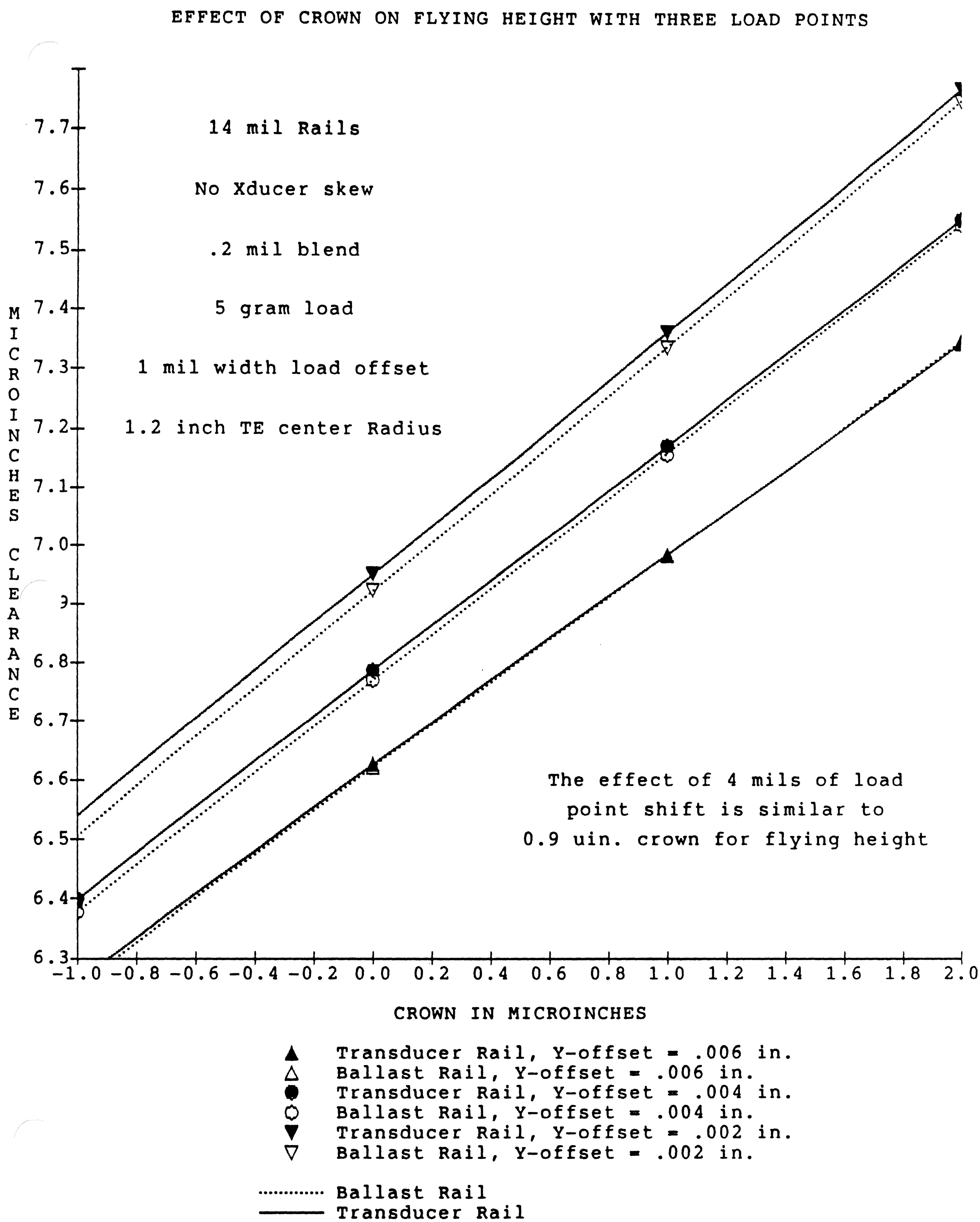

EFFECT OF CROWN ON FLYING HEIGHT WITH THREE LOAD POINTS
14 mil Rails
No Xducer skew
.2 mil blend
5 gram load
1 mil width load offset
1.2 inch TE center Radius
MICROINCHES CLEARANCE
7.7
7.6
7.5
7.4
7.3
7.2
7.1
7.0
6.8
6.7
6.6
6.5
6.4
6.3
-1.0
-0.8
-0.6
-0.4
-0.2
0.0
0.2
0.4
0.6
0.8
1.0
1.2
1.4
1.6
1.8
2.0
The effect of 4 mils of load
point shift is similar to
0.9 uin. crown for flying height
CROWN IN MICROINCHES
Transducer Rail, Y-offset = .006 in.
Ballast Rail, Y-offset = .006 in.
Transducer Rail, Y-offset = .004 in.
Ballast Rail, Y-offset = .004 in.
Transducer Rail, Y-offset = .002 in.
Ballast Rail, Y-offset = .002 in.
Ballast Rail
Transducer Rail

RAIL CLEARANCE AS A FUNCTION OF TRAILING EDGE CENTER DISK RADIUS

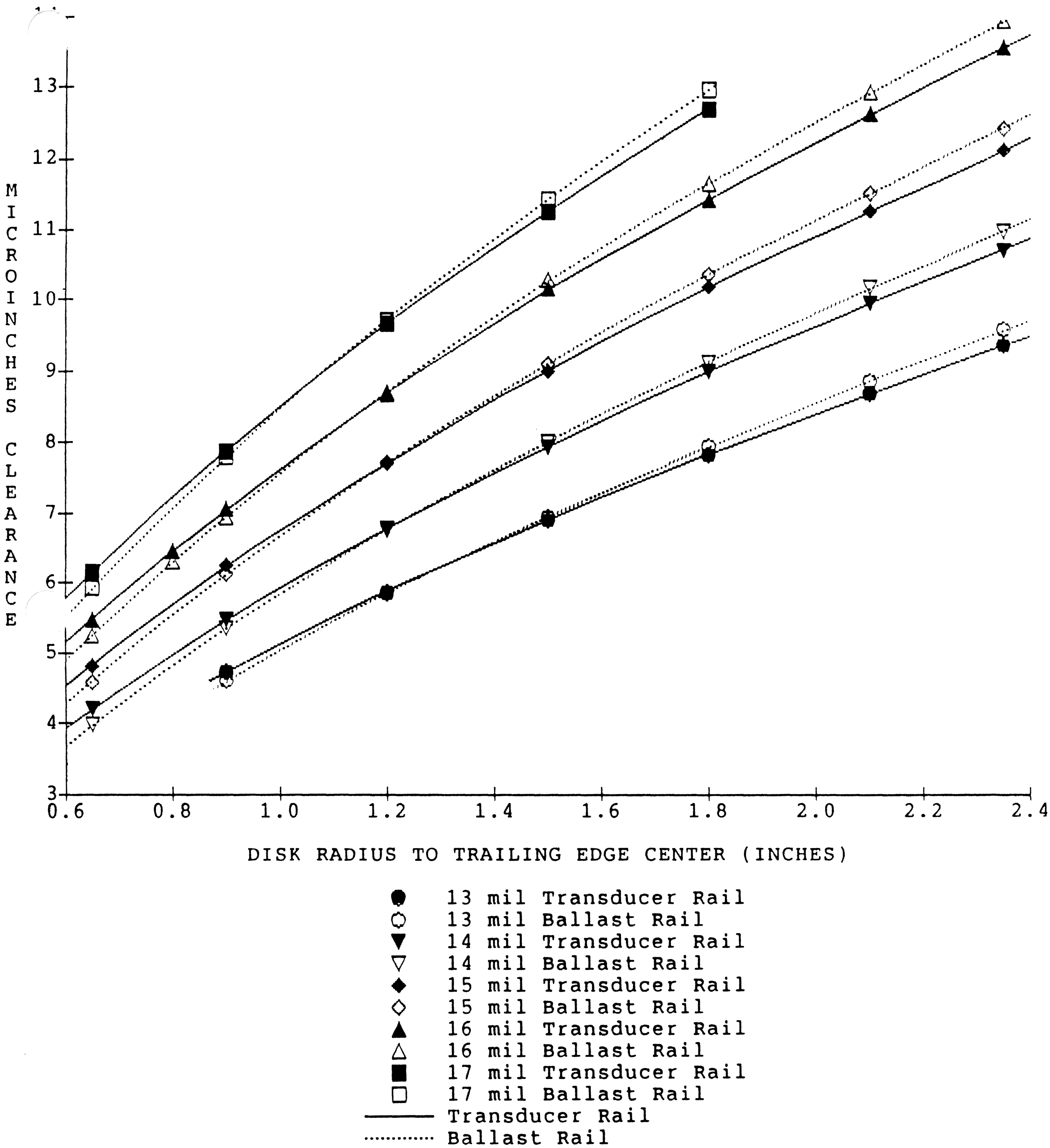

PITCH VS RADIUS WITH ZERO TRAILING EDGE SKEW FOR SEVERAL RAIL WIDTHS

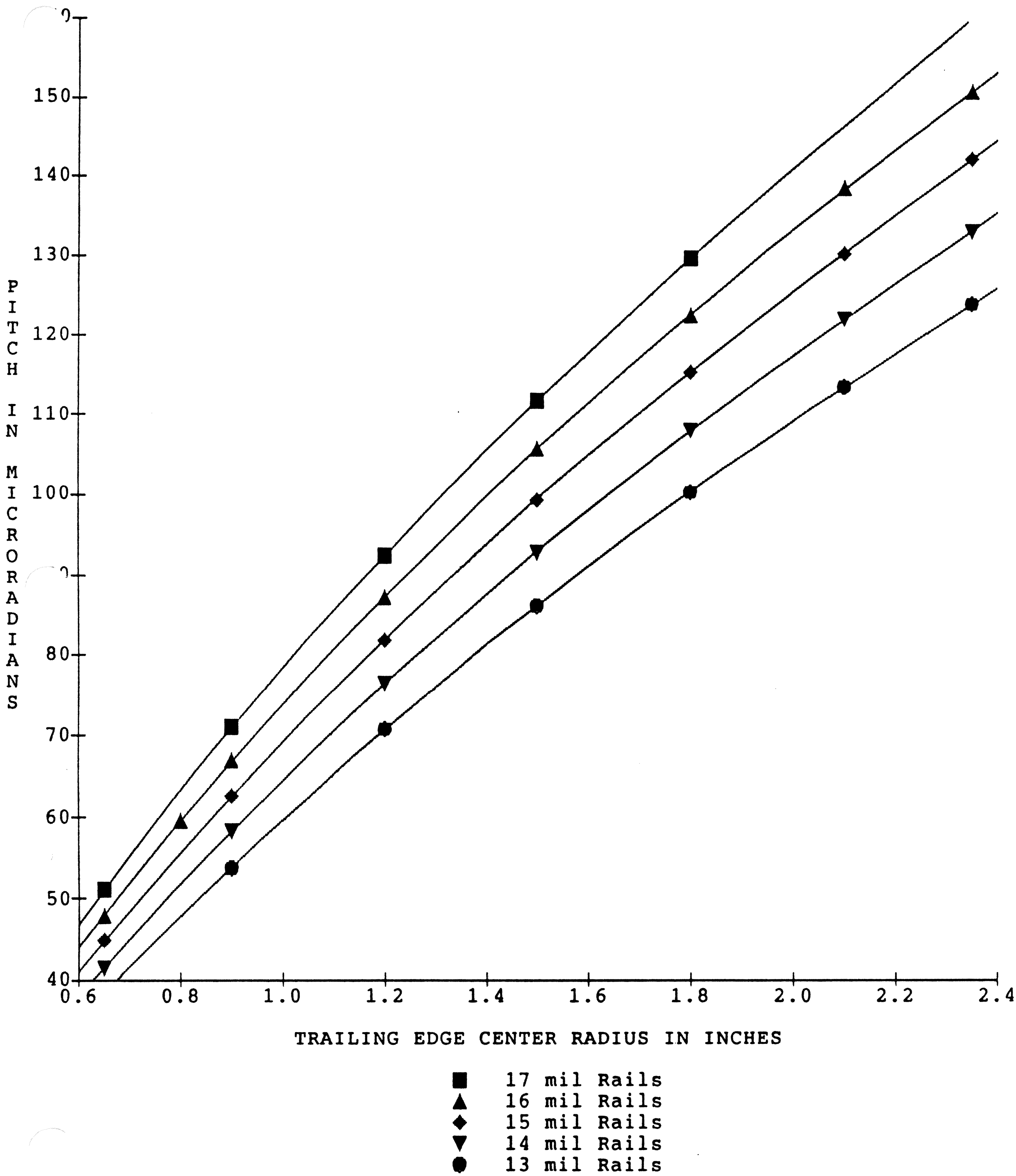

FLYING HEIGHT VS SKEW FOR UNCROWNED MICROSLIDERS AT 1.2 INCH RADIUS

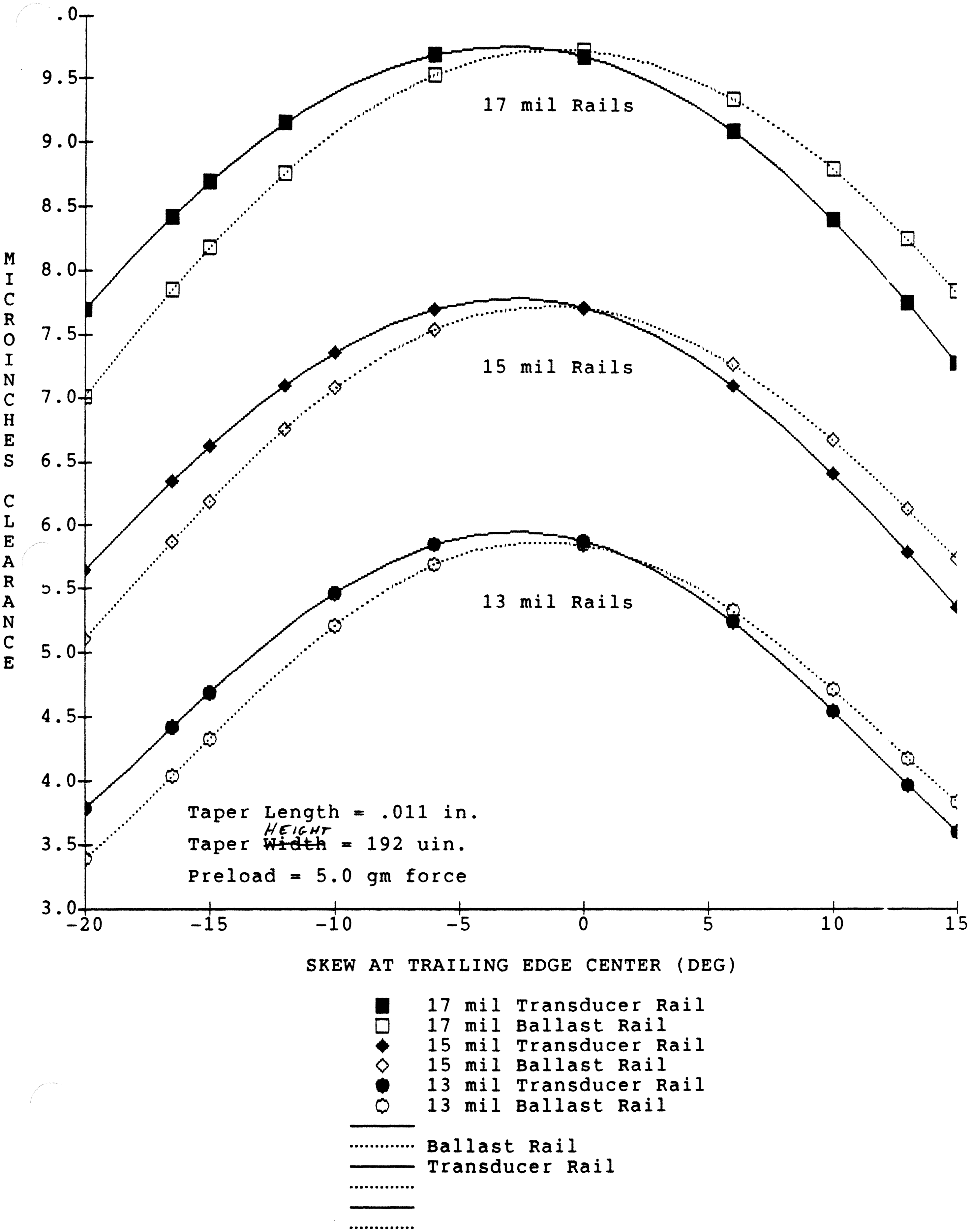

PITCH VS SKEW FOR THREE UNCROWNED MICROSLIDER RAIL WIDTHS AT 1.2 INCH RADIUS

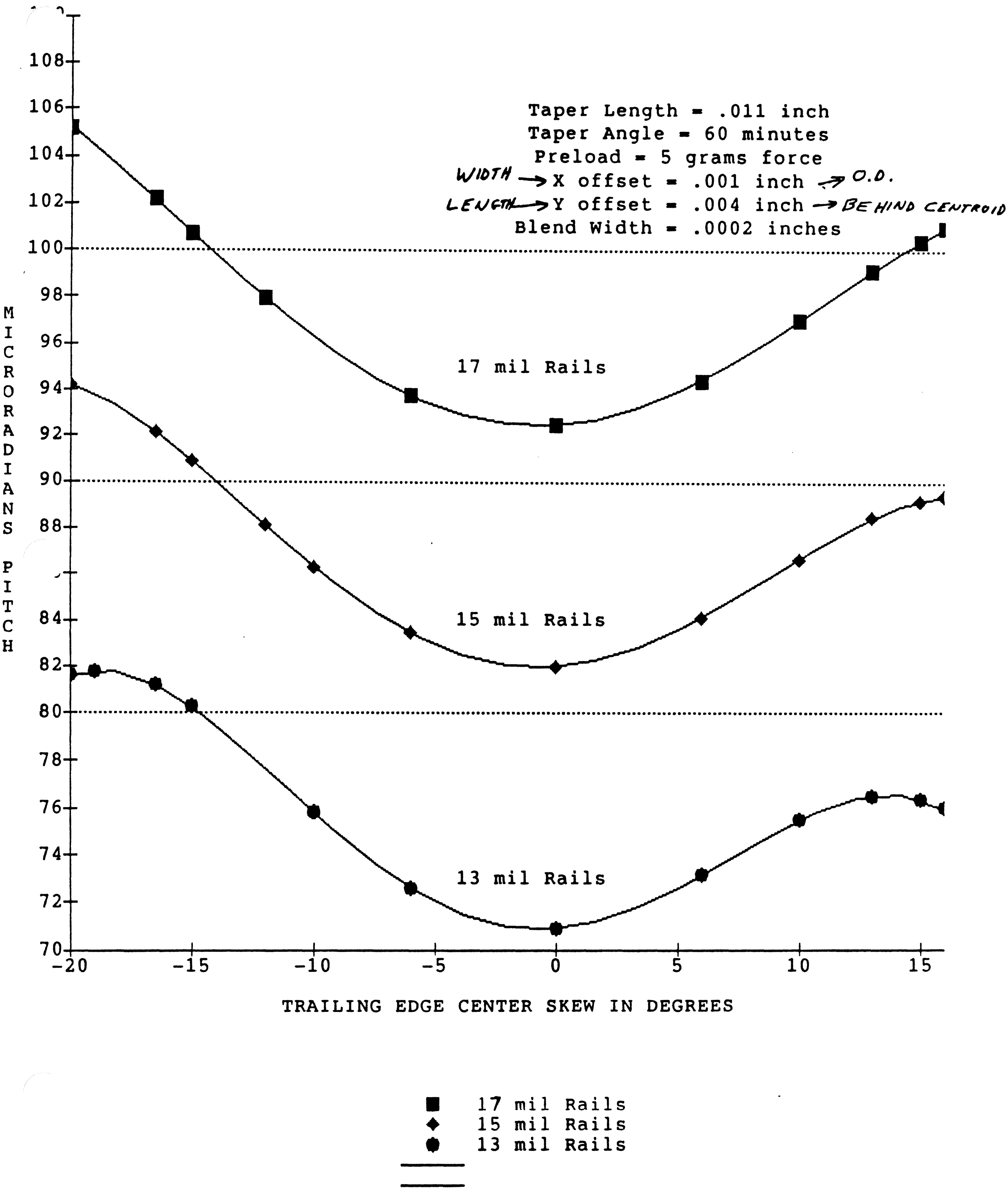

TOPOGRAPHICAL MAPS AND CONSTANT FLYING HEIGHT OPTIMIZATION

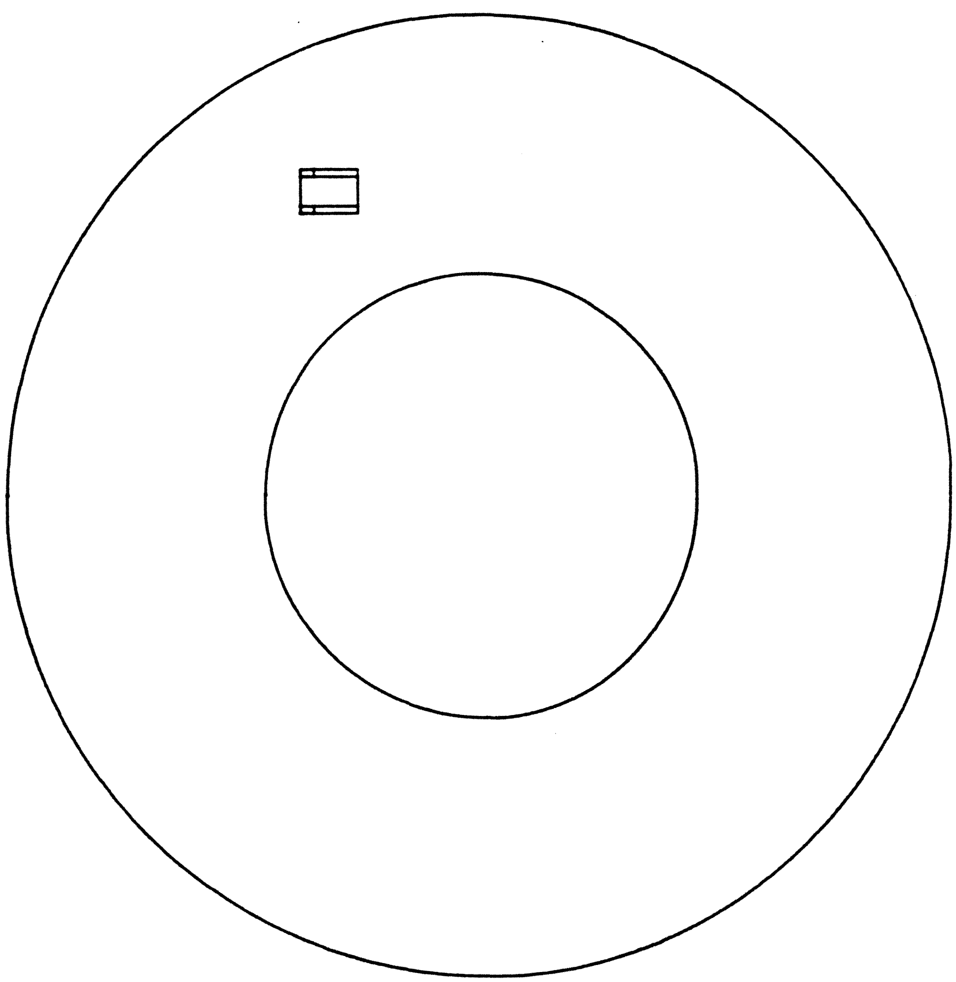

MICROHEAD PITCH IN MICROINCHES VS RADIUS AND SKEW

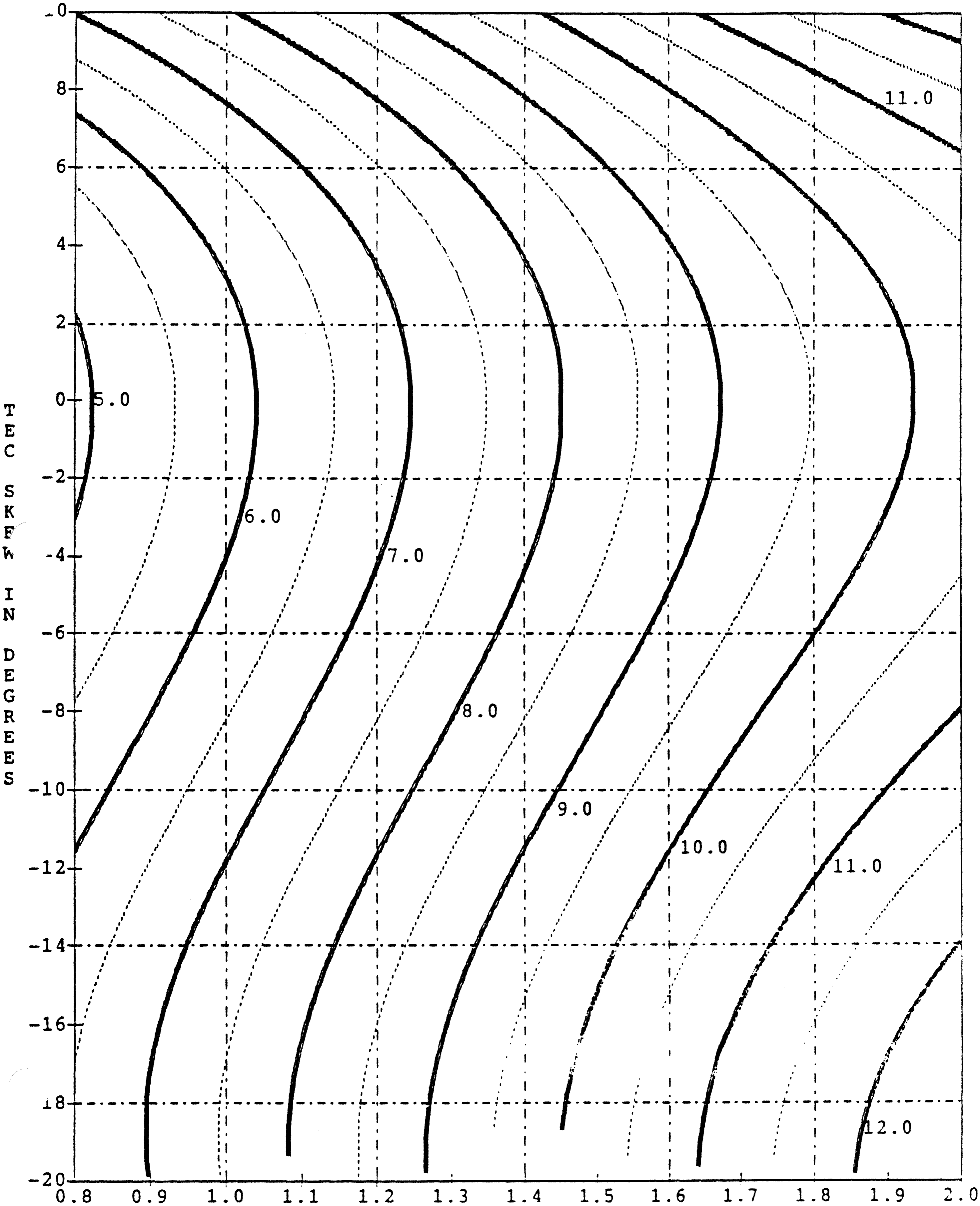

MICROHEAD BALLAST RAIL FLYING HEIGHT VS RADIUS AND SKEW

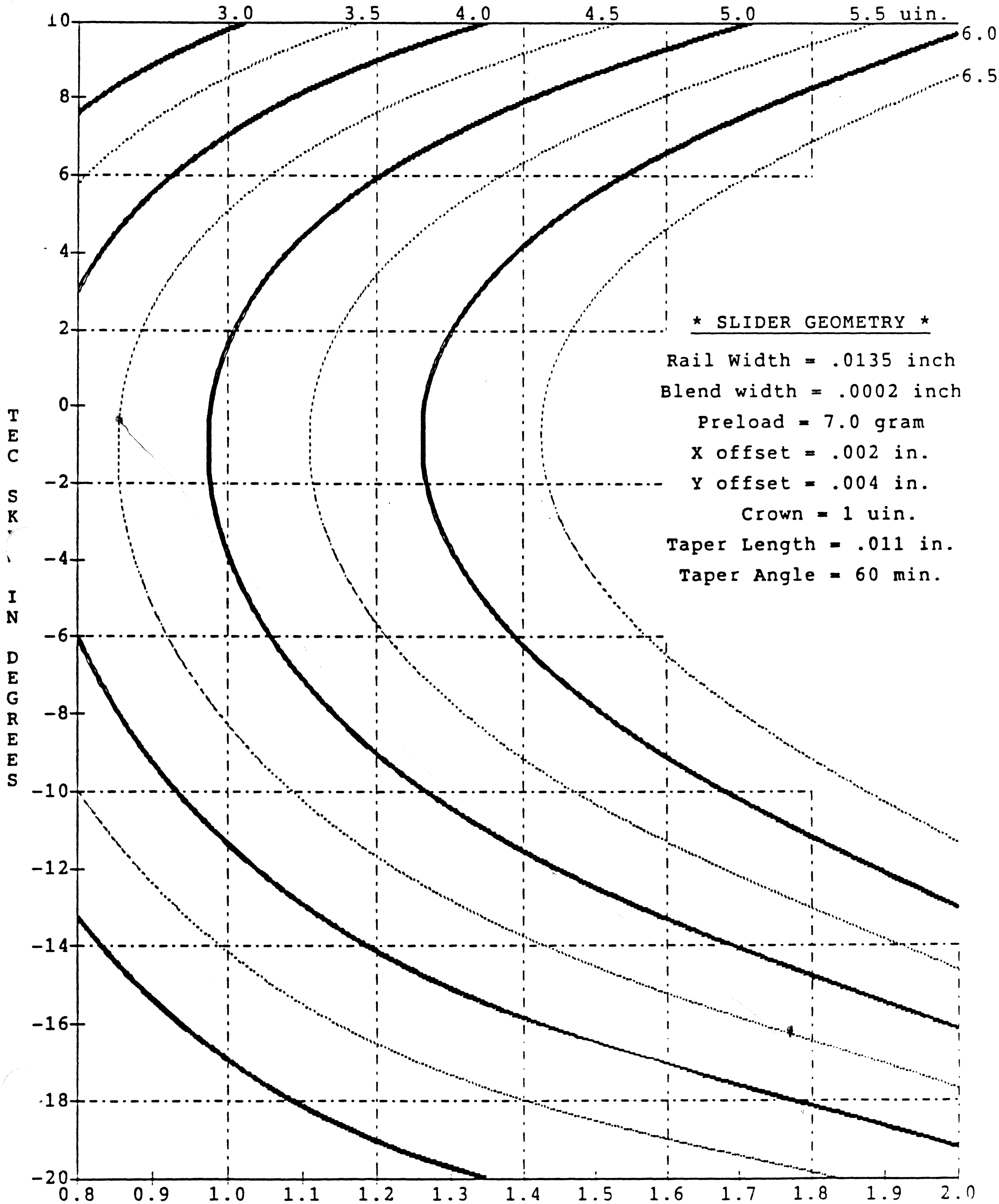

MICROHEAD TRANSDUCER RAIL FLYING HEIGHT VS RADIUS AND SKEW

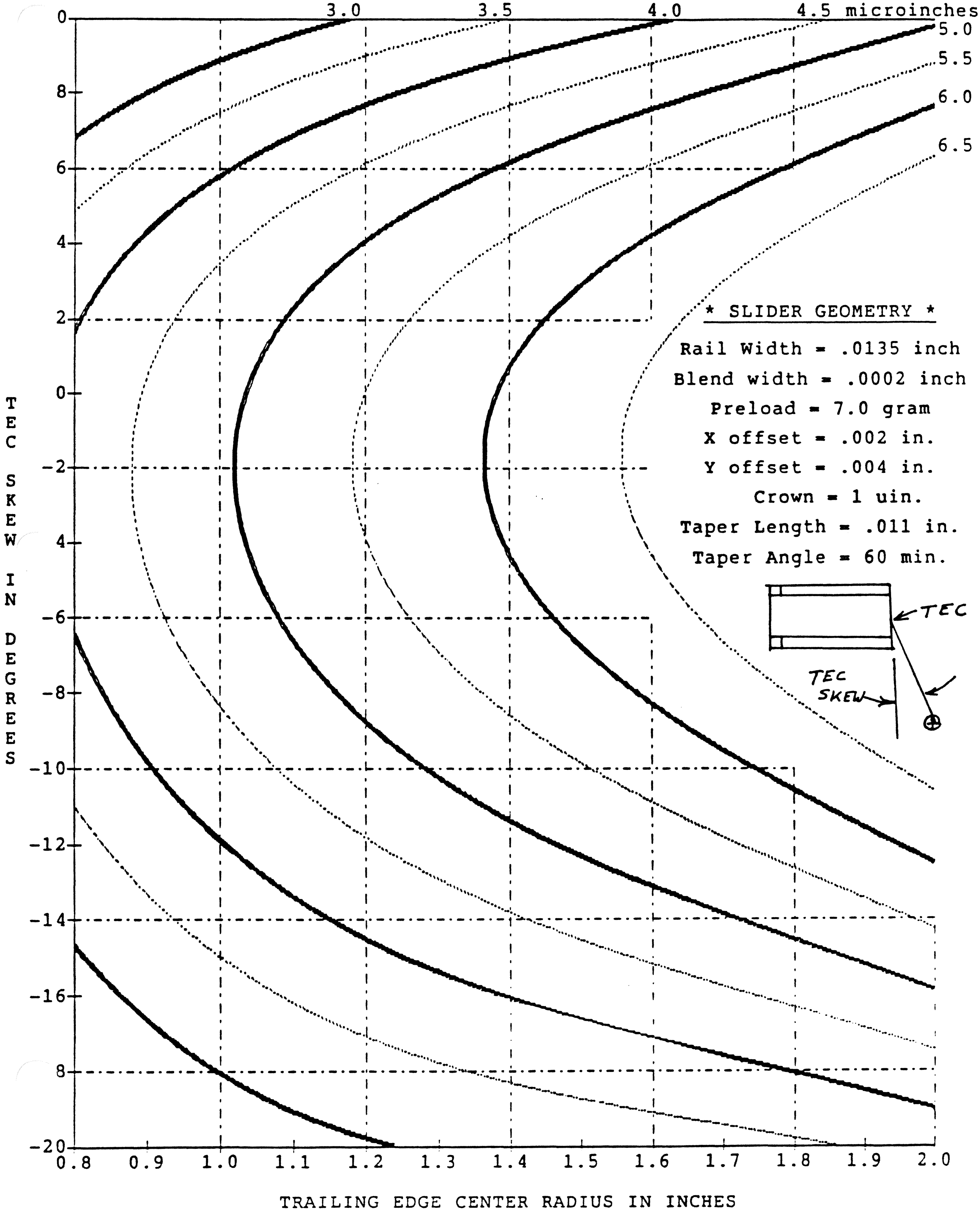

TOPOGRAPHICAL MAPS AND CONSTANT FLYING HEIGHT OPTIMIZATION

Topographical maps such as the three which follow show flying height and attitude of a specific slider geometry as a function of radius and skew. By designing a rotary actuator with skew as a function of radius in mind, flying height vs radius can be controlled.

These maps were created by taking some thirty finite difference method steady-state flying height results, and fitting a fourth order polynomial in 2 dimensions to values representing clearance, pitch, and roll. Such a polynomial is in the form:

```
f(r,theta) = c1 + c2*r + c3*theta + c4*(r^2) + c5*r*theta
               + c6*(theta^2) + c7*(r^3) + c8*(r^2)*theta
               + c9*r*(theta^2) + c10*(theta^3) + c11*(r^4)
               + c12*(r^3)*theta + c13*(r^2)*(theta^2)
               + c14*r*(theta^3) + c15*(theta^4)
```

A statistics package (RS/1) was used to evaluate the significance level (1-confidence) of each term. Terms which were not associated with high confidence were discarded, and the polynomial was evaluated again after each discard until all terms were associated with high confidence.

This resulting 'trimmed' polynomials associated with each value (clearance, pitch, and roll) were used to make these topographical maps.

Note the skew convention used shown on the transducer rail clearance map. If the segment connecting the trailing edge center to the center of disk rotation does not pass through the slider body, the skew here is said to be positive.

EXAMPLE OF AN ARM LENGTH AND BEND ANGLE OPTIMIZATION

It is desired to fly with the transducer rail at a constant value of 4.5 microinches above the disk. The drive in question is at the innermost track when the trailing edge center radius is approximately 0.88 inches, and the outermost radius will be 1.80 inches.

After some work, it is decided a good head geometry would have a 13.5 mil (.0135 inch) rail width, and a 7 gram suspension load.

A topographical map of a typical head meeting these constraints (attached) shows that desired skew angles are:

Trailing edge center radius (inches)	Trailing edge center skew (degrees)
0.88	-3.1
0.90	-5.1
1.00	-8.6
1.20	-11.7
1.40	-13.6
1.60	-15.1
1.80	-16.4

Because of other constraints, it is desired to have the distance between the actuator pivot point and center of disk rotation set to 2.20 inches. The problem is to find the best effective arm length A and bend angle such that the skew vs radius is as close as possible to the above values, which were taken from the appropriate topographical map.

SOLUTION:

By setting L to 2.20 inches, and performing a least squares fit to the desired skew values, the best effective arm length is 2.1798 inches with a bend angle of 5.1835 degrees. This results in the following results, which is within 2.1 degrees for each specified radius!

Radius (in.)	Achieved Skew (deg)	Desired Skew	Error
.88	-5.113	-3.1	-2.013
.9	-5.410	-5.1	-0.310
1.0	-6.883	-8.6	1.717
1.2	-9.786	-11.7	1.914
1.4	-12.672	-13.6	0.928
1.6	-15.567	-15.1	-0.467
1.8	-18.494	-16.4	-2.094

The map which follows shows the achieved skew vs radius and the separation from the broken line associated with a constant 4.5 microinches. Except for the extreme outer radius, the flying height would be within a half microinch of ideal in this example.

TRANSDUCER RAIL TRAILING EDGE HEIGHT

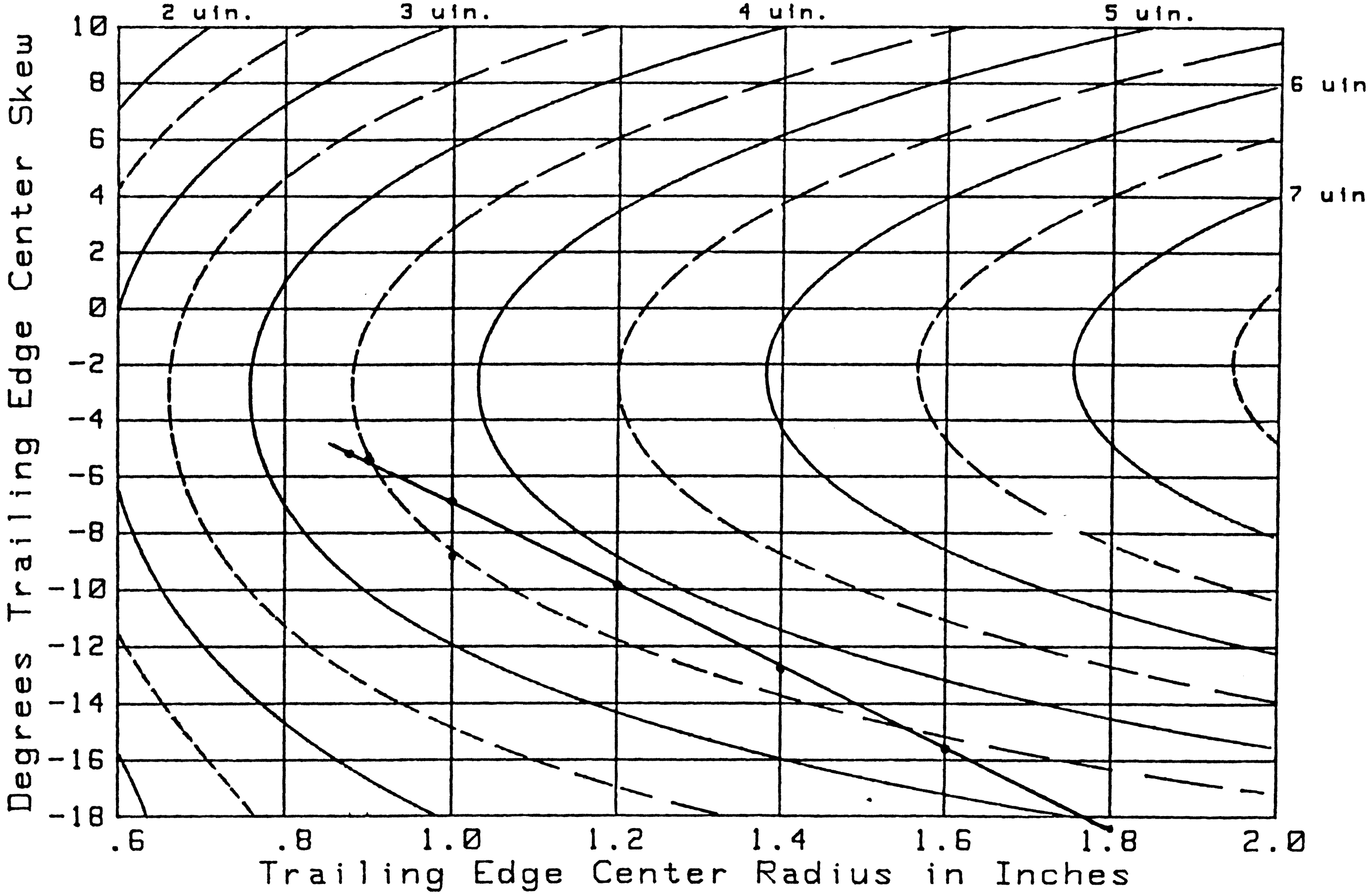

MICROSLIDER -- 13.5 mil rails -- 1 uin crown

7 gm load -- X=.002 -- Y=.004

MONTE-CARLO ANALYSIS

(EXAMPLE)

USING GAUSSIAN RANDOM NUMBERS IN MONTE-CARLO VALUE ASSIGNMENTS

Commonly used random numbers have an equal probability of occuring anywhere along the range of zero to one. This is usually the random number you get when you type the RND (or similar) function in many computer languages.

A Gaussian random number may have any real value. You may obtain a Gaussian random number by assigning a value p to the common random number described above, and then calculate a number z such that:

$$\int_{-\infty}^{z} \frac{1}{\sqrt{2\pi}} e^{-x^2/2} dx = p$$

In this case, z is the Gaussian random number.

One may use Gaussian random numbers to simulate many processes (when these processes have near-normal distributions) by measuring the mean and standard deviation of a process, and generating values with these same characteristics. These are done by first multiplying the Gaussian random number by the measured standard deviation and then adding the measured mean.

For example, if the measured mean of slider preload is 9.450 grams force (excuse the units) with a standard deviation of 0.394, and one wanted to represent six (6) preloads, then a method could be created as follows:

Random number p →	Associated Gaussian z →	Times Measured s →	Plus Measured $\bar{x}$
.101798	-1.27137	-.50092	8.94908
.736529	.63268	.24928	9.69928
.324752	-.45445	-.17905	9.27095
.348546	-.38925	-.15336	9.29664
.868522	1.11943	.44106	9.89106
.278903	-.58610	-.23092	9.21908

In most cases, at least 35 trials are recommended to get a good idea of the resulting mean. Depending on what other results are needed and how accurately the results should be calculated, many more trials may be needed.

Verification of simulated and existing results are always a good idea (if possible) before using the model to simulate a changed process.

MONTE-CARLO ANALYSIS EXAMPLE

We wish to see width of the flying height and attitude distribution for a .112 inch slider at a trailing edge center radius of 1 inch, with no skew at the trailing edge. The system nominal and distribution widths are defined as:

	MEAN	STD. DEV.	
Test parameters:			
RPM:	3600	10	
TEC Radius:	1 in.	.01	
TEC Skew:	0 deg.	1.	
Slider parameters:			
Rail Width:	14 mils	.2	
Crown:	1 uin.	.4	
Taper Length:	11 mils	.8	
Blend Width:	.2 mils	.1	
Load parameters:			
Load Force:	7 gm f.	.45	
Load pt. length offset:	4 mils	.8	(toward TE)
Load pt. width offset:	2 mils	.7	(toward OD)

For purposes of this example, we will assume the taper angle has a fixed value of one (1) degree, and blending is linear, with a 40 microinch per mil slope. (Example, if the blend with is .3 mils on a given slider, then the height is 12 microinches.) The blend is assumed to be the same and constant on each side of each rail. Camber is assumed to be zero.

Also, it is assumed that each rail has the same width, and that crown on the active and ballast rails are the same. In other words, the slider bodies are perfectly symmetrical, with the exception of the load point location. (In reality, such symmetry will result in an underestimation of the slider roll distribution.)

Another assumption made to reduce complexity is that the suspensions harbor no torques in the loaded positions. In short, to make this model fit real life, approximately 24 variables would be required for an excellent agreement.

n = 2400

*** FLYING HEIGHTS ***

	Ballast Rail	Transducer Rail
Minimum:	3.8643	3.8098
Mean:	5.2218	4.9998
Maximum:	6.4524	6.0883
Est. Std. Dev.:	0.3355	0.3307

** ATTITUDE **

	ROLL	PITCH
Minimum:	-1.0396	4.2603
Mean:	-0.2220	6.3180
Maximum:	0.4625	8.7519
Est. Std:	0.1986	0.6529

MICROSLIDER FLIGHT ANALYSIS

	Head type:	MICROHEAD	<MONTE-CARLO>
	RPM:	3600	S =10.000
	TEC radius:	1 inch	S = 0.0100
	Rail width:	14.000 mils	S = 0.2000
	Load force:	7.000 grams force	S = 0.4500
WIDTH →	X offset:	2.000 mils	S = 0.7000
LENGTH →	Y offset:	4.000 mils	S = 0.8000
	Crown:	1.000 microinch	S = 0.4000
	TEC Skew:	0.00 degrees	S = 1.0000
	Taper Length:	11.000 mils	S = 0.8000
	Blend:	0.2000 mils	S = 0.1000

<TERMINATE>

Transducer rail T.E. clearance:	5.016 µin.
Ballast rail T.E. clearance:	5.240 µin.
Pitch:	6.301 µin.
Roll:	-0.224

MONTE-CARLO TABLE OF RESULTS FOR 70% MICROSLIDER

Isolated Variable Method:

X1 RPM s	X2 Rad s	X3 Rail s	X4 Crown s	X5 Blend s	X6 Skew s	X7 Taper s	X8 Force s	X9 Xc s	X10 Yc s	Y1 Ht $\bar{x}$	Y2 Hb $\bar{x}$	Y3 Alpha $\bar{x}$
0	.0	.0	.0	.0	.0	.0	.0	0.	0.	5.016	5.240	6.301
10	.01	0.2	0.4	0.1	1.0	0.8	0.45	0.8	0.7	5.000	5.222	6.318
10	.0	.0	.0	.0	.0	.0	.0	0.	0.	5.016	5.240	6.301
0	.01	.0	.0	.0	.0	.0	.0	0.	0.	5.017	5.241	6.303
0	.0	0.2	.0	.0	.0	.0	.0	0.	0.	5.013	5.237	6.298
0	.0	.0	0.4	.0	.0	.0	.0	0.	0.	5.012	5.236	6.295
0	.0	.0	.0	0.1	.0	.0	.0	0.	0.	5.006	5.228	6.286
0	.0	.0	.0	.0	1.0	.0	.0	0.	0.	5.006	5.230	6.309
0	.0	.0	.0	.0	.0	0.8	.0	0.	0.	5.015	5.240	6.297
0	.0	.0	.0	.0	.0	.0	0.45	0.	0.	5.029	5.254	6.316
0	.0	.0	.0	.0	.0	.0	.0	0.8	0.	5.015	5.240	6.586
0	.0	.0	.0	.0	.0	.0	.0	0.	0.7	5.017	5.240	6.301

Variables:

X1: Revolutions/minute
X2: Trailing edge center (TEC) radius (inches)
X3: Rail width (mils)
X4: Crown (uin.)
X5: Blend Width (mils)
X6: TEC skew (deg.)
X7: Taper length (mils)
X8: Preload (gm force)
X9: Load (mils from TE)
X10: Load (mils OR or CL)

Fixed values:
Length = .112 inch
Taper angle = 1 deg.
Rail Camber = 0.
Blend angle = 2 deg. 20 minutes
Ballast Rail Width - Transducer Rail Width = 0.
No residual flexure torques in loaded position

Y1: Xducr Rail microinch
Y2: Ballast Rail Height
Y3: Pitch microinches

MONTE-CARLO TABLE OF RESULTS FOR 70% MICROSLIDER

Isolated Variable Method:

X1 RPM s	X2 Rad s	X3 Rail s	X4 Crown s	X5 Blend s	X6 Skew s	X7 Taper s	X8 Force s	X9 Xc s	X10 Yc s	Y1 Ht s	Y2 Hb s	Y3 Alpha s
10	.01	.2	.4	.1	1.0	.8	.45	0.8	0.7	.3307	.3355	.6529
10	.0	.0	.0	.0	.0	.0	.0	0.	0.	.0099	.0104	.0142
0	.01	.0	.0	.0	.0	.0	.0	0.	0.	.0352	.0401	.0527
0	.0	0.2	.0	.0	.0	.0	.0	0.	0.	.1294	.1383	.0865
0	.0	.0	0.4	.0	.0	.0	.0	0.	0.	.1796	.1855	.4741
0	.0	.0	.0	0.1	.0	.0	.0	0.	0.	.0951	.1038	.0566
0	.0	.0	.0	.0	1.0	.0	.0	0.	0.	.0472	.0729	.0243
0	.0	.0	.0	.0	.0	0.8	.0	0.	0.	.0189	.0197	.0984
0	.0	.0	.0	.0	.0	.0	0.45	0.	0.	.1883	.1929	.2756
0	.0	.0	.0	.0	.0	.0	.0	0.8	0.	.0613	.0560	.3195
0	.0	.0	.0	.0	.0	.0	.0	0.	0.7	.1115	.0841	.0181

Variables:

X1: Revolutions/minute
X2: Trailing edge center (TEC) radius (inches)
X3: Rail width (mils)
X4: Crown (uin.)
X5: Blend Width (mils)
X6: TEC skew (deg.)
X7: Taper length (mils)
X8: Preload (gm force)
X9: Load (mils from TE)
X10: Load (mils OR or CL)

Fixed values:
Length = .112 inch
Taper angle = 1 deg.
Rail Camber = 0.
Blend angle = 2 deg. 20 minutes
Ballast Rail Width - Transducer Rail Width = 0.
No residual flexure torques in loaded position

Y1: Xducr Rail microinch
Y2: Ballast Rail Height
Y3: Pitch microinches

STANDARD DEVIATIONS FOR TRANSDUCER CLEARANCE
(ISOLATED VARIABLE METHOD)

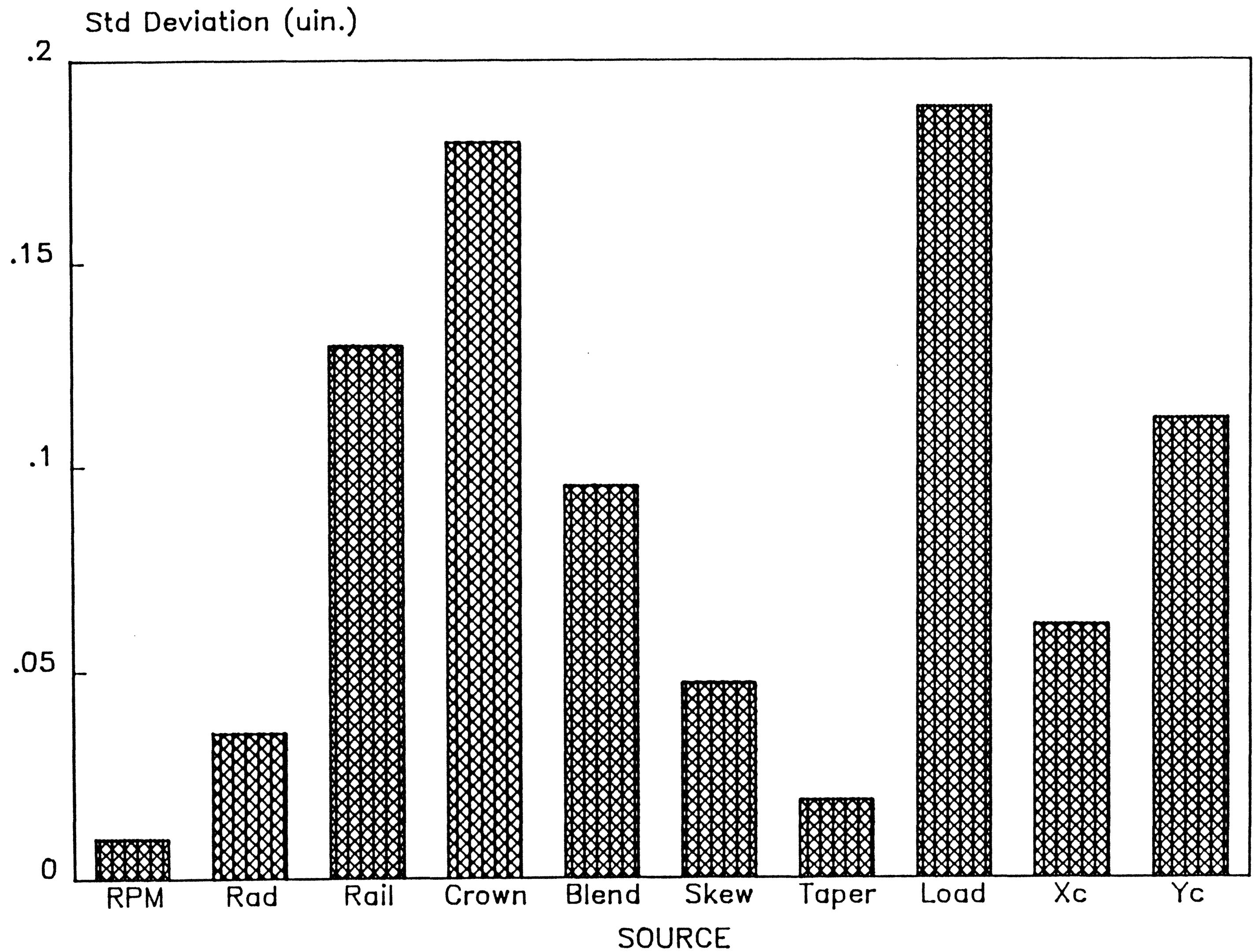

TEN VARIABLE MONTE-CARLO

STANDARD DEVIATIONS FOR PITCH
(ISOLATED VARIABLE METHOD)

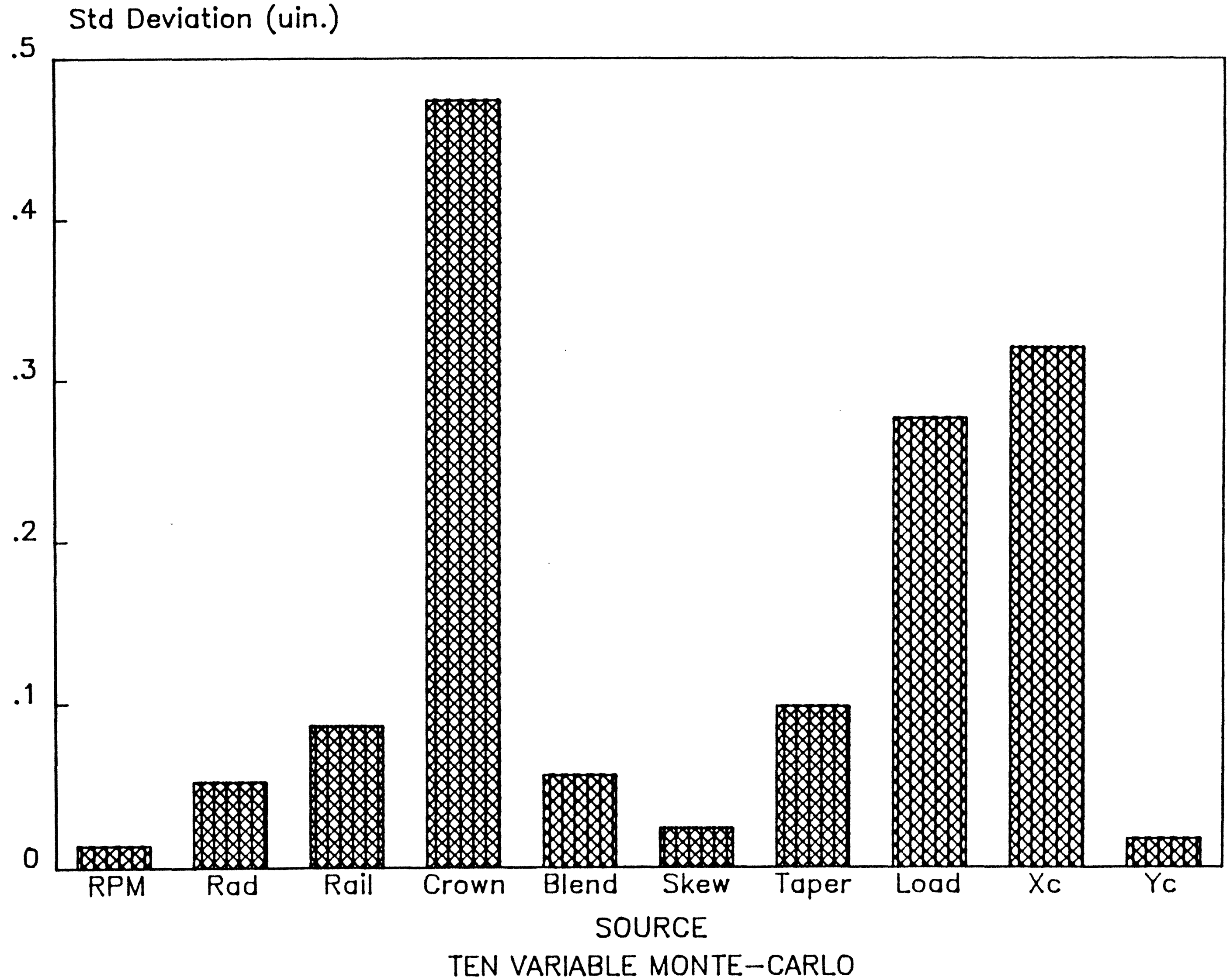

IN A LINEAR SYSTEM, THE SUM OF VARIANCE FROM EACH CAUSAL COMPONENT WOULD EQUAL THE SYSTEM VARIANCE.

AN AIR BEARING IS NOT A LINEAR SYSTEM.

ISOLATED VARIABLE METHOD LINEAR VARIANCE COMPARISON CHART

Source of Variance	Transducer Rail Height	Ballast Rail Height	uin. Pitch
RPM	.000098	.000108	.000202
Radius	.001299	.001608	.002777
Rail Width	.016744	.019127	.007482
Crown	,032256	.034410	.224771
Blend Width	.009044	.010774	.003204
Skew	.002228	.005314	.000590
Taper Length	.000357	.000388	.009683
Preload	.035457	.037210	.075955
Dimple x Pos.	.003758	.003136	.102080
Dimple Y Pos.	.012432	.007073	.000328

Sum/Combination: .11367/.10936 .11915/.11256 .42707/.42628

Note: All values in units of microinches squared.

MONTE-CARLO TABLE OF RESULTS FOR 70% MICROSLIDER

Variable Elimination Method:

X1 RPM s	X2 Rad s	X3 Rail s	X4 Crown s	X5 Blend s	X6 Skew s	X7 Taper s	X8 Force s	X9 Xc s	X10 Yc s	Y1 Ht s	Y2 Hb s	Y3 Alpha s
10	.01	.2	.4	.1	1.0	.8	.45	0.8	0.7	.3307	.3355	.6529
0	.01	.2	.4	.1	1.0	.8	.45	0.8	0.7	.3304	.3352	.6530
10	0.	.2	.4	.1	1.0	.8	.45	0.8	0.7	.3299	.3348	.6516
10	.01	0.	.4	.1	1.0	.8	.45	0.8	0.7	.3071	.3035	.6493
10	.01	.2	0.	.1	1.0	.8	.45	0.8	0.7	.2864	.2872	.4557
10	.01	.2	.4	0.	1.0	.8	.45	0.8	0.7	.3154	.3188	.6506
10	.01	.2	.4	.1	0.	.8	.45	0.8	0.7	.3232	.3322	.6523
10	.01	.2	.4	.1	1.0	0.	.45	0.8	0.7	.3299	.3345	.6455
10	.01	.2	.4	.1	1.0	.8	0.	0.8	0.7	.2811	.2820	.5961
10	.01	.2	.4	.1	1.0	.8	.45	0.0	0.7	.3261	.3317	.5591
10	.01	.2	.4	.1	1.0	.8	.45	0.8	0.0	.3149	.3221	.6510

Variables:

X1: Revolutions/minute
X2: Trailing edge center (TEC) radius (inches)
X3: Rail width (mils)
X4: Crown (uin.)
X5: Blend Width (mils)
X6: TEC skew (deg.)
X7: Taper length (mils)
X8: Preload (gm force)
X9: Load (mils from TE)
X10: Load (mils OR or CL)

Fixed values:
Length = .112 inch
Taper angle = 1 deg.
Rail Camber = 0.
Blend angle = 2 deg. 20 minutes
Ballast Rail Width - Transducer Rail Width = 0.
No residual flexure torques in loaded position

STANDARD DEVIATIONS FOR TRANSDUCER CLEARANCE (VARIABLE ELIMINATION METHOD)

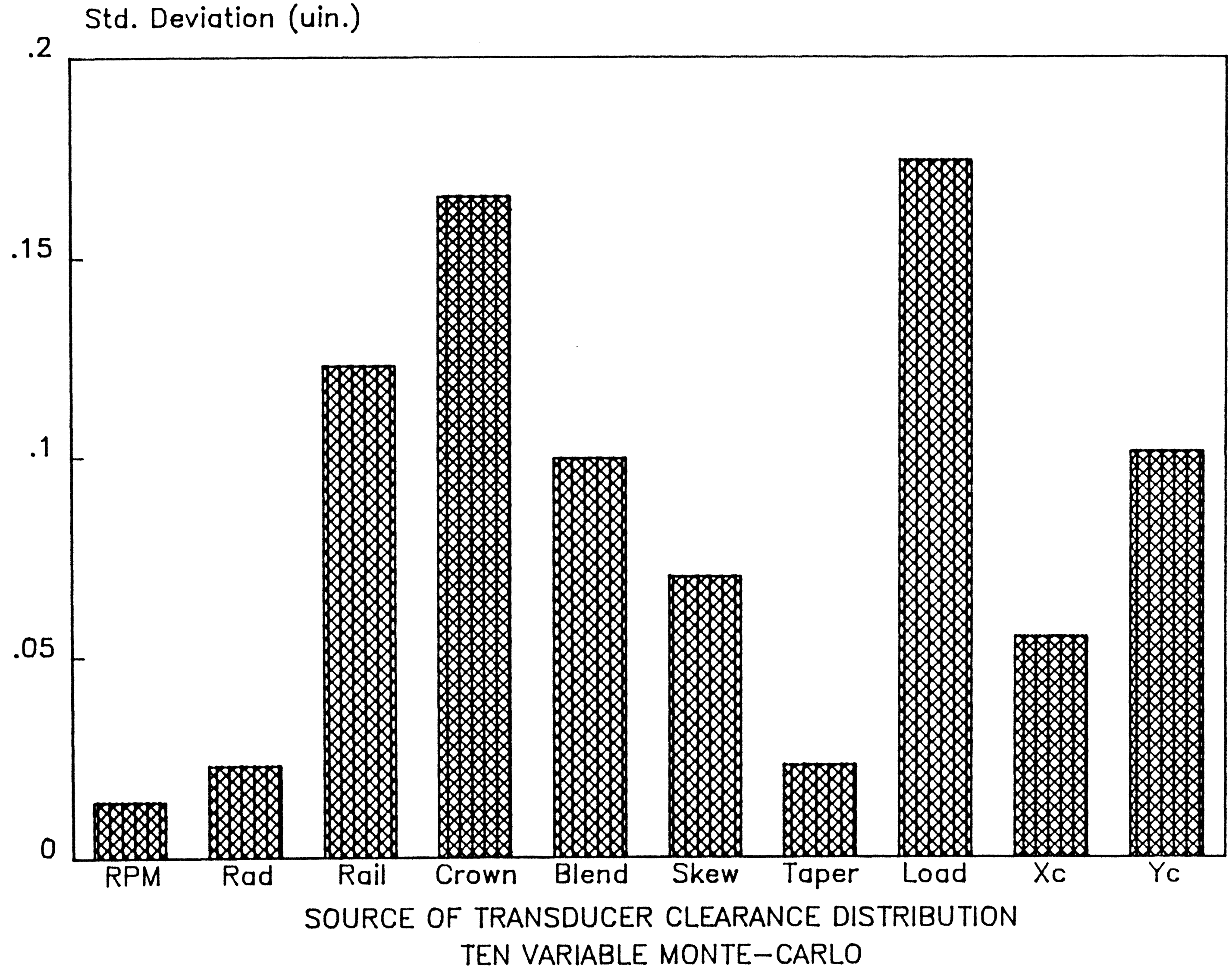

POTENTIAL Ht DISTRIBUTION IMPROVEMENT FROM COMPLETE CONTROL OF DIFFERENT PARAMETERS

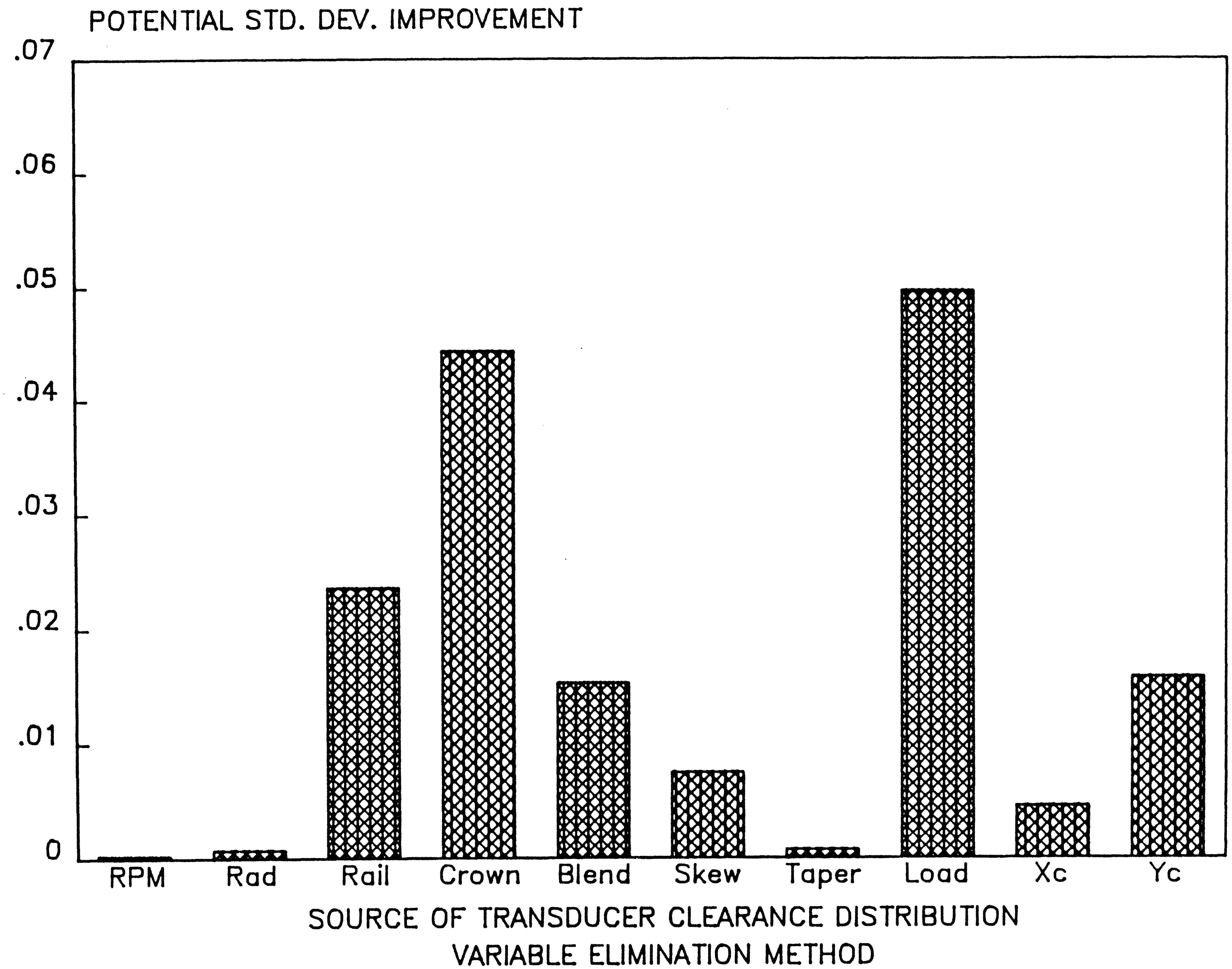

Dynamic Head Loading Short Course Outline

- *Historical Perspective*
  - *In the Beginning...*
  - *Early Dynamic Loading*
  - *Contact Start/Stop*
  - *Removable Winchester*
- *Dynamic Loading for Reliability*
  - *Rotary Dynamic Load Designs*
  - *Tolerance Considerations*
  - *Testing & Analysis*
- *Applicability To the Portable Marketplace*
  - *Ruggedization*
  - *Reliability*
  - *Low Power*
  - *Disadvantages*
  - *Other Advantages*
- *Conclusions*

Historical Perspective

Dynamic Loading is Not That New

In the Beginning...

First Air Bearing Magnetic Head Tested on June 2, 1953

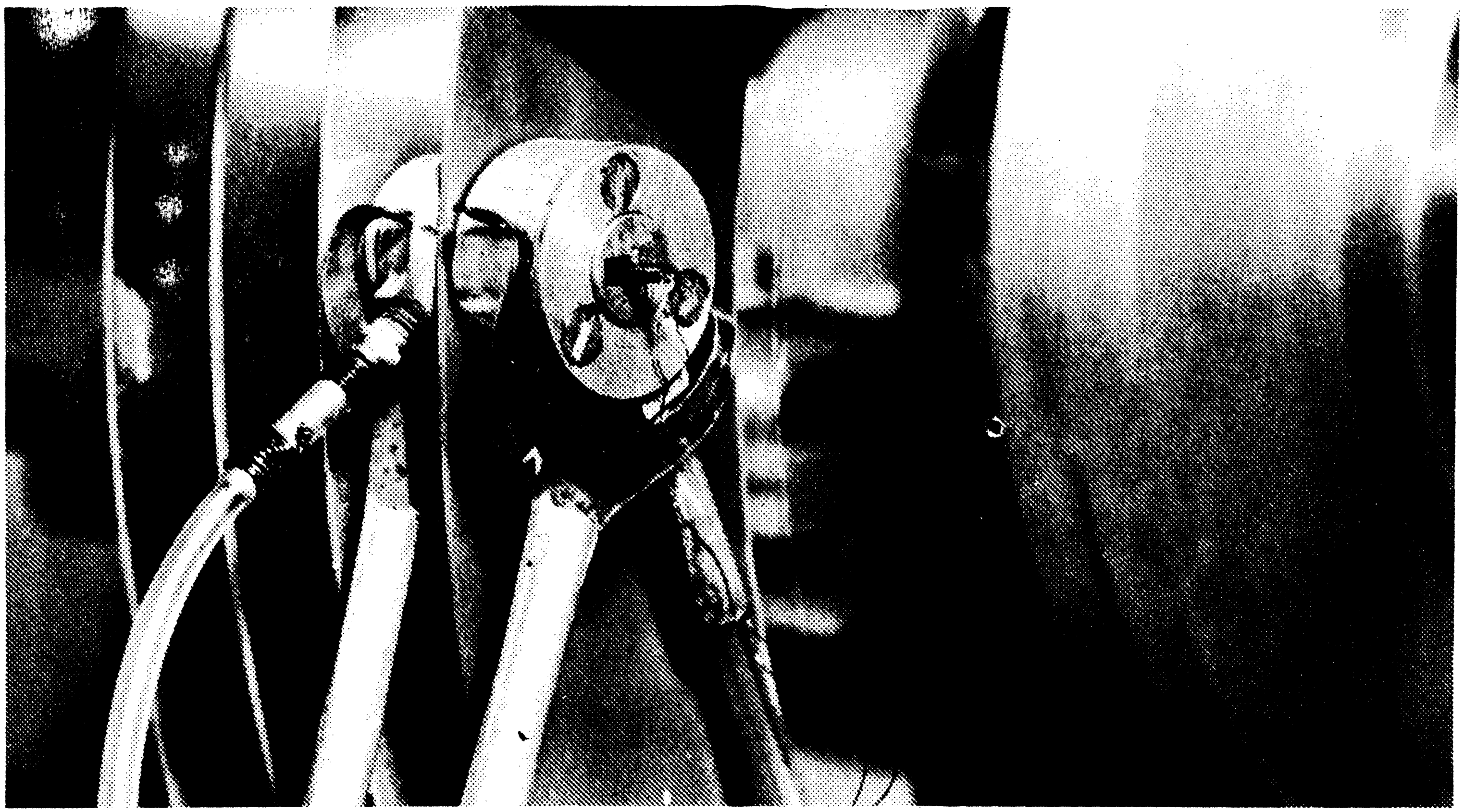

Source: (Review IBM JRNL RES & DEV)

Artist Conception of the Finished Random Access File

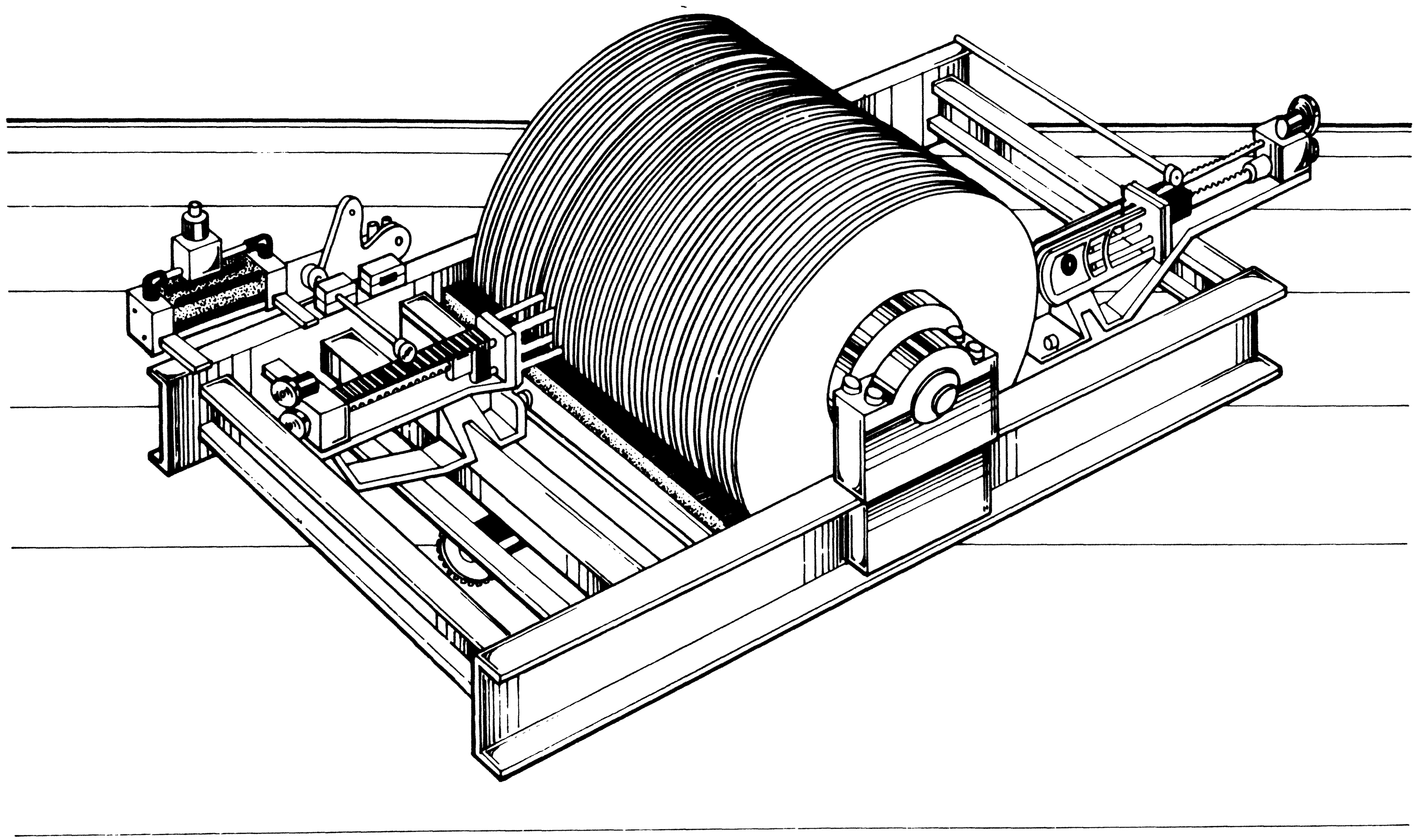

Source: (Review IBM JRNL RES & DEV)

Development of Technologies

Year of First Ship	1957	1961	1962	1963	1966	1971	1973	1976	1979	1979	1981
Product	350	1405	1301	1311	2314	3330	3340	3350	3310	3370	3380
Areal Density (Mb/in.^{2})	0.002	0.009	0.026	0.051	0.22	0.78	1.69	3.07	3.8	7.8	>12
Linear Bit Density (bpi)	100	220	0.026	0.051	2200	4040	5636	6425	8530	12134	15200
Track Density (tpi)	20	40	50	**	100	192	300	478	450	635	>800
Head-to-Disk Spacing (μin)	800	650	250	125	85	50	18	**	13	**	<13
Bearing Type	hydrostatic		hydrodynamic		**	**	**	**	**	**	**
Bearing Contour	flat	**	cylindrical		**	**	taper flat		**	**	**
Fixed/Removable	fixed	**	**	removable pack		**	module pack		**	**	**
Heads	2 heads/ actuator		1 head/ surface		**	**	2 h/s	**	1 h/s	2 h/s	**

** Same as in preceeding column

Source: (Review IBM JRNL RES & DEV)

Hydrodynamic Head Evolution

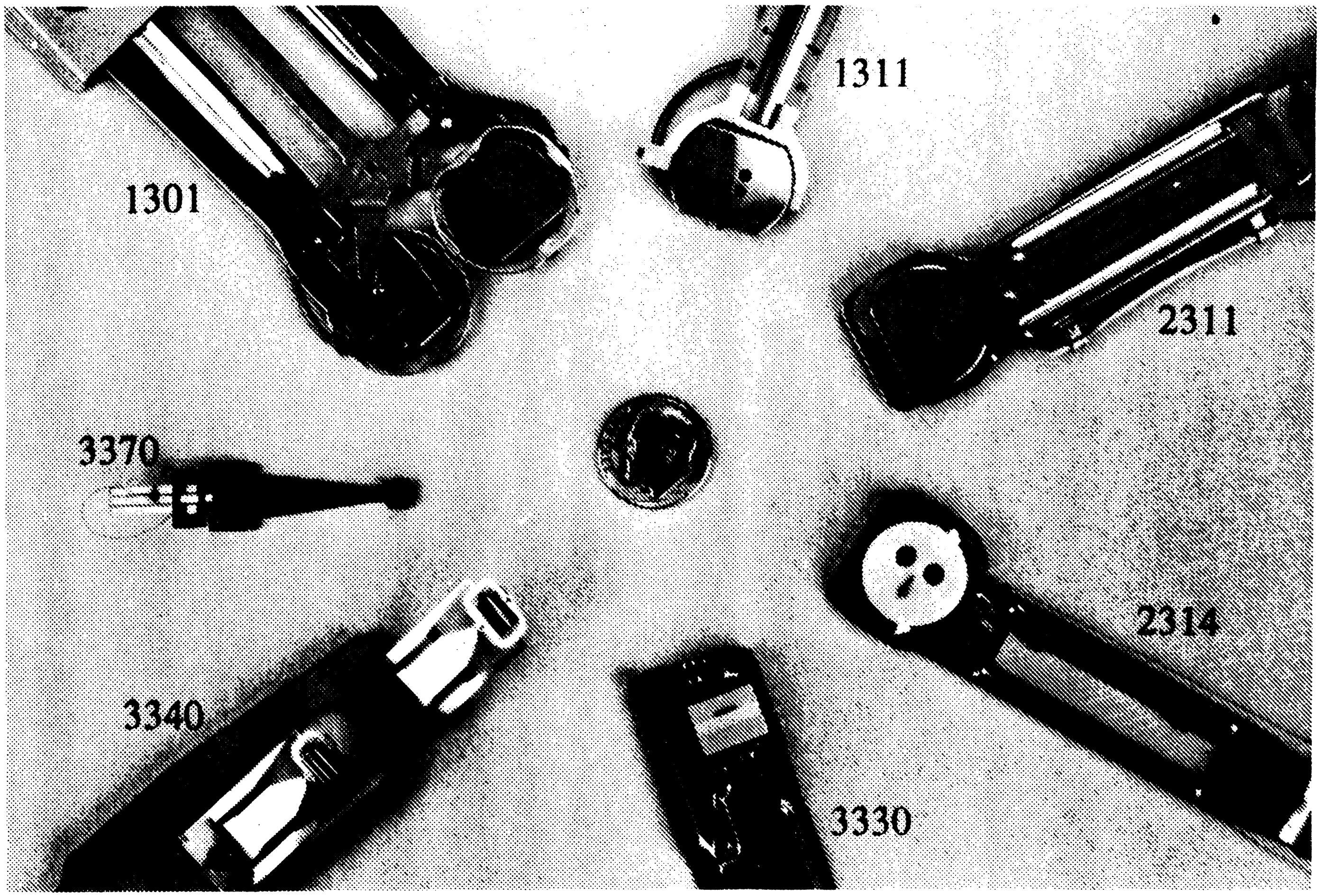

Source: (Review IBM JRNL RES & DEV)

Early Dynamic Loading

Torsion Bar Loading

Sept. 29, 1970 S. F. BROWN ET AL **3,531,788**

APPARATUS FOR LOADING AND UNLOADING A SLIDER ASSEMBLY

Filed Sept. 30, 1968

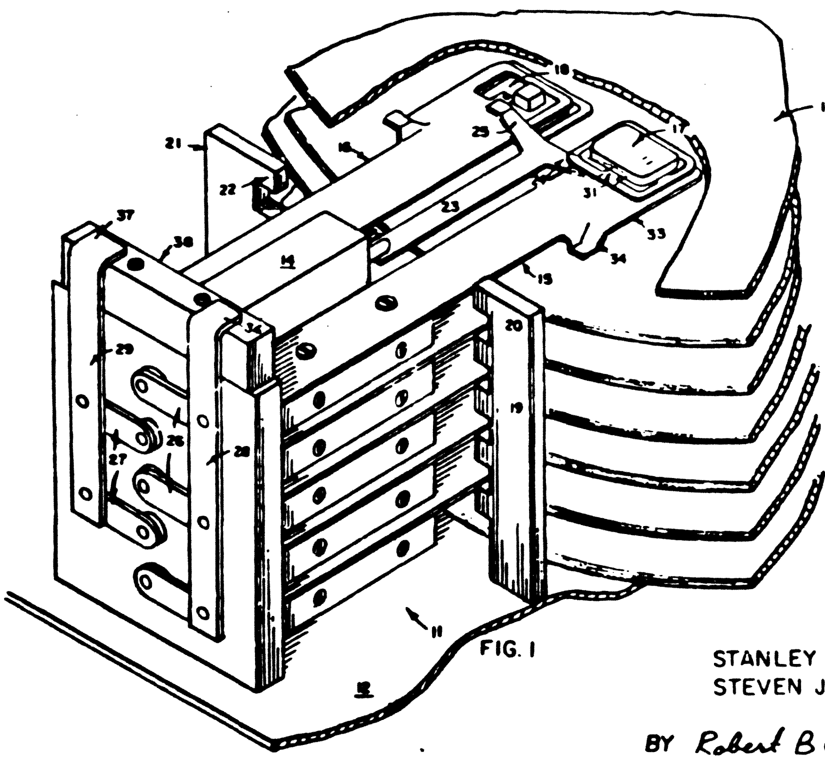

FIG. 1

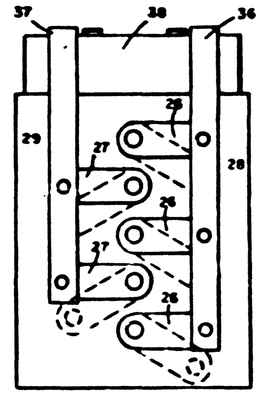

FIG. 2

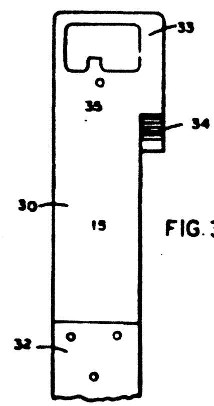

FIG. 3

INVENTORS
STANLEY F. BROWN
STEVEN J. MACARTHUR

BY Robert B Crouch

Early Dynamic Loading

Passive Ramp Structure

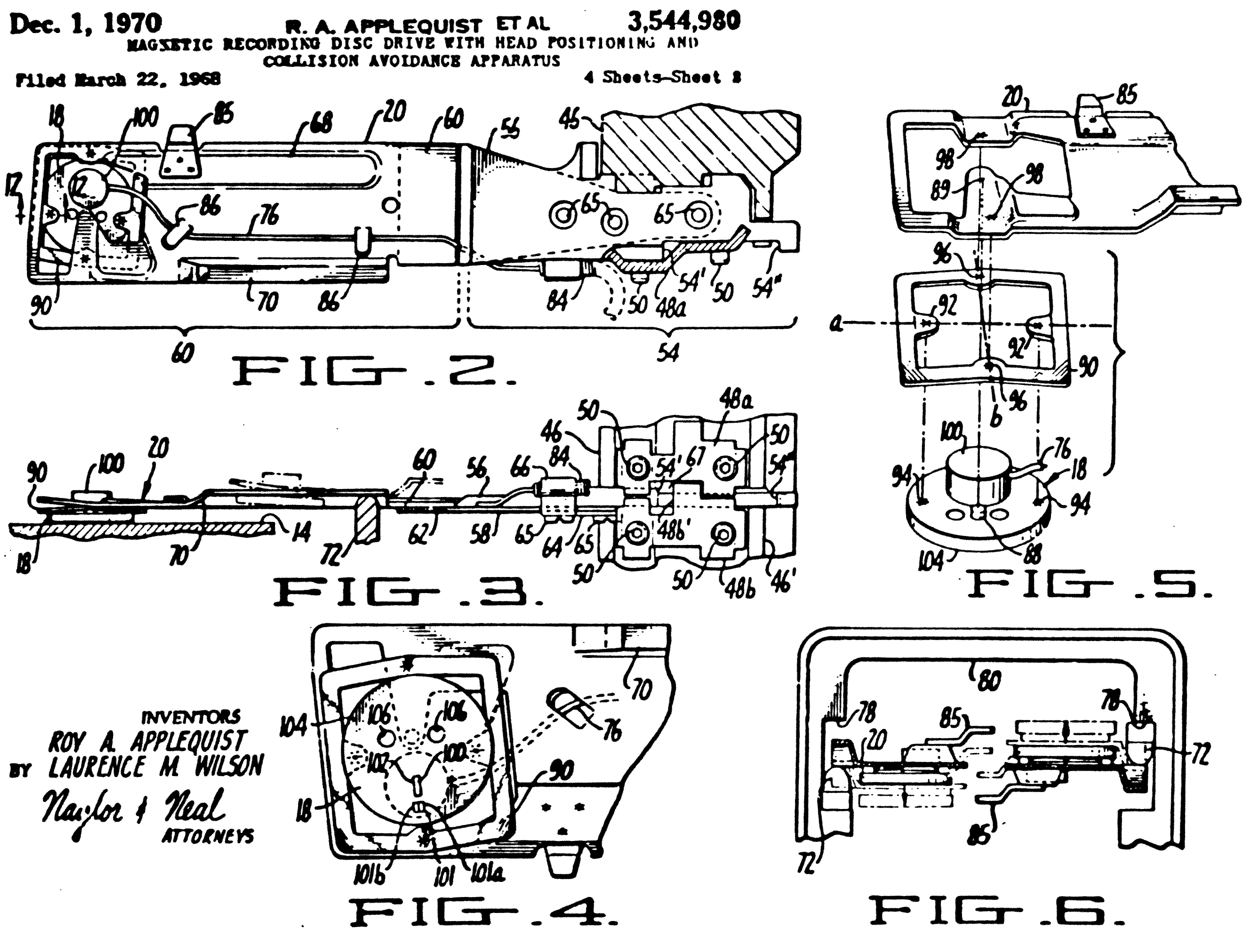

2314 & 3330 Ramp Loading

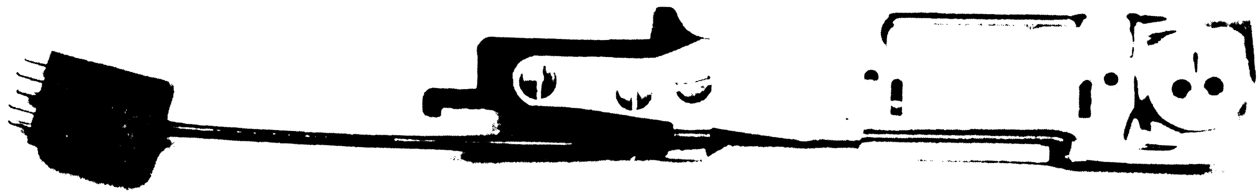

Introduction of Contact Start/Stop

3340/3350 & 3370/80

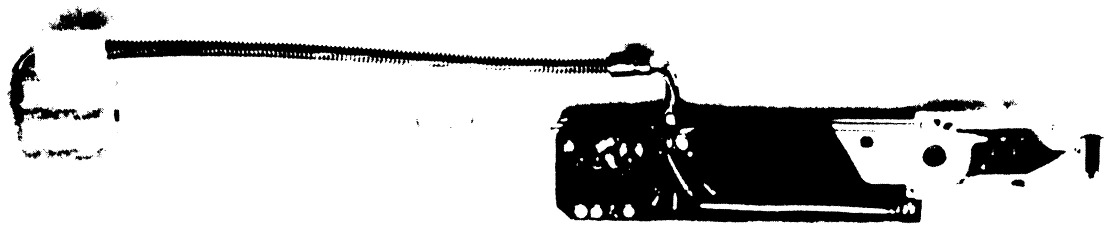

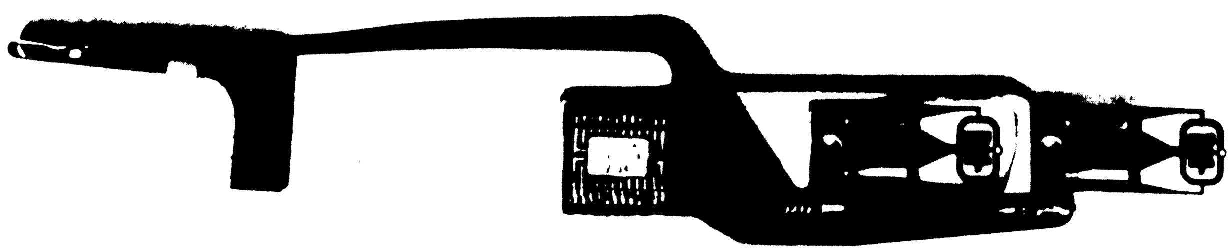

Removable Winchester Designs

CDC Lark

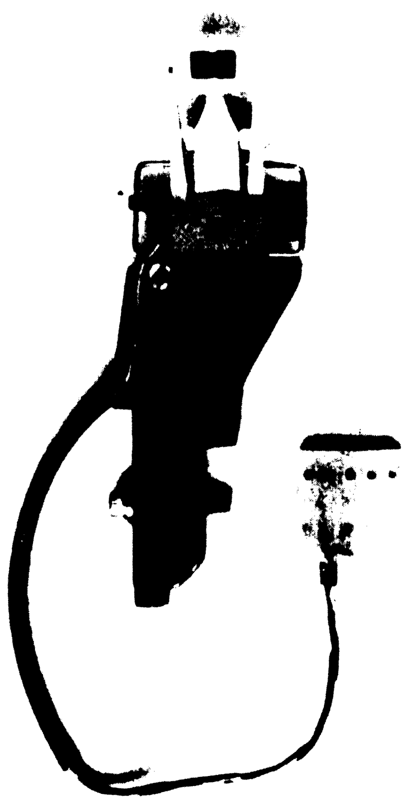

DEC Aztec

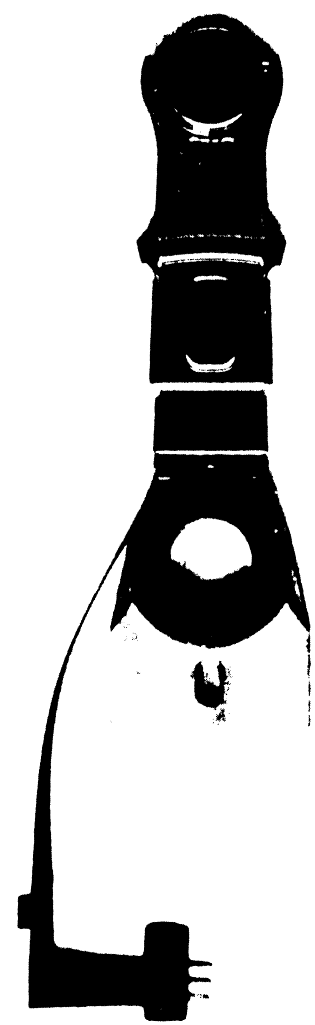

DMA

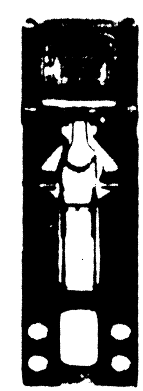

Amcodyne

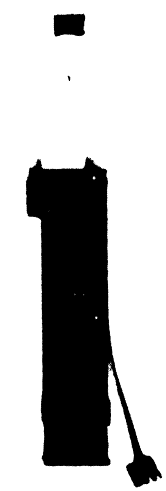

Dynamic Whitney Head Loading

Linear Implementation (Amcodyne)

U.S. Patent Aug. 13, 1985 Sheet 3 of 3 4,535,374

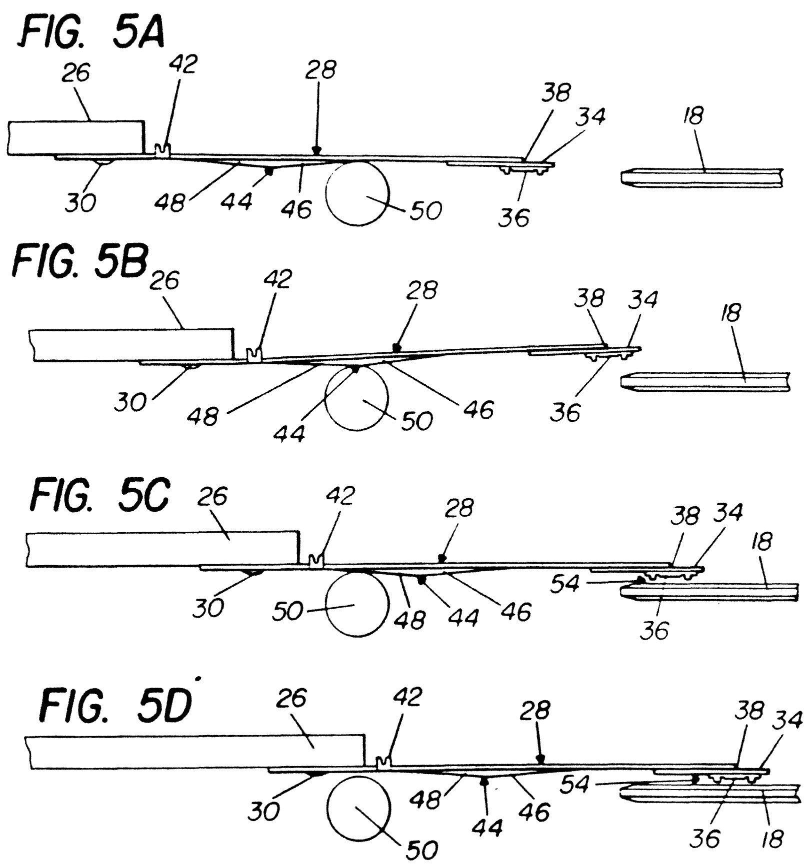

Dynamic Whitney Head Loading

Launch Energy vs RPM For Various Carriage Speeds

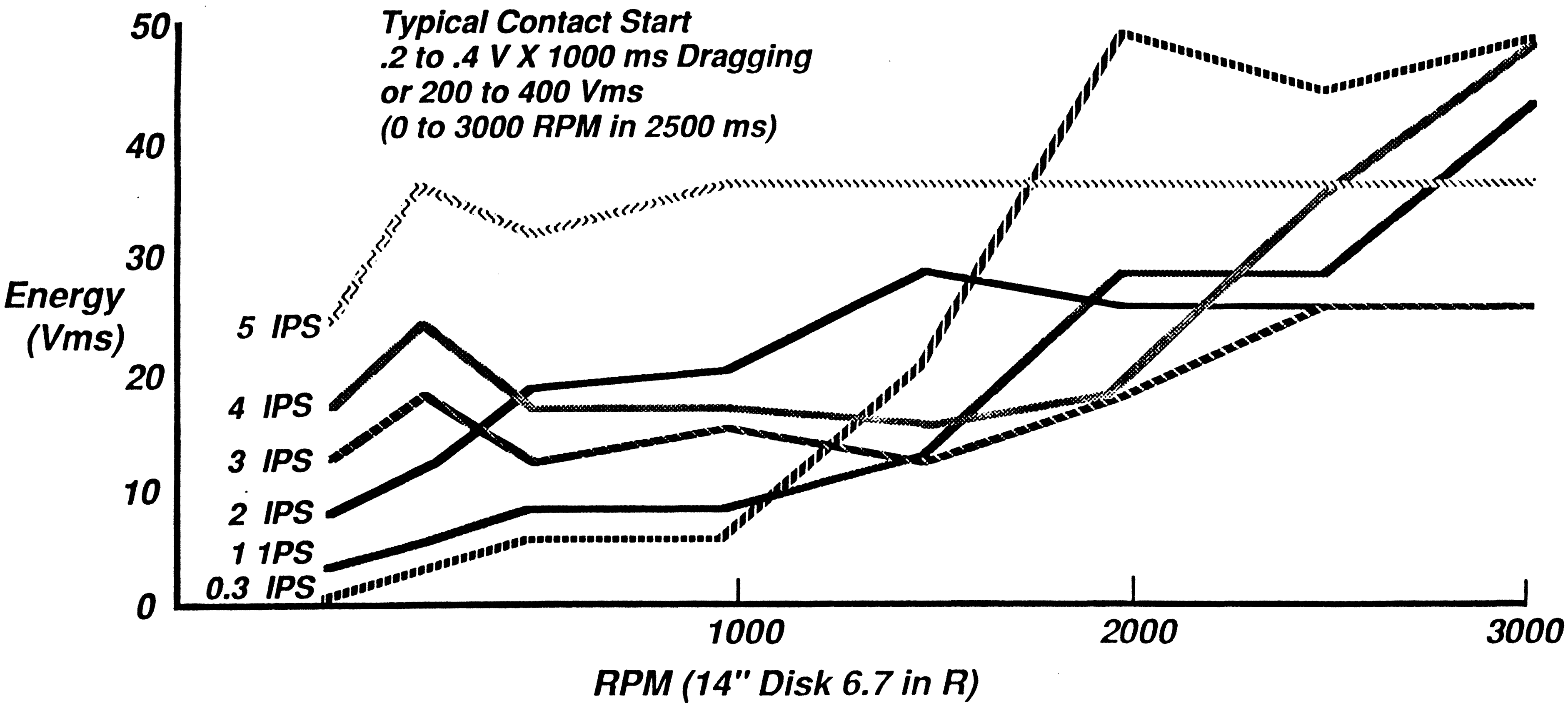

Source: KMA 4/16/82
(Amcodyne)

Removable Whitney Test Results (Amcodyne)

- Life Tests (60,000 L/UL)
  No Head/Disk Degradation
- High Speed Movies
  Smooth Landing
- Field Performance
  80,000 hr MTBF

Early Fixed Drives with Dynamic Loaded Heads for Reliability

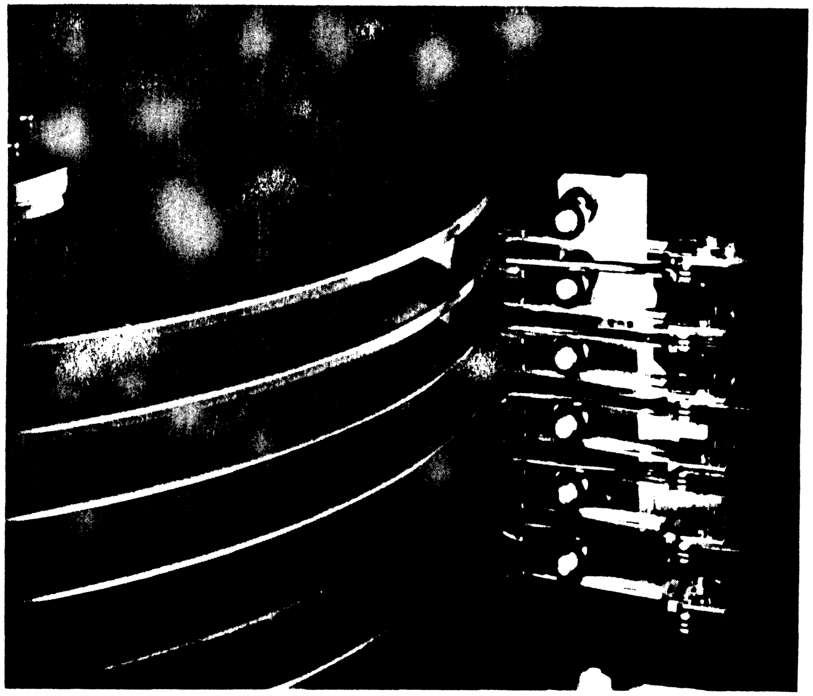

Amcodyne

Lapine

Dynamic Loading for Reliability

Rotary Dynamic Loading

Rotary Dynamic Loading Hardware Implementations with Buttons

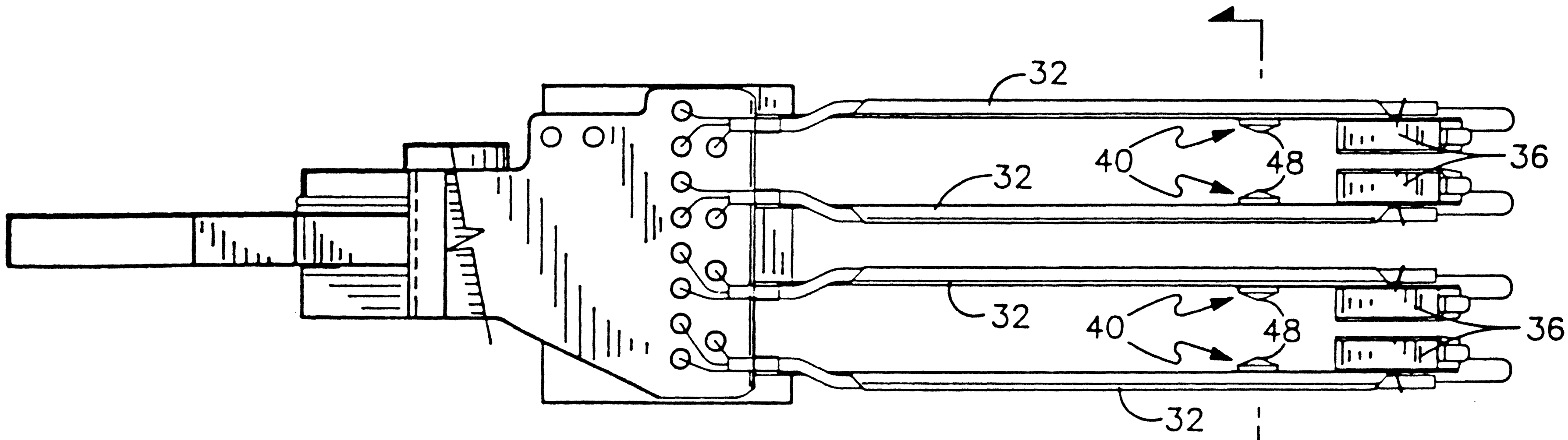

FIG.2

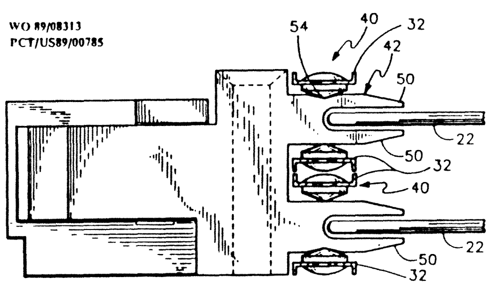

FIG.4A

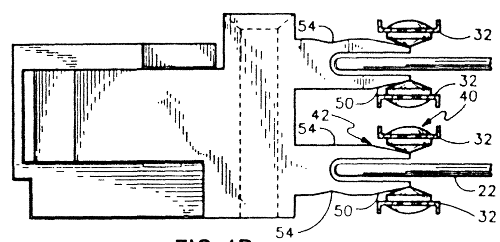

FIG.4B

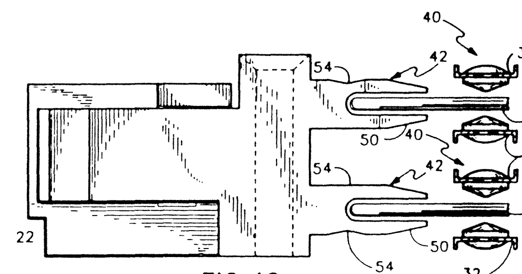

FIG.4C

Source: PrairieTek '86

Low Profile Rotary Dynamic Loading

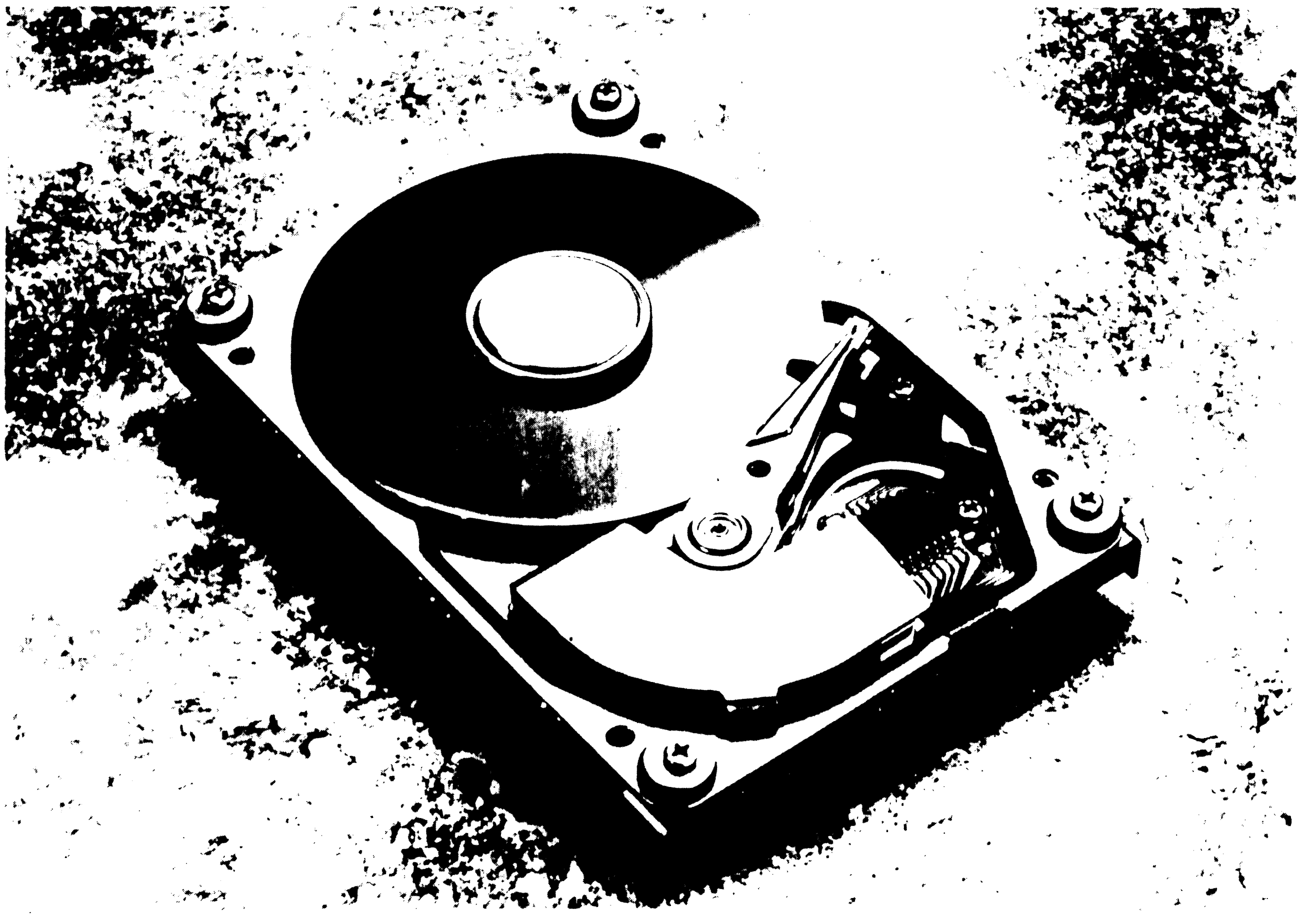

Rotary Dynamic Loading Hardware Implementation

Low Profile

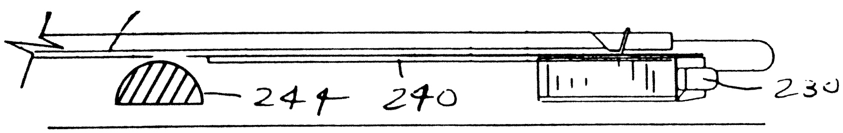

FIG.15A

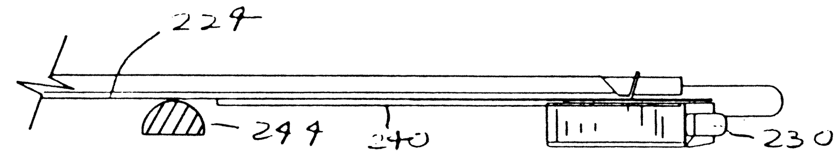

FIG.15B

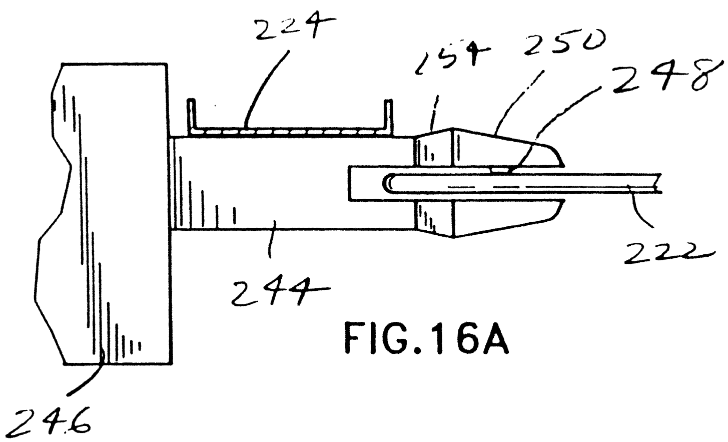

FIG.16A

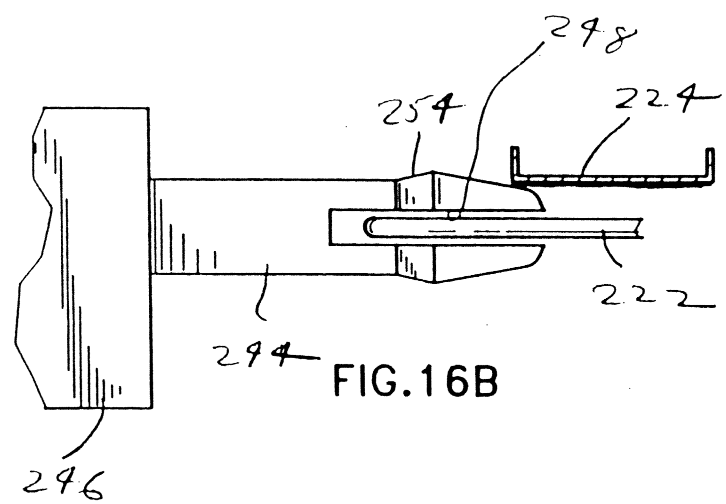

FIG.16B

Source: PrairieTek '86

Dynamic Loading Tolerance Considerations

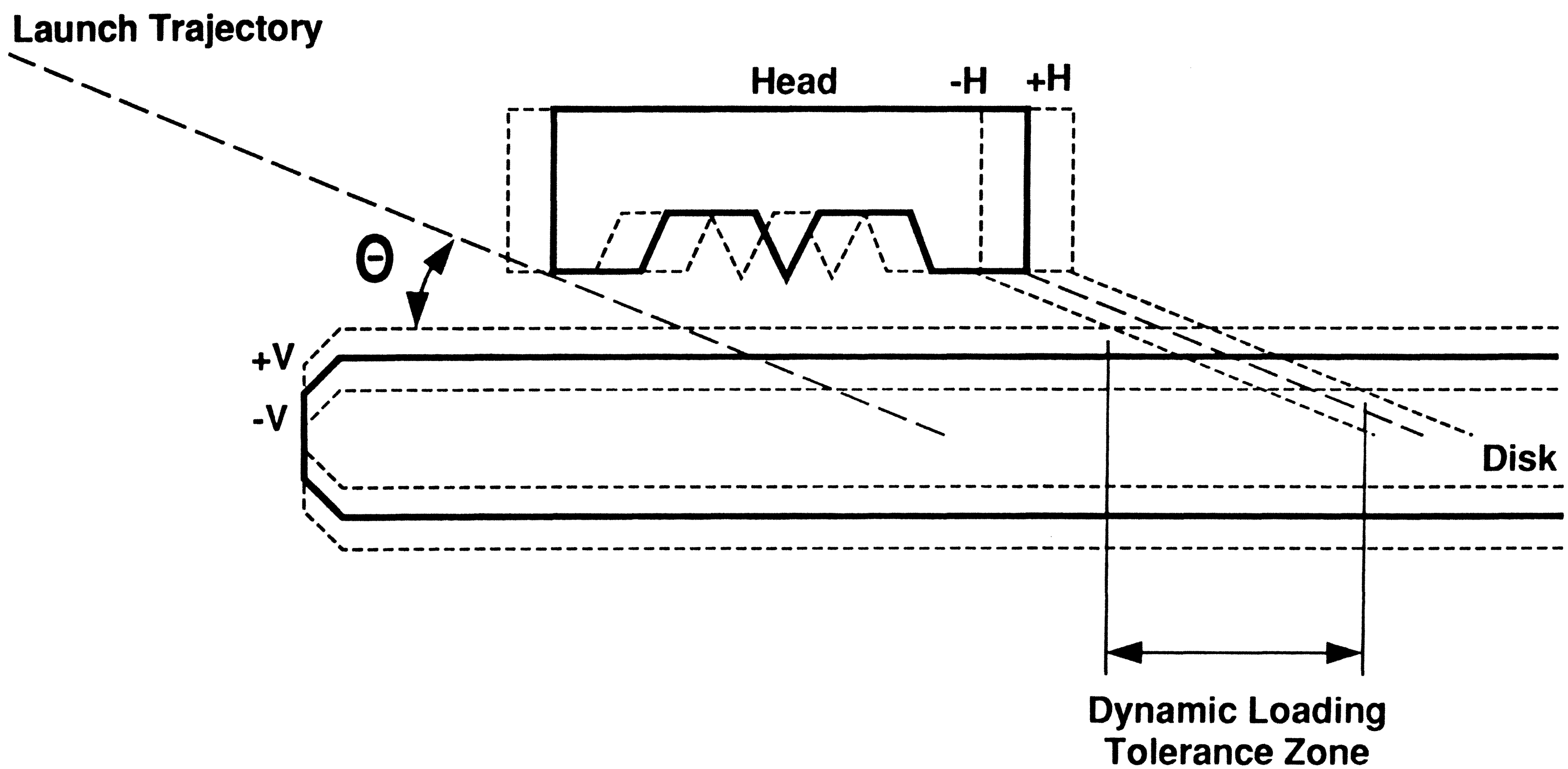

Dynamic Loading Life Test Results

Typical Dynamic Load Slider After 250,000 Load/Unloads

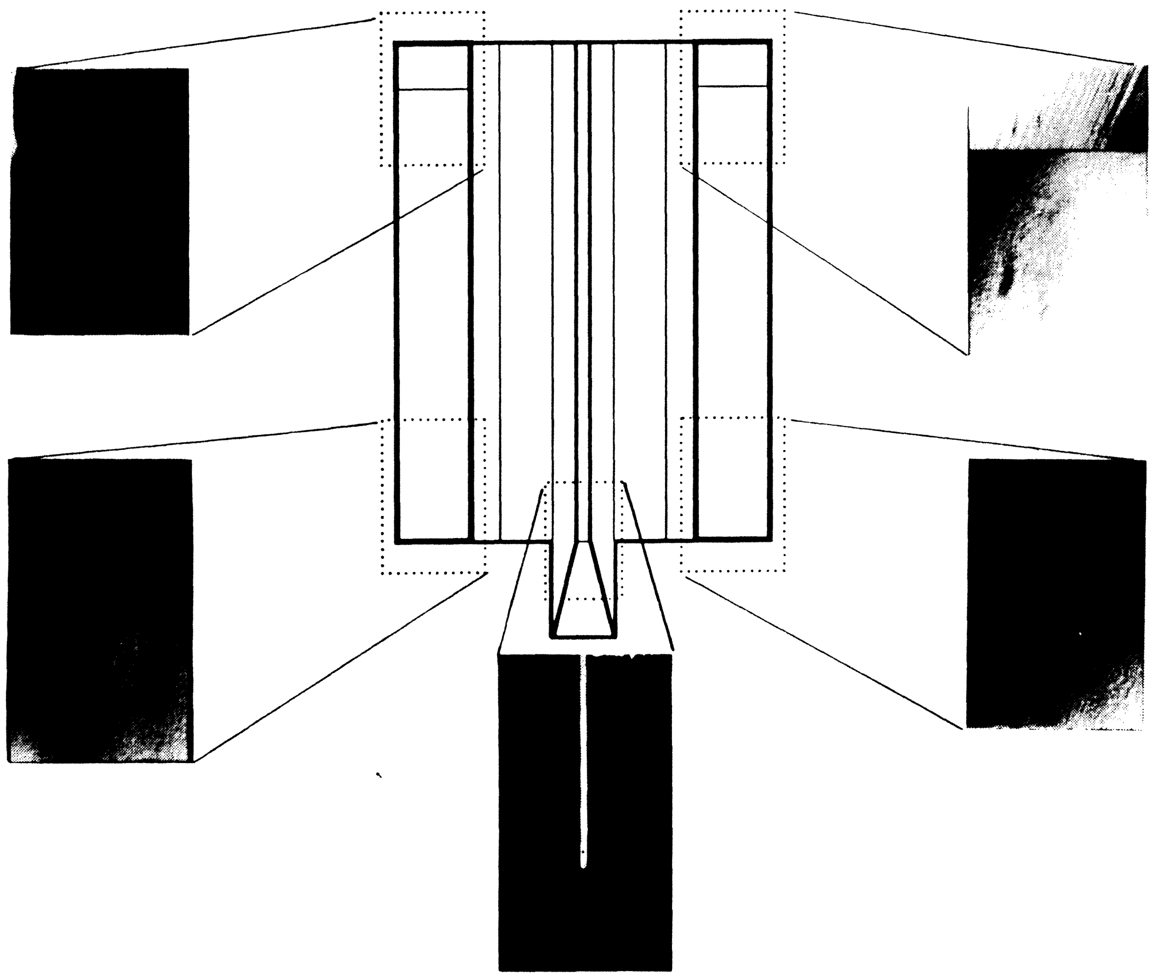

Dynamic Loading DVT Life Test

- *10 Drives (40 heads)*
- *343,000 Load/Unload*
- *No Additional Errors*
- *No Other Drive Problems*

Dynamic Loading Trajectories

Loading Motion of the Slider for Different Initial Times, TEIR.

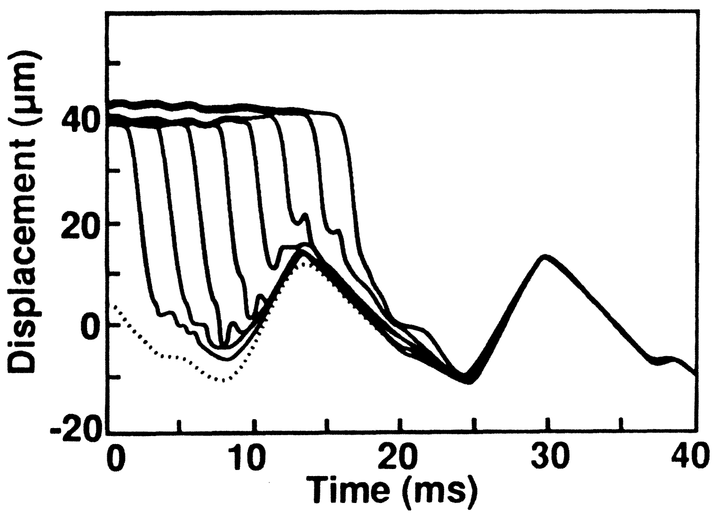

With Runout

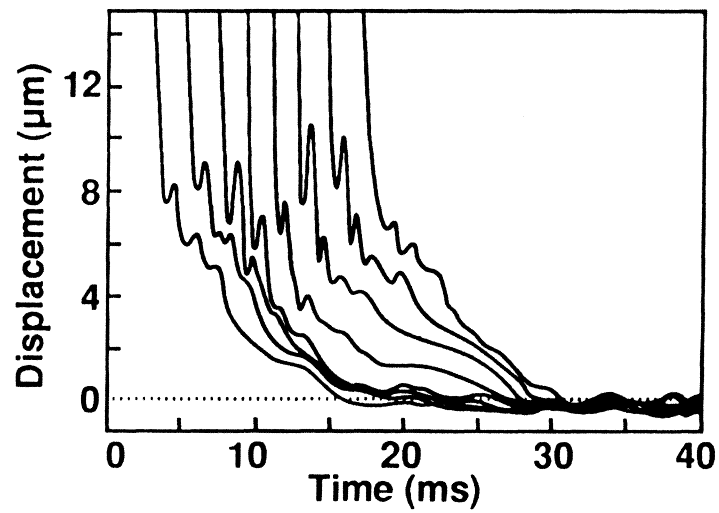

Runout Subtracted out

Source: Yamada & Bogy

Dynamic Loading High Speed Movie Frames

Dynamic Loading on a Glass Disk

Applicability of Dynamic Loading to the Portable Marketplace

Is Dynamic Loading a Future Requirement?

Applicability to the Portable Marketplace

Ruggedization

- Non-Operating Shock
- Non-Operating Vibration
- High Humidity & Temperature

Applicability to the Portable Marketplace

Reliability

- Passive Ramp vs Scissor Load
- No Stiction
- No Mechanical Wear

Applicability to the Portable Marketplace

Low Power

- Start Torque (Stiction & Friction)
- Unlimited Power Downs (with fast spin-up)

Applicability to ιhe Portable Marketplace

Disadvantages

- *Interdisk Spacing*
- *Power Down Unload Requirements*

Applicability to the Portable Marketplace

Other Advantages

- Manufacturability
- Unload Detent
- Allows Higher Areal Densities

Applicability to the Portable Marketplace

Disadvantages

- Interdisk Spacing
- Power Down Unload Requirements

Conclusions

Dynamic Loading

- ***Works Well***
- ***Increases Reliability***
- ***Increases Durability***
- ***Efficiently Uses Data Surface***
- ***Lowers Power Requirements***
- ***Eliminates Barriers to Higher Areal Density***
- ***Allows Removability in Miniaturized HDA***
- ***Appropriate Solution to Portable Computing Requirements***

IIST Short Course on the Head-Disk Interface

Low Flying Height

Dick Henze
Hewlett-Packard Laboratories
Dec. 12-14, 1989

What Does "Low Flying Height" Mean?

4-6 microinches?

2-3 microinches??

Less than 1 microinch???

*) Operation in a "similar" manner to todays products!

Reduced spacings achieved via the evolution of "conventional" components and process controls.

No continual high speed contacts

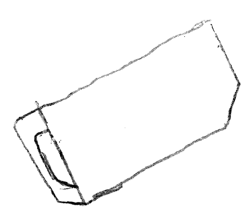

What's Required?

* Further development of components:

Disks	Sliders
Process control	Suspensions

* Product and process engineering which assimilates these components to satisfy a product definition:

Density	Reliability
Performance	Cost

* The product definition can vary widely

Form factor will affect:

Speed	OD/ID ratio
Skew angle range	Power consumption

DISKS

For lower flying heights:

* Decreased surface roughness of intentional texture

- Tradeoff with friction/stiction
- Isotropic micro-textures, primarily on glass and glass-ceramic
- Relationships between lube thickness and texture roughness
- Measurement issues remain
- Therefore, process control issues especially vital

* Reduced RVA characteristics

- Allows reduced dynamic flying heights
- Tribology role not fully understood
- Clamp Distortion
-

* Some parallel developments:

Reduced thickness **Alternate substrate materials**

Representative Disk Textures

(4 microinch scale) 200x

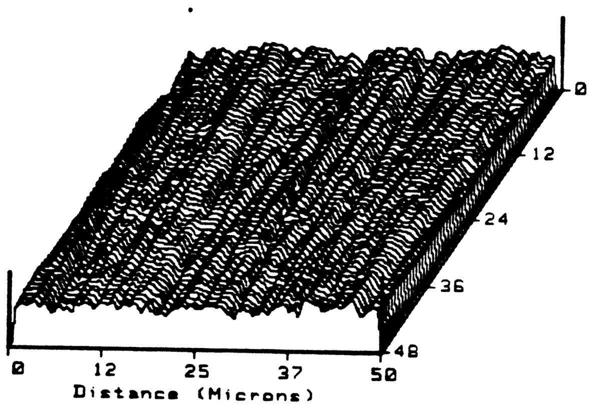

Circumferential texture on NiP plated aluminum carbon/lube
RMS roughness 5.79 nm

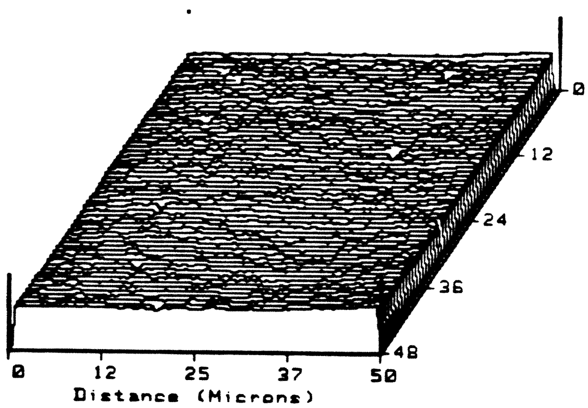

Polished glass
carbon/no lube
RMS roughness 1.58 nm

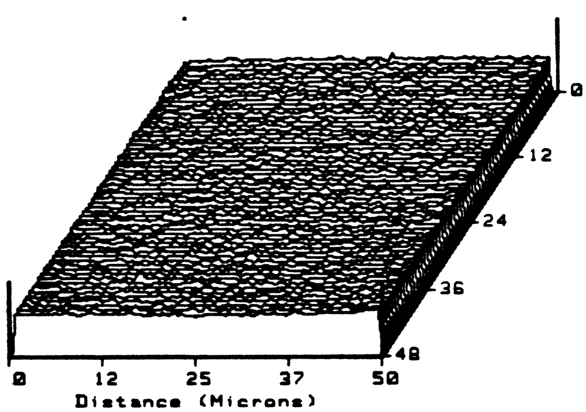

Isotropic microtexture on glass
carbon/lube
RMS roughness 1.68 nm

Strain Gage Friction Force (SG) and Acoustic Emission RMS Output (AE) vs. Velocity, With Touch Down and Acoustic Emission Velocities Marked

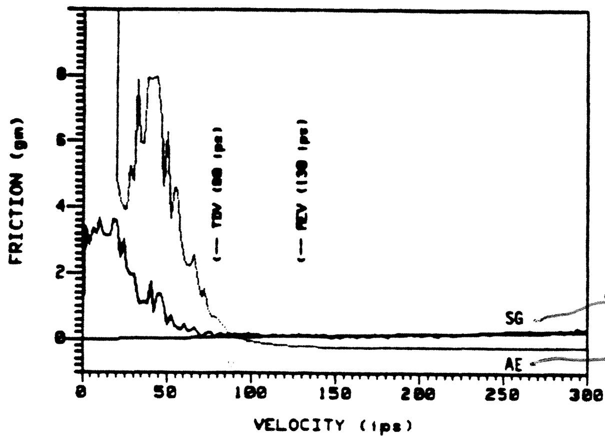

Circumferential texture on NiP plated aluminum carbon/lube

strain gauge
Accoustic emmission

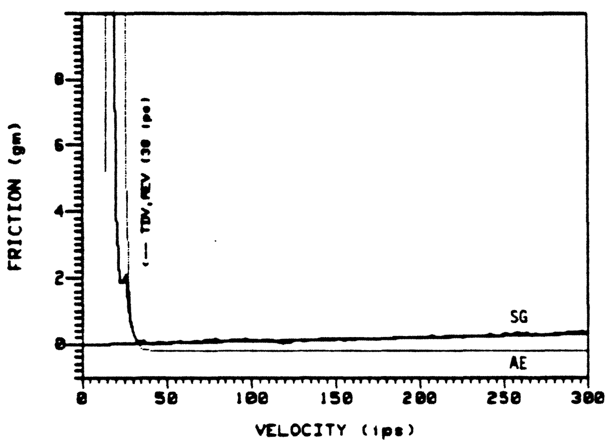

Polished glass carbon/no lube

Why is landing speed so high?

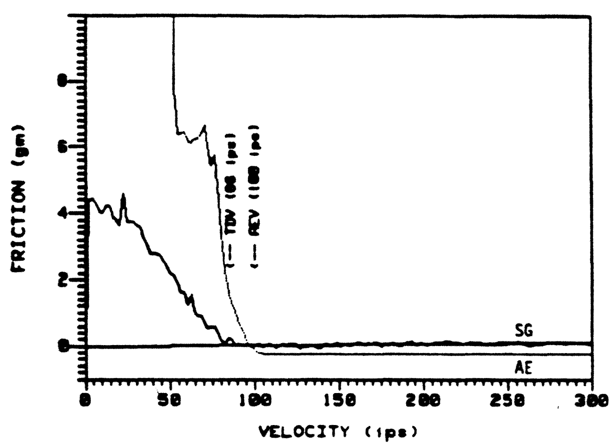

Isotropic microtexture on glass carbon/lube

Initial Once-around Friction Plots Showing Magnitude and Modulation of Friction Force

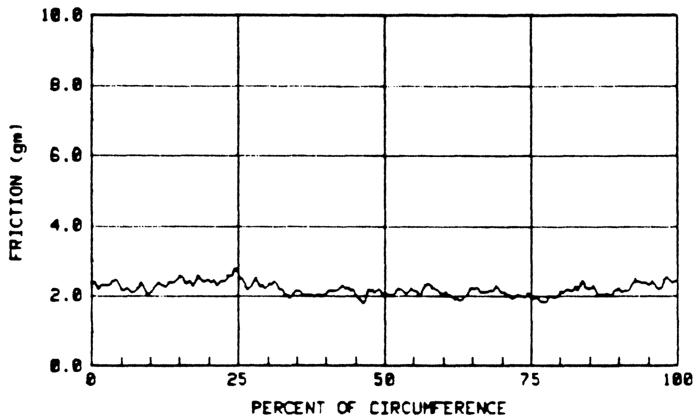

circumferential texture on
NiP plated aluminum
carbon/lube

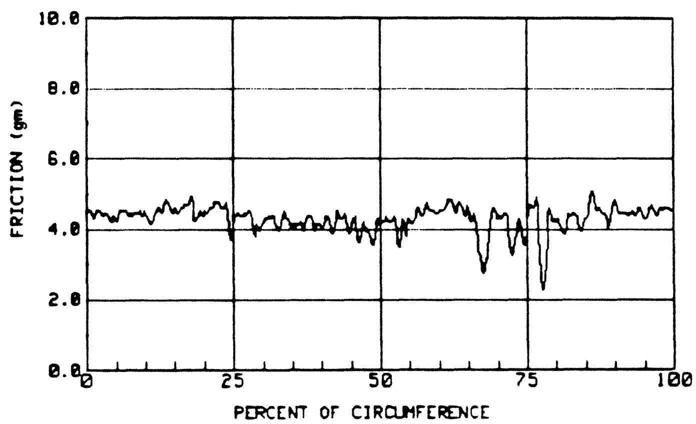

Polished glass
carbon/no lube

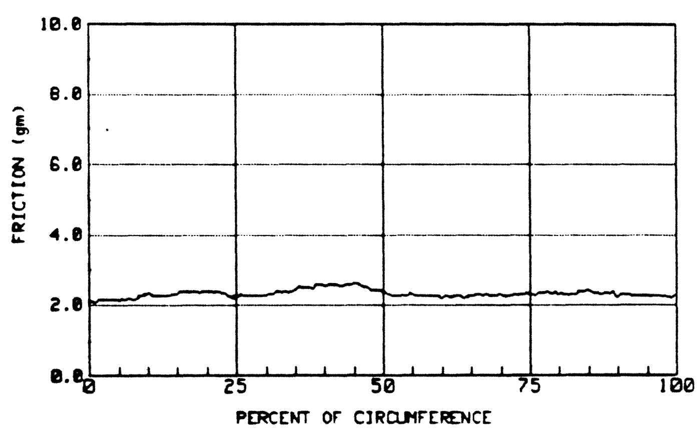

Isotropic microtexture
on glass
carbon/lube

Average Friction Force and Strain Gage Touchdown Velocity vs. Start/Stop Cycles For Each Texture

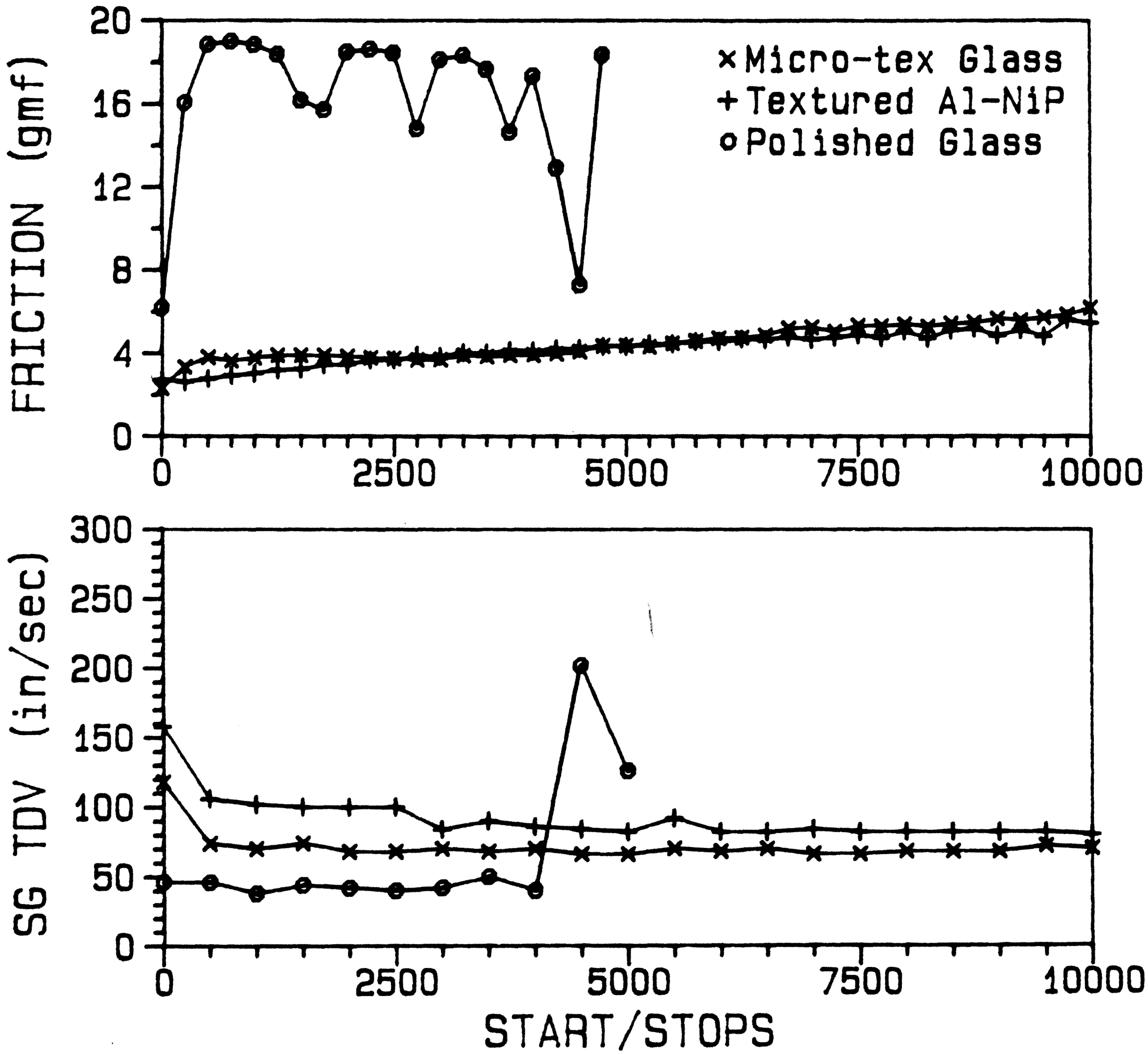

Storage Technology Department
Hewlett-Packard Laboratories

Schematic of Flying Height Measurement With and Without Texture

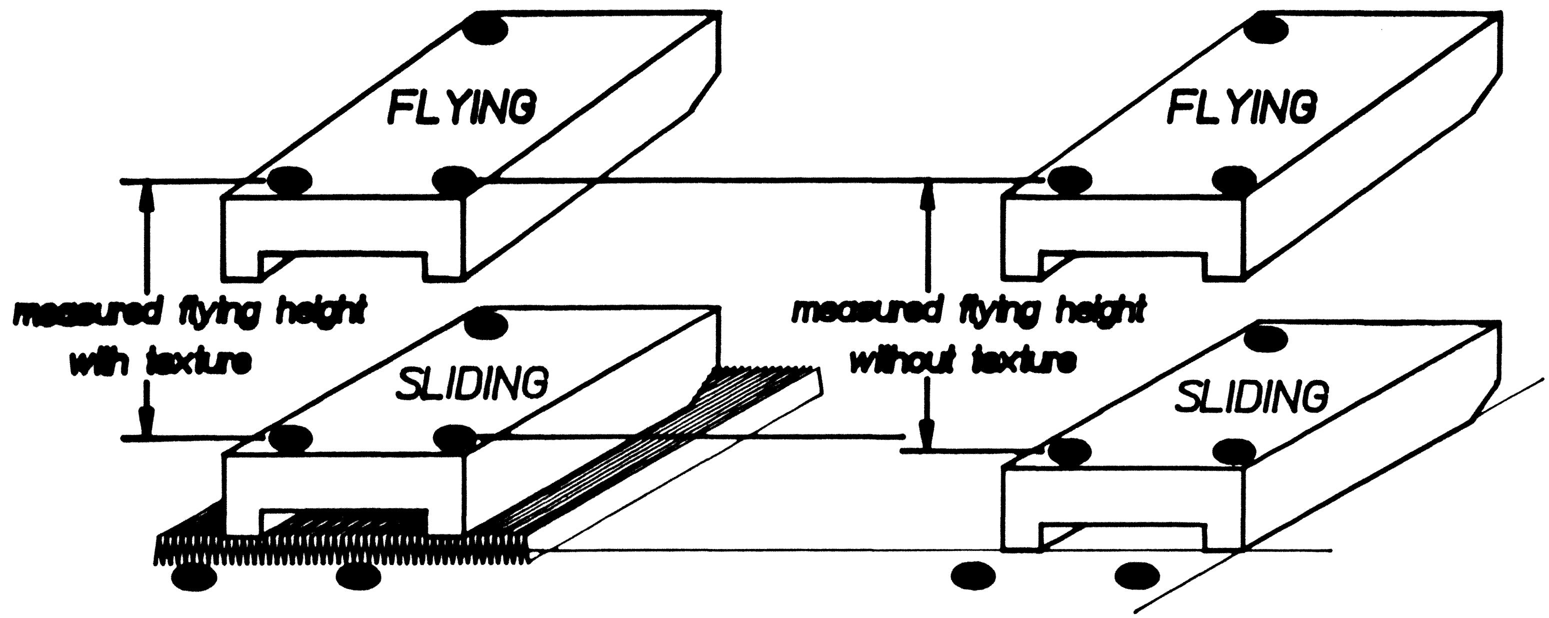

EFFECT OF TEXTURE ON LIT MEASUREMENT
WITH NO AERODYNAMIC EFFECTS

Need interferometer
Vibrometer can give same data

Storage Technology Department
Hewlett-Packard Laboratories

Measured Flying Height Vs. Speed for Polished Glass and Conventional Texture With 3 Sigma RMS Roughness Values Superimposed

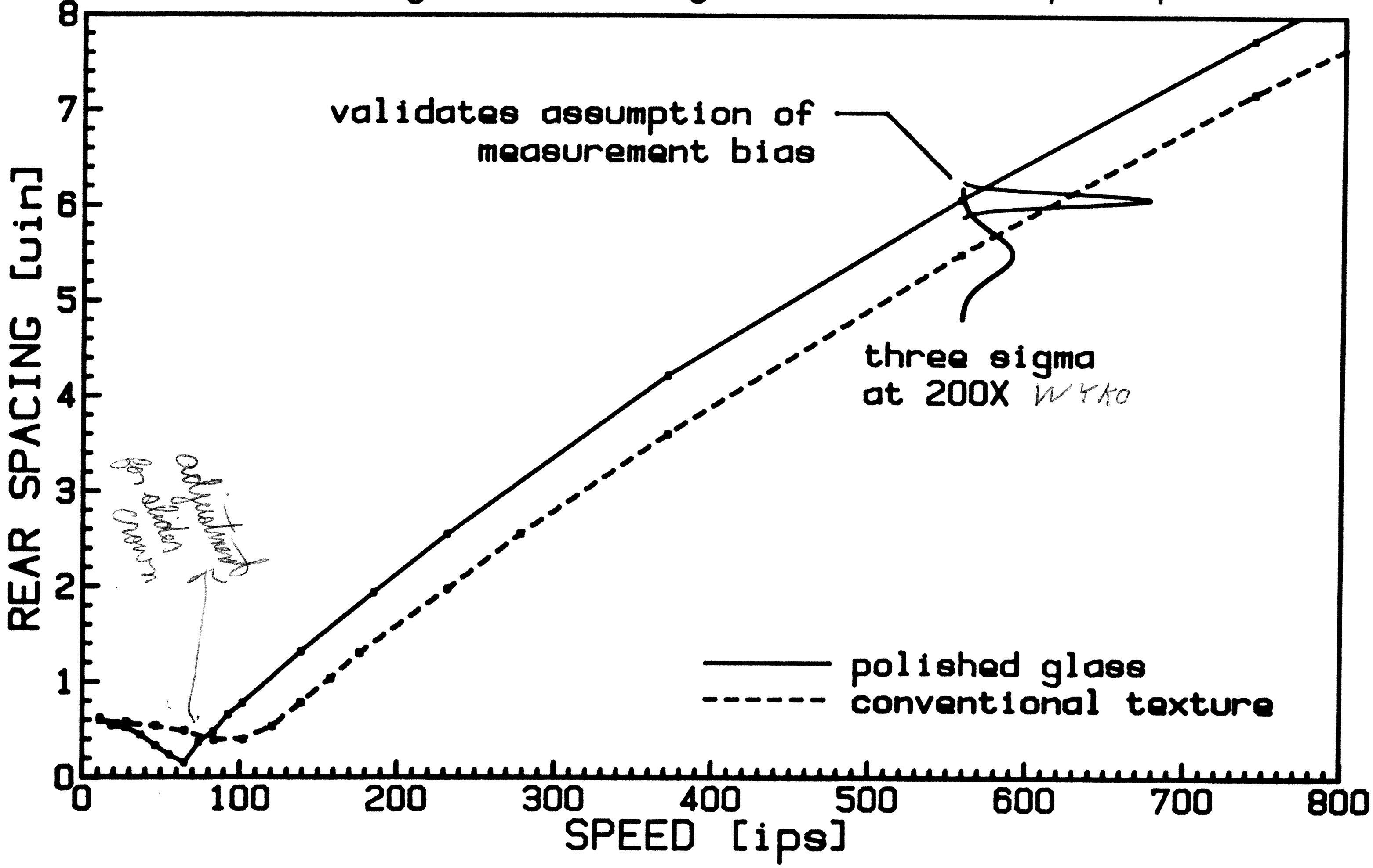

Measured Flying Height Vs. Speed for Polished Glass and Isotropic Microtexture With 3 Sigma RMS Roughness Values Superimposed

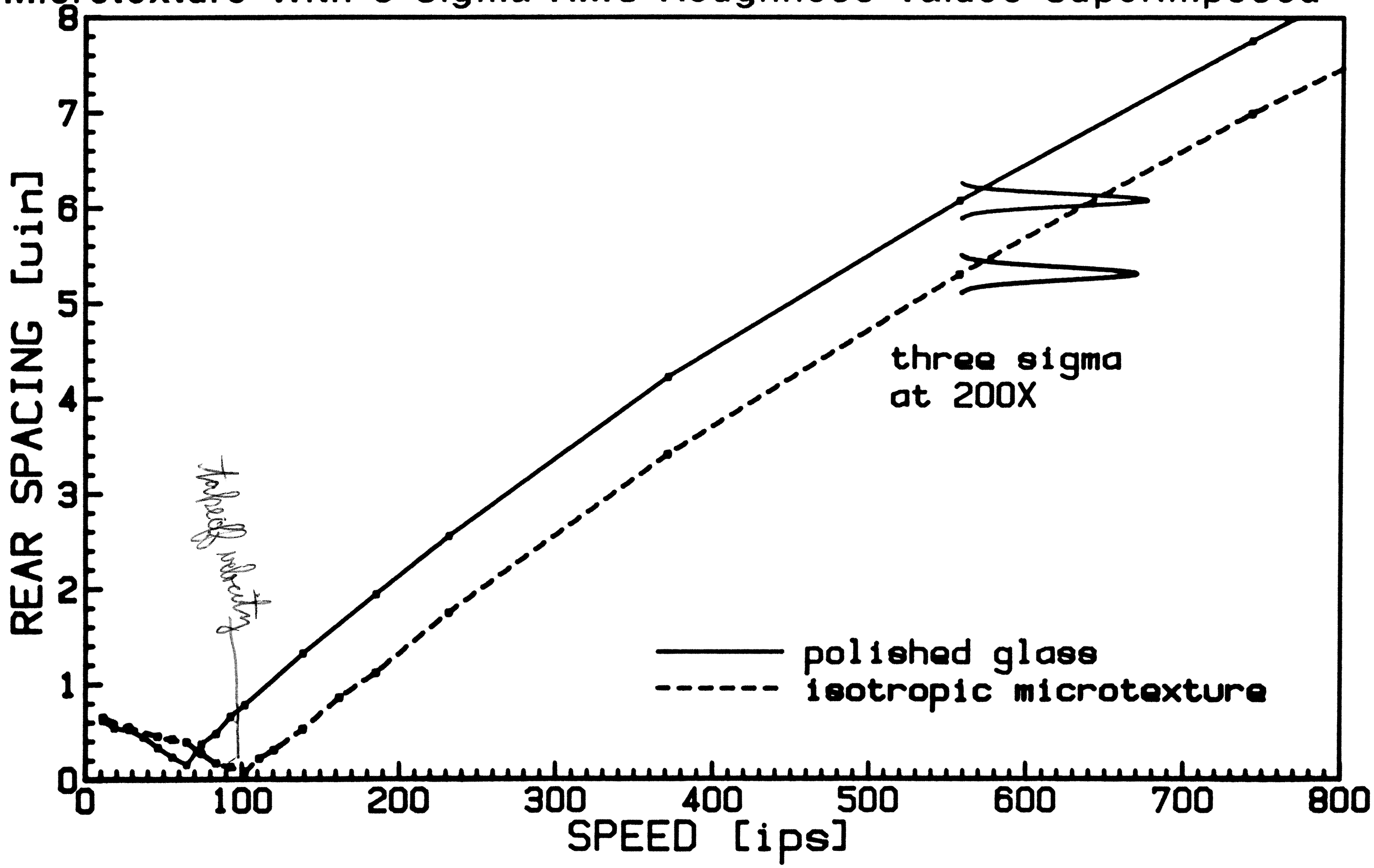

only advantage of slotted rails - allow wider rail to be used at same FHT
makes head less sensitive to skew

SLIDERS

* **Skew angle sensitivity is increased at lower flying heights** - Watch for increased roll when minimizing variation

Air bearing surface geometries address this issue

Conventional taper flat sliders

Transverse slotted (cross-cut) designs

Transverse pressure contour stepped edge (Jim White) designs

↓ **Flatter flying height profile**
Less roll variation

↓ **Increased complexity**
More expensive

Where is the practical tradeoff between cost and performance?

* **Problems are intensified in small drives**
  - **Reduced speed ⟶ reduced bearing stiffness**
  - **Larger OD/ID ratios**

Flying Height Measurements Showing the Combined Effect of Radius and Skew Angle for a Typical 5-1/4 Drive With Taper Flat and Slotted Sliders

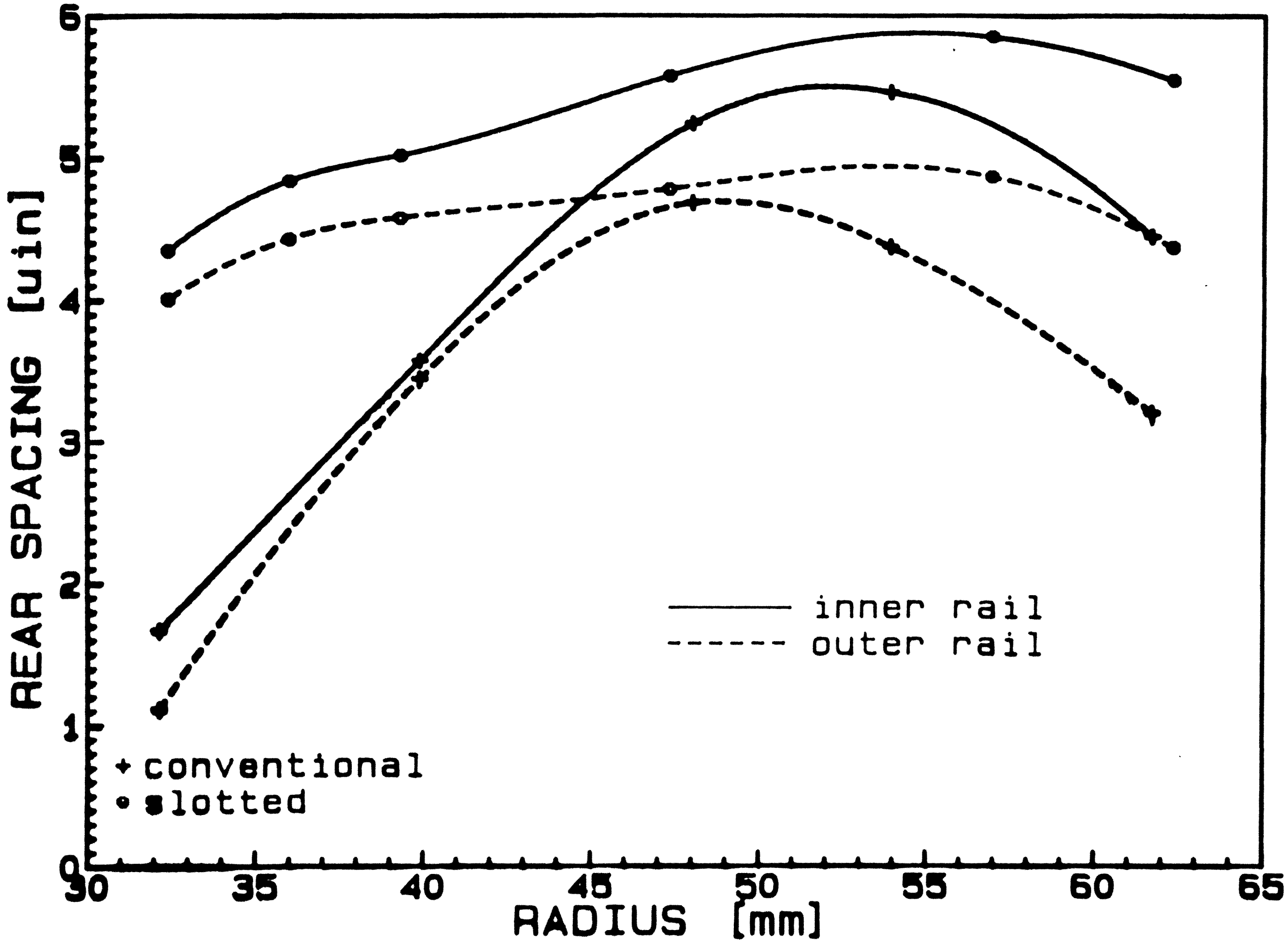

Modeling Results Showing the Combined Effect of Radius and Skew Angle for a Typical 3-1/2 Drive With TPC and Slotted (Cross-cut) Sliders

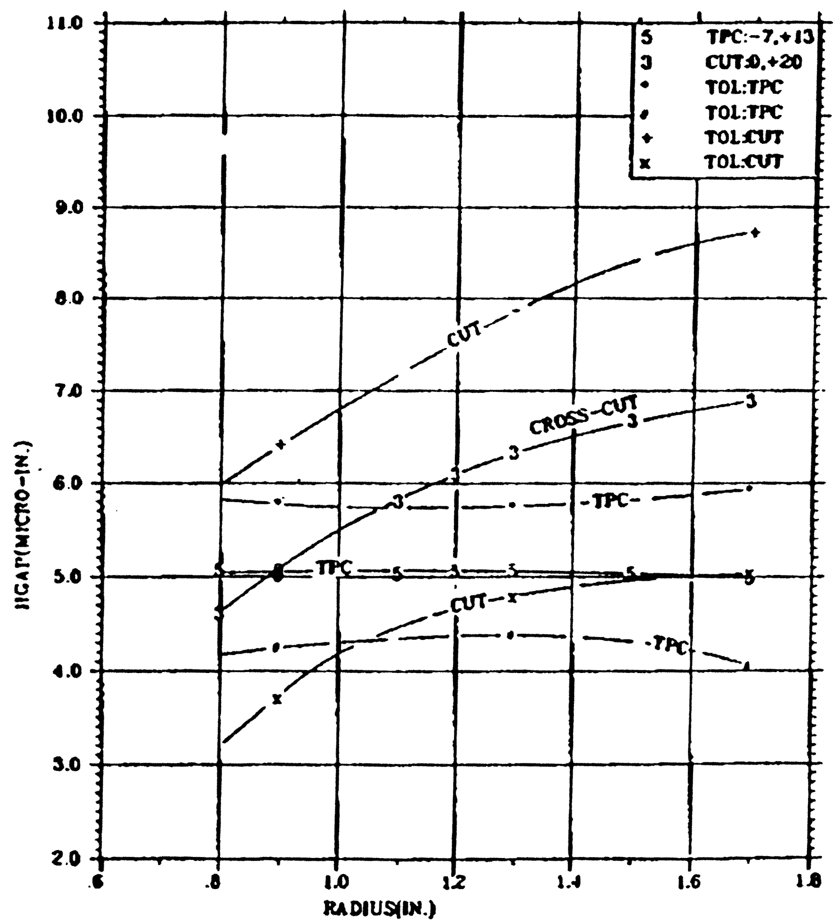

Data courtesy of Dastek
Source: Dr. James W. White

SLIDERS (cont)

* Behavior is more sensitive to actual ABS characteristics:

edge blend — crown

cross-curvature — twist

Is there quantitative agreement between your model and empirical data?

* Parallel development: reduced size sliders

  - actuator inertia reduced
  - disk area saved
  - frictional forces reduced from reduced loading forces
  - dynamic flying height reduced
  - lower cost
  - requires proper stiffness and relationship with suspension

* All of the above relates to negative pressure or zero-load sliders as well

PROCESS CONTROL

* Glide testing

Pros:

- Slider is part of the transducer, so the results can be tied to what you really care about
- Relatively efficient means for scanning entire disk surface
- Can be extremely sensitive

Cons:

- Calibration process, flying behavior and piezo output
- Contact/noncontact
- How "realistic" is the calibration event?
- The "sacred" standard

What features do you need to detect?

Dealing with reduced glide margins and customer expectations

Using interferometer

Glide Head Over 2 mm Calibration Bump - 664 ips

Diameter
2.5μ" high

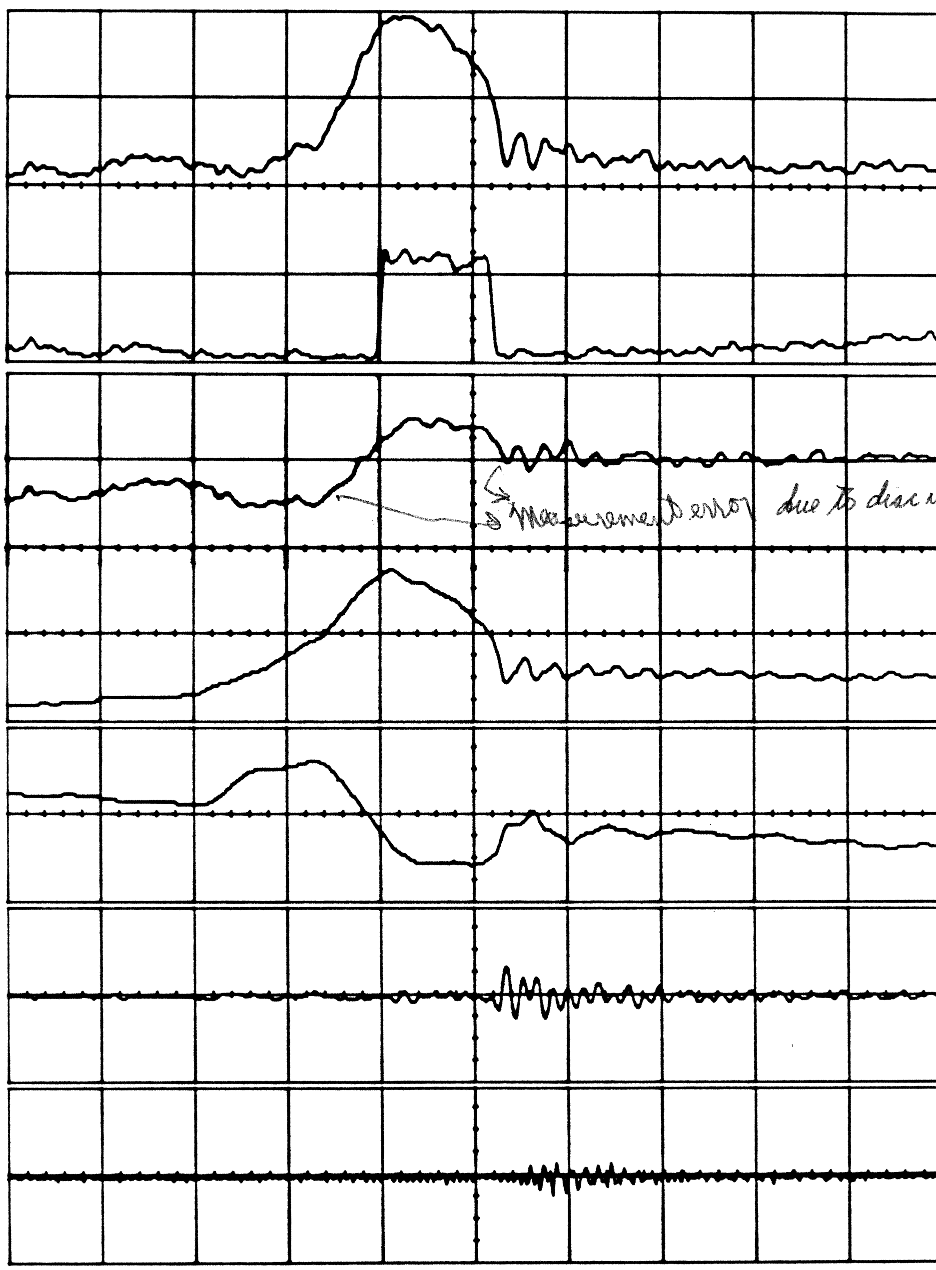

Glide Head Over 2 mm Calibration Bump - 332 ips

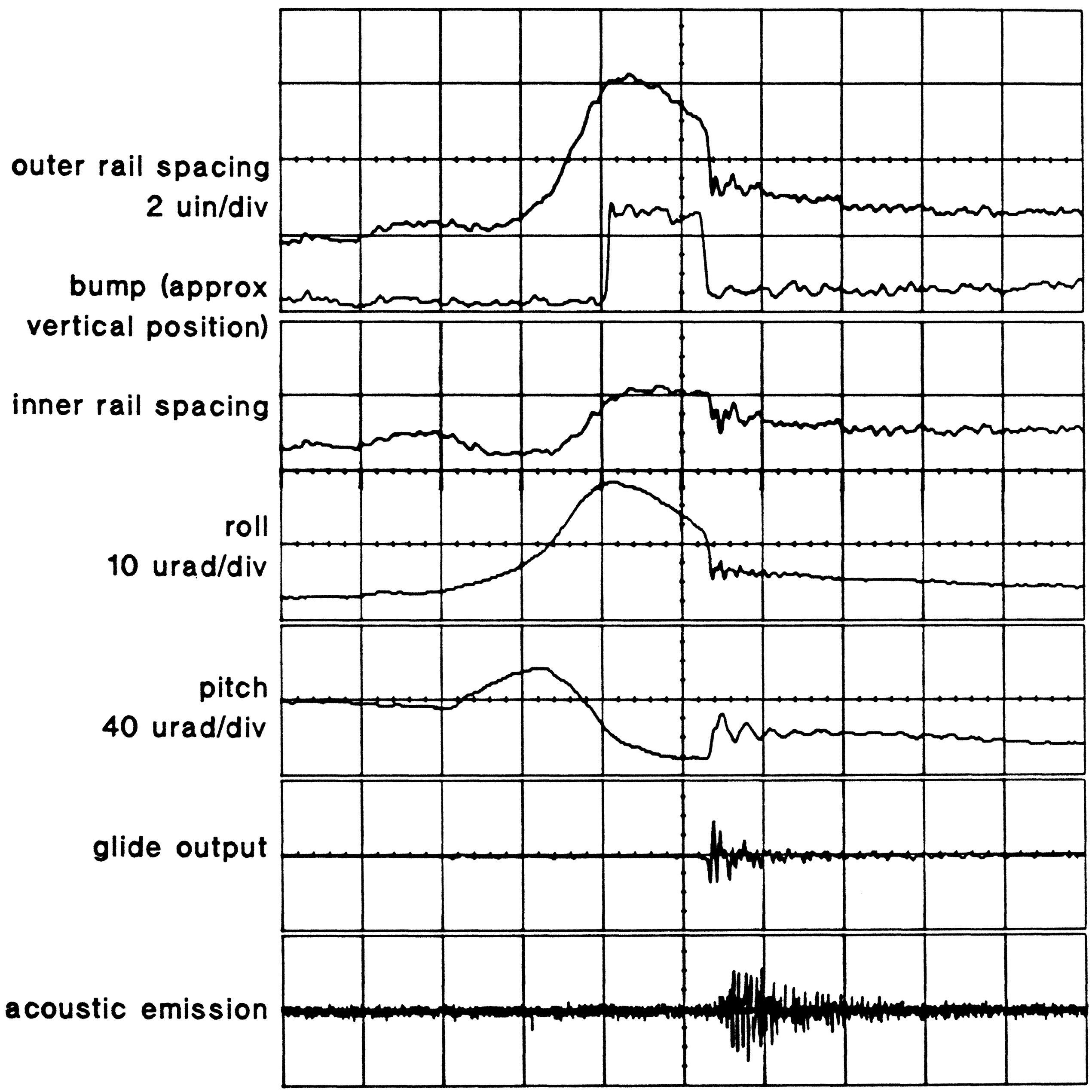

Glide Head Over 2 mm Calibration Bump - 155 ips

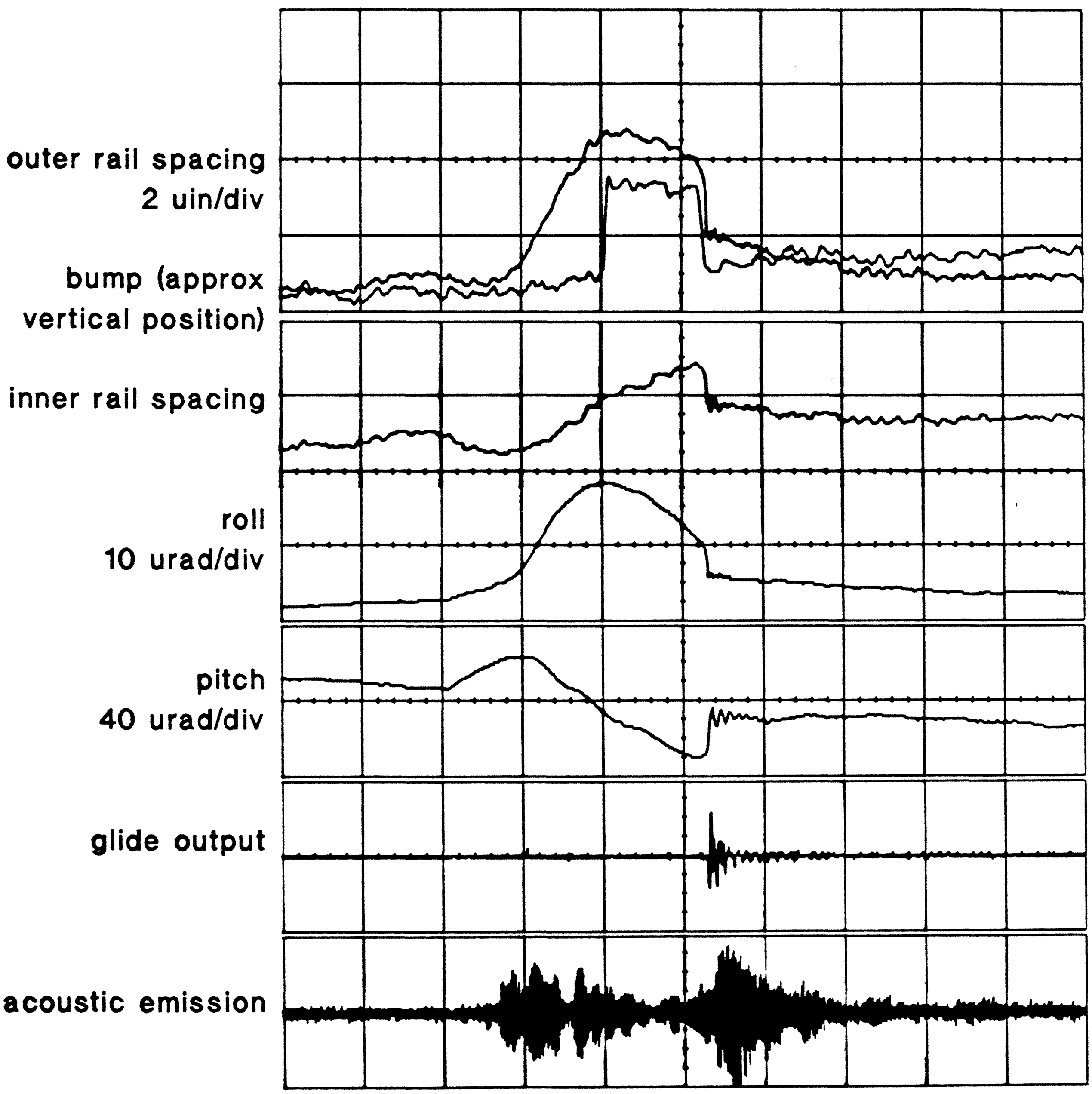

PROCESS CONTROL (cont)

* Augmentation with other techniques

- Acoustic emission
- Laser Doppler vibrometry

Variable skew
Variable RPM
Easy on off Head/Disc

* Readback signal modulation

- A very important bottom line
- Magnetics coupled in

* Disk surface monitors

- Runout, velocity, acceleration probes
- Optical scattering for smaller features
- What about smallest features, scratches, etc.?

SUSPENSIONS

Type 4 in line

Suspension dynamics during seeks and crash stops can cause significant vertical displacement of the slider

Vertical Displacement at the Slider Trailing Edge vs. Suspension Base Excitation for an In-line Suspension

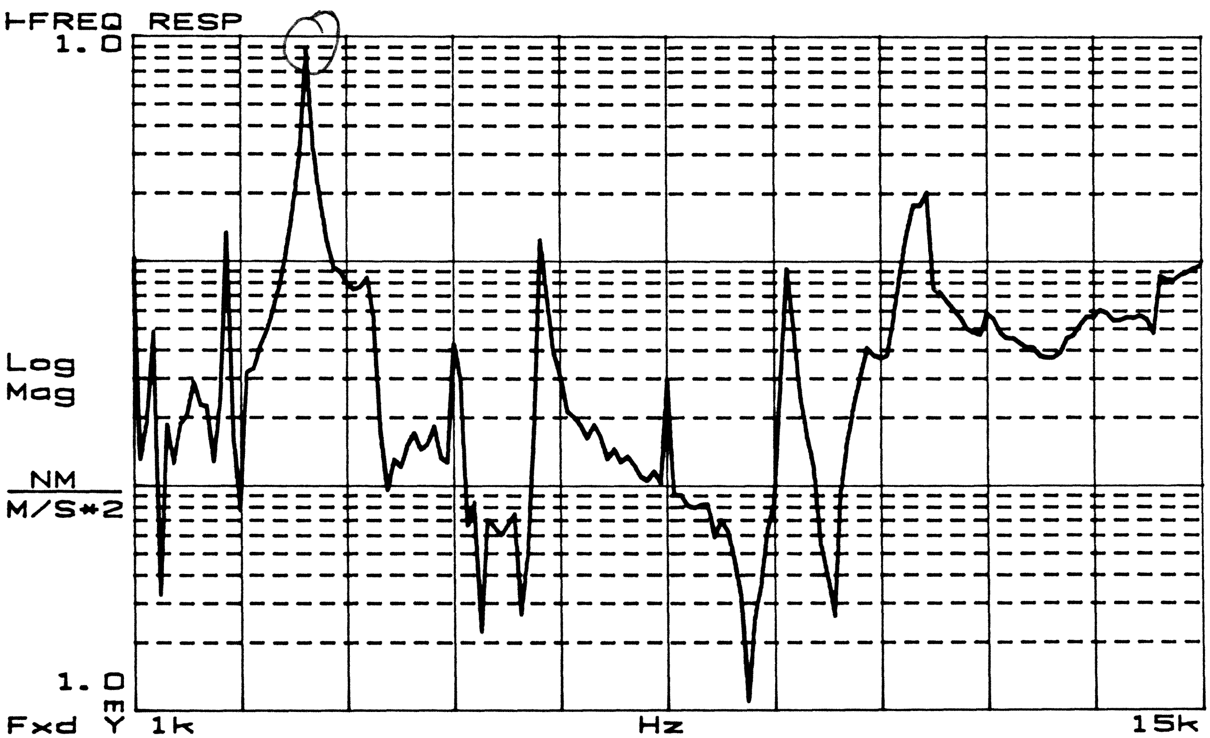

Design and control of load beam and gimbal resonances will become more important at lower flying heights

KOMAG

275 South Hillview Drive
Milpitas, CA 95035
Tel. (408) 946-2300
Telex 759164

THE DISK

H. C. Tong
Komag, Inc.

KOMAG

275 South Hillview Drive
Milpitas, CA 95035
Tel. (408) 946-2300
Telex 759164

THE DISK

GENERAL VIEW

SUBSTRATE/UNDERLAYER

TEXTURING

MEDIA

OVERCOAT

LUBRICANT

THE NEXT GENERATION --- GLASS DISK

KOMAG

275 South Hillview Drive
Milpitas, CA 95035
Tel. (408) 946-2300
Telex 759164

DISK TECHNOLOGY REQUIREMENTS

High Performance:

* Optimum Hc and Mrt
* High S/N
* Low Flying Height
* Thin and Light Weight
* Highest Quality Control
* Optimized surface mechanical parameters
    - Roughness
    - Flatness

KOMAG

275 South Hillview Drive
Milpitas, CA 95035
Tel. (408) 946-2300
Telex 759164

Excellent Reliability:

* Excellent Wear Resistance
* Excellent Corrosion Resistance

Lowest Cost:

* Simplest Manufacturing Steps
* High Yield Automation
* Low Cost High Performance Materials

KOMAG

275 South Hillview Drive
Milpitas, CA 95035
Tel. (408) 946-2300
Telex 759164

Future demand for Increased volume storage requires thinner disks

DISK SIZE	NOW	FUTURE
5 1/4	75 mil	50 mil
3 1/2	50 mil	31.5 mil
2 1/2	35 mil	25 mil

3 1/2" Al Substrate - 50 mil

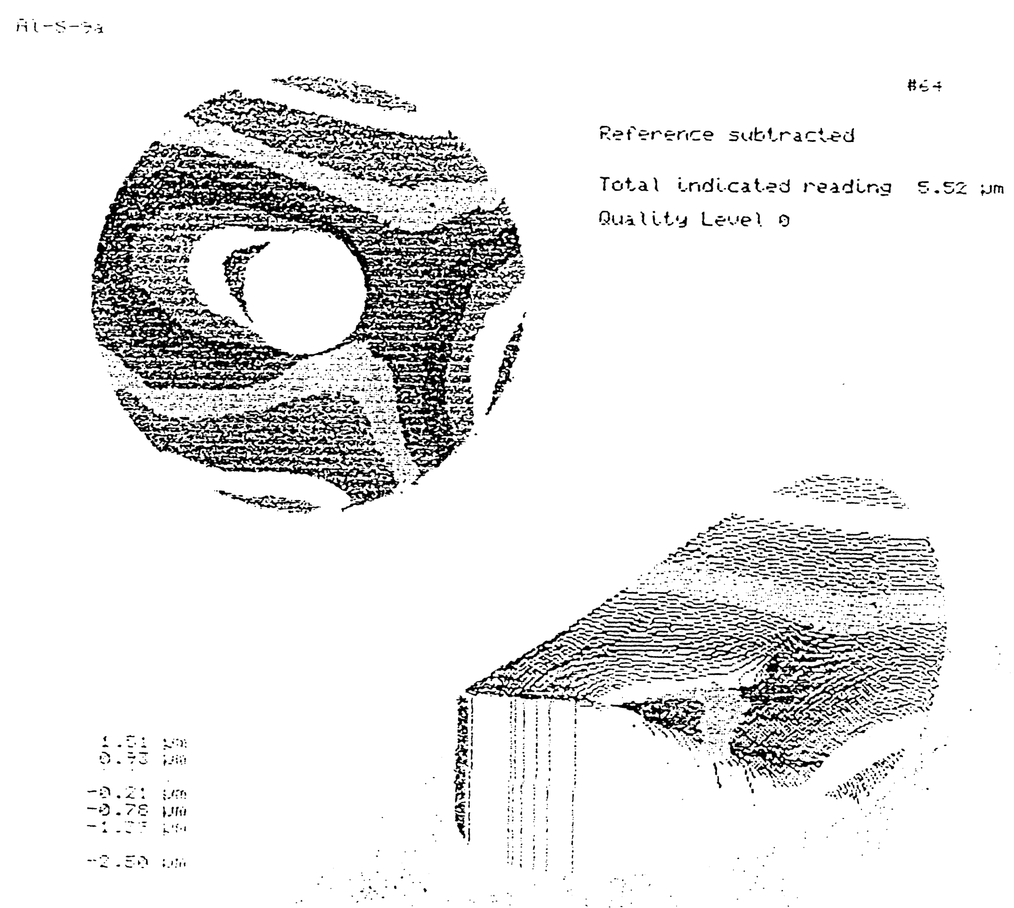

Flatmaster Front Referenced Plot

Ref: 2

KOMAG

3 1/2" Glass Substrate - 50 mil

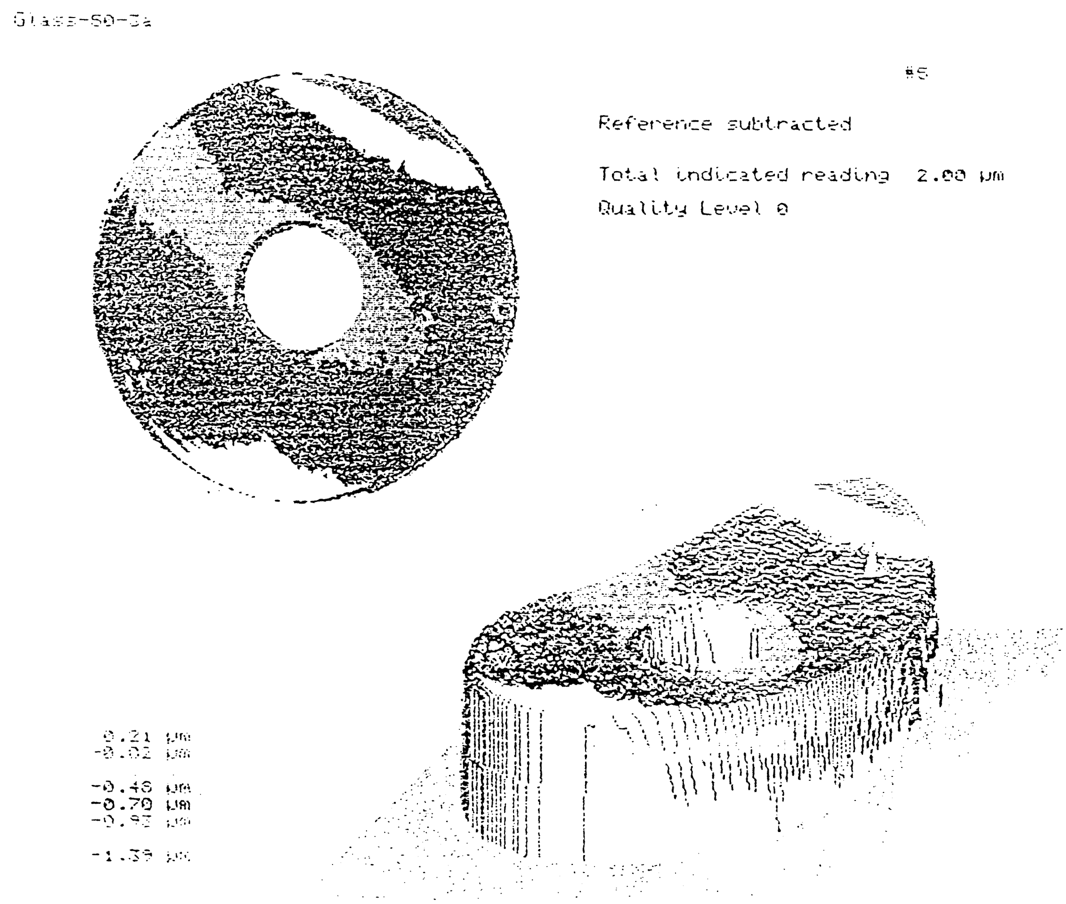

Flatmaster Front Referenced Plot

Ref: 2

KOMAG

3 1/2" Al Substrate - 31.5 mil

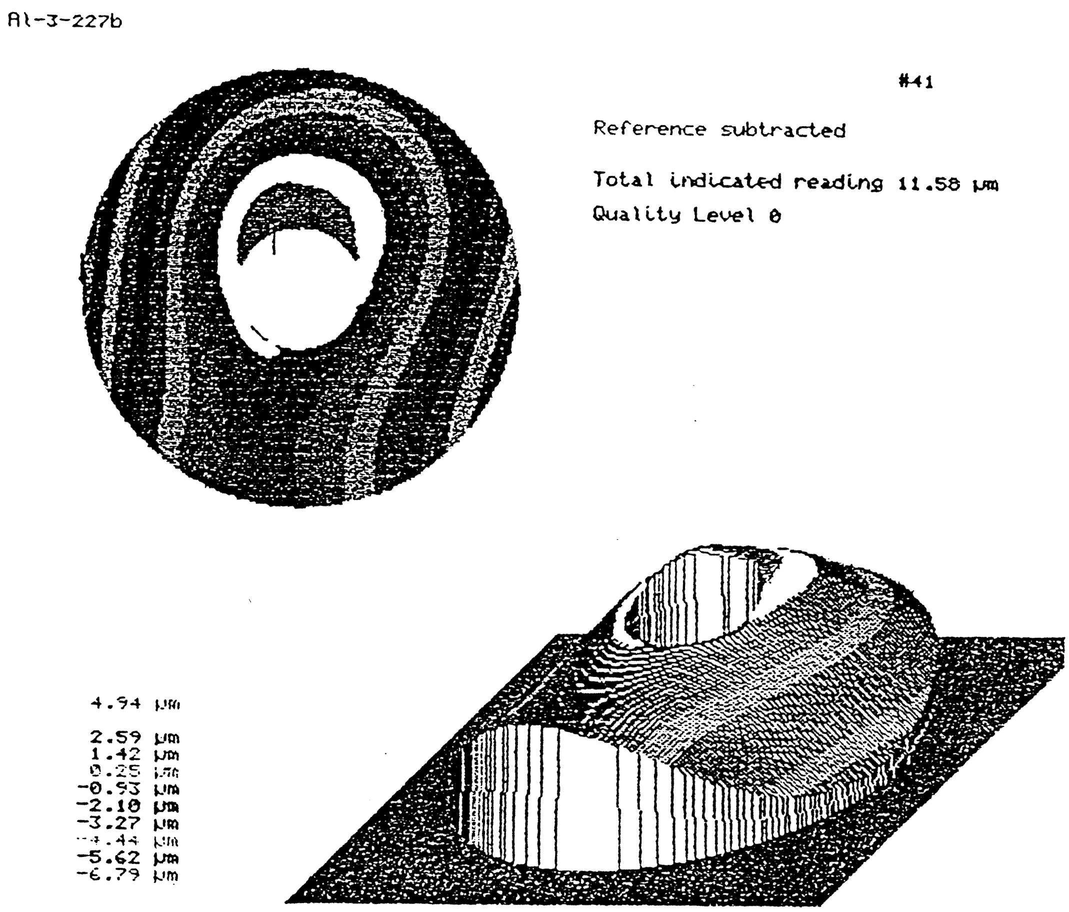

Flatmaster Front Referenced Plot

Ref: 2

KOMAG

3 1/2" Glass Substrate - 31.5 mil

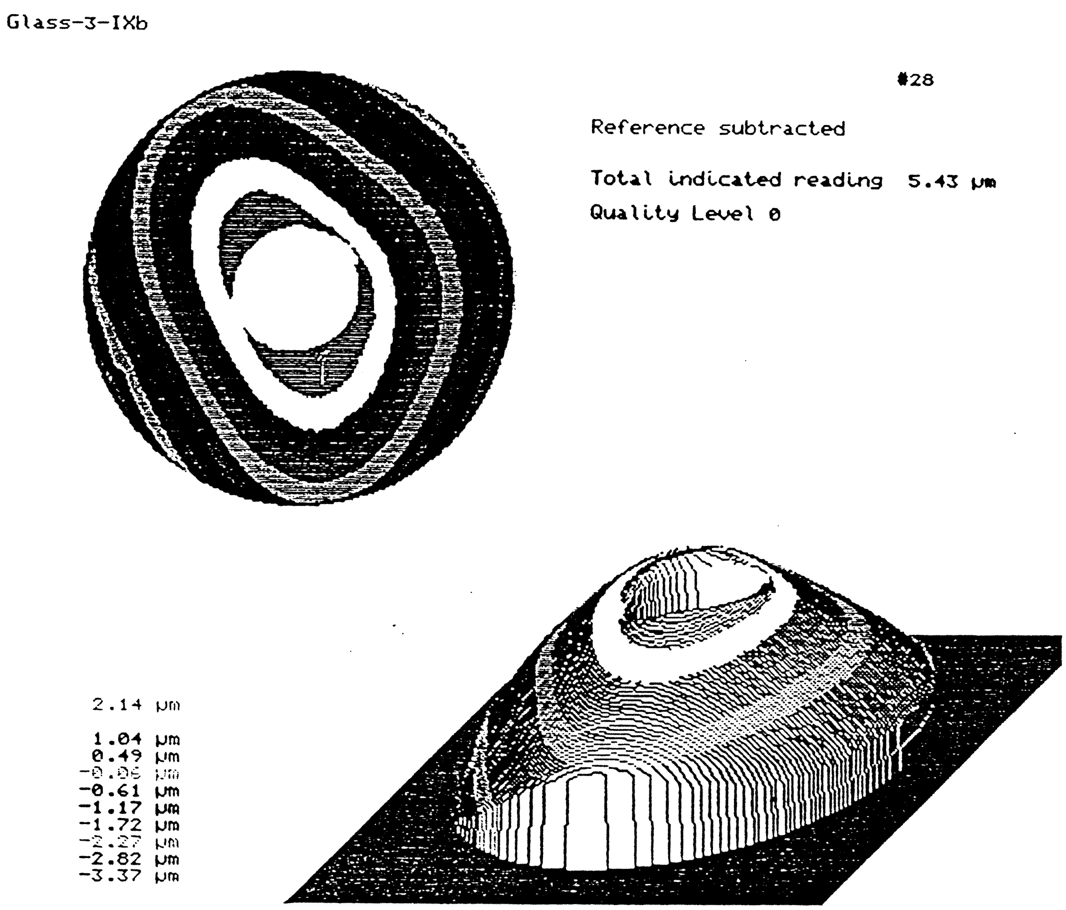

Flatmaster Front Referenced Plot

Ref: 2

KOMAG

KOMAG

275 South Hillview Drive
Milpitas, CA 95035
Tel. (408) 946-2300
Telex 759164

UNDERCOAT TECHNOLOGY:

FUNCTION:

RIGIDITY IMPROVEMENT
PROVIDE EASIER TEXTURING SURFACE

COMMON TYPE:

	Koop Hardness
AL-Mg ALLOY(5086):	
1. ELECTROLESS NiP	600-650
2. ANODIZED LAYER	-
GLASS: NO UNDER COATING IS NEEDED.	600

ISSUES:

DISK FLATNESS MAY BE INDUCED BY STRESS OR HANDLING INDUCED DISK.

INDUCED DEFECTS SUCH AS NODULES, PITS, ETC. WHICH MAY CAUSE MISSING PULSES/EXTRA PULSE, AND GLIDE HEIGHT FAILURES.

KOMAG

275 South Hillview Drive
Milpitas, CA 95035
Tel. (408) 946-2300
Telex 759164

SUBSTRATE

FUNCTION:

Provide a flat rigid base for a magnetic recording media.

SUBSTRATE MATERIALS

Selection criteria:

* Low cost.
* Surface finish
* Physical Properties such as modulus, rigidity, etc
* Dynamic properties, RVA, etc.
* Easy manufacturing.
* Adhesion to next layer.
* Thermal expansion
* Environmental stability

CURRENT SUBSTRATE:

5086 AL-ALLOY

KOMAG

275 South Hillview Drive
Milpitas, CA 95035
Tel. (408) 946-2300
Telex 759164

Al-Mg Aluminum-Magnesium

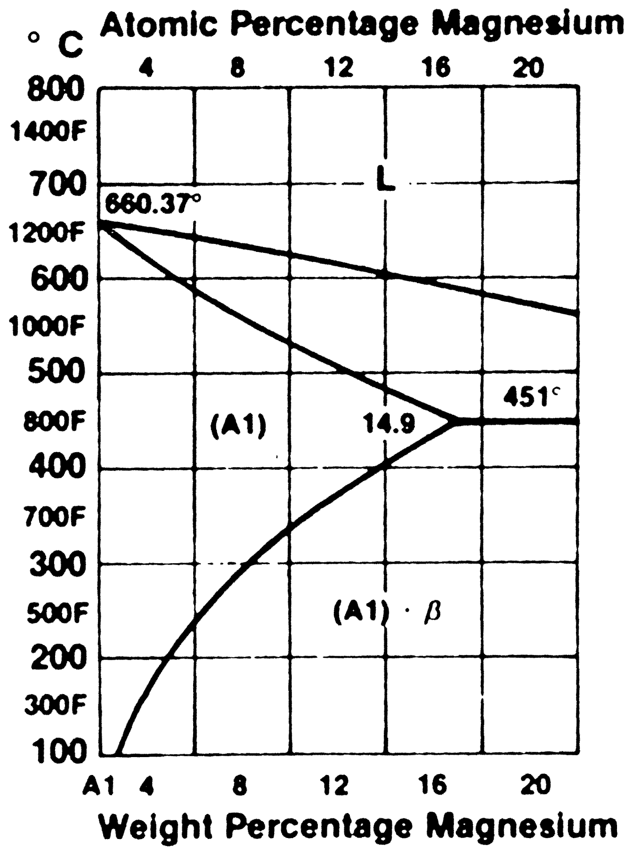

Chemical Composition

ALUMINUM ALLOY- 5086

SILICON	0.40 max
IRON	0.50 max
COPPER	0.10 max
MANGANESE	0.20 to 0.7
CHROMIUM	0.05 to 0.25
ZINC	0.25 max
TITANIUM	0.15 max
Others	0.05 each-0.15 max
Remaining	Aluminum

Source: ASM Handbook 8th Edition Volume 1.

Mechanical Properties of Glass and Al-5086 Disk Substrate:

Properties	Glass	Aluminum
Specific Gravity (g/mm)	2.41	2.70
Young's Modulus (Kg/mm)	7050	7220
Shear Modulus (Kg/mm)	3000	3008
Poisson's Ratio	.18	.20
Knoop Hardness (Kg/mm)	640	50-60 Al 600-650 NiP
Thermal Expansion Coefficient	49	231

KOMAG

275 South Hillview Drive
Milpitas, CA 95035
Tel. (408) 946-2300
Telex 759164

TEXTURING TECHNOLOGY:

FUNCTION:

1. REDUCE STICTION OF THE LUBED DISK, AND
2. PROVIDE SUFFICIENT BEARING SURFACES FOR WEAR RESISTANCE.

ISSUES:

DISK FLATNESS: RVA

DEFECTS: PITS, NUDULES, ETC.

INFLUENCE GHT BUDGET

TEXTURE CAN INFLUENCE TRANSITION ZIG-ZAG PATTERN

3. Texture induced space loss

Mechanical Texture - NiP

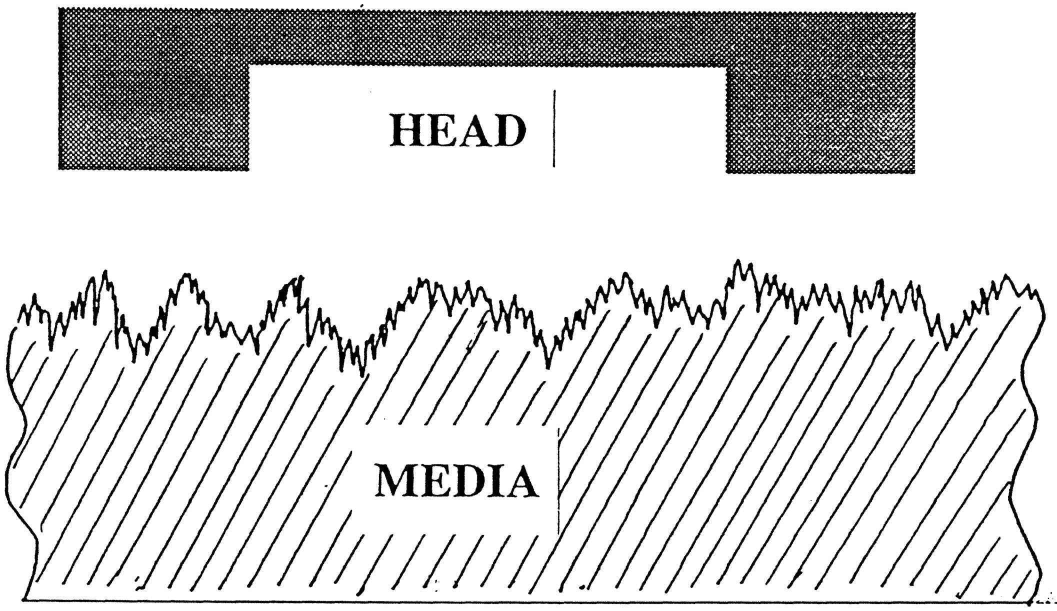

Chemical Texture - Glass

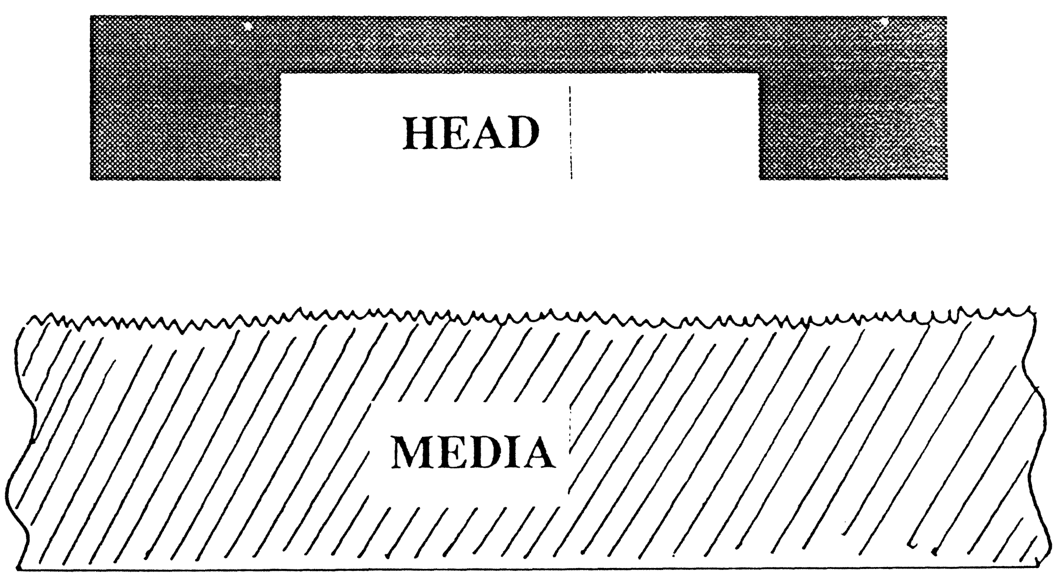

KOMAG

Mechanical Texture - NiP

X5000

X60000

Ref: 2

KOMAG

Chemical Texture - Glass

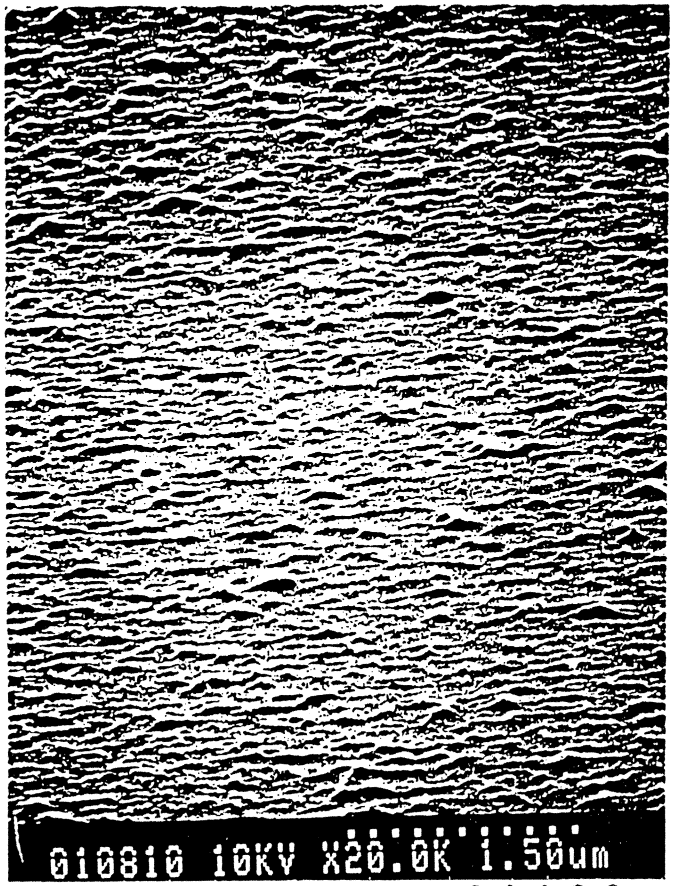

×20000

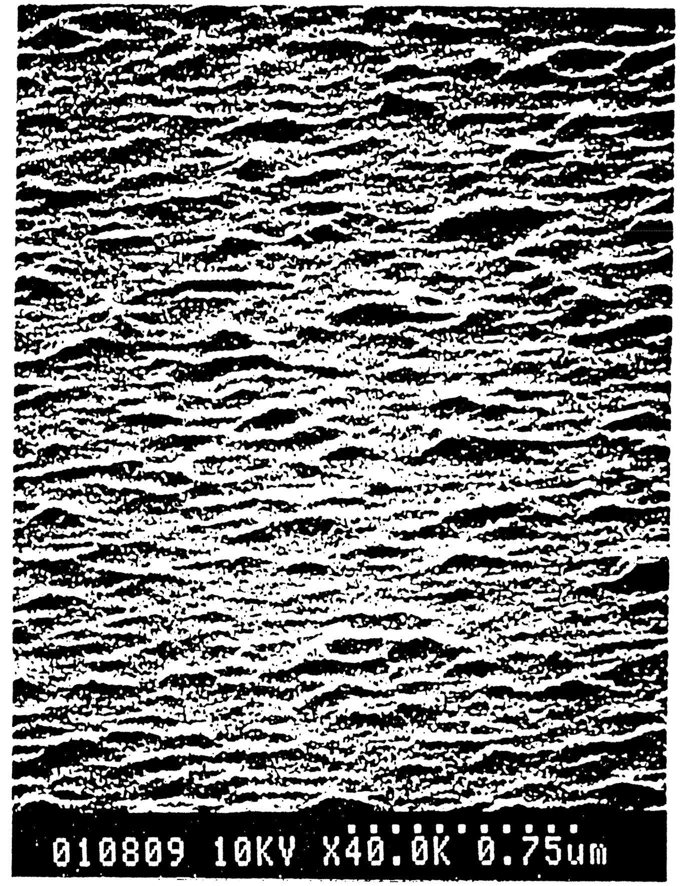

×40000

Ref: 2

KOMAG

Media surface asperity

a. Texture induced

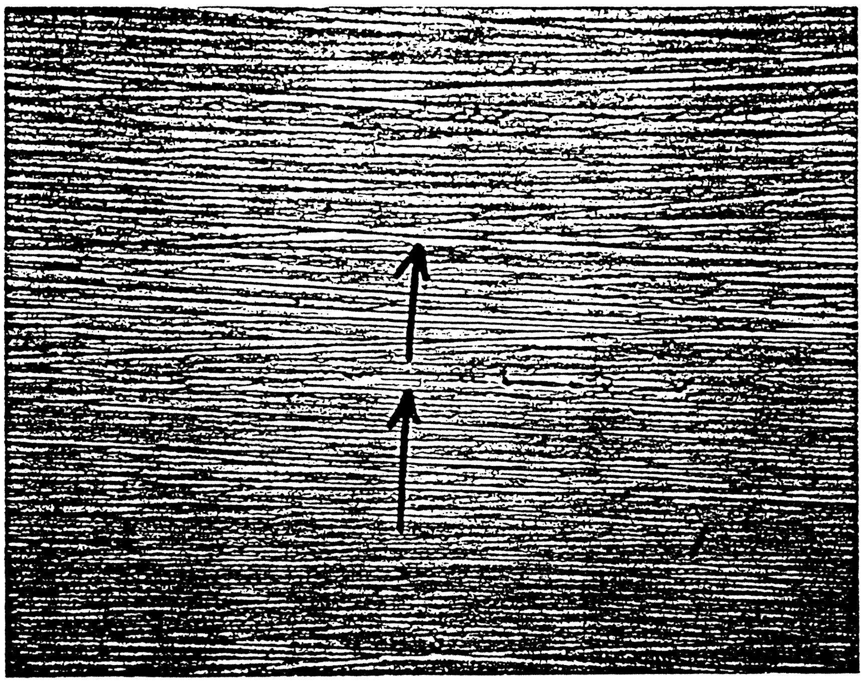

400x Magnification

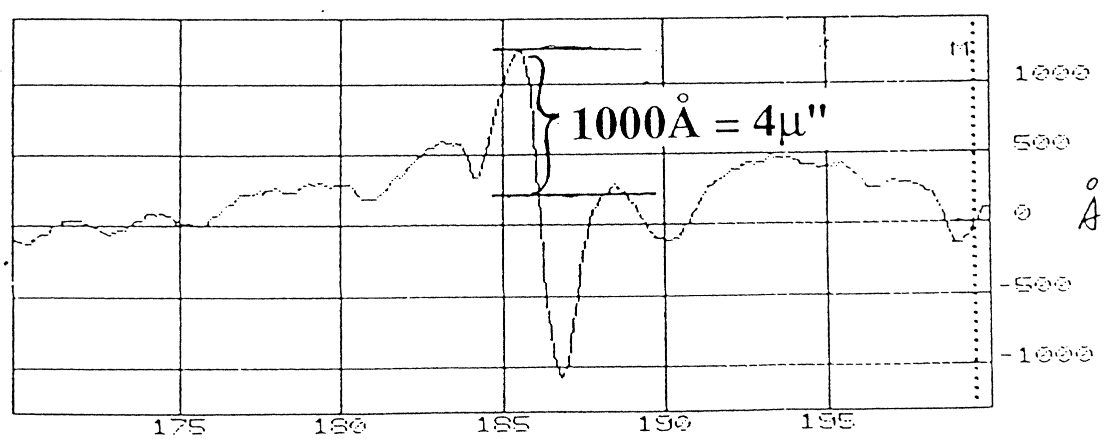

Ref: 2

Dektak scan (µm)

KOMAG

KOMAG

275 South Hillview Drive
Milpitas, CA 95035
Tel. (408) 946-2300
Telex 759164

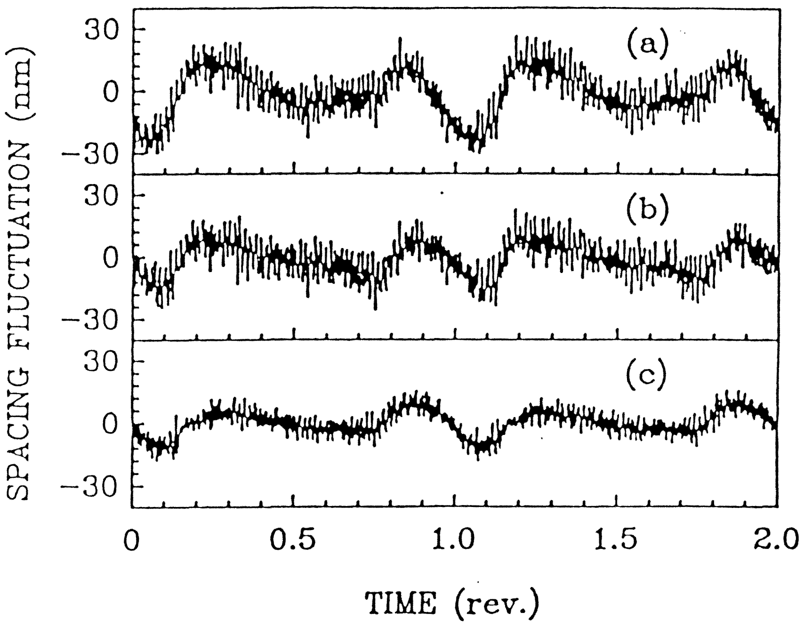

Head-disk spacing fluctuation due to the disk surface curvature. (a) experimental data, uncorrected; (b) experimental data, corrected; (c) theoretical prediction based on the disk profile.

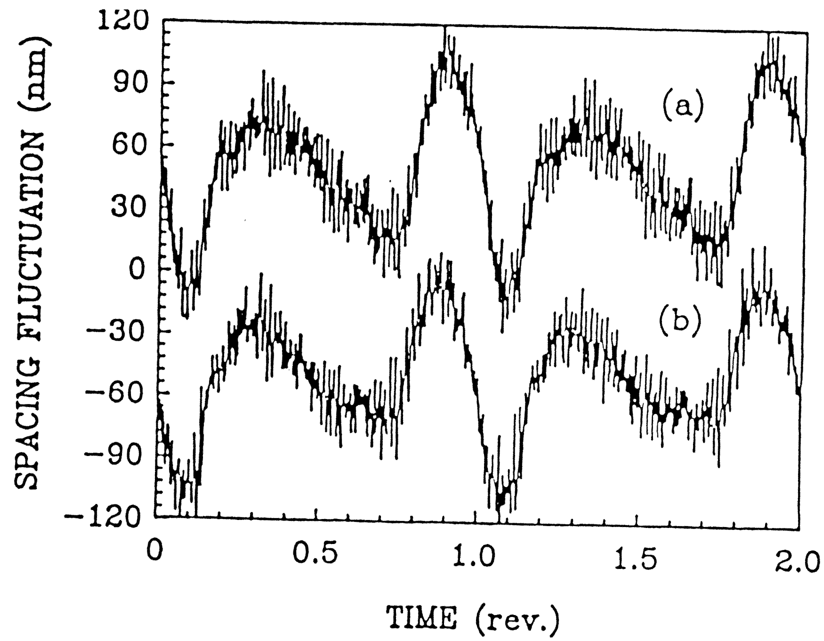

Slider-disk spacing fluctuation at the slider's leading edge. (a) Experimental data, corrected; (b) theoretical prediction.

Ref: 3

KOMAG

275 South Hillview Drive
Milpitas, CA 95035
Tel. (408) 946-2300
Telex 759164

Scan File Name:82t3.dat with 600 data points.
Scan Time:09:05, Scan Date:10-27-89, Scan Length:1200uM, Scan Speed:LOW .
Ra= 35.9A, RMS= 45.6A, Sk= -0.005, Ku= 0.03
Max= 94.3A (at 104.0um), Min=-170.9A (at 334.0um), RMax= 265.2 A.

Original Profile From Dektak

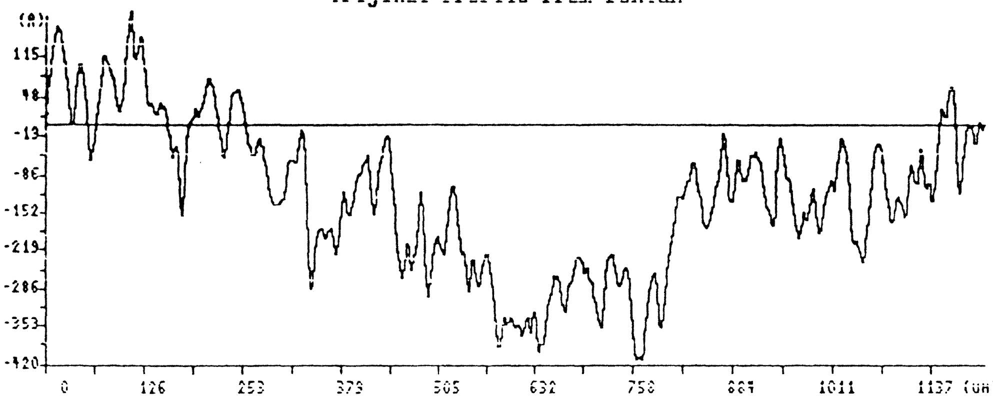

Filtered Profile

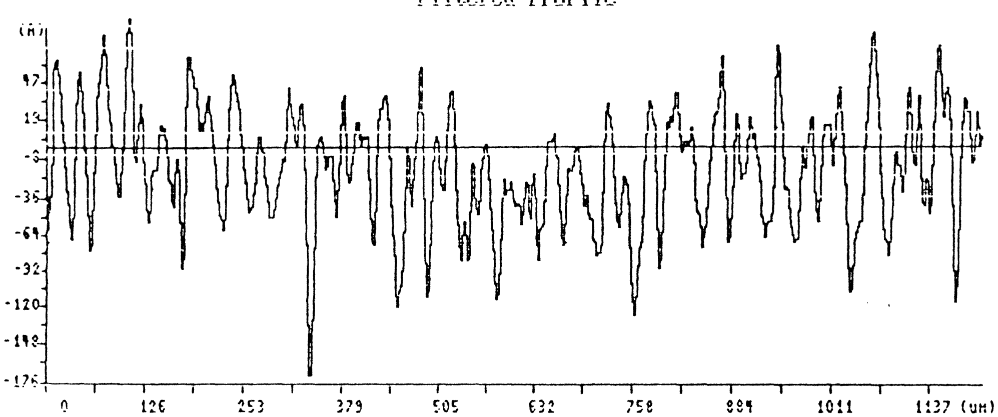

Bearing Area Ratio

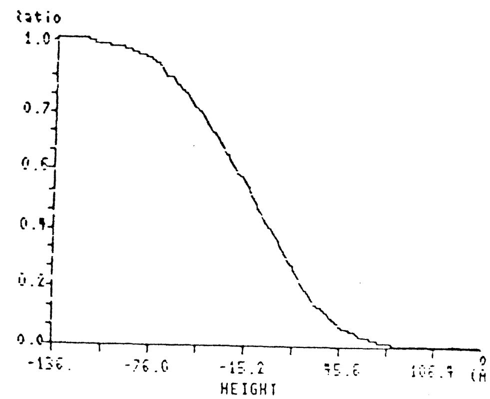

Line Density

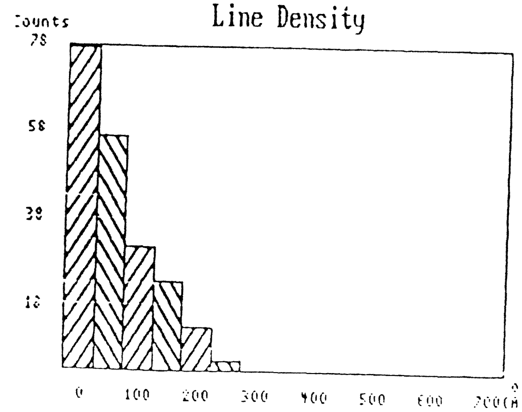

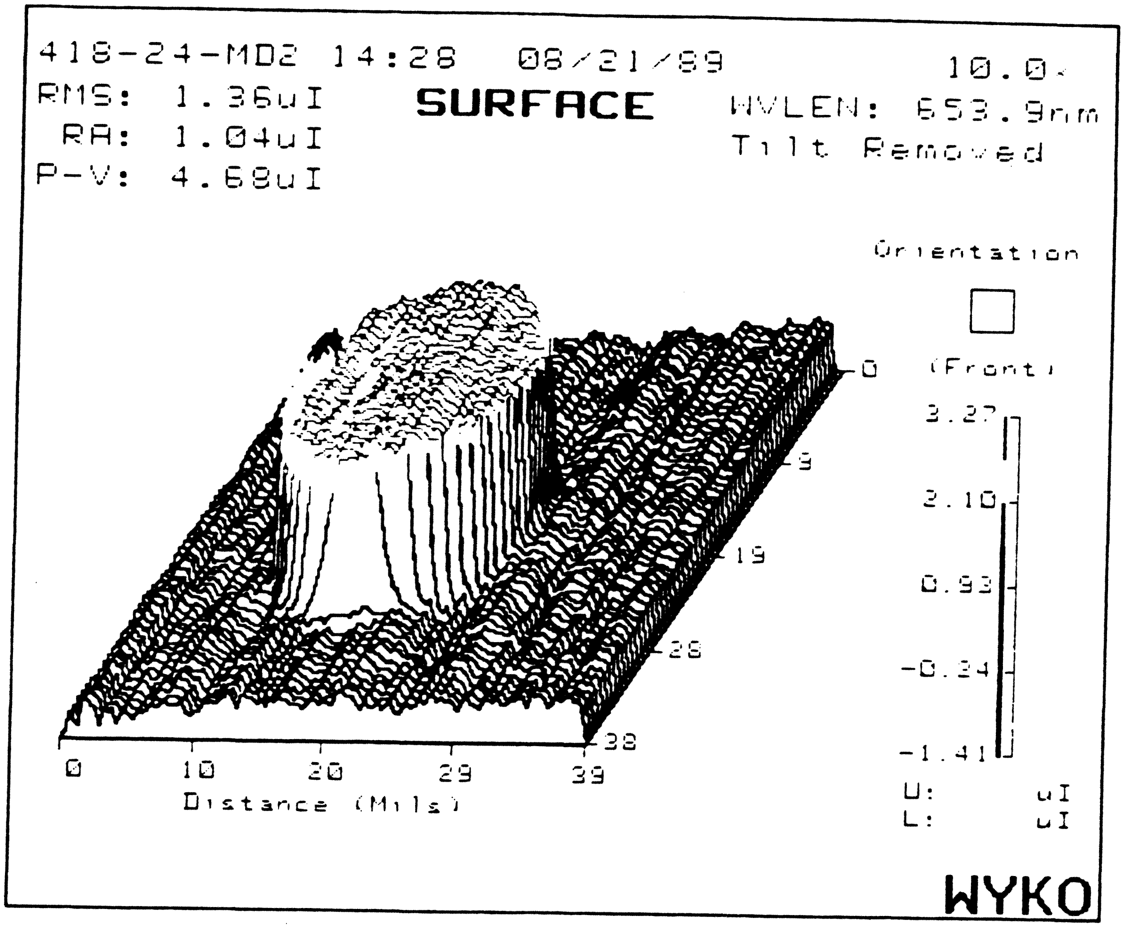
418-24-MD2 14:28 08/21/89
10.0×
RMS: 1.36uI
RA: 1.04uI
P-V: 4.68uI
SURFACE
WVLEN: 653.9nm
Tilt Removed
Orientation
(Front)
3.27
2.10
0.93
-0.24
-1.41
0
9
19
28
38
0
10
20
29
39
Distance (Mils)
U: uI
L: uI
WYKO

AKASHIC

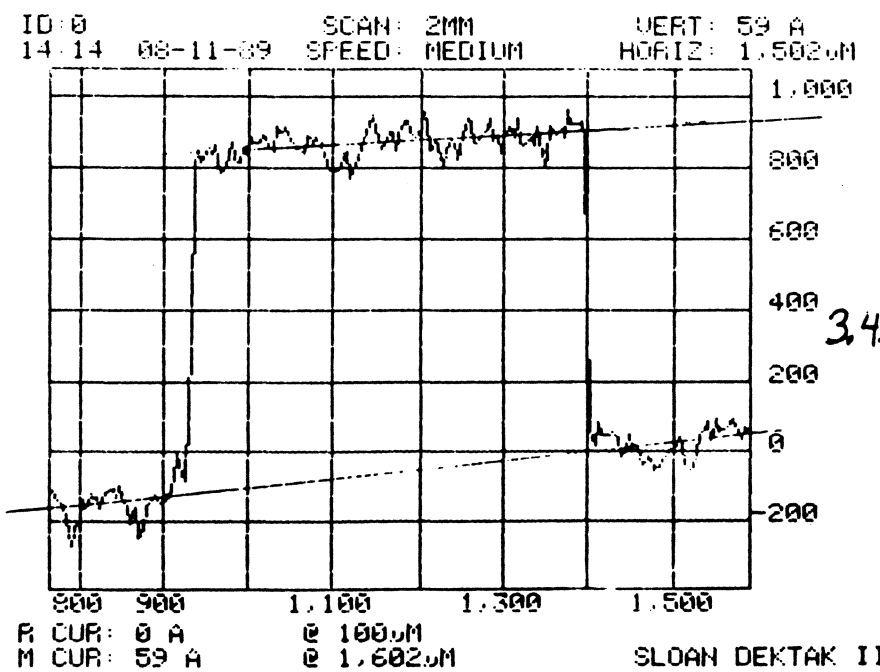
ID:0
14:14 08-11-89
SCAN: 2MM
SPEED: MEDIUM
VERT: 59 A
HORIZ: 1,502uM
1,000
800
600
400
200
0
-200
800
900
1,100
1,300
1,500
R CUR: 0 A @ 100uM
M CUR: 59 A @ 1,602uM
SLOAN DEKTAK II

3.4μ"

Set	Right	Center	Left	Avg	Sd Dev
1	4.6	4.9	5.1	4.9	0.25
2	5.3	5.9	5.3	5.4	0.35
3	5.1	-	5.8	5.4	0.50
Total				5.2	0.43

Conclusions:

A) The <u>best</u> repeatability we can expect from the Dektak is +/- 0.3 u".

B) The bump heights measured via a Dektak are subjective due to:

1) The operator must "eyeball" a line through the top of the peak and the base.

2) The height scale on the side of the print out must be interpolated to determine the height.

Inconsistencies in measurement techniques could easily cause 0.5 u" differences in height.

Enclosures:

A) Dektak measurement technique.

GLIDE ISSUES

Transducer

Acoustic vs. Piezo

Data courtesy Bernard Flusche Jr., Akashic

Maxtor

Both Signals Simultaneously

Pz

AE

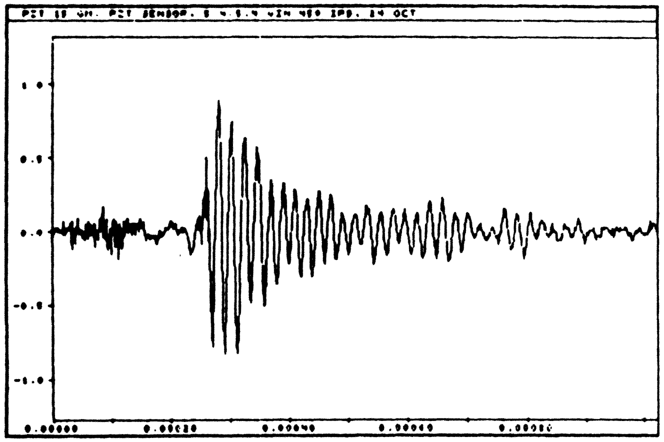

.1μ" Above Bump

5.4μ"

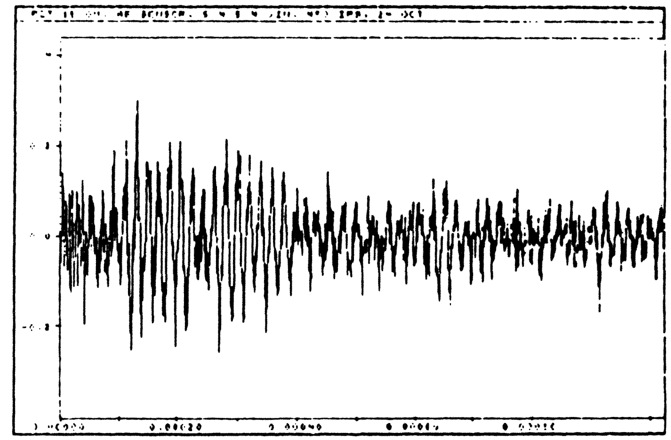

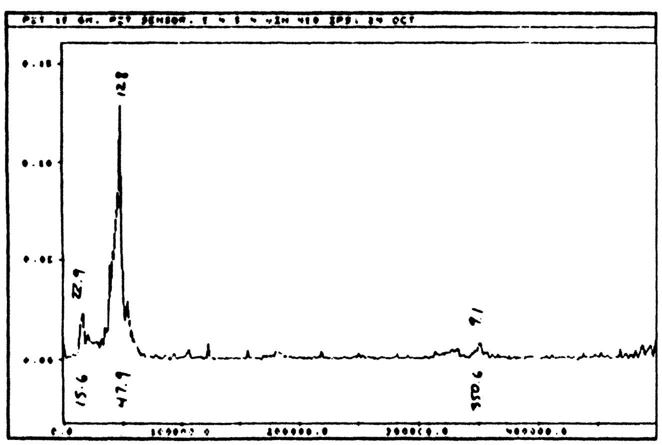

Spectrum

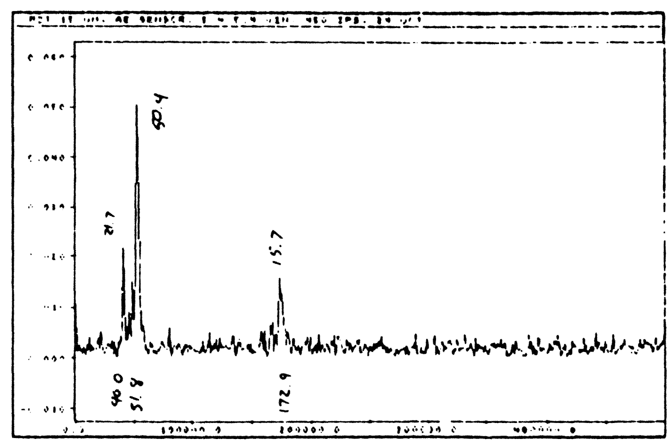

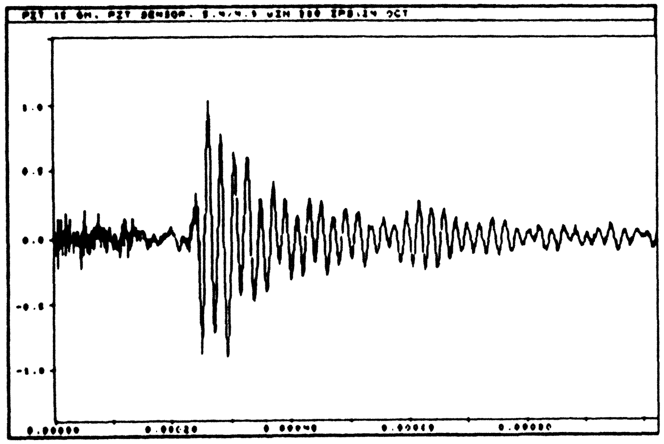

At
Bump
Ht

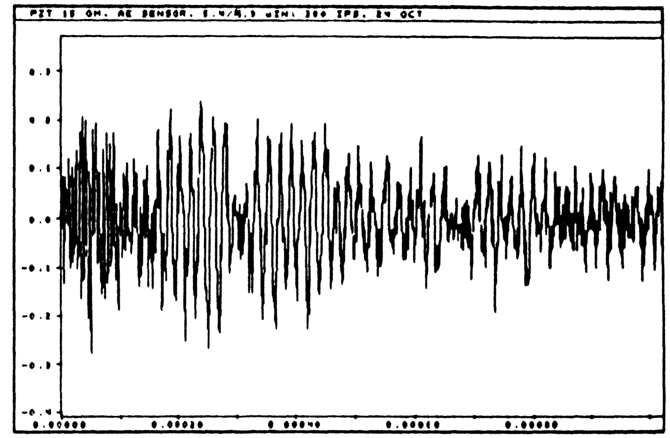

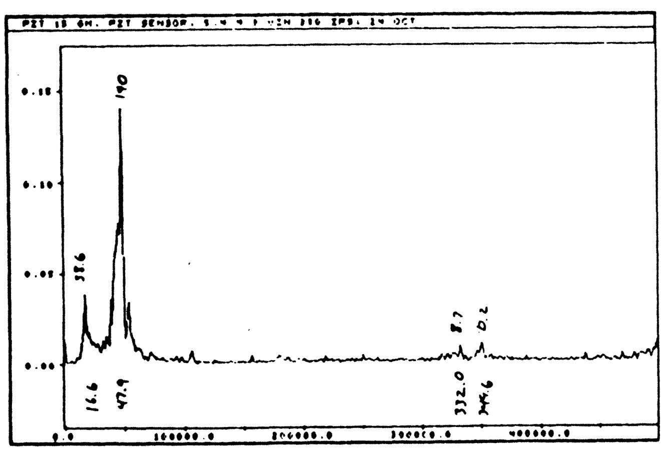

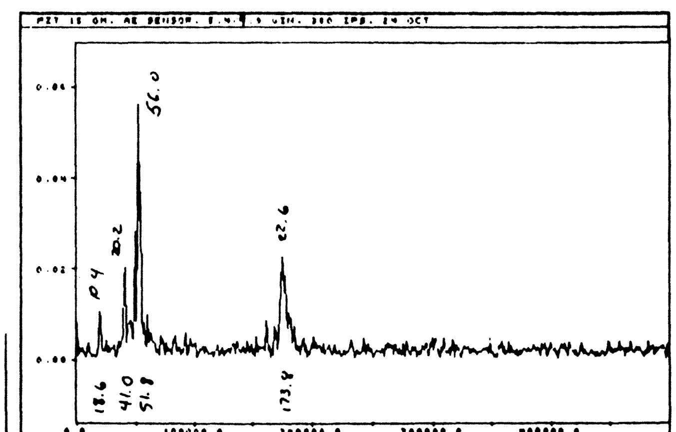

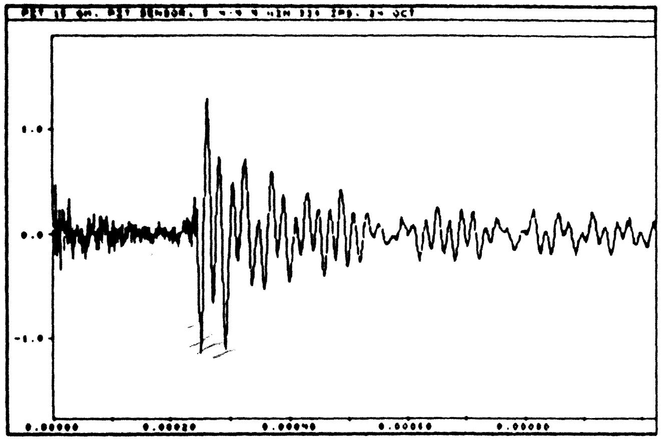

Below Bump Ht

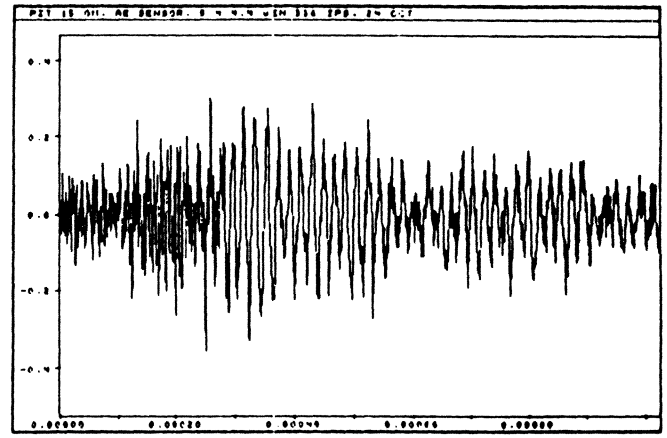

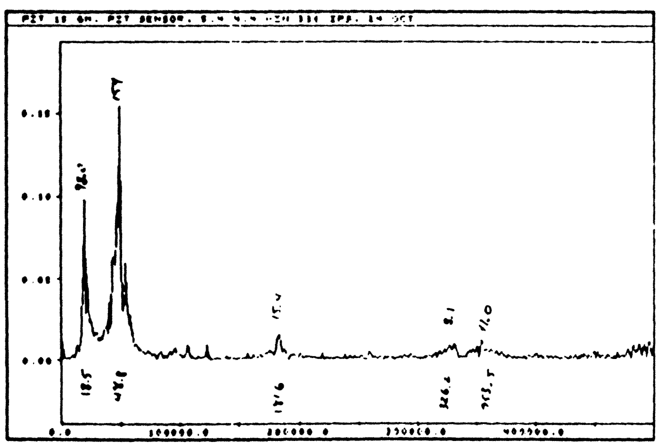

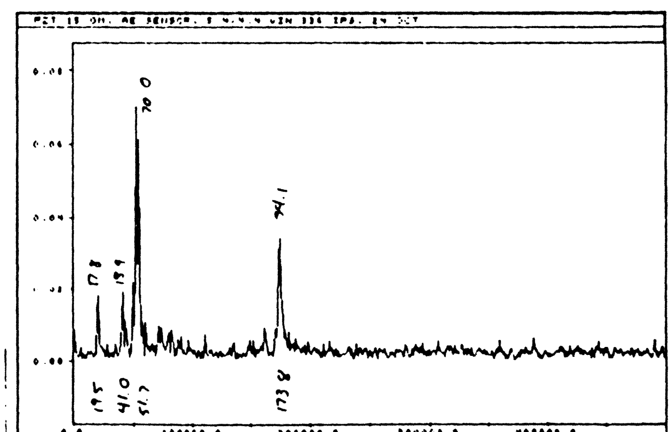

GLIDE ISSUES

Channel

Bandwidth

Response

Data courtesy Bernard Flusche Jr., Akashic

Maxtor

Voltage Gain vs Frequency

(Sine wave)

AKASHIC

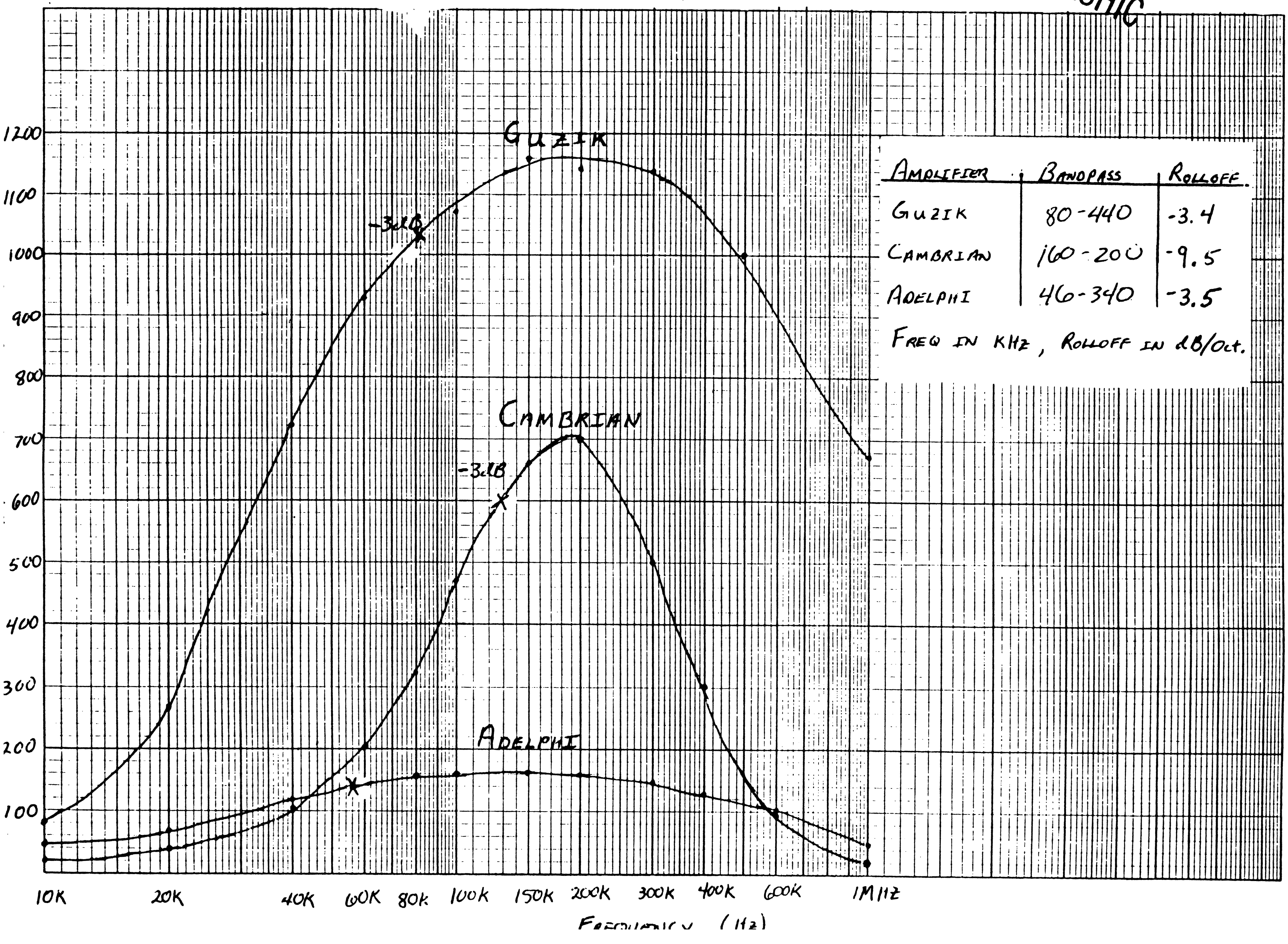

SIGNAL VS LINEAR VELOCITY

AKASHIC

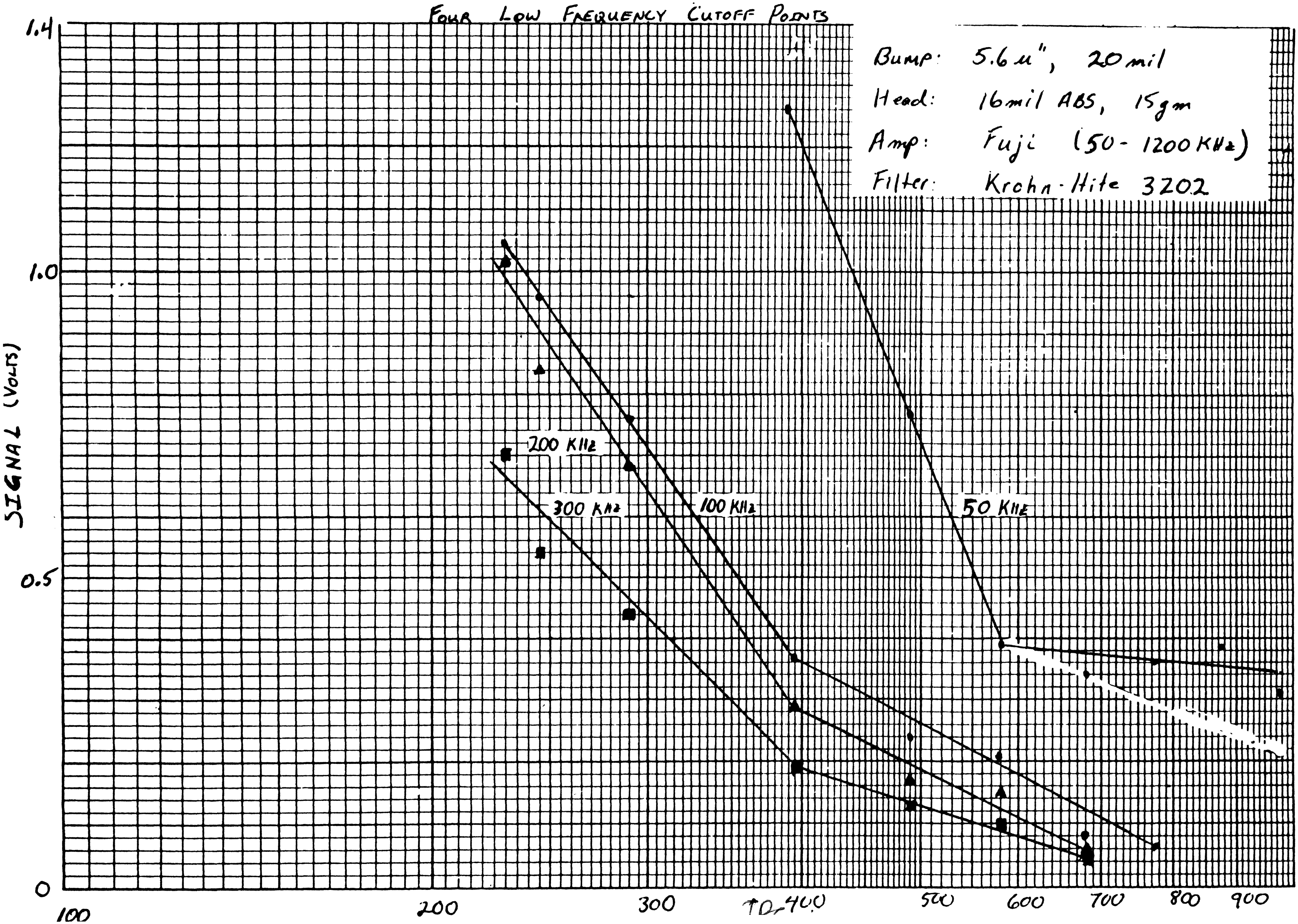

AKASHIC

Signal Sources

TR-22 by T.G. Jeong and D.B. Bogy

- Air Bearing Frequencies

  10 - 30 KHz

- Sensor Resonance Frequencies

  PZT - 180 KHz
  AE - 500 KHz

- 3370 Slider Resonance Frequencies
  (Finite Element Analysis)

Mode 1	313 KHz
Mode 2	414 KHz
Mode 3	613 KHz
Mode 4	682 KHz

GLIDE ISSUES

Detection

- Threshold
- Other

Repeatability

Data courtesy Bernard Flusche Jr., Akashic

Maxtor

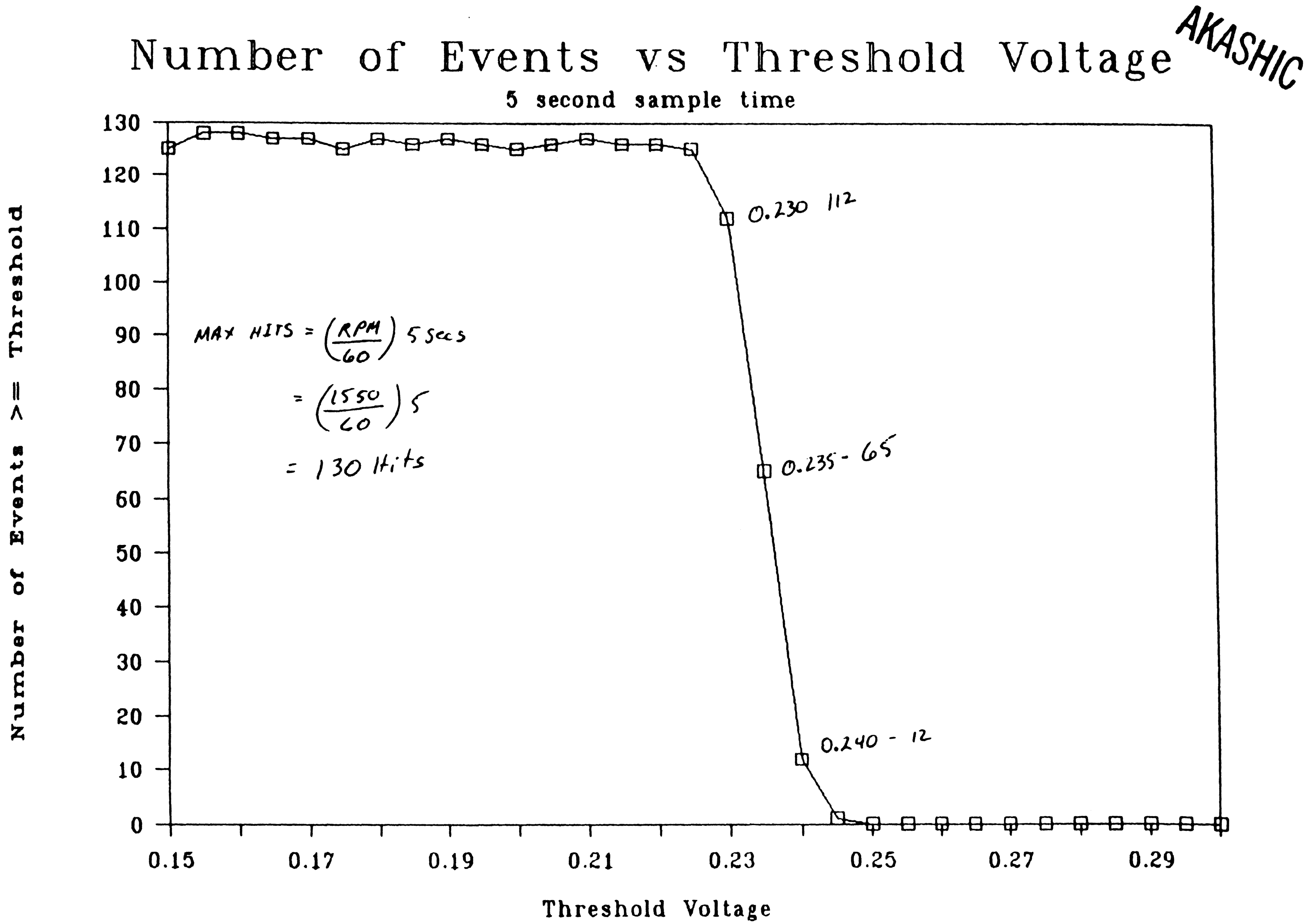
AKASHIC
Number of Events vs Threshold Voltage
5 second sample time
Number of Events >= Threshold
Threshold Voltage
0
10
20
30
40
50
60
70
80
90
100
110
120
130
0.15
0.17
0.19
0.21
0.23
0.25
0.27
0.29
0.230 112
0.235 - 65
0.240 - 12
MAX HITS = (RPM/60) 5 secs
= (1550/60) 5
= 130 Hits

AKASHIC

Probability Distributions

Rail centered on bump at 1840 mils

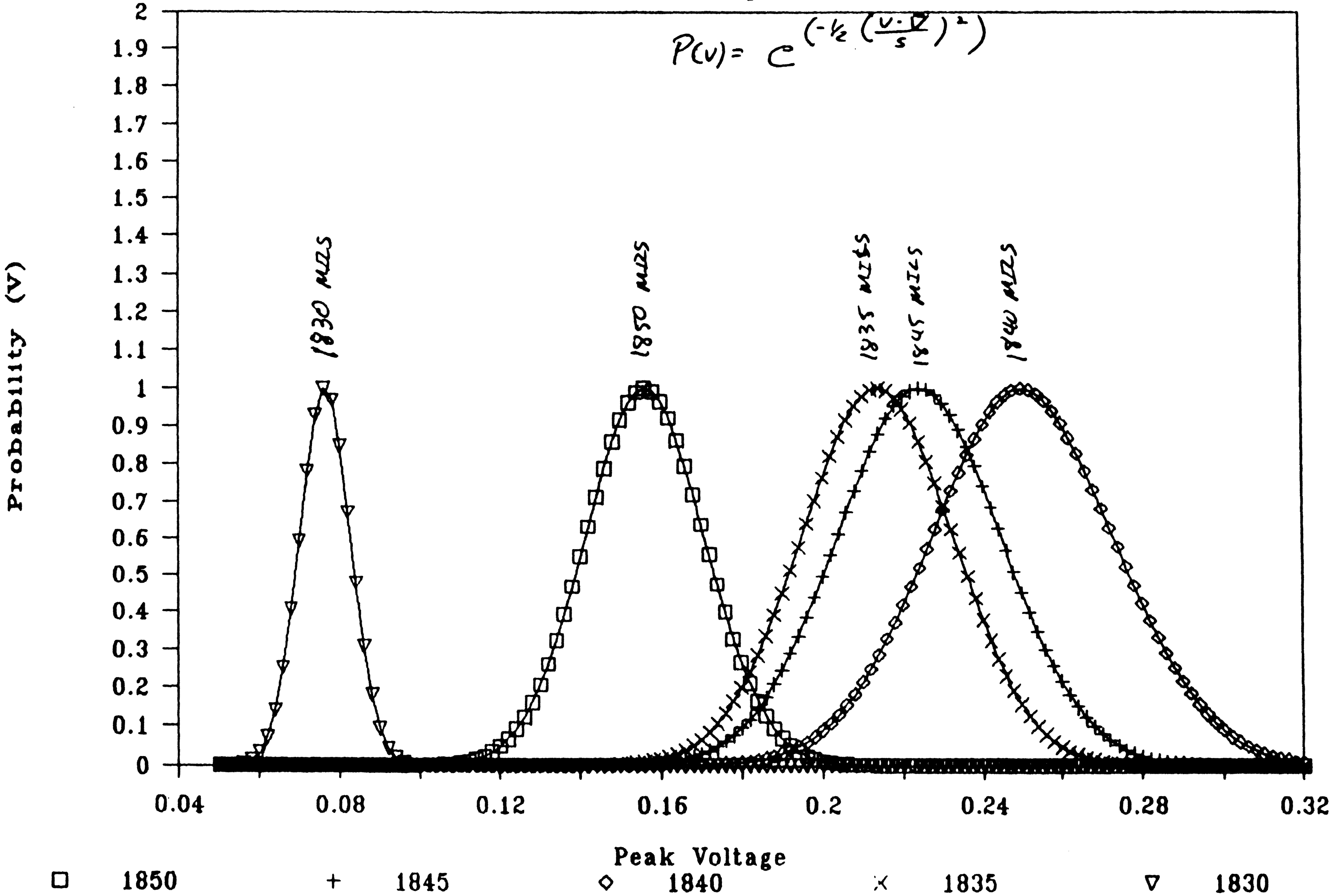

Glide Issues

Calibration & Correlation

Flying Height:	PPL low software, Adelphi, Spot size, location, cal factors, Slider matl
Head:	ABS, Load, Gimbal
Bump Height:	Wyko, Dektak, ?
Transducer:	Acoustic, Piezo
Channel:	BW, Response
Detection:	Threshold, Other
Repeatability:	30-100% ampl. var.

Maxtor

OVERVIEW

- Why Lower?
- How Close Can We Get?
- Glide Issues
- Contact Recording

Maxtor

CONTACT RECORDING OBJECTIVES

- Transducer-Magnetic Film Spacing 0 - 2uin.
- Reliable Operation (>5 Years)
- Negligible or Manageable Wear
- Meet Stiction Requirements
- Low Cost

Maxtor

courtesy of Victor Dunn, Maxtor

CONTACT RECORDING MODEL

A

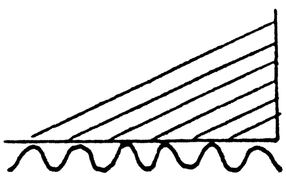

B

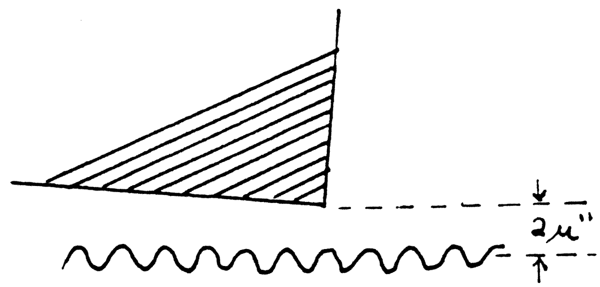

- RUBBING CONTACT
- NO NEED TO CONTROL F.H.
- ELIMINATE HEAD CRASH
- TRIBOELECTRIC EFFECT

- FLY HEIGHT 1μ" - 2μ"
- LESS WEAR
- LESS HEAT GENERATED (DATA INTEGRITY)

CRITICAL ISSUES

- ø WEAR

  PHYSICAL CONTACT WILL ACCELERATE WEAR OF OVERCOAT, ABS, AND MAGNETIC LAYER

- ø RELIABILITY

  TEMPERATURE INCREASES MAY AFFECT DATA

  (Tc ~ 1000oC)

  MAGNETOSTRICTIVE EFFECT

- ø STICTION

  SMOOTHER HEADS AND DISKS SURFACES INCREASE LONG TERM STATIC FRICTION

TRIBOLOGY OF HEAD/MEDIA INTERFACE

GOAL: MINIMIZE FRICTION, WEAR, AND HEAT

FRICTION

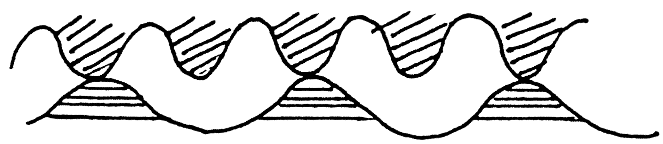

$$\text{AREA OF CONTACT (A)} = \frac{\text{load (L)}}{\text{yield pressure } (P_m)}$$

FRICTION FORCE (F) = (A) X SHEAR TO MOVE ASPERITIES (T)

$$\text{FRICTIONAL COEFFICIENT } (\mu) = \frac{F}{L} = \frac{T}{P_m}$$

TO REDUCE FRICTION:

- o REDUCE HEAD LOAD (L)
- o USE HARD MATERIAL WITH HIGH (P_m)
- o USE LUBRICANT TO REDUCE (T)

LONG-TERM STATIC FRICTION

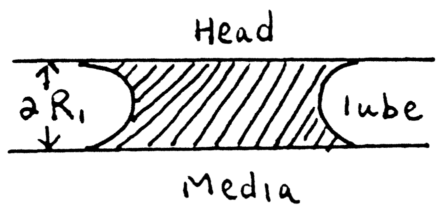

$$\Delta P = \gamma(1/R1 + 1/R2) = \gamma/R1$$

$$Fs = \Delta P \times A = \frac{\gamma A}{R1}$$

TO REDUCE LONG TERM STATIC FRICTION (FS)

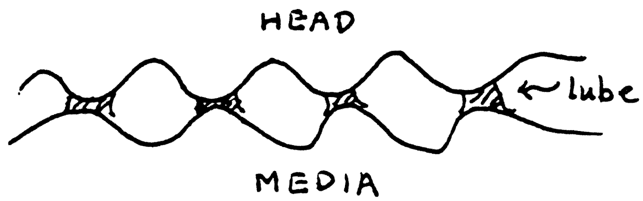

- o DECREASE HEAD/MEDIA CONTACT AREA (A) (TEXTURE SURFACE)
- o REDUCE AMOUNT OF LIQUID LUBRICANT
- o USE SEMI-SOLID LUBRICANT
- o INCREASE CONTACT ANGLE OF LUBRICANT

HEAT

FRICTIONAL WORKDONE = F X DISTANCE

HEAT EQUIVALENT (Q) = $\frac{\mu \; L \; G \; U}{J}$ CALORIES/SEC.

TO REDUCE HEAT (Q):

- REDUCE FRICTIONAL COEFFICIENT (μ)
- REDUCE HEAD LOAD (L)
- REDUCE SURFACE VELOCITY (U)

WEAR

ADHESIVE WEAR (SLOW) HARD - HARD

ABRASIVE WEAR (FAST) HARD - SOFT

activation energy of matl

$$V = \frac{k\ L\ X}{3\ H}$$

REDUCE VOLUME (V) OF WEAR BY:

- o REDUCE HEAD LOAD (L)
- o INCREASE HARDNESS OF OVERCOAT AND ABS SURFACE (H)
- o USE LUBRICANT TO REDUCE WEAR COEFFICIENT (k)
- o REDUCE SURFACE VELOCITY

CONCLUSIONS ON HEAD/MEDIA INTERFACE REQUIREMENTS

- SURFACES OF MEDIA AND ABS MUST BE VERY HARD TO REDUCE FRICTION, WEAR AND HEAT

- LOW MASS HGA SYSTEM TO REDUCE WEAR AND FRICTION; BUT NEED TO FOLLOW SURFACE CONTOURS

- MINIMAL AMOUNT OF LUBRICANT TO BALANCE WEAR AND STICTION

- FLAT AND "SMOOTH" MEDIA SURFACE.

COEFFICIENTS OF FRICTION

μ	SURFACE A	SURFACE B	LUBRICANT
0.1	DIAMOND	DIAMOND	NO
0.05-0.1	DIAMOND	DIAMOND	YES
0.2	SAPPHIRE	SAPPHIRE	NO
0.04	TEFLON	TEFLON	NO
0.9-1.0	GLASS	GLASS	NO
0.1-0.6	GLASS	GLASS	YES
1.0	IRON	IRON	NO
0.7	NICKEL	NICKEL	NO

HARDNESS OF MATERIALS

MATERIAL	MOH HARDNESS
DIAMOND	1 0
BORON CARBIDE (B4C)	>9
SILICON CARBIDE	>9
CORUNDUM (AL203)	9
QUARTZ	7
ZIRCONIA (Zr02)	6
APATITE CA3(P04)2	5
CALCITE CAC03	3
TALC SILICATE (HYDRATED MAGNESIUM)	1

LUBRICANTS

PERFLUOROETHERS

FOMBLIN Z $CF_3-(O-CF_2-CF_2)_m-(O-CF_2)_n-O-CF_3$

FOMBLIN YR $CF_3-(O-CF(CF_3)-CF_2)_m-(O-CF_2)_n-O-CF_3$

REACTIVE LUBE

$$X-CF_2-O-(CF_2-O)_n-(CF_2-CF_2-O)_m-CF_2-X$$

X = ACID, ALCOHOL, EPOXIDE, ESTER

TEFLON WAX $CF_3-(CF_2-CF_2)_n-CF_3$

SILICONE $CH_3-Si(CH_3)_2-O-(Si(CH_3)_2-O)_n-Si(CH_3)_2-CH_3$

Friction vs. RPM

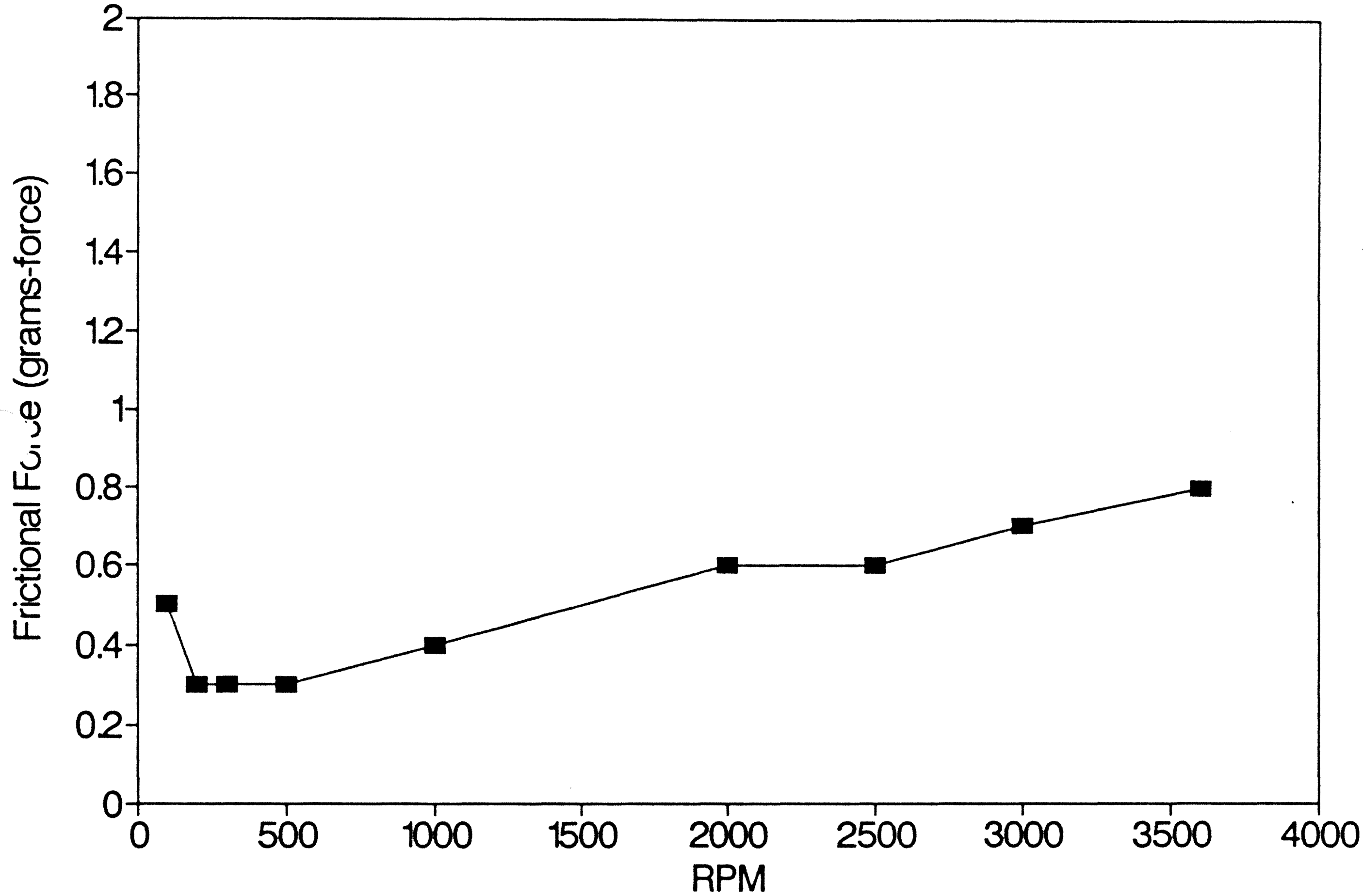

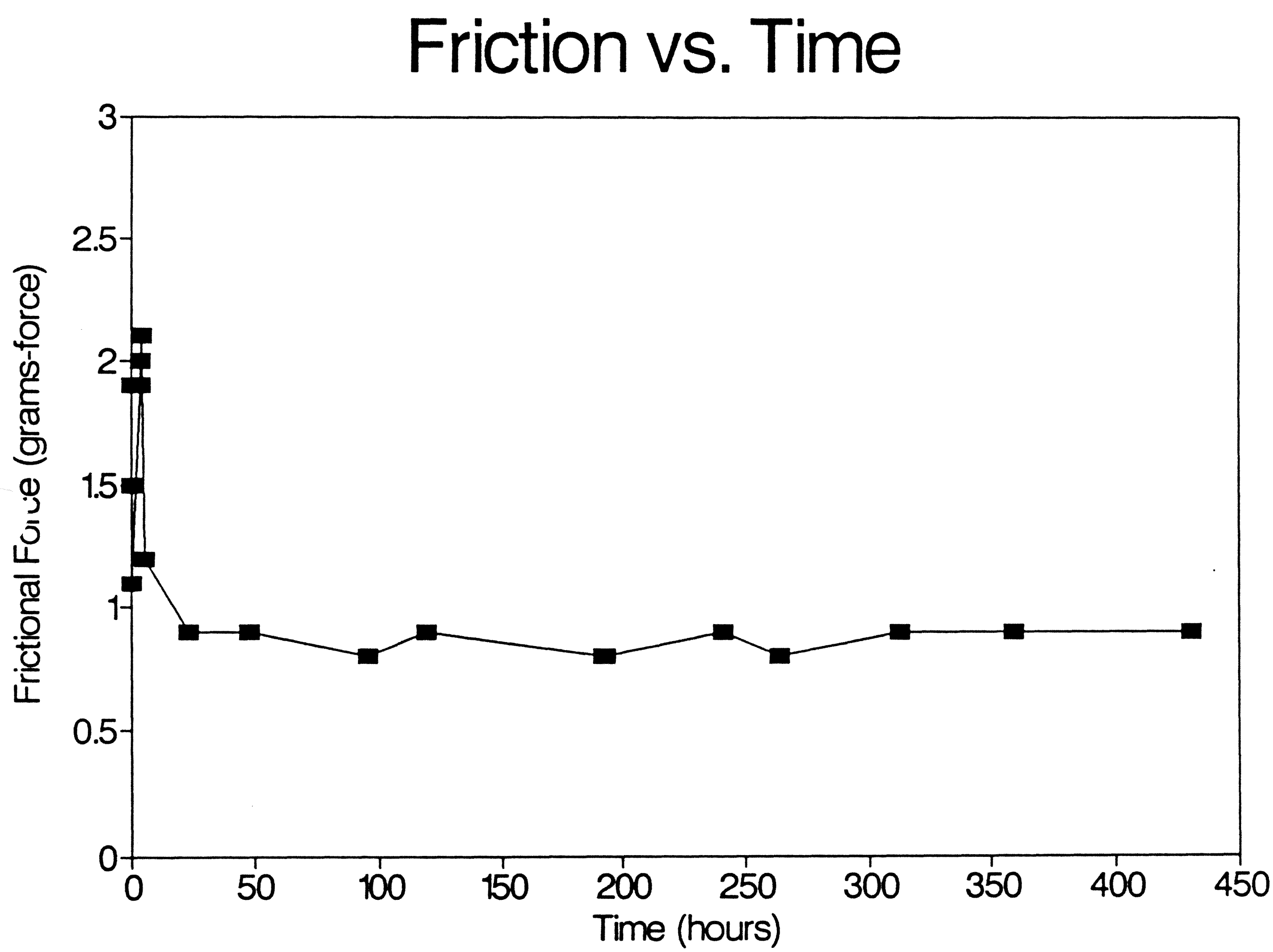

Friction vs. Time
Frictional Force (grams-force)
3
2.5
2
1.5
1
0.5
0
0
50
100
150
200
250
300
350
400
450
Time (hours)

Flying Height
vs. Time

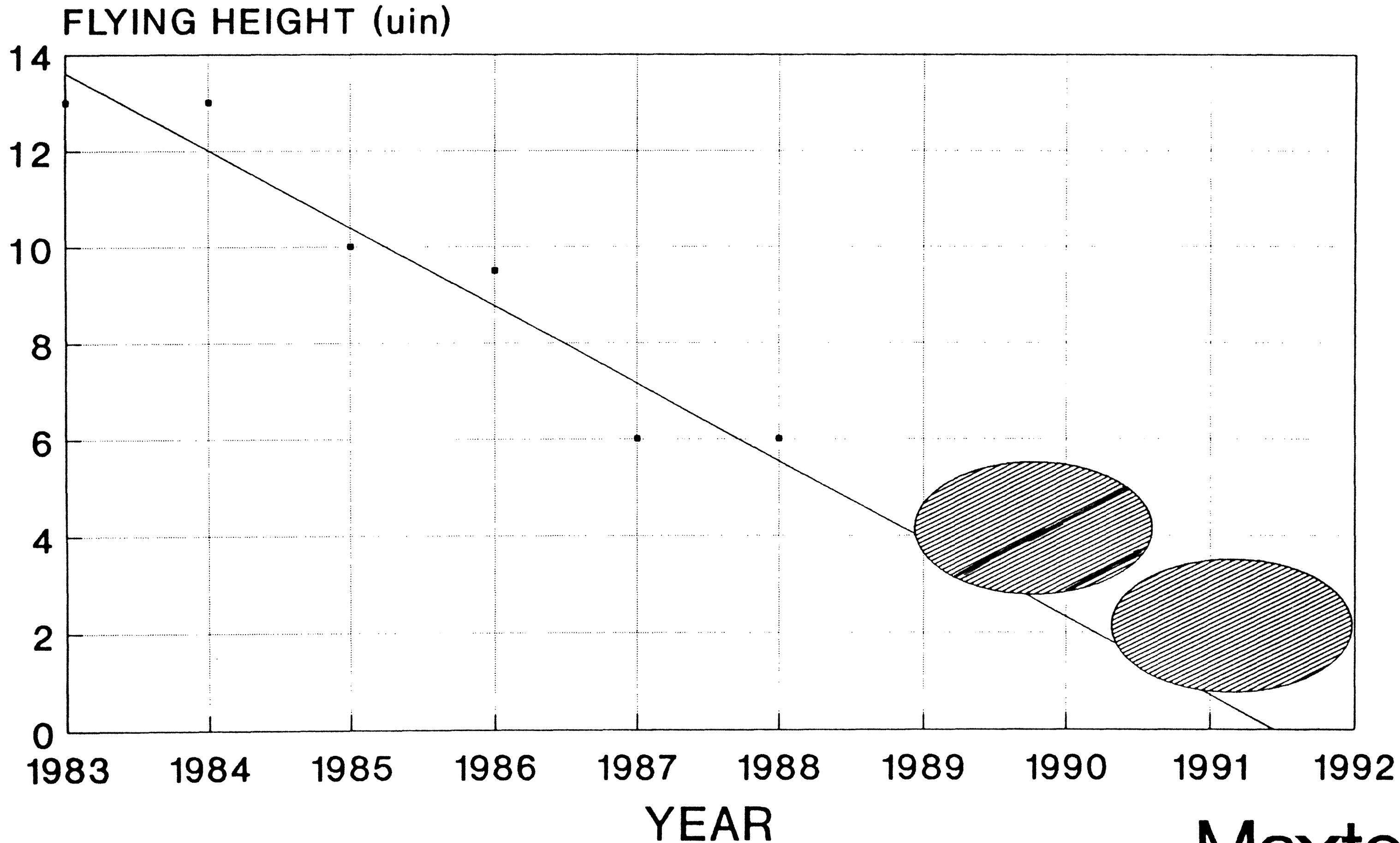

Maxtor

THANKS

Dr. Victor Dunn, Maxtor

Dr. Don Huber, Maxtor

Mr. Bernard Flusche Jr., Akashic

Maxtor

THE HEAD DISC INTERFACE

INTRODUCTION

GORDON HUGHES

SEAGATE TECHNOLOGY

- HEAD-DISC TRENDS, 1980-1989.

  1980: HORIZONTAL RECORDING ON OXIDE MEDIA,

  0.5 μM FLY HEIGHT, 3340-STYLE HGAs

  NOW: HORIZONTAL THIN FILM MEDIA

  0.2 μM FLY HEIGHT, THREE "3380-ISH" SLIDERS

...MAYBE VERTICAL RECORDING,

WHEN FLY HEIGHTS REACH 3 MICROINCHES?

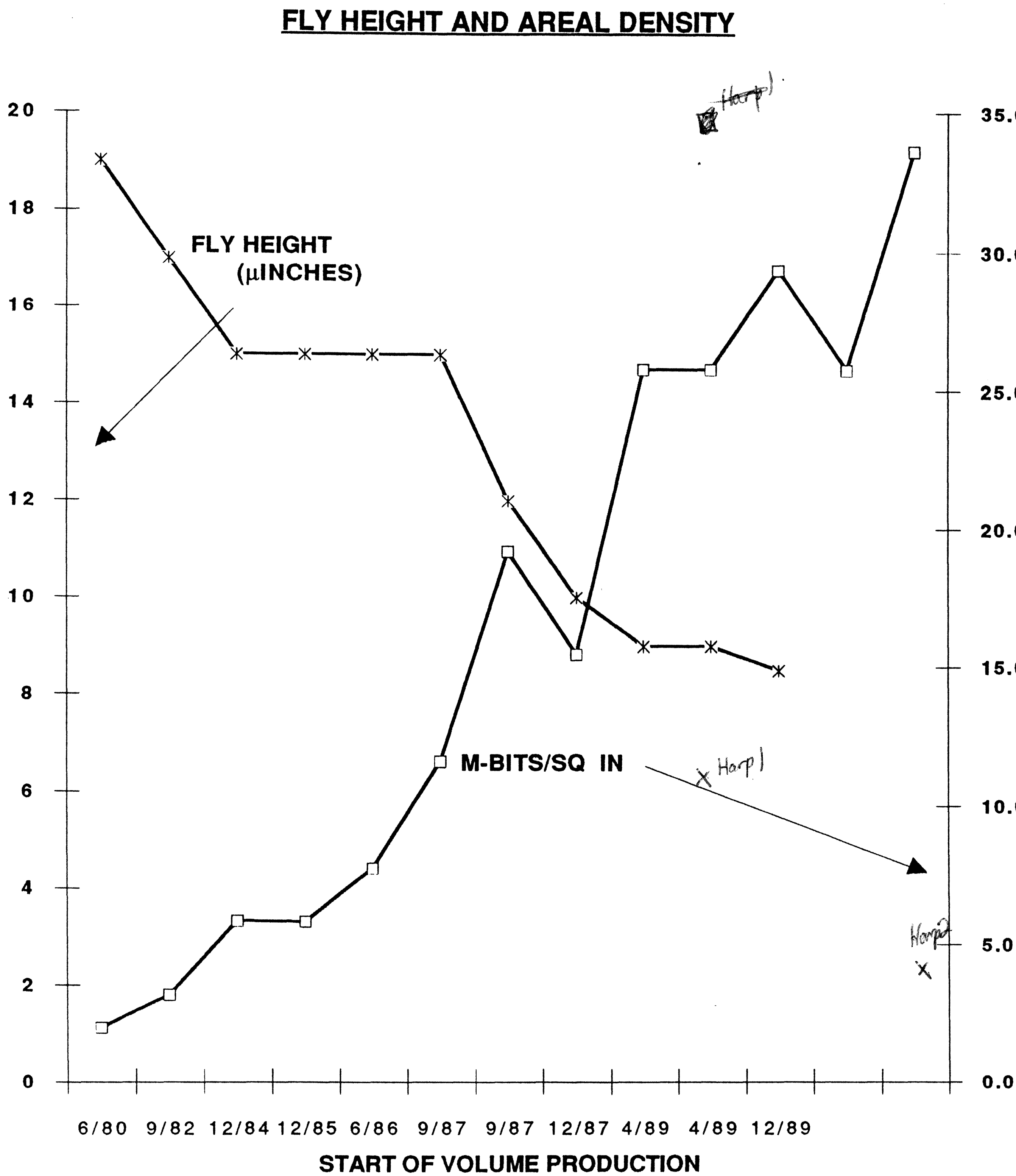

FLY HEIGHT AND AREAL DENSITY
FLY HEIGHT (μINCHES)
M-BITS/SQ IN
20
18
16
14
12
10
8
6
4
2
0
35.0
30.0
25.0
20.0
15.0
10.0
5.0
0.0
6/80 9/82 12/84 12/85 6/86 9/87 9/87 12/87 4/89 4/89 12/89
START OF VOLUME PRODUCTION

THE HEAD-DISC SYSTEM: COMPONENTS, TERMINOLOGY

THE HEAD:

= SLIDER + FLEXURE + READ/WRITE CORE

BASIC SLIDERS:

4 MM BY 3 MM BY 5/8 MM GEOMETRY:

- TI CARBIDE ALUMINA, THIN FILM CORE
- Ceramic → MnZn MONOLITHIC FERRITE SLIDER & CORE
- CaTi COMPOSITE SLIDER, MnZn CORE
- 70% AND 50% DOWNSIZED VERSIONS,
  FOR LOWER FLY, FASTER ACCESS

HEAD-GIMBAL ASSEMBLY (HGA)

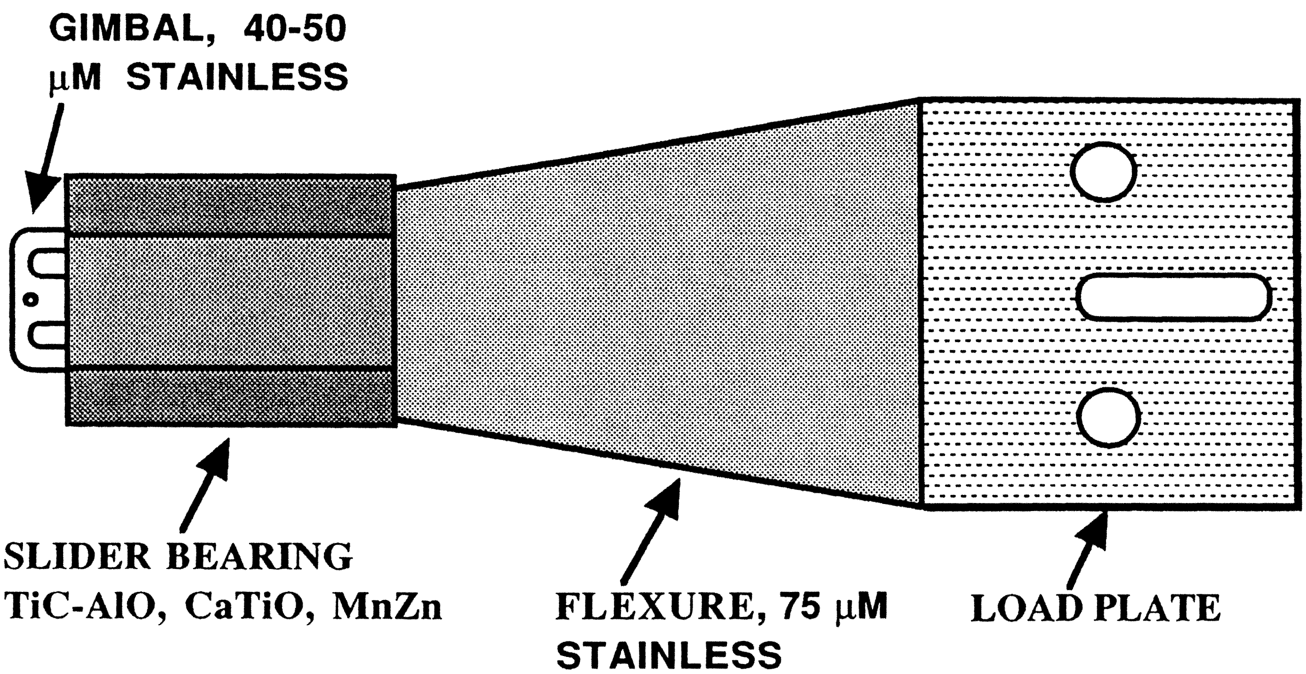

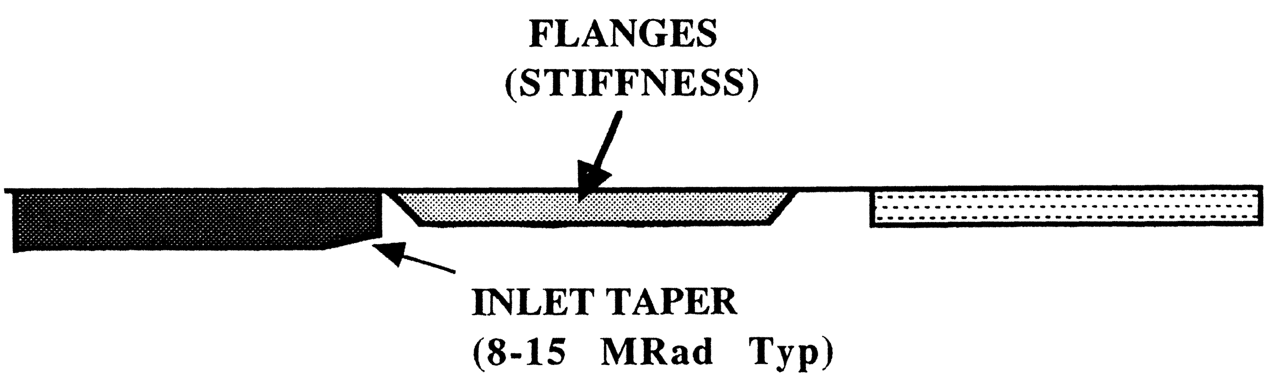

THE INTERFACE:

AIR BEARINGS. TERMINOLOGY:

FLY HEIGHT, PITCH, ROLL, YAW, G'S

AIR BEARING FLIGHT DESIGN, TOLERANCING,

YAW STABILITY UNDER TRACK ACCESS.

SLIDING CONTACT LUBRICATION

DURING START-STOP & ASPERITY CONTACT

DESIGN DISC/HEAD TRIBOLOGY,

TO MINIMIZE WEAR.

TESTS: DIGITAL SPECTRORADIOMETER,

ACOUSTIC EMISSION, HEAD/DISC WEAR...

THE HEAD-DISC INTERFACE

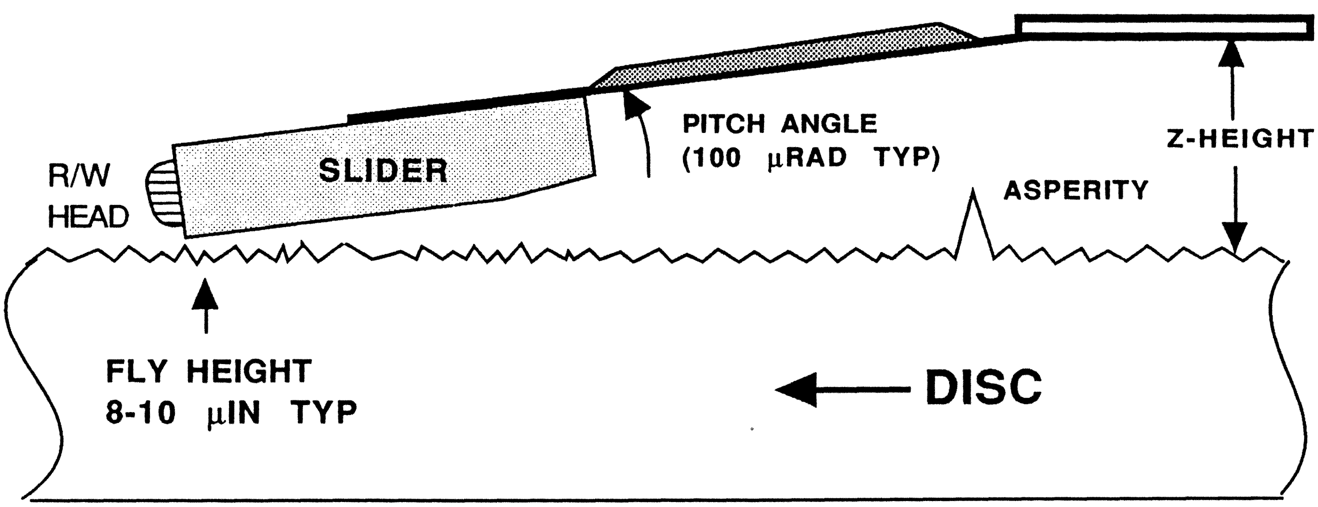

FLIGHT ATTITUDE TERMINOLOGY

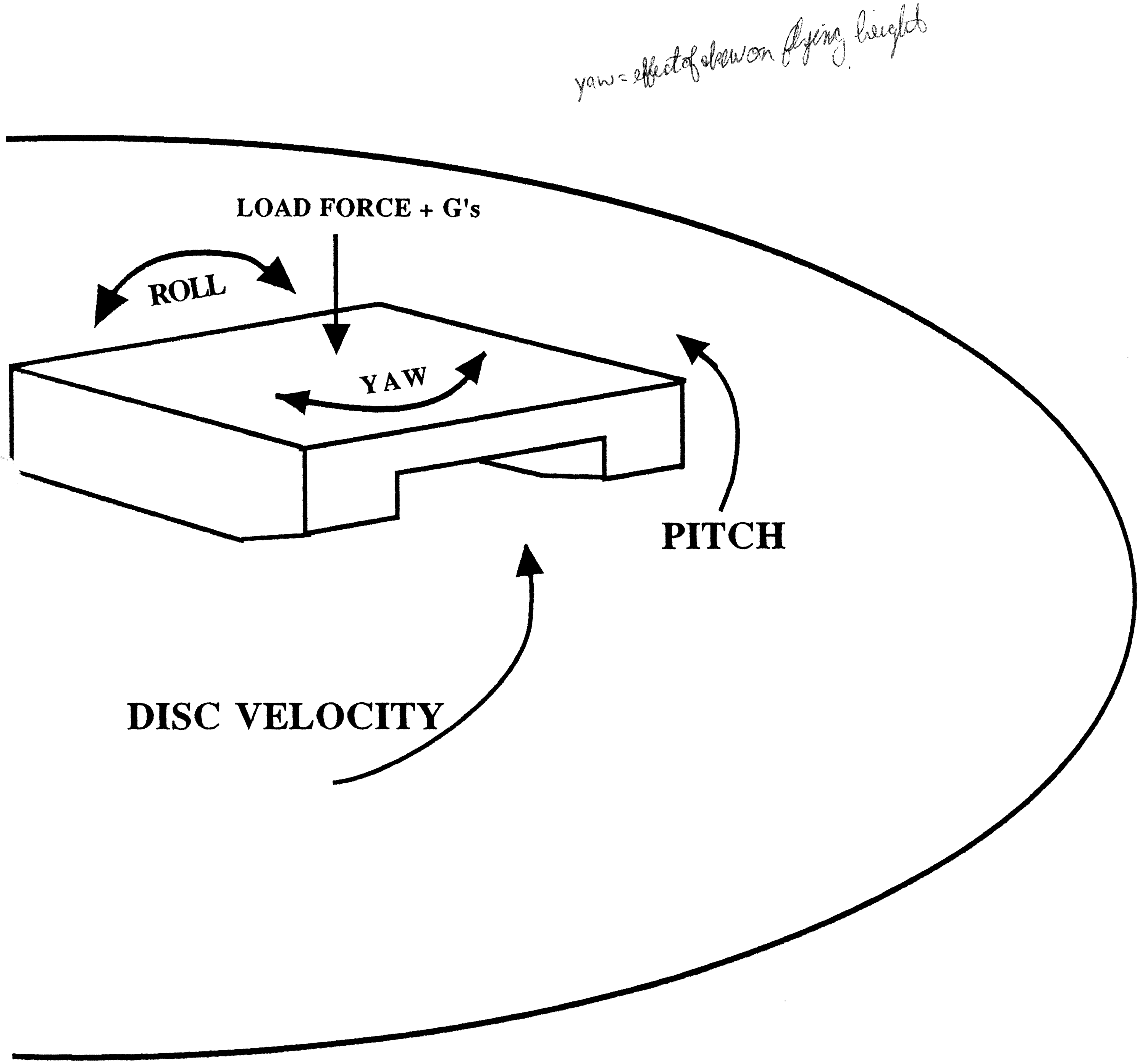

TYPICAL VALUES: FLY HEIGHT 9-12 μIN, PITCH 100 μRADIANS, ROLL 20 μRAD, YAW -10° TO +20°

DISC:

= SUBSTRATE + UNDERLAYER + MAGNETIC MEDIA

+ TRIBOLAYER + LUBE + CONTAMINANT

SIZES: 130 MM x 25 MM x 0.075 INCH ALUMINUM

95 MM x 20 MM x 0.050 INCH ALUMINUM

65 MM x 20 MM x 0.035 INCH Al OR GLASS.

UNDERLAYER: Cr ON Ni-PHOSPHORUS TYPICAL

MAGNETIC MEDIA: SPUTTERED Co ALLOYS:

CoCrTa, CoPt, CoNi, 50-100 NM THICK

...SOME PLATED DISCS: CoNi, CoP

TRIBOLAYER: AMORPHOUS CARBON, 35 NM THICK

...SOME ZIRCONIA

LUBE: PERFLUOROPOLYETHERS,

WITH REACTIVE END GROUPS

(FIRST LAYER BONDS TO DISC)

CONTAMINANTS:

AEROSOLS, DRIVE MATERIALS OUTGASSING

• STANDARD SYSTEM DESIGN: "WINCHESTER"

TWO-RAIL RECTANGULAR SLIDER,

WITH TAPER AIR INLETS

(MONOLITHIC IS THREE RAIL DESIGN).

TAKEOFF AND LAND IN DISC CONTACT

(CSS = CONTACT START-STOP).

CURRENT COMMERCIAL SPECS: 13-20 K CSS CYCLES

Variant: RAMP LOAD ON SPINNING DISC

OBJECTIVE: 100 K CSS CYCLES, SHOCK RESISTANCE

(FOR LAPTOP PC DISC DRIVEs)

• SYSTEM DESIGN ISSUES:

FOR HIGH AREAL DENSITY:

LOW FLY, SMALL SLIDER, THIN MEDIA

FOR START/STOP WEAR DURABILITY:

GOOD TRIBOLOGY DESIGN OF DISC ROUGHNESS,

LUBE CHEMISTRY AND THICKNESS,

SLIDER MATERIAL

• TRIBOLOGY

THE MOST DIFFICULT ISSUE,

AND THE MOST EMPIRICAL.

TRADITIONALLY "BLAMED" ON THE DISC.

DISC SURFACE ROUGHNESS,

CARBON OVERCOAT,

ORGANIC LUBE,

CONTAMINATION CONTROL

BUT ACTUALLY ENTIRE HEAD-DISC SYSTEM.

EXAMPLE:

MARCHON'S MRM '89 TRIBOCHEMICAL WEAR:

...O_2 ON CARBON SURFACE OXIDIZES INTO Co_X,

USING SLIDER ASPERITY IMPACT ENERGY,

AND CATALYTIC PROPERTIES OF SLIDER

MATERIAL.

TRIBOLOGY, CONTINUED

GOOD FACTORS: FEWEST REVOLUTIONS TO TAKE OFF, STABLE FLIGHT RECOVERY FROM ASPERITY CONTACT, COMPATIBLE HEAD AND DISC MATERIAL SCIENCE, LOWER LOAD FORCE FOR SLOWER DISC VELOCITIES, SLIDER SIZE, MASS, LOAD HEIGHT OFF DISC.

TESTING:

- TO CSS SPEC,
- WITH ULTRASONIC DETECTORS
  - ACOUSTIC EMISSION,
  - SLIDER BODY OSCILLATIONS
- THERMAL CYCLING (-40° TO +70°C),
- IR/FTIR SPECTROSCOPY, SEM EDAX,
- GC/MASS SPECTROMETER...

HEAD-DISC WEAR PHYSICS (SIMPLIFIED)

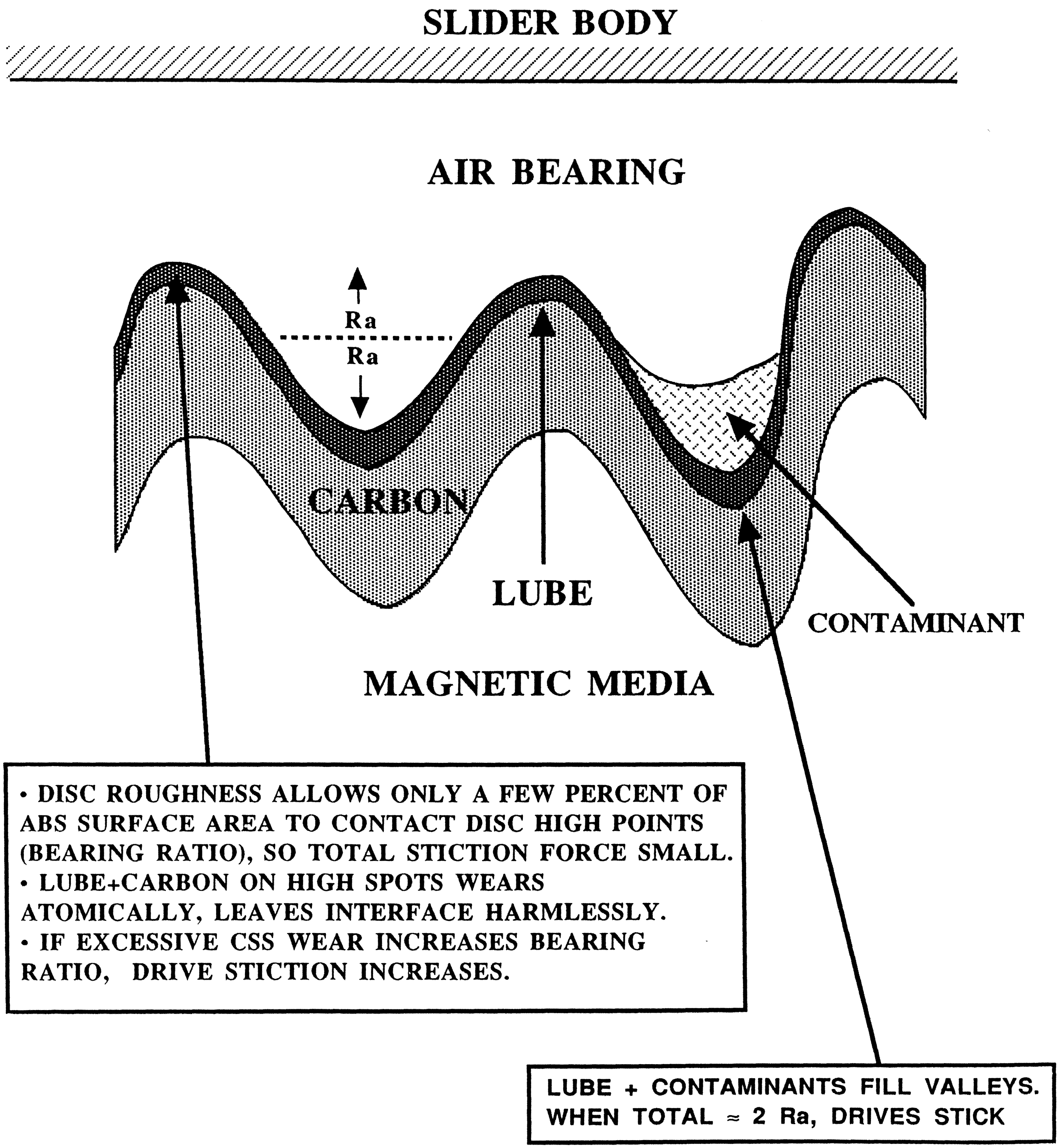

IIST Short Course
"The Head Disc Interface"
December 12-14, 1989

Analysis and Instrumentation Tools

Peter R. Goglia, Ph.D.
Seagate Technology
Minneapolis, Minnesota

Analysis and Measurement Techniques — Peter R. Goglia

1 Introduction

  1.1 Sliding

  1.2 Mixed

  1.3 Flying

2 Flying Height Modeling

  2.1 Reynolds Equation

  2.2 Impact Modeling

3 Head Disc Separation Budget; Full Flying Regime

  3.1 Head Roughness

  3.2 Disc Geometry Effects

    3.2.1 Circumferential

      3.2.1.1 Low Frequency: Synchronous Acceleration

      3.2.1.2 High Frequency: High-Pass Run-Out and Roughness

    3.2.2 Radial

      3.2.2.1 Curvature

      3.2.2.2 Slope

  3.3 Disc Dynamic Effects: Asynchronous Acceleration

  3.4 Track Seek Acceleration Effects

  3.5 Temperature and Altitude Effects

4 Measurement

  4.1 Static and Dynamic Fly Height

    4.1.1 White Light

    4.1.2 Fringe Sensing Laser Interferometric

    4.1.3 Laser Doppler Vibrometer

    4.1.4 Capacitance Probe Heads

      4.1.4.1 Embedded Probe Heads

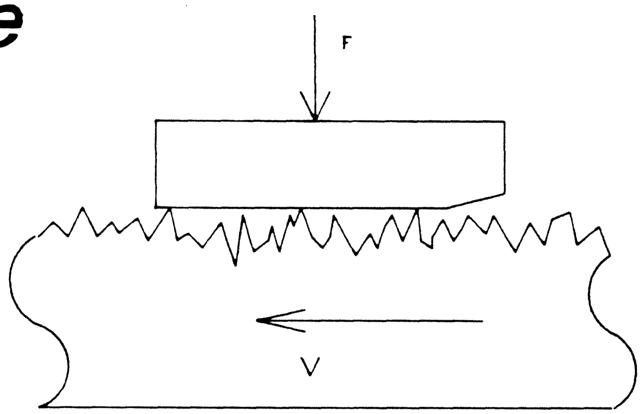

Full Sliding Regime

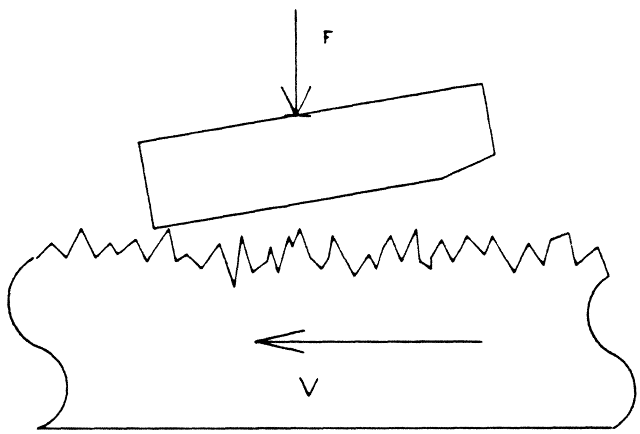

Mixed Lubrication Regime

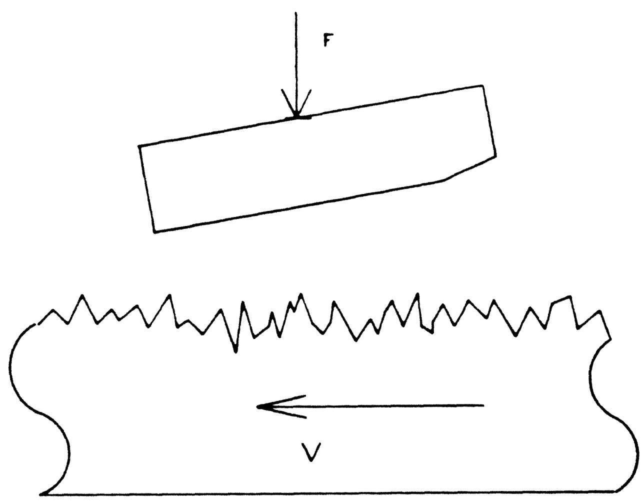

Full Flying Regime

Seagate

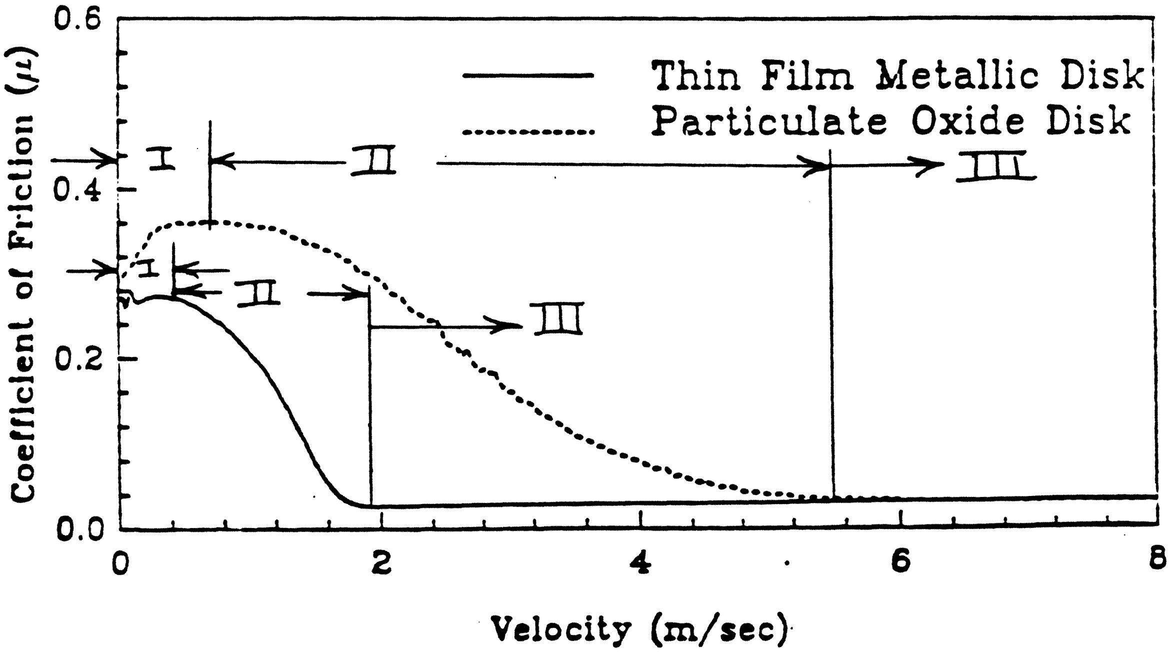

Figure 4. Coefficient of friction vs. disk velocity

I. Full Sliding
II. Mixed Lubrication
III. Full Flying

Trauner, D., Y. Li, and F.E. Talke, "Frictional Behavior of Magnetic Recording Disks", CMRR Preprint

Seagate

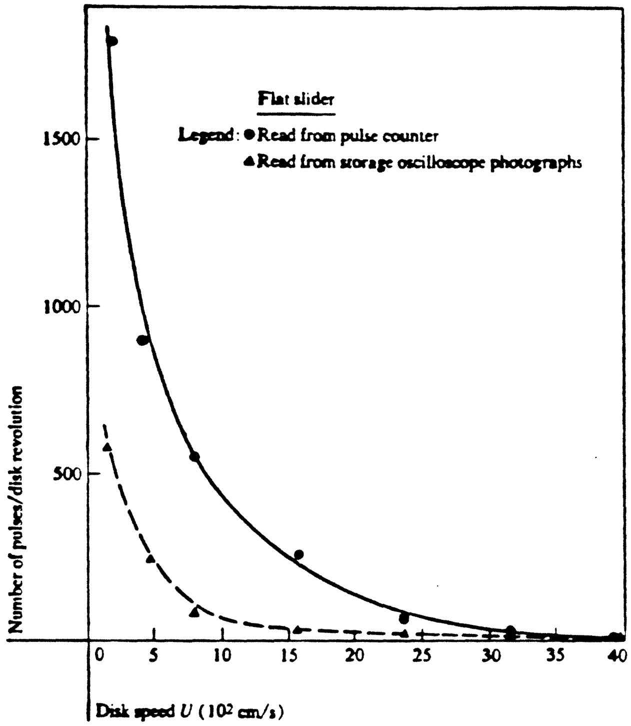

Figure 8 Contact pulses for a nearly flat tripad slider.

Tseng, R.E. and F.E. Talke, "Transition from Boundry Lubrication to Hydrodynamic Lubrication of Sliding Bearings", IBM J. Res. Dev., Nov. 1974

Seagate

Air Bearing Modeling

Codes

-Reynold's Equation with first or second order slip

-Boltzman's Equation

-Finite Difference Solution (Column method, ADI, Factored Implicit)

-Static and Dynamic Solutions (Three degrees-of-freedom)

-Commercial Codes Available

Geometry Input

-Automatic Node Point Generation

-Catamaran, Negative Pressure and Custom Geometries

-Head Contouring (Taper, Crown, Cross Curvature and Edge Blend)

Excitations

-Disc Waviness

-Disc Step

-Disk Vibration

-Periodic Forces and Moments on Slider

-Periodic Displacement on Slider

Seagate

Reynolds Equation with First Order Slip

$$\frac{\partial}{\partial X}\left(PH^3\frac{\partial P}{\partial X}+6K_nH^2\frac{\partial P}{\partial X}\right)+\frac{\partial}{\partial Y}\left(PH^3\frac{\partial P}{\partial Y}+6K_nH^2\frac{\partial P}{\partial Y}\right)$$

$$=\Lambda_x\frac{\partial PH}{\partial X}+\Lambda_y\frac{\partial PH}{\partial Y}+\sigma\frac{\partial PH}{\partial t}$$

where:

$$X=\frac{x}{L};\quad Y=\frac{y}{L};\quad P=\frac{p}{P_a};\quad H=\frac{h}{h_{\min}}$$

and

$K_n=\dfrac{\lambda_a}{h_{\min}}$ = Knudsen Number

$\Lambda_y=\dfrac{6\mu LV_y}{P_a h_{\min}^2}$ = Bearing Number in the Y Direction

$\Lambda_x=\dfrac{6\mu LV_x}{P_a h_{\min}^2}$ = Bearing Number in the Y Direction

$\sigma=\dfrac{12\mu L^2}{P_a h_{\min}^2}$ = Squeeze Number

$$\mu=\frac{\mu_{bulk}}{1+6\lambda/h}$$

Seagate

Governing Equations for Rigid Body Slider Motion

$$M\ddot{z} + K_z(z - z_0) + K_z\bar{y}(\theta - \theta_0) + K_z\bar{x}(\psi - \psi_0)$$

$$= F_z + \int\int(P-1)dx\,dy$$

$$I_\theta\ddot{\theta} + K_z\bar{y}(z - z_0) + (K_\theta + K_z\bar{y}^2)(\theta - \theta_0) + K_z\bar{y}\bar{x}(\psi - \psi_0)$$

$$= M_\theta + \int\int(P-1)(y - y_g)dx\,dy$$

$$I_\psi\ddot{\psi} + K_z\bar{x}(z - z_0) + (K_\psi + K_z\bar{x}^2)(\psi - \psi_0) + K_z\bar{y}\bar{x}(\theta - \theta_0)$$

$$= M_\psi + \int\int(P-1)(x - x_g)dx\,dy$$

where

M = Slider Mass
I_θ and I_ψ = Slider Moments of Inertia
K_z, K_θ and K_ψ = Flexure Stiffness Coeff.
θ = Pitch Angle
ψ = Roll Angle
z = Vertical Displacement of the Pivot Point
x_g, y_g = Coordinates of the Slider Center of Mass
$\bar{x}$ and $\bar{y}$ = Distances between the slider Center of Mass and Pivot Location

Seagate

PHYSICAL CONDITIONS

SKEW	:	0.0000
VELOCITY	:	1000.0000
RADIUS	:	0.0000
LOAD	:	6.0000
P_OFFSET	:	0.0000
CAV_DPTH	:	0.0004
H_LENGTH	:	0.1600
H_WIDTH	:	0.1140
TAPER_H	:	0.0002
TAPER_L	:	0.0140

HEAD CONTOUR

NPAB
4/28/88

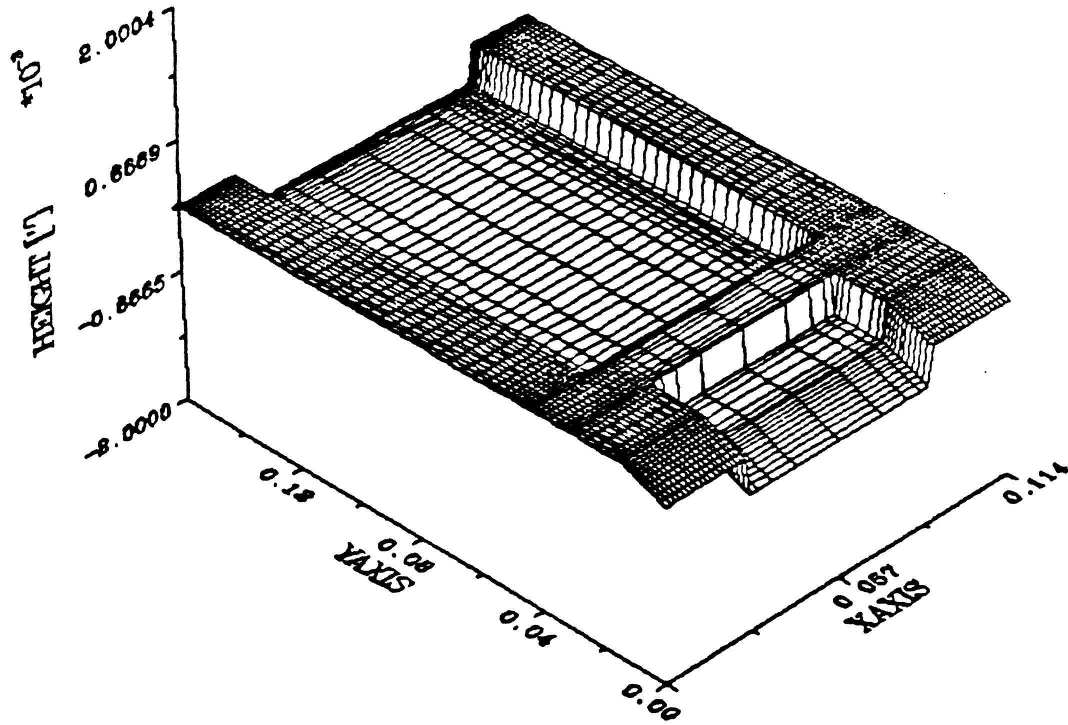

WRM

iist

12-13-89

Seagate

PHYSICAL CONDITIONS

SKEW	:	0.0000
VELOCITY	:	1000.0000
RADIUS	:	0.0000
LOAD	:	6.0000
P_OFFSET	:	0.0000
CAV_DPTH	:	0.0004
H_LENGTH	:	0.1600
H_WIDTH	:	0.1140
TAPER_H	:	0.0002
TAPER_L	:	0.0140

ENVIRONMENTAL CONDITIONS

VISCOSITY	:	2.6427
MFP	:	2.6736
PRESSURE	:	14.7000

FLY CONDITIONS

FLYING_H	:	6.2099
PITCH	:	-137.6766
ROLL	:	-0.0066
NET_LOAD	:	-0.2330
NET_XMOM	:	-0.0178
NET_YMOM	:	0.0001
PEAK_PR	:	3.0310

PRESSURE PROFILE

NPAB
4/28/88

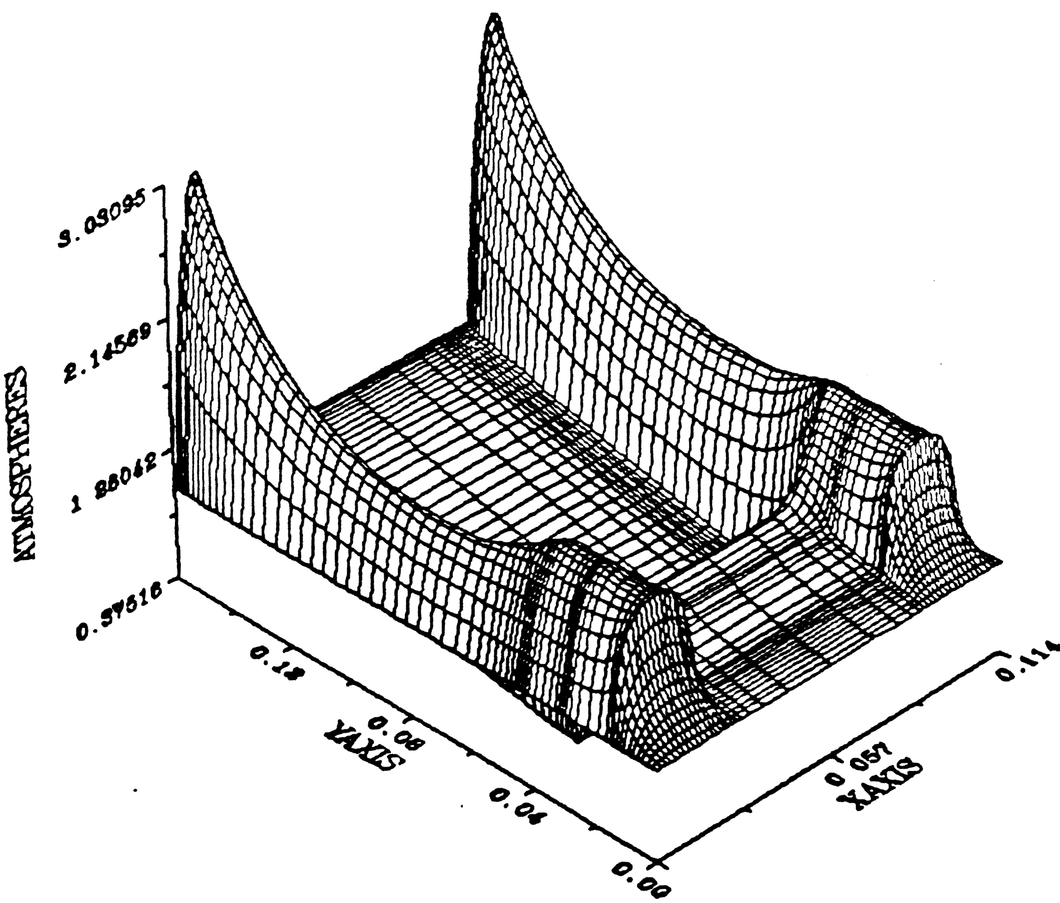

WRM

iist

12-13-89

Seagate

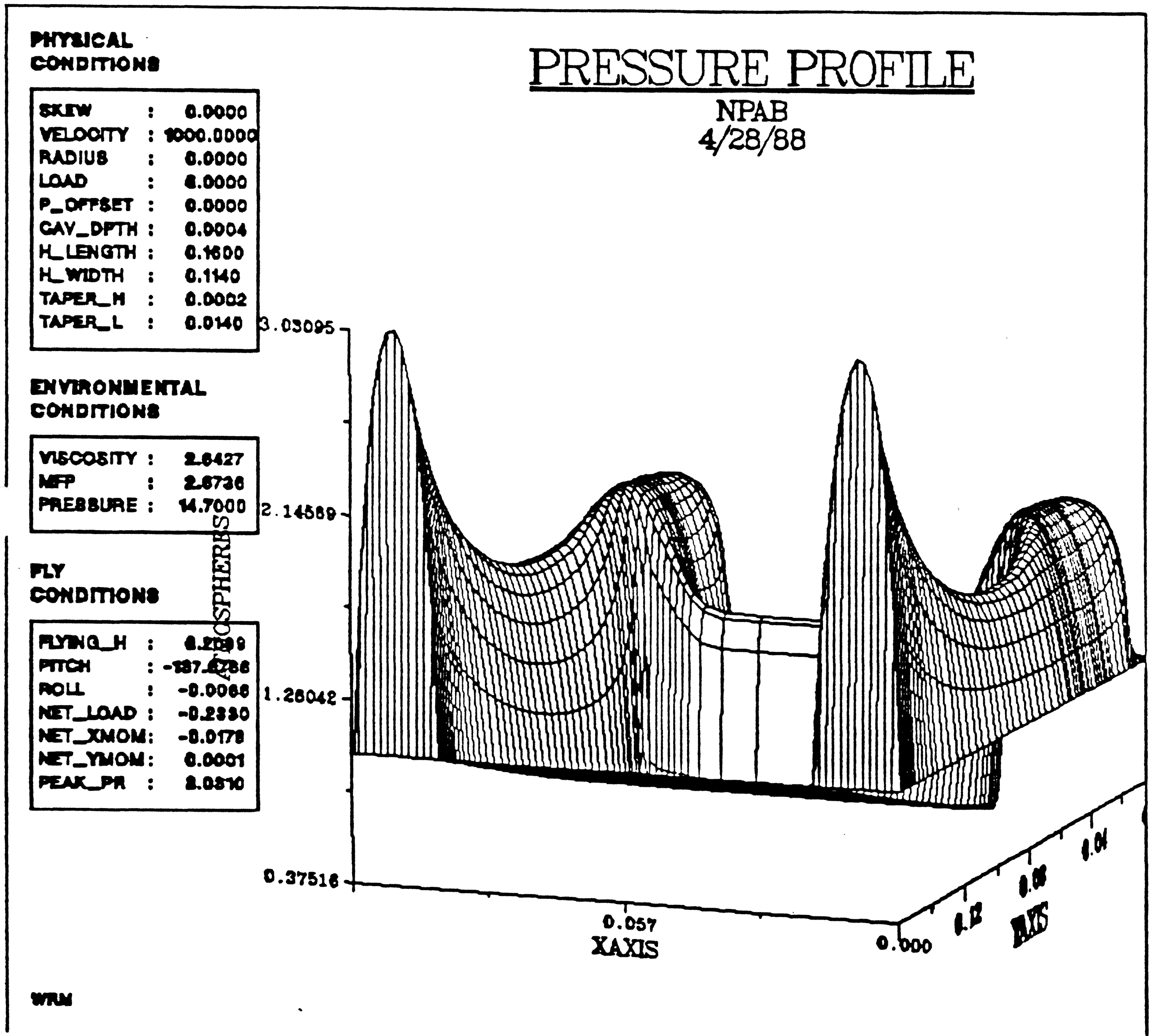

PHYSICAL CONDITIONS
SKEW : 0.0000
VELOCITY : 1000.0000
RADIUS : 0.0000
LOAD : 8.0000
P_OFFSET : 0.0000
CAV_DPTH : 0.0004
H_LENGTH : 0.1600
H_WIDTH : 0.1140
TAPER_H : 0.0002
TAPER_L : 0.0140
ENVIRONMENTAL CONDITIONS
VISCOSITY : 2.6427
MFP : 2.6736
PRESSURE : 14.7000
FLY CONDITIONS
ROLL : -0.0066
NET_LOAD : -0.2330
NET_XMOM : -0.0178
NET_YMOM : 0.0001
PEAK_PR : 3.0310
WRM
PRESSURE PROFILE
NPAB
4/28/88
3.03095
2.14569
1.26042
0.37516
0.057
XAXIS
0.000
YAXIS

Seagate

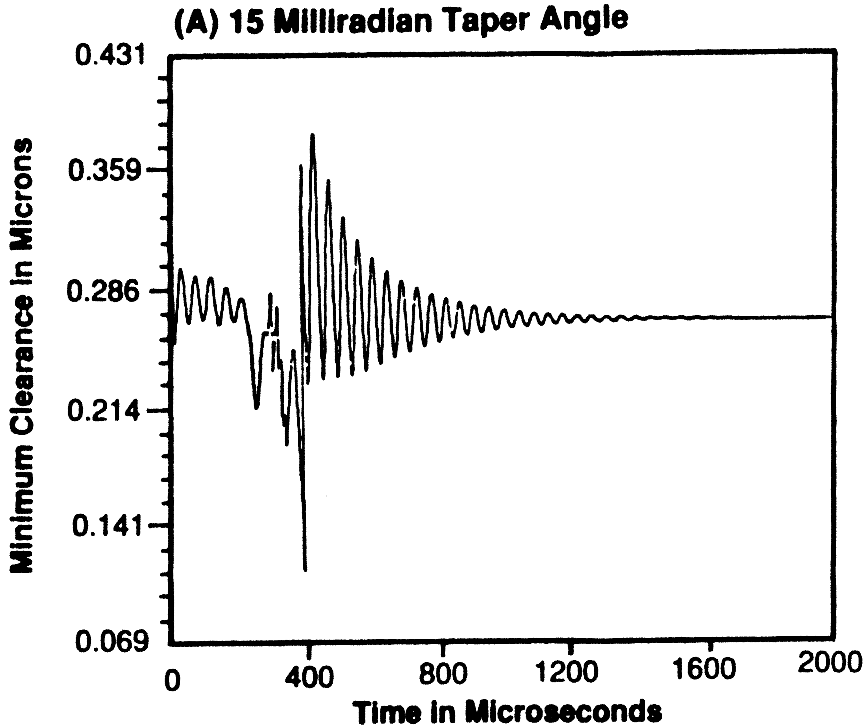

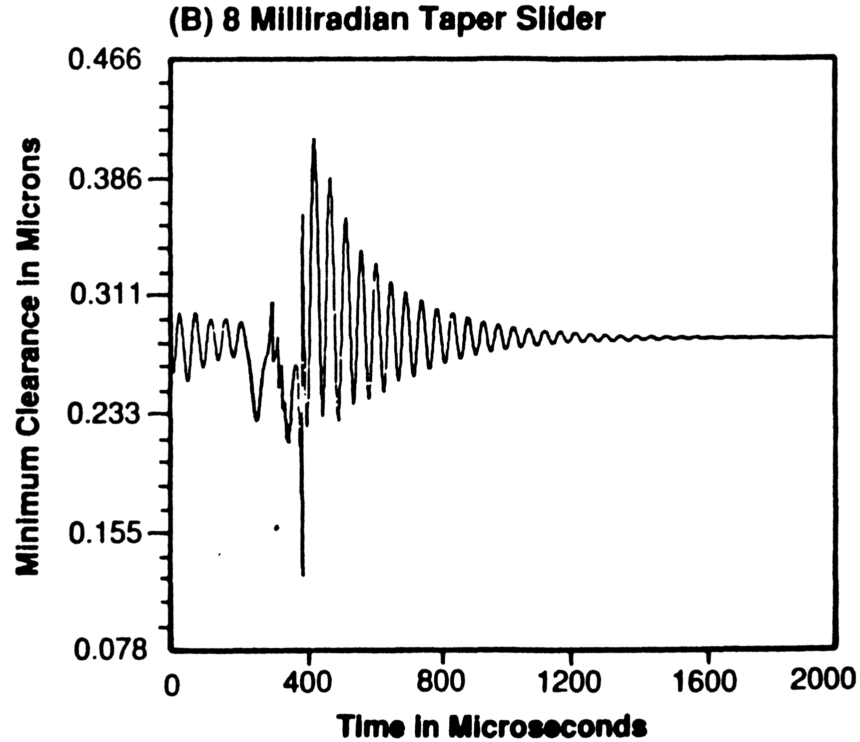

Transient vertical response of 8 and 15 milliradians slider to 0.25 μm step height on disk surface.

Seagate

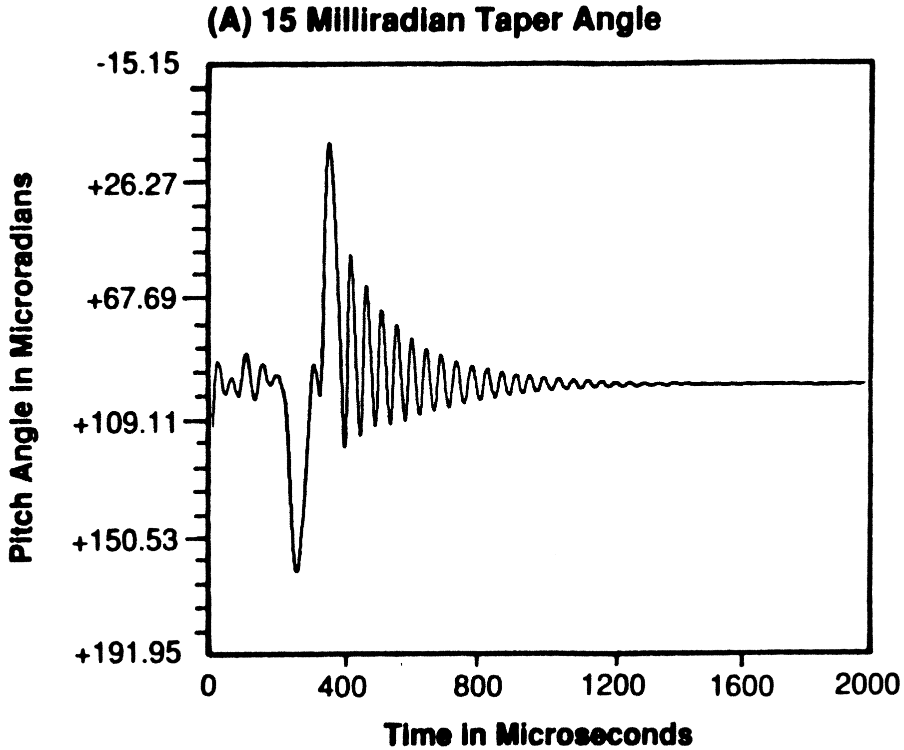

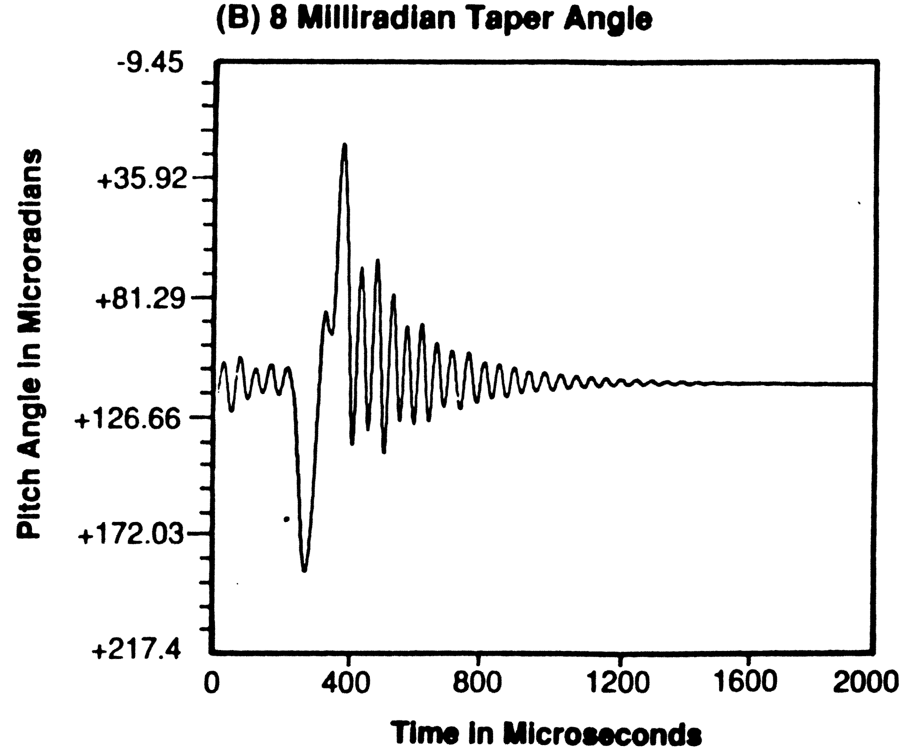

Transient pitch angle response of 8 and 15 milliradians slider to 0.25 μm step height on disk surface.

Seagate

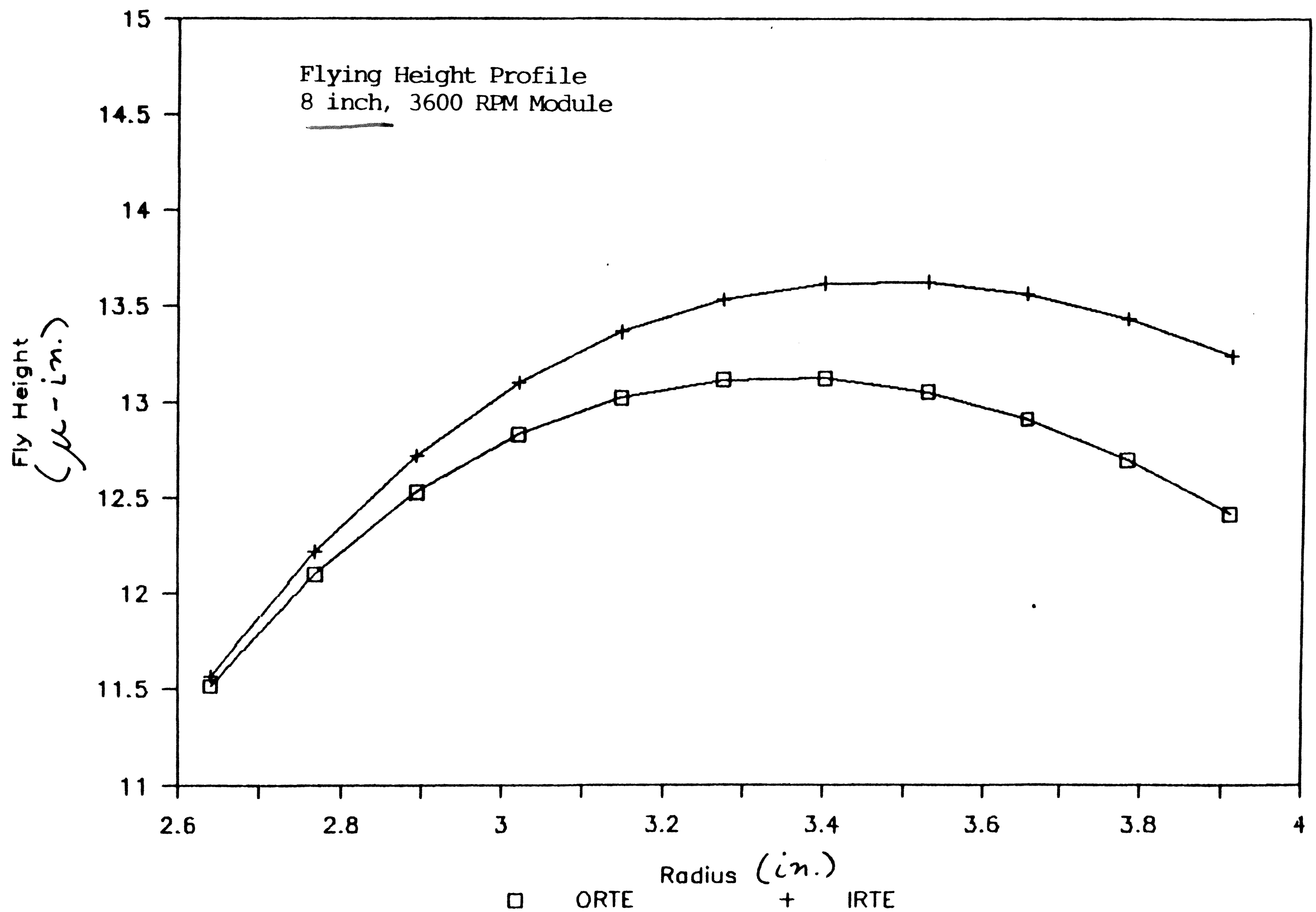

iist

12-13-89

Seagate

Applications of Numerical Air Bearing Simulation

- Simulation of new head designs to screen for feasable design alternatives.
- Design test heads such as "Glide" (FIT) or "Burnish" heads with specific characteristics.
- Natural frequency analysis.
- Air Bearing stiffness and damping v.s. frequency.
- Guide for disk and head constraints at the time a new drive module is designed.
- Analysis of head flying height sensitivity to manufacturing tolerences.
- Mapping of head design and/or operation parameter space by application of statistical design of experiments methods applied to numerical modeling.
- Prediction of flying height loss due to component, drive and environmental factors. (Reliability margin)

Seagate

Impact Modeling of the Head Disc Interface

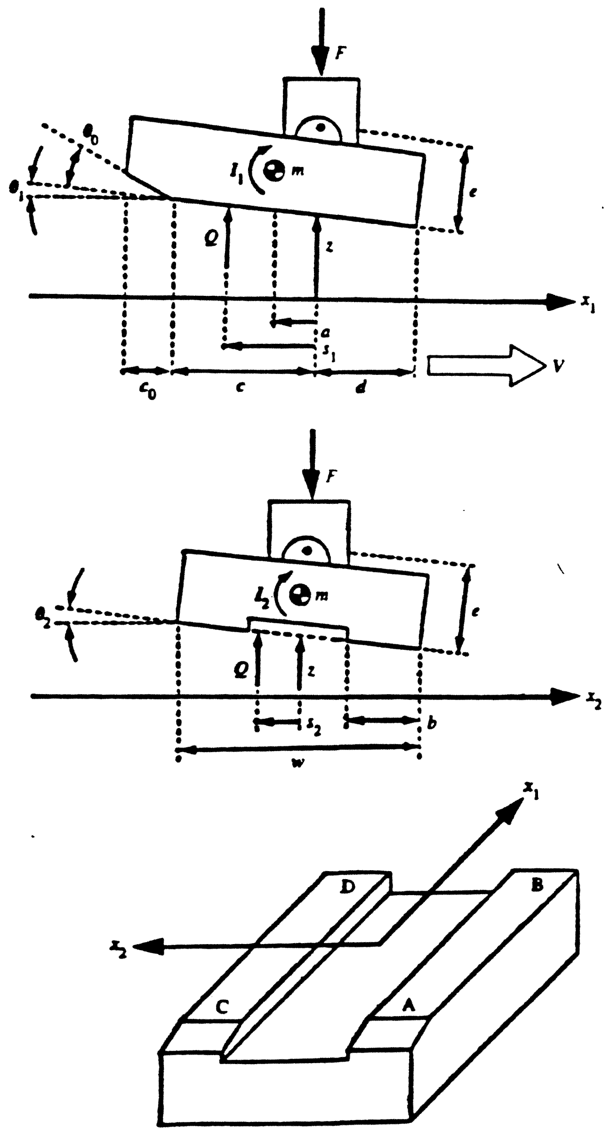

iist

Benson, R. C., Chiang, C., Talke, F. E., "The Dynamics of Slider Bearings During Contacts Between Slider and Disk," IBM J. Res. Dev., Vol. 33, No.1, Jan. 89.

12-13-89

Seagate

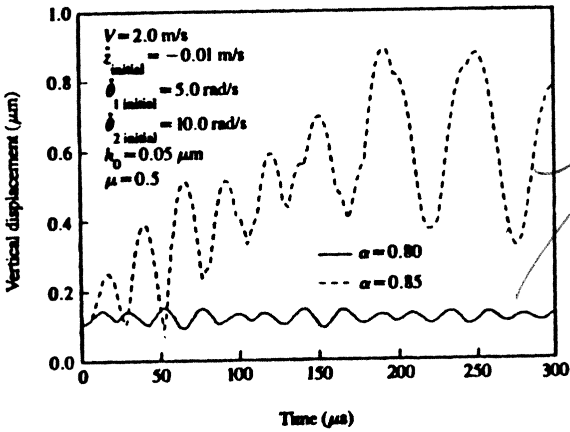

Figure 4

Vertical displacement of slider vs. time for $\alpha = 0.80$ and $\alpha = 0.85$.

different coef of restitution

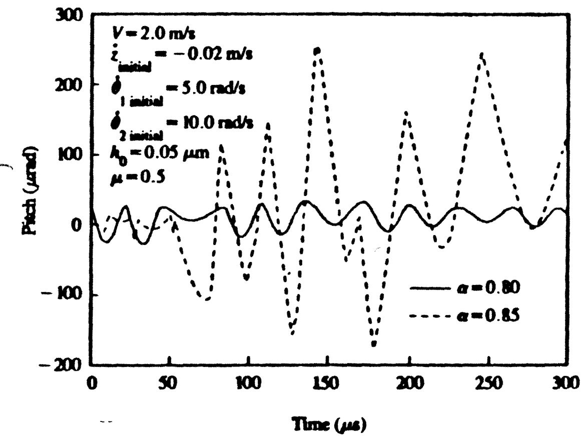

Figure 5

Pitch of slider vs. time for $\alpha = 0.80$ and $\alpha = 0.85$.

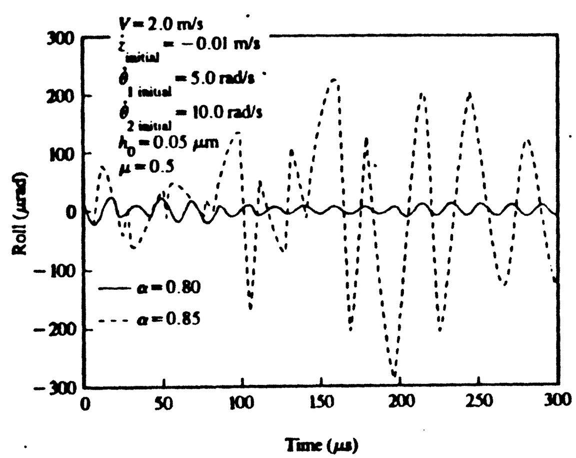

Figure 6

Roll of slider vs. time for $\alpha = 0.80$ and $\alpha = 0.85$.

Seagate

AC = Leading edge
BD = Trail

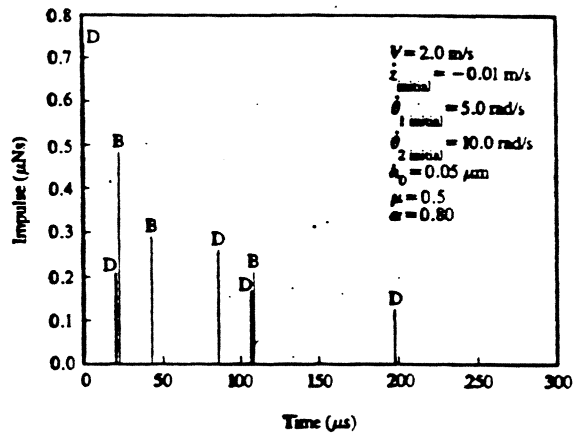

Figure 7

Slider/disk impact history for $\alpha = 0.80$.

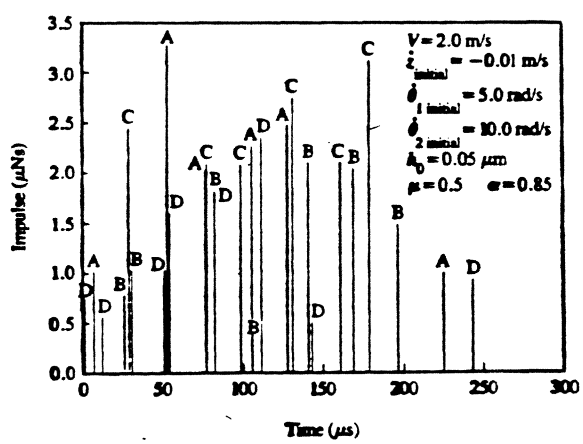

Figure 8

Slider/disk impact history for $\alpha = 0.85$.

Seagate

Head Disc Spacing Budget Analysis

An Optimization Tool
in
Drive Design for Reliability

iist *12-13-89*

What Is
Head/Disk Separation Budget?

The head/disk separation budget (HDSB) relates the distribution of specified mechanical parameters in a disk drive to the distribution of minimum flying height.

The flying height loss contributions due to all parameters are combined statistically.

How Is the Head/Disk Separation Budget Used?

Specifications for the heads, disks, and drive mechanical parameters are selected to achieve adequate head/disk separation in the initial phase of drive design.

Parameters are measured at the component and drive level during the design cycle to confirm the separation margin.

Tradeoffs in the parameters and tolerances are made based on the separation margin requirement.

Head/Disk Separation Loss Budget Methodology

Loss of head/disk separation can be caused by several primary factors:

A. Disk Surface Roughness

B. Circumferential Disk Surface Variations and Spindle Vibration

C. Radial Disk Surface Variations

D. Temperature and Altitude Changes

E. Head Roll During Seek and Emergency Retract Stop Contact

F. HDA Stacking Tolerances

G. Head and Arm Manufacturing Tolerances

Head/Disk Separation Loss

A. Losses caused by disk surface roughness. The head attempts to fly over a perfectly flat surface defined by the arithmetic mean centerline of the disk surface finish. Protrusions above this reduce the spacing on a one-for-one basis.

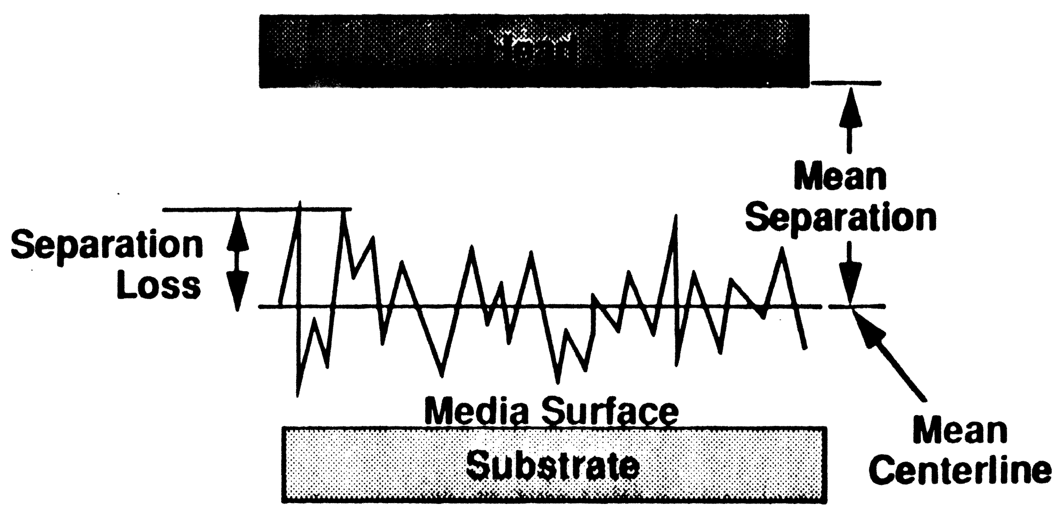

Head/Disk Separation Loss

B. Losses incurred by the head failing to dynamically respond to larger scale circumferential disk surface variations or spindle induced vibrations. Circumferential variations are assumed to be sinusoidal in shape. Head response to variations and vibrations is modeled.

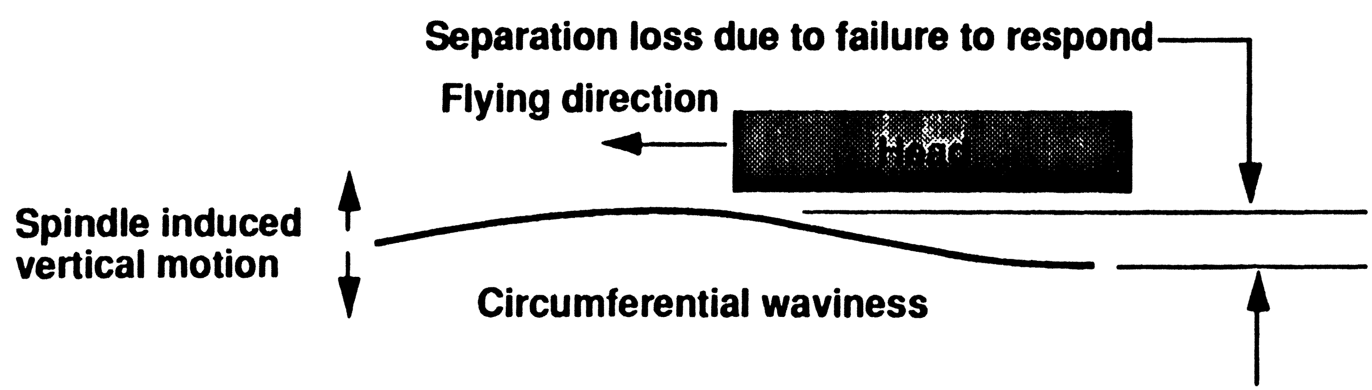

97340-6

How Effect of Circumferential Waviness Is Determined

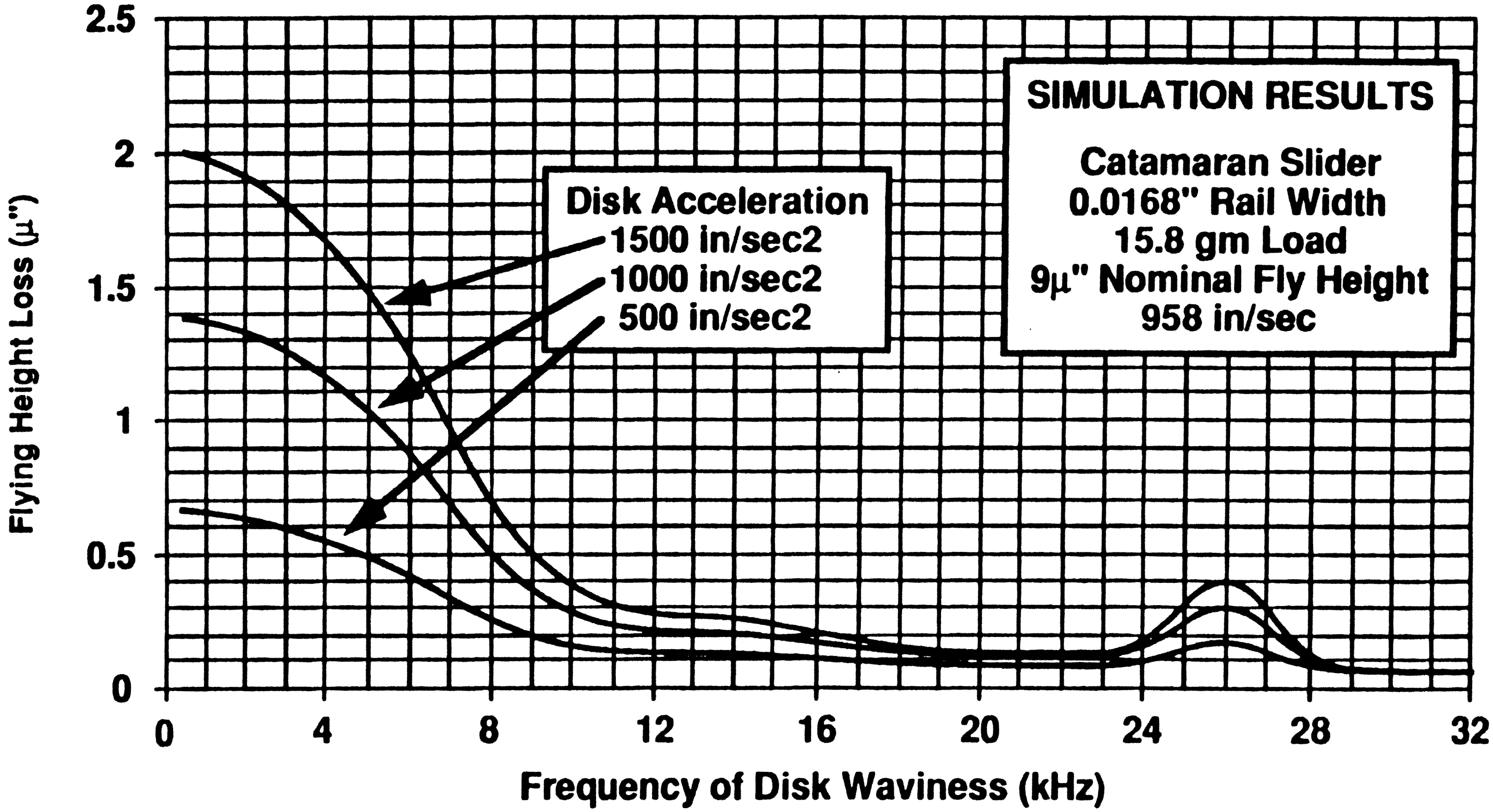

97340-7

Factors Affecting Spacing Loss Due to Circumferential Disk Variations

1. Length of the slider
2. Axial synchronous acceleration
3. Disk surface velocity

Spacing loss is primarily a geometric effect when a straight surface tries to negotiate a curved surface.

Separation Loss Due to Disk Acceleration Calculated from Geometric Model

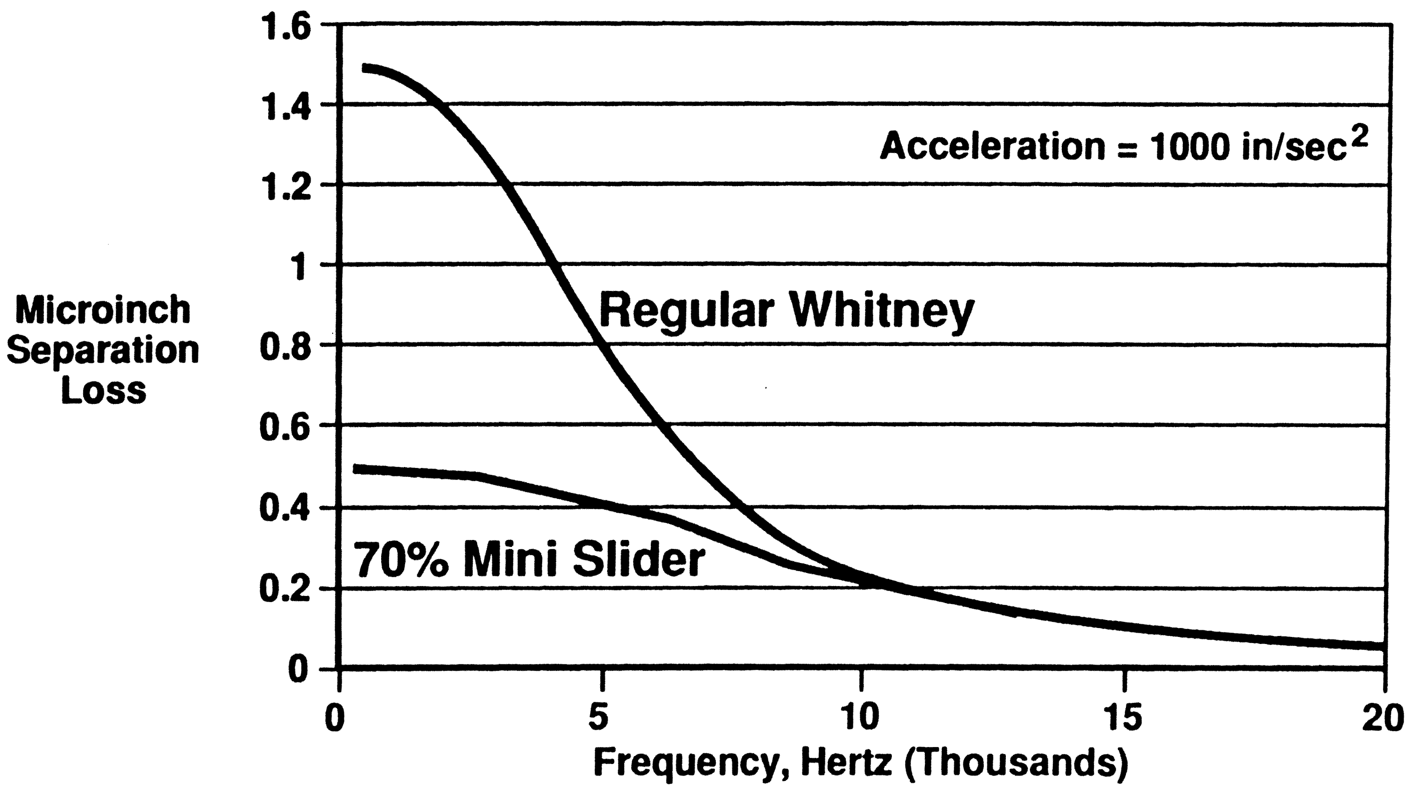

97340-9

Head/Disk Separation Loss

C. Static spacing losses incurred by very large scale radial disk surface variations. The slider straddles a curved surface – either convex or concave. Each pad essentially flies on the side of a hill. One edge of each pad is closer to the disk surface than the other edge. The mean spacing is reduced by one half the chord height over the width of the pad (w).

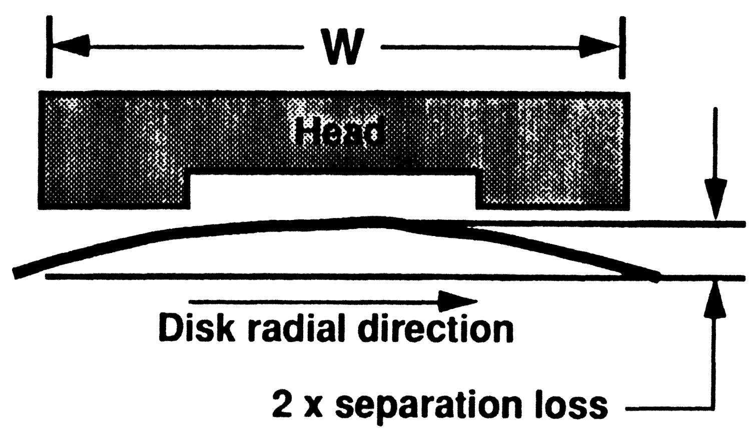

97340-10

Factors Affecting Spacing Loss Due to Radial Disk Surface Variations

1. Width of the slider
2. Width of the rails
3. Skew of the slider
4. Length of the slider excluding taper
5. Local curvature of the disk surface
6. Local slope of the disk surface

Loss can be calculated using an air-bearing simulation code or by using an approximate geometric model.

97340-11

Head/Disk Separation Loss

D. Altitude and temperature extremes over the operating range of the head/disk interface affect the flying height of the head through variations in the mean free path of air and its viscosity.

1 μ" over spec range

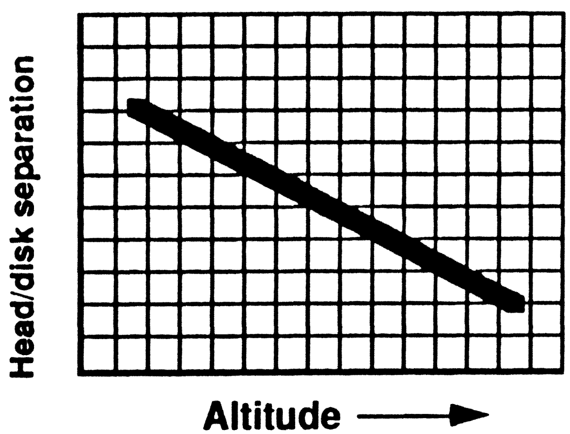

.01-.02 μ" over op temp

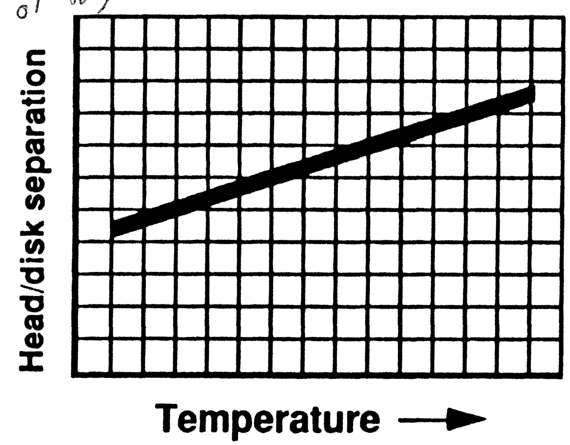

97340-12

Head/Disk Separation Loss

E. A rolling moment is transmitted to the head, through the flexure, during head seek, or when the actuator contacts the crash stop. This causes one edge of the head to roll closer to the disk, reducing the spacing. Presently, neither friction between the head and disk, nor inertia of the head about the roll axis are considered. Only radial acceleration forces are considered.

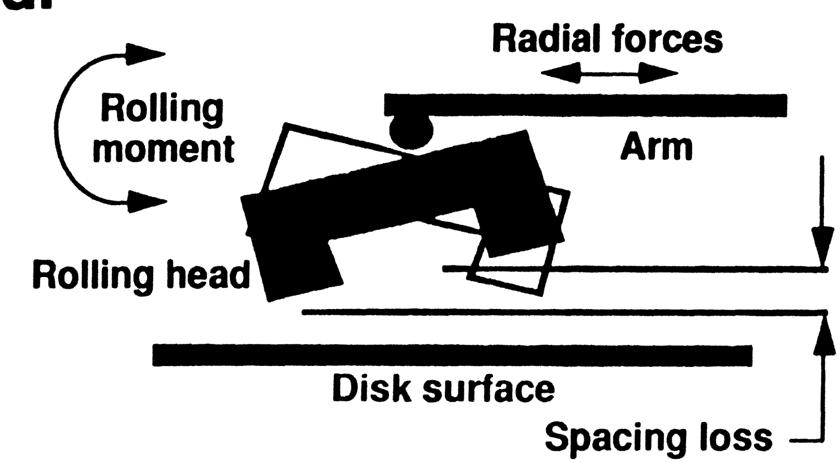

97340-13

Head/Disk Separation Loss

F. HDA head/disk stacking tolerances cause the vertical position of the arm to vary slightly from nominal. This causes variations in the head load in the vertical direction due to gimbal deflections. This causes either an increase or decrease in fly height. Also, presentation of the HGA at an angle induces a rolling moment in the head which always decreases flying height.

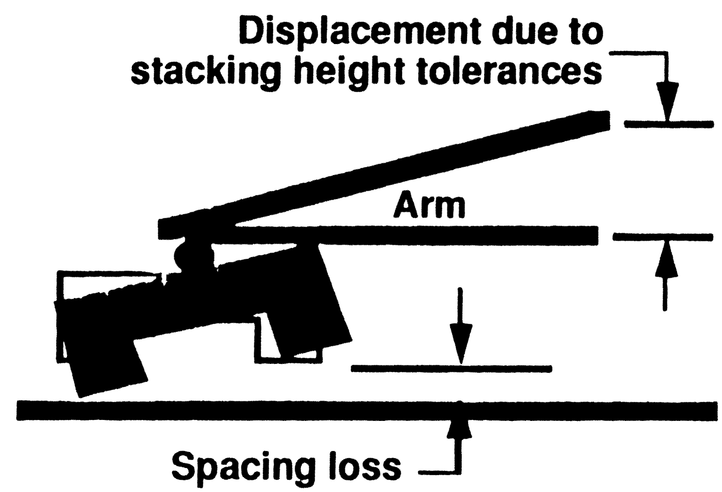

97340-14

Head/Disk Separation Loss

G. Head and arm manufacturing tolerances result in a variation from HGA to HGA in mean flying height over a perfectly smooth surface. (i.e. the component flying height specification limits)

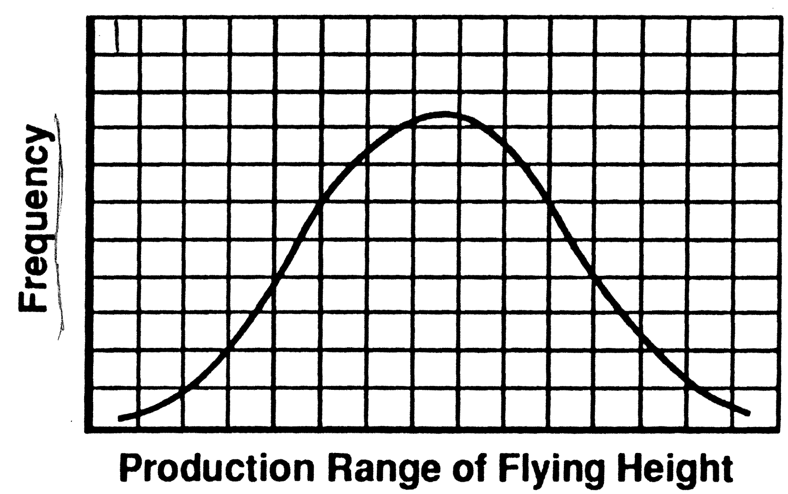

Typical Drive — Thin Film Media/Thin Film Heads

REDUCTION SOURCE	Target Value	±	LOSS	3sigma	sigma	sigma2
Head/Arm Mfg Tolerances (μ")	10.5	1.5	0.00	1.50	0.50	0.25
HDA Stacking Tolerances (")	0.002	0.01	0.05	0.30	0.10	0.01
Disk Radial Curvature (")	1200	2400	0.30	0.20	0.07	0.00
Disk Radial Slope (")	0.08	0.08	0.70	0.70	0.23	0.05
Disk HF Displacement (")	0.3	0.2	0.30	0.20	0.07	0.00
Circumferential Waviness ("/s2)	450	400	0.60	0.50	0.17	0.03
Disk Roughness (μ")	0.5	0.5	1.20	0.00	0.00	0.00
Head Roughness (μ")	0.2	0.05	0.20	0.05	0.02	0.00
Track Seek Acceleration (g's)	50	5	0.90	0.05	0.02	0.00
Temp/Pres Effect (μ")	Design	Design	0.90	NA	NA	NA
		NOMINAL	5.15			

Disk RPM = 3600

Sum of sigma2	0.35
Root-sum sigma2	0.59
3 x Root-sum-sigma2	1.78
MOST PROBABLE LOSS TOLERANCE	1.78
MOST PROBABLE ACTUAL SPACING LOSS	6.93
SPACING LOSS MARGIN	3.57

97340-16

Contribution of Sources to Nominal Separation Loss

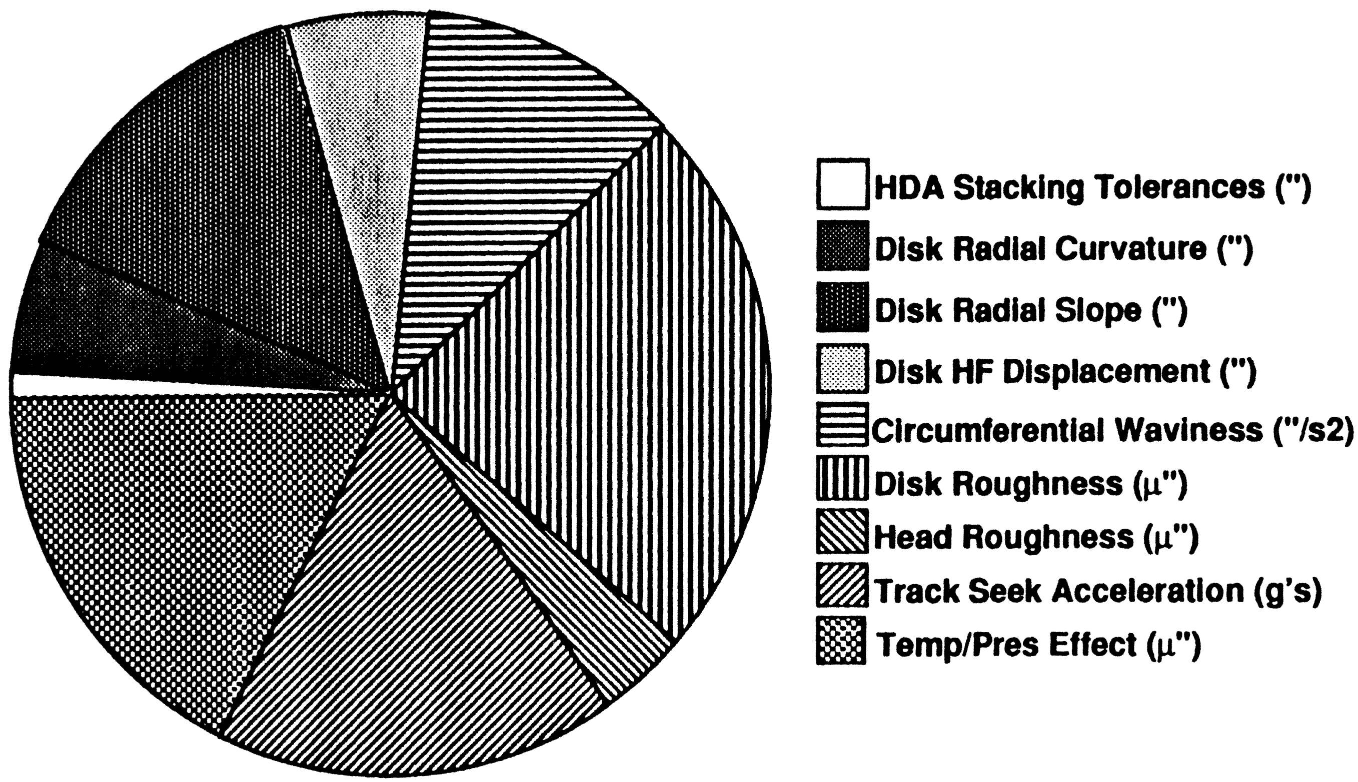

97340-17

Contribution of Sources to Variability in Separation Loss

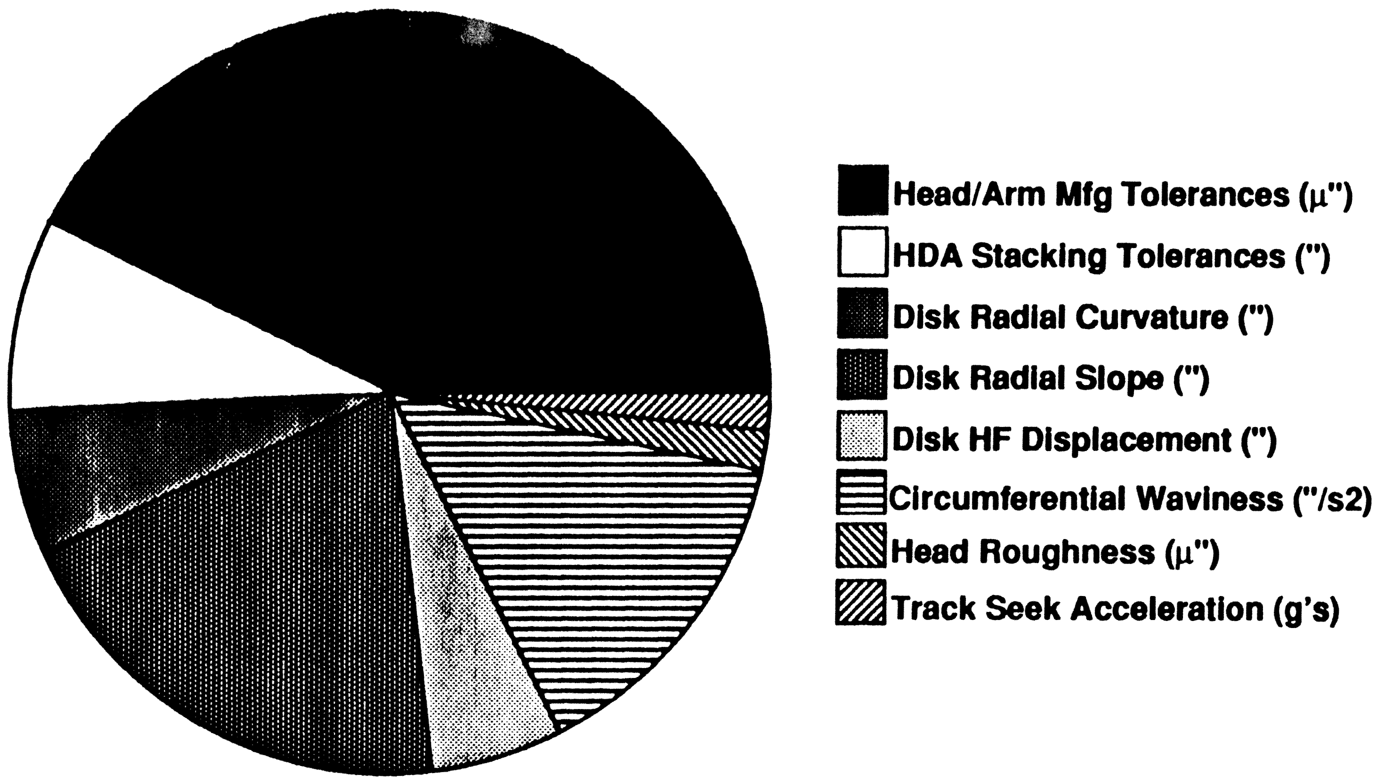

97340-18

Conclusions

It is shown that the head/disk spacing analysis can be used to accomplish the following drive design objectives:

1. Set specifications for head, disk, and drive mechanical parameters to ensure adequate spacing margin.
2. Enable proper design tradeoffs in the parameters and tolerances during the design cycle.
3. Provide a road map for design improvements for the next generation design to maximize head/disk interface reliability.

97340-19

Conclusions

4. Allows specification of the glide height for media surface qualification for a specific product. Required glide height should be the sum of all the spacing losses from the disk alone from the sample budget shown. Since the calculated margin is guaranteed in the presence of those losses from the disk, a disk finished to that glide height will also have the same margin.

Seagate

White Light Flying Height Measurement

Manual Fringe Interpretation

- -Resolution 0.5 micro-inches (1 operator)
- -Fast Production Test
- -Can be Set-up for Skew, Speed and Radius Variability

Spectrophotometric (Digital) Analysis

- -Resolution better than 0.1 micro-inches
- -Moderate Speed
- -Automated for Batch Measurements
- -Small Measurement Spot; to .0005"
- -Set-up for Skew, Speed and Radius Variability

iist 12-13-89

Seagate

Manual Fringe Interpretation

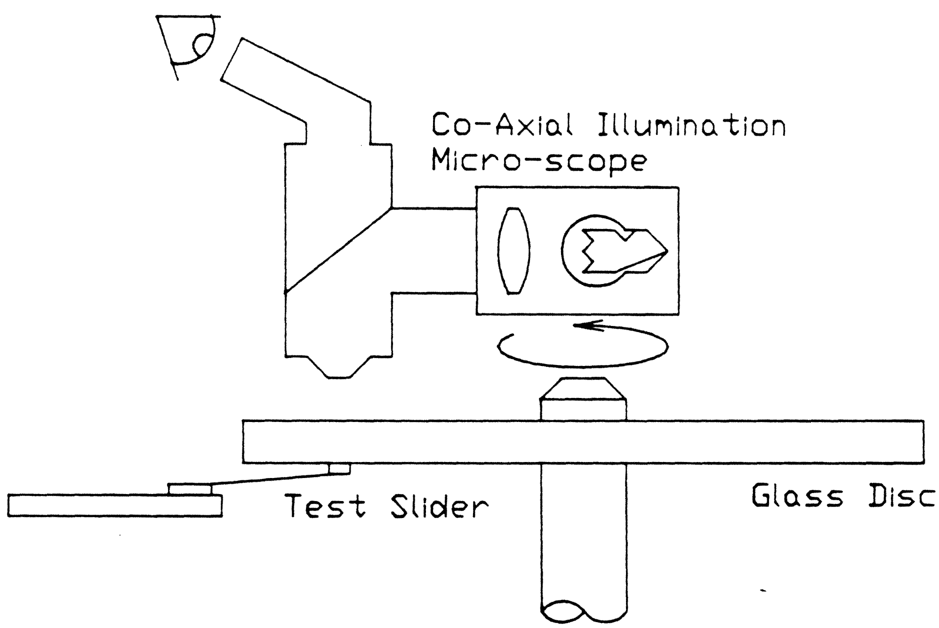

iist

12-13-89

Seagate

Spectrophotometric White Light Flying Height Analysis

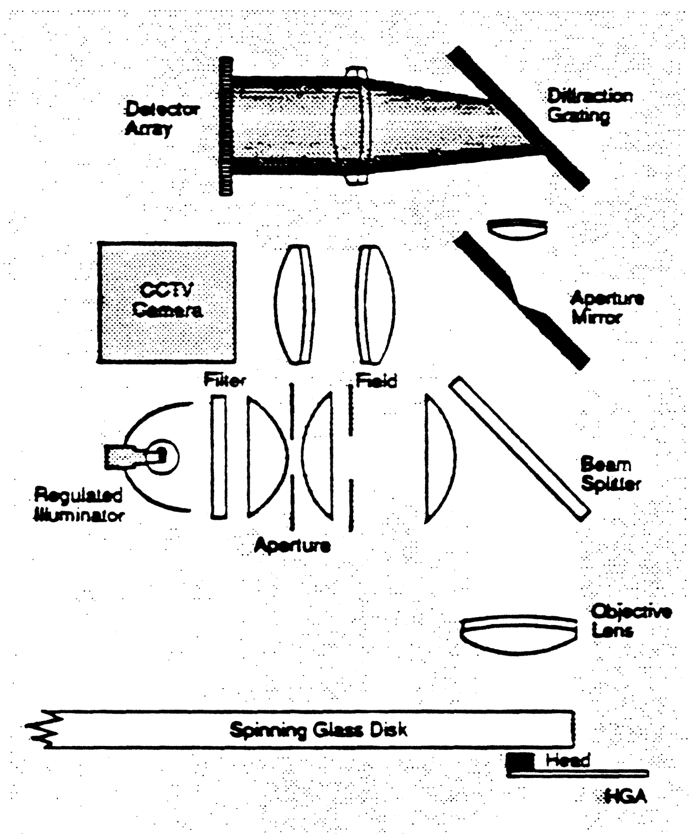

Figure 2

PPL Optics

Re-printed with permission from
"Advances in Flying Height Measurement,"
by W. McBain and B. F. Norton
Pacific Precision Labs, 1989

iist

12-13-89

Seagate

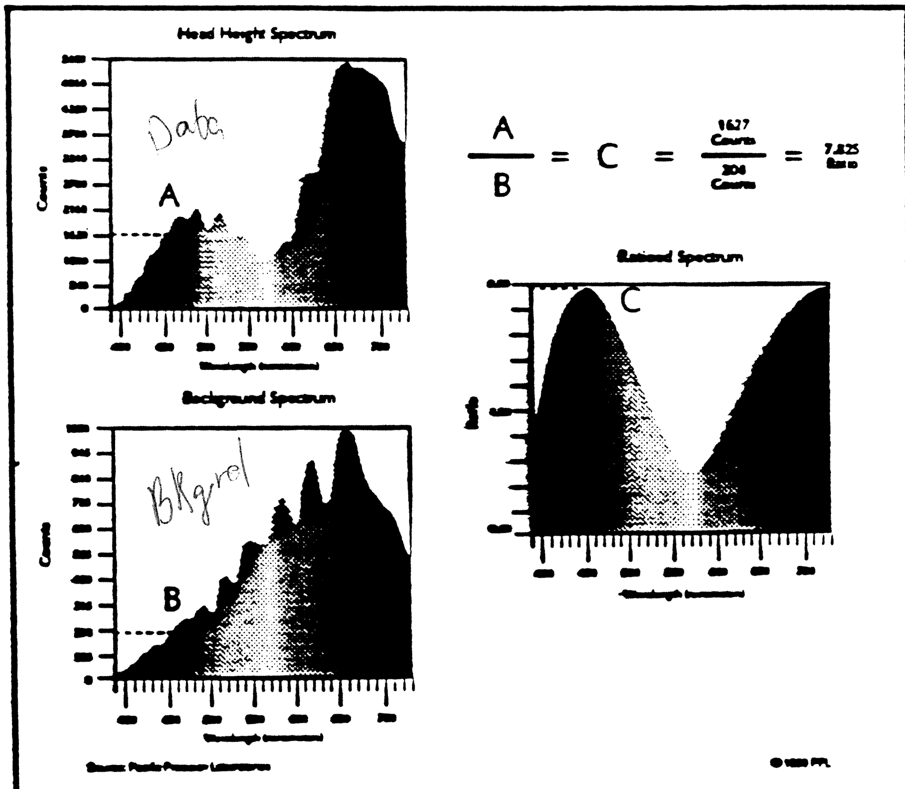

Figure 3 A, B, and C

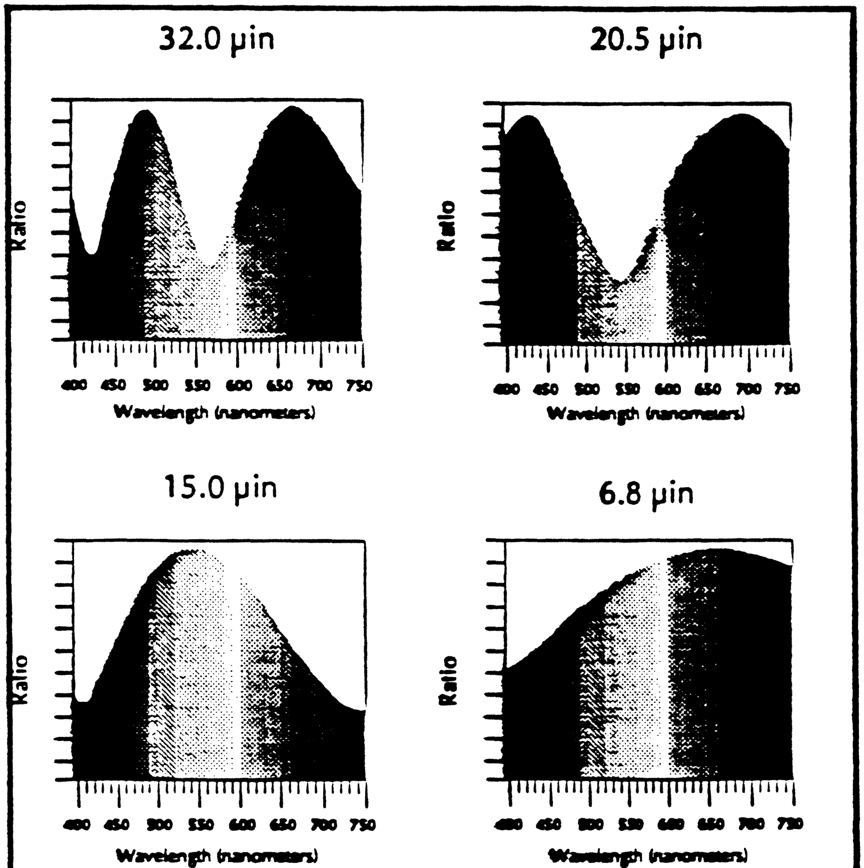

Figure 4

Ratioed Curve
3.8 µin Flying Height

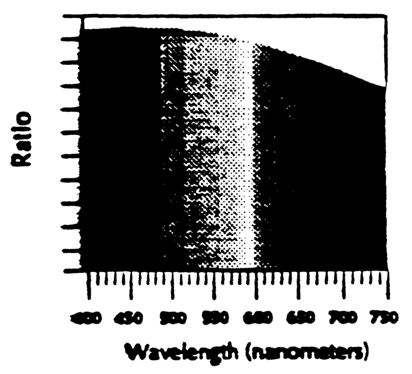

Figure 5

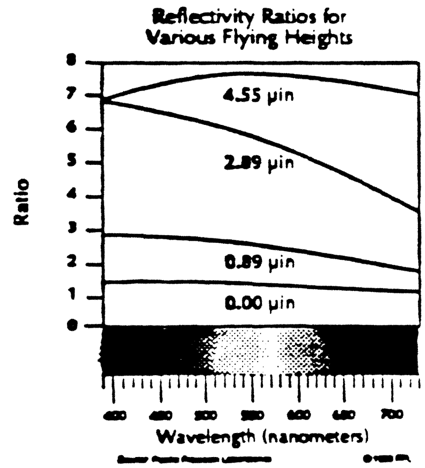

Figure 6

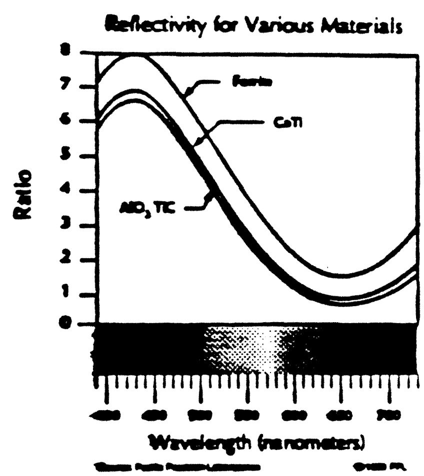

Figure 7

Seagate

Laser Interferometer
Fringe Intensity

- Better than 0.1 micro-inch Resolution
- Static and Dynamic Measurements
- Dynamic Measurements only at Linear Region of the Intensity Curve

Seagate

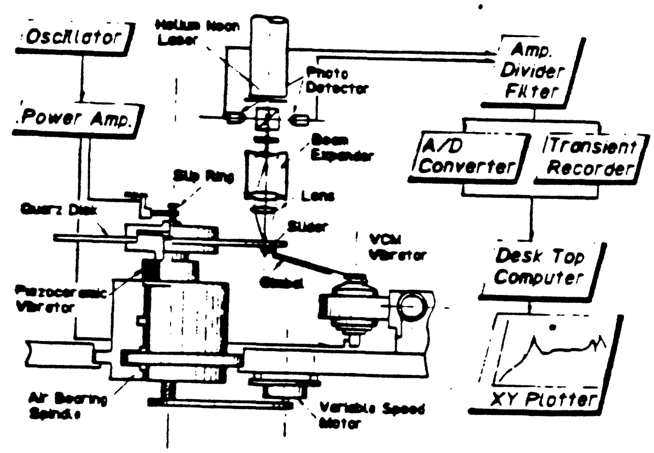

Fig. 1(a) Experimental apparatus.

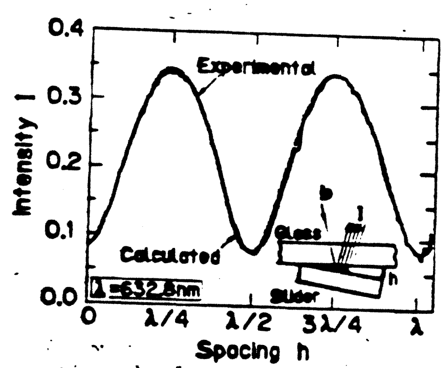

Fig. 1(b) Confirmation of interference intensity based on fixed spacing

Ohkubo, T., T. Hayashi and Y. Mitsuya, "Accurate Measurement and Evaluation of Dynamic Characteristics of Flying Head Slider for Large-Capacity Fast-Access Magnetic Disk Storage," IEEE Trans. Mag., Vol. MAG-23, No. 5, Sept. 1987, pp3456-58.

iist 12-13-89

Seagate

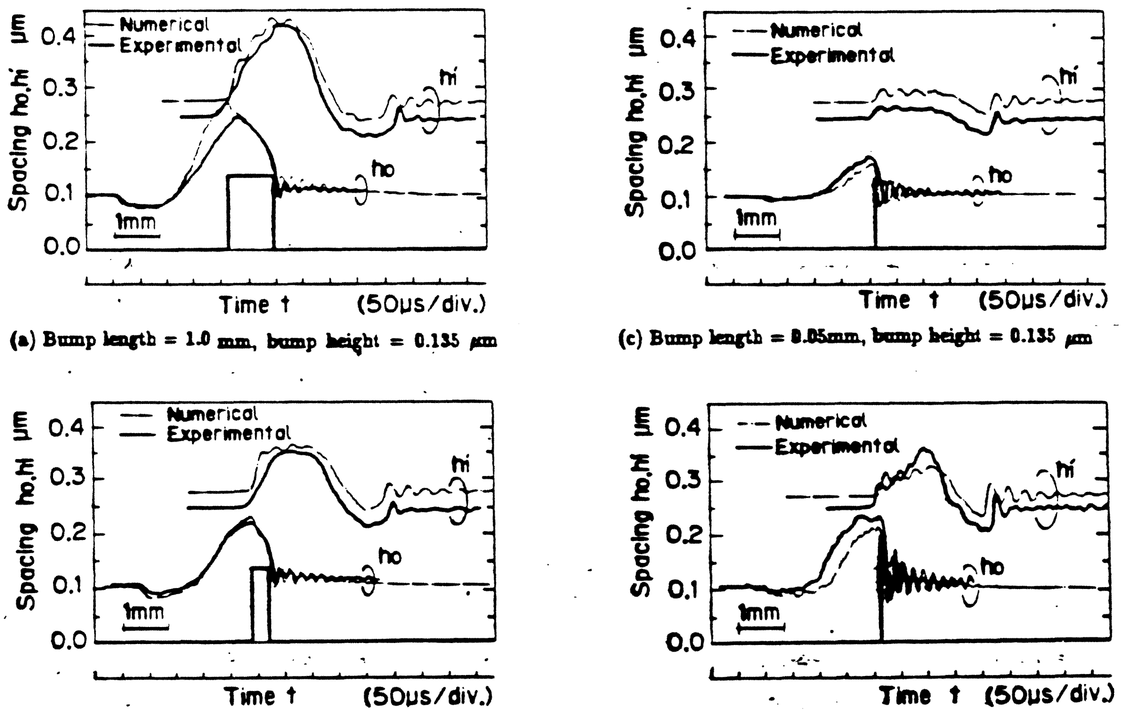

(a) Bump length = 1.0 mm, bump height = 0.135 μm

(b) Bump length = 0.4 mm, bump height = 0.135 μm

(c) Bump length = 0.05mm, bump height = 0.135 μm

(d) Bump length = 0.05mm, bump height = 0.19 μm

Fig. 5 Transient response due to rectangular bump

Seagate

Laser Doppler Vibrometer

Description:

- Measures Velocity Component of Vertical Head or Disc motion
- Fixed Reference Frame (Carries Common Mode Head and Disc Motion
- Wide Bandwidth (500 KHz)
- Can High-pass Filter for Good Resolution of Dynamics

Application:

- Head Natural Frequency Measurement
- Module Level Head and Disc Mesurements
- Disc RVA

Seagate

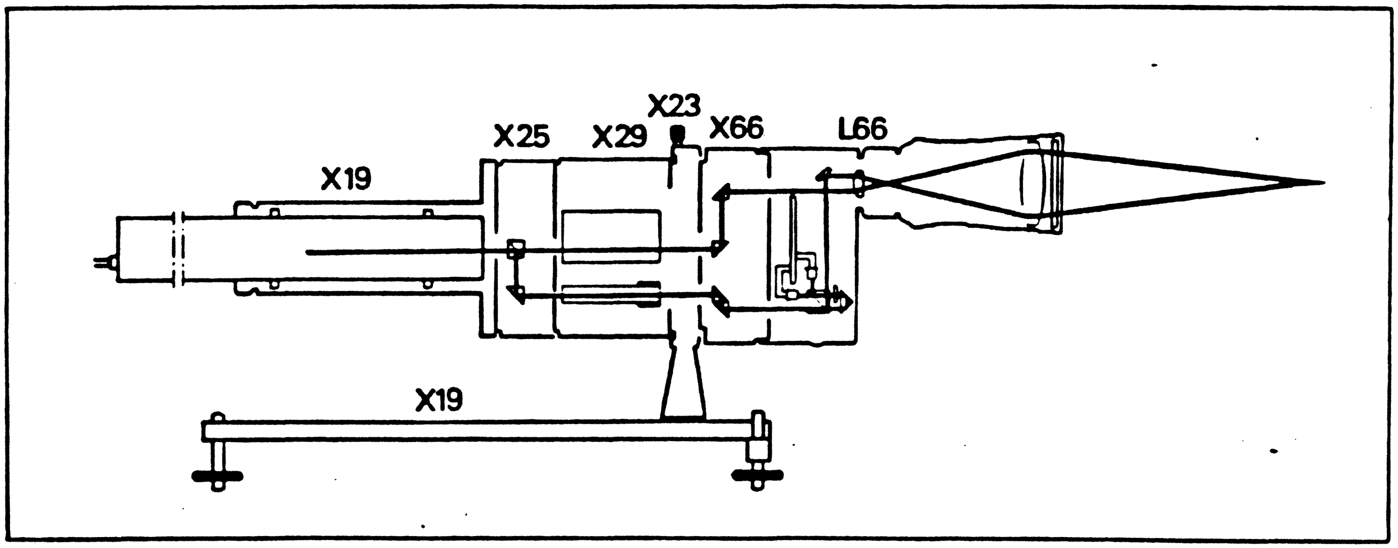

Fig. 2. Diagram of the 55X Laser Doppler Vibrometer

Seagate

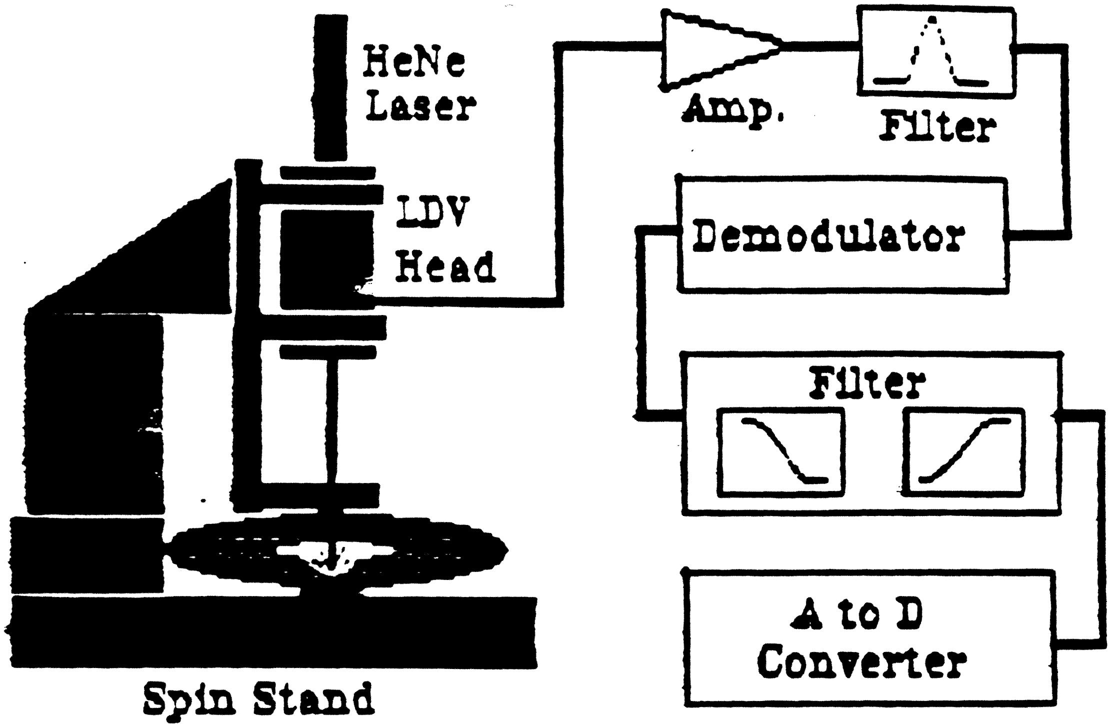
HeNe
Laser
LDV
Head
Spin Stand
Amp.
Filter
Demodulator
Filter
A to D
Converter

Seagate

Laser Doppler Vibrometer

4-T

18 Nov 1987 15:16:45
NO. OF DATA POINTS = 1024
NO. OF AVE.=25 CAL.FAC.= .765
RADIUS = 2.4
SPINDLE RPM = 3606
LEVELING IN EFFECT
RMS DISPLACEMENT(UIN) 68.549
RMS VELOCITY(IN/SEC) 3.07E-02
RMS ACCEL(KIN/SEC2) .0439

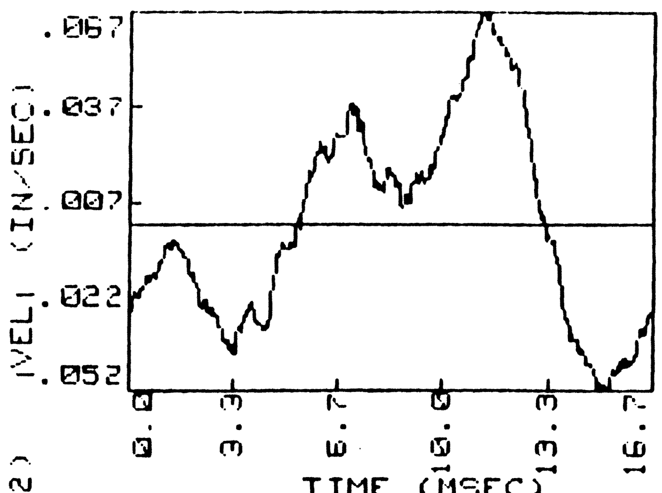

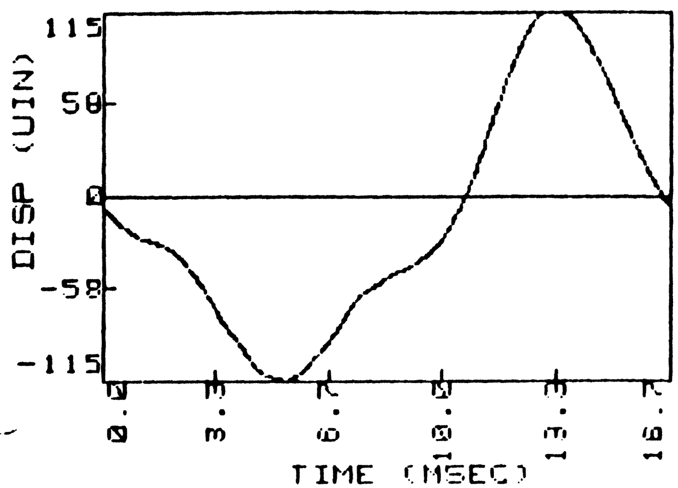

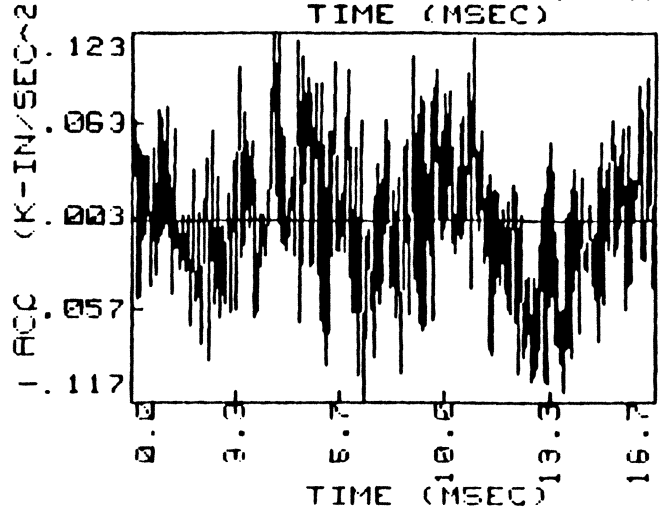

iist

12-13-89

Seagate

Laser Doppler Vibrometer

TIME BETWEEN POINTS (H1)= 18.0 uSEC.
CALIBRATION FACTOR (C1)= .7650
SPINDLE SPEED = 3605 RPM

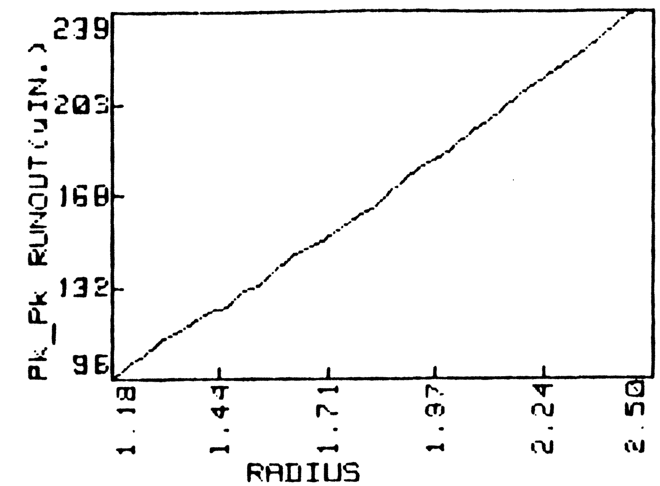

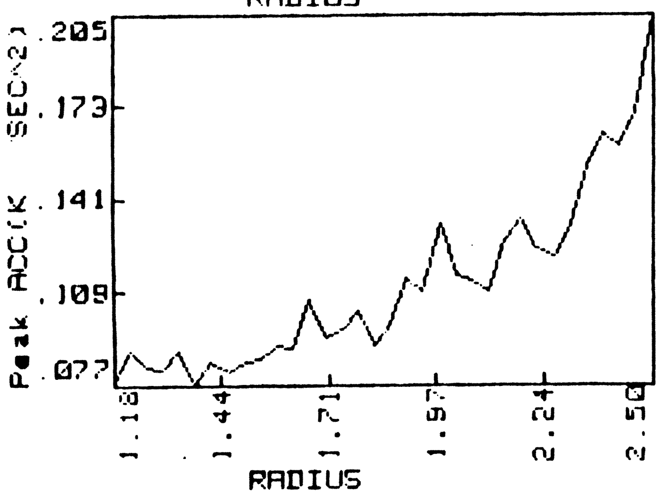

iist

12-13-89

Capacitance Probe Heads

Capabilities:

- On Track Dynamic Flying Height
- Seek and Emergency Retract Flying Dynamics
- In Module or Spin Stand

Seagate

Capacitance Probe Heads

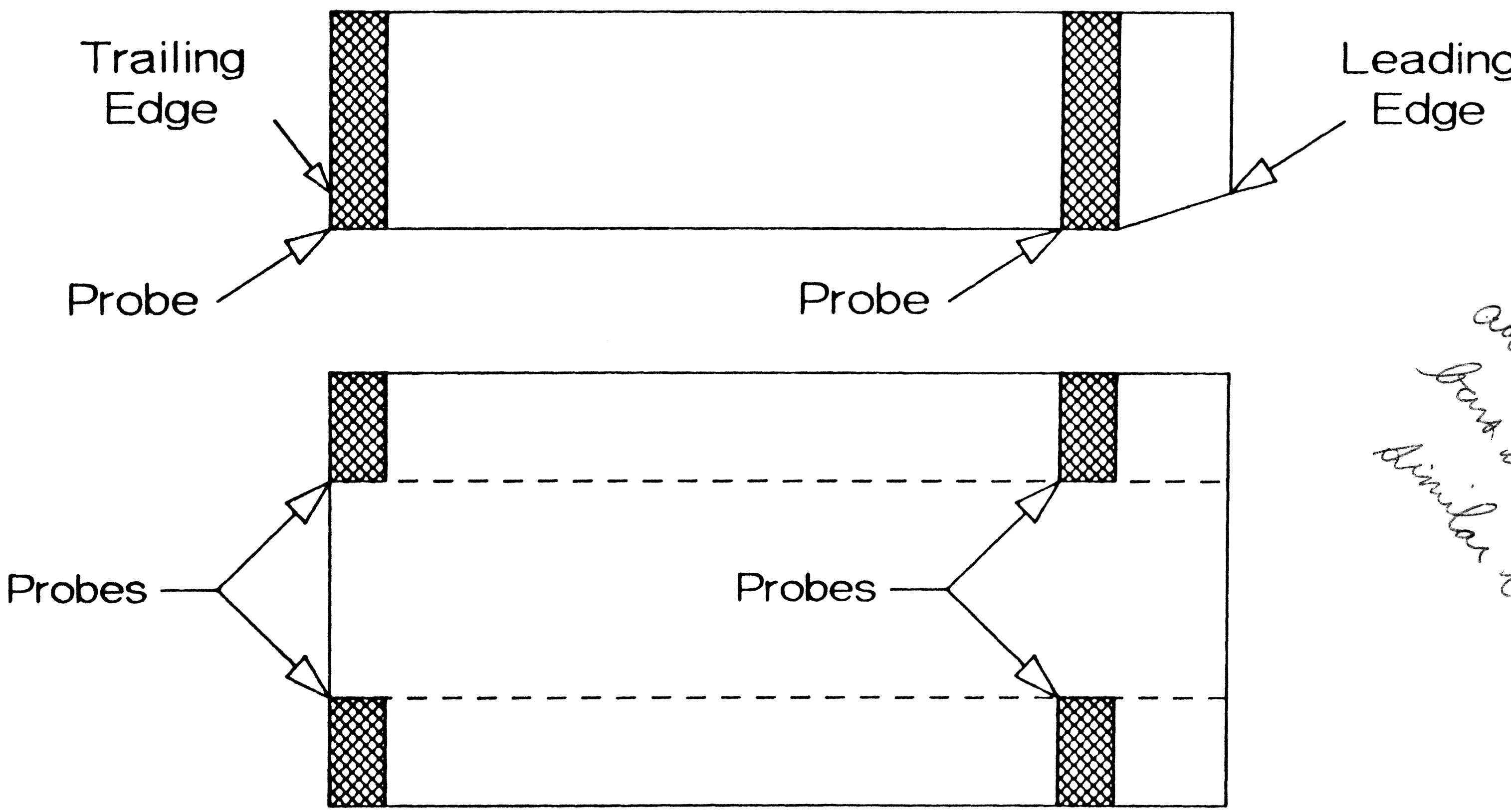

adding ferrite bars into corner of CaTi similar to composite

iist

Probe Locations

12-13-89

Seagate

Capacitance Probe Heads

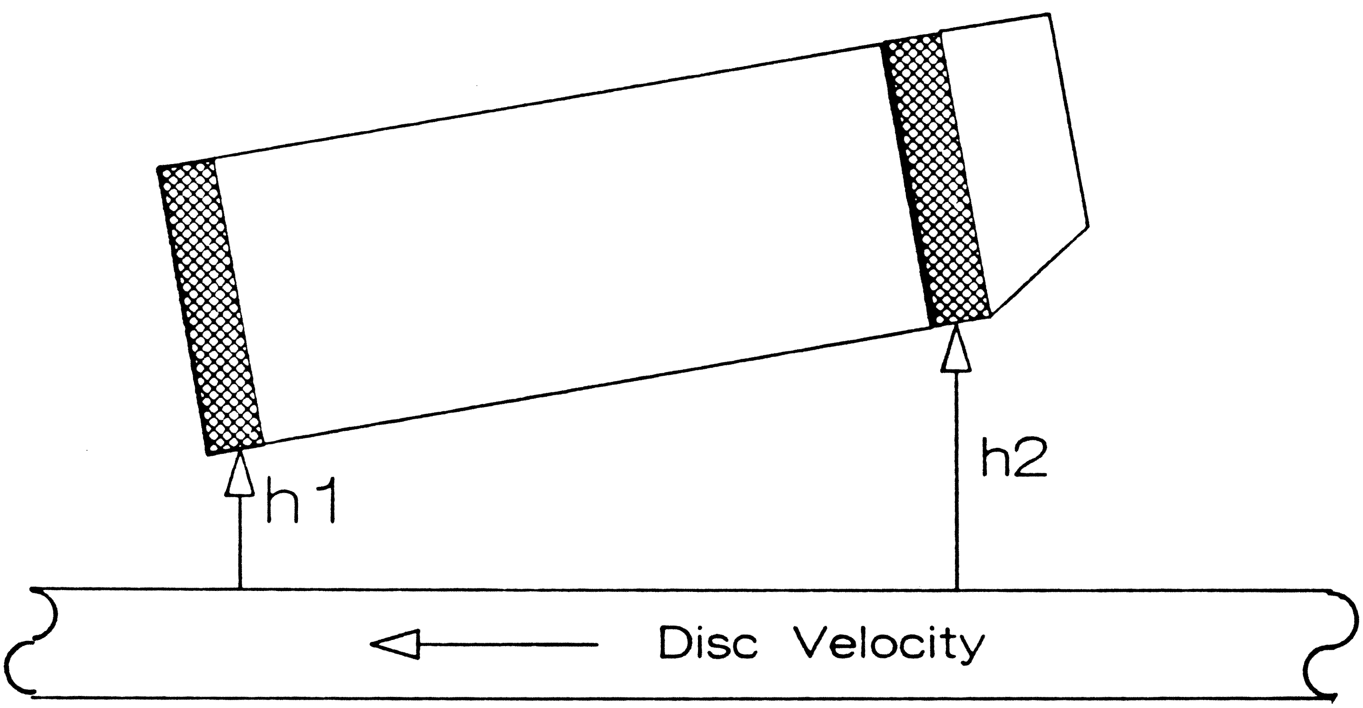

$$\Delta\Phi = R\Delta C\omega$$

$$C = \frac{e_0 A}{h_i}$$

iist

12-13-89

Seagate

Capacitance Probe Heads

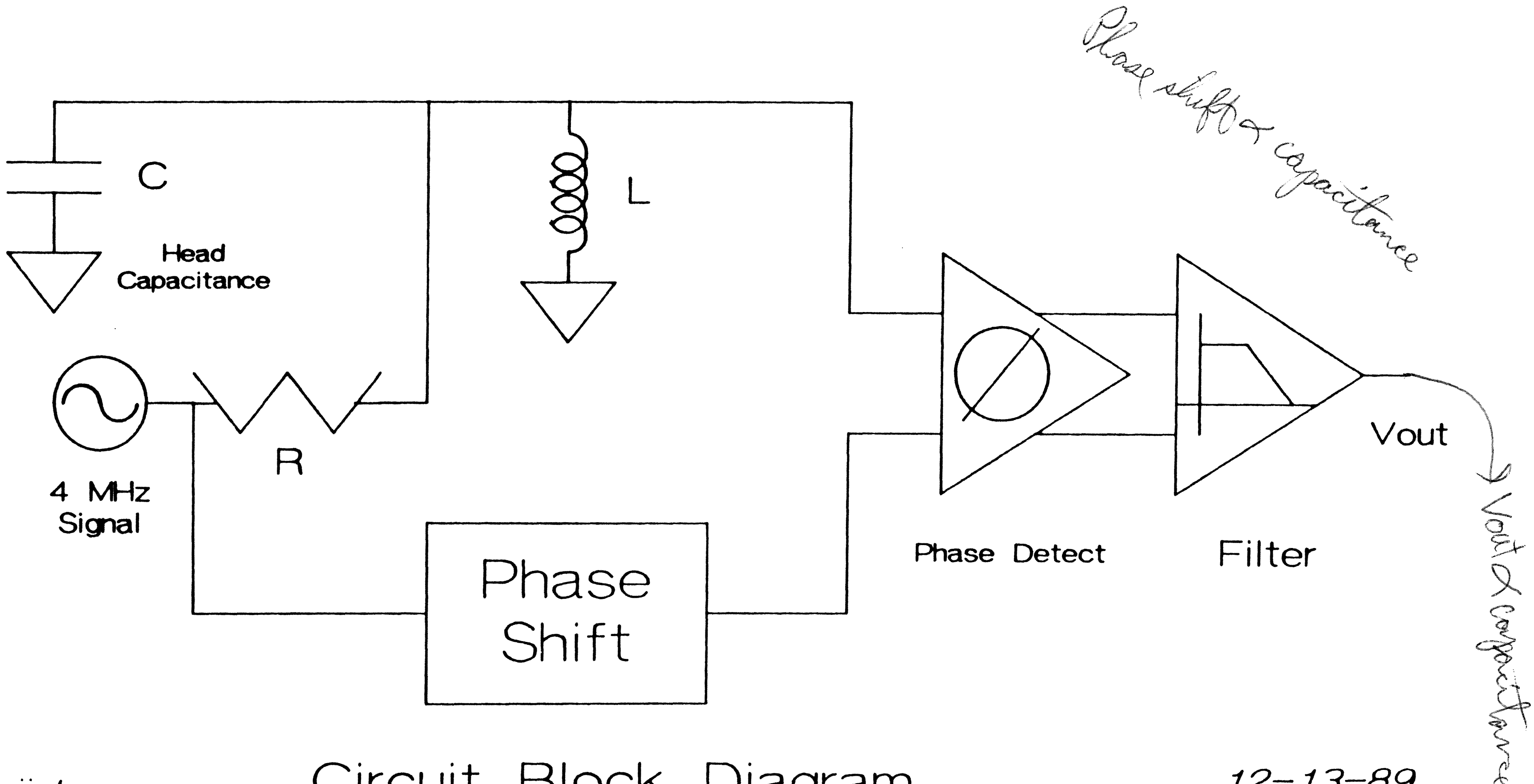

iist Circuit Block Diagram *12-13-89*

CAPACITANCE PROBE HEADS

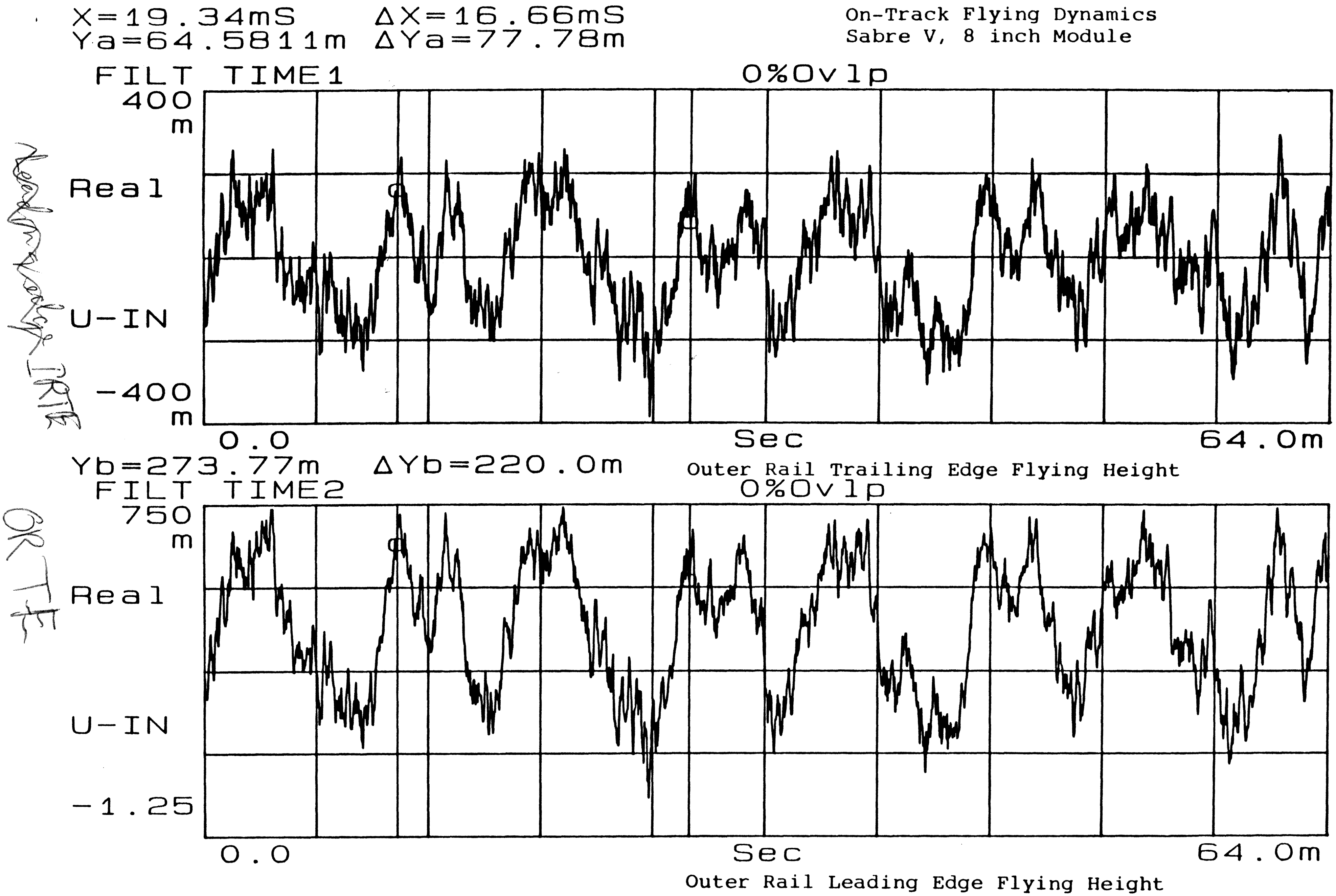

CAPACITANCE PROBE HEAD

X=3.875mSec
Ya=-46.434mU-IN

80 -Track Seek
Sabre V, 8 inch Module

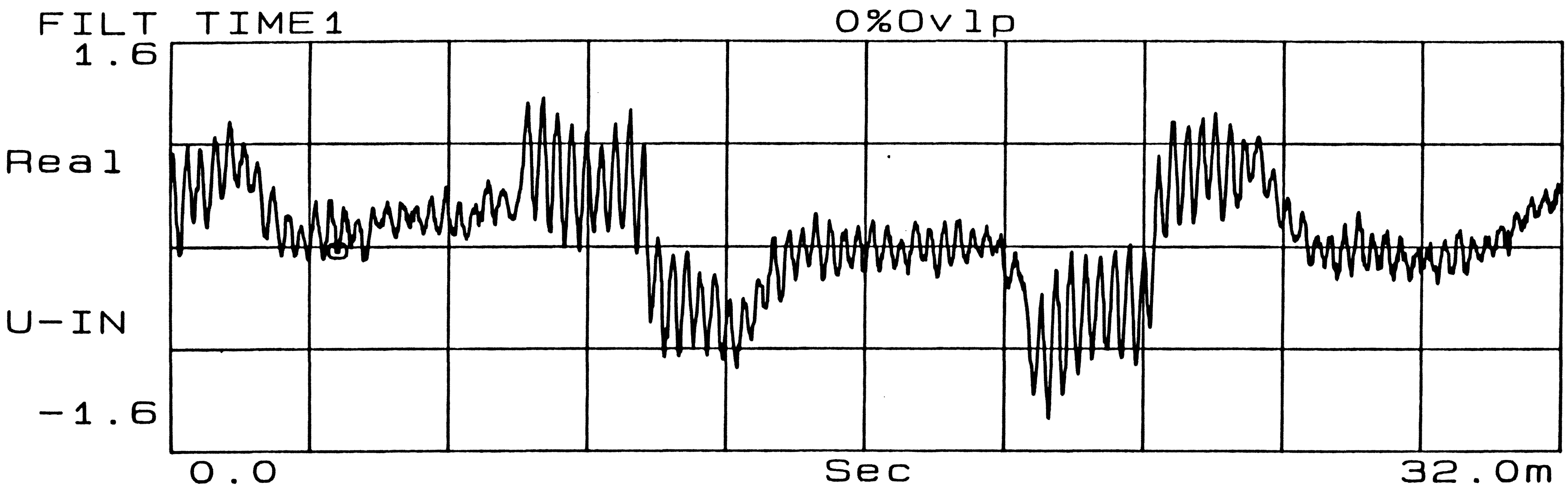

Outer Rail Trailing Edge Flying Height

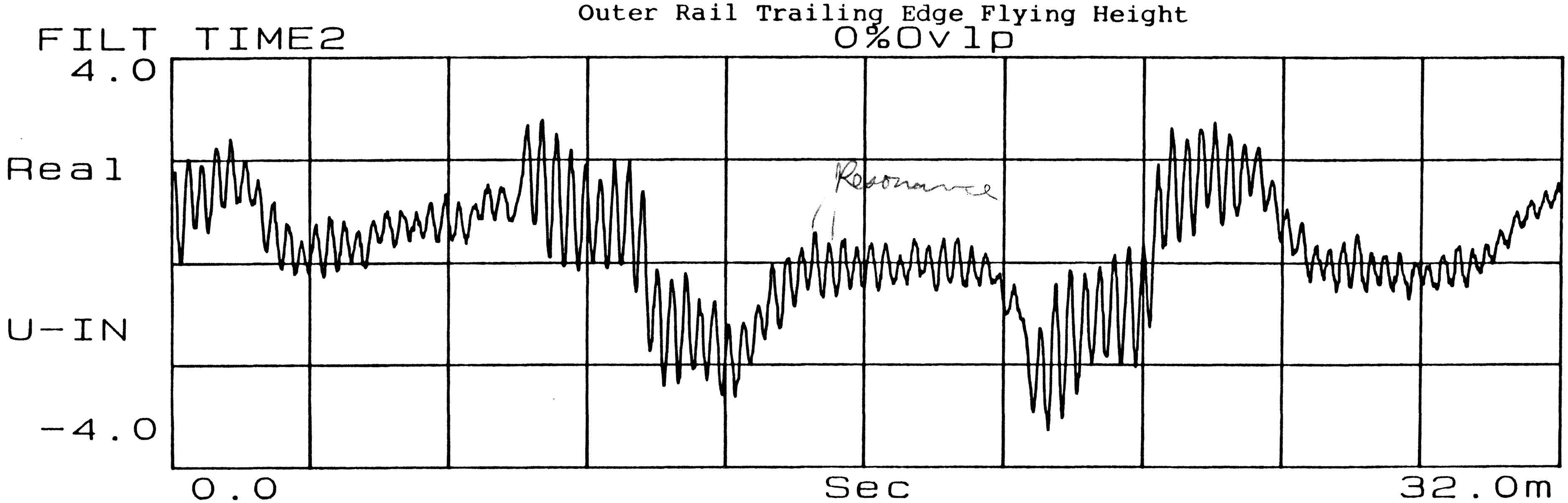

Outer Rail Leading Edge Flying Height

Multiple seeks

CAPACITANCE PROBE HEAD

X=3.875mSec
Ya=78.5405mU-IN

512 Track Seek
Sabre V 8 inch Module

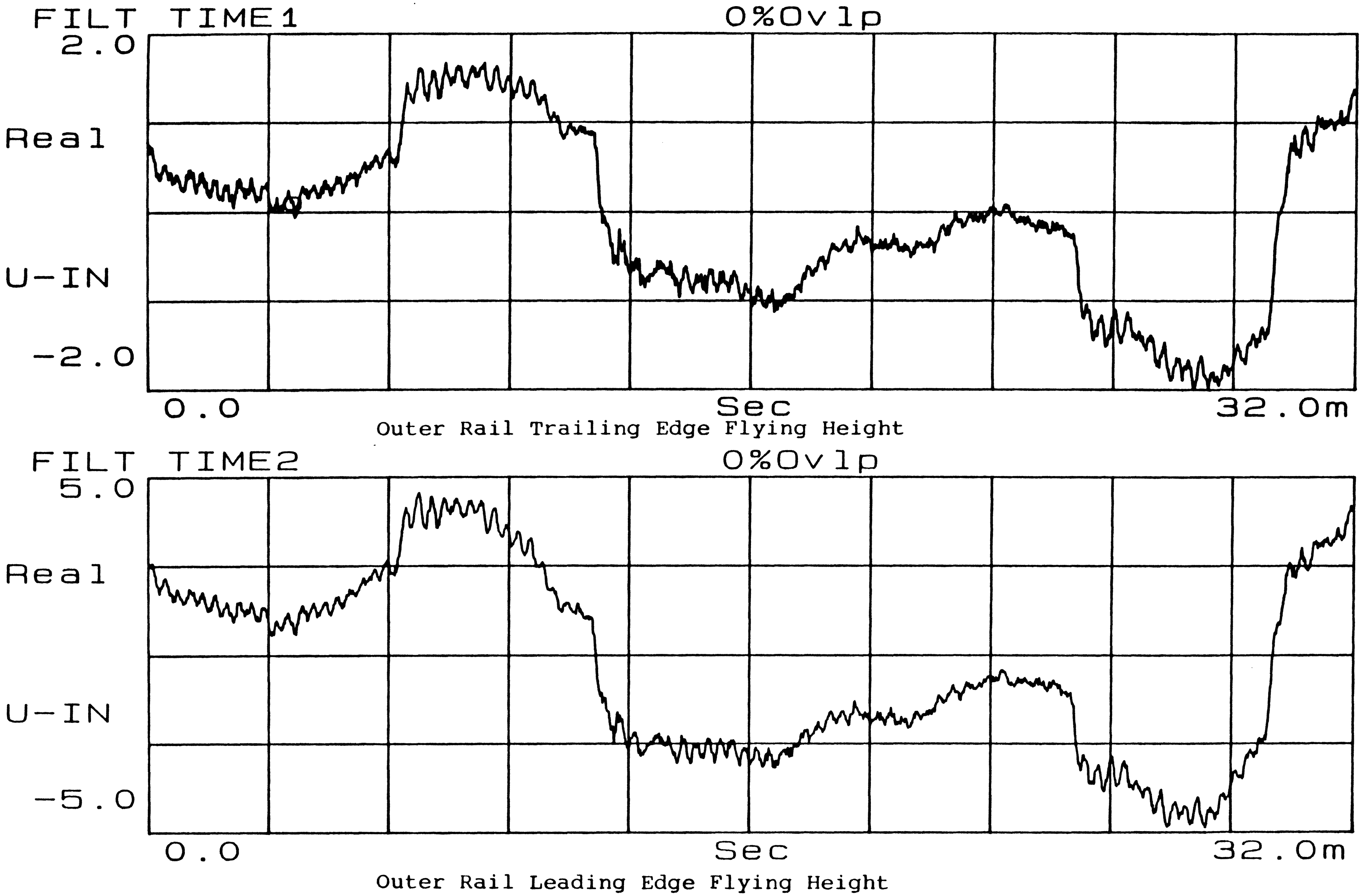

Longer seeks

CAPACITANCE PROBE HEAD

Head Take-Off During Start-up
Sabre V, 8 inch Module

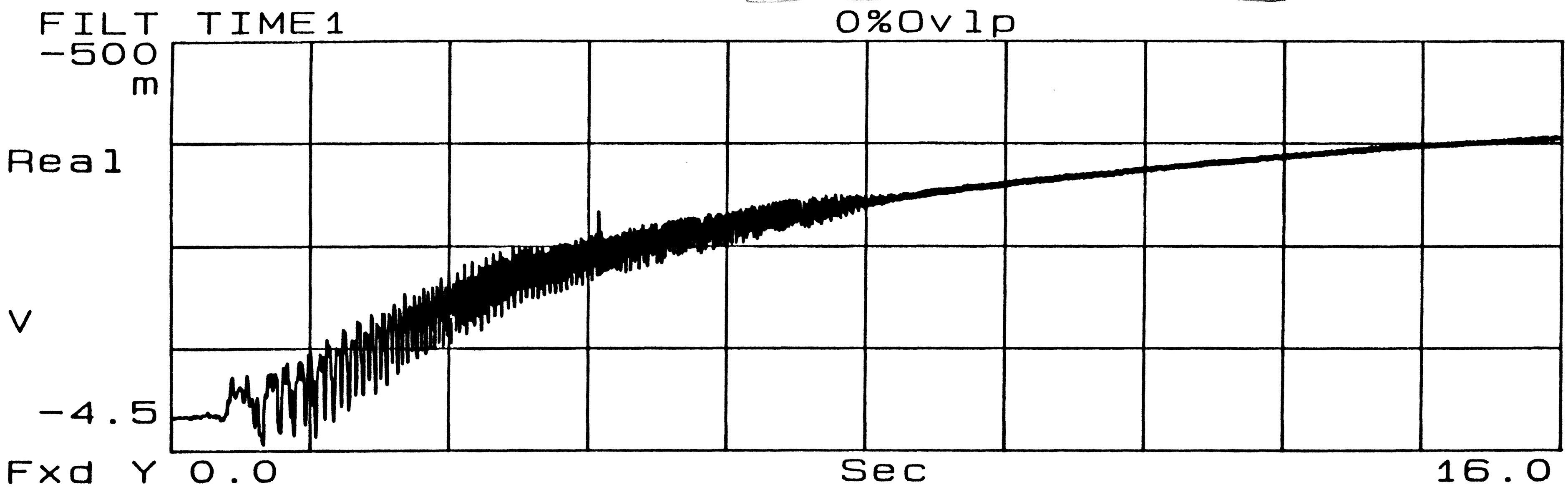

Outer Rail Trailing Edge

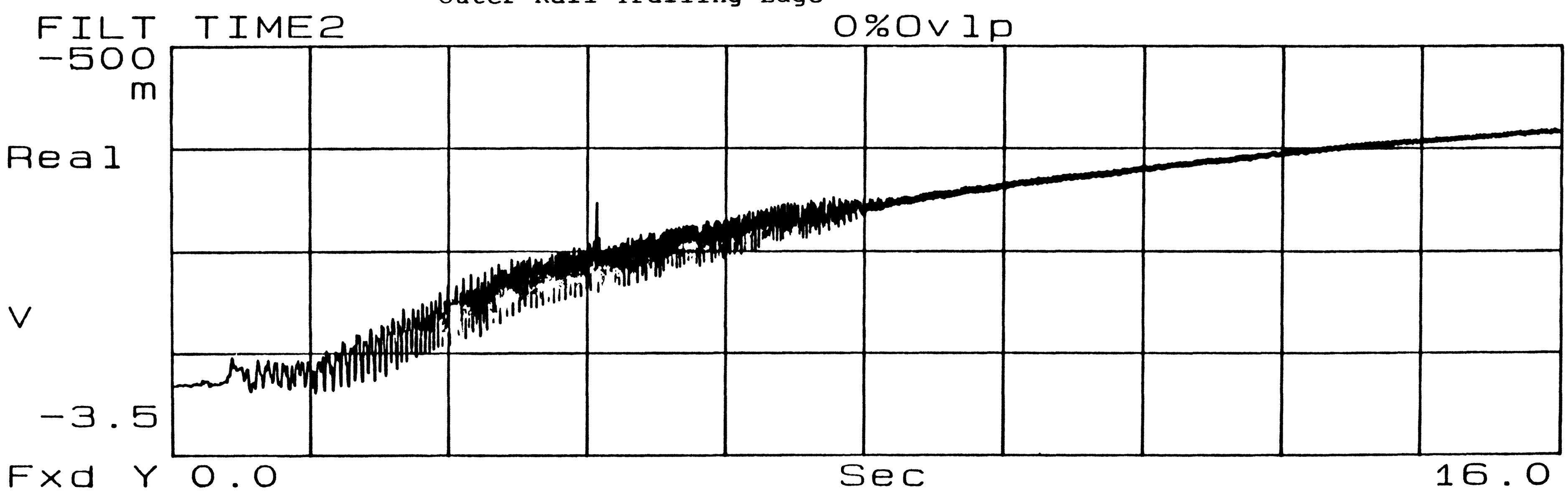

Outer Rail Leading Edge

Seagate

Capacitance Probe Heads

Summary:

- Moderate Bandwidth (50KHz)
- Small Measurement Area (.010 X Rail Width)
- High Resolution (better than .02u")
- Signal Proportional to Capacitance (proportional to 1/h)
- Linear Over Small Range

Seagate

MULTICHANNEL LASER DISPLACEMENT MEASUREMENT SYSTEM

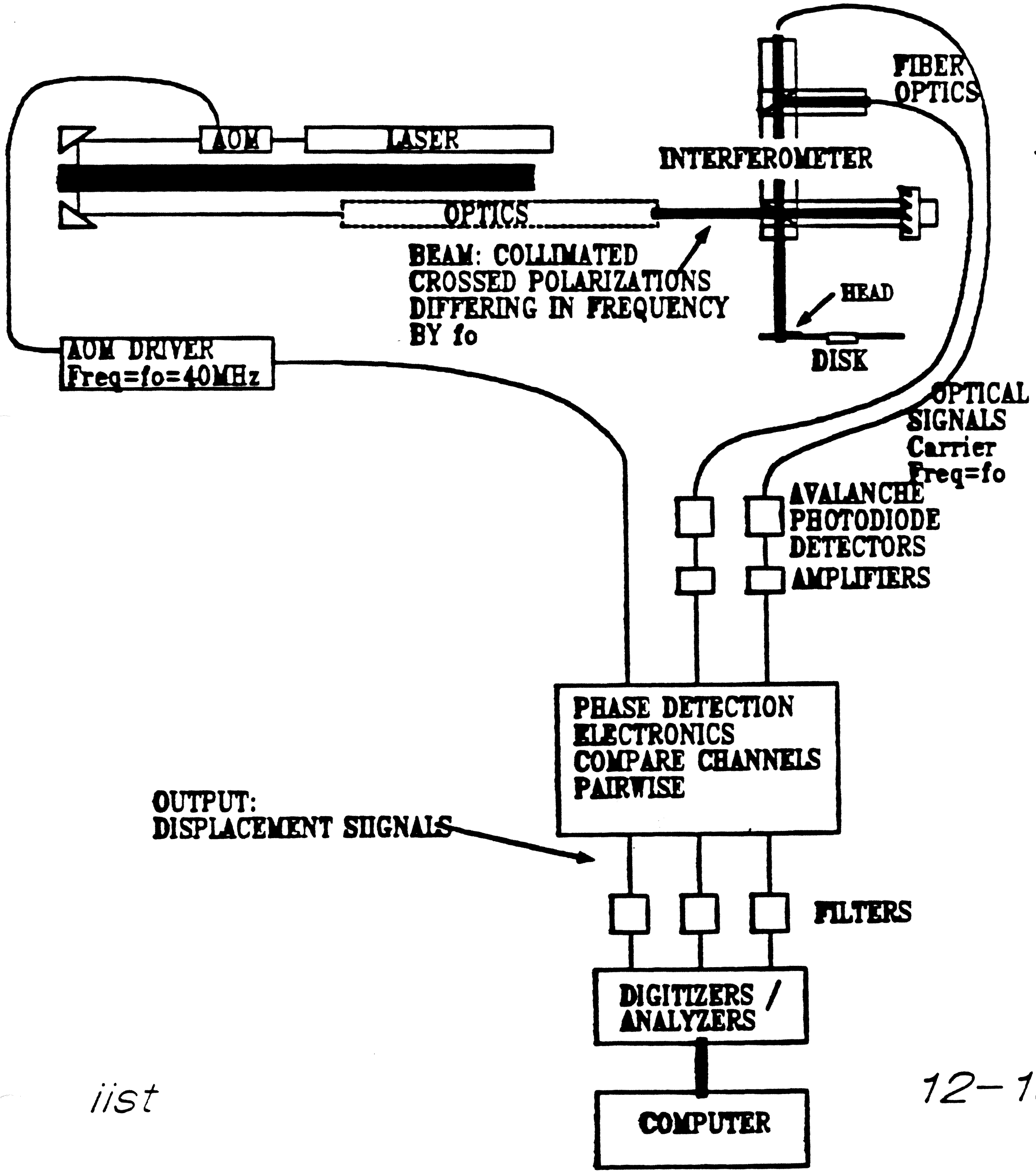

iist

12-13-89

Multi-Channel Laser Displacement Probe (MLDP)

Capabilities:

- On-Track Static and Dynamic Flying Height
- Gimbal Dynamics
- Capacitance Probe Head Calibration
- Disc RVA and High Frequency Displacement

Seagate

Berkeley

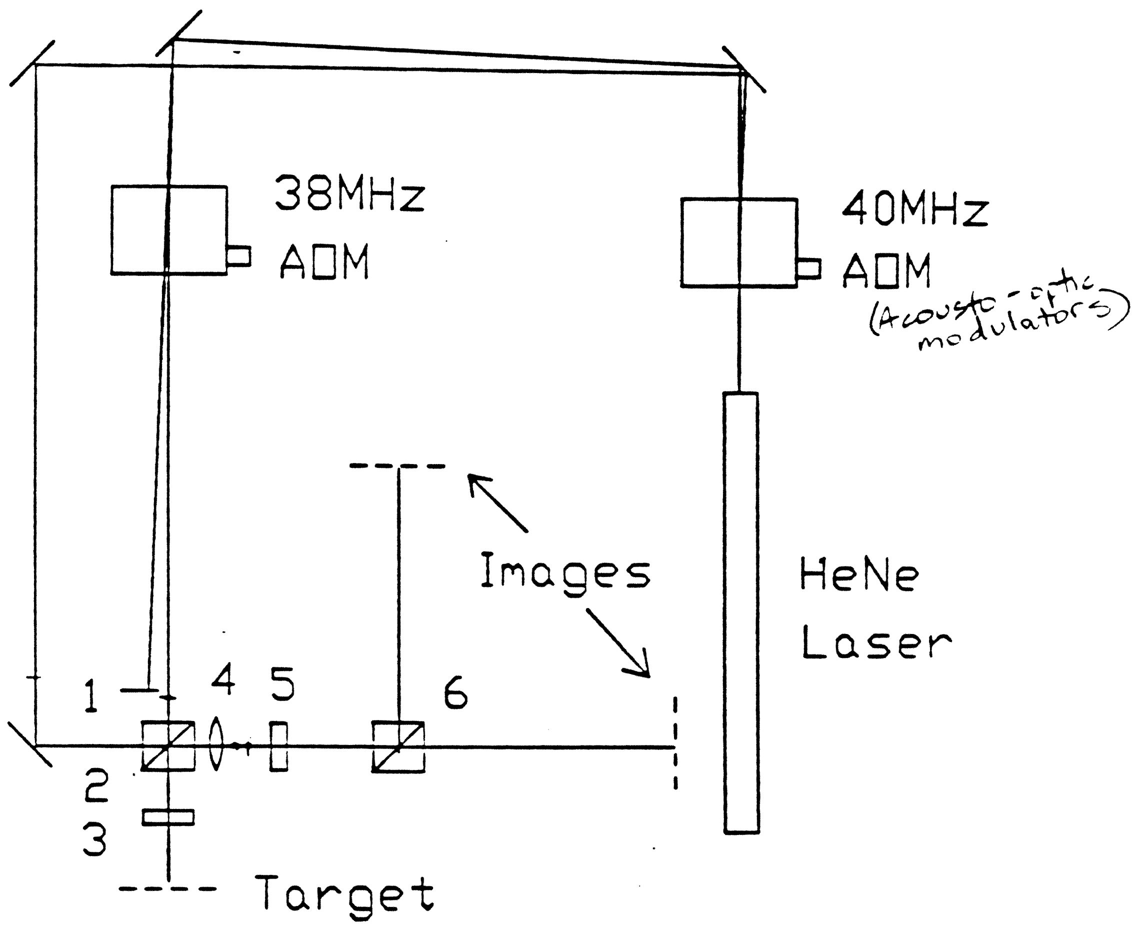

1 stop
2,6 polarizing beamsplitters
3 quarter wave plate
4 lens system
5 half wave plate

iist *12-13-89*

D. Bogy 3/14/88

12-13-89

HP R. J. Davidson

Seagate

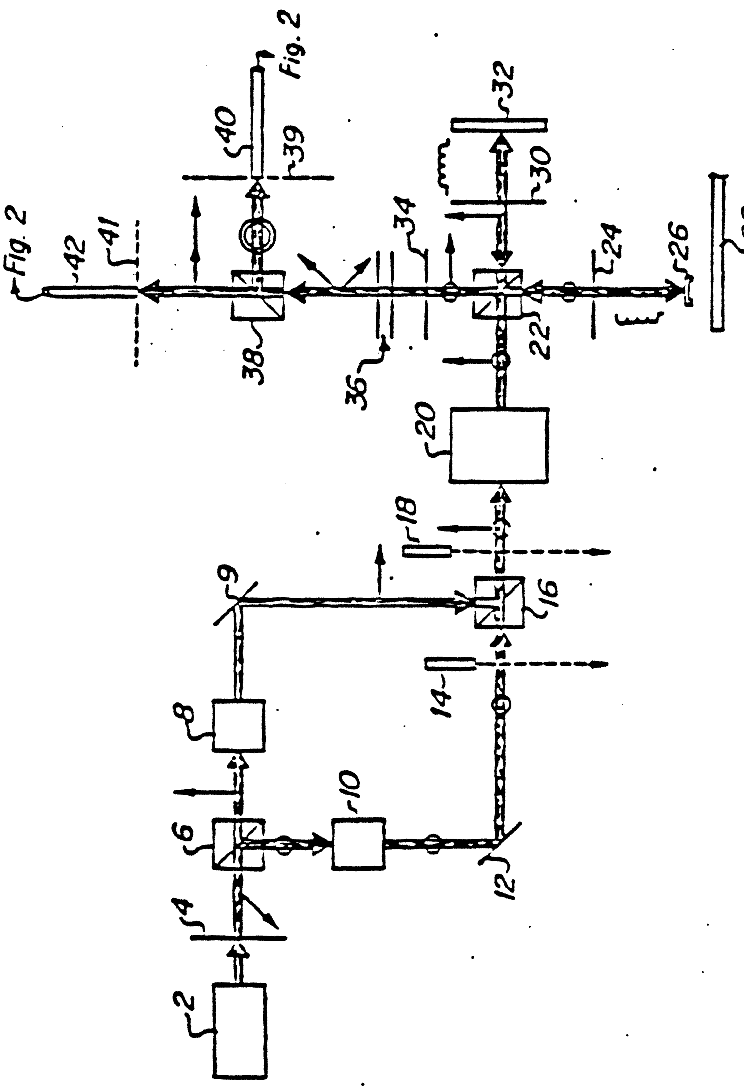

Fig 1

iist

Seagate

MLDP Static Calibration

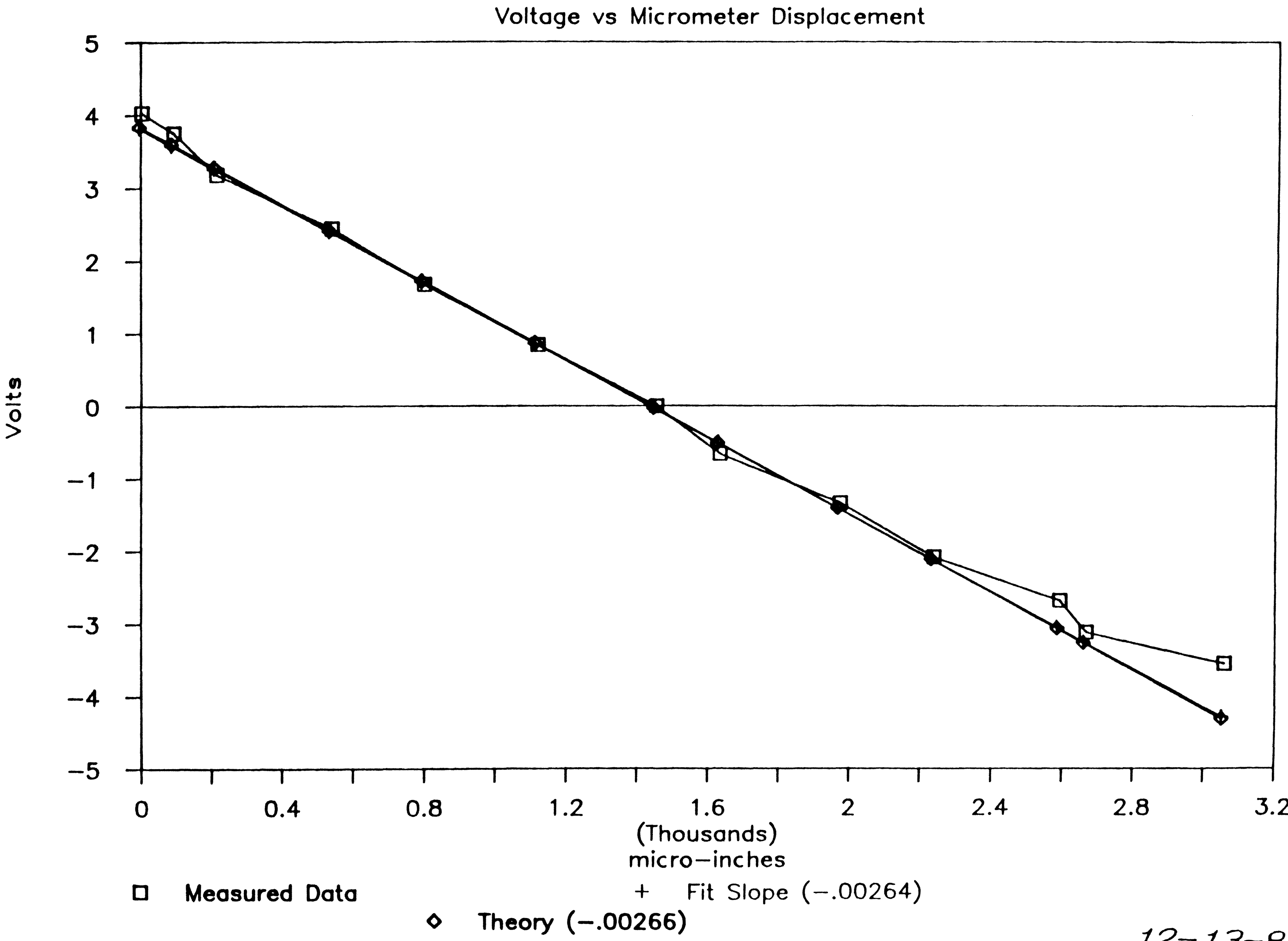

12−13−89

iist

Seagate

Multi-Channel
Laser Displacement Probe

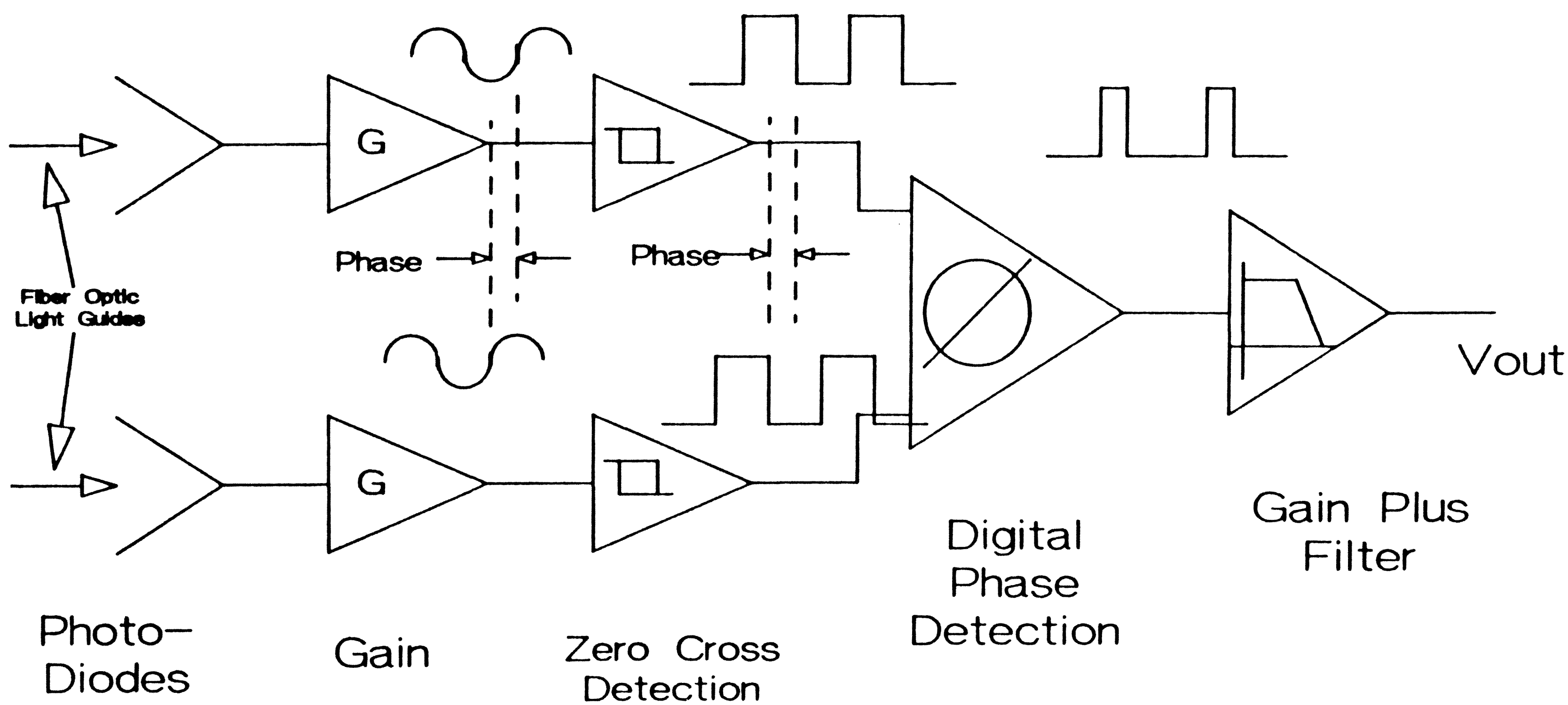

iist Circuit Block Diagram *12-13-89*

Seagate

Multi-Channel Laser Displacement Probe

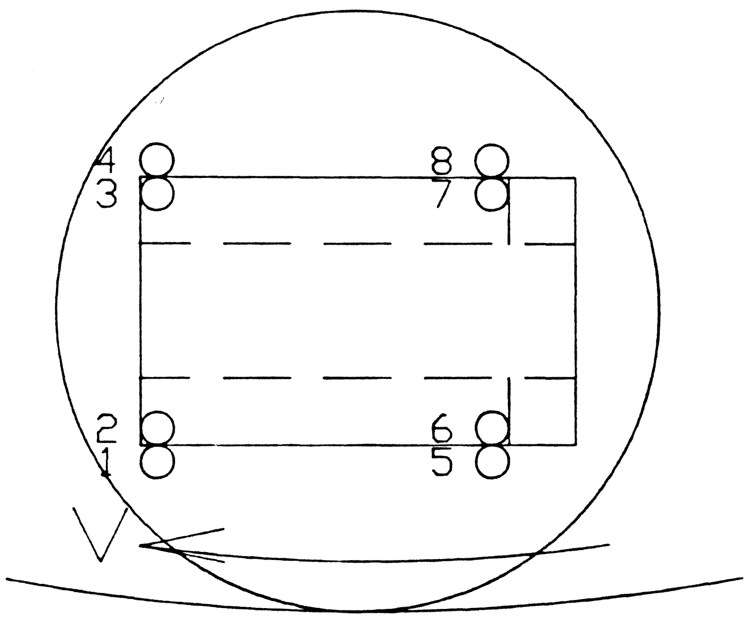

Location of Measurement Spots for Four Corner Flying Height Measurement

iist

12-13-89

Seagate

Multi-Channel Laser Displacement Probe (MLDP)

Summary:

- Wide Bandwidth (>200KHz)
- Small Measurement Spot (.004")
- High Resolution (better than .02u")
- Direct Displacement Signal
- Multiple Simultaneous Channels
- Measures Standard Heads on Standard Discs

Seagate

Acoustic Emission Sensing of Head Disc Interference

- Head Disc Contact Durung Operation Causes Vibration of Head and Other Components
- Vibrations are Transmitted Through Solids as Ultrasonic Waves
- These can be Sensed by Acoustic Emission Sensors Coupled to the Solid Surface

iist

12-13-89

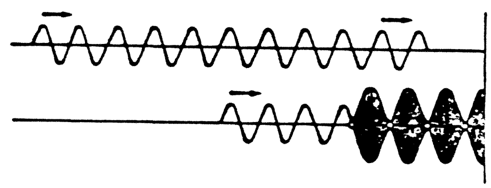

Fig. 1.9 Standing wave through reflection on free wall. Plotted is the amplitude of the particles. At the free wall it has an antinode.

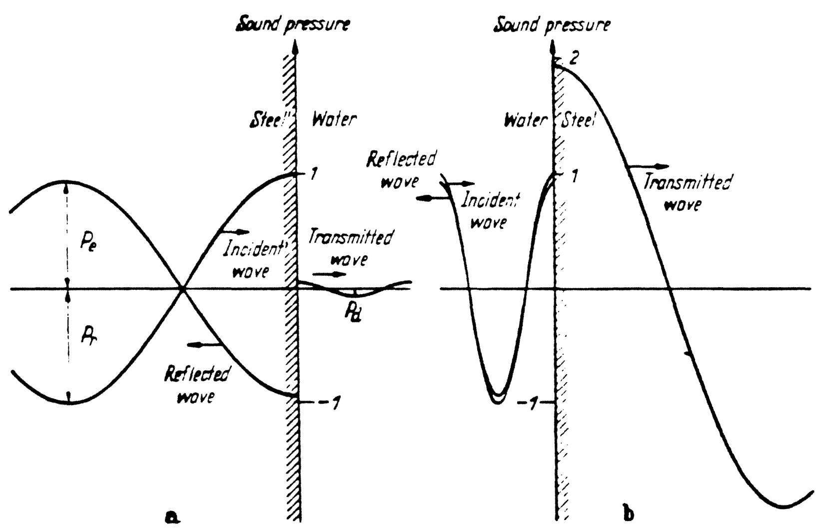

Fig. 2.1 Sound pressure values in the case of reflection on the interface steel/water, incident wave in steel (*a*) or in water (*b*).

Seagate

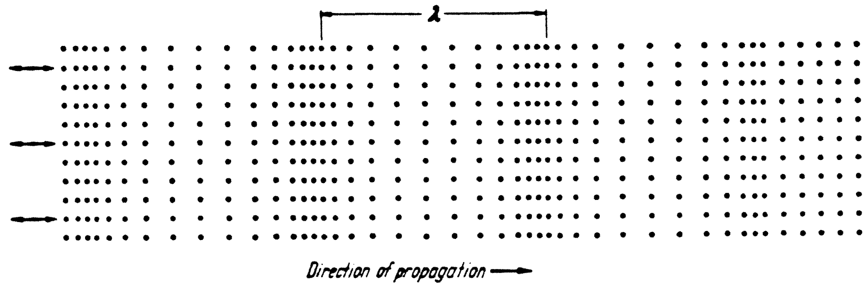

Fig. 1.3 Longitudinal wave.

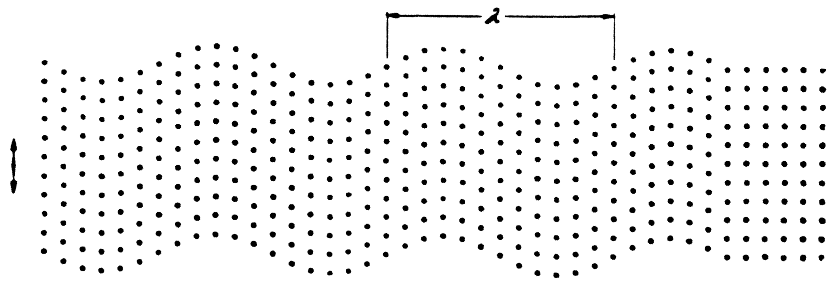

Fig. 1.4 Transverse wave.

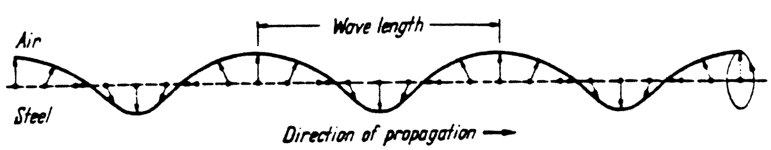

Fig. 1.5 Surface wave on steel. On the right, oscillation ellipse of a particle and sense of rotation (calculated according to [34], ratio of axes 0.44:1).

Ultrasonic Testing of Materials, J. Krautkramer and H. Krautkramer, 3rd revised Ed., Springer-Verlag, NY, 1983.

Seagate

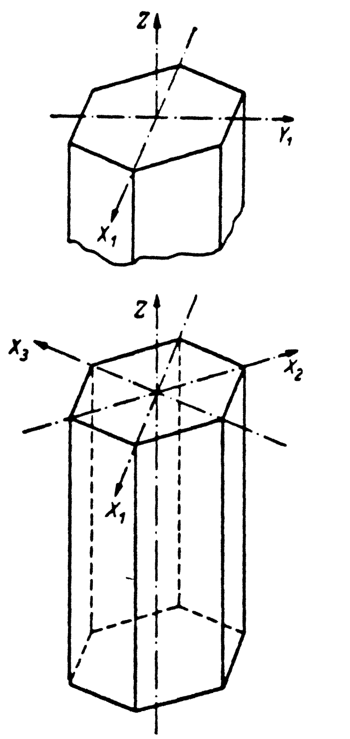

Fig. 7.1 Position of crystal axes in quartz (idealized crystal).

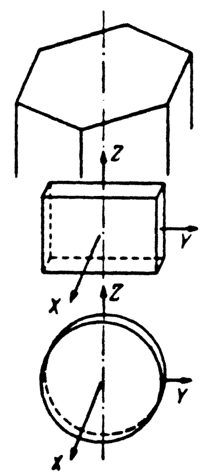

Fig. 7.2 Orientation of sections for rectangular and round X-cut quartz plates.

Seagate

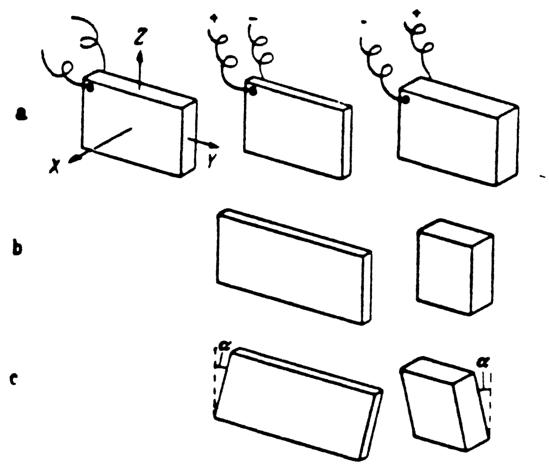

Fig. 7.3 Deformation of an X-cut quartz plate with dimensions $x \times y \times z = 5 \times 30 \times 20$ mm, at a voltage of 1000 V, drawn on an exaggerated scale of 1,000,000:1. (*a*) Change of thickness alone; (*b*) with additional change of width (*Y*-direction); (*c*) with additional shear (in the *Y*, *Z* plane).

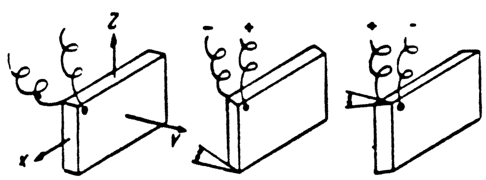

Fig. 7.4 Deformation of a Y-cut quartz plate, dimensions and voltage as above, angle of shear exaggerated on a scale 200,000:1. To this must be added the shear in the *Z*-*X*-plane, as in the case of the X-cut.

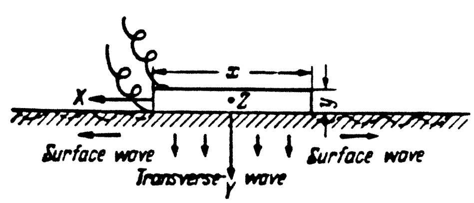

Fig. 7.5 In the solid material the Y-cut quartz plate generates a transverse wave normal to the surface, and a surface wave in the X-direction. The latter is particularly strong in the case of steel if $x:y \sim 7:1$.

Seagate

HP 5183T DIGITIZING OSCILLOSCOPE   Fri, 1 Dec 1989, 09:25:35

"760_rep" ; ADC ; Compressed 16X
X : 1.6384E-3 (s)/div ; Zoom 16384 ; Position 1
Y : 50.00E-3 (V)/div ; Center 0E+0

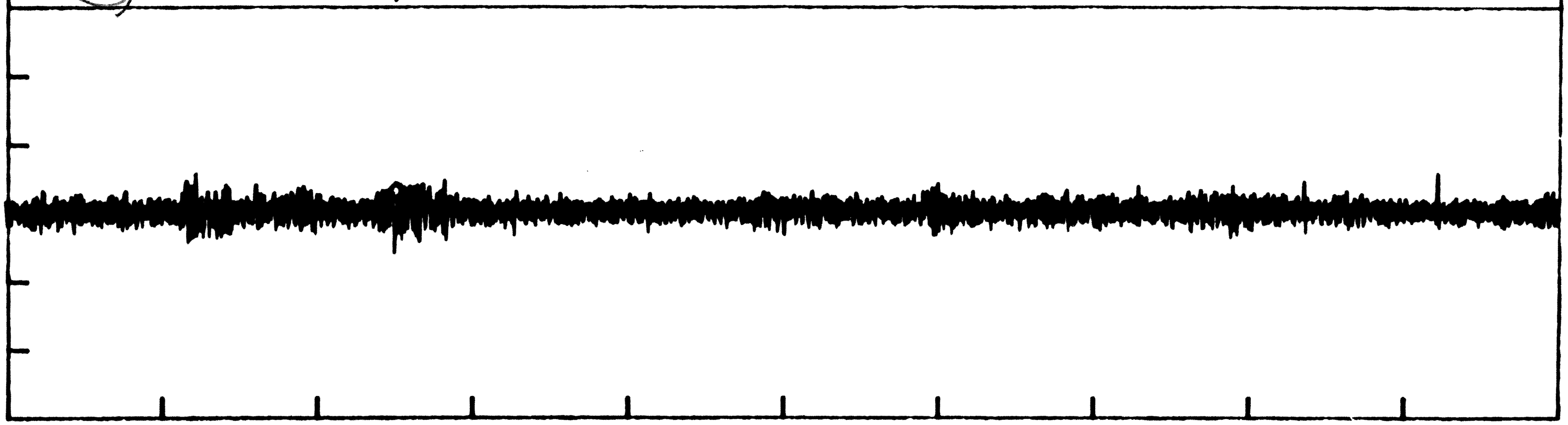

"110_rep" ; ADC ; Compressed 16X
X : 1.6384E-3 (s)/div ; Zoom 16384 ; Position 1
Y : 250.0E-3 (V)/div ; Center 0E+0

110 Torr in vacuum

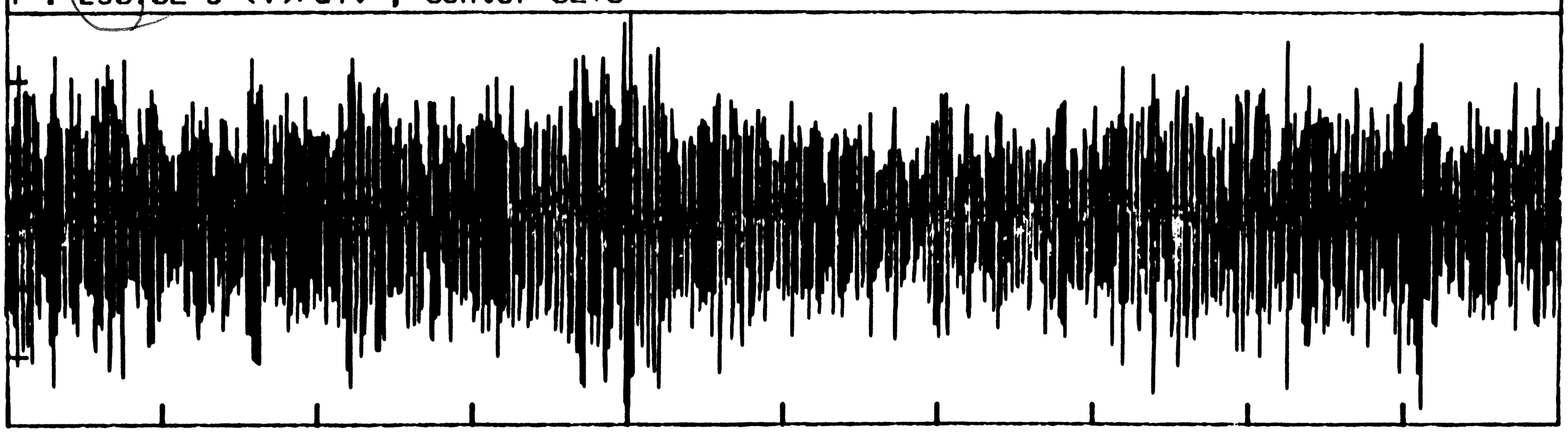

iist   12-13-89

Seagate

HP 5183T DIGITIZING OSCILLOSCOPE **Fri, 1 Dec 1989, 09:37:24**

* : 320.068359375E+3 Hz; 39.38368E+0 dBV
o : 419.189453125E+3 Hz; 40.52895E+0 dBV

"ANALYSIS1" ; Subtract ; Compressed 4X
X : 50.0000000000E+3 (Hz)/div ; Zoom 2048 ; Position 1
Y : 10.00000E+0 (dB)/div ; Center 22.4135E+0

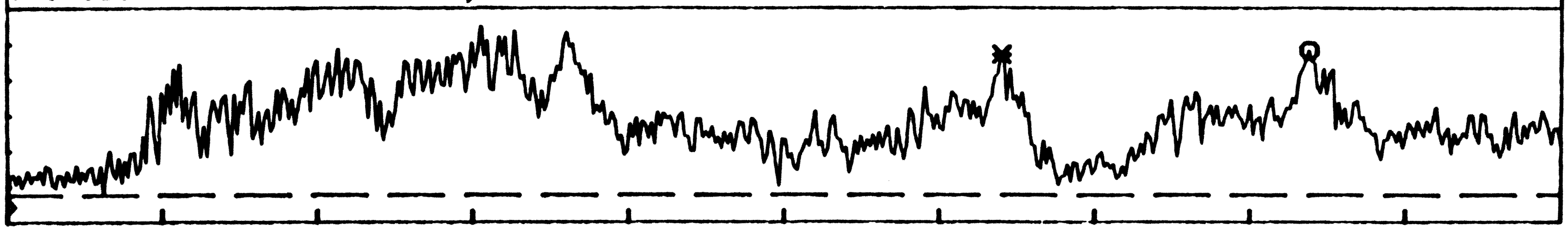

"110_IV_0" ; FFT Spectrum in dBV; Window Hann ; Compressed 4X
X : 50.0000000000E+3 (Hz)/div ; Zoom 2048 ; Position 1
Y : 10.00000E+0 (dB)/div ; Center -56.3578E+0

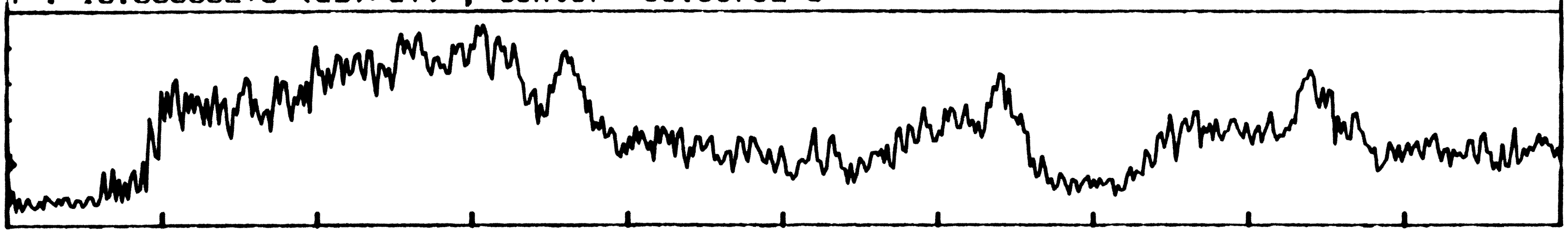

"760_IV_0" ; FFT Spectrum in dBV; Window Hann ; Compressed 4X
X : 50.0000000000E+3 (Hz)/div ; Zoom 2048 ; Position 1
Y : 10.00000E+0 (dB)/div ; Center -73.3026E+0

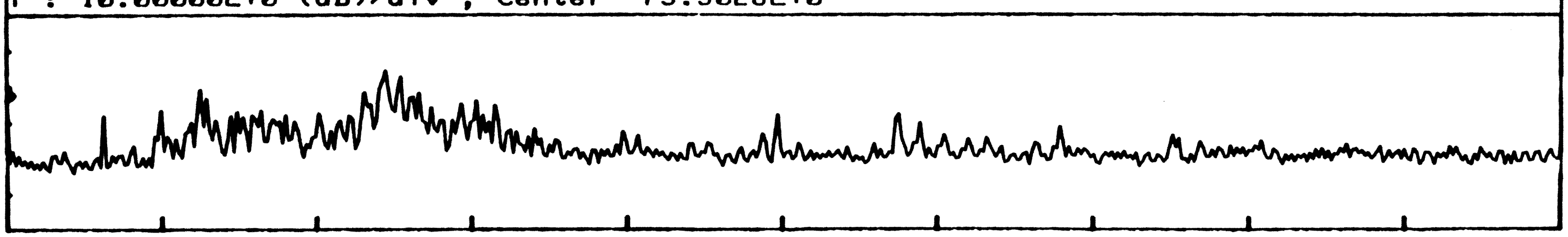

Seagate

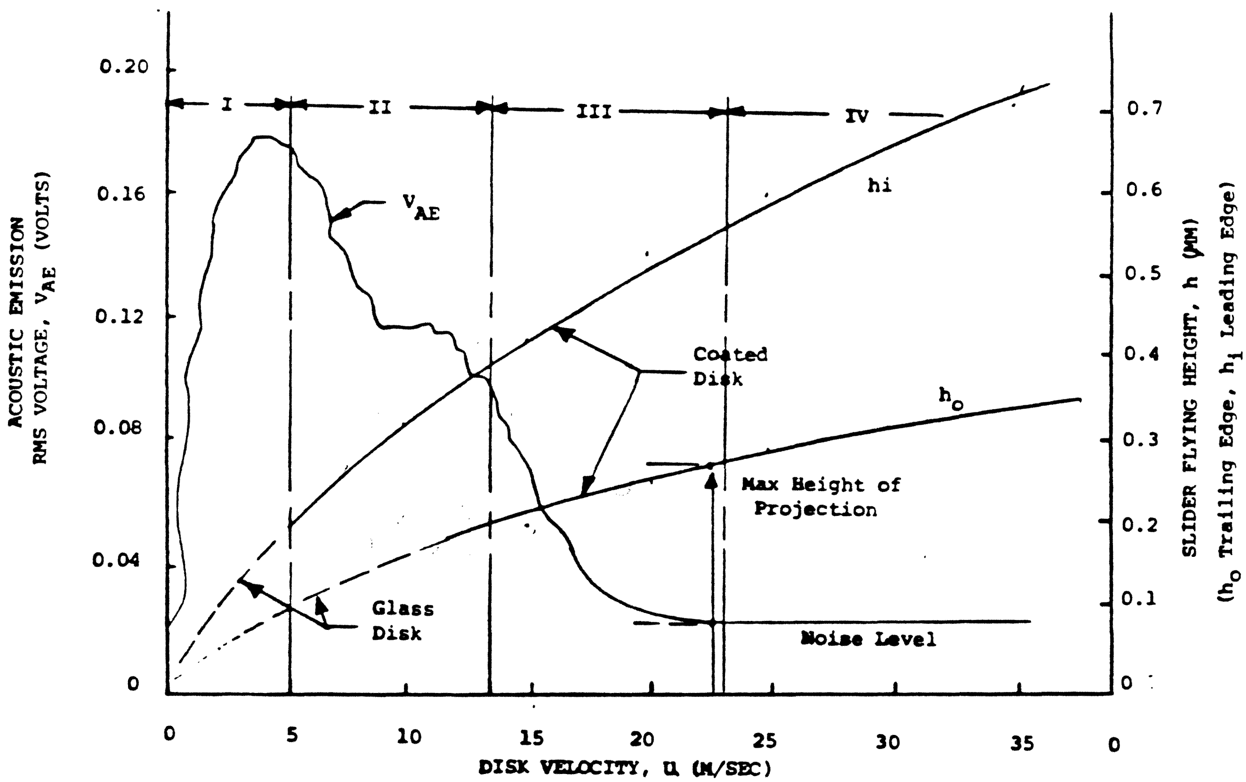

ACOUSTIC EMISSION VOLTAGE AND SLIDER FLYING HEIGHT VERSUS DISK VELOCITY

FIGURE 1 (KITA, etal)

Seagate

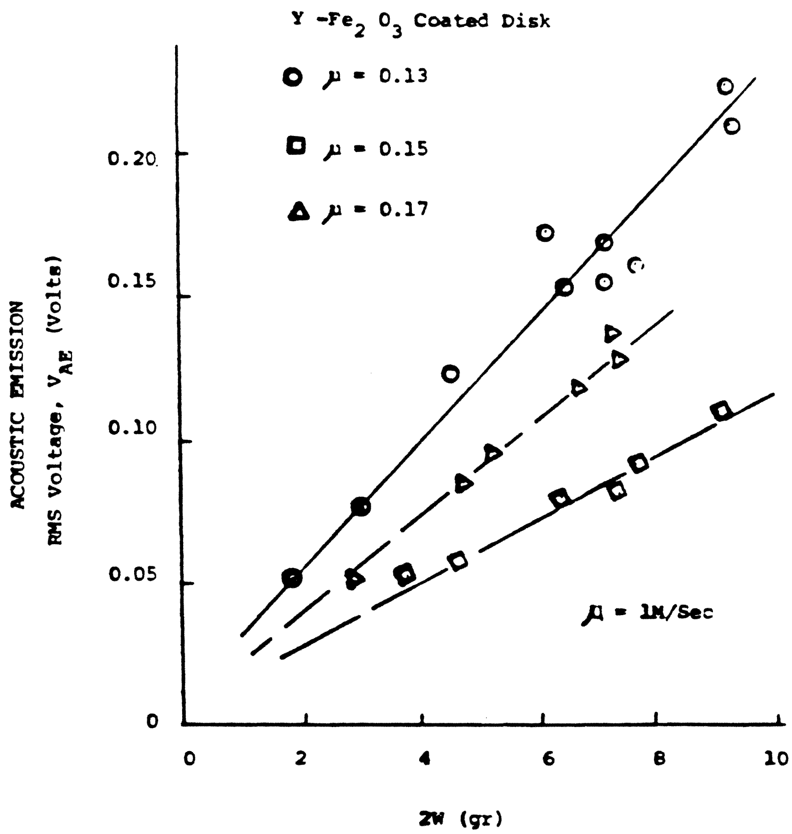

ACOUSTIC EMISSION VOLTAGE VERSUS LOAD APPLIED TO SLIDER FOR DIFFERENT COEFFICIENTS OF FRICTION

FIGURE 2

(KITA, ETAL)

Seagate

Measurement of Flying Height Variation by Readback Signal Demodulation

iist

12-13-89

Seagate

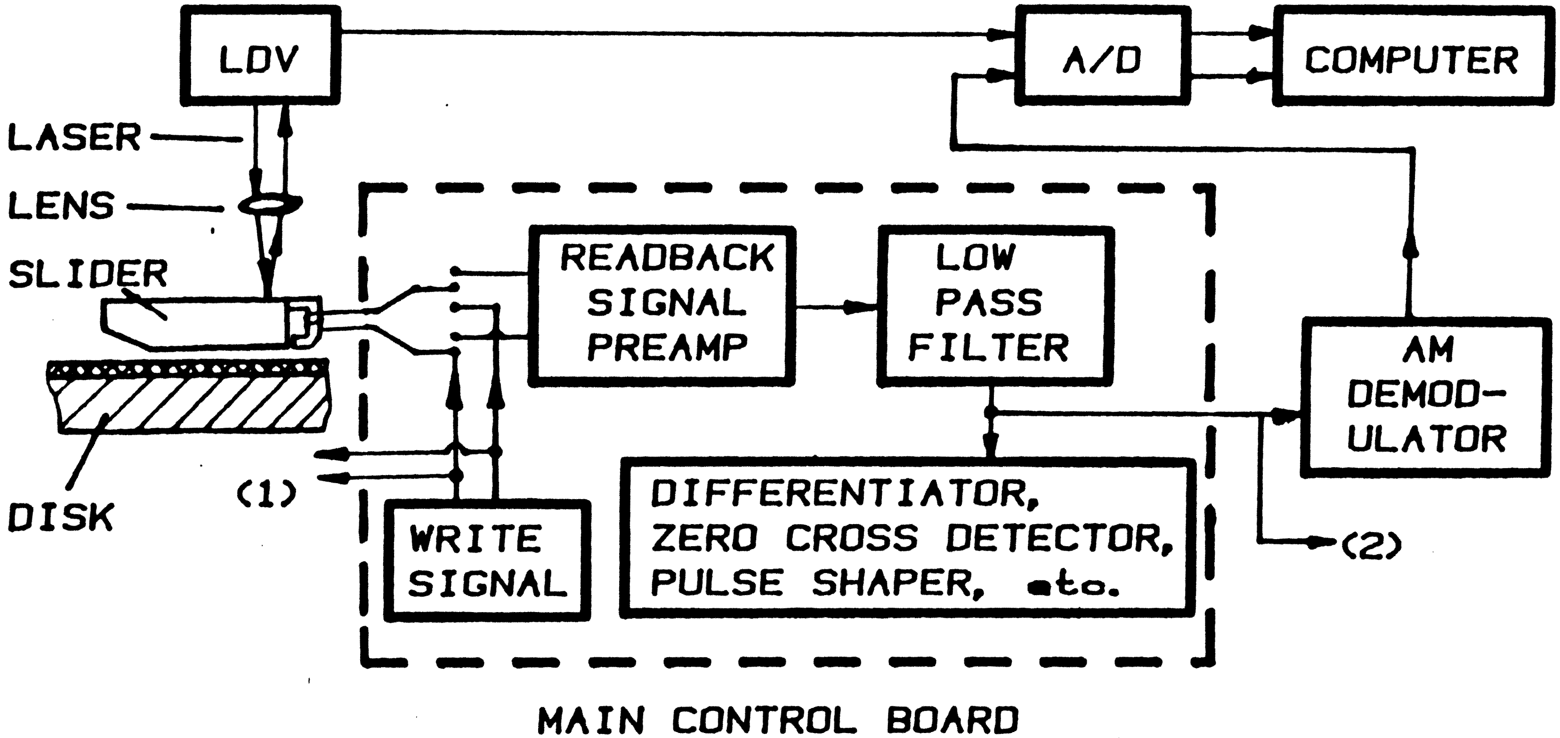

Fig. 2 Schematic of the measurement system. The "main control board" is one of the two circuit boards that comes with a Seagate ST 412 disk file.

Seagate

$$e(t) = 4\pi\left(10^{-8}\right)N\alpha W\left(\frac{\mu}{\mu+1}\right)Mv\left(1-e^{-2\pi\delta/\lambda}\right)G(\lambda)$$

$$\cdot e^{-2\pi d/\lambda}\cos\left(\frac{2\pi vt}{\lambda}\right)$$

Wallace Equation

where
- e = voltage of the readback signal (V)
- t = time (s)
- N = number of turns of the readback coil
- α = head effeciency $(0<\alpha<1)$
- W = head width (cm)
- μ = core permiability
- M = peak remnant magnetization of the medium (emu/cc)
- v = tangential velocity (cm/s)
- δ = medium thickness (cm)
- λ = wavelength of the recorded signal
- $G(\lambda)$ = gap length factor
- d = head to medium spacing (cm)

$$E = C \cdot e^{-2\pi d/\lambda}$$

where

- E = The amplitude of the readback signal e(t)
- C = a constant derived from the remaining terms in the Wallace Equation

The modulation due to spacing variations are:

$$A = \frac{E(d)-E(d_0)}{E(d_0)}$$

The spacing variation itself, then is:

$$y(t) = -\frac{v}{2\pi f}\ln(1+A(t)) = -\frac{v}{2\pi f}\ln\left(\frac{E(d)}{E(d_0)}\right)$$

Shi, W. K., L. Y. Zhu, and D. B. Bogy, "Use of Readback Signal Modulation to Measure Head/Disk Spacing Variations in Magnetic Disk Files," IEEE Trans. Mag., Vol. MAG-23, No. 1, Jan. 1987.

Wallace, R. I. Jr.,"The Reproduction of Magnetically Recorded Signals," The Bell Tech. J., pp. 1145-1173, 1951.

Seagate

- Oscillation of recording head at its natural frequency due to a disturbance causes modulation of the read-back signal

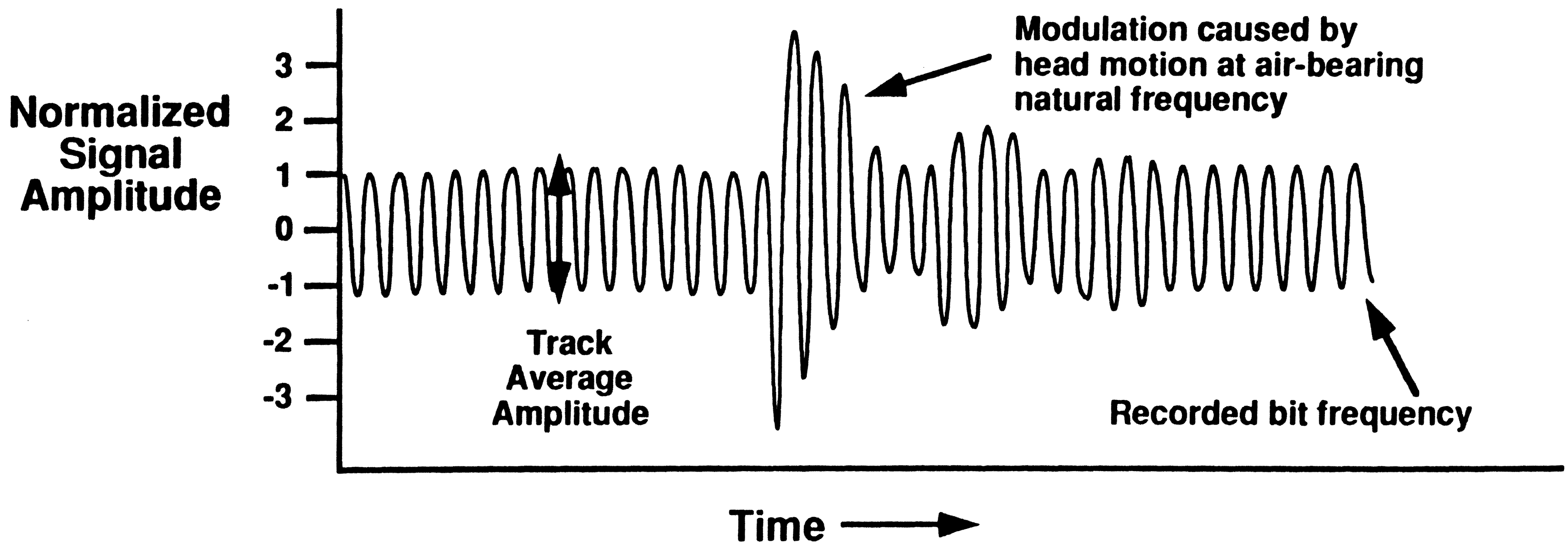

Seagate

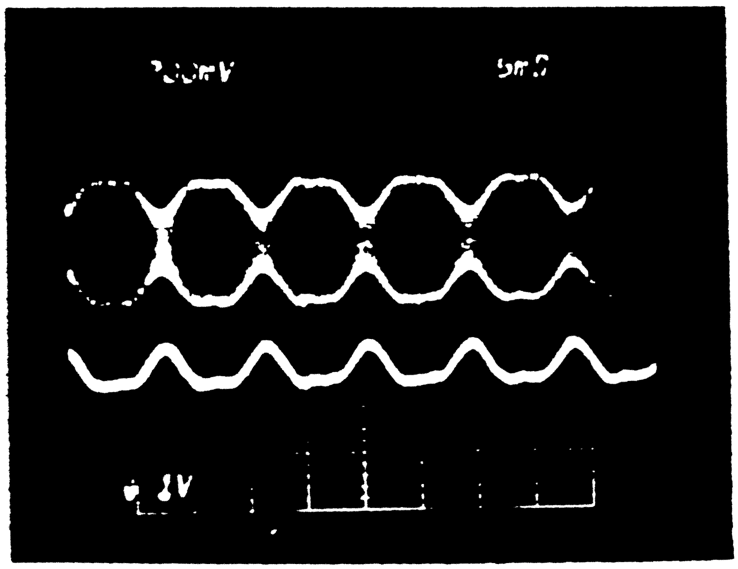

Fig. 5 Modulated carrier and envelope. Top: modulated carrier (2.5 MHz readback signal). Bottom: output of the AM demodulator.

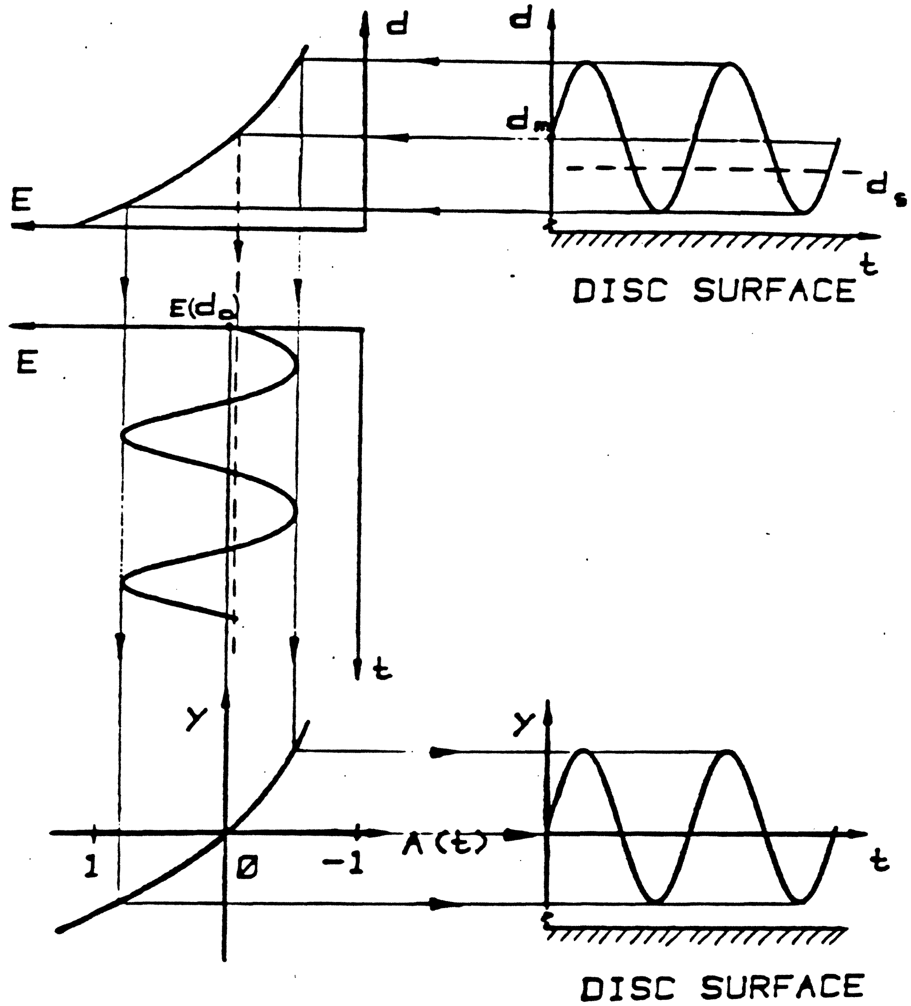

Fig. 13. Measurement of the steady-state spacing oscillation. In the direction of arrows, plots of: d(t), eqn.(2), E(t), eqn.(8) and y(t). Note: 1) The mean spacing d_m is the "zero" of LDV output, but does not appear directly in the RSM result; 2) The mean of E(t) is taken as $E(d_o)$ to compute A(t), but the corresponding d_o has no physical significance; 3) The steady flying height d_s appears in neither the LDV nor RSM result, and d_m is usually above d_s due to the nonlinear air bearing.

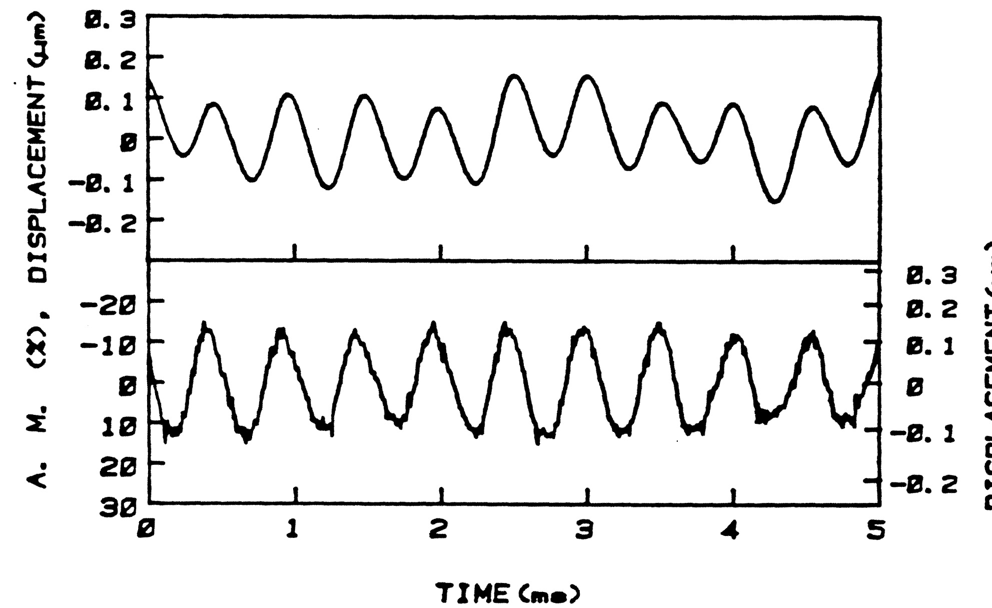

Fig. 6 Response to a harmonic excitation on the flexure. Top: LDV measurement of slider displacement. Bottom: RSM measurment of amplitude modulation (left scale) and spacing variation (rignt scale).

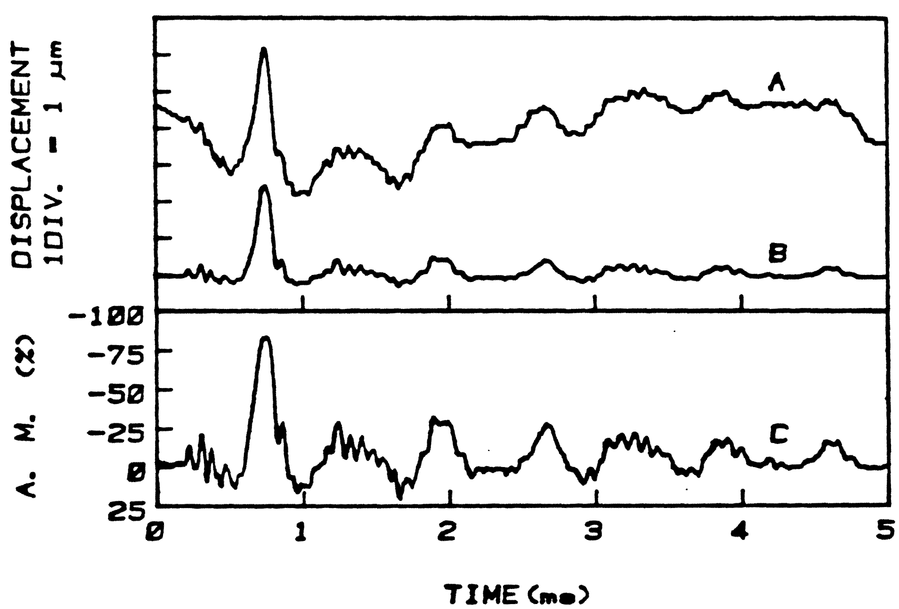

Fig. 7 Impulse excitation on the flexure. Trace A: LDV measurement of slider displacement. Trace B: RSM measurement of spacing variation, calibrated from trace C by use of Eqn. (6). Trace C: RSM measurement in terms of amplitude modulation.

Seagate

Glide Head Sensing of Head Disc Interference

- Highly Sensitive Head/Disc Contact Detection
- PZT Crystal Couples to Contact Induced Plate Mode Bending the Slider Body
- Each Oscillation Burst Represents One Contact Event

iist *12-13-89*

Seagate

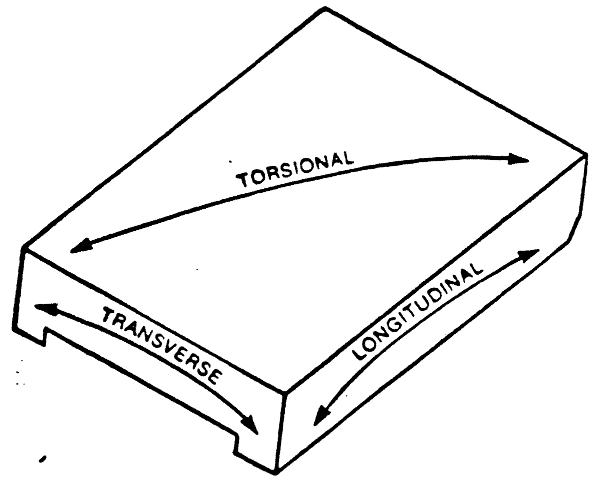

Figure 1. 3380-type slider with arrows indicating the torsional, longitudinal and transverse fundamental plate vibrational modes.

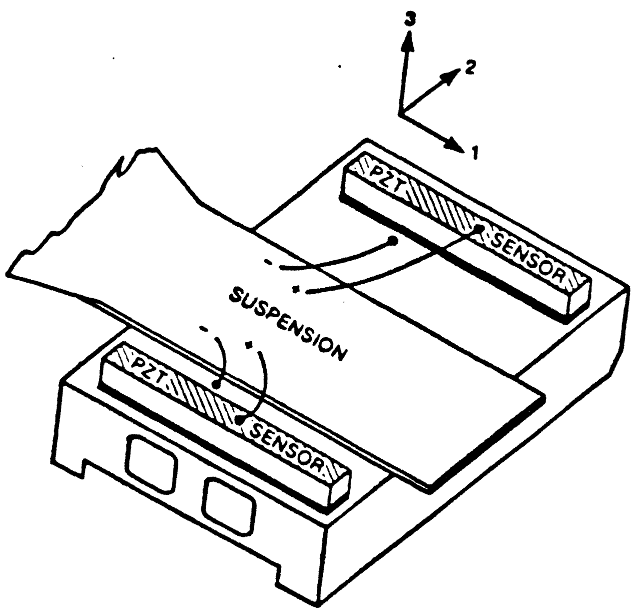

Figure 2. Mounting arrangement of PZT transducers on 3380-type slider on suspension.

iist 12-13-89

Wallash, A., "Reproduction of Slider Vibrations During Head/Disk Interactions Using PZT Sensors," Intermag, 1988, Paper GF-11.

Seagate

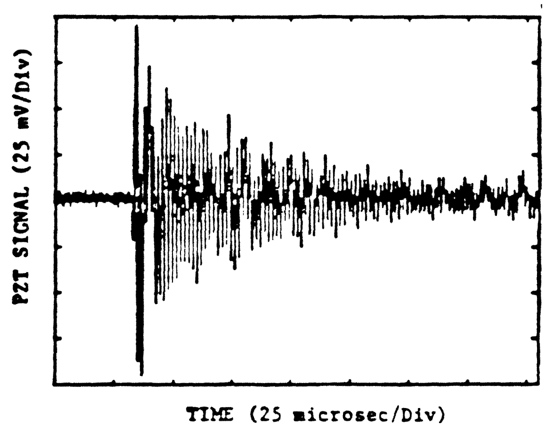

Figure 3. PZT signal due to typical disk asperity while flying.

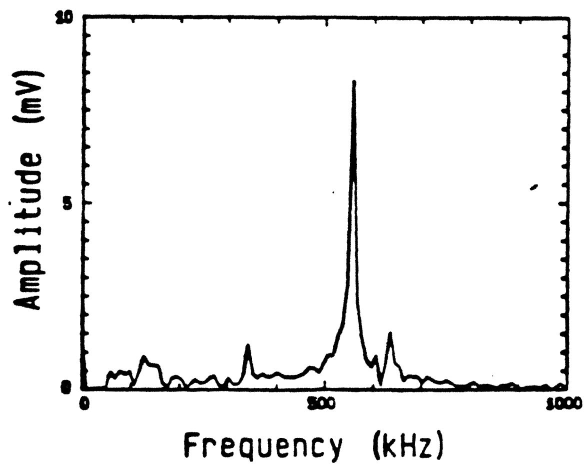

Figure 4. FFT of typical PZT signal shown in Fig. 3. Peaks at 330, 550 and 634 kHz.

Seagate

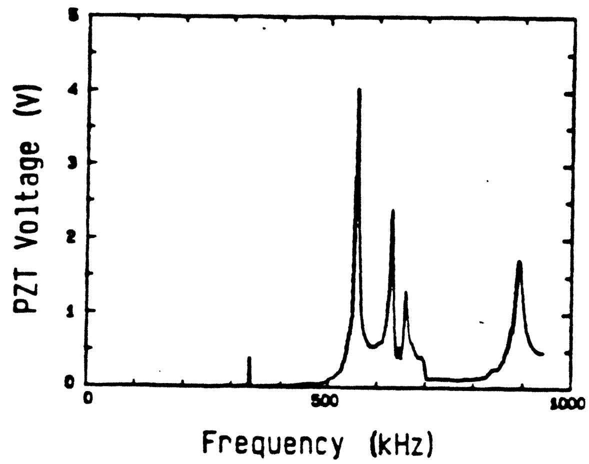

Figure 5. Output PZT amplitude versus frequency of input voltage.

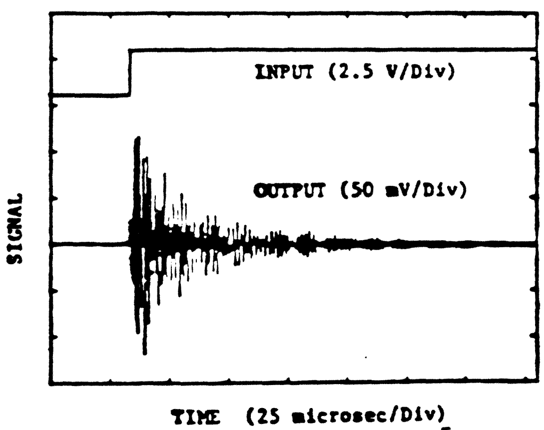

Figure 6. Input voltage and Output PZT signal versus time.

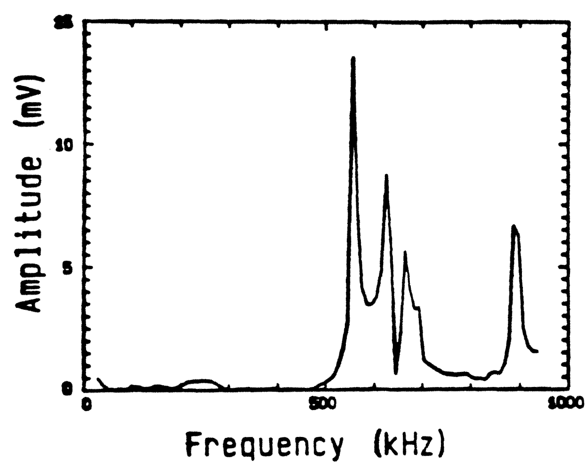

Figure 7. FFT of Output PZT signal caused by square wave input.

Seagate

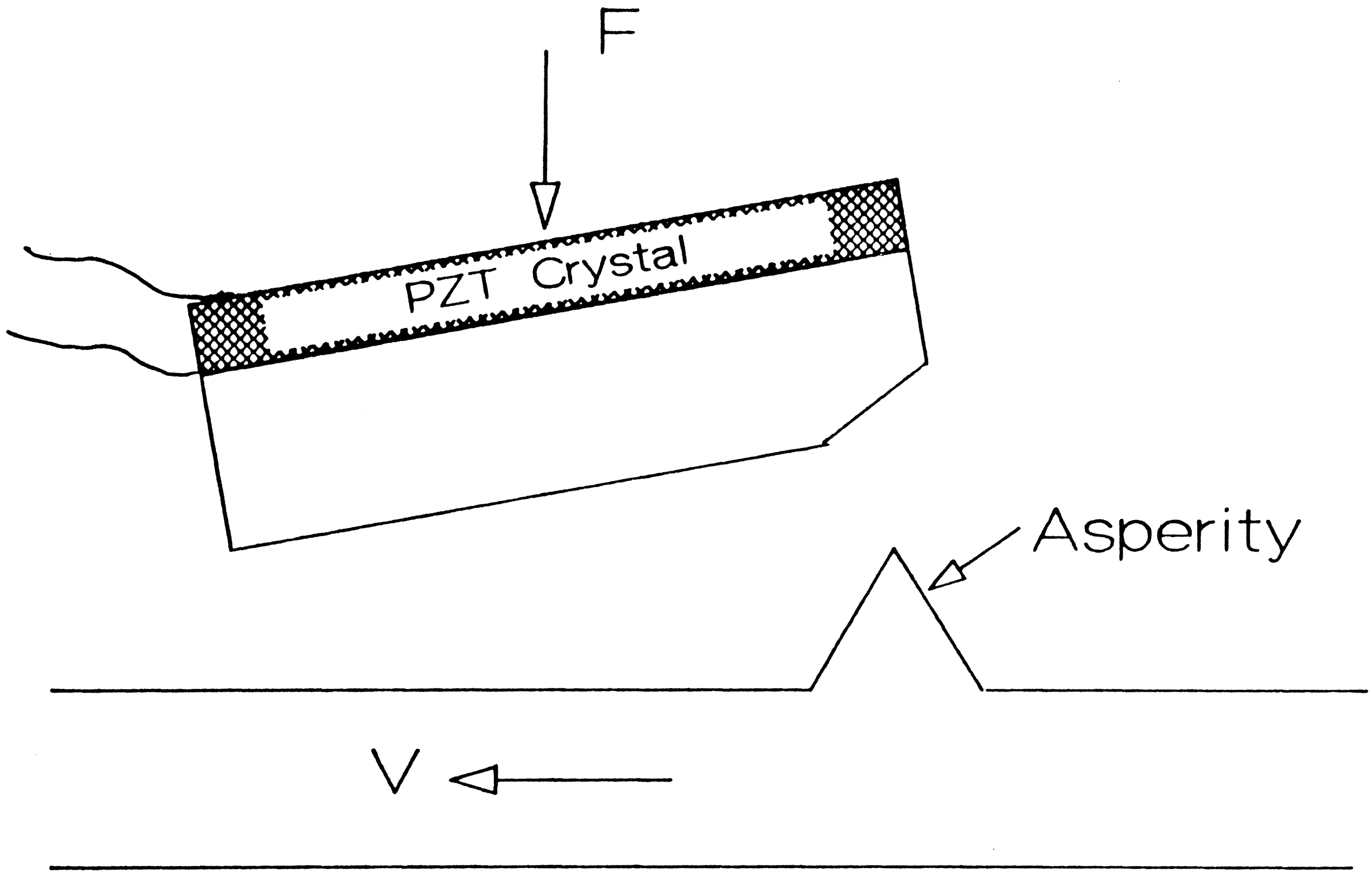

Contact Detection by Head Plate Mode Bending
Coupled to Piezo Crystal

Seagate

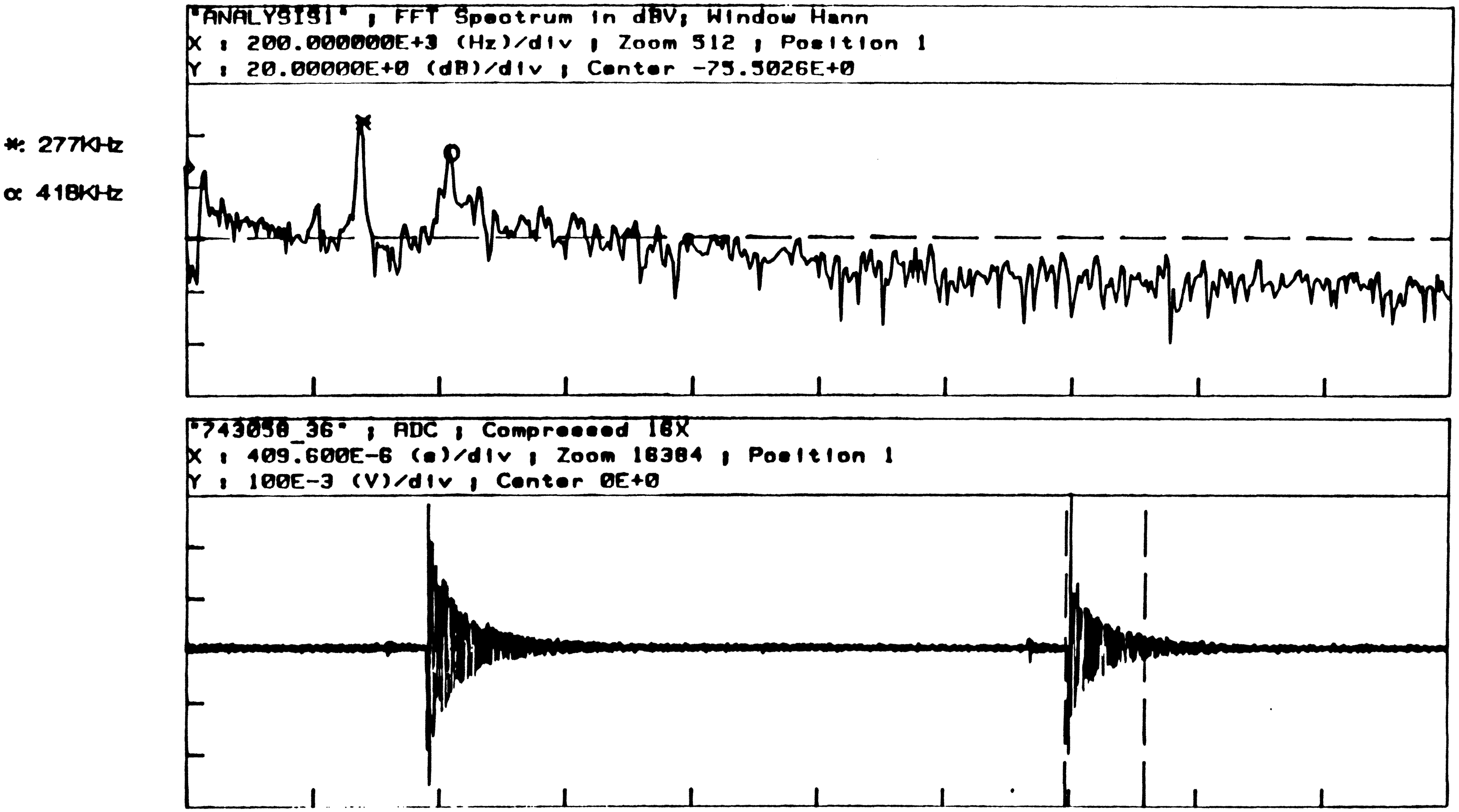

Head Response to Head–Disc Contact

a) Frequency Spectrum

b) Time Trace

Seagate

Glide Head Calibration

-Set S/N Ratio Above the Background Noise
  *Simple to Impliment
  *Hard to Correlate Testers
  *Disc Dependent

-Asperity Disk
  *Gives Reference to Head Flying Height
  *Asperity Subject to Wear

-Reference Excitation
  *Good way to Account for PZT Crystal Variability
  *Must also Calibrate Flying Height

Boyer, D., "Glide Test Calibration for Rigid Disk Magnetic Media," Sensors, Sept. 86, pp 80-83.

Core Recession/Protrusion

Monolithic MIG Head

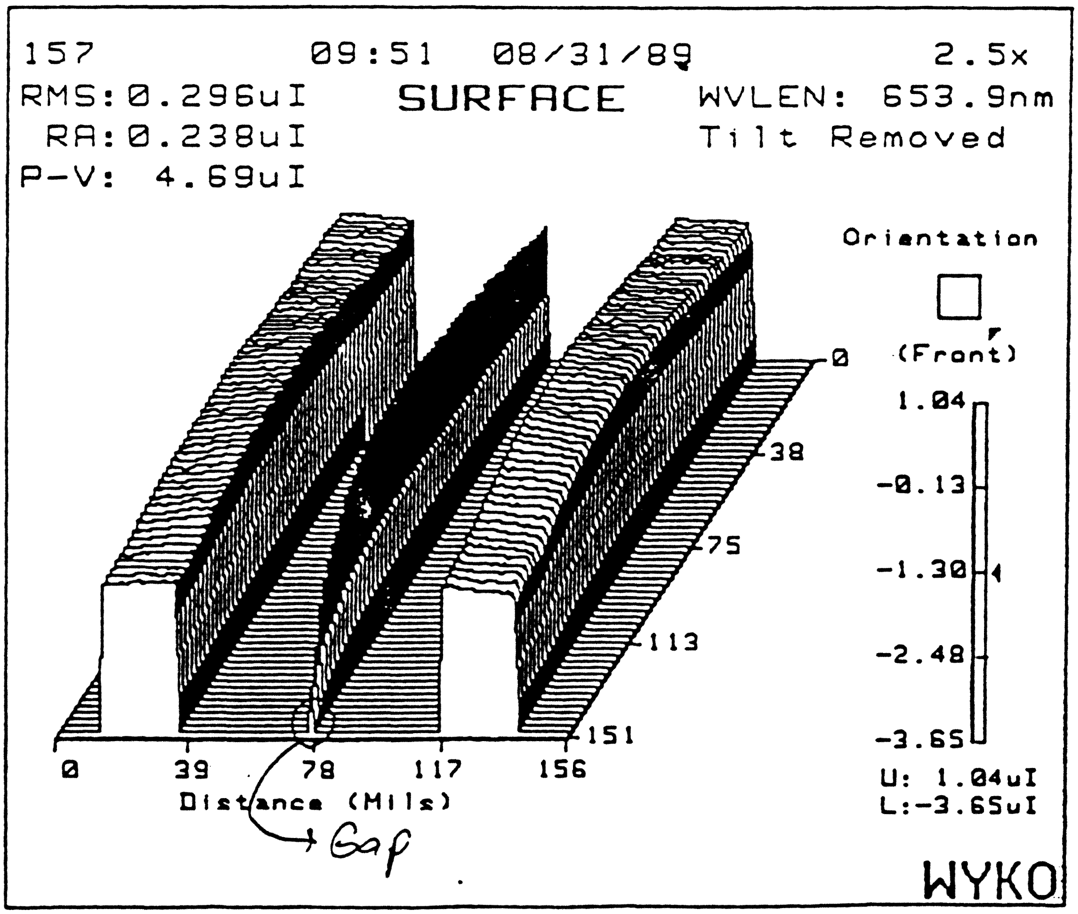

Maxtor

How Close Can You Get?

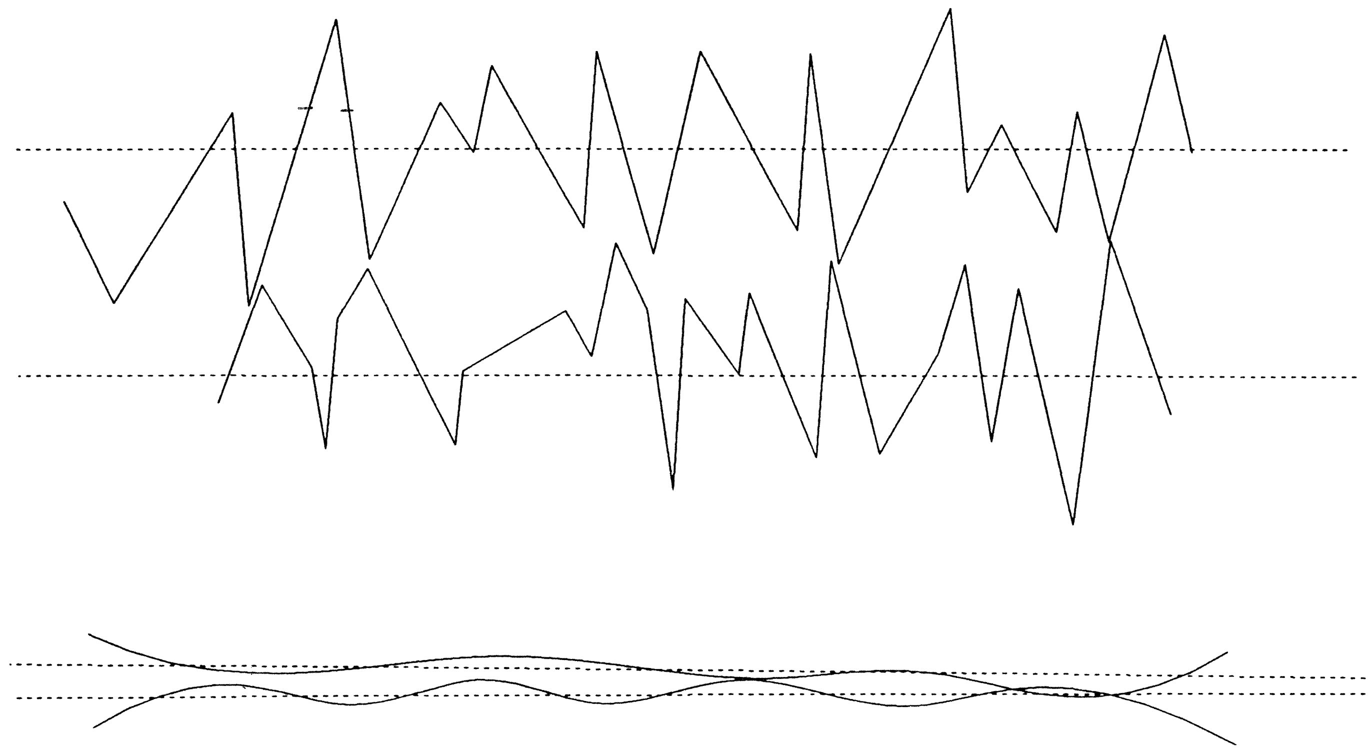

Maxtor

Flying Variations
Today (u")

	Today 2Sigma
•HEAD VARIATIONS	
gram load	0.3
gimbal point	0.1
roughness	0.5
flatness	0.4
camber	0.2
crown	0.37
twist	0.2
pole tip recession/	-1

Maxtor

)Typical Values for Std TF Heads and Metal Disks(

Flying Variations

Today and in 2 Years (u")

	Today 2Sigma	+2 Years 2Sigma
•HEAD VARIATIONS		
gram load	0.3	0.2
gimbal point	0.1	0.07
roughness	0.5	0.25
flatness	0.4	0.2
camber	0.2	0.1
crown	0.37	0.15
twist	0.2	0.15
pole tip recession	-1	-0.5

Typical Values for Std TF Heads and Metal Disks

Maxtor

Flying Variations
Today

	Today 2Sigma
•DISK VARIATIONS	
disk roughness	1.25
disk waviness	0.14
disk curvature	0.15
glide	3
•SYSTEM VARIATIONS	
stackup	0.2
tilt	0.1
runout	0.14
pressure & temp	0.4

Typical Values for Std TF Heads and Metal Disks

Maxtor

Flying Variations

Today and in 2 Years (u")

	Today 2Sigma	+2Years 2Sigma
•DISK VARIATIONS		
disk roughness	1.25	0.2
disk waviness	0.14	0.05
disk curvature	0.15	0.05
glide	3	1
•SYSTEM VARIATIONS		
stackup	0.2	0.1
tilt	0.1	0.05
runout	0.14	0.05
pressure & temp	0.4	0.4

Typical Values for Std TF Heads and Metal Disks

Maxtor

Flying Variations

Today and in 2 Years (u")

Today = Metal Disk & Std TF Head

+2 Years = Glass Disk & Minature Head

	Today 2Sigma	+2Years 2Sigma	Today $2Sigma^2$	+2Years $2Sigma^2$
•HEAD VARIATIONS				
gram load	0.3	0.2	0.09	0.04
gimbal point	0.1	0.07	0.01	0.0049
roughness	0.5	0.25	0.25	0.0625
flatness	0.4	0.2	0.16	0.01
camber	0.2	0.1	0.04	0.01
crown	0.37	0.15	0.1369	0.0225
twist	0.2	0.15	0.04	0.0225
pole tip recession	-1	-0.5	1	0.25
•DISK VARIATIONS				
disk roughness	1.25	0.2	1.5625	0.04
disk waviness	0.14	0.05	0.0196	0.0025
disk curvature	0.15	0.05	0.0225	0.0025
glide	3	1	na	na
•SYSTEM VARIATIONS				
stackup	0.2	0.1	0.04	0.01
tilt	0.1	0.05	0.01	0.0025
runout	0.14	0.05	0.0196	0.0025
pressure & temp	0.4	0.4	0.16	0.16
	$\sqrt{SUM}$		1.9	0.8

Typical Values for Thin Film Heads

Maxtor

Contribution of Variances Today and in 2 Years

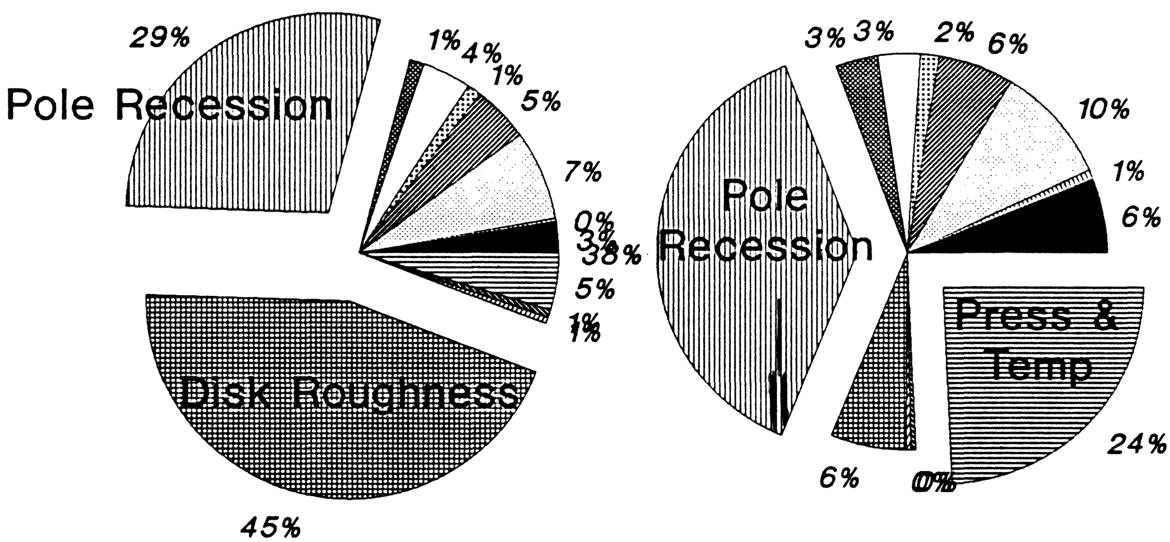

Metal Disk Standard Head *Glass Disk Small Head*

	Today +/-2sigma in u"	+2 Years +/-2sigma in u"
Total (Flying)	1.9	.8
Head Alone	1.3	.7
Contact	1.8	.7

Maxtor

OVERVIEW

- Why Lower?
- How Close Can We Get?
- Glide Issues
- Contact Recording

Maxtor

GLIDE ISSUES

- Flying Height
- Head
- Bump Height
- Transducer
- Channel
- Detection
- Repeatability

Data courtesy Bernard Flusche Jr., Akashic

Maxtor

GLIDE ISSUES

Flying (Height

Repeatability

PPL vs. Adelphi

Measurement Variables
- Spot Size
- Spot Location
- Calibration Factors

Data courtesy Bernard Flusche Jr., Akashic

Maxtor

AKASHIC

Head Flying Characteristic Distributions

• 20 Sets of heads tested at 400 IPS

Head	Location	Ave. (u")	Std Dev. (u")
Up	Lead	7.77	0.57
Up	Trail	4.71	0.42
Up	Roll	0.34	0.47
Up	Pitch	3.06	0.73
Dn	Lead	7.65	0.51
Dn	Trail	4.69	0.62
Dn	Roll	0.61	0.66
Dn	Pitch	2.96	0.52

AKASHIC

Flying Height
Measurement Repeatability

- A PZT head (16 mil rails) was flown on the PPL at 400 IPS.
- 25 separate measurements were made with the head being removed and remounted for each measurement.

Corner	Avg. Ht. (u")	3 Sigma (u")
Lead Inner	7.48	0.027
Lead Outer	6.97	0.060
Trail Inner	4.15	0.054
Trail Outer	5.08	0.060

GLIDE ISSUES

Head

- ABS Geometry
- Load
- Gimbal Location

Maxtor

GLIDE ISSUES

Bump Height

Wyko vs. Dektak

Average vs. Peak

Data courtesy Bernard Flusche Jr., Akashic

Maxtor

Atomic-Scale Tribology

C. Mathew Mate

IBM Research Division
Almaden Research Center
San Jose, California 95120-6099

(Seminar for IIST Short Course, December 14, 1989)

IBM

The question remains though, what is happening on the atomic scale?

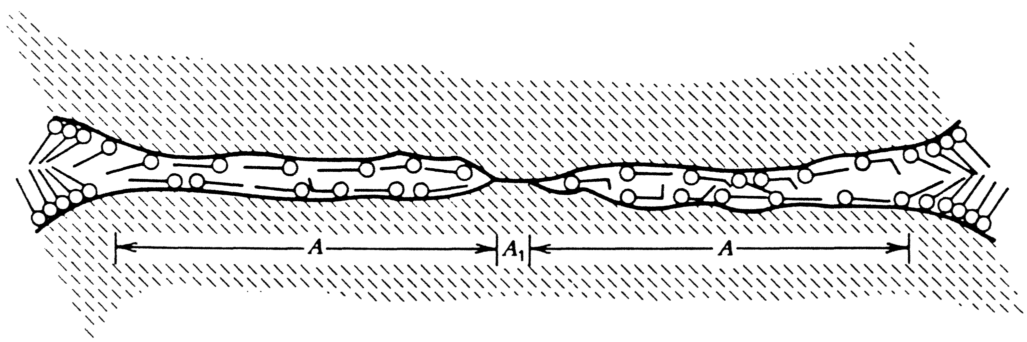

Outline and Researchers

1. Atomic Force Microscope

    - S. Chiang, R. Erlandsson, H.J. Mamin, C.M. Mate, G.M. McClelland, D. Rugar

2. Topography

    → Wear

    - C.M. Mate, I.L. Sanders

    → Micro-Indentation

    - G.S. Blackman, C.M. Mate, M.R. Philpott

3. Magnetic Force Microscopy

    - S.E. Lambert, H.J. Mamin, D. Rugar, J.E. Stern, B.D. Terris

4. Atomic-Scale Friction

    - S. Chiang, R. Erlandsson, C.M. Mate, G.M. McClelland

Outline and Researchers

5. Lubricant Films

→ Wear of Langmuir-Blodgett Films

→ Thickness of Liquid Lubricant Films

→ Disjoining Pressure of Lubricant Films

→ Bonded Lubricants

- G.S. Blackman, A.B. Jaffe, L.J. Lin, M.R. Lorenz, C.M. Mate, V.J. Novotny, M.R. Philpott

The Atomic Force Microscope (AFM)

- First introduced by Binnig, Quate, and Gerber, Phys. Rev. Lett. 56 (1986) 930.

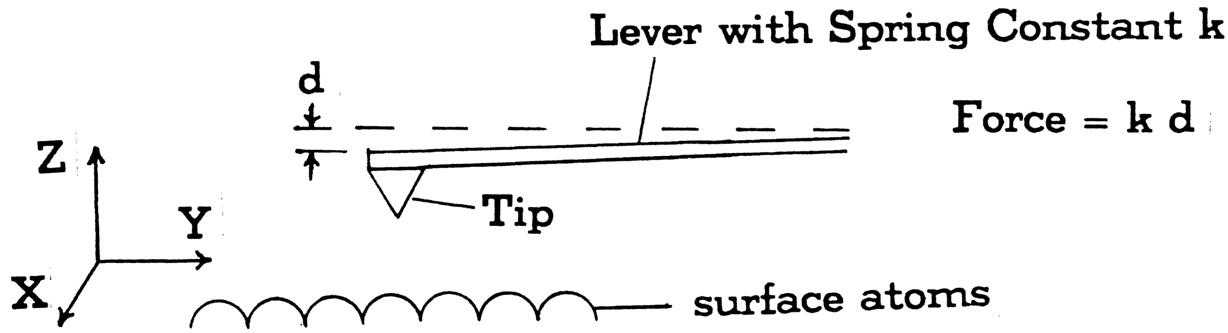

- Need to measure the lever deflection, d, while scanning the tip in X and Y.
- Need to measure deflections with better than a 1 Å precision in order to achieve atomic resolution.
- Then choose a spring constant, k, that enables one to measure atomic scale forces (i.e., 10^{-7}N to 10^{-11}N).

AFM Detection Methods

Tunnelling

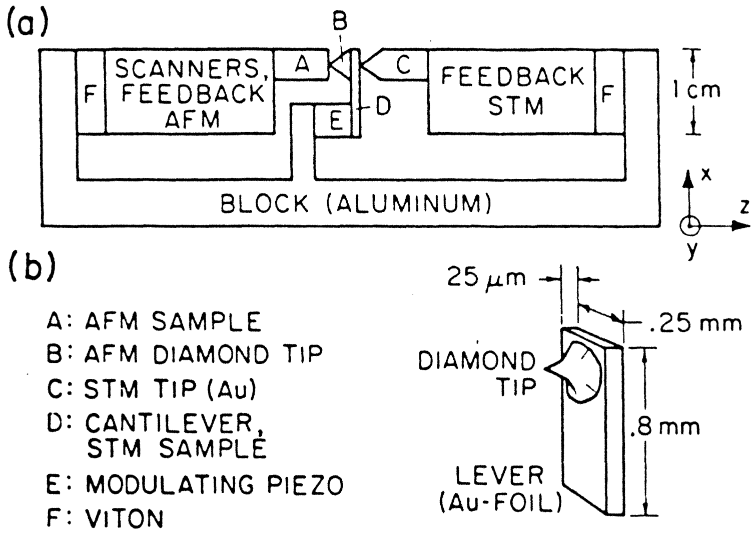

Optical Deflection

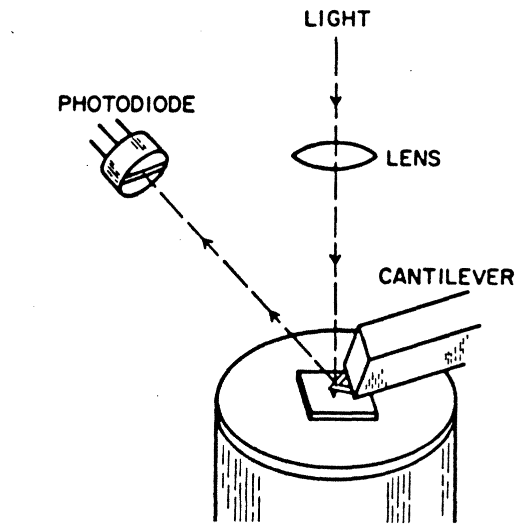

Capacitance

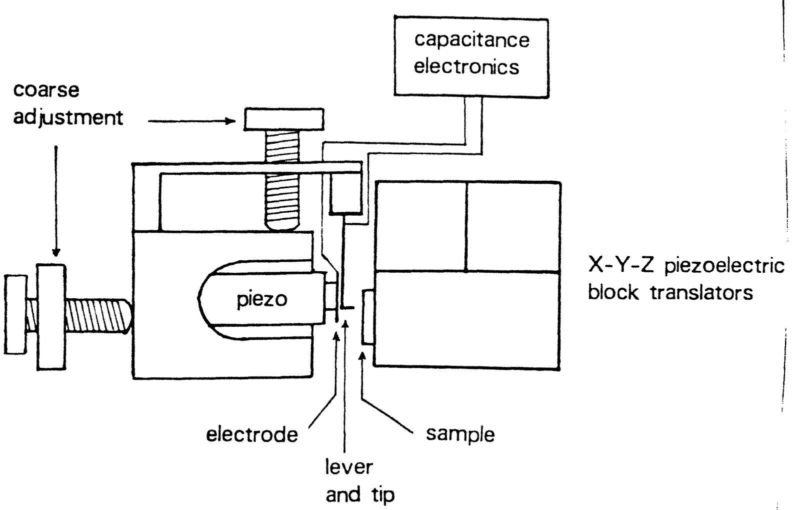

Optical Interference

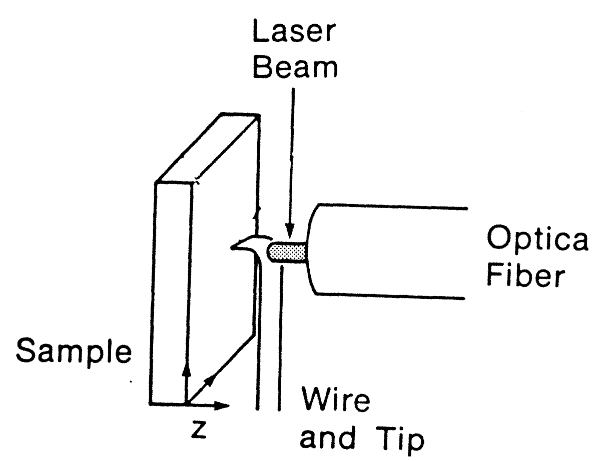

Tip is electrochem etched

08/89 (C. Mathew Mate)

Optical Interference Detection AFM

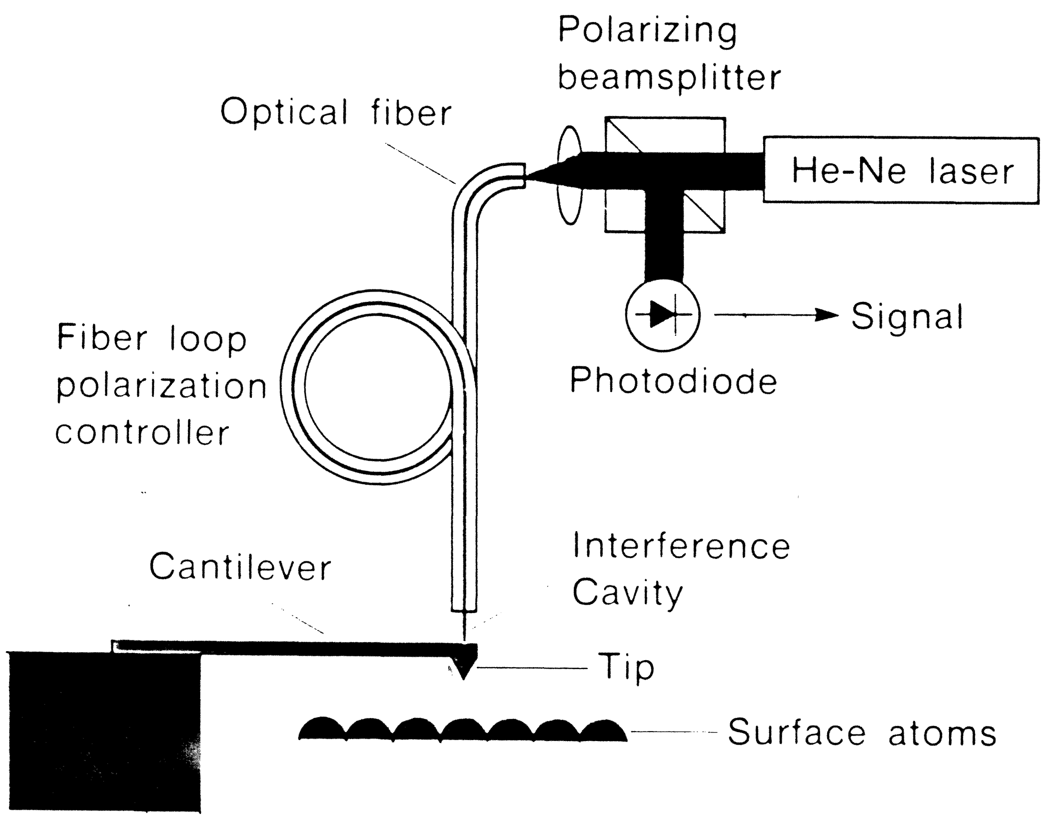

1. Rugar, Mamin, Erlandsson, Stern, and Terris, Rev. Sci. Instrum. 59(1988) 2337.

2. Erlandsson, McClelland, Mate, and Chiang, J. Vac. Sci. Technol. A6 (1988) 266.

Attractive Forces at 5 Å

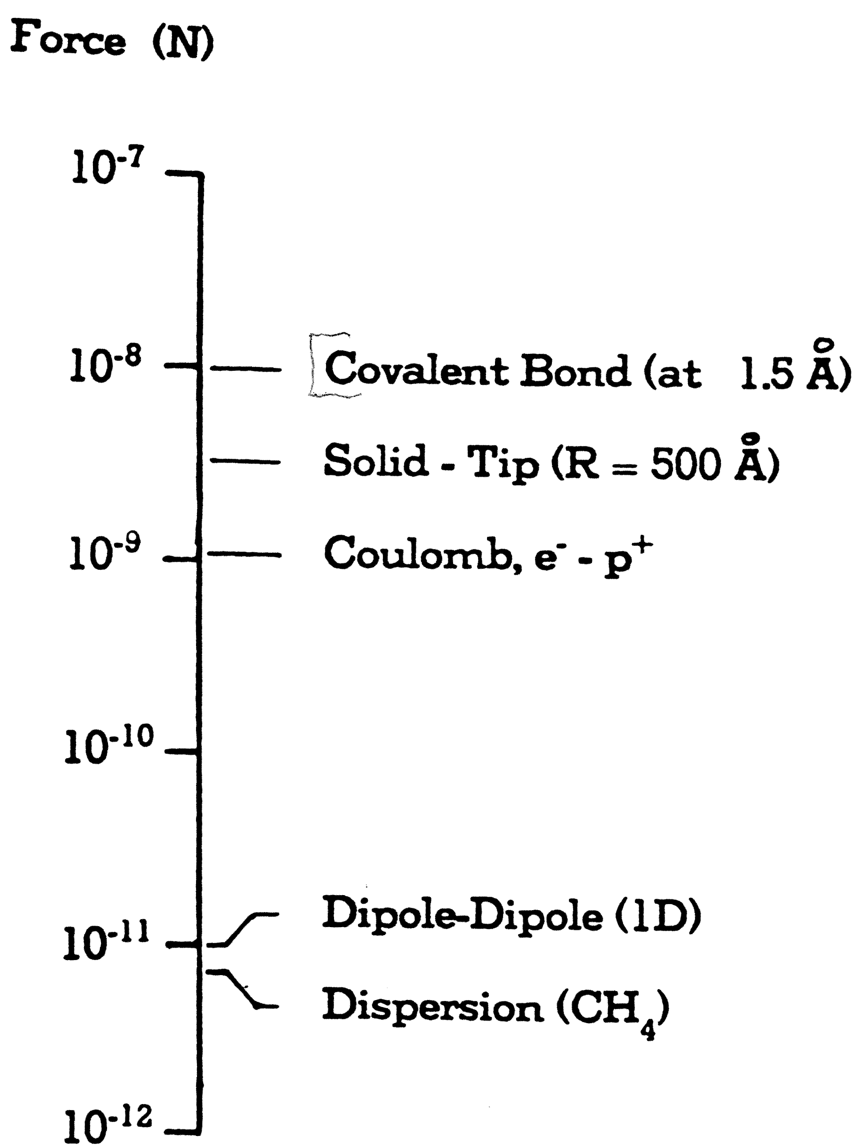

(How to adjust force on tip)

Principle of AC Force Microscopy

(Repulsive Contact)

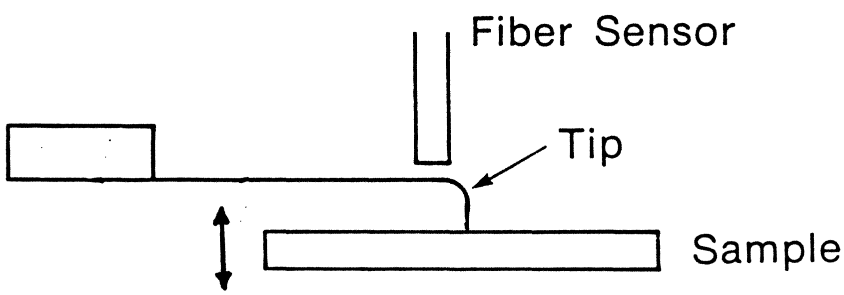

- Vibrate sample at a frequency far below cantilever resonance. Monitor motion induced onto tip.

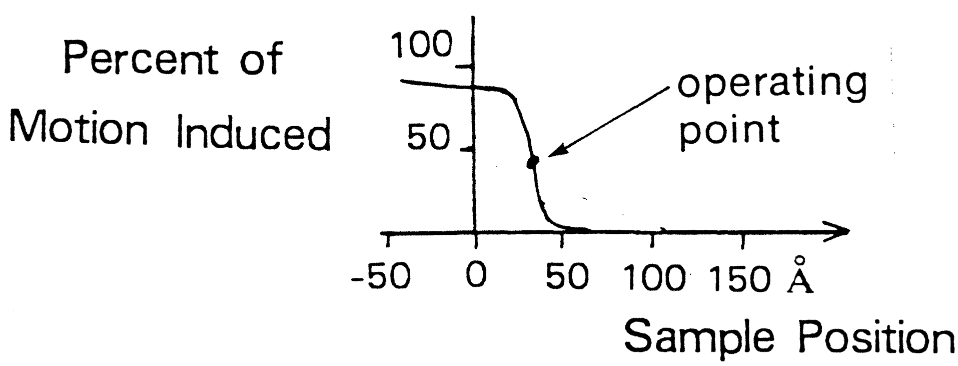

- Plot contours of constant repulsive force gradient.

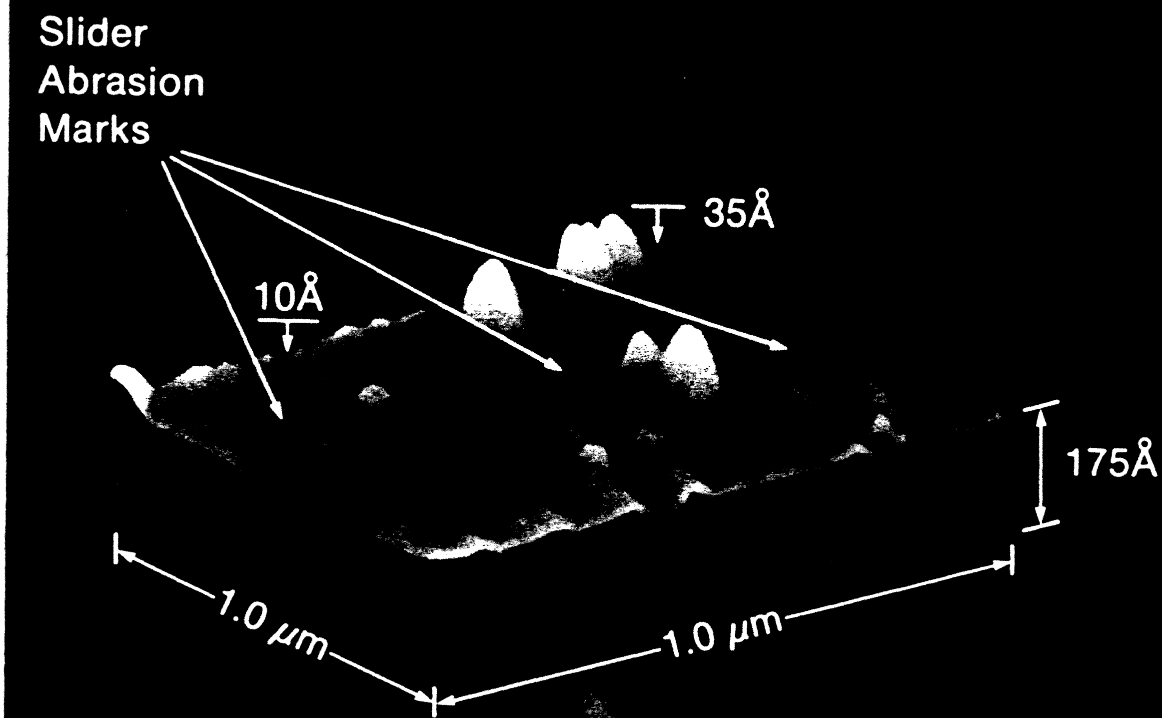

(a) Amorphous Carbon Overcoat After CSS Cycling

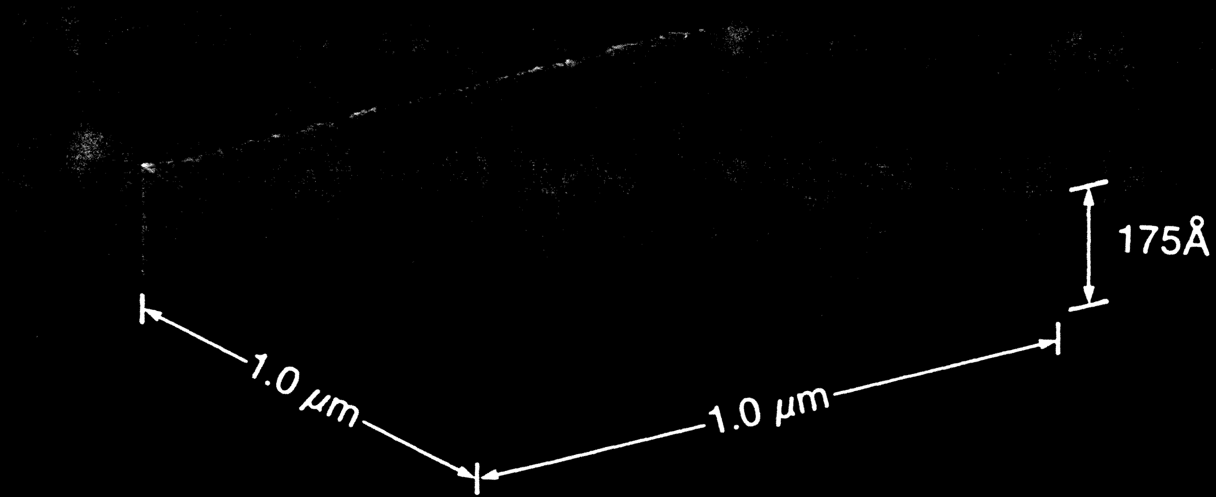

(b) Amorphous Carbon Overcoat

Mate 10/88

100 Å Tips

Micro-Hardness of Gold

(2500Å gold on mica)

Still developing tips to use on C

5mm=1000Å

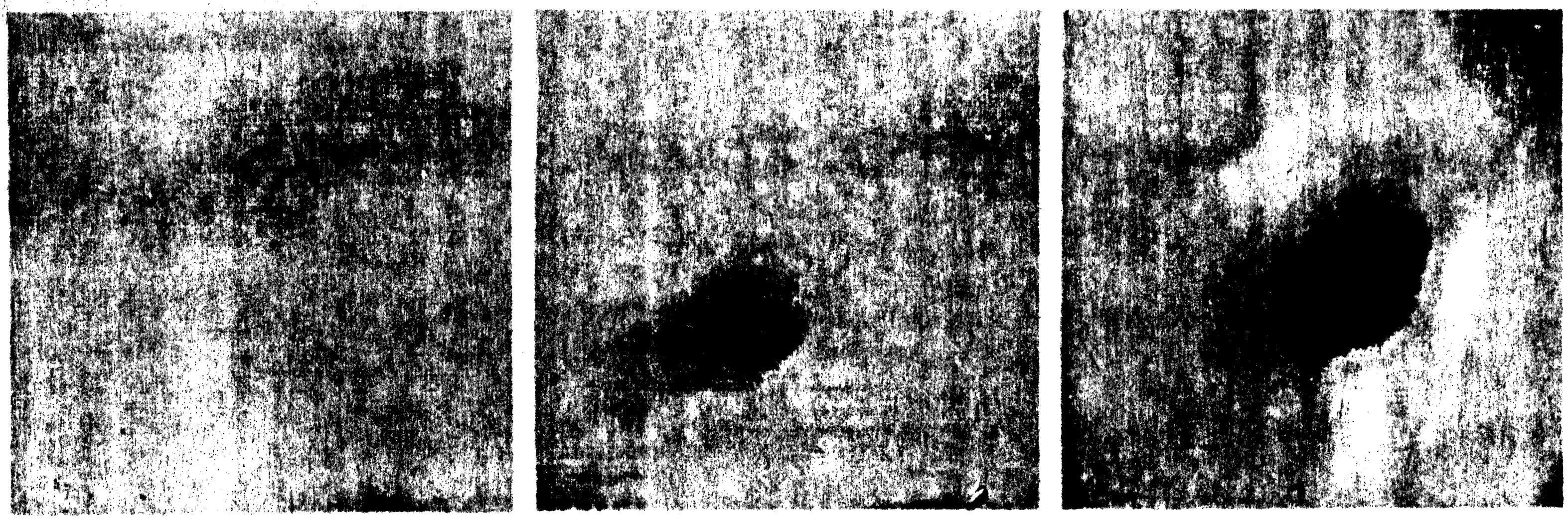

Load	3.4×10^{-5} N	6.7×10^{-5} N	1.0×10^{-4} N
Hardness	—	1.6 GPa	1.0 GPa
	—	1.6×10^{4} atm	1.0×10^{4} atm

Langmuir-Blodgett Films

Cadmium Arachidate, $[CH_3(CH_2)_{18}CO_2]_2^- Cd^{2+}$

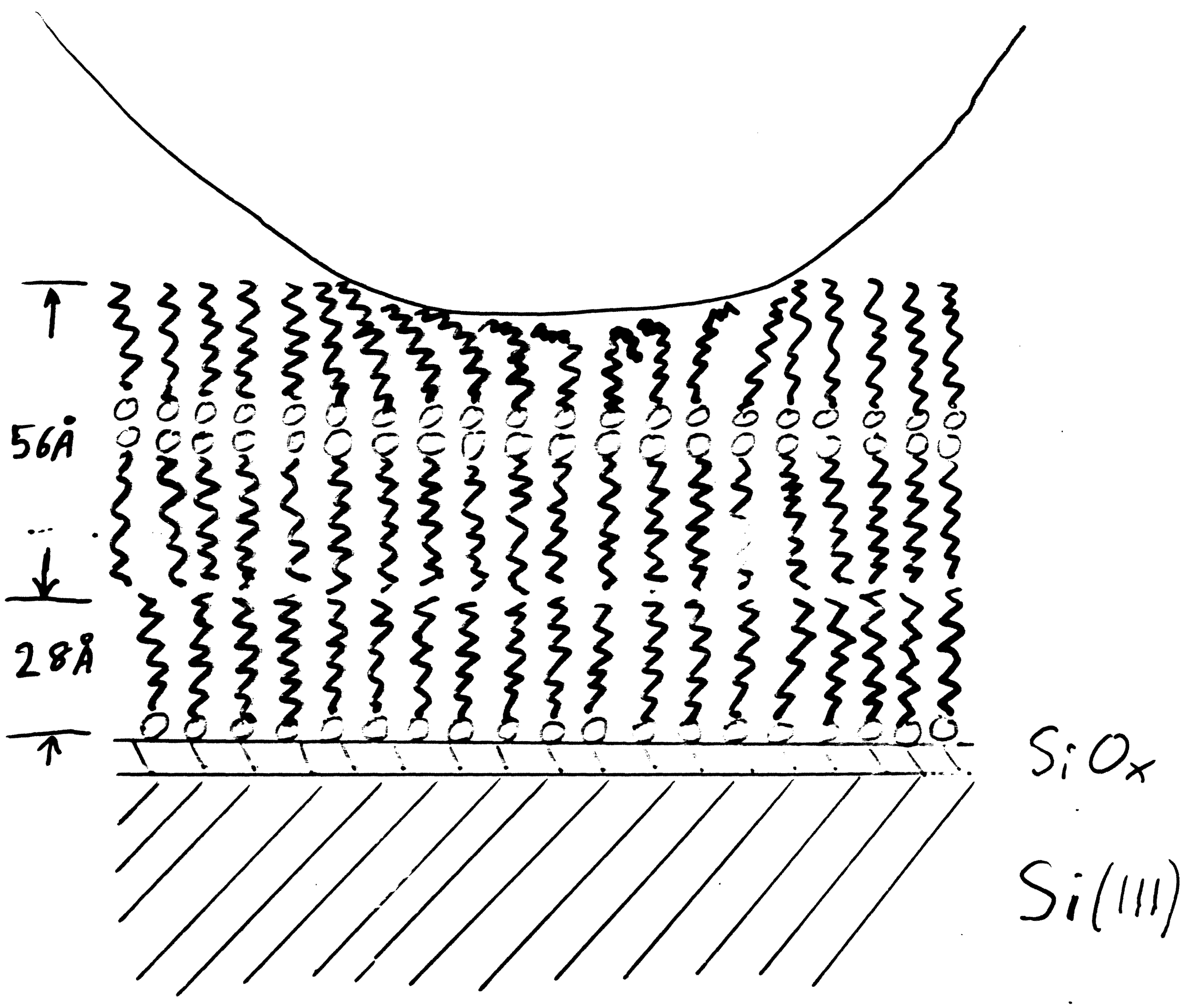

alternate force calibration

Principle of AC Force Microscopy

(Attractive forces or magnetic forces)

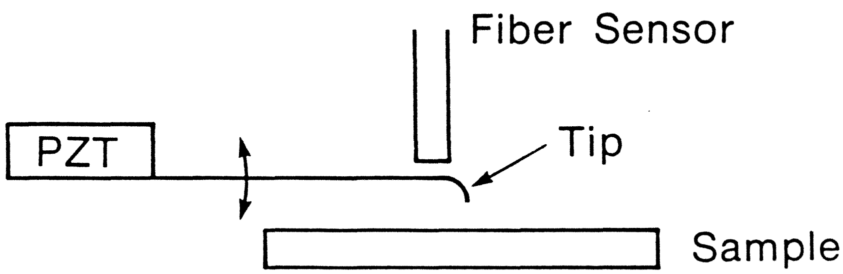

- Vibrate cantilever near resonance

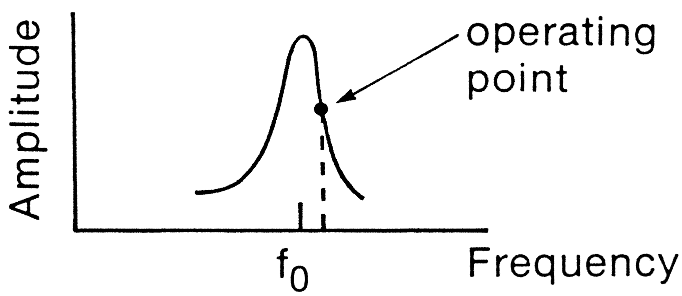

- Resonant frequency shifts

$$f_0 = \frac{1}{2\pi}\sqrt{k/m}$$

$$k = k_{Lever} + \partial F/\partial z$$

- Force gradient modulates vibration amplitude

Indentation of Seven Layers of Cadmium Arachidate on Si (111)

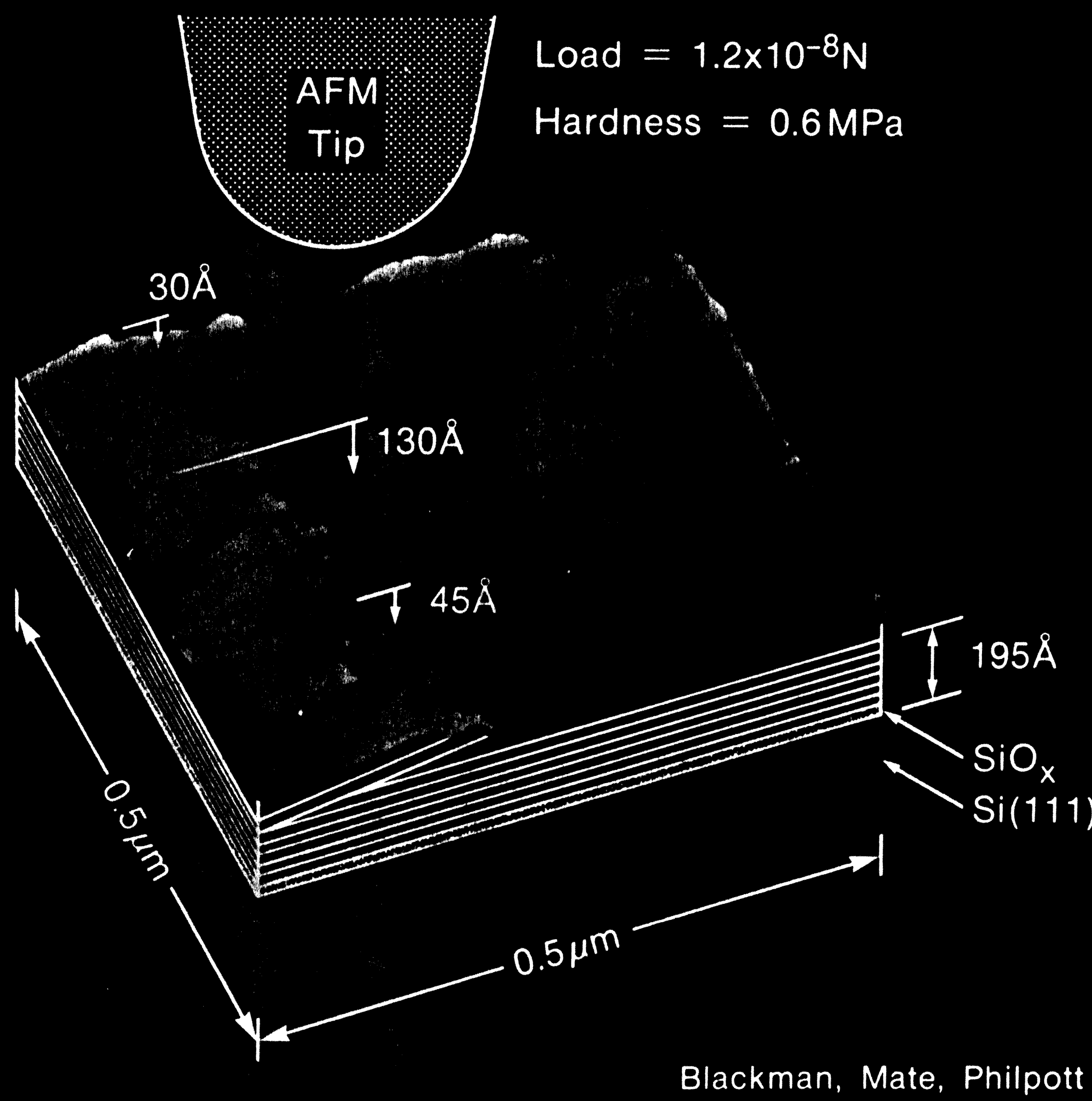

Magnetic Force Microscopy

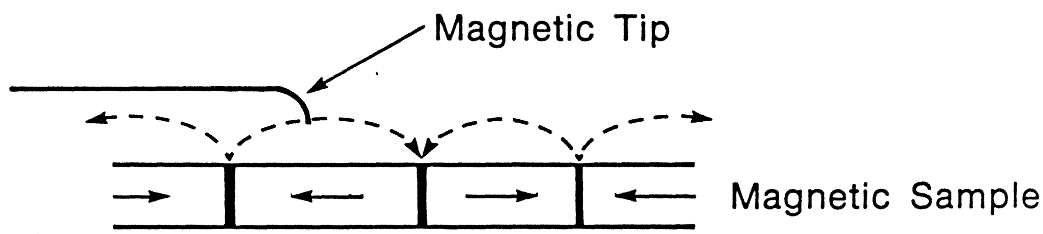

- Tip interacts with fields generated by sample

$$\vec{F} = \nabla \, (\vec{m}_{tip} \cdot \vec{B}_{sample})$$

- Typical values

$$B = 10\text{–}1000 \text{ gauss}$$

$$m_{tip} = 1700 \text{ emu/cm}^3 \times (1000 \text{ Å})^3$$
$$= 2\times10^{-12} \text{ emu}$$

$$F_z = 10^{-8} - 10^{-12} \text{ Newtons}$$

$$\frac{dF_z}{dz} = 10^{-3} - 10^{-6} \text{ N/m}$$

2 μm Bits on Co-alloy Disk

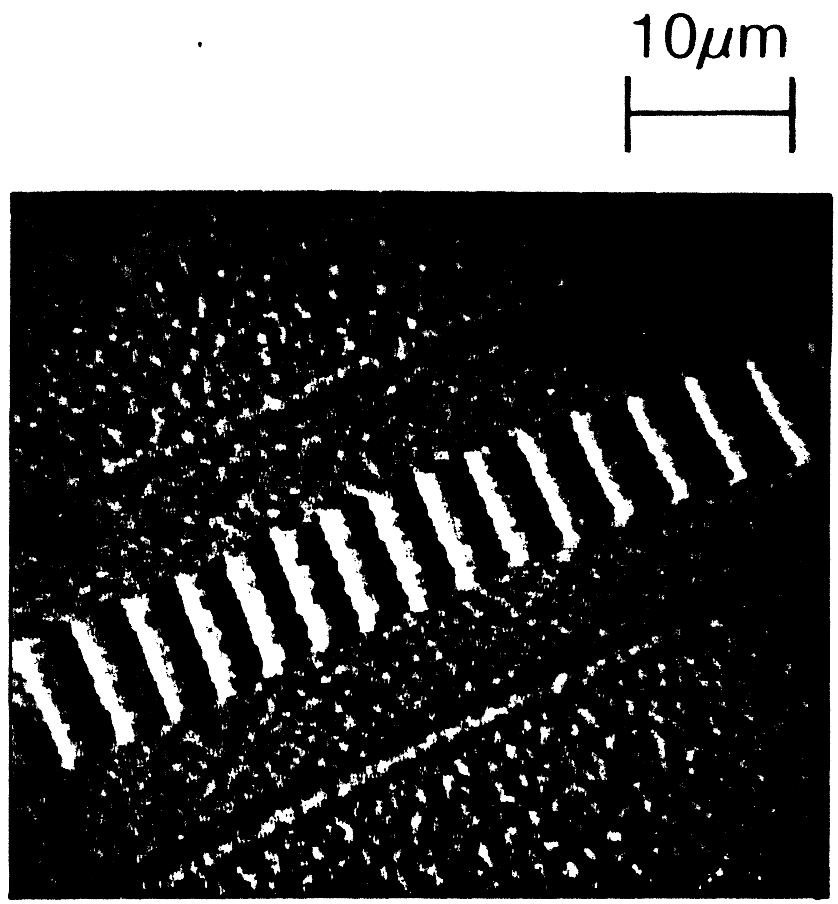

Mamin, Rugar, et al.

IBM Almaden Research Ctr.

Force Microscope Imaging of Disk Magnetization

5μm Bits on Co-alloy Disk

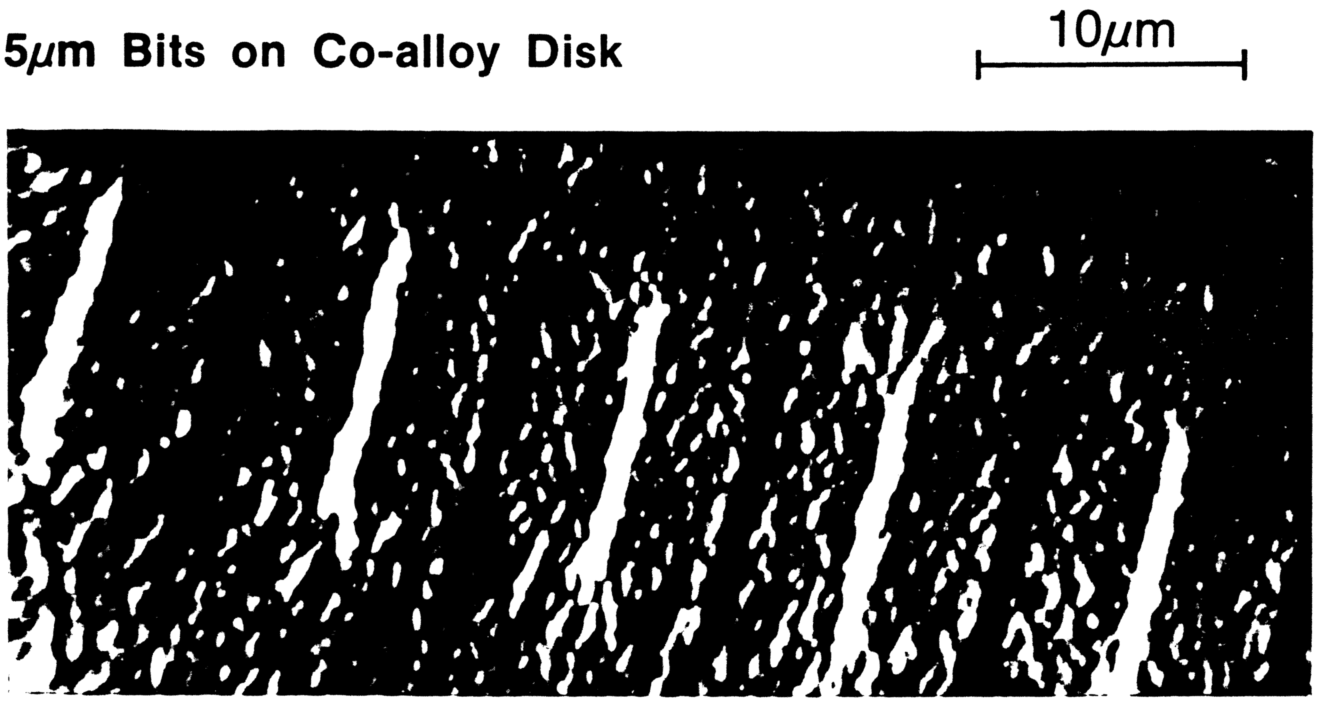

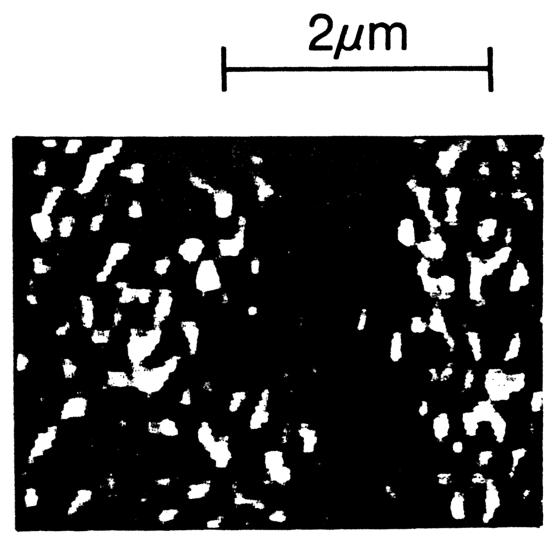

Transition Detail Revealed using Coated Tip

Mamin, Rugar, et al.

IBM Almaden Research Ctr.

The New rk Times
Science Ti s Section
Tuesday, August 16, 1988

A Pervasive Molecule Is Captured in a Photograph

By MALCOLM W. BROWNE

A century and a quarter after chemists first deduced the shape of the benzene ring from its chemical behavior, microscopists have at last obtained a direct image of this distinctive and vital molecular structure.

It turns out that a molecule of benzene, which is an ingredient of gasoline, looks very much the way chemists visualized it at a time when carriages were propelled by horses rather than gasoline.

Microscopic pictures of benzene molecules, acclaimed by chemists as a technical tour de force, were recently made at the I.B.M. Almaden Research Center in San Jose, Calif., using an ultrapowerful scanning tunneling microscope. The computer-generated images, based on data obtained from a microscopic beam of electrons scanned across a thin film of benzene, clearly show the doughnut-like shape that gives the benzene ring its unique chemical properties. The images contained no surprises but the technique developed to make them will help chemists understand how certain reactions are speeded up by substances called catalysts, which do not participate in the reactions themselves.

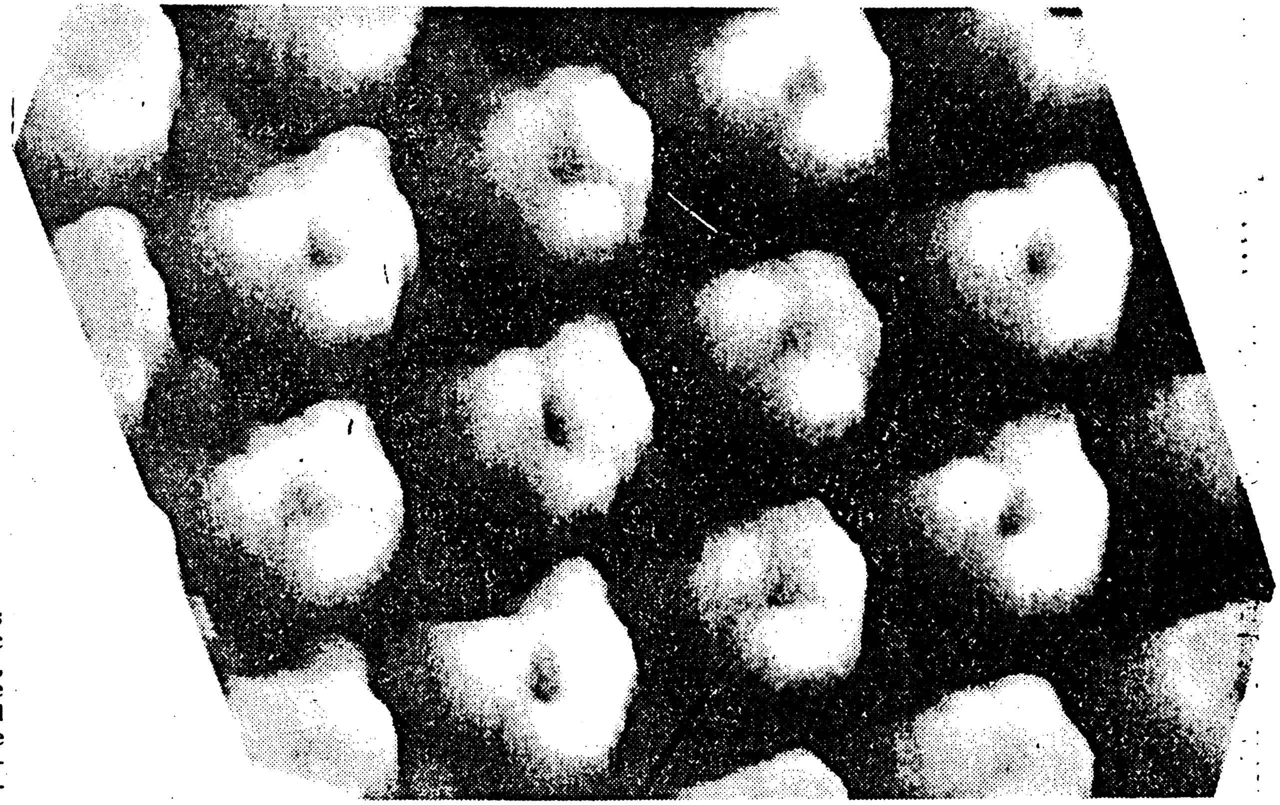

I.B.M.

First photograph of ring-shaped benzene molecules, in rows, made with a scanning tunneling microscope. The photograph supports century-old deductions about the molecular structure of benzene.

The benzene molecule consists of six carbon atoms linked in a hexagonal ring by two kinds of electronic bonds. Surrounding this ring are six hydrogen atoms, each linked to one of the carbon atoms. In itself, benzene is a clear, inflammable liquid that is both poisonous and carcinogenic. But the hydrogen atoms surrounding the benzene ring can be replaced by other atoms or molecules to yield a bewildering variety of combinations, including vanilla and almond flavoring, explosives, plastics, dyes and medicines.

Most chemicals, in fact, are based in part on benzene rings. The American Chemical Society, which records all chemical substances as they are discovered or created, reported last week that its master list had grown to 9,196,187 entries. Of these, at least 6,436,928 — some two-thirds of all known chemicals — contain one or more benzene rings. Such compounds are classified by chemists as "aromatic," a term referring to chemical structure rather than odor.

By the mid-19th century, European chemists were aware that each carbon atom has four electronic linkage points called valence bonds when it is linked with other carbon atoms or hydrogen. When six carbon atoms arranged in a straight line are joined by single valence bonds, eight bonds are left over as vacant attachment points. If each is linked to a hydrogen atom, the formula of the resulting chain, called "hexane," is C_6H_{14}.

(In recent decades chemists have found it convenient to describe the bonding together of atoms in terms of quantum-mechanical "molecular orbitals" — overlapping shells of the orbital electrons of linked atoms — rather than "valence bonds.")

But 19th-century chemists discovered another molecule containing six carbon atoms that was more difficult to describe in terms of straight-chain architecture; analysis showed that it contained only six hydrogen atoms rather than eight.

The solution to the puzzle was the benzene ring. The realization that the carbon atoms in benzene had to be linked in a ring rather than a straight chain has been widely attributed to the German chemist Friedrich August Kekulé von Stradonitz, although Kekulé's claim to this landmark discovery has recently been challenged.

Since then, the chemistry of aromatic molecules — molecules based on benzene rings — has evolved as a

Continued on Page B9

Also see Ohtani, Wilson Chiang, Mate, Physical Review Letters 60 (1988) 2398

Experimental Geometry for Measuring Frictional Forces

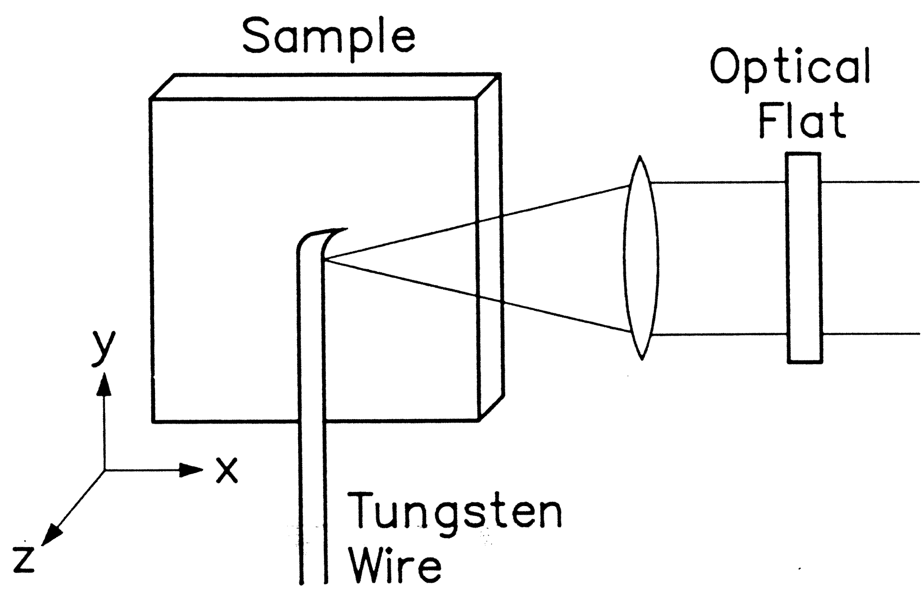

Lateral Tungsten Tip Motion at Three Loads While Oscillating Graphite Sample

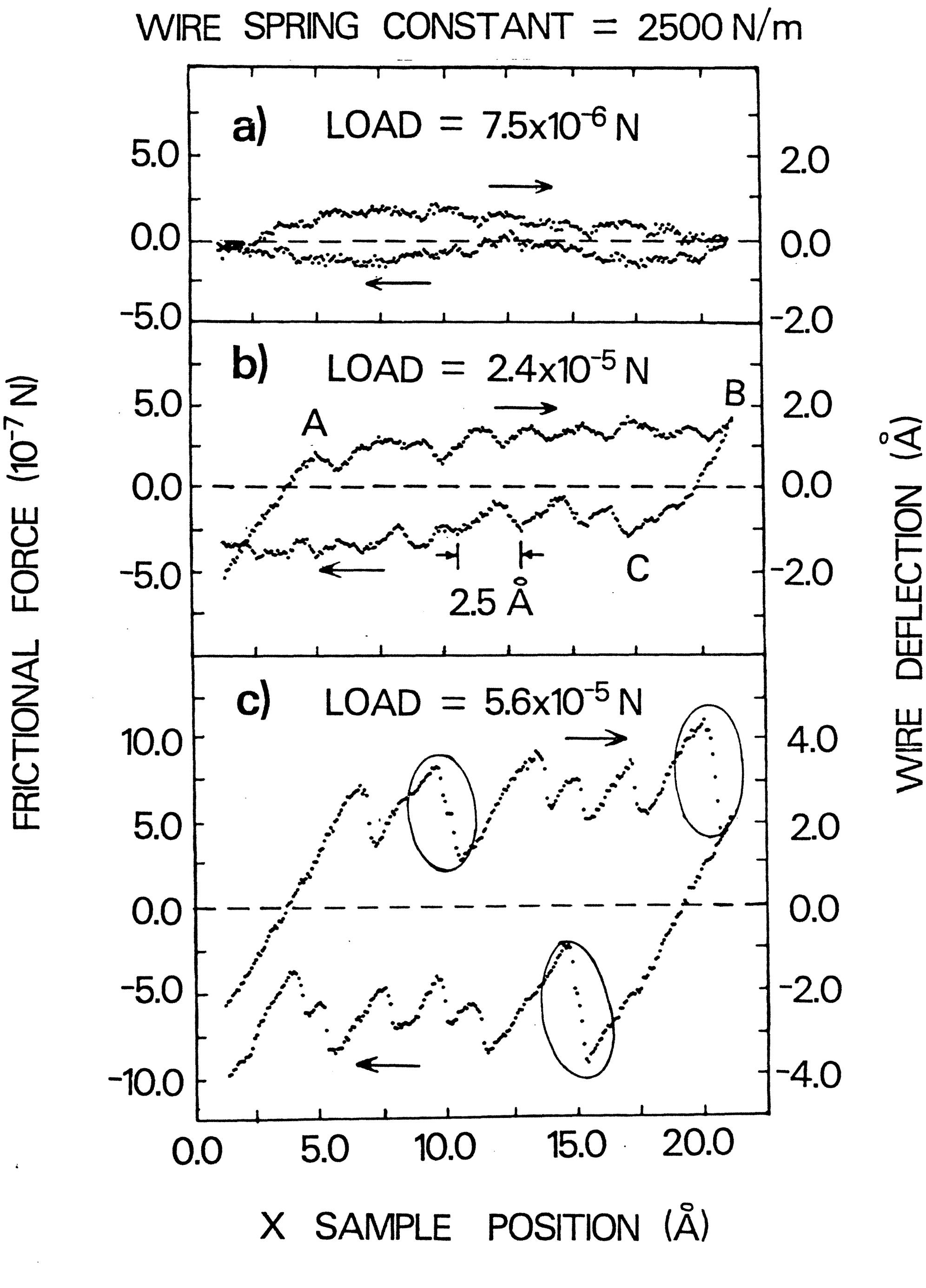

Mate, McClelland, Erlandsson, Chiang, Phys. Rev. Lett. 59 (1987) 1942.

Frictional Forces on a Tungsten Tip on Graphite

Load = 5.5×10^{-5} N

3 D image of previous data

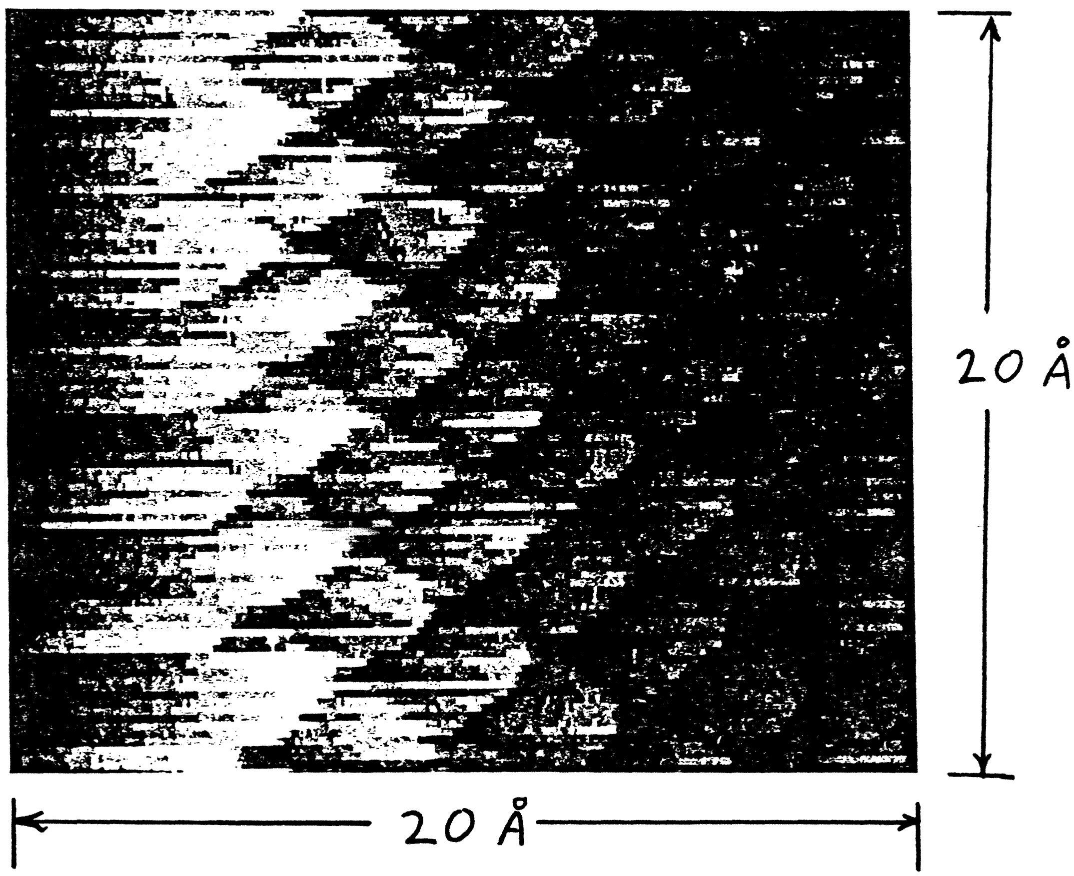

[redacted]

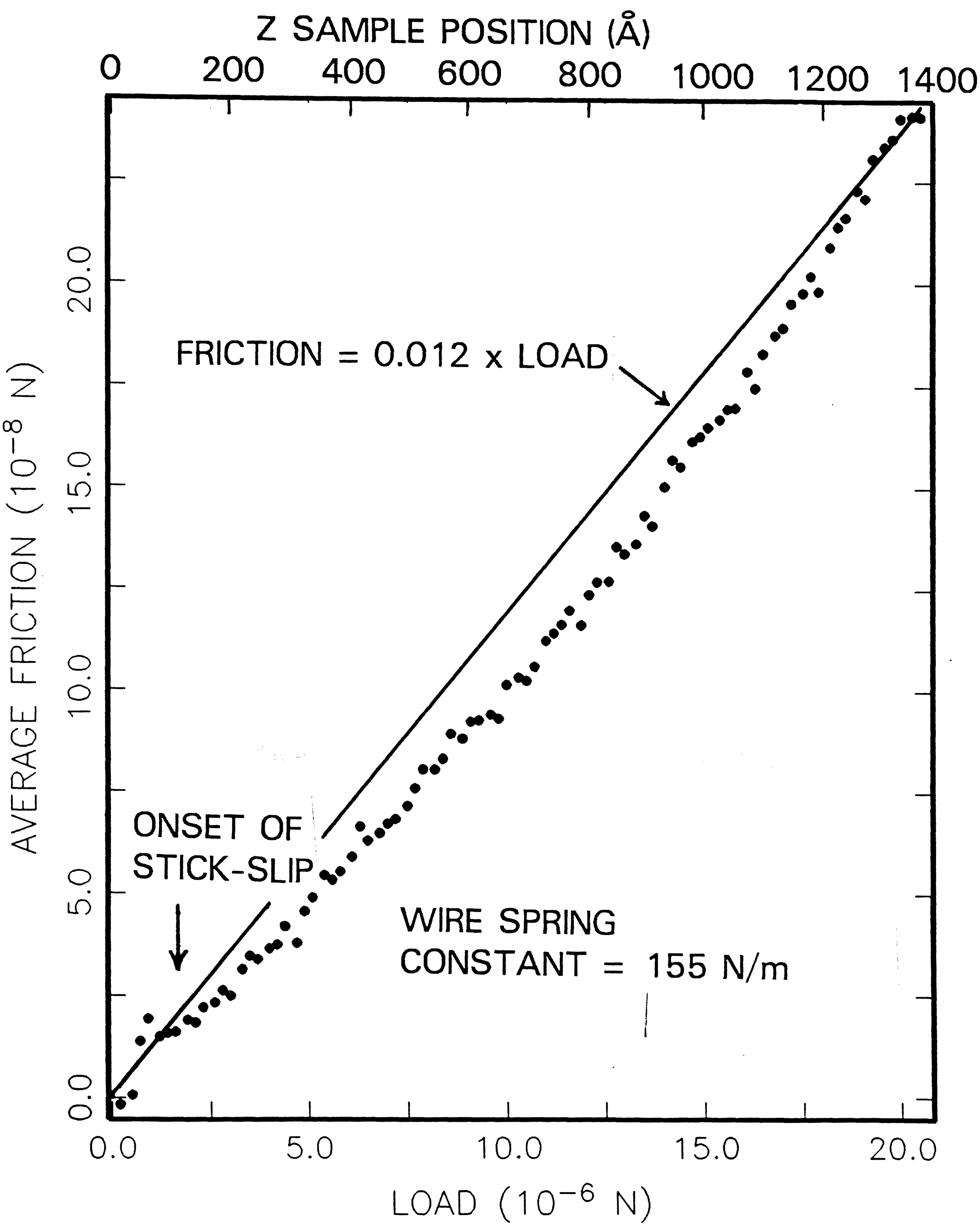

Z SAMPLE POSITION (Å)
0
200
400
600
800
1000
1200
1400
AVERAGE FRICTION (10−8 N)
0.0
5.0
10.0
15.0
20.0
FRICTION = 0.012 x LOAD
ONSET OF
STICK-SLIP
WIRE SPRING
CONSTANT = 155 N/m
0.0
5.0
10.0
15.0
20.0
LOAD (10−6 N)

- **The frictional force varies as $(\text{Load})^{1.2}$.**
- In standard models of friction, the frictional force is assumed to be proportional to contact area: $F = sA$.
- Two standard models for the actual contact area are
  - → Hertzian Contact -
    Contact area varies as $(\text{Load})^{2/3}$

  - → Asperity Contact -
    Contact area is proportional to Load.

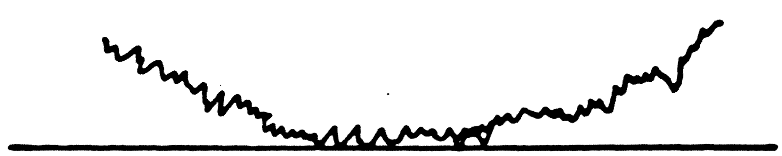

 07/87 (C. Mathew Mate)

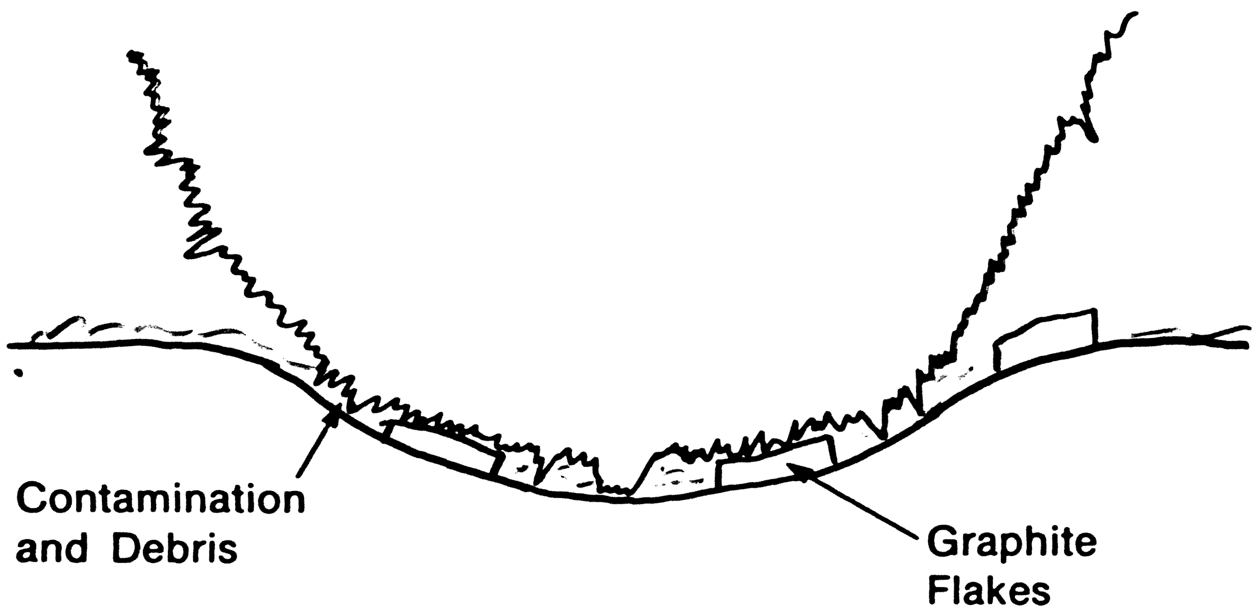
Contamination
and Debris
Graphite
Flakes

Atomic Scale Friction on Mica

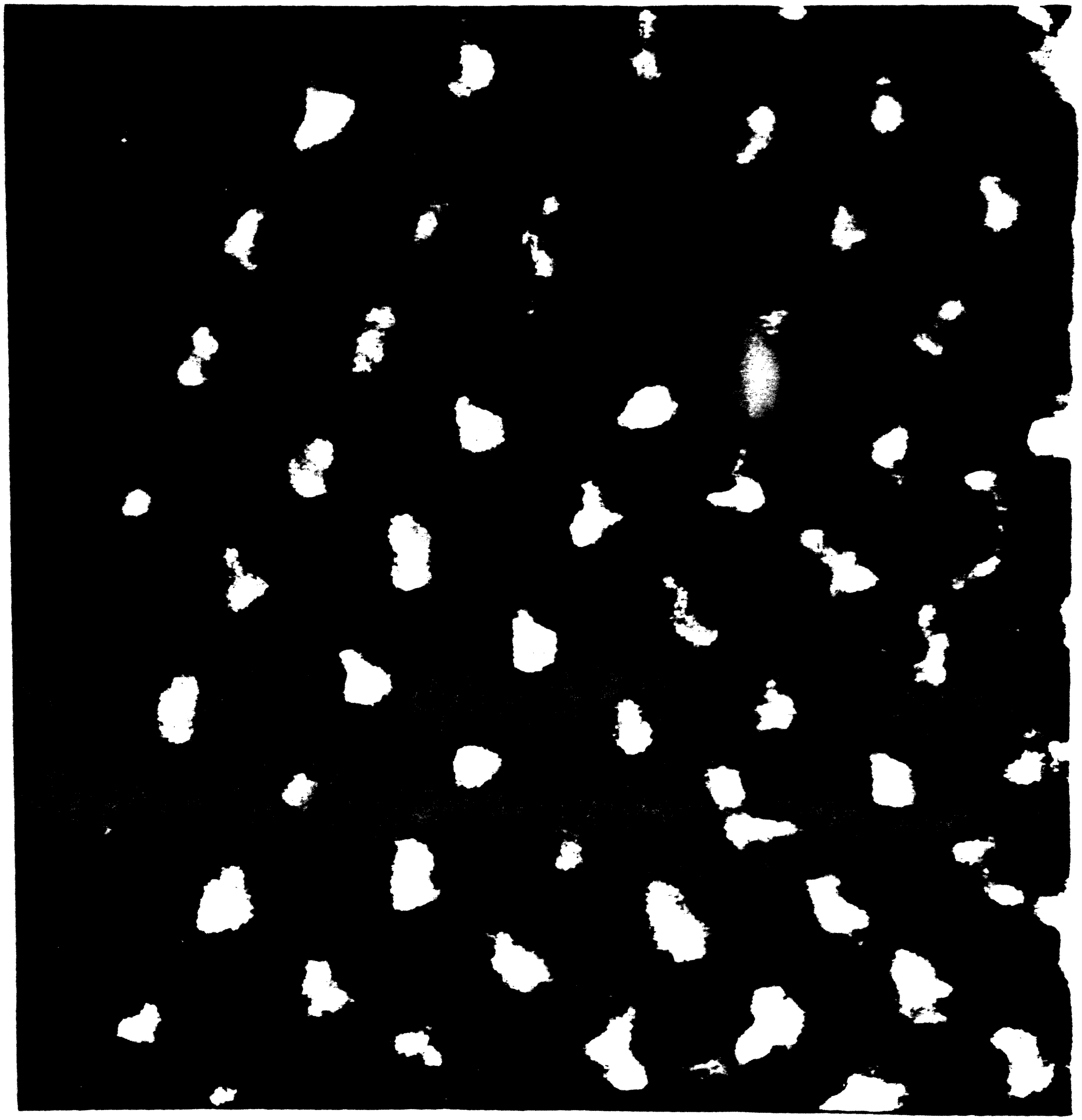

R. Erlandsson, G. Hadziioannou, C.M. Mate, G.M. McClelland, and S. Chiang, J. Chem. Phys. 89 (1988) 5190.

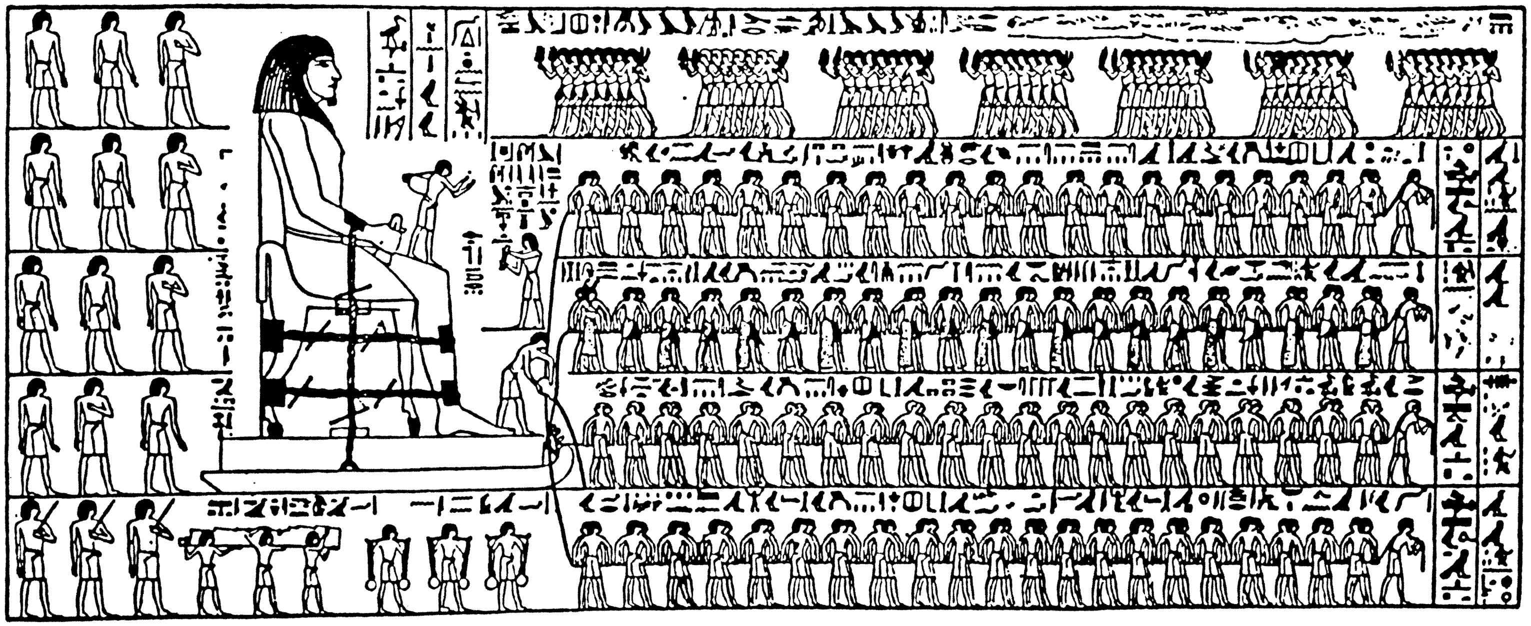

Figure 3 *Part of a mural painting in a grotto at El Bersheh (c. 1900 B.C.) showing slaves dragging a colossus on a sledge while one man pours lubricating oil in its path.*

LUBRICATION

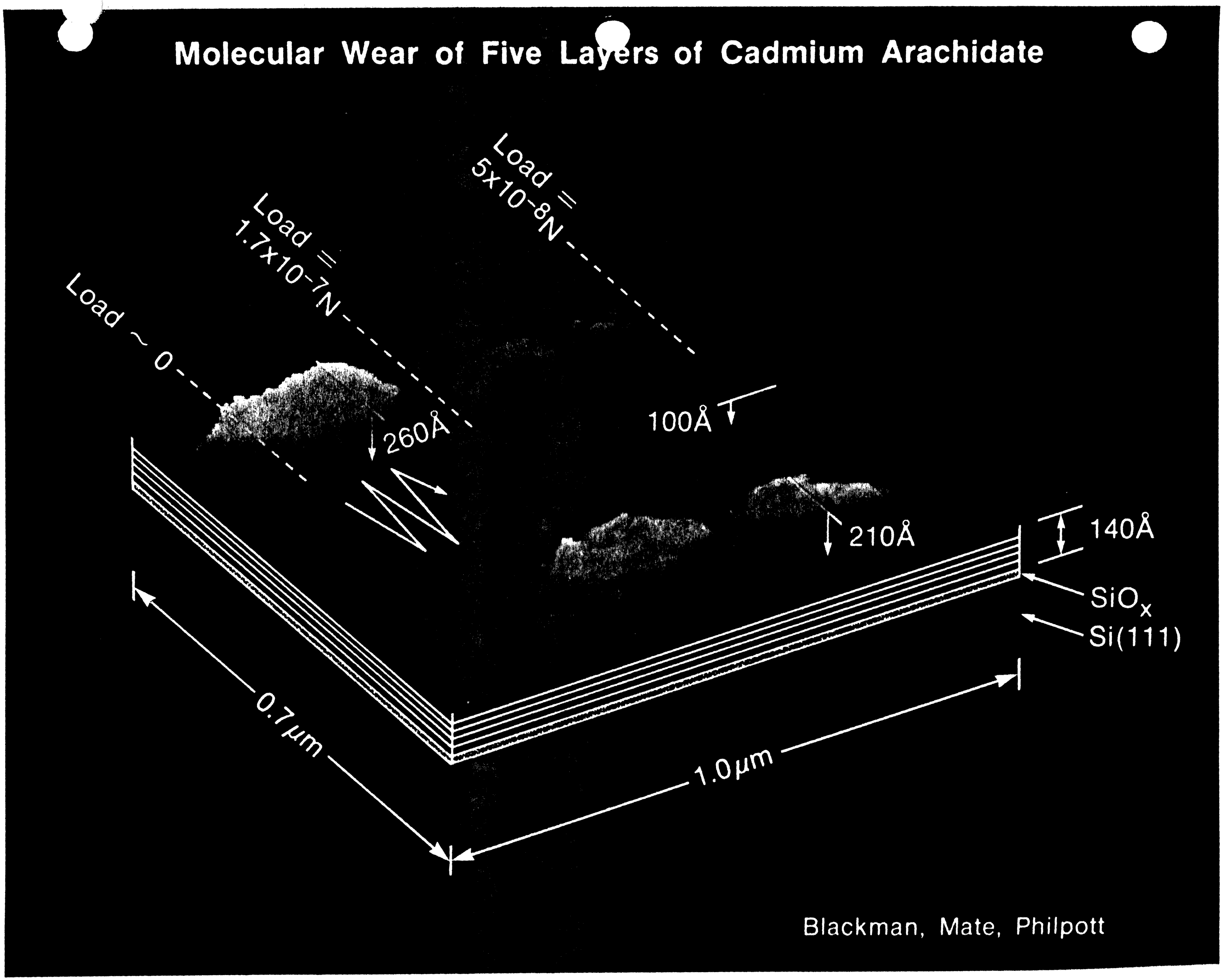

Molecular Wear of Five Layers of Cadmium Arachidate
Load ~ 0
Load = 1.7x10-7N
Load = 5x10-8N
260Å
100Å
210Å
140Å
SiOx
Si(111)
0.7μm
1.0μm
Blackman, Mate, Philpott

Sweeping of Molecular Debris on a Cadmium Arachidate Monolayer

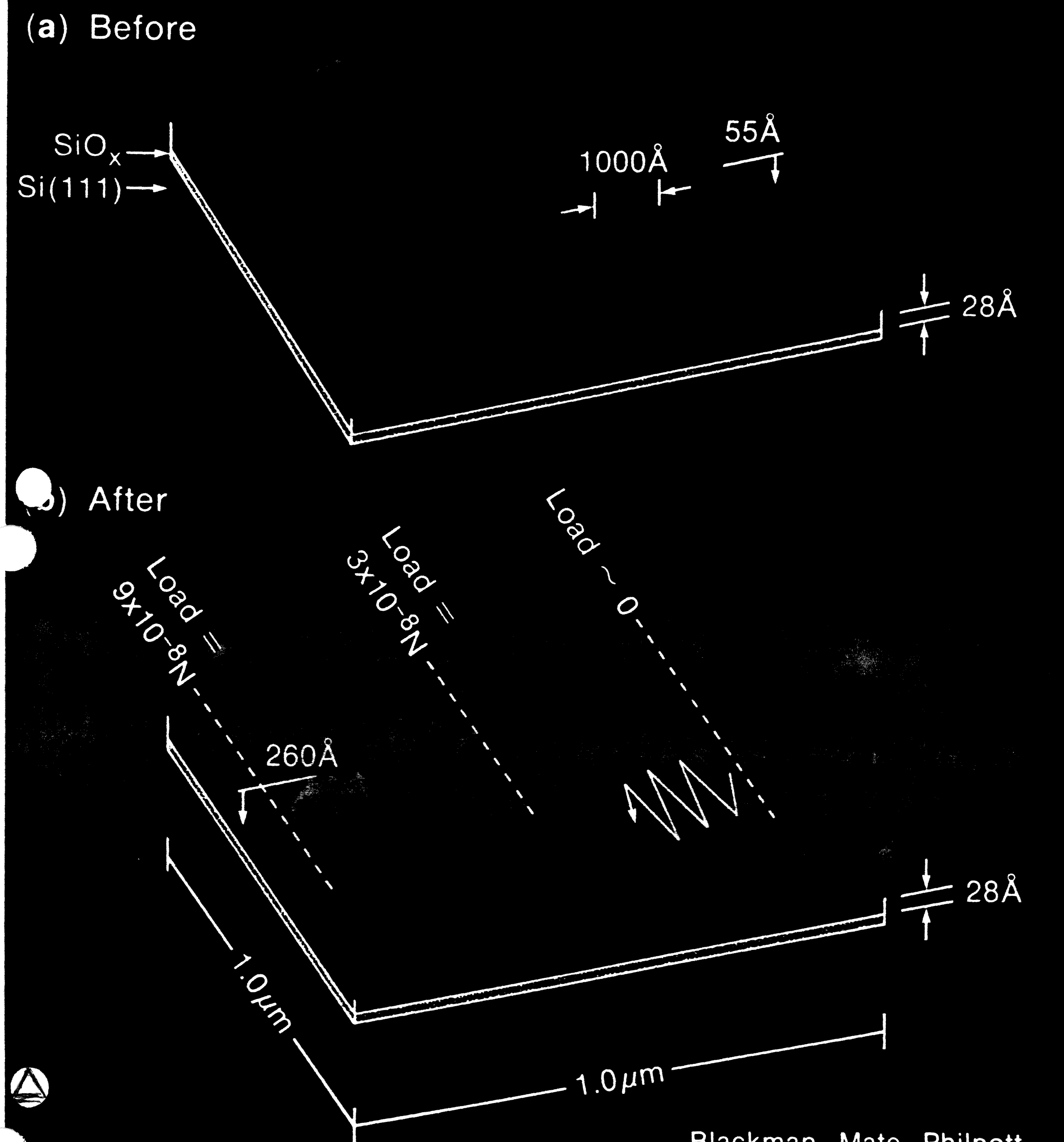

Blackman, Mate, Philpott

When you have monolayer, it stays after wear.

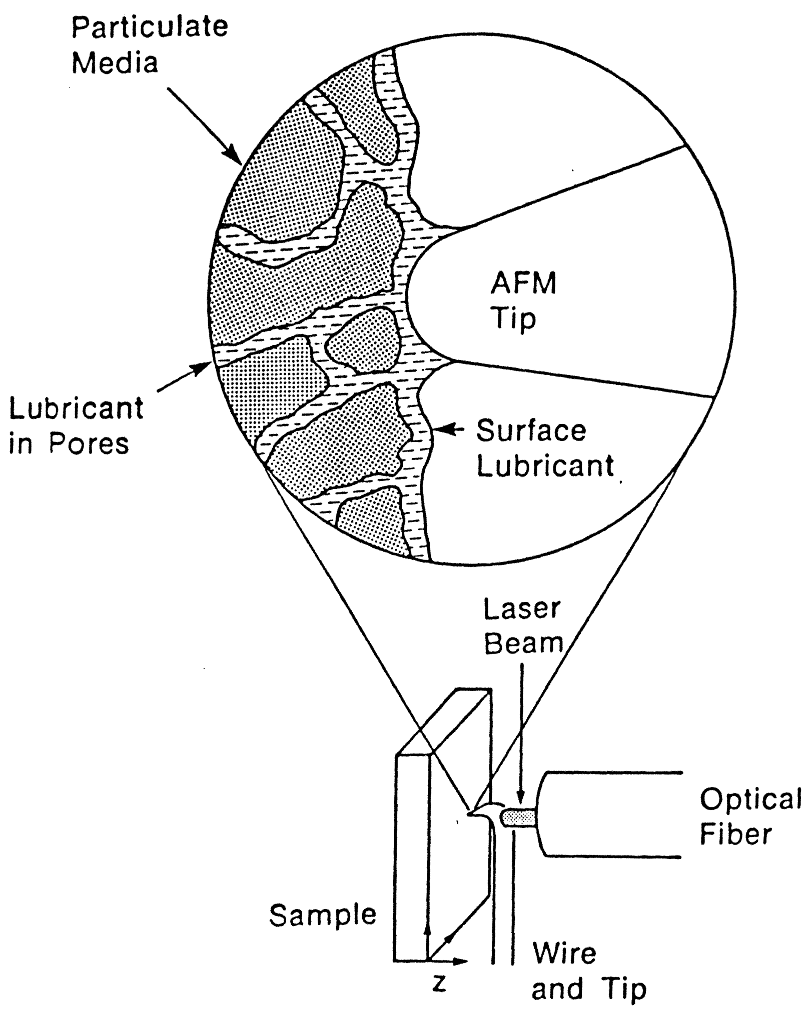

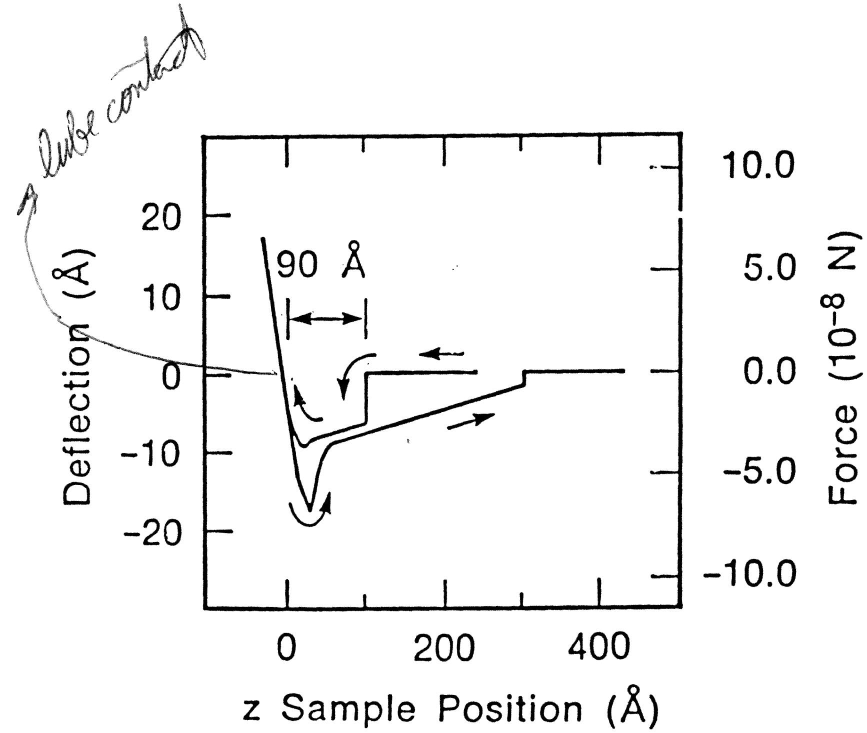

Starting here - Real lube on real discs

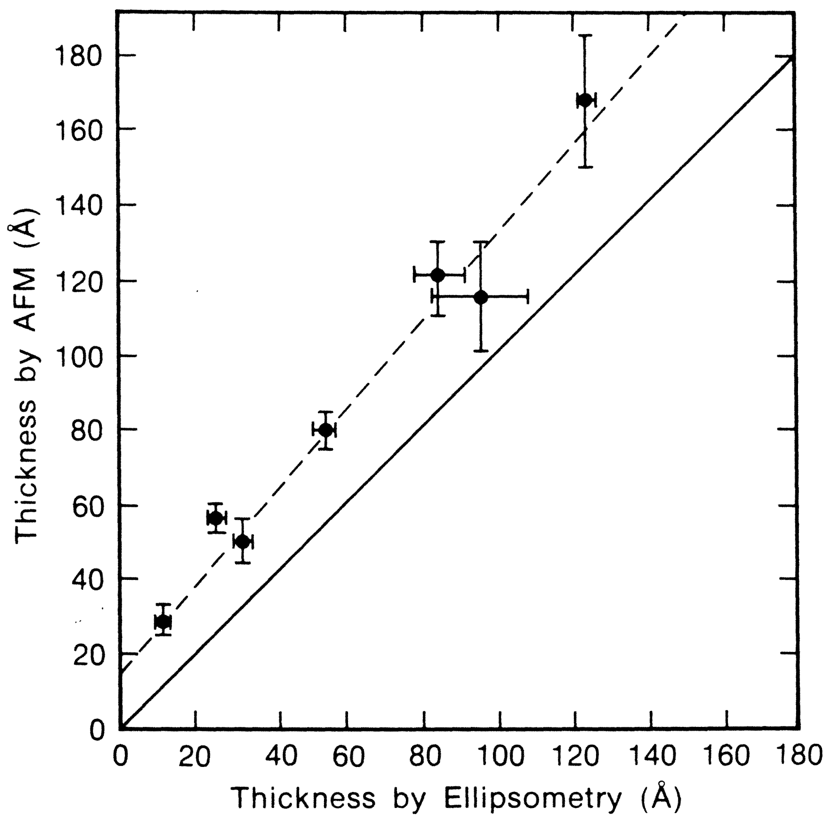

Offset caused by layers of lube on tip

Mate, Lorenz, Novotny, J. Chem. Phys. 90 (1989) 7550.

AFM Measurement of Lubricant on a Particulate Disk Surface

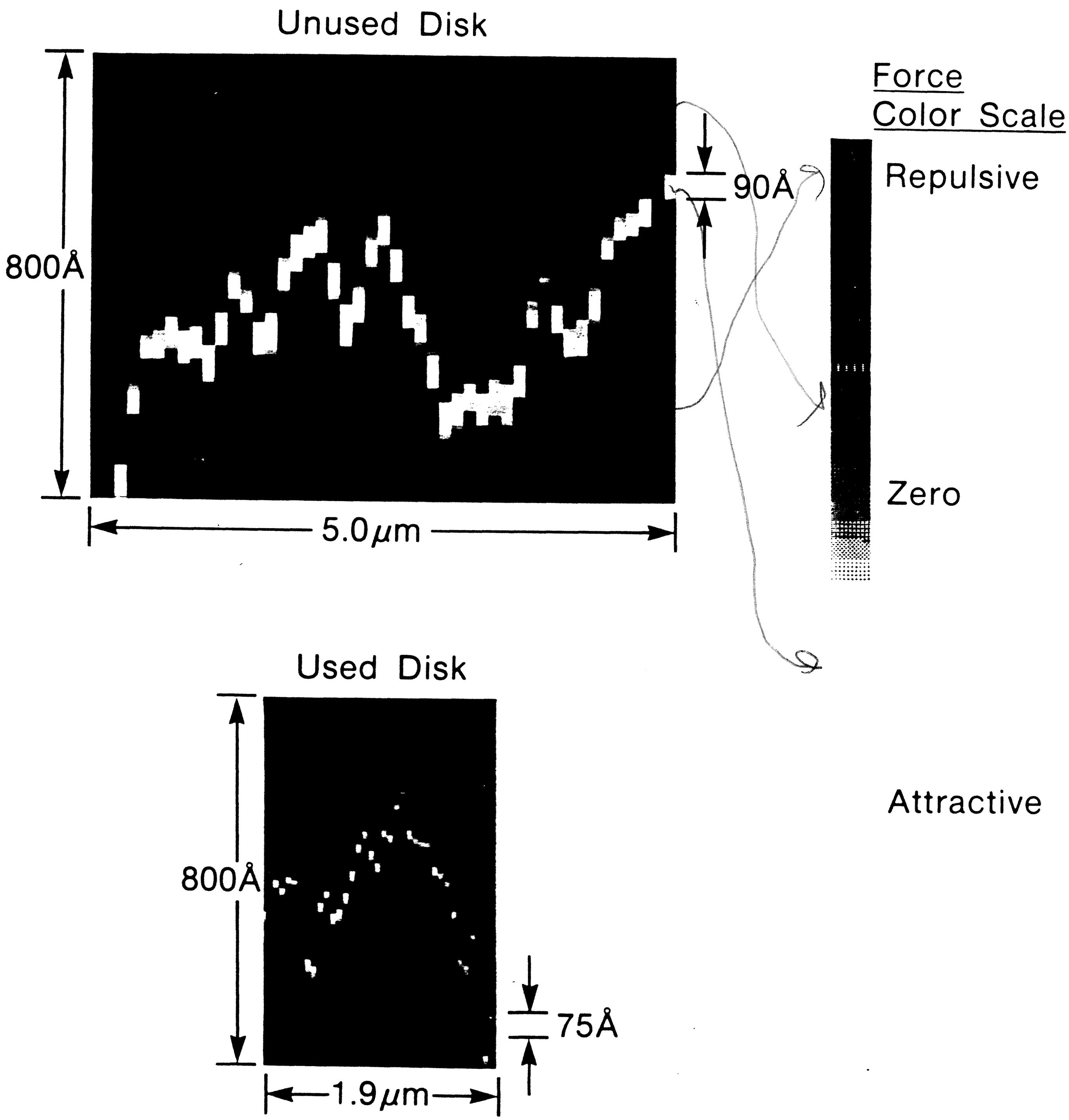

Mate, Lorenz, Novotny, IEEE Trans. on Magnetics, in press.

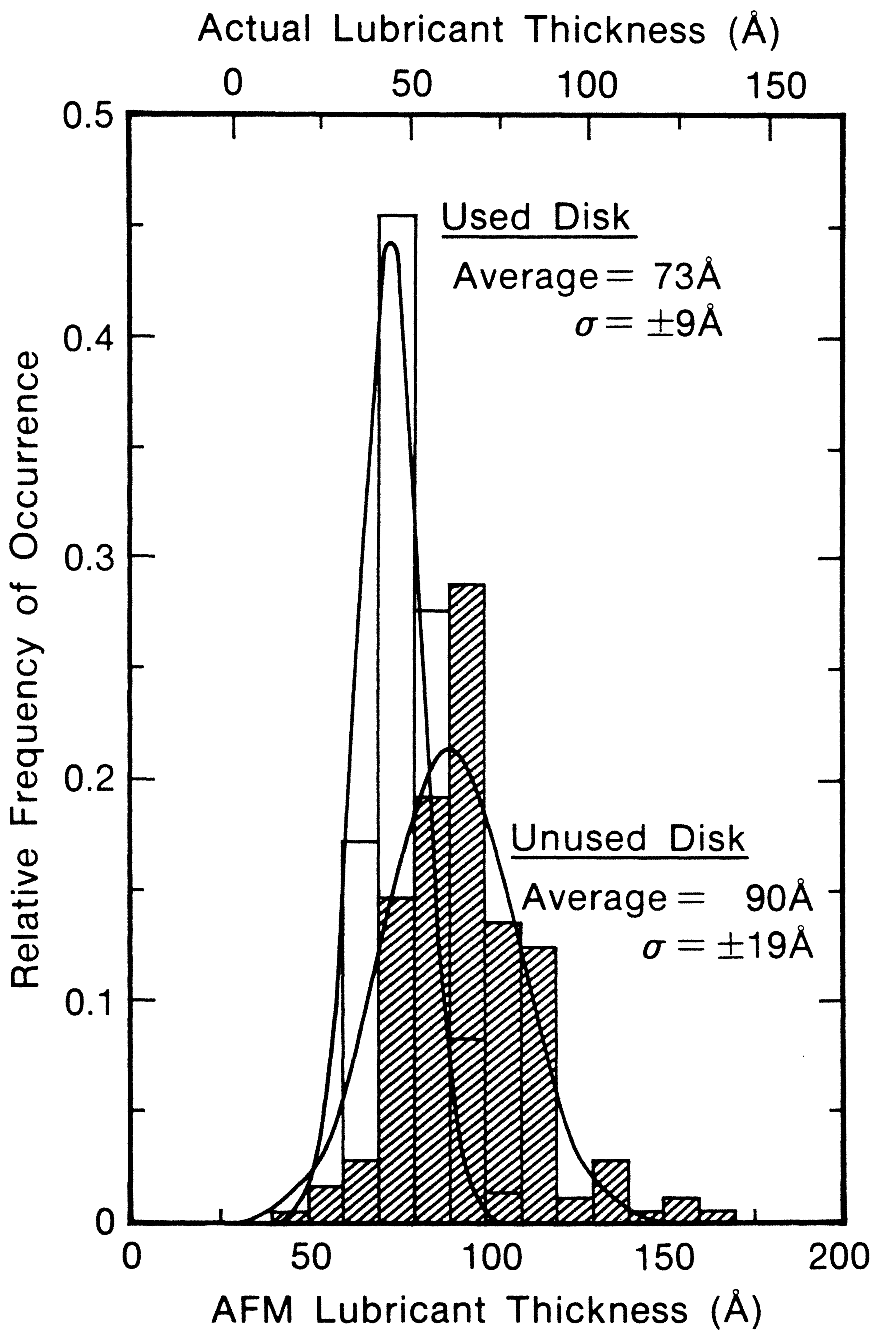
Actual Lubricant Thickness (Å)
0
50
100
150
0.5
0.4
0.3
0.2
0.1
0
Relative Frequency of Occurrence
Used Disk
Average = 73Å
σ = ±9Å
Unused Disk
Average = 90Å
σ = ±19Å
0
50
100
150
200
AFM Lubricant Thickness (Å)

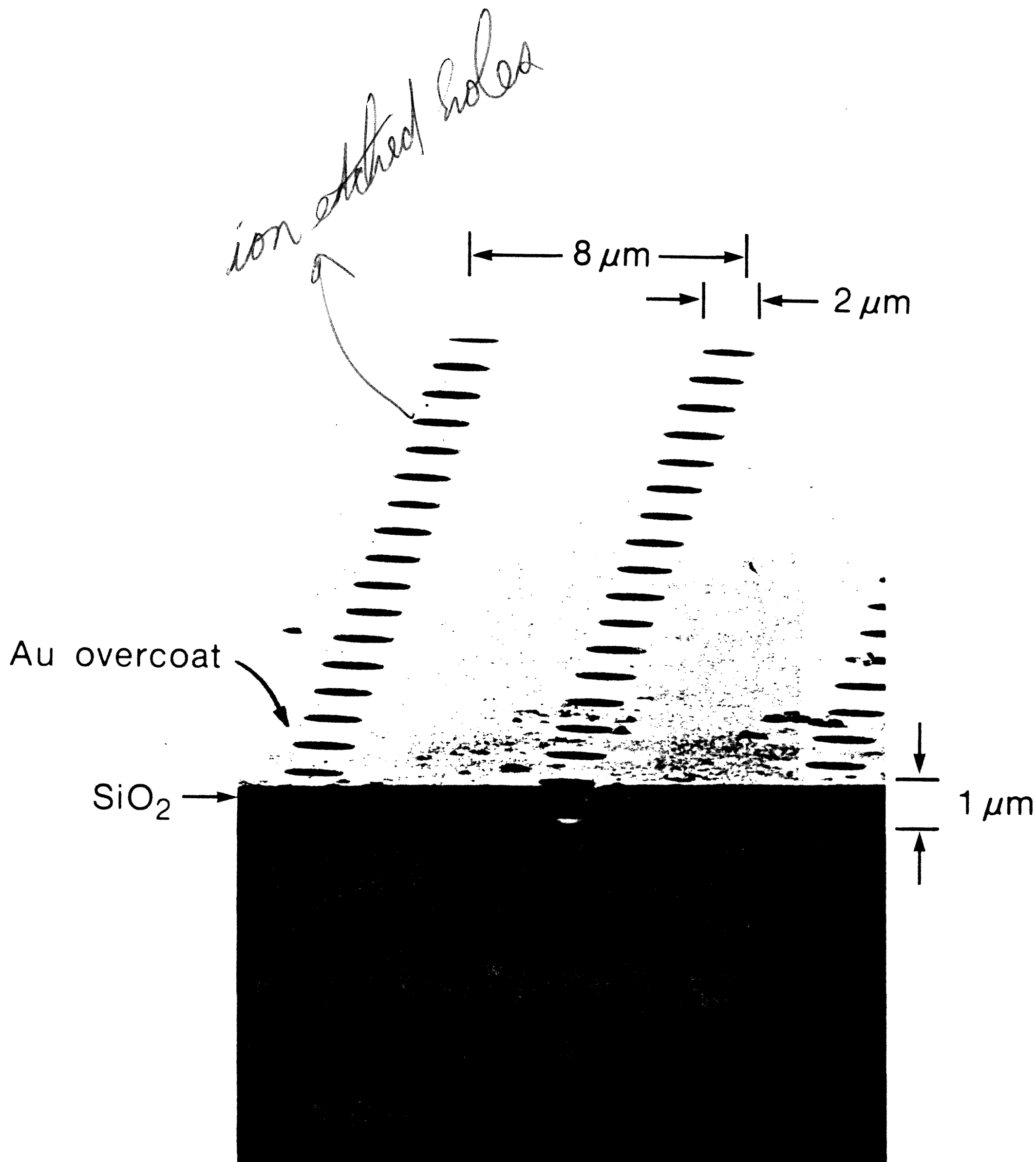

Lubricant is added over surface

A

Polymer Liquid/Air Interface on a Patterned Substrate

equil between amt of lube in hole & on surface

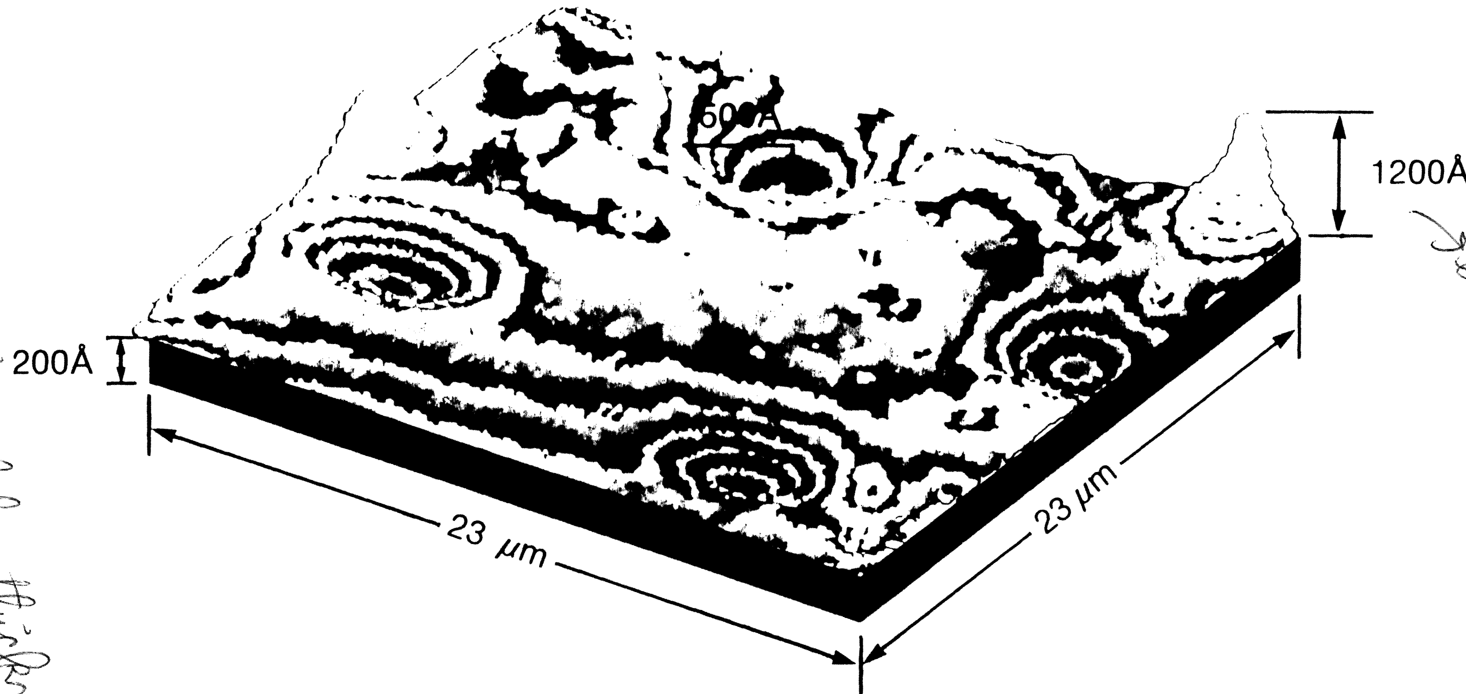

lube mound

lube thickness

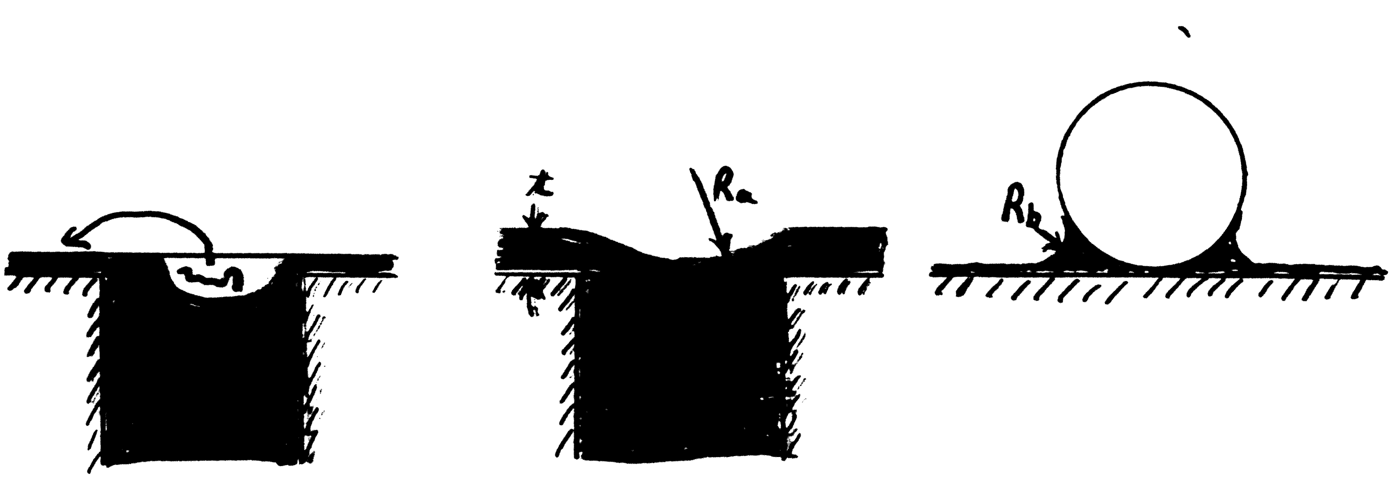

Equilibrium occurs when

$$dG_{tot} = dG_S + dG_H = 0$$

$$\frac{dg_S}{dt} A_S dt + \frac{dg_H}{dR} A_H dR = 0$$

Now $A_S dt = -A_H dR$, by mass conservation

$$\text{Disjoining Pressure} \equiv -\frac{dg_S}{dt}$$

$$\text{Capillary Pressure} \equiv \frac{dg_H}{dR} = \frac{2\gamma}{R_a}$$

$$= \frac{\gamma}{R_b}$$

$\Rightarrow$ Disjoining Pressure = Capillary Pressure, at equilibrium

Disjoining Pressure

- **Formal Definition:** The derivative of the Gibbs free energy per unit area with respect to liquid film thickness, i.e.,

$$P_d(t) = \frac{-dg}{dt}.$$

- **Informal Definition:** The extra attraction or repulsion that molecules on the surface of the liquid film experience relative to what the molecules on the surface of the bulk liquid experience.

$$P_d = \frac{F'}{A}$$

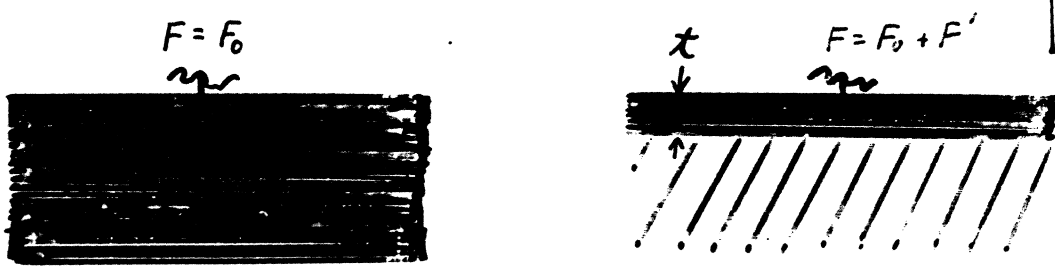

Radius of Curvature, R	$\Delta P = \frac{2\gamma}{R}$	Liquid Thickness Between Holes
510 μm	7.7×10^2 dynes/cm^2	1800 Å
230	1.7×10^3	200
1.9	2.1×10^5	50

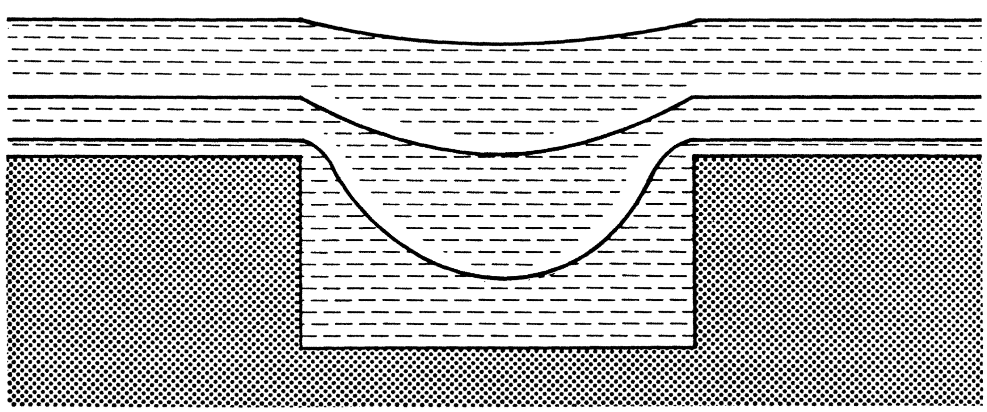

Break Free Length (BFL)

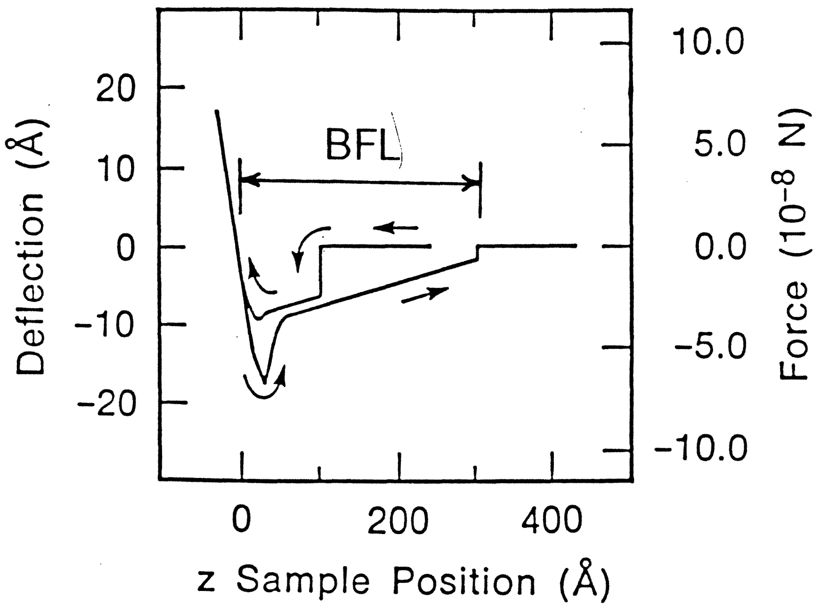

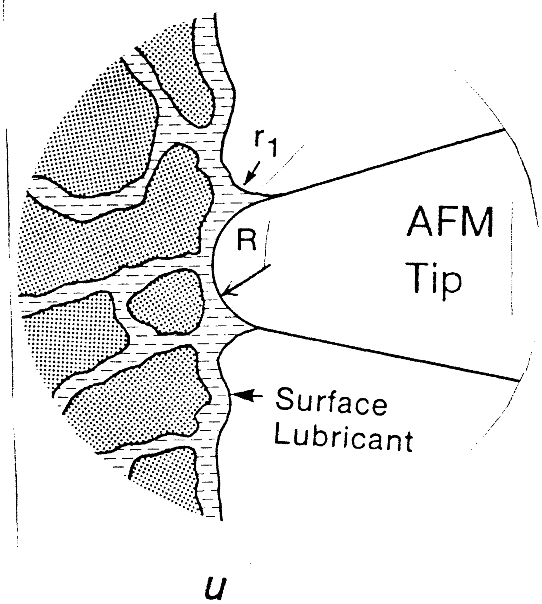

Force from the capillary or Laplace pressure,
if R $\gg$ r_1 and $\theta \sim 0$

$$F = 4\pi R\gamma_L(1 + \frac{u}{2r_1})$$

Break Free Length occurs at

$$u = -2r_1 = -\frac{2\gamma_L}{Capillary\ Pressure}$$

$$= -\frac{2\gamma_L}{Disjoining\ Pressure}$$

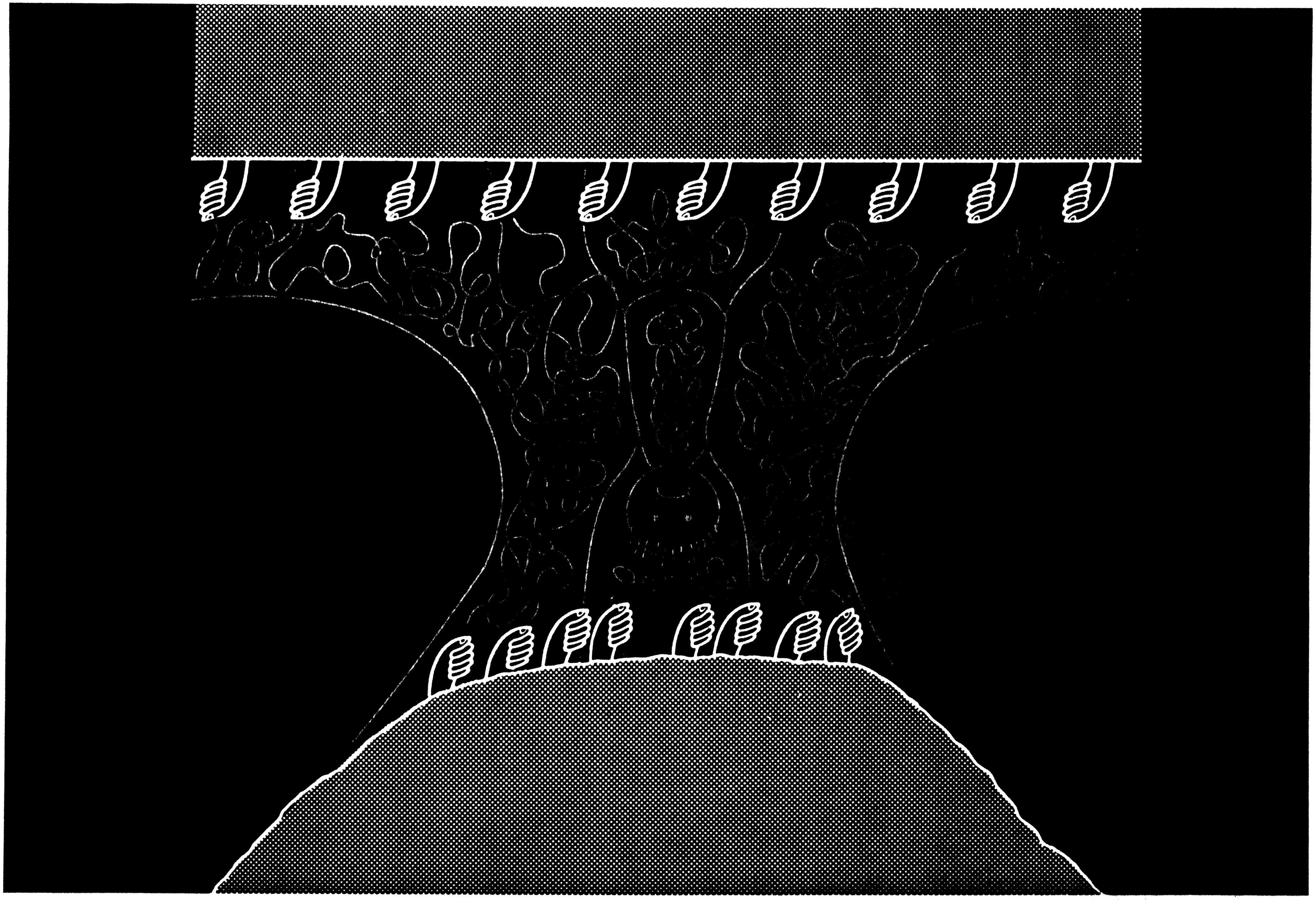

LUBRICANT ON CARBON FILMS AND PARTICULATE DISKS

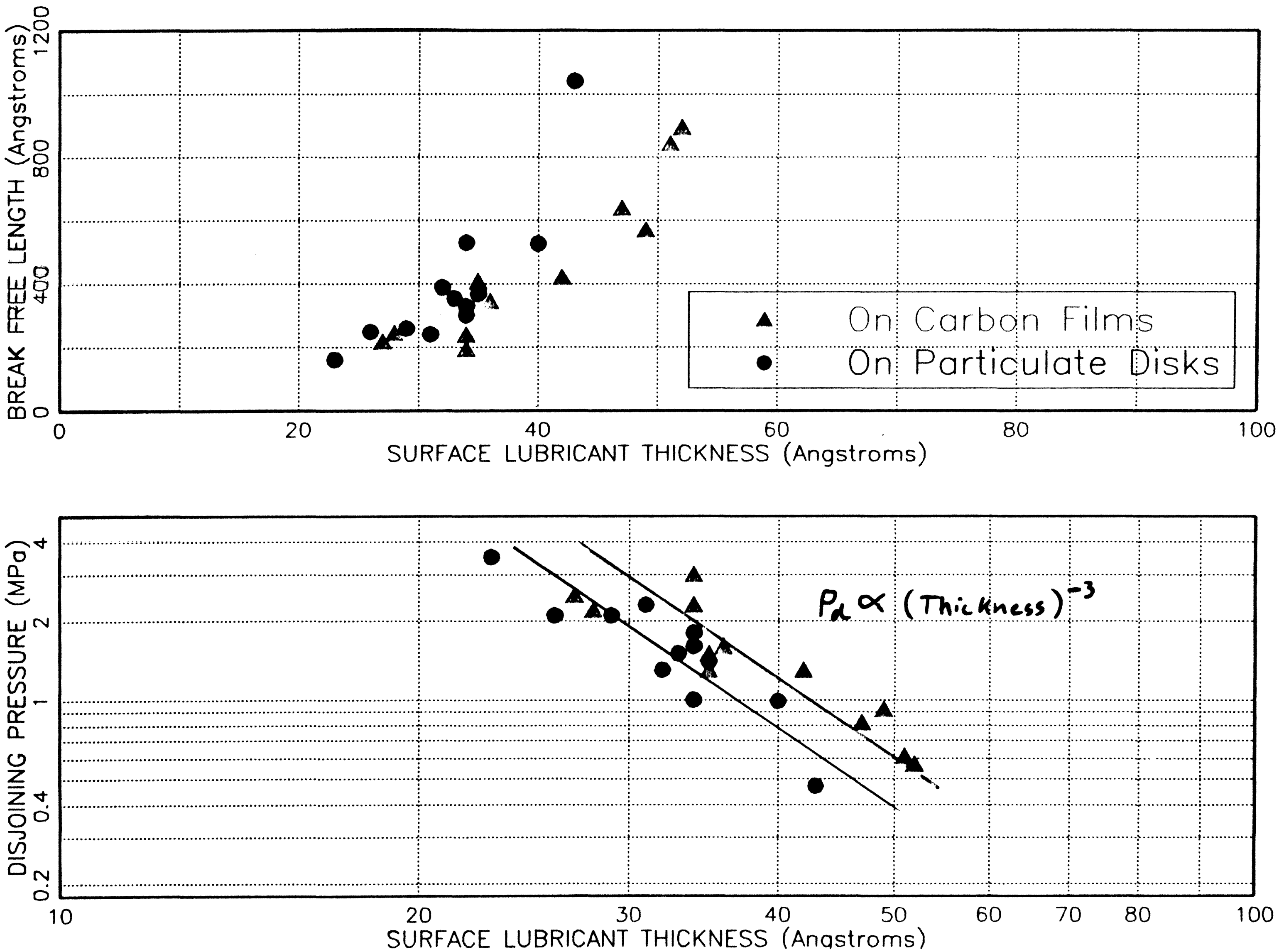

Mate, Blackman 10/89

SURFACE LUBRICANT THICKNESS vs. TOTAL LUBRICANT

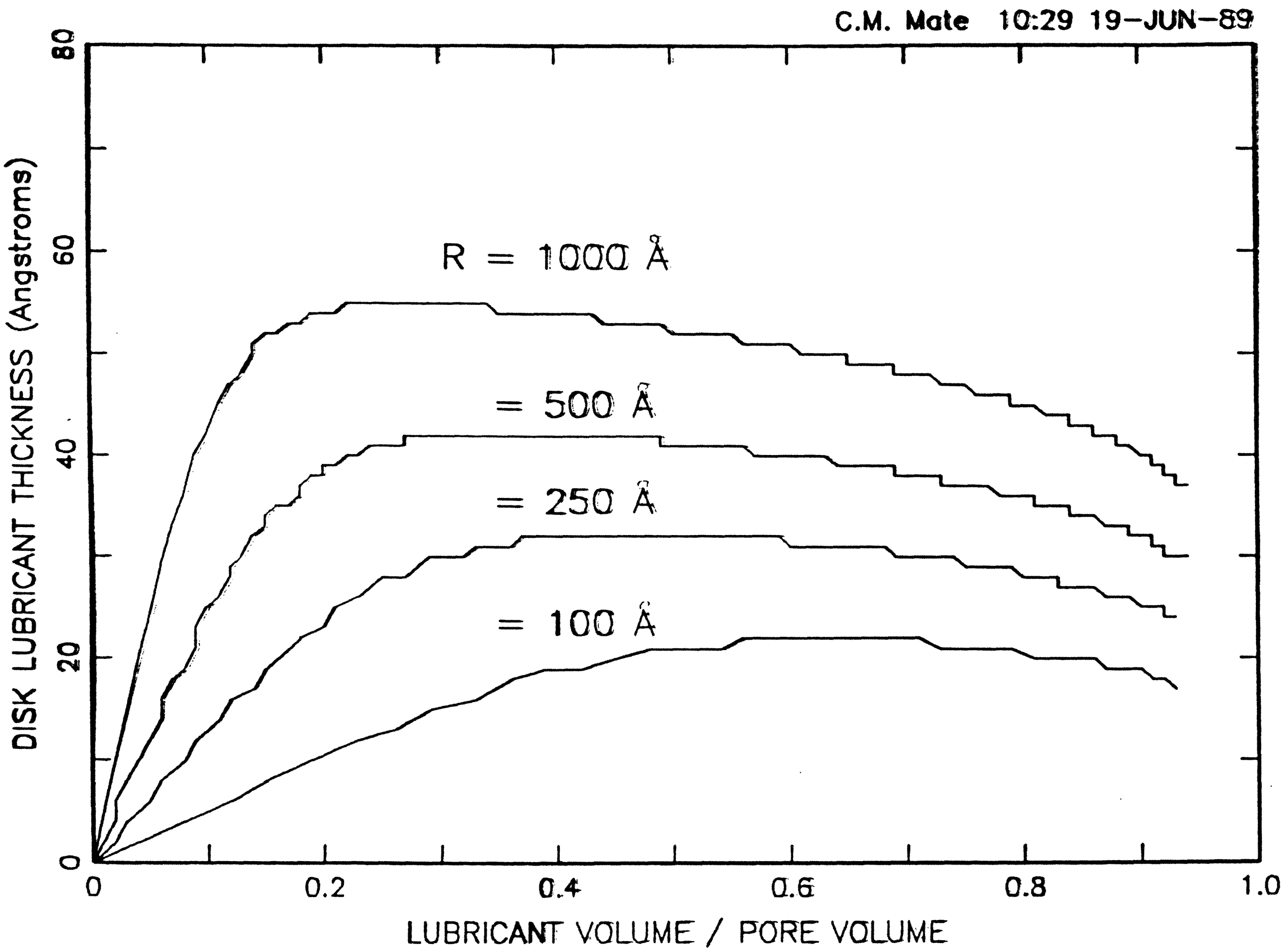

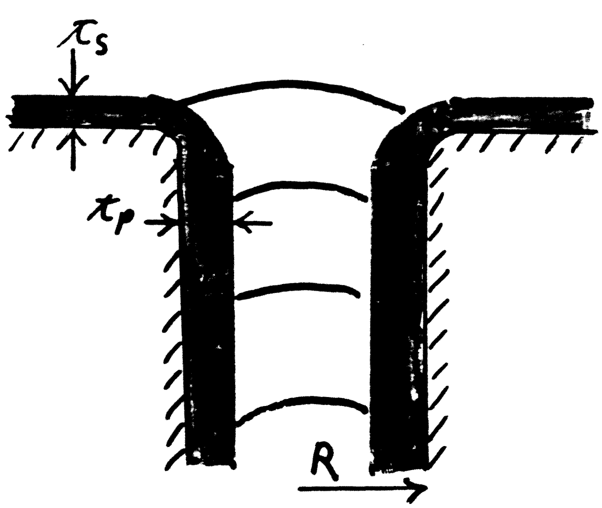

$$P_d(t_s) = P_d(t_p) + \frac{\gamma}{R - t_p}$$

Where:

$$P_d(t) = (5x10^{10}\ \text{Å}^3 \cdot Pa)\ t^{-3}$$

SURFACE LUBRICANT THICKNESS vs. TOTAL LUBRICANT

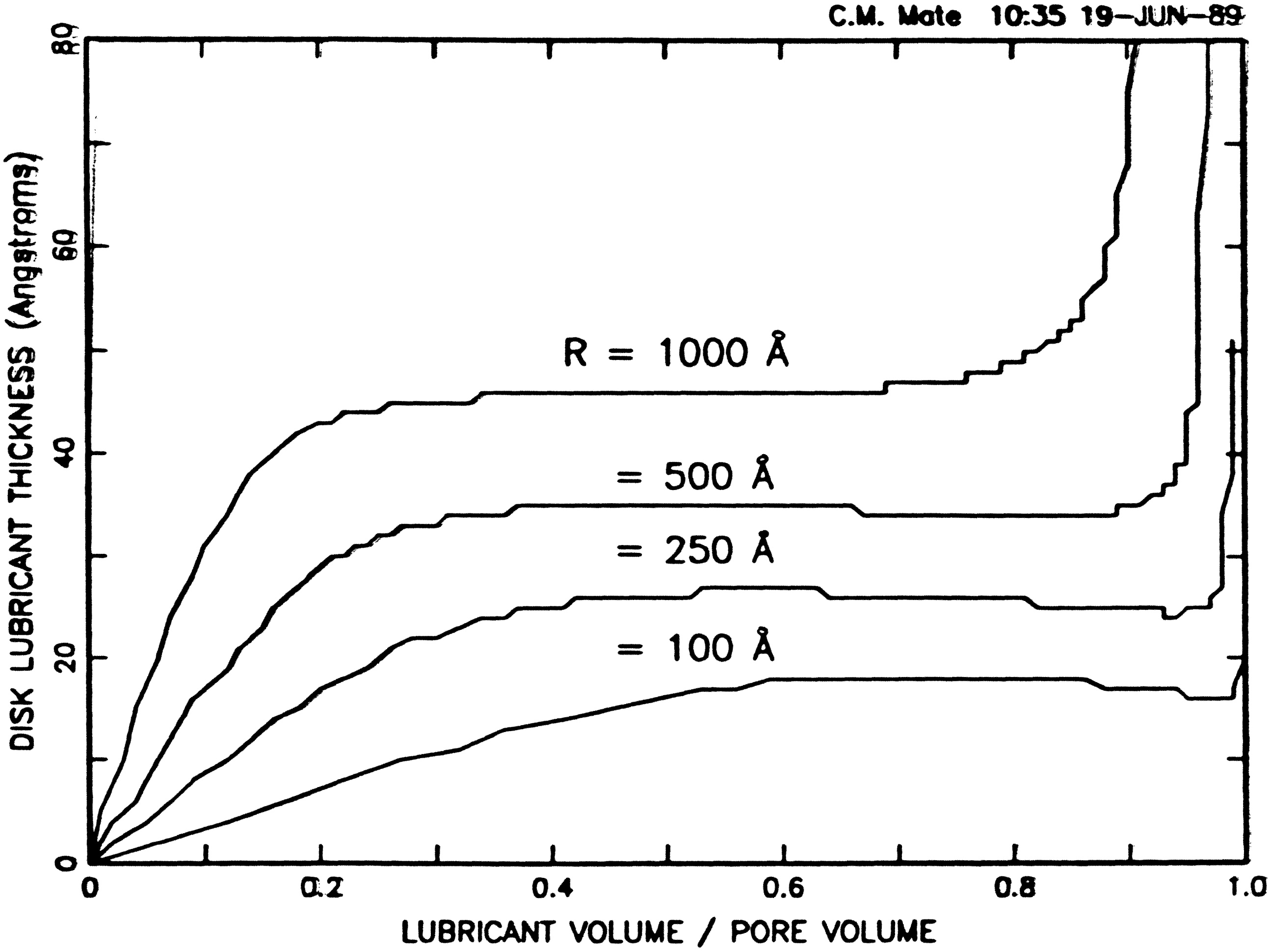

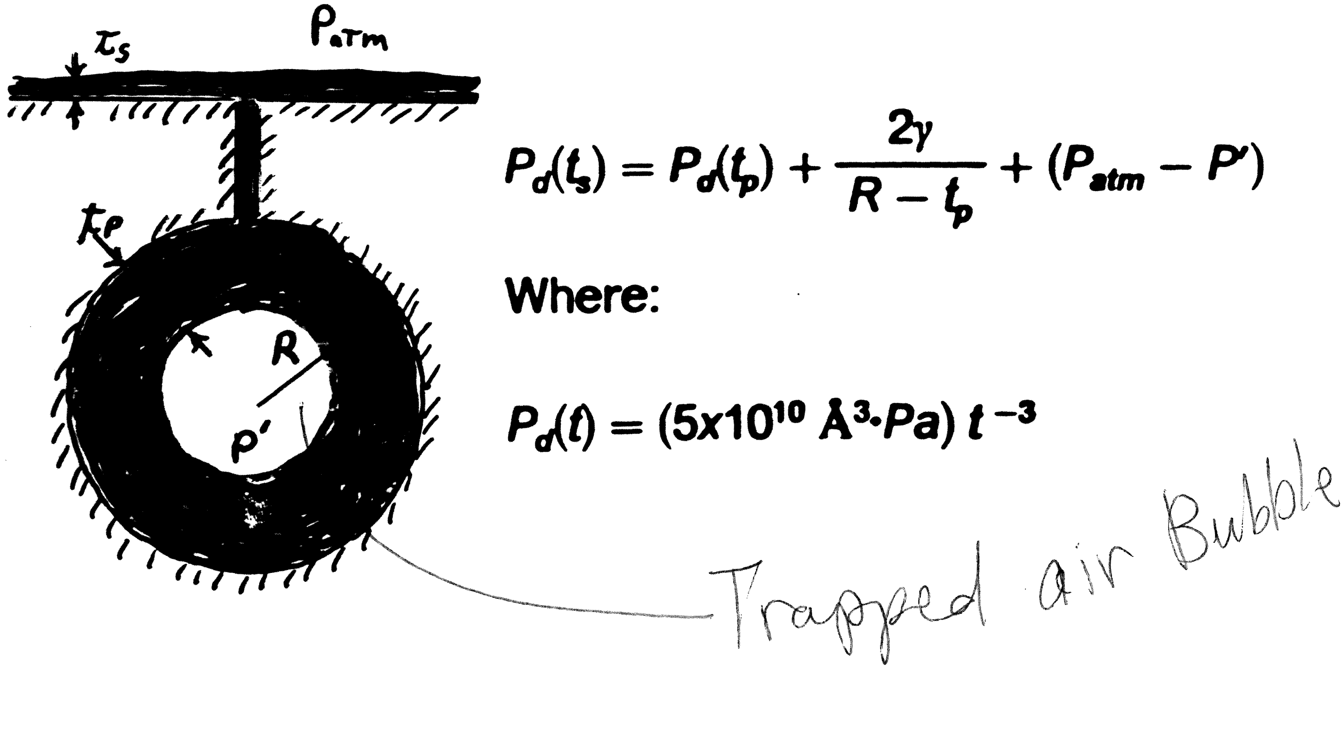

$$P_d(t_s) = P_d(t_p) + \frac{2\gamma}{R - t_p} + (P_{atm} - P')$$

Where:

$$P_d(t) = (5x10^{10}\ \text{Å}^3 \cdot Pa)\ t^{-3}$$

SURFACE LUBRICANT THICKNESS vs. TOTAL LUBRICANT

ON A PARTICULATE DISK

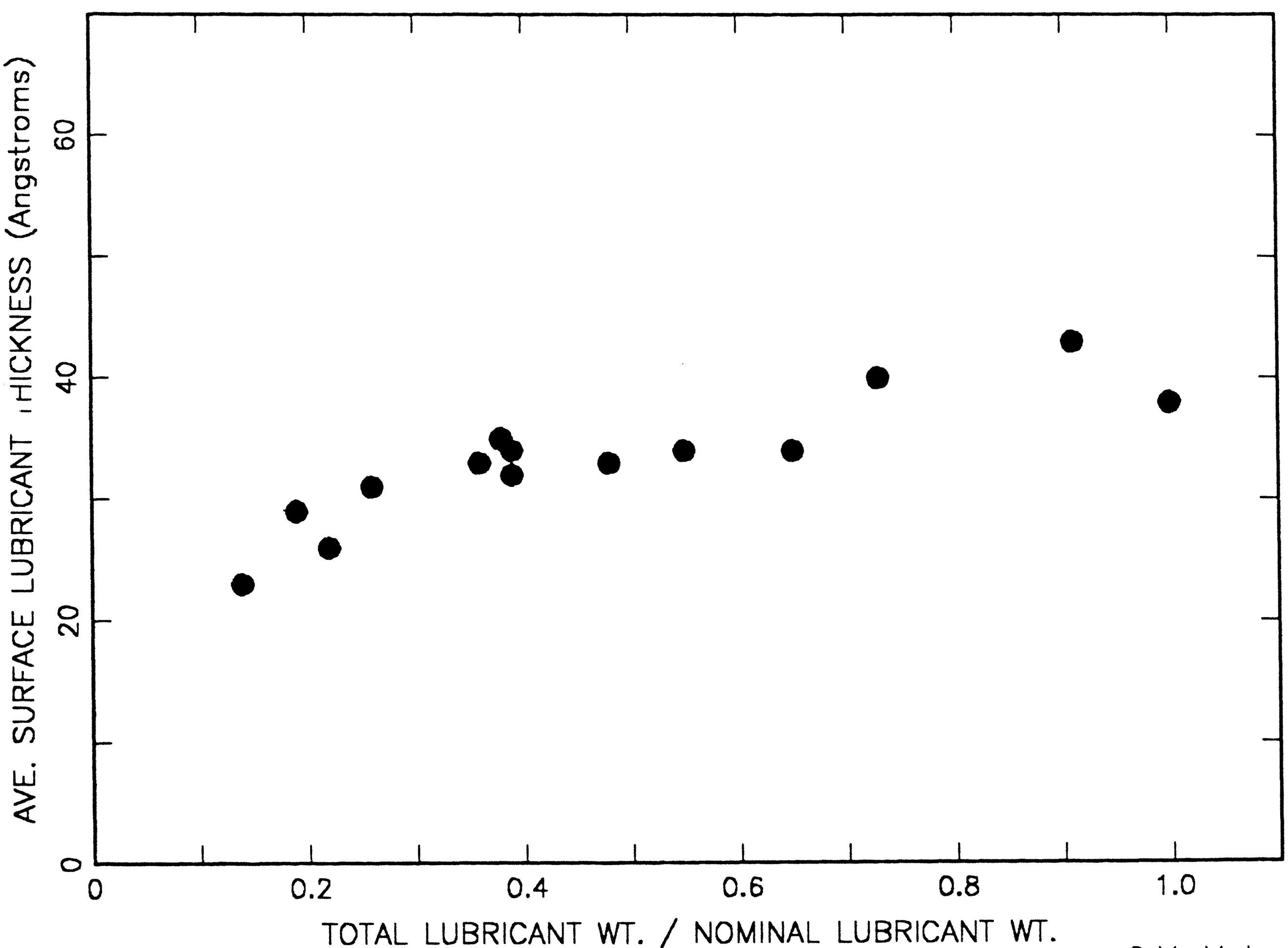

C.M. Mate

Bonded lube = functional end group

Blunter tip

sharper tip

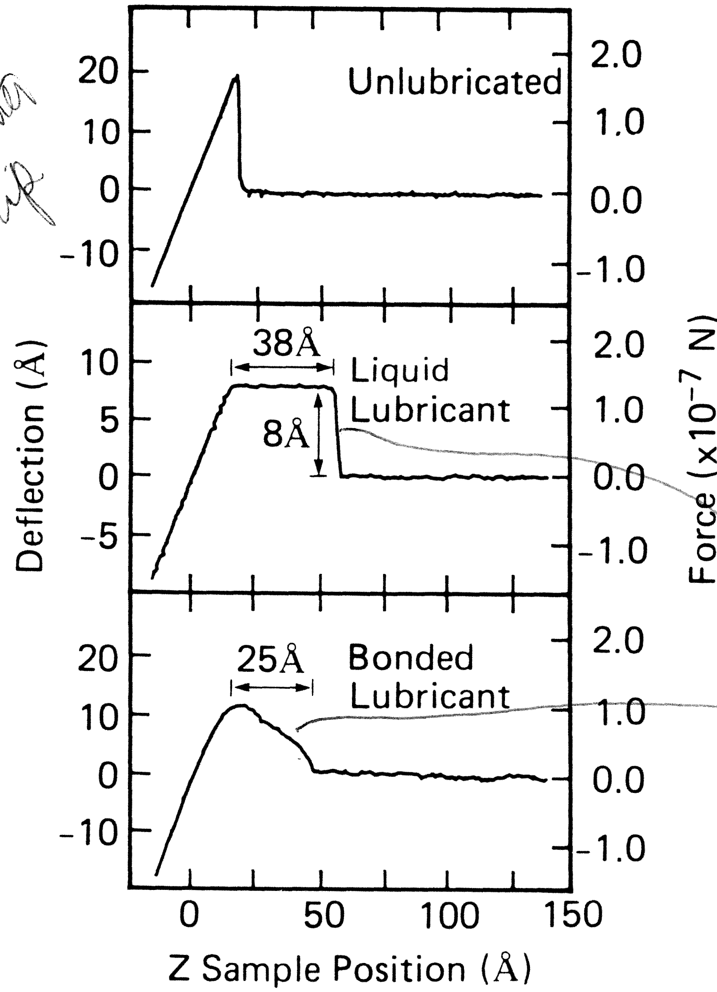

lube sticks to disc, therefore faster pull away

C.M. Mate, L.J. Lin

Conclusions

AFM is allowing us to understand the tribology of the slider-disk interface on the sub-nanometer scale.

In particular:

→ AFM can determine the morphology of the slider and disk surfaces.

→ AFM can be used as a micro-indenter.

→ Atomic-scale features are observed on the friction force for an AFM tip dragging across layered compounds.

→ AFM can determine the thickness and distribution of molecular thin films of lubricants on surfaces.

→ AFM can determine the disjoining pressure of lubricant films.

→ The equilibrium lubricant thickness on porous particulate disks is determined by the balance of capillary and disjoining pressures.

→ AFM indicates that lubricants bonded to surfaces lose their liquid character.

ADVANCED TRIBOLOGY TECHNIQUES

V. Novotny
IBM Research Division
Almaden Research Center
San Jose, California

Presentation at IIST Short Course on Head-Disk Interface

Santa Clara University, Dec. 1989

Tribology

--study of interfacial processes of bodies in motion.

In magnetic recording, tribology is more and more important as the flying height is lowered.

Tribology in magnetic recording is unique:

- **High velocity flying** $\lesssim$ **60m/sec**
- **High velocity sliding** $\lesssim$ **10m/sec**
- **Intermittent contact in flying**
- **Very thin lubricant layers** $\lesssim$ **50 Å**
- **Extremely high shear rates** $10^8 \rightarrow 10^{10}\ sec^{-1}$

Outline

- Properties of importance in tribology
- "Classical" measurement techniques
- "Advanced" measurement techniques
- Emphasis on lubricant characterization

Disclaimers:

- This is not a comprehensive review
- Reference list is not complete

PROPERTIES OF IMPORTANCE IN TRIBOLOGY

1. Static and dynamic friction

2. Wear rates

3. Contacts
   - areas
   - number
   - frequency
   - energy and momentum transfer
   - mass transfer

4. Interfacial temperatures

5. Lubricant properties
   - distribution
   - dynamics--displacement, loss, migration
   - conformation
   - viscosity at high shear rates
   - degradation

6. Contamination
   - organics and water
   - particulate

FRICTIONAL MEASUREMENTS

Tangential deflection measured with

- **Strain gauges**
- **Optical sensing**
- **Accelerometry**
- **Atomic force technique**

Surface Force Apparatus

FRICTION MEASUREMENTS

WITH STRAIN GAUGES

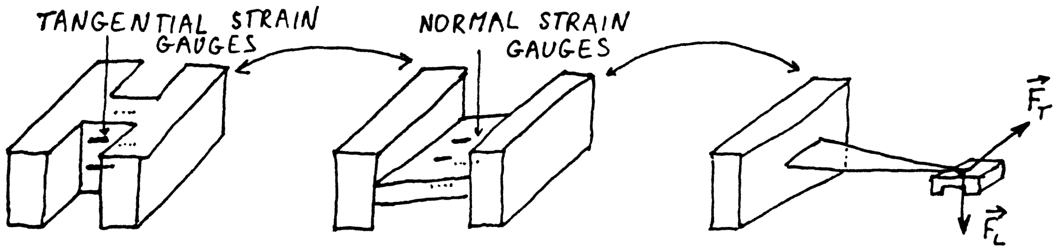

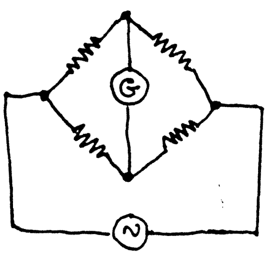

f_S = STATIC FRICTION COEFFICIENT

f_D = DYNAMIC FRICTION COEFFICIENT

$$f_{S,D} = \frac{|\vec{F}_{T\,S,D}|}{|\vec{F}_L|}$$

FOR LUBRICATED MEDIA : $f_S \gtrsim 0.3$

$f_D \approx 0.1 \rightarrow 0.2$

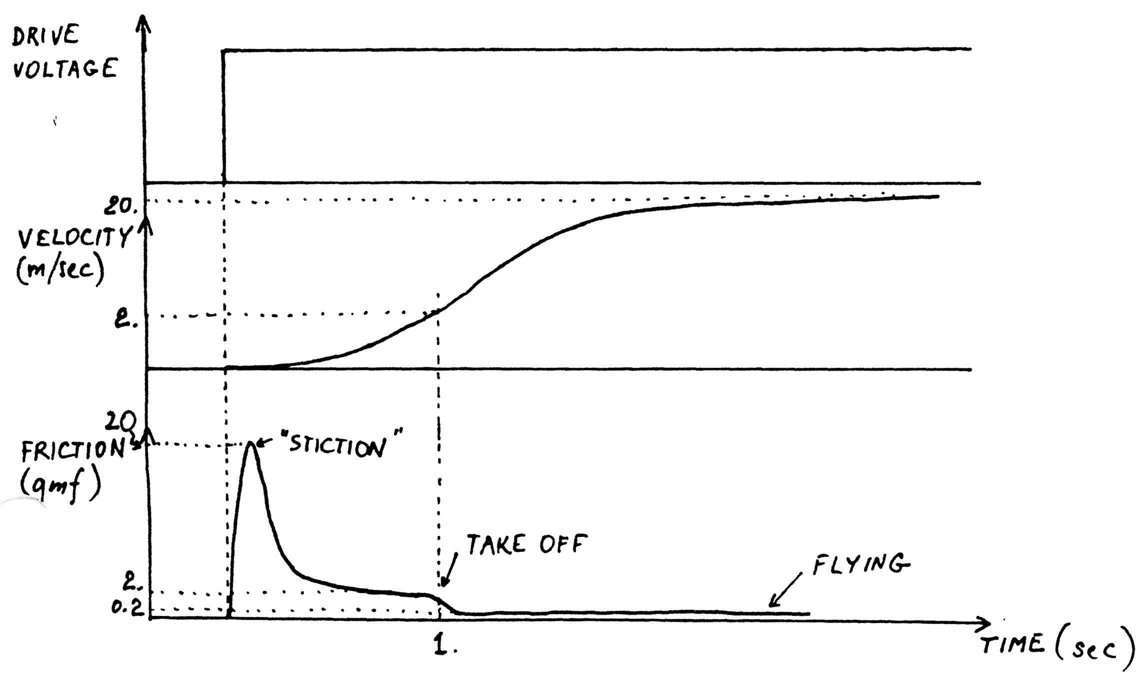

WEAR RATE MEASUREMENTS

In-situ (I)
Ex-Situ (E)
Dynamic (D)
Static (S)

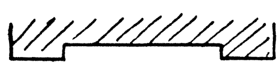

← slider

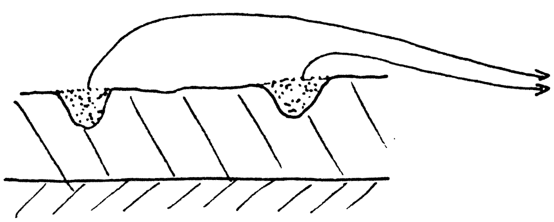

wear area A; number of cycles N

Wear rate $W = \frac{A}{N}$

WEAR MEASUREMENTS

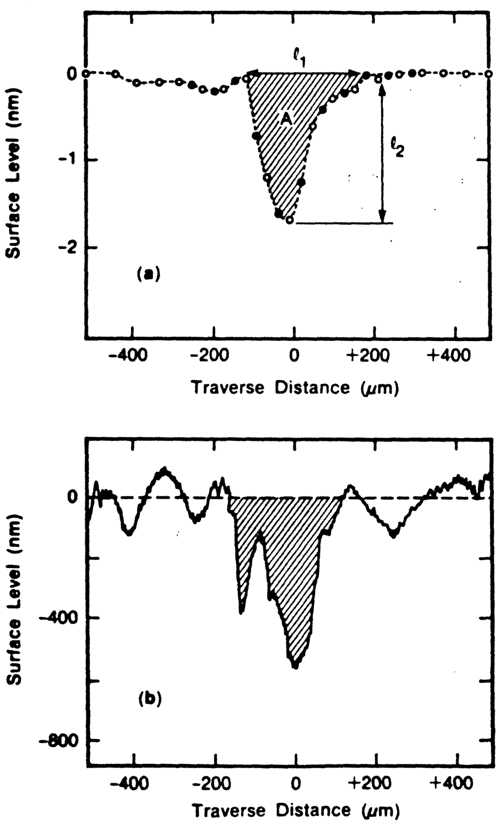

FIG. 2. An example of the wear track measurement by (a) ellipsometer and an illustration of the parameters used to characterize wear traces, and (b) profilometer. The regions outside the wear track indicate the typical surface roughness.

WEAR RATE	W
WEAR VOLUME	V
WEAR CROSS-SECTIONAL AREA	A
LENGTH OF THE TRACK	L
NUMBER OF CYCLES	N
RADIUS	r

$$W = \frac{V}{L} = \frac{2\pi r A}{2\pi r N} = \frac{A}{N}$$

WEAR COEFFICIENT	R
LOAD	F
INDENTATION HARDNESS	H

$$R = \frac{HW}{F}$$

special head

THE HERTZIAN CONTACT OF A SPHERICAL CAP ON A FLAT SURFACE

SPHERICAL CAP RADIUS	s
CONTACT RADIUS	a
TOTAL FORCE	F_T
POISSON'S RATIO	ν_i
YOUNG'S MODULUS	E_i

$$a^3 = 3s\,F_T\,(k_1 + k_2)/4$$

$$k_i = (1 - \nu_i^2)/E_i \qquad i = 1, 2$$

WEAR EXAMPLE

PIN ON DISK TEST

CARBON OVERCOATED DISK, UNLUBRICATED

TiC/Al_2O_3 SLIDER - SPHERICAL CAP WITH RADIUS $s = 10$ cm

LOAD $F_L = 0.15$ N, ADHESION FORCE $F_A \simeq 0.03$ N

$A = 0.75\ \mu m^2$

$N = 2.86 \times 10^4$ cycles

$W = A/N = 0.25 \times 10^{-4}\ \mu m^2/cycle = 25\ nm^2/cycle$

$H = 22$ GPa

$F_T = F_L + F_A = 0.15 + 0.03 = 0.18$ N

$R = HW/F_T = 22 \times 10^9 \times 0.25 \times 10^{-16}/0.18 = 0.3 \times 10^{-5}$

$10^{-5} \lesssim R \lesssim 5 \times 10^{-3}$ THREE BODY ABRASIVE WEAR

$E_{1disk} \cong 100$ GPa $\quad \nu_{1disk} \cong 0.25 \quad k_1 = (1-\nu_1^2)/E_1 = 0.94 \times 10^{-11}$

$E_{2slider} \cong 450$ GPa $\quad \nu_{2slider} \cong 0.25 \quad k_2 = (1-\nu_2^2)/E_2 = 0.20 \times 10^{-11}$

$a^3 = 3 \cdot s\, F_T\, (k_1 + k_2)/4 = 0.15 \times 10^{-12}$

$a = 0.54 \times 10^{-4}\ m = 54\ \mu m$

CALCULATED TRACK WIDTH $\approx 110\ \mu m$

MEASURED TRACK WIDTH $\approx 200\ \mu m$

WEAR RATE MEASUREMENTS

• Scanning microellipsometry	I,D	Ref.
• Mechanical profilometry	E,S	
• Optical interferometry	E,S	e.g. WYKO
• Atomic force microscopy	E,S	
• Optical integrating sphere	E,S	Ref.
• Particle size and concentration	I,D	

CONTACT MEASUREMENTS

- PZT sensing
- Magnetoresistive sensing
- Optical imaging
- Mass transfer - surface analysis techniques

SCANNING MICROELLIPSOMETRY

- IN-SITU, DYNAMIC TRIBOLOGY

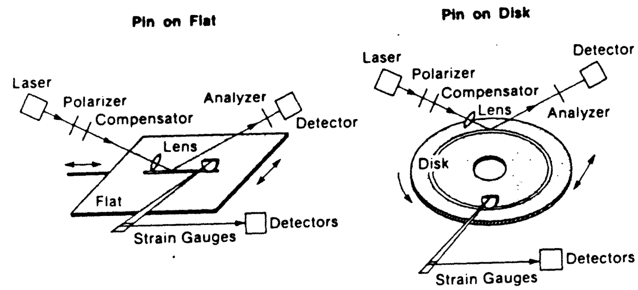

Figure 1. Low-speed pin-on-flat and pin-on-disk tribological setups with in situ scanning microellipsometry to profile wear of LB films.

SPATIAL RESOLUTION $20\mu m \times 60\mu$

THICKNESS RESOLUTION $\lesssim 0.5$Å

THICKNESS ACCURACY ~ 1 Å

TYPICAL OPTICAL CONSTANTS OF CARBON OVERCOATED THIN FILM DISK

TABLE I. The optical constants measured by ellipsometry and optical spectroscopy at $\lambda = 633$ nm.

Parameter	Value
Real part of magnetic film refractive index, n_s	2.3
Imaginary part of magnetic film refractive index, k_s	4.4
Real part of carbon film refractive index, n	2.0
Imaginary part of carbon film refractive index, k	0.6

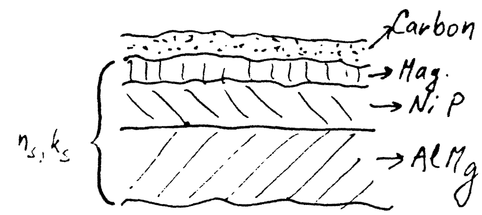

$$\Psi = f_1(n_s, k_s, n, k, d, \phi, \lambda)$$

$$\Delta = f_2(n_s, k_s, n, k, d, \phi, \lambda)$$

f_1, f_2 – FUNCTIONS DERIVED FROM PROPERTIES OF REFLECTED AND REFRACTED LIGHT

n_s, n – REAL PART OF REFRACTIVE INDEX OF SUBSTRATE AND FILM

k_s, k – IMAGINARY " " " " " " "

d – FILM THICKNESS

ϕ – ANGLE OF INCIDENCE

λ – WAVELENGTH

WEAR RATES OF CARBON OVERCOATED DISKS

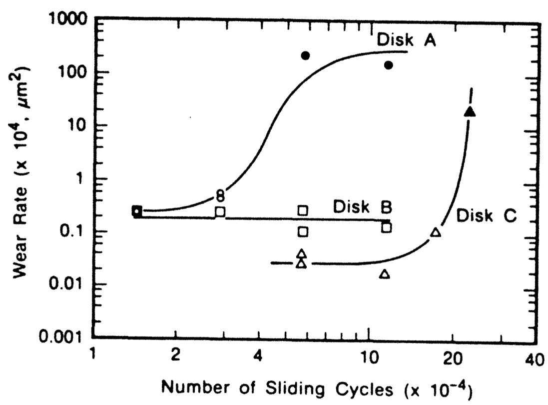

FIG. 5. The wear rate on three different carbon overcoated thin-film recording disks under a 0.15-N load. The open symbols correspond to wear of the overcoat while the solid symbols correspond to wear of the underlying layers.

@ TiC sliders

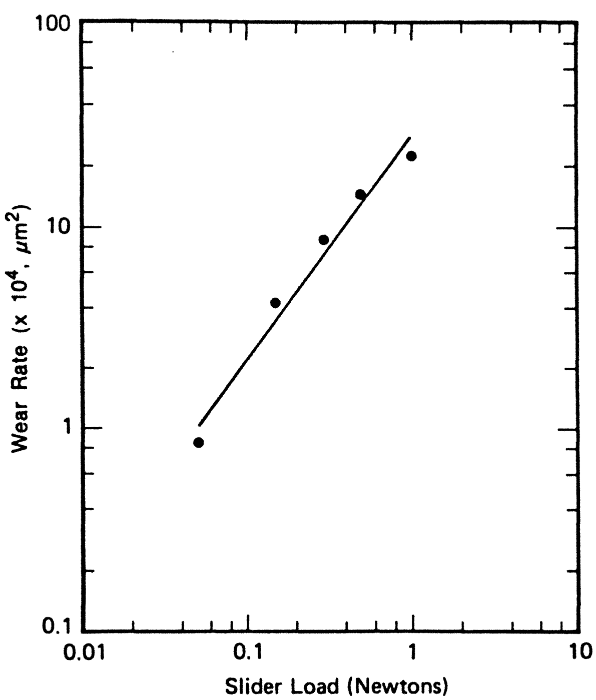

FIG. 6. The average wear rate of the overcoat as a function of the slider load.

OPTICAL INTERFEROMETRY

WYKO

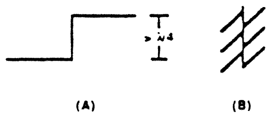

Fig. 1. (A) Step height too large to measure with a single wavelength λ. (B) Fringes in region of step show possible ambiguity in fringe order.

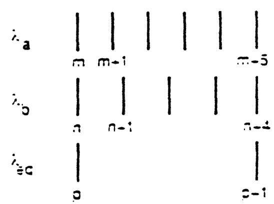

Fig. 3. Synthesis of beat wavelength λ_{eq} using shorter wavelengths λ_a and λ_b.

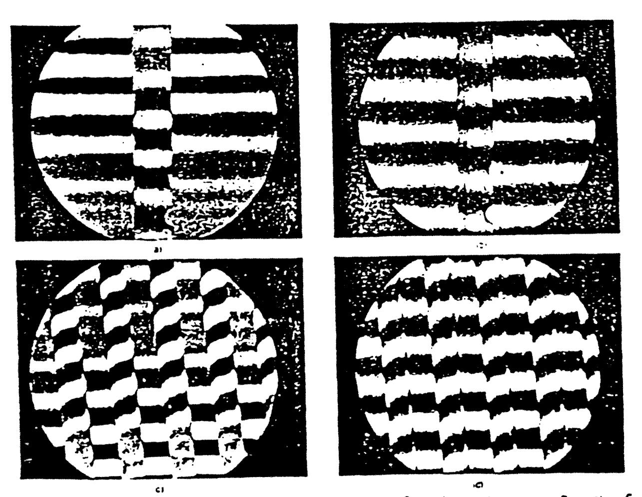
Fig. 2. Black and white photographs of (A) white light fringes of an optical wavefront, (B) same fringes with a narrowband filter in place, (C) white light fringes of a grating, and (D) images of grating with narrowband filter in place

Wyko has moving mirror to determine direction

Ball bearing

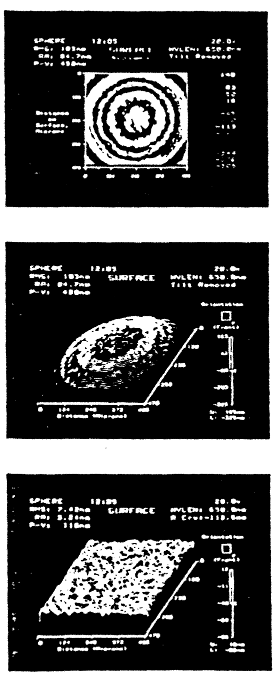
A color contour map and three-dimensional plot of a ball bearing surface measured with a 20X magnification head. The bottom figure is a plot of the same surface with the curvature removed by software. This plot shows an rms roughness of 7.12 nm over the measured region.

Polypropylene

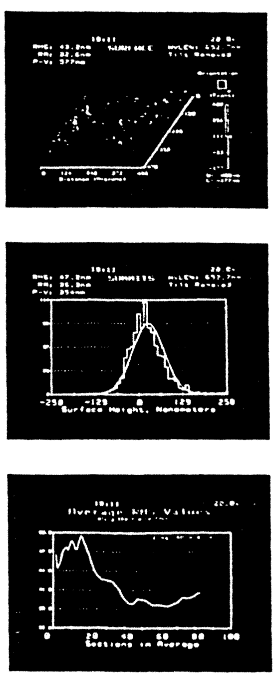

A three-dimensional plot of a polypropylene surface measured with a 20X magnification head. The middle figure is a histogram of the summits of the surface. The bottom figure shows a plot of the cumulative average rms values measured along the y direction.

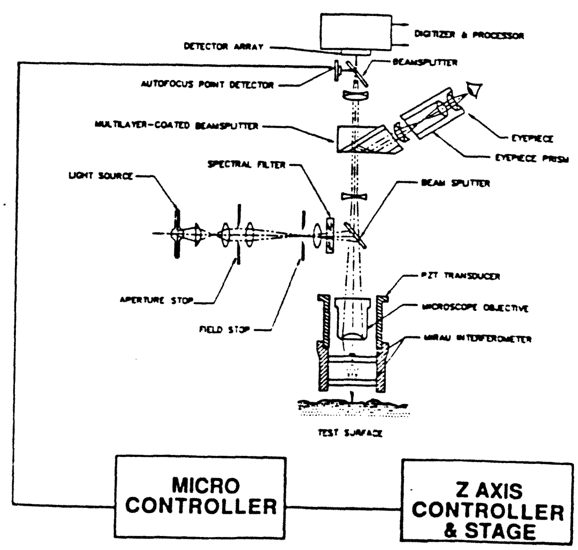

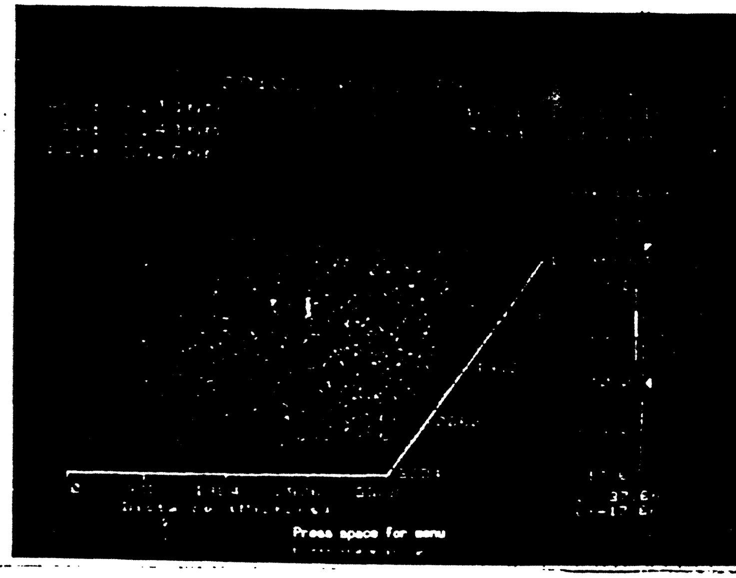

OPTICAL INTERFEROMETR

PIN ON DISK TEST
Au/Pd OVERCOATED

INITIAL OPTICALLY DETECTABLE
WEAR TRACK

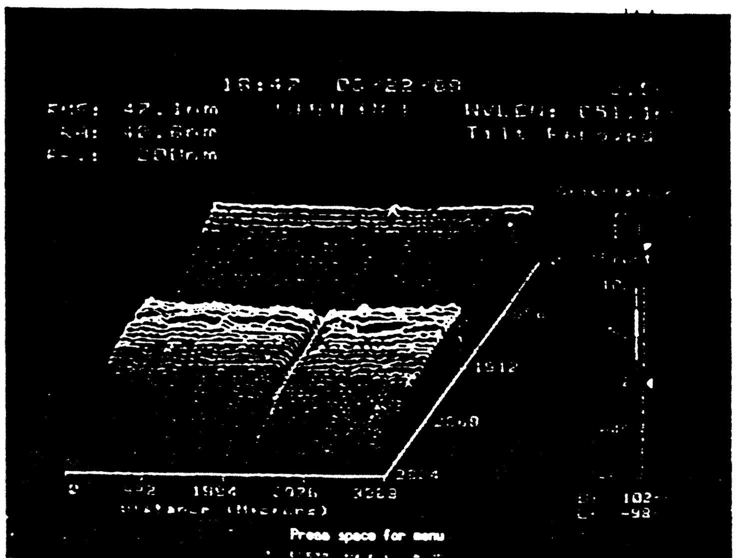

INTERMEDIATE WEAR TRACK
WITH ASHED STEP AND
Au/Pd OVERCOAT

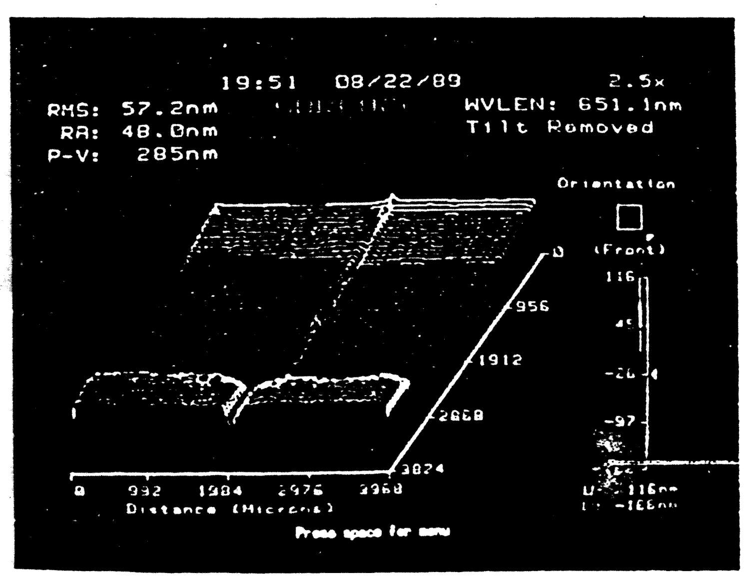

WEAR TRACK AT FRICTIONAL
FAILURE
WITH ASHED STEP AND
Au/Pd OVERCOAT

OPTICAL MEASUREMENTS OF WEAR (B. Phipps)

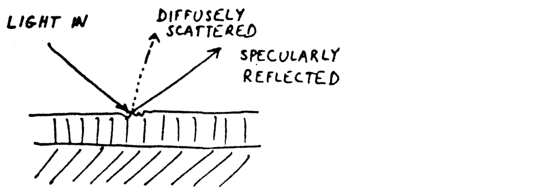

THIN FILM DISK WITH CARBON OVERCOAT
PIN ON DISK SLIDING TEST

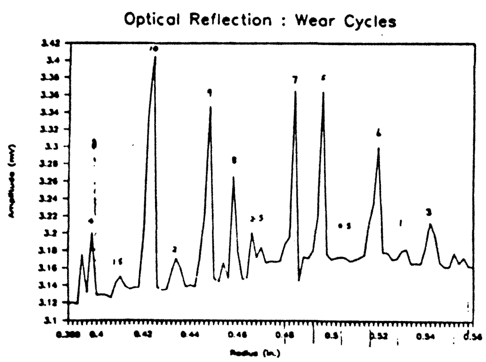

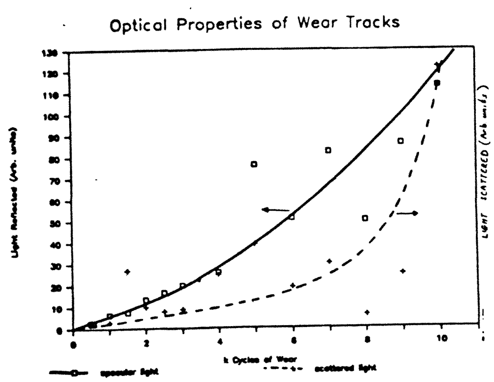

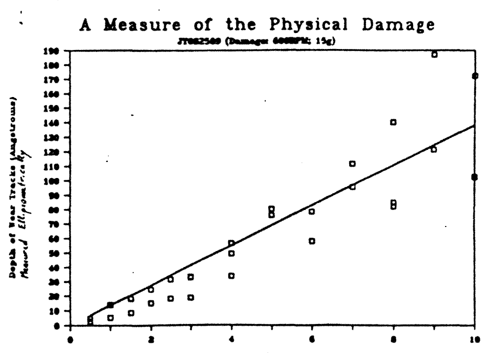

SENSITIVE IN-SITU DETECTION OF WEAR PARTICLES

1. ACTIVE LASER CAVITY SCATTERING

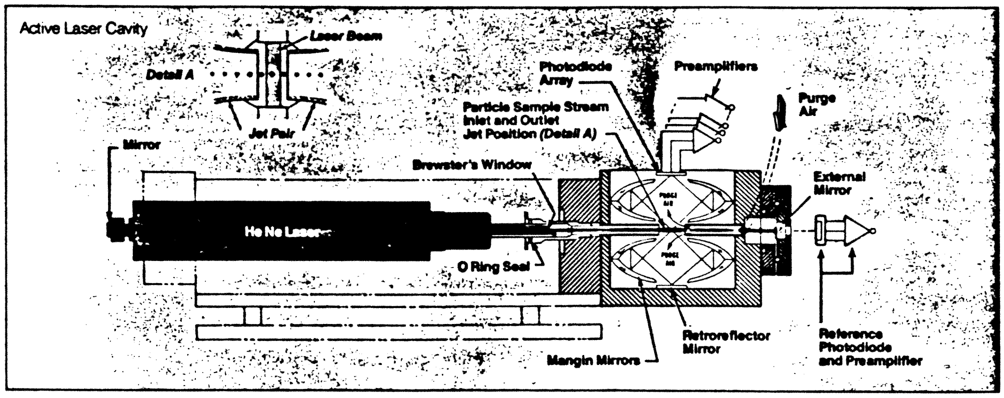

PARTICLE SIZE 0.05 - 5.0 μm
8 CHANNELS
>80% COUNTING EFFICIENCY

2. CONDENSATION NUCLEUS COUNTER

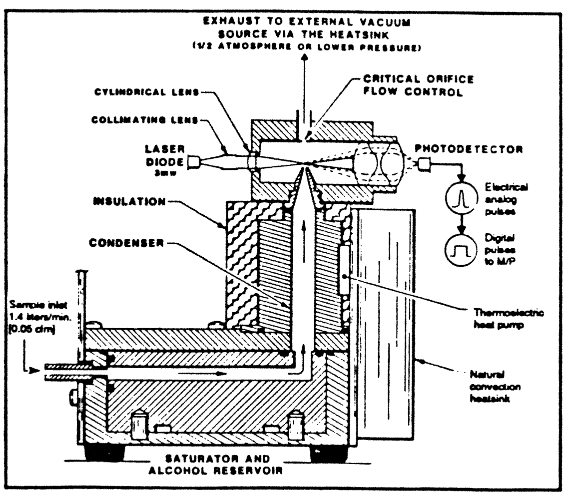

liquid condenses around particles

PARTICLE SIZE > 0.01 μm
NO SIZE INFORMATION

EVEN THE MOST SENSITIVE PARTICLE DETECTION METHODS DETECT GENERALLY ONLY LATER STAGES OF WEAR.

PIEZOELECTRIC AND CAPACITIVE DETECTION OF WEAR

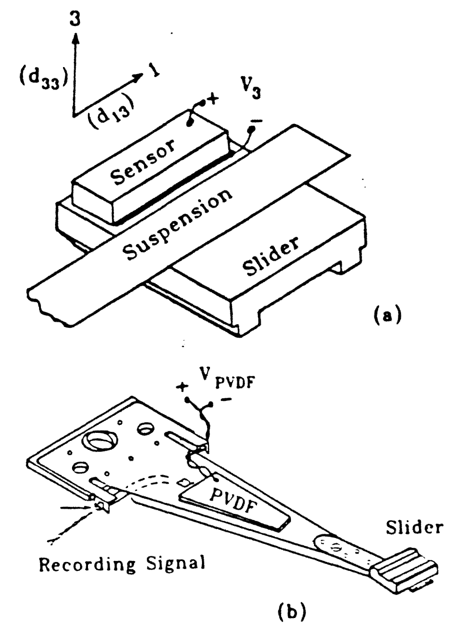

Fig. 1. Sensor configuration. Piezoelectric transducer mounted on a 3380 slider (a), and PVDF, a plastic piezoelectric bonded to a 3380 suspension (b).

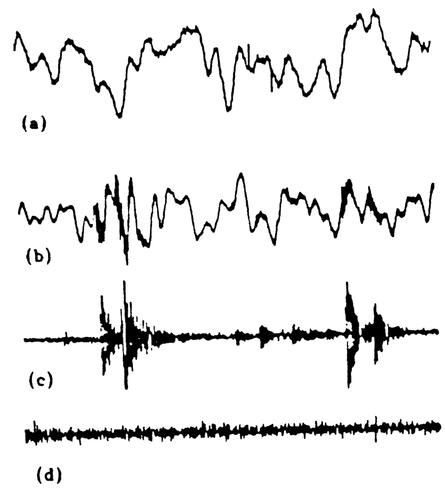

Fig. 2. Simultaneously acquired capacitive and piezoelectric waveforms from a 3380 slider flying on a particulate disk (1.0 msec full trace). Unfiltered capacitance (a) and piezoelectric (b), and 100 kHz-400 kHz filtered piezoelectric (c) and capacitance (d) signals.

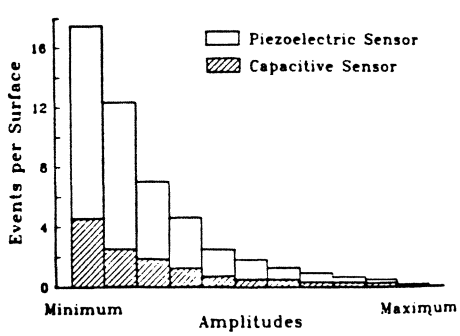

Fig. 4. Histograms of piezoelectric and capacitive sensor signal amplitudes for 12 particulate disk surfaces where the minimum threshold is set for each at just above the baseline.

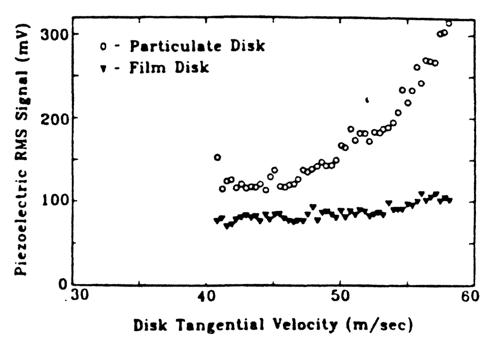

Fig. 12. RMS amplitudes of the filtered (100 kHz-300 kHz) piezoelectric signals from a film and particulate disk, both obtained by varying the radius at 60 Hz rotation frequency.

MEASUREMENT OF LUBRICANT PROPERTIES

• Scanning microellipsometry	I,D	Ref.
• Atomic force microscopy	E,S	Ref.
• Infrared micro profiling	E,S	Ref.
• Scanning X-ray photoemisison	E,S	Ref.
• Force apparatus	I,S	Ref.

CONTAMINATION MEASUREMENTS

- Surface analysis techniques - XPS, Auger, SIMS, laser desorption and mass spectrometry

- Particle detection
  - SEM
  - TEM replica
  - Optical

Key Lubricant Characteristics

→ • Distribution on macro and micro scale

→ • Conformation

→ • Migration on surfaces and transport in pores

• Displacement from sliding and flying tracks

• Loss and transfer to slider

• Degradation

Branching greatly affects performance

LUBRICANT STRUCTURE, MOLECULAR WEIGHT, VISCOSITY AND SIZE

FOMBLIN Y09 Branched

$$CF_3 - (O - \underset{\displaystyle CF_3}{CF} - CF_2)_{\sim 0.9} - (O - CF_2)_{\sim 0.1} - O - CF_3$$

FOMBLIN Z15

$$CF_3 - (O - CF_2 - CF_2)_{\sim 0.4} - (O - CF_2)_{\sim 0.6} - O - CF_3$$

Lub. Type	Wt. Avg. Mol. Wt. M_w	Viscosity at 25°C η(mPa sec)	Size = 2× Rad. of Gyration 2 Rg (Å)
Y 09	9,300	1,500 → 2,900	32
Z15	15,600	250	~40

DENSITY OF Y09 AND Z15 IS ~1.9 g/cm^3

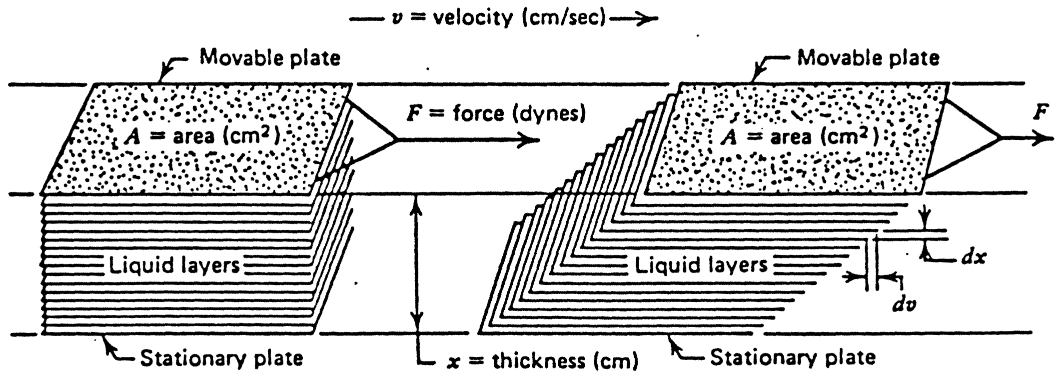

τ = shear stress = F/A (dynes / cm²)
D = shear rate = v/x (sec⁻¹)
η = viscosity = shear stress / shear rate = τ/D (dyne sec/cm²) or (poise)

Fig. 1-1 Schematic diagram of a parallel plate arrangement illustrating the relationship of the quantities involved in simple (Newtonian) flow.

$$\text{D (shear rate)} = \frac{dv}{dx} = \frac{v\text{ (velocity)}}{x\text{ (thickness)}}$$

$$\tau\text{ (shear stress)} = \frac{F\text{ (force)}}{A\text{ (area)}}$$

$$\eta\text{ (viscosity)} = \frac{\tau\text{ (shear stress)}}{\text{D (shear rate)}}$$

TRIBOLOGY OF LANGMUIR - BLODGETT LAYERS

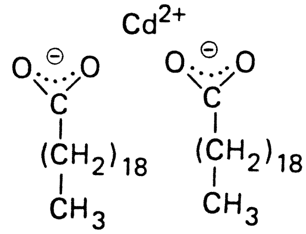

CADMIUM ARACHIDATE (see previous lecture

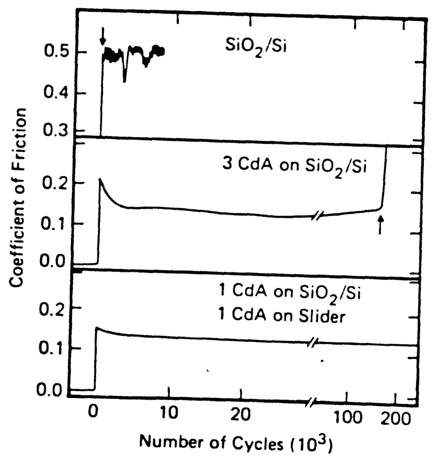

Figure 3. Dependence of dynamic friction coefficient on the number of sliding cycles for the couple consisting of SiO_2/Si and ceramic Al_2O_3/TiC rectangular slider: (a) uncoated SiO_2, (b) SiO_2 with three CdA layers, and (c) SiO_2 and slider with one CdA layer each. The load was 150 mN, and an arrow indicates failure with an optically detectable wear track.

← wear track →

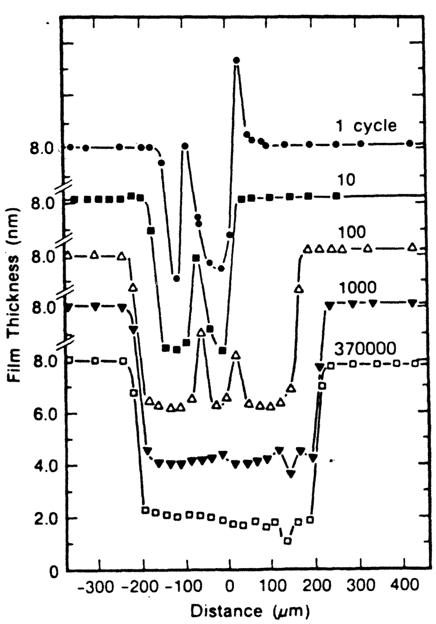

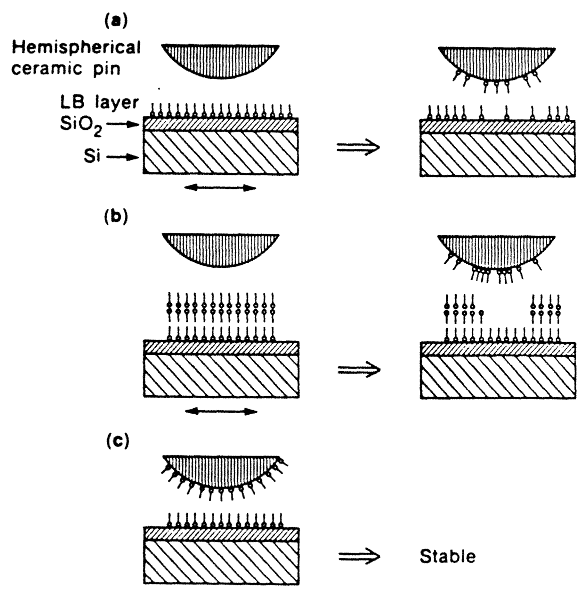

Figure 5. Schematic representation of tribological experiments: (a) with flat or disk coated with an LB monolayer; (b) with flat or disk coated with multilayers; (c) with both surfaces coated with a monolayer.

INFRARED MICROPROFILING

SPATIAL RESOLUTION ~ 200 μm

THICKNESS SENSITIVITY ~ 3 Å (FOR PPFPO)

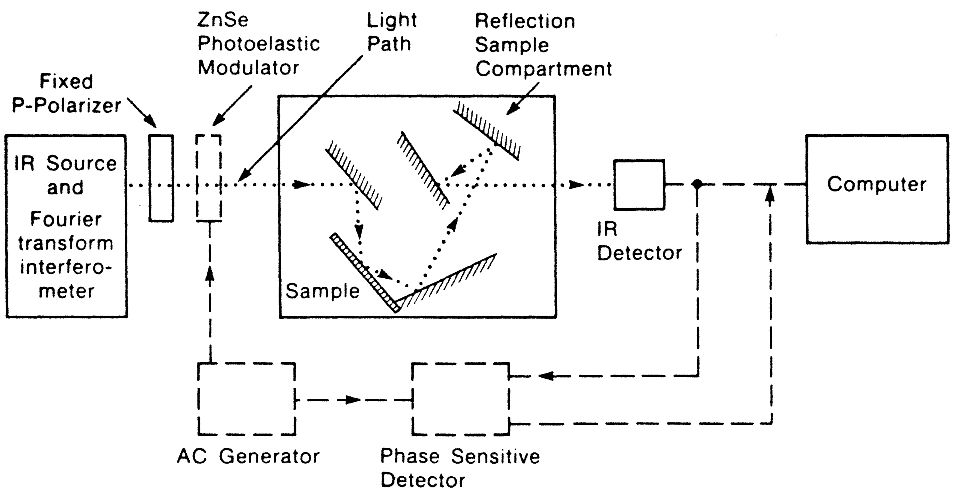

FIG. 2. Schematic diagram of the experimental set-up for the reflection experiments with fixed *p*-polarization and modulated polarization. The components marked by the solid lines are common to both experiments. The dashed line components pertain only to the modulated polarization set-up.

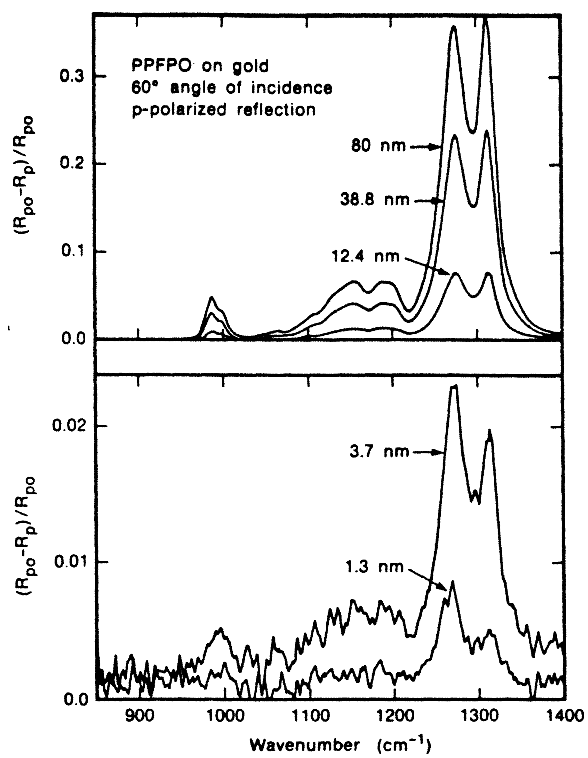

FIG. 8. Reflection spectra of PPFPO on gold substrates for several different polymer thicknesses obtained in *p*-polarized reflection experiments.

PPFPO

POLY PERFLUORO-PROPYLENE OXIDE

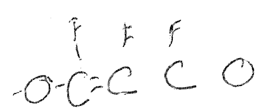

LUBRICANT CONFORMATION

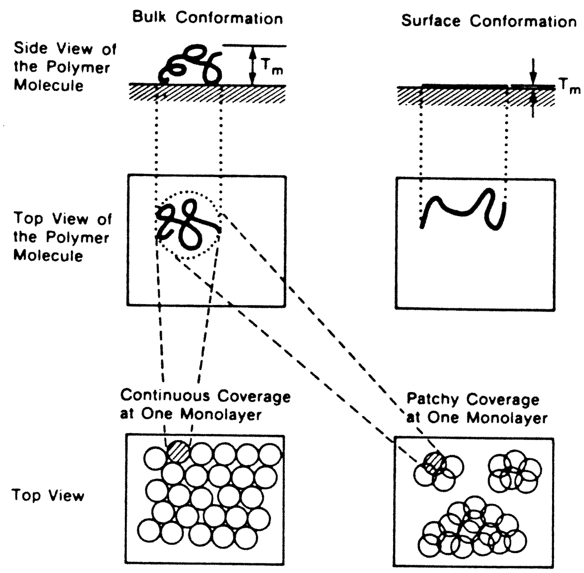

FIG. 1. Schematic representations of the conformation of the liquid polymer molecule on the solid surface showing two extrema—bulk and surface conformations and corresponding definitions of a polymer monolayer thickness. Also shown are possible distributions of molecules on the surface at monolayer coverage.

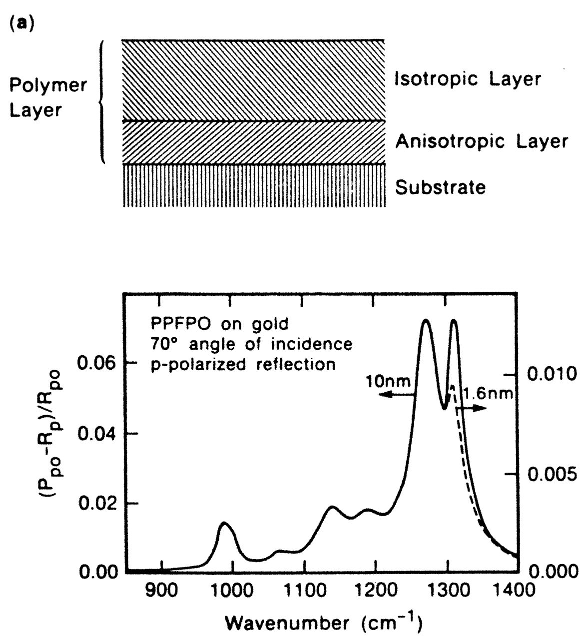

FIG. 12. (a) Schematics of the two layer model of polymer film. (b) The calculated spectra of PPFPO on gold substrate with the two layer model.

SCANNING X-RAY PHOTOEMISSION SPECTROSCOPY (XPS)

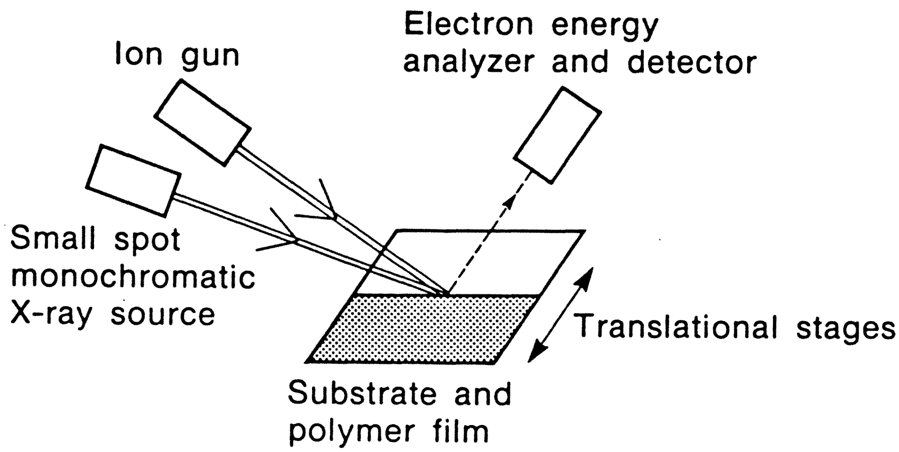

SPATIAL RESOLUTION 150 μm → 5 μm

THICKNESS RESOLUTION ~1 Å

XPS OF LUBRICANT

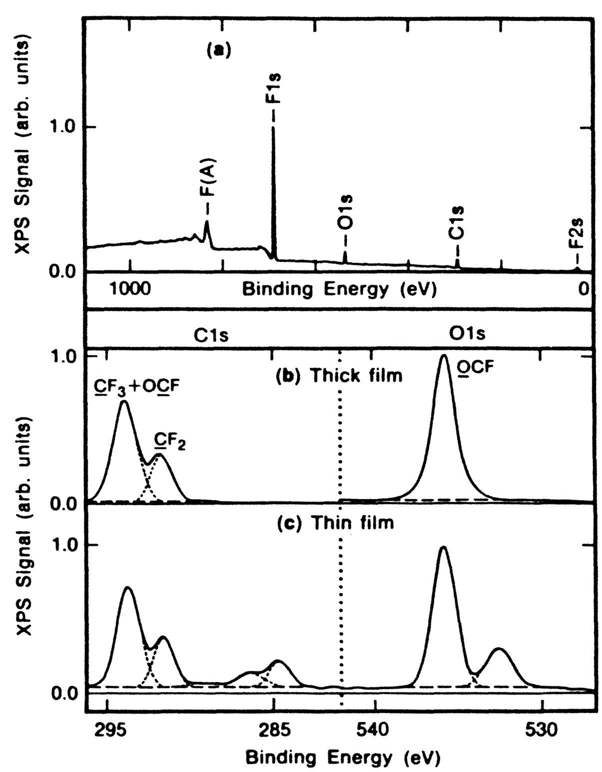

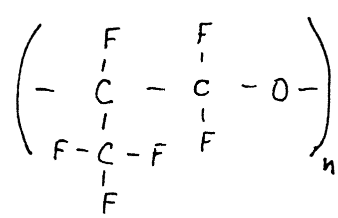

FIG. 5. X-ray photoemission spectra of PPFPO including survey in (a), carbon and oxygen regions for 15 nm film in (b) and the same regions for 3 nm film in (c).

XPS ANALYSIS OF MULTILAYERS

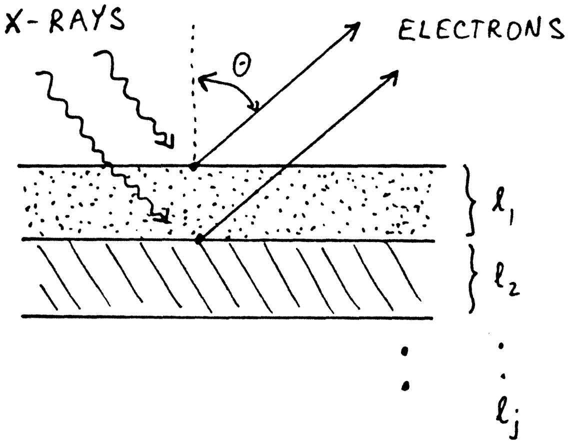

S_{ij} - SIGNAL FROM ELEMENT i IN THE LAYER j

S_i - " " " " AT THE TOP OF THE STRUCTURE

c_{ij} - CONCENTRATION OF ELEMENT i IN THE LAYER j

λ_{ijo} - ESCAPE DEPTH " " " " " " "

b_j - BRIGHTNESS OF ELEMENT j

$$S_{ij} \sim c_{ij}\, b_j\, \lambda_{ij} \left(1 - e^{l_j/\lambda_{ij}}\right)$$

$$S_i = S_{in} \prod_{j=1}^{n-1} e^{-l_j/\lambda_{ij}}$$

$$\lambda_{ij} = \lambda_{ijo} \cdot \cos\theta$$

$$R_{ij} = \frac{(s_i/b_i)}{(s_j/b_j)}$$

SIMPLIFIED MODEL OF LUBRICANT ON THE DISK

LUBRICANT THICKNESS $= \lambda \cdot \cos\theta \, \ln(aR + 1)$

$$R = \frac{S_{C_{1s}\,LUBE}}{S_{C_{1s}\,DISK}}$$

$a \approx 2.$

POLYMER MIGRATION

PPFPO

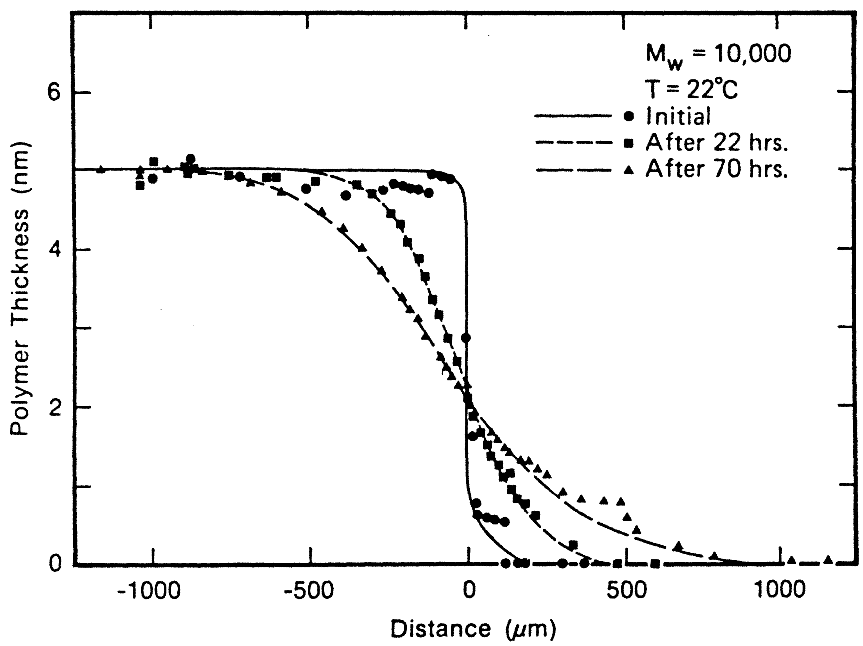

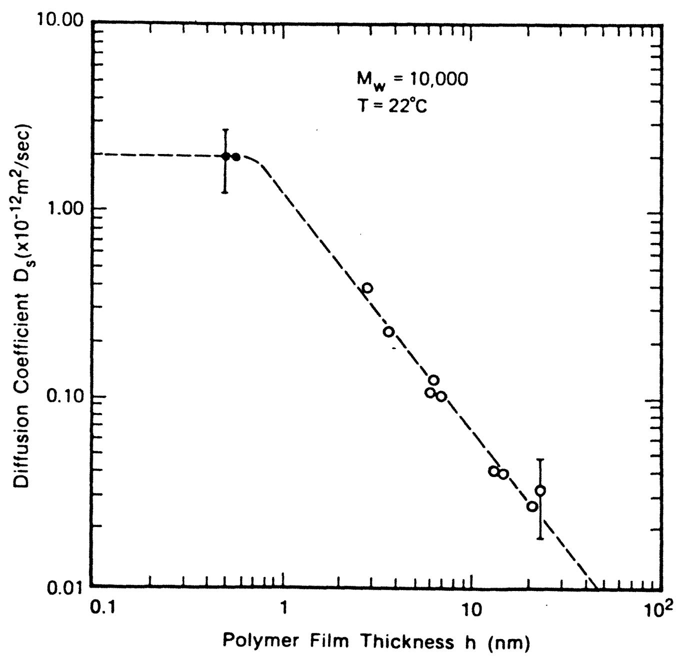

TIMESCALE FOR LUBE RECOVERY

$D = 2 \times 10^{-12}\ m^2/sec$

ASPERITY SIZE $x = 0.2\ \mu m$

$t = x^2/2D = 4 \times 10^{-14} / 4 \times 10^{-12} = 10^{-2}\ sec = 10\ msec$

$R = 3600\ rpm$ $t_R = \frac{1}{60}\ sec = 16\ msec$

FORCE APPARATUS

FORCE RESOLUTION 10n N (10^{-6} gmf)
DISTANCE RESOLUTION $\lesssim$ 1 Å

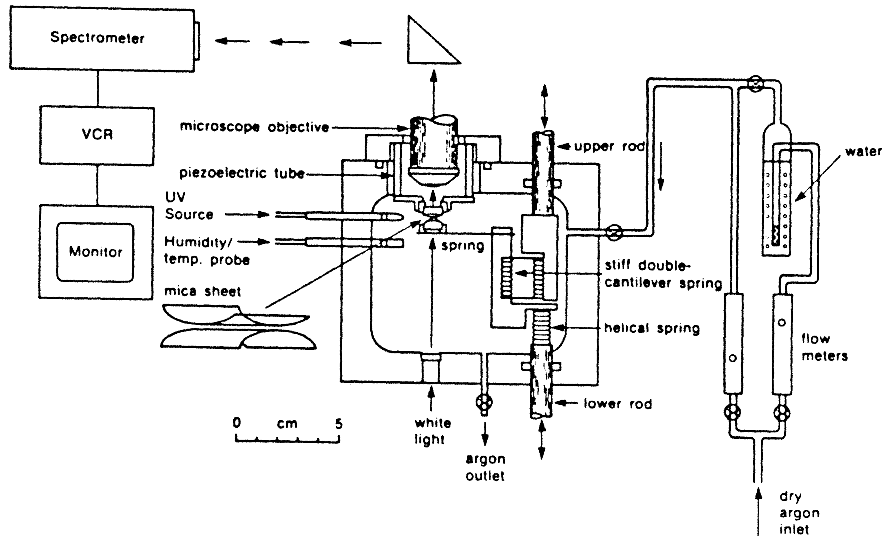

RELAXATION EFFECTS IN THIN LUBRICANT LAYERS (A. HOMOLA)

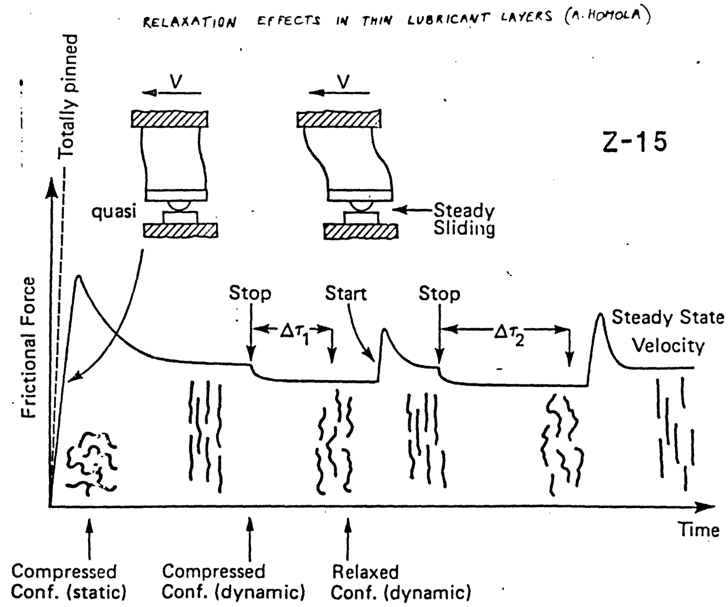

SHEAR STRESS VS. SHEAR RATE (A. Homola)

Shear Stress vs Shear Rate for Z-15

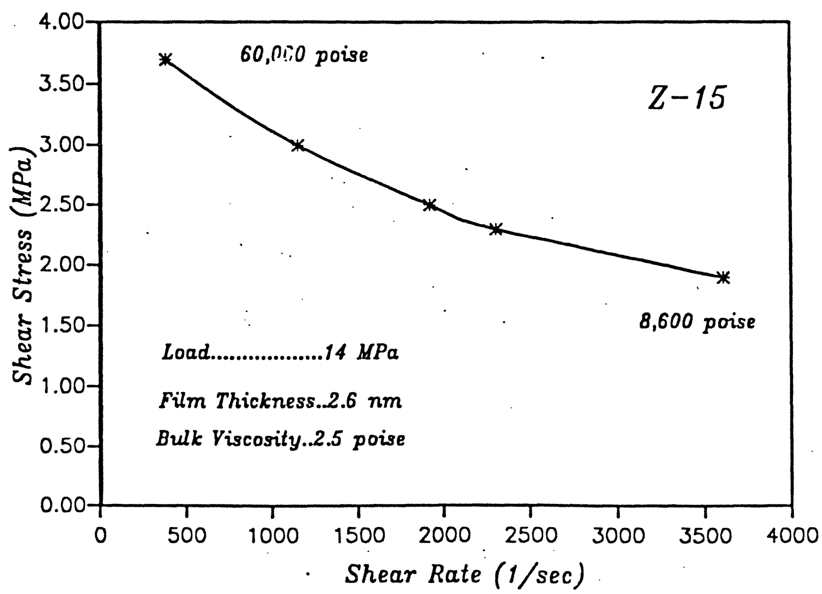

Shear Stress vs Shear Rate for Y09

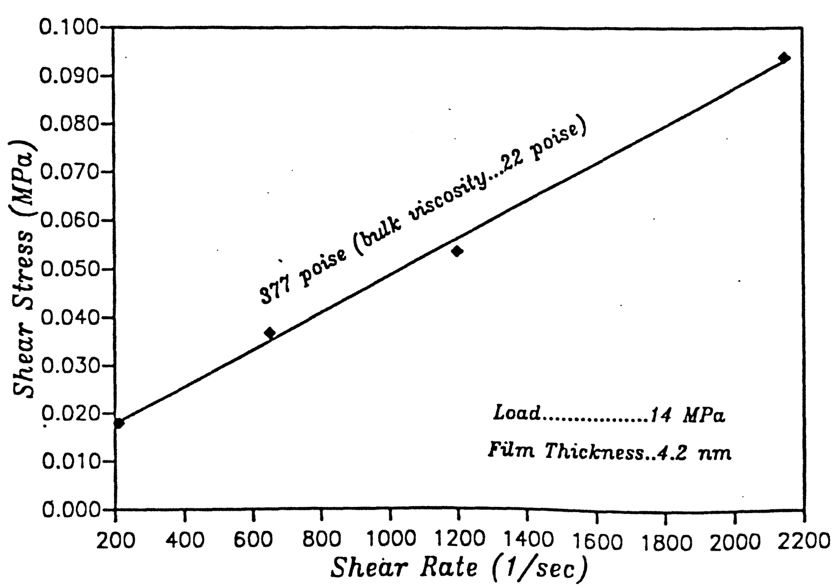

ORGANIC CONTAMINATION MEASUREMENTS

USUALLY MASS SPECTROMETRY (MS) METHODS HAVE THE HIGHEST SENSITIVITY

STATIC SECONDARY ION MASS SPECTROMETRY (SIMS)
LASER DESORPTION + MASS SPECTROMETRY (LAMMA, LIMS,..)
LASER DESORPTION + POSTIONIZATION + MASS SPECTROMETRY

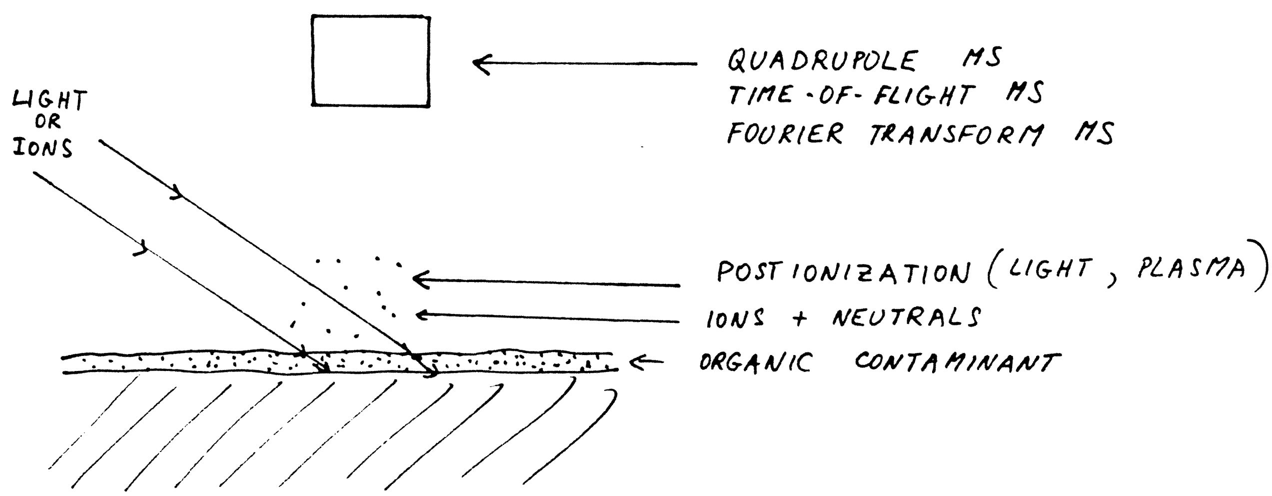

TYPICAL PROBLEMS

- FRAGMENTATION (METAL FILM OR SCREEN CAN PARTLY ALLEVIATE IT)
- DIFFICULT QUANTIFICATION

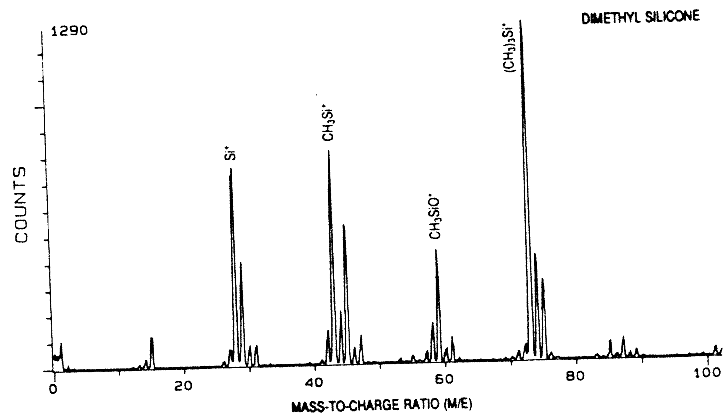

Figure 1. This Static SIMS spectrum of pure dimethylsilicone, (molecular weight=2,500,000) is dominated by the 73 peak.

SUMMARY

- Tribology is the key area in modern magnetic recording
- "Classical" techniques of friction and wear were reviewed
- "Advanced" techniques of lubricant and contaminant characterization were outlined
- Many tribological properties are not adequately measured and many of them are not measured in-situ and dynamically

REFERENCES

The Design and Verification of Reliable Head-Disk Interfaces

by
DeLloy Forbes
Project Mgr. - Head/Media Development
Hewlett-Packard Co.
Disk Mechanism Division

CAPACITY PER FORM FACTOR

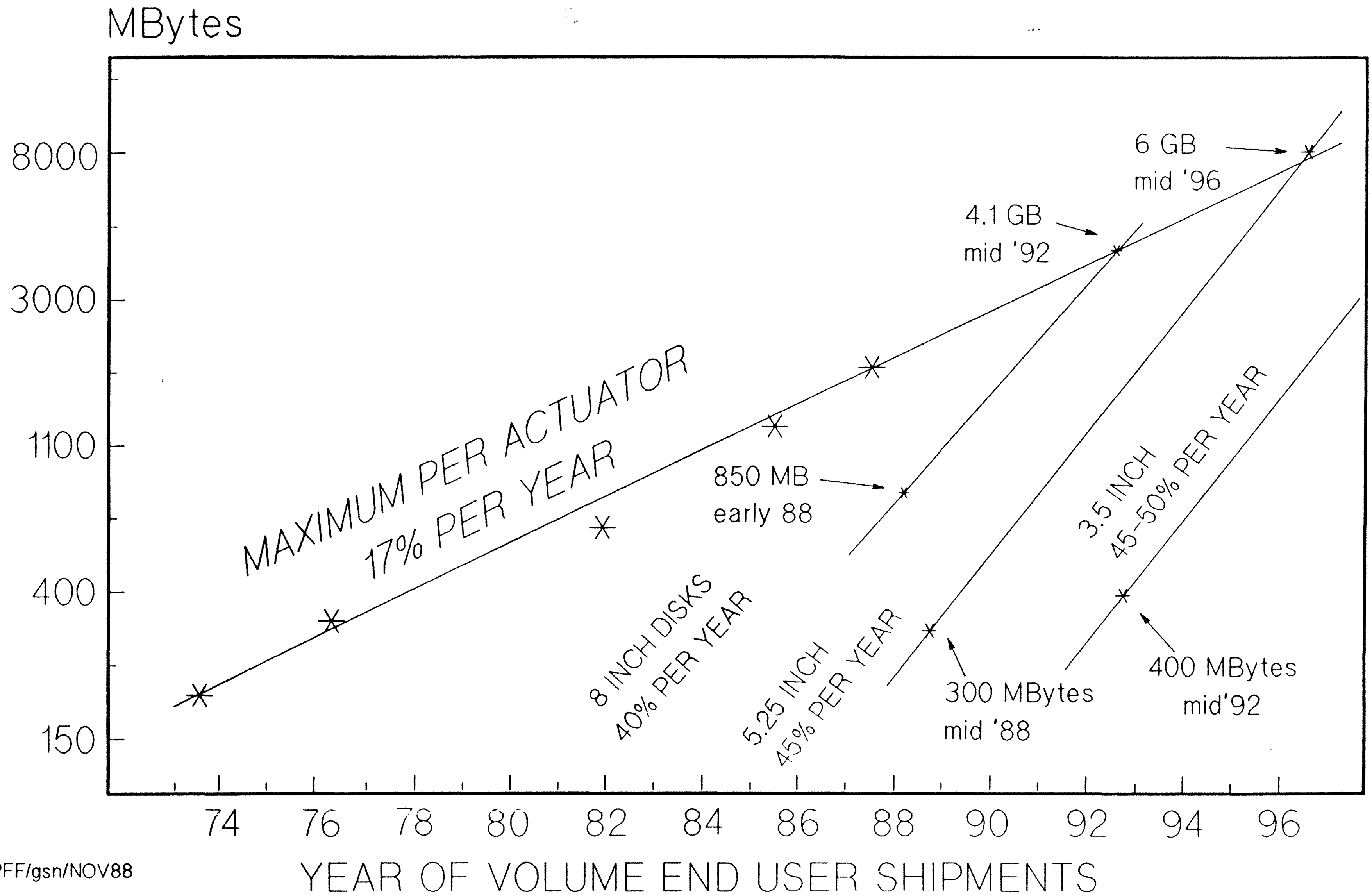

CPFF/gsn/NOV88

Areal Recording Density
OEM Market

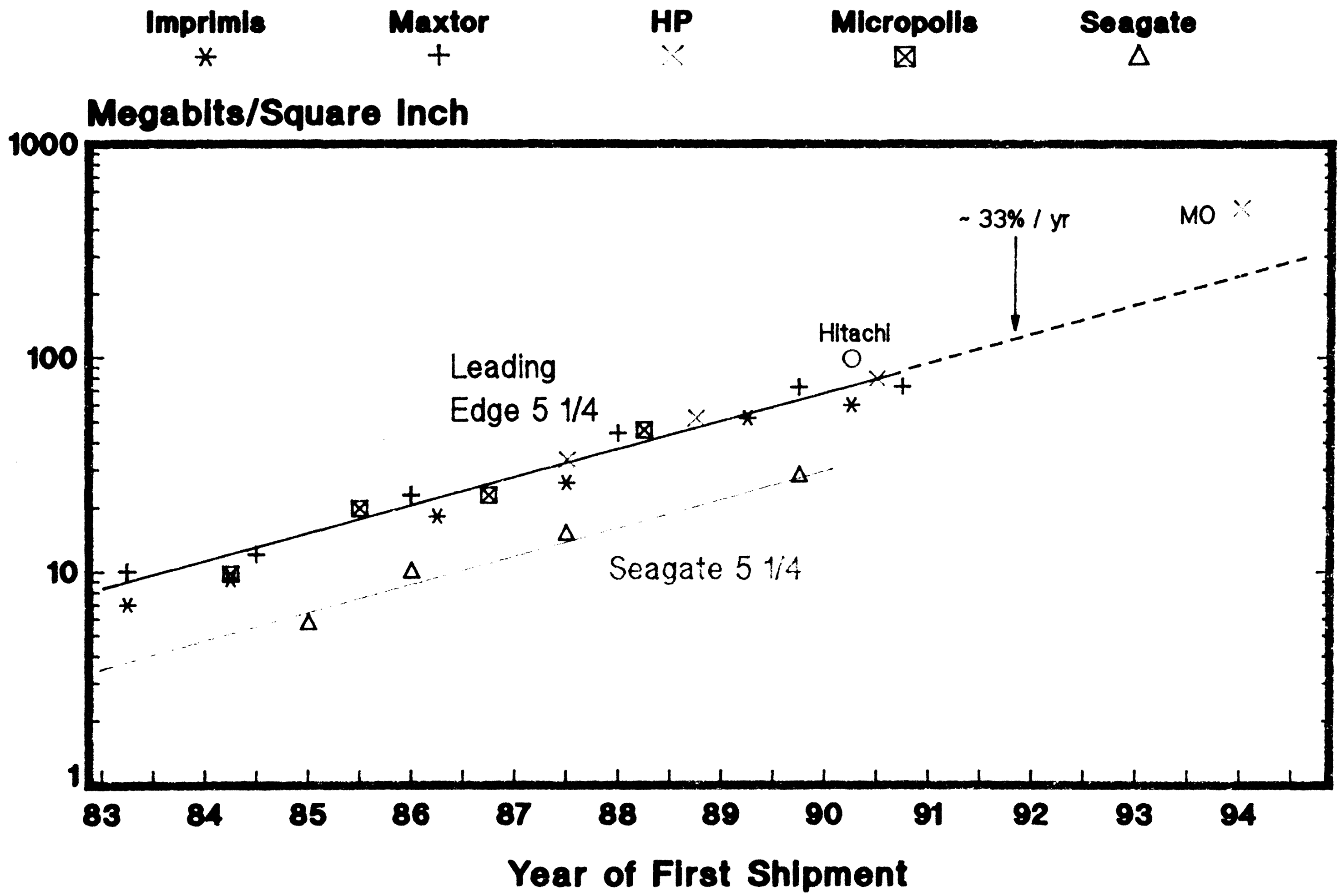

Channel Margin

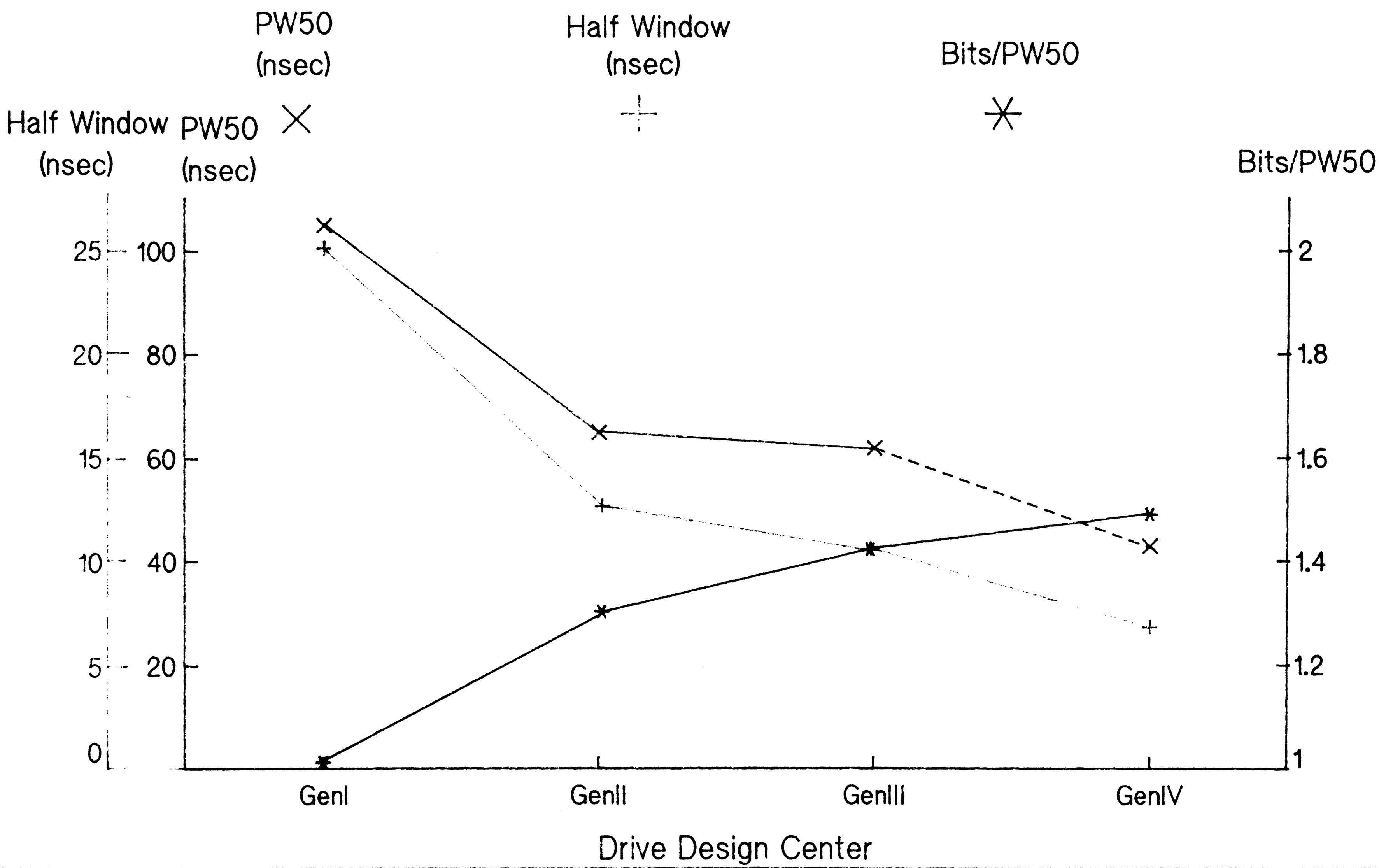

HEAD TECHNOLOGY BOUNDARIES

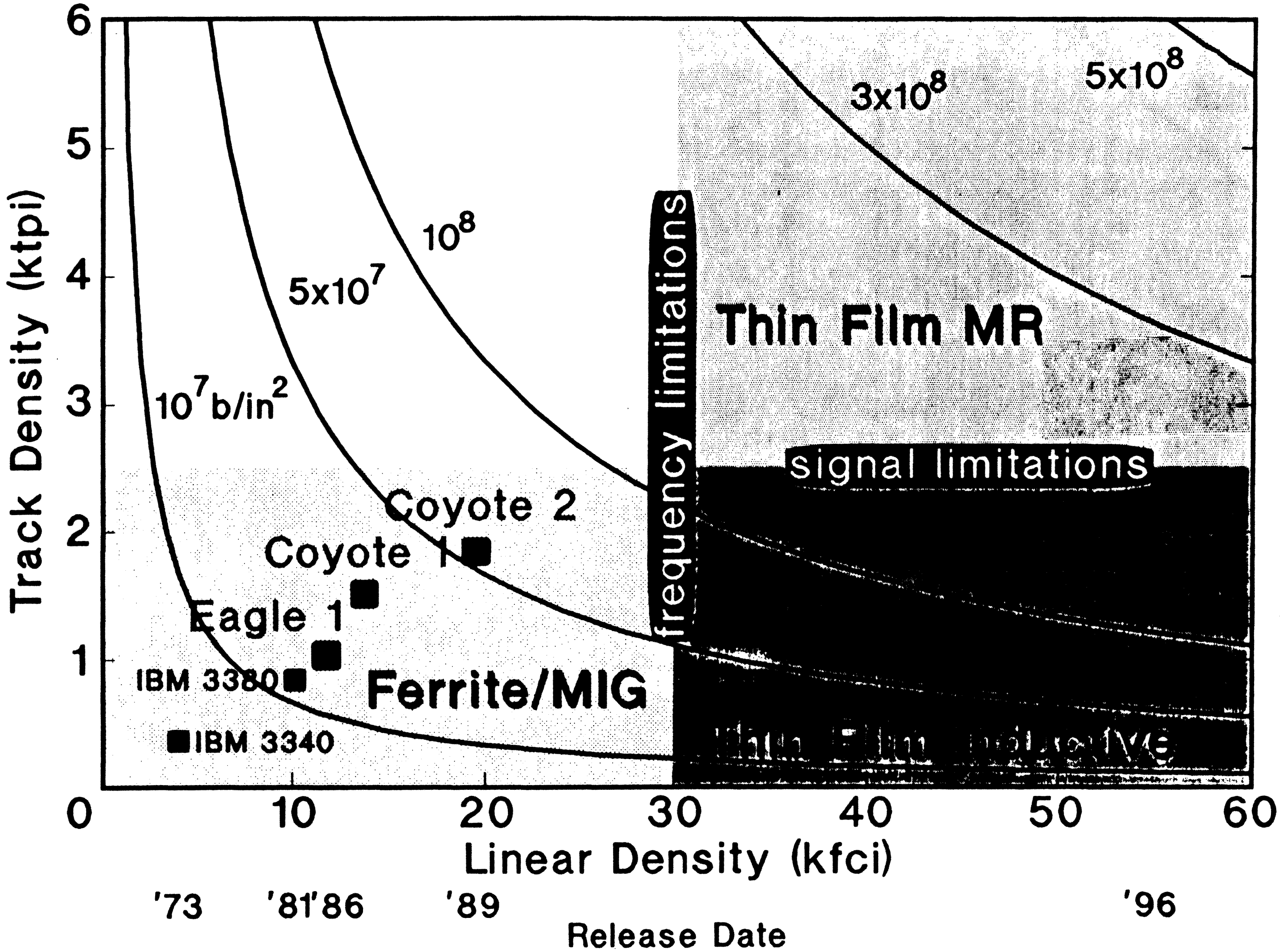

1,000,000,000 = 160,000 mb/in²
1 Gig / 95mm disc surface
1.36 Gig formatted Hard drive (8 disc)

Thin Film Department, CPL/HPL

SLN 7/89 fcti079

HEWLETT PACKARD

HEAD/MEDIA PRODUCT PARAMETERS

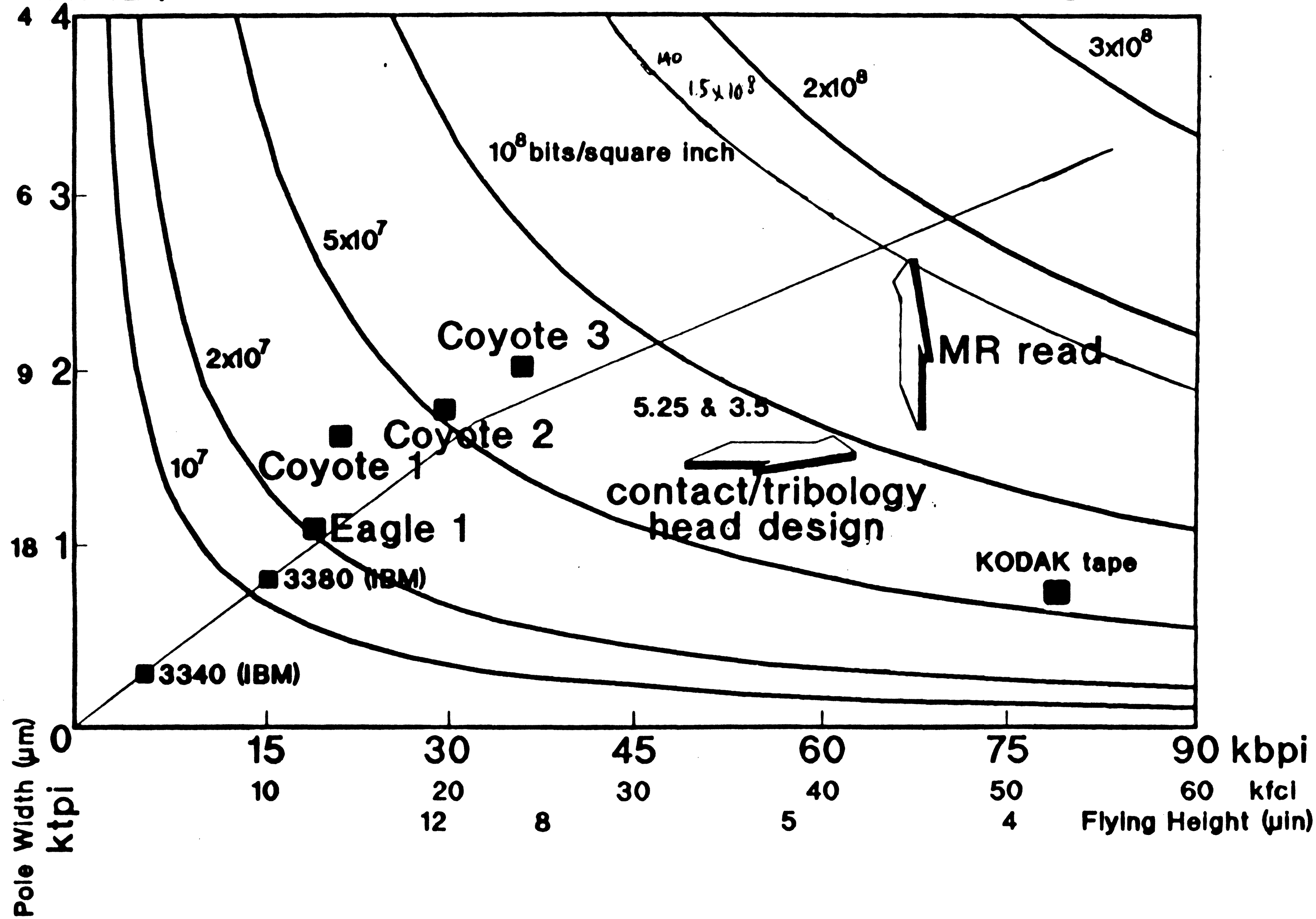

Head / Media Trends

Conclusion: Major H/M challenge of next few years is significantly lower Flying Heights (current 6 Uin ⟶ 4 Uin)

Implications:

1. Smoother disks
   - smoother, flatter substrates
   - more uniform texture
   - sub-3 Uin glide (*major issue).
2. Tighter tolerance heads
   - all dimensions/factors affecting flying height.
3. Lower defect density disks.
4. Semi-Contact Recording
   - tougher disks
   - harder, more elastic substrates
   - tougher overcoats
   - near-zero magnetostiction
   - durable thin-film structures
   - more compatible thin-film heads
   - Electrical Storm eliminated
   - Barkhausen noise controlled to very low levels.
5. Better error tolerance/error correction.

Disk Drive Reliability

Two Parts:

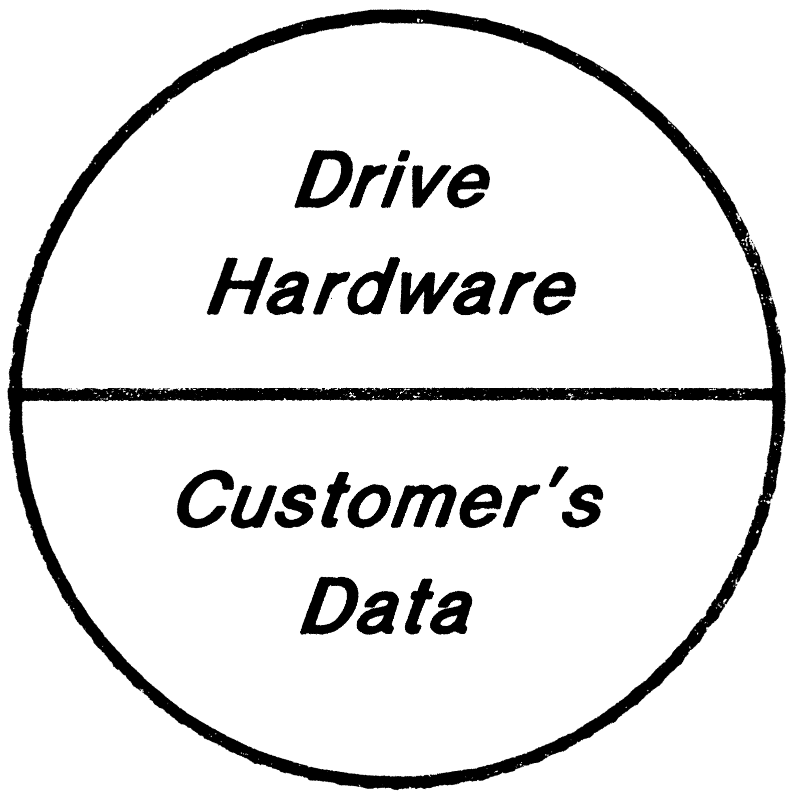

Disk Drive Reliability

Two Parts:

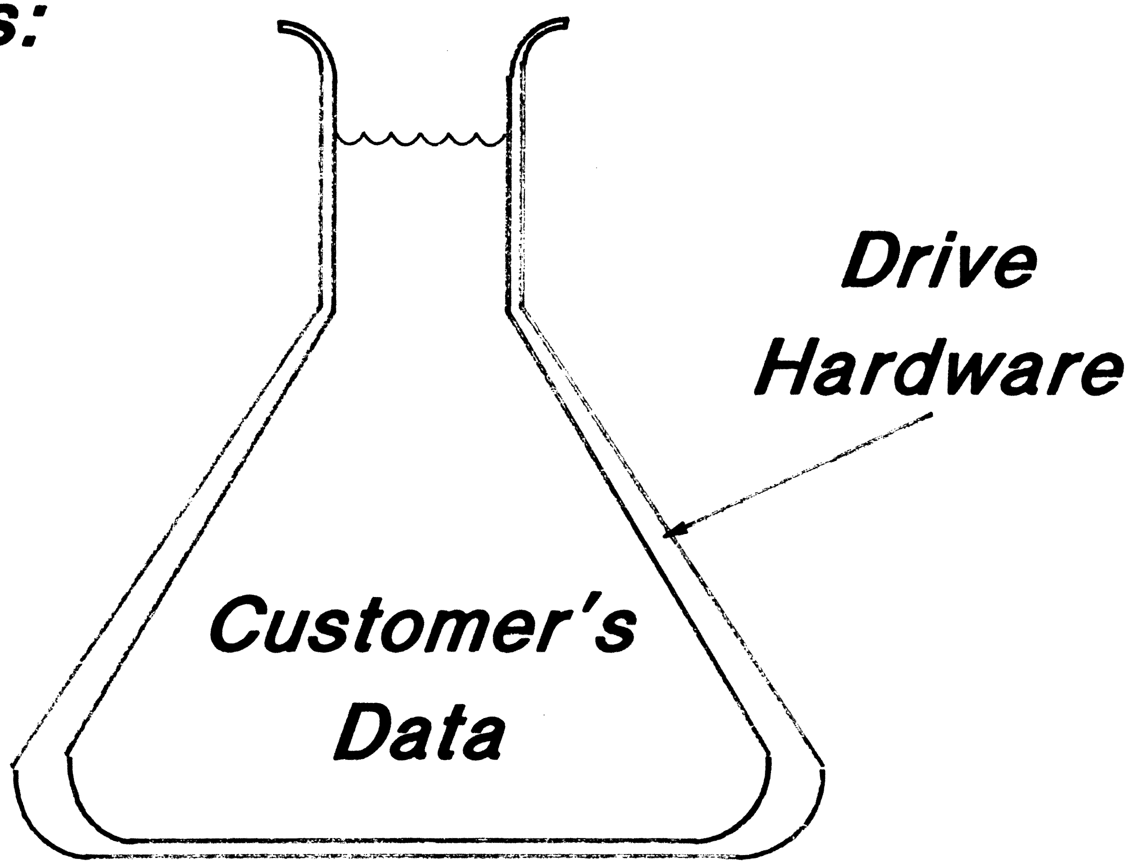

Reliability

The manifestation of depth of understanding in all details of applying product technology to the requirements of the marketplace.

Unreliability

The occurrence of residual unresolved and/or non–understood design, process or market application problems.

"It is my experience that the ability to uncover and understand the unexpected problem areas associated with the application of advancing disk drive technologies is the ultimate limiting factor in the rate of improvement of the overall marketplace art.... Attempts to exceed this rate without similar increased commitment to in-depth, detailed problem identification and resolution is wishful thinking and will only be met by program delays and/or market disasters."

Scott Anderson
R&D Manager - HP/DMD
April 1988

FACTORS OF HEAD-MEDIA RELIABILITY

(Five-Whys Format) DF, 12-3-89

```
1   Hardware Reliability (H/M)
2   ├── Landing Zone
3   │   ├── Stiction
4   │   │   ├── Wringing of Head to Disk
5   │   │   │   └── Disk Wear
6   │   │   │       ├── Drag distance
7   │   │   │       ├── Touch-down velocity
8   │   │   │       ├── Disk surface
9   │   │   │       │   ├── Texture
10  │   │   │       │   │   ├── profile
11  │   │   │       │   │   ├── depth
12  │   │   │       │   │   └── uniformity
13  │   │   │       │   └── Flatness
14  │   │   │       │       ├── radial curvature
15  │   │   │       │       ├── circumferential curvature
16  │   │   │       │       └── RVA
17  │   │   │       ├── Disk Materials
18  │   │   │       │   ├── Overcoat
19  │   │   │       │   │   ├── hardness
20  │   │   │       │   │   └── durability
21  │   │   │       │   ├── Lube
22  │   │   │       │   │   ├── thickness
23  │   │   │       │   │   ├── bonding
24  │   │   │       │   │   ├── migration
25  │   │   │       │   │   ├── recovery
26  │   │   │       │   │   ├── reservior
27  │   │   │       │   │   └── type
28  │   │   │       │   └── Substrate hardness
29  │   │   │       ├── Head gram-load
30  │   │   │       │   ├── mean
31  │   │   │       │   └── variation (hd/hd)
32  │   │   │       ├── Head profile
33  │   │   │       │   ├── ABS crown/contact area
34  │   │   │       │   ├── edge-blend/cross-curve
35  │   │   │       │   └── taper
36  │   │   │       ├── Head slider material
37  │   │   │       └── Humidity, lack of
38  │   │   └── "Glueing" of head to disk
39  │   │       ├── Contamination
40  │   │       │   ├── Outgassing
41  │   │       │   │   └── silicones
42  │   │       │   └── Formation of tars
43  │   │       └── Humidity, excess (max spec.)
44  │   └── Head Crash
45  │       ├── Disk wear
46  │       └── Corrosion
47  │           ├── Overcoat
48  │           │   ├── porosity
49  │           │   ├── thickness
50  │           │   └── damage/interuption
51  │           │       ├── shock
```

```
52   │           │       └───particle contamination
53   │           ├───Lube
54   │           │   └───(lines 22-27)
55   │           ├───Magnetic layers
56   │           │   ├───material corrosivity
57   │           │   └───thickness
58   │           └───Corrosive contamination
59   │               ├───surface
60   │               └───sub-surface
61   └───Data Zone
62       ├───Head/Media Interaction
63       │   └───Head Slap
64       │       ├───shock, operating
65       │       └───vibration, operating
66       └───Flying Height Margin
67           ├───Asperities
68           ├───Contamination
69           ├───Disk Surface
70           │   ├───flatness
71           │   └───RVA
72           └───Fly Height Tolerance
```

73 **Data Reliability (H/M)**

```
74   ├───Defects
75   │   ├───Native (from disk vendor)
76   │   ├───H/M Interaction
77   │   │   └───(lines 63-65)
78   │   ├───Corrosion
79   │   │   └───(lines 47-60)
80   │   └───Contamination
81   │       ├───particle
82   │       ├───outgassing/fluid
83   │       └───smudge/tar formations
84   ├───H/M Separation
85   │   ├───Contamination
86   │   │   └───(lines 81-83)
87   │   └───Disk Asperities
88   ├───Erasure
89   │   ├───Stress-Demagn.
90   │   │   ├───Hard particles
91   │   │   └───H/M interaction
92   │   │       └───(lines 63-65)
93   │   └───Magnetic contamination
94   ├───Noise
95   │   ├───Barkhausen noise (popcorn) [TF head]
96   │   ├───Wiggle (head write instability)
97   │   ├───Electrical Storm [TF head]
98   │   │   ├───Core/Coil resistance
99   │   │   └───Preamp input bias
100  │   └───Media write noise
101  └───Offtrack
102      ├───Headshift
103      ├───Thermal Cycle
104      └───Disk Shift / Slippage
```

"The trick to developing highly reliable head/disk interfaces . . . is to realize there are no tricks – just sound, careful, complete engineering."

Head/Media Designer's "Molecule"

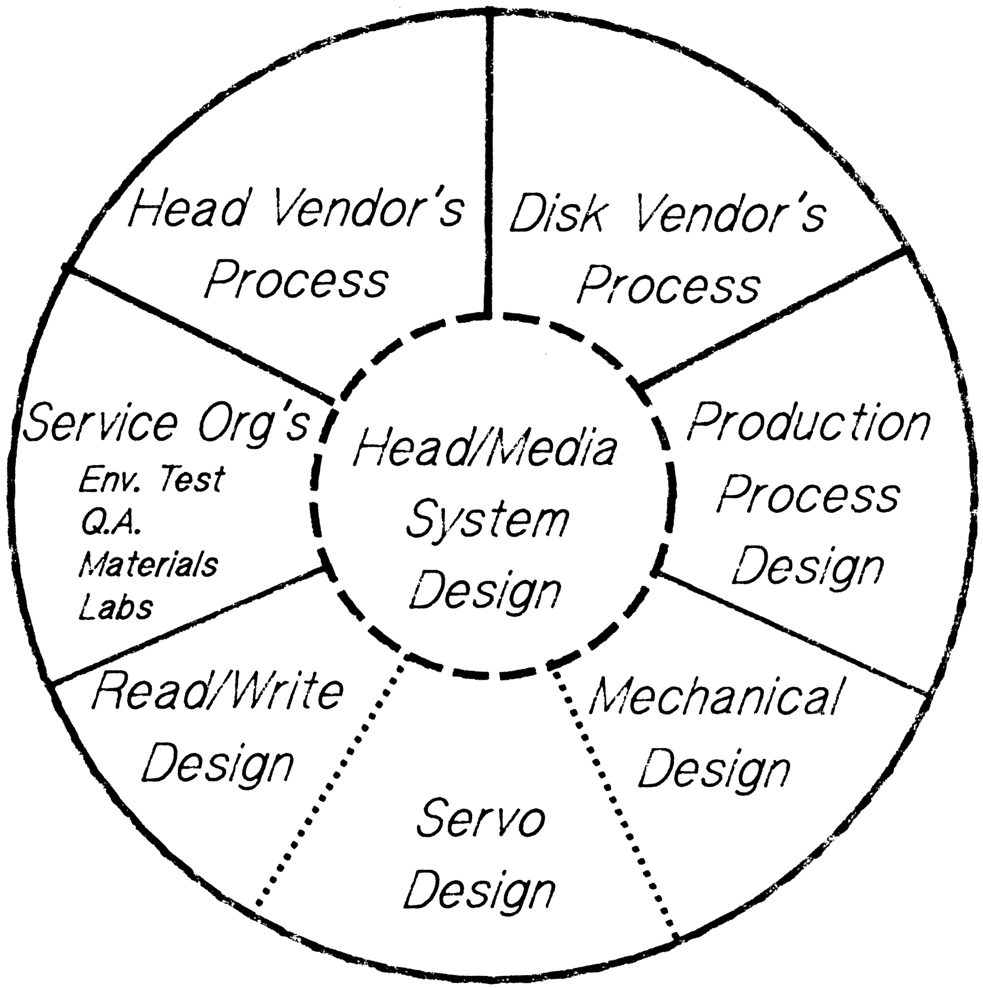

The Three Phases of H/M Development

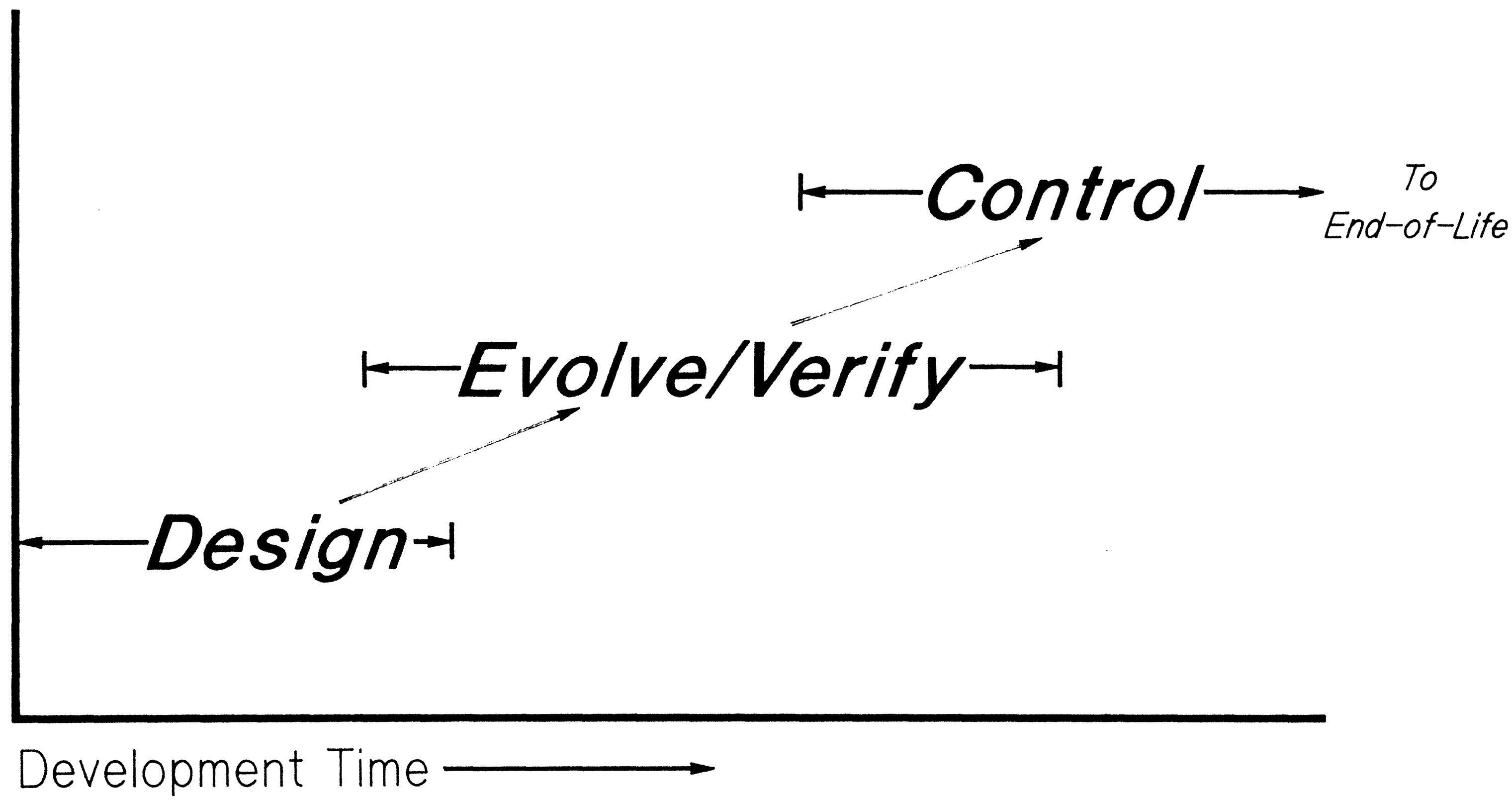

Three Phases of Development
Phase 1 – Design

Objective: To provide the best design allowed/enabled by:

* understanding of requirements
* best available design practices, methods
* best available design talent
* most effective tools
* acceptable amounts of New Technology Risk
* (in the shortest time)

Three Phases of Development
Phase 2 – Evolve/Verify

Objective:

To evolve the design of the product, its component parts, and to evolve/refine the processes producing those parts until the program goals are met for performance, reliability, producability, and cost (and do so on time).

Test–Fix–Test

"Reliability cannot be achieved by adhering to detailed specifications. Reliability cannot be achieved by formula or by analysis. Some of these may help to some extent, but there is only one road to reliability. Build it, test it, and fix things that go wrong. Repeat the process until the desired reliability is achieved. It is a feedback process and there is no other way."

David Packard, July 1972

Three Phases of Development
Phase 3 - Control

Objective:

To establish a "system" which, once all of the program goals for performance, reliability, producability, and cost are met, assures they will continue to be met for the life of the product.

The Head-Media Technologist's Toolbox

"DRAWERS":

1. Project Management
2. Engineering Methods
3. Computer-Aided Design
4. Computer Models
5. Databases / Data Analysis
6. Verification Tests, Gauges
7. Stimulus / Response
8. Stress / Environment
9. Failure Analysis

The Head-Media Technologist's Toolbox

DRAWER #1: Project Management Tools

1. Industry Trend Analysis
2. Lessons Learned Book
3. Phase Review Process
4. Peer Design Reviews
5. Design Defect Tracking
6. Total Quality Control (TQC) Process
7. Design Verification Testing (DVT)
8. Design Maturity Testing (DMT)
9. Duane Chart Reliability Measurement
10. Careful Change Process

The Head-Media Technologist's Toolbox

DRAWER #2: Engineering Methods

1. Statistical Design
2. Full-Distribution Design
3. Process Capability Analysis
4. Sensitivity Analysis
5. Design-Space Verification
6. Text-Fix-Text
7. Statistical Design of Experiments
8. Strife Test - Component Level
   - Drive Level
9. Model / Component Test / Drive Test Integration & Correlation

The Head-Media Technologist's Toolbox

DRAWER #3: Computer-Aided Design

1. 2D & 3D Mechanical Design (ME30)
2. Finite Element Analysis
3. Geometric Modeler
4. 3D Magnetic Field Fuction Models

The Head-Media Technologist's Toolbox

DRAWER #4: Computer Models

1. Head Magnetic Field-Function
2. Flying Height
3. H/M Write Models
4. H/M Read Models
5. Offtrack Models
6. Channel Simulation
7. Data Separation / TDA Analysis Simulation
8. Magnetic Hysteresis Models
9. Micromagnetic Model (noise)
10. Electrical Circuit Analysis
11. Monte-Carlo Simulation

The Head–Media Technologist's Toolbox

DRAWER #5: Data Bases / Data Analysis

1. Relational Databases
2. PC Databases
3. Versatile Search/Sort Capability
4. Convenient Statistical Capability
   (incl. parameter regressions)
5. Graphical Summaries
   (histograms, control charts, Cpk charts, etc.)
6. Automated Data Collection Facility

The Head-Media Technologist's Toolbox

DRAWER #6: Verification Tests, Gauges

Heads:
1. X-Y Stage Microscope
2. Optical Measurement System
3. Gramload Tester
4. Head Profile (Wyco, etc.)
5. Head Coil Resistance, Inductance
6. Head Field Measurement
7. Static Fly Height (PPL, Adelphi)
8. Dynamic Fly Height

The Head-Media Technologist's Toolbox

DRAWER #6: Verification Tests, Gauges

Disks:
1. Vibrating Sample Magnetometer
2. Laser Doppler Vibrometer
3. Disk RVA Measurement
4. Disk Surface Profile (WYCO, etc.)

The Head-Media Technologist's Toolbox

DRAWER #6: Verification Tests, Gauges

Head/Disk:
1. Friction Tester
2. Touch-down Velocity Tester
3. Head/Disk Parametric Tester
4. Disk Defect Tester
5. Write/Read Noise/Peak-shift Tests
6. Phase-Margin Testers
7. Time-Domain Analysis Testers
8. Component C.S.S. Testers
9. Disk Drive Prototypes (for tests)

The Head-Media Technologist's Toolbox

DRAWER #7: Stimulus / Response

1. Dynamic Signal Analyzer - w/ Photonic Sensor
   (resonance-mode characterization)
2. High-Speed Camera - w/Glass Disk

The Head–Media Technologist's Toolbox

DRAWER #8: Stress / Environment

1. Environmental Chambers (Temp., Humidity)
2. Vibration Tables, Transducers
3. Shock/Drop Tables
4. Altitude Chamber
5. Variable Power Supplies
6. Corrosive Atmosphere Tester
7. Misc. Stress Sensors
   (temp., humidity, vibration, shock, voltage, etc.)

The Head-Media Technologist's Toolbox

DRAWER #9: Failure Analysis

1. Disk Decoration Processes
2. Microscopes (w/ X-Y and r,Θ stages)
3. Microscope Cameras
4. H/M Parametric Tester
5. Disk Defect Tester
6. Bright-light Inspection

The Head–Media Technologist's Toolbox

DRAWER #9: Failure Analysis Laboratory

1. Scanning Electron Microscope w/ EDS
2. Fourier Transform Infrared (FTIR)
3. Electron Spectroscopy / Chemical Analysis (ESCA)
4. AUGER Electron Spectroscopy
5. X-Ray Flourescence Spectrometry (XRF)
6. 3-D Profilometers (WYCO, Federal 3000, etc.)

DDT Defect Status

Status	Description
0	Cause unknown
1	Root cause has been isolated
2	Solution has been designed and reviewed
3	Solution has been implemented for testing
4	Solution has been verified
5	Problem and solution have been recorded in a lessons learned data base so that it will never recur

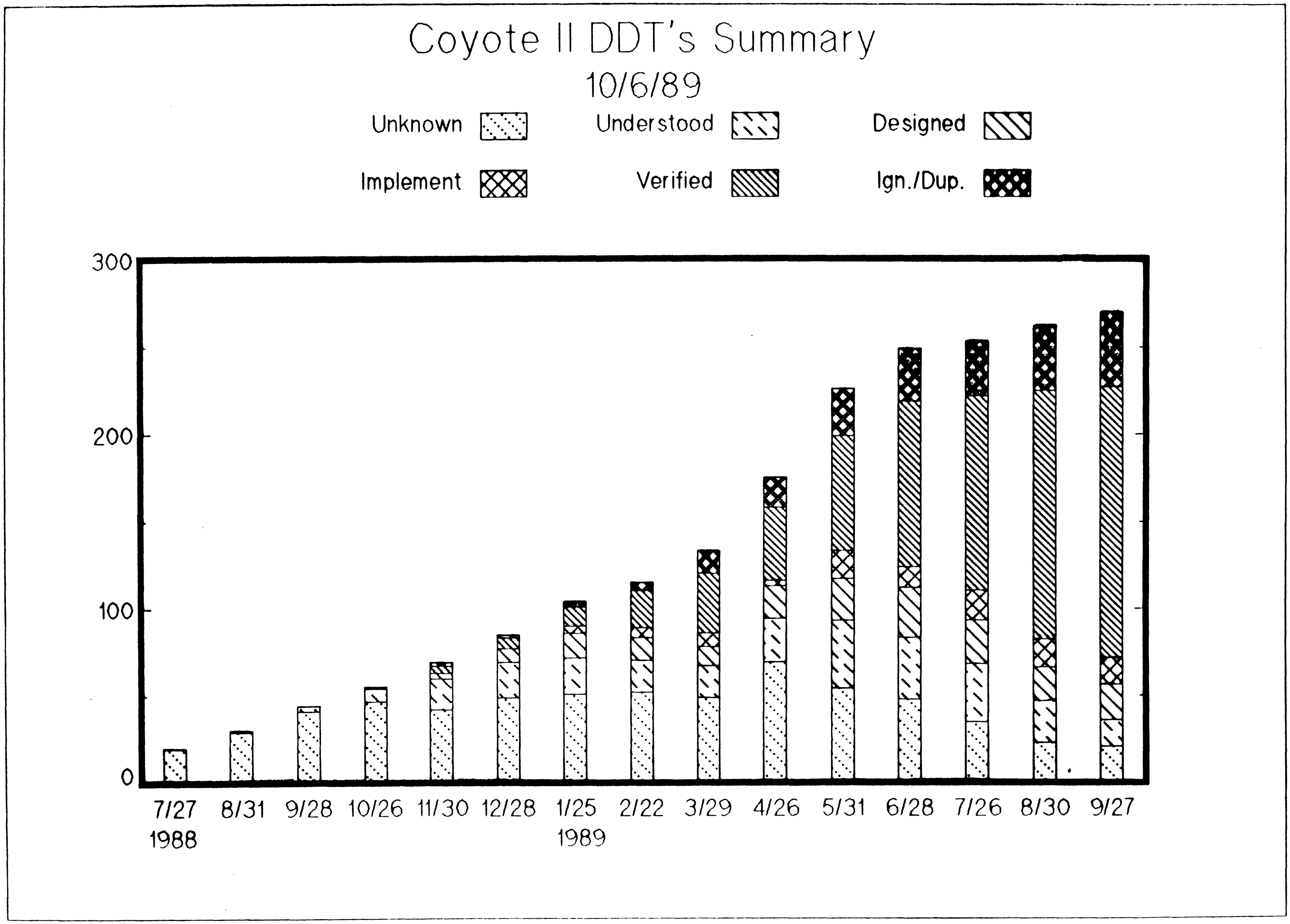
Coyote II DDT's Summary
10/6/89
Unknown
Understood
Designed
Implement
Verified
Ign./Dup.
300
200
100
0
7/27
1988
8/31
9/28
10/26
11/30
12/28
1/25
1989
2/22
3/29
4/26
5/31
6/28
7/26
8/30
9/27

Reliability Methods

Advantages of Design Defect Tracking:

- Measurable goals and results - visible priorities
- Track problem status - can't be forgotten
- Gives a roadmap of action
- Fewer surprises after release
- Problems documented for future reference
- Provides critical information for management decisions

TQC Methodology

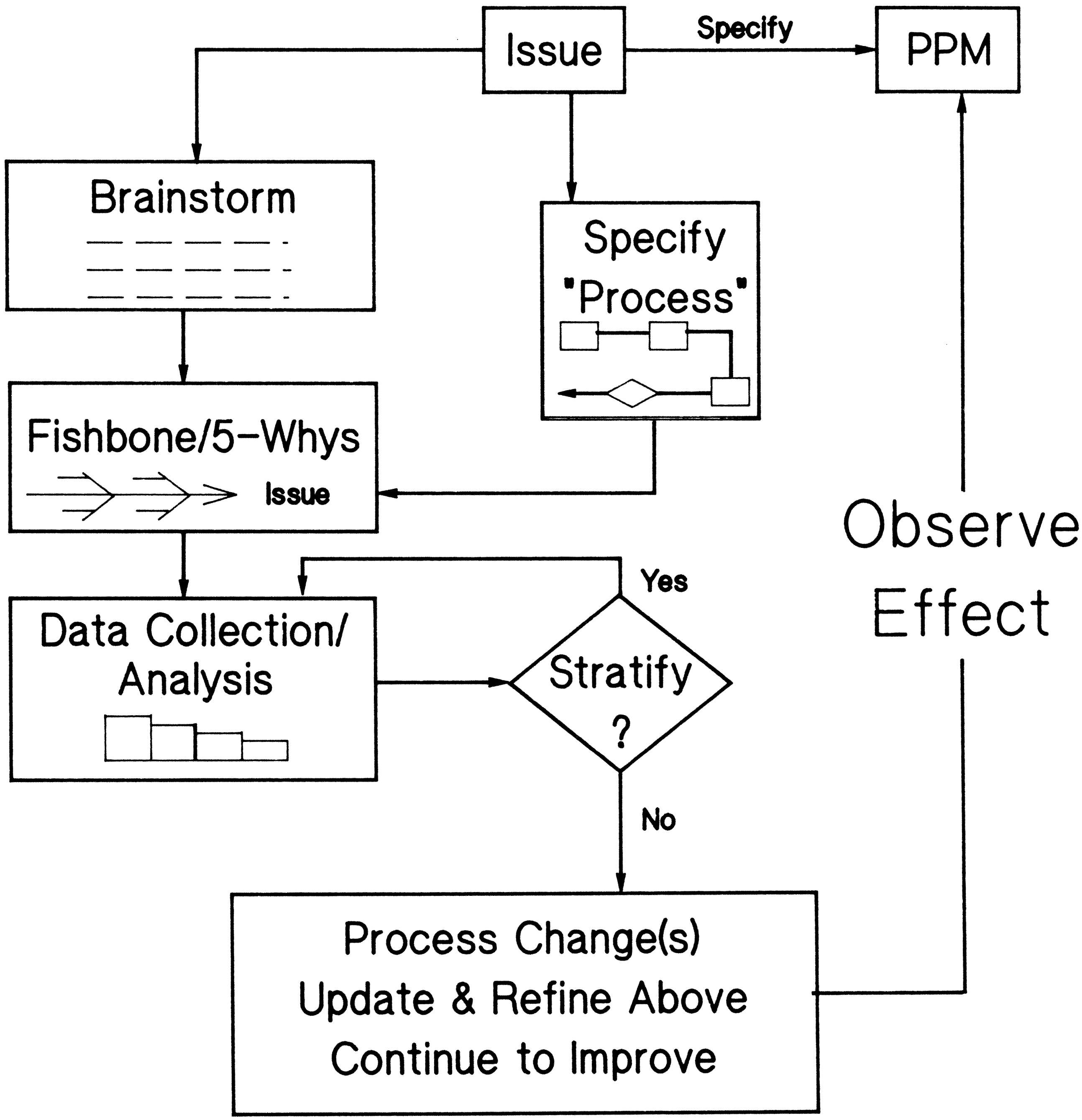

FISHBONE

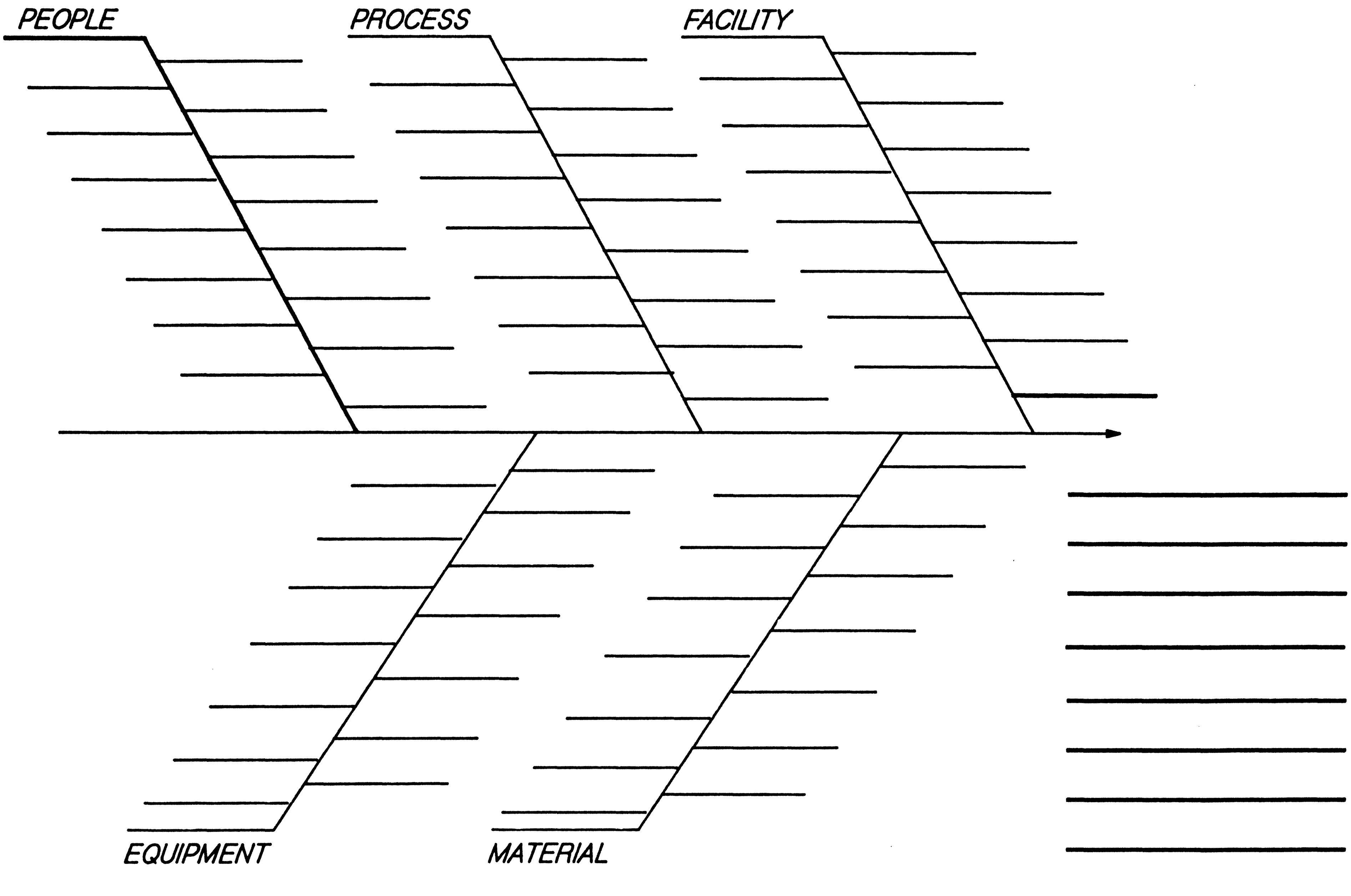

Ask Why Five Times

The disk drive failed.	Why?
Bad microprocessor board.	Why?
Eprom died.	Why?
Electromigration on buried metalization layer.	Why?
Violation of current density design rule.	Why?
Chip designer didn't catch the violation.	Why?

Reliability Methods

Strife (Stress + Life) Testing

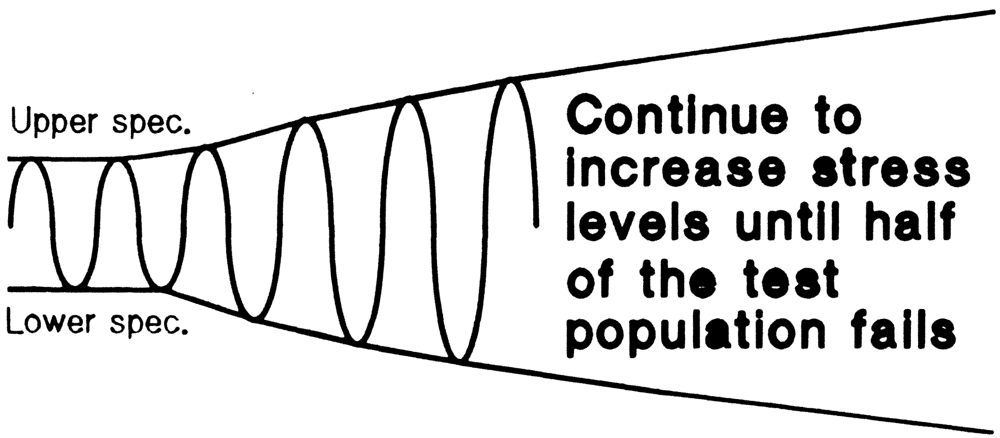

Note: Critical to find and understand the root cause of every problem

Typical Strife Stresses

- Temperature (high, low)
- Rate of temperature change
- Humidity
- Vibration
- Power cycling
- Power line variations
  - . Voltage
  - . Frequency
  - . Power line dropout
- Altitude

Model - Component Test - Drive test

"Tripod"

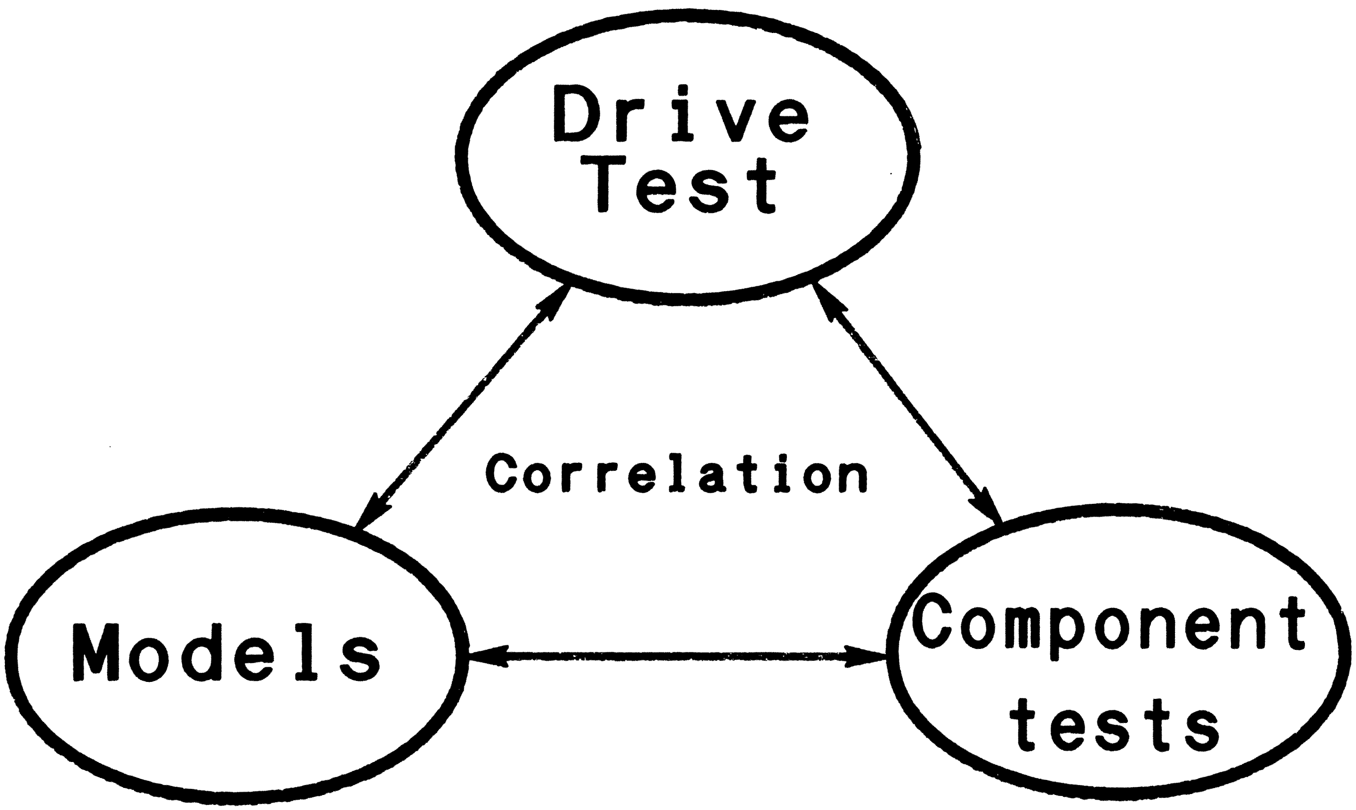

Integrated H/M Modeling/Measurement System

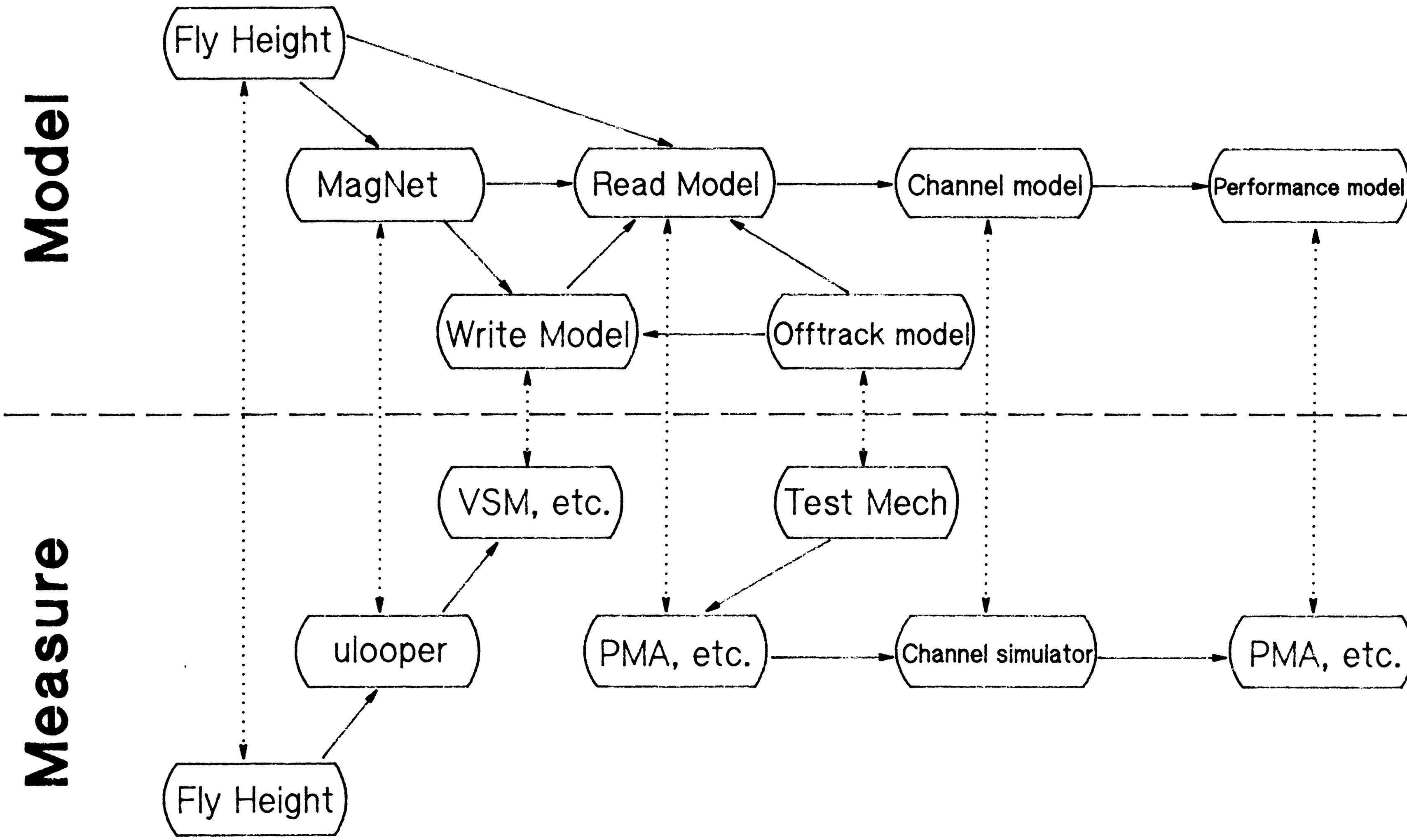

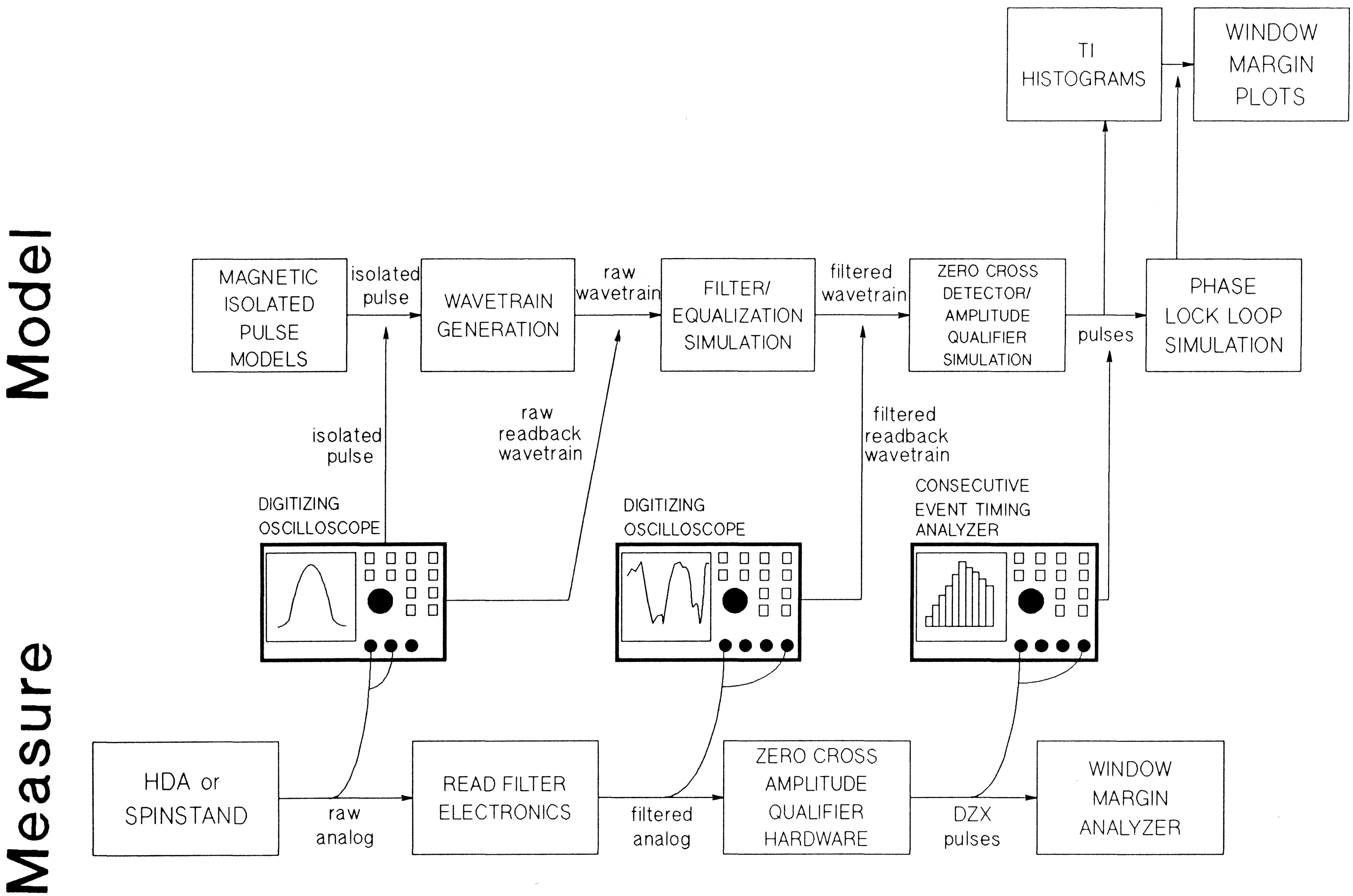
Model
Measure
TI HISTOGRAMS
WINDOW MARGIN PLOTS
MAGNETIC ISOLATED PULSE MODELS
isolated pulse
WAVETRAIN GENERATION
raw wavetrain
FILTER/ EQUALIZATION SIMULATION
filtered wavetrain
ZERO CROSS DETECTOR/ AMPLITUDE QUALIFIER SIMULATION
pulses
PHASE LOCK LOOP SIMULATION
isolated pulse
raw readback wavetrain
filtered readback wavetrain
DIGITIZING OSCILLOSCOPE
DIGITIZING OSCILLOSCOPE
CONSECUTIVE EVENT TIMING ANALYZER
HDA or SPINSTAND
raw analog
READ FILTER ELECTRONICS
filtered analog
ZERO CROSS AMPLITUDE QUALIFIER HARDWARE
DZX pulses
WINDOW MARGIN ANALYZER

Cost of "Nonquality":

Impacts:

* Production Yields
* Production Capacity
* Production Linearity
* Process Complexity
* Process Overhead
* Warranty Costs
* Customer Satisfaction
* "Perceived" Quality
* Cost of Lost Opportunity

etc., etc., etc.

Conclusions & Summary

Bad News:

* No magic or shortcuts to quality & reliability!

  - requires commitment, attention to detail.
  - requires large capital investment.
  - requires large expense commitments.
  - requires a close working relationship with head and disk vendors.

Conclusions & Summary

Good News:

* "QUALITY IS ^ FREE"
NOT

But the ROI is EXCEPTIONAL!

(apologies to Phil Crosby!)

Very, Ultra, Super Low Flying and Contact

Presented at

The IIST December 1989 Shortcourse

by Ron Dennison   Maxtor

OVERVIEW

- Why Lower?
- How Close Can We Get?
- Glide Issues
- Contact Recording

Maxtor

OVERVIEW

- Why Lower?
- How Close Can We Get?
- Glide Issues
- Contact Recording

Maxtor

OEM Price per Megabyte

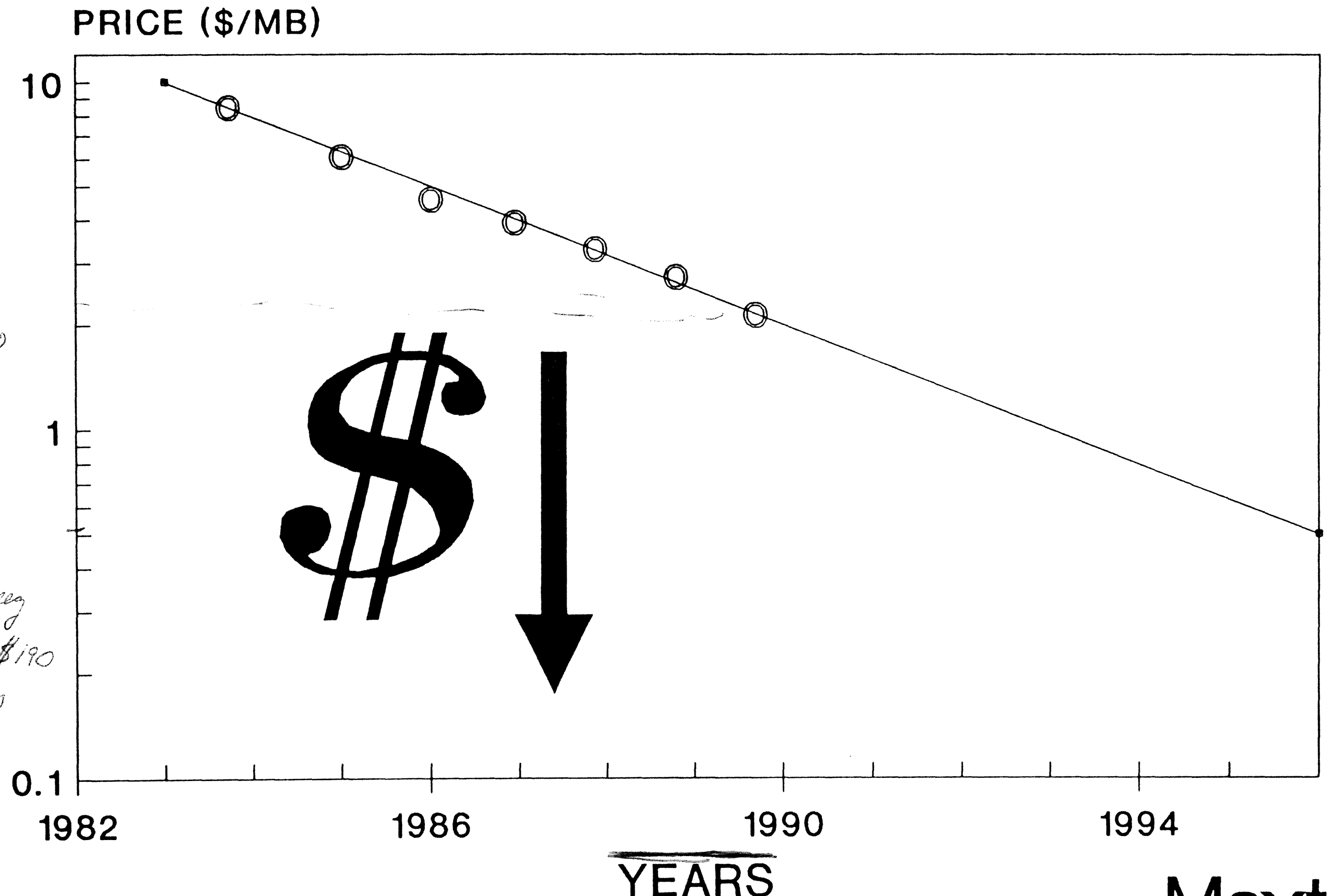

$2.50/meg
380 meg = $950

.5

50¢/meg
380meg = $190
40meg = $20

Maxtor

Megabits per Square Inch
vs. Time

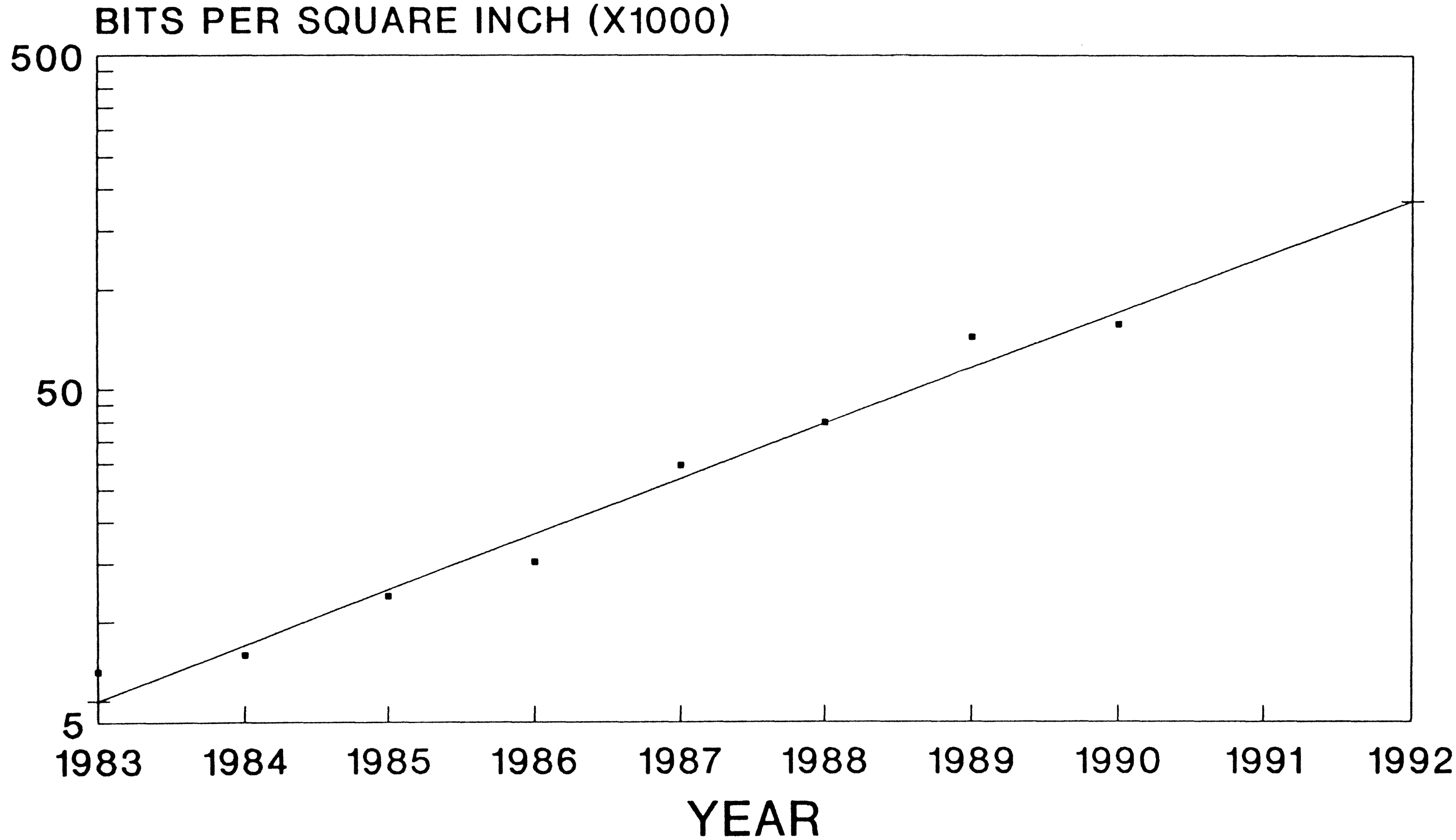

YEARS ARE DATES OF MAXTOR
FIRST PRODUCT INTRODUCTION

Maxtor

Bitshift Basics

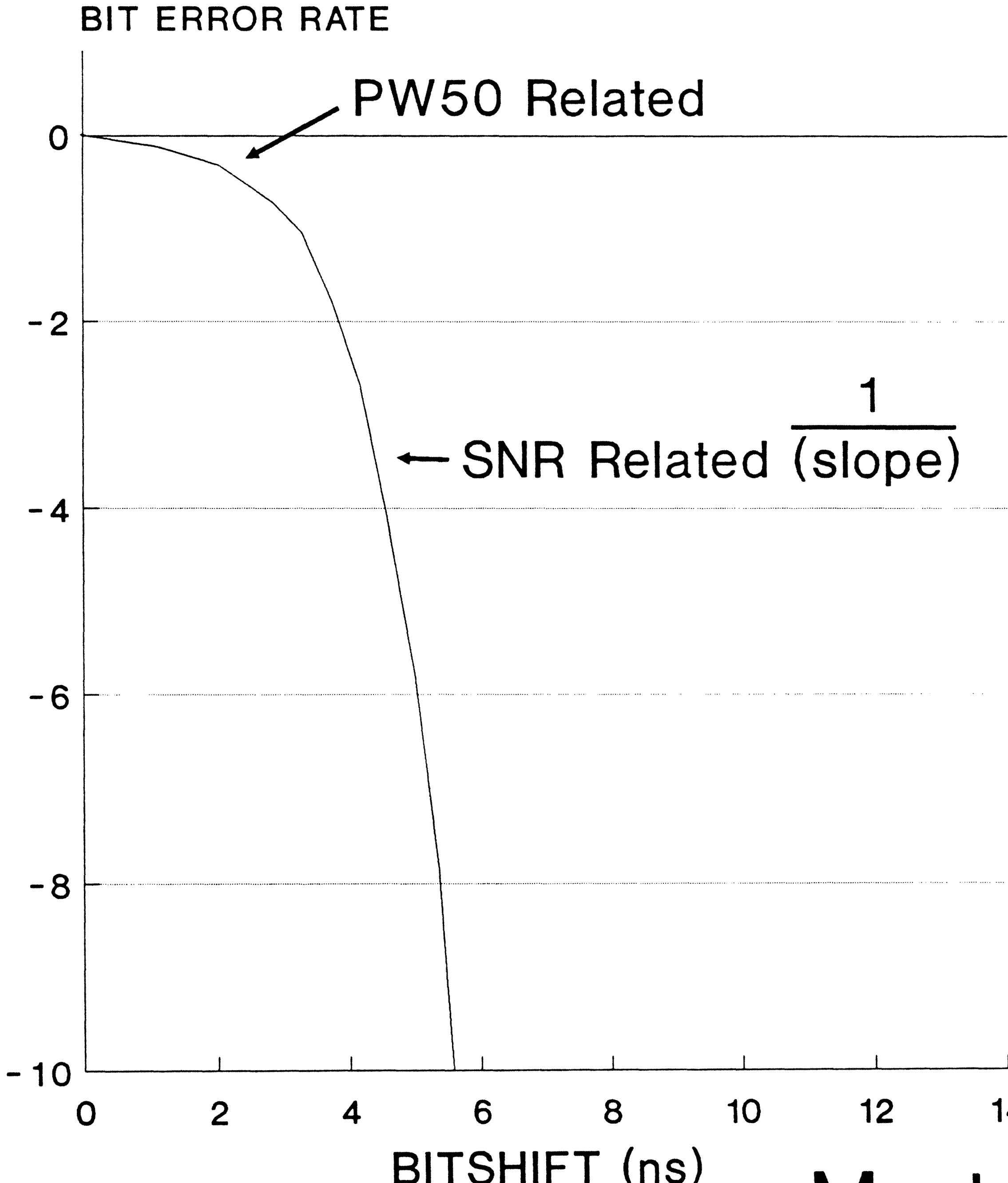

Maxtor

PW50 and/or SNR
System Capability Improvement

- Code Selection/Implementation
- ECC
- Specialized Channel Designs
- Head/Media Changes
- FLYING LOWER!!

Maxtor

Wavelength
vs. Spacing Loss

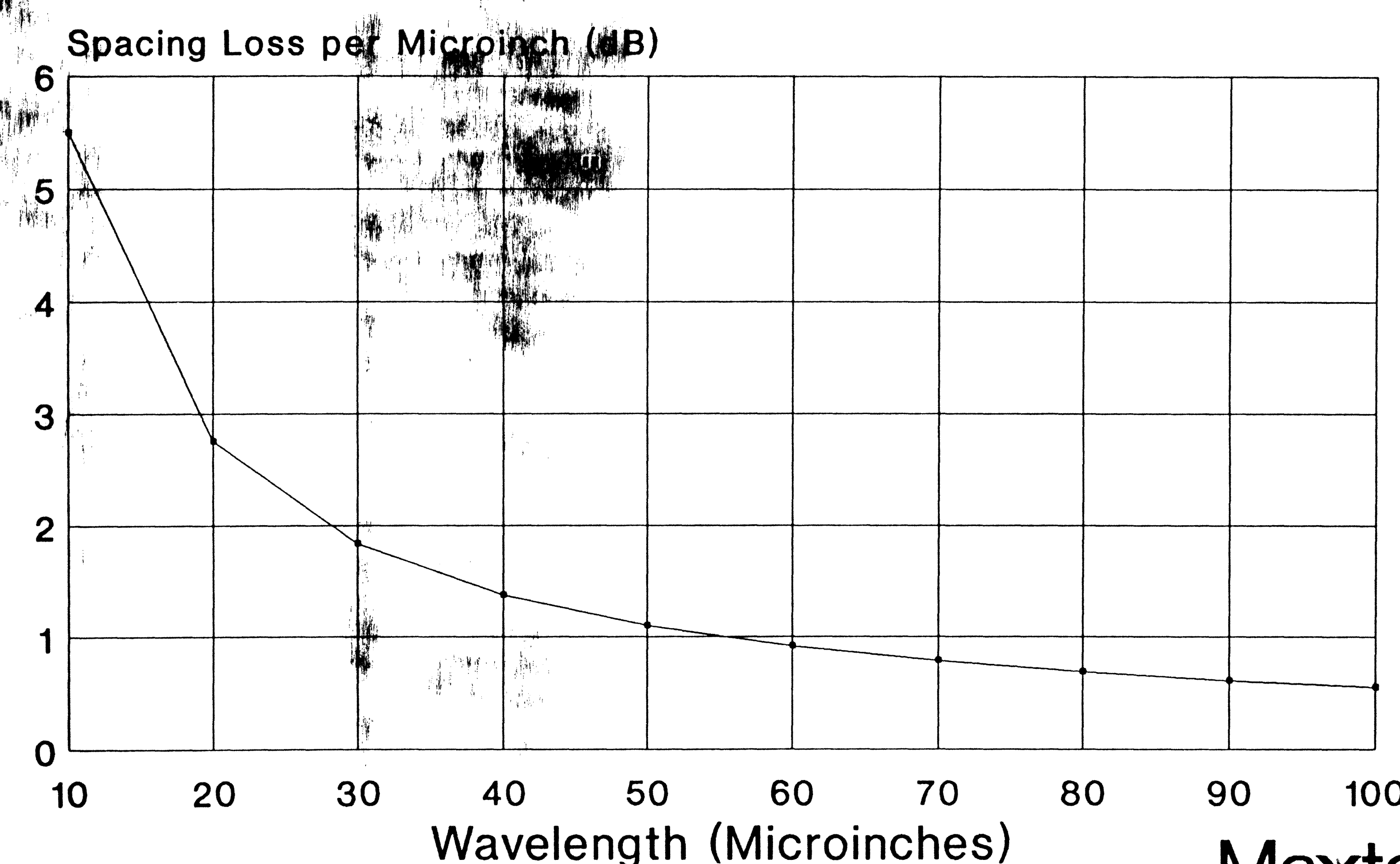

Maxtor

Data Transfer Rate
vs. Spacing Loss

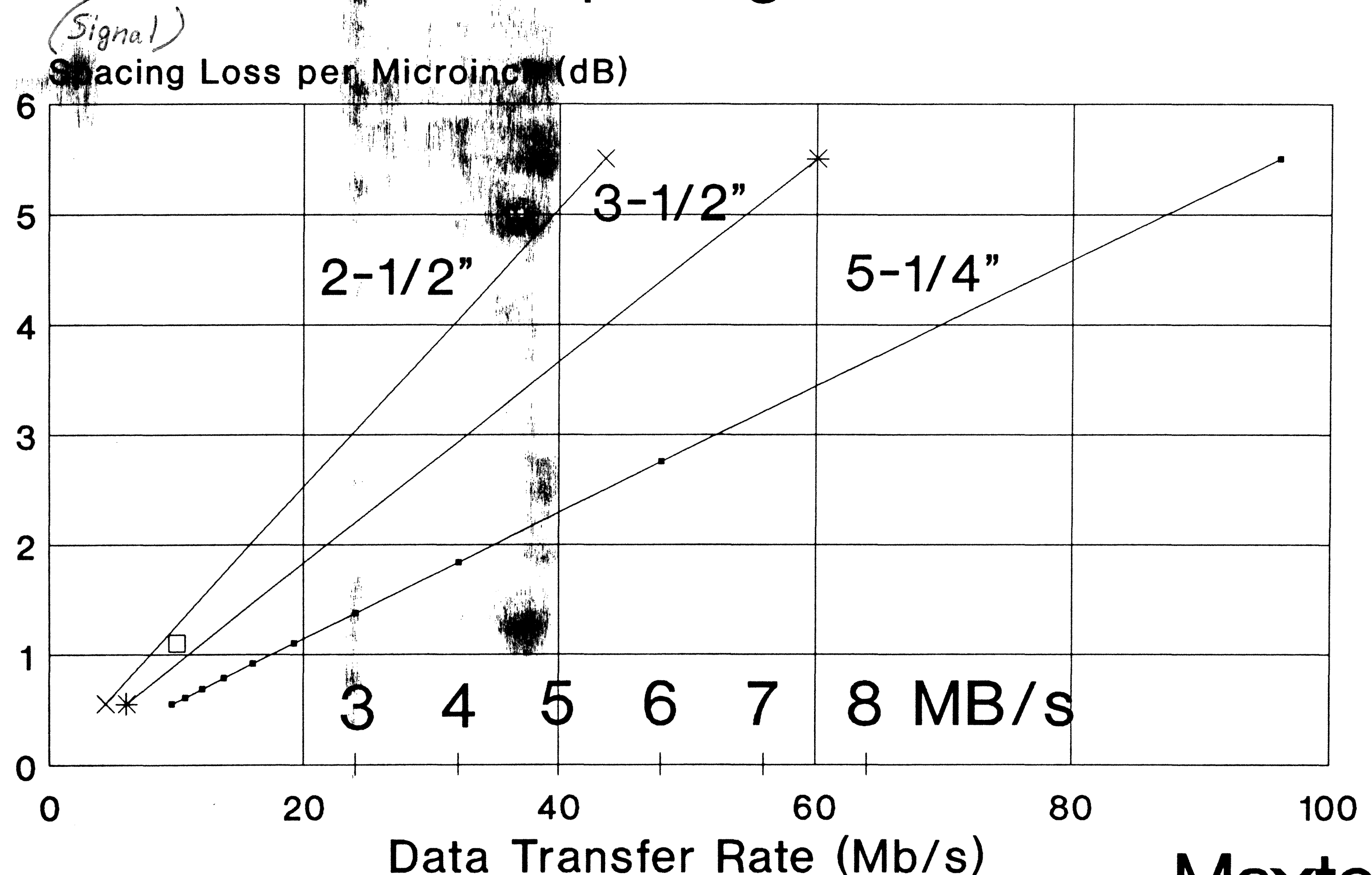

Maxtor

PW50 vs. Flying Height

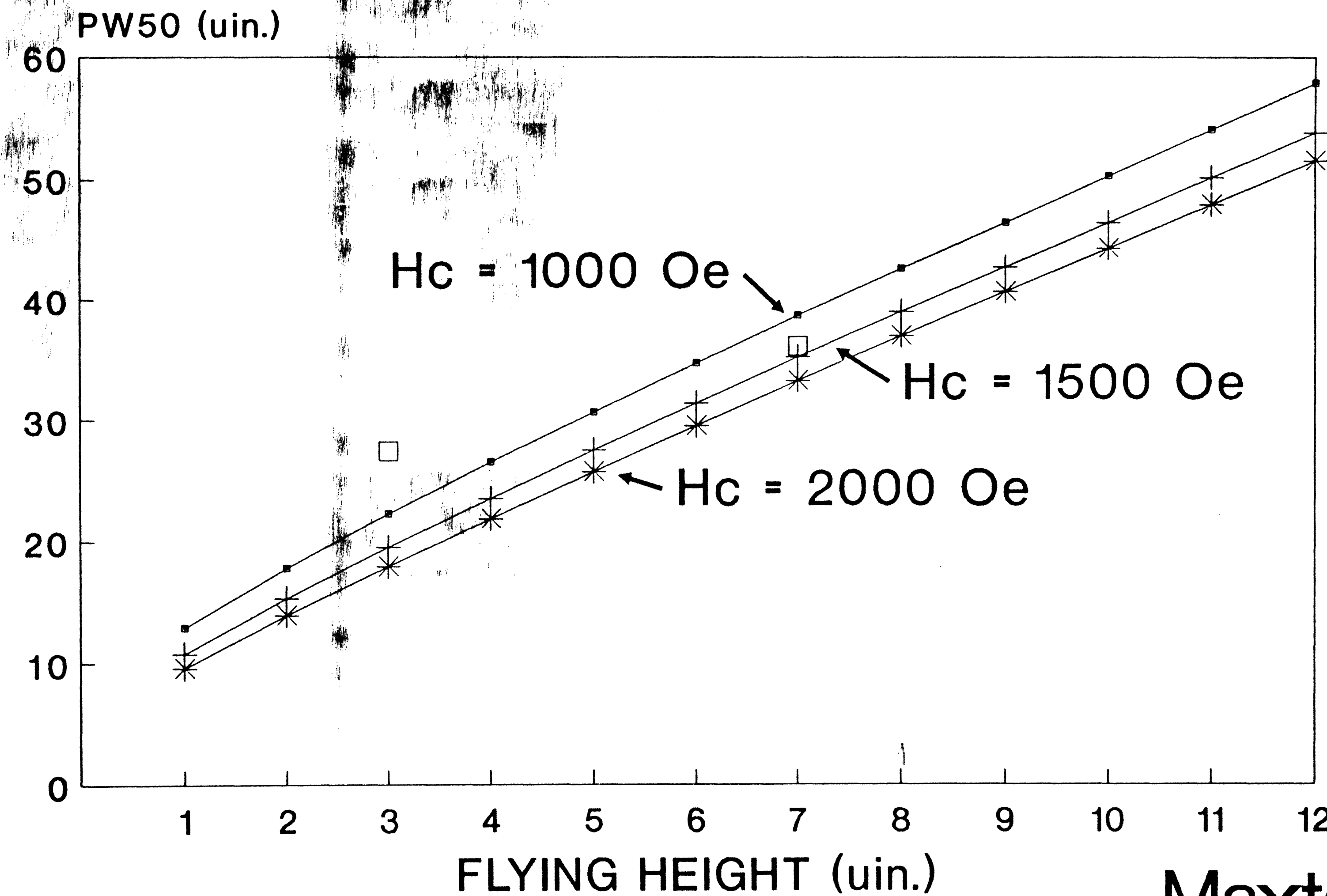

Maxtor

Improved PW50 and SNR

How Used?

PW50

$$\frac{1}{Tb} = \frac{A}{T50} (m/n) (d+1)^{1-Q} SNR^{Q}$$

→ Quality ≅ 1/3

$$\frac{FCInew}{FCIold} = \frac{T50old}{T50new} * \frac{SNRnew^{1/3}}{SNRold^{1/3}}$$

THUS 1/3 T50 → 3 x FCI

SNR

$$SNR \propto \sqrt{Wt}$$

→ track width

THUS 5dB SNR → 3 x TPI

Maxtor

OVERVIEW

- Why Lower?
- How Close Can We Get?
- Glide Issues
- Contact Recording

Maxtor

TYPICAL SURFACES

GLASS
vs.
METAL

Maxtor

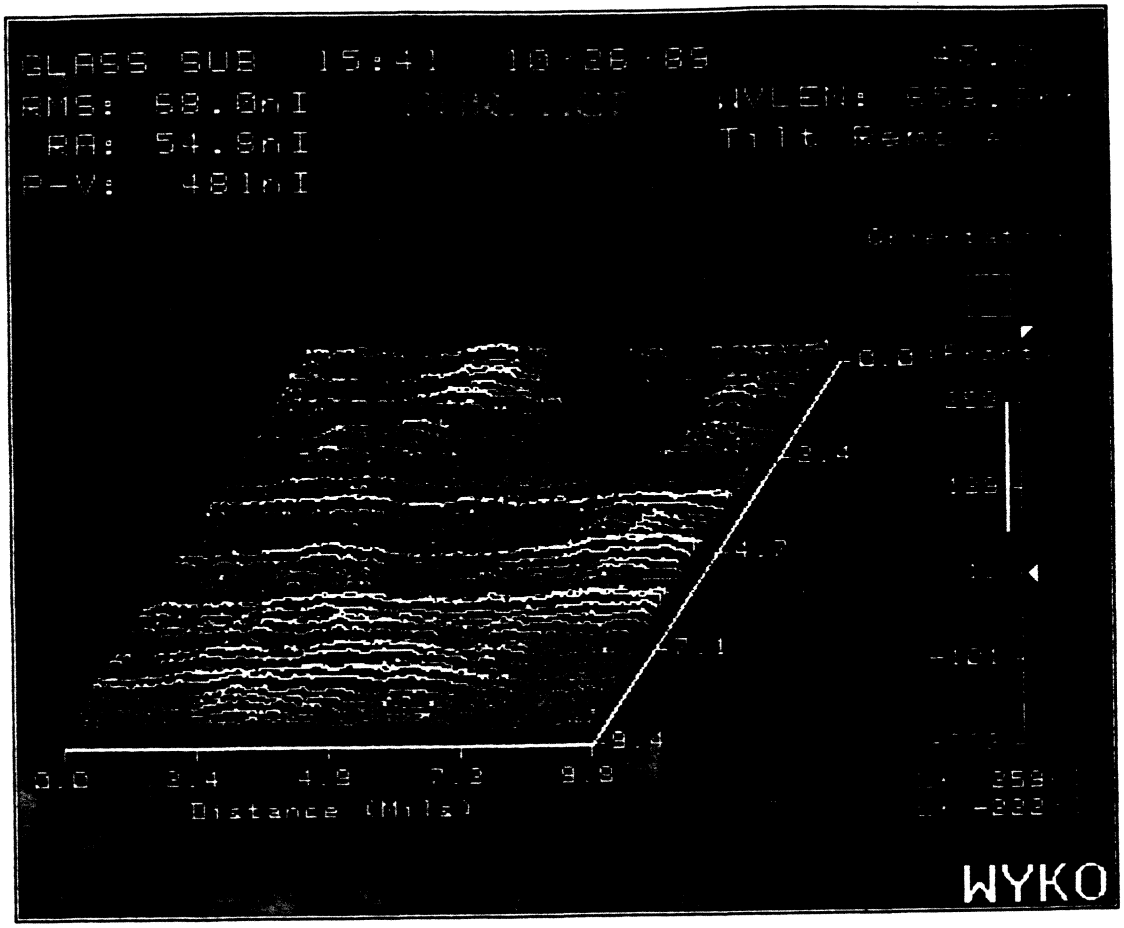
GLASS SUB 15:41 10-26-89
RMS: 58.0nI
RA: 54.8nI
P-V: 481nI
WVLEN:
0.0 2.4 4.9 7.3 9.8
Distance (Mils)
WYKO

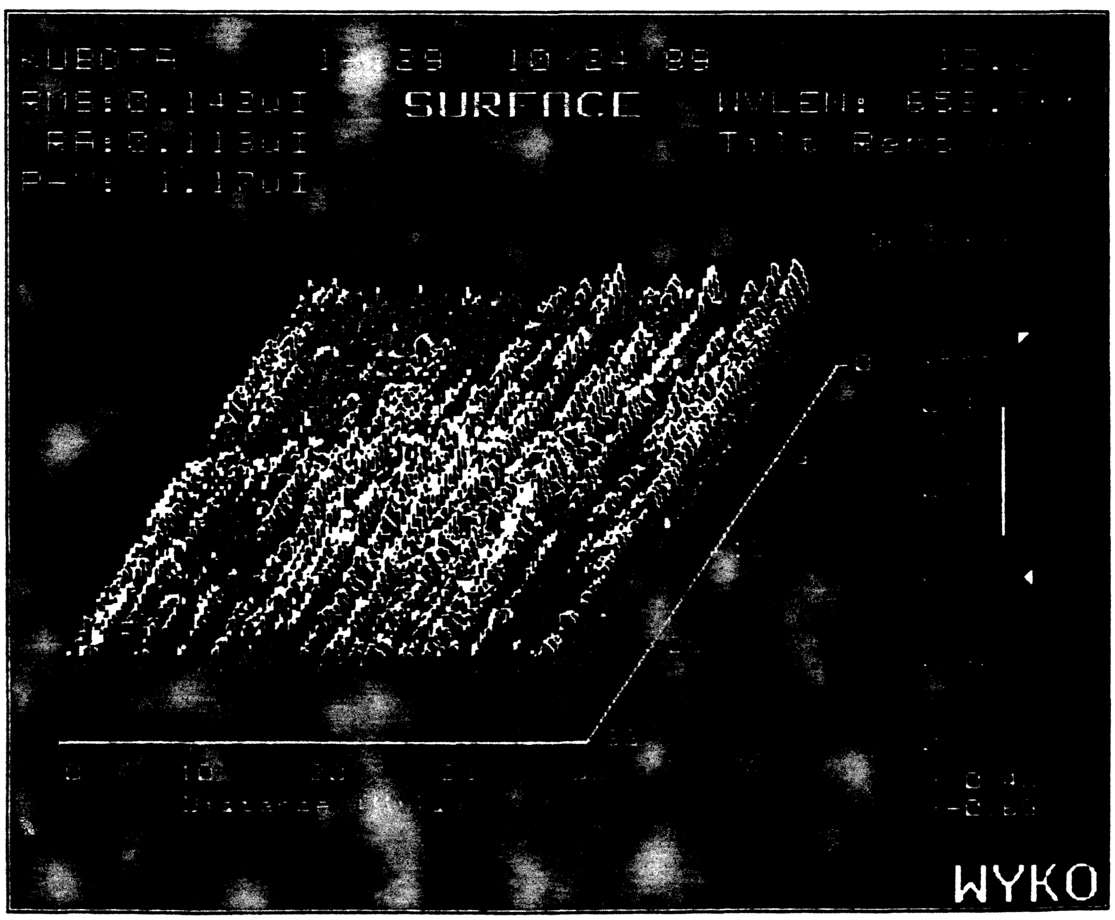
10-24-89
RMS:0.143uI
SURFACE
WVLEN:
RA:0.113uI
P-V: 1.17uI
WYKO

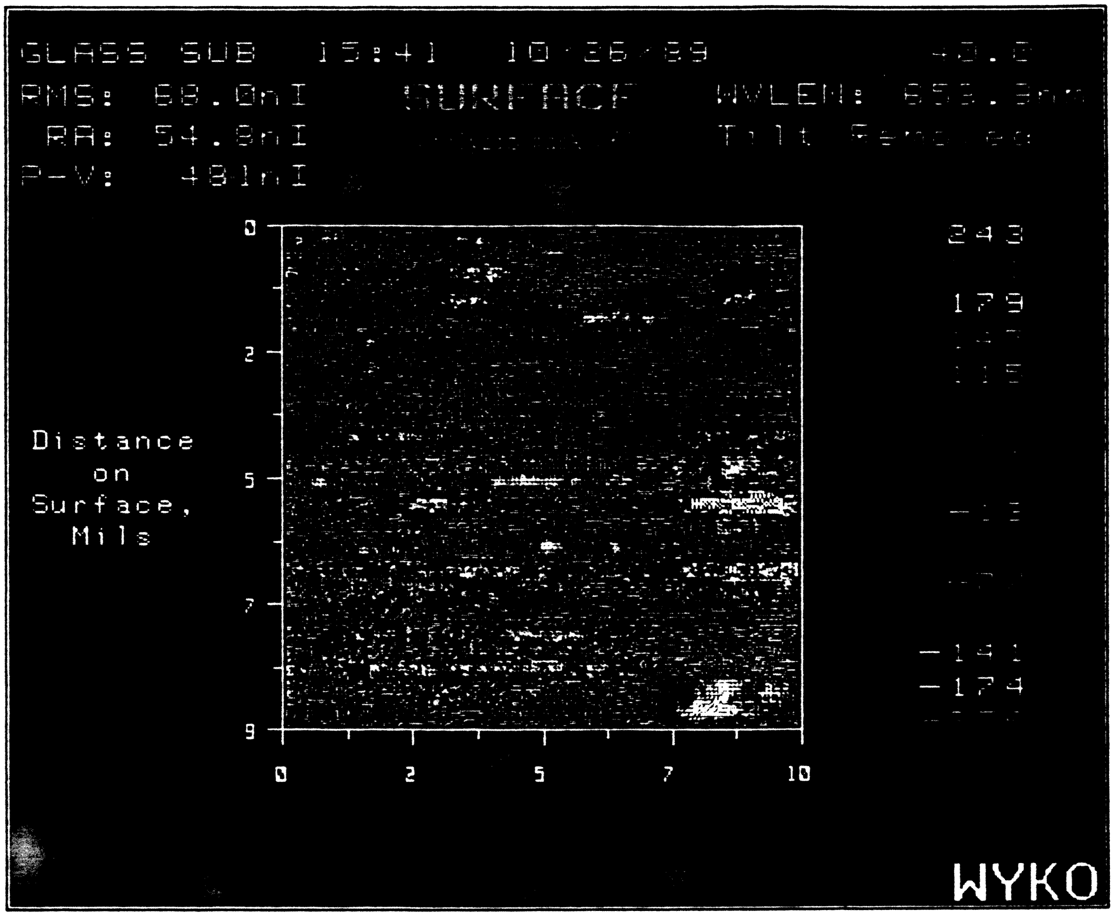
GLASS SUB 15:41 10-26-89
RMS: 68.0nI
RA: 54.8nI
P-V: 481nI
SURFACE
WVLEN: 653.3nm
Tilt Removed
Distance on Surface, Mils
243
179
-141
-174
WYKO

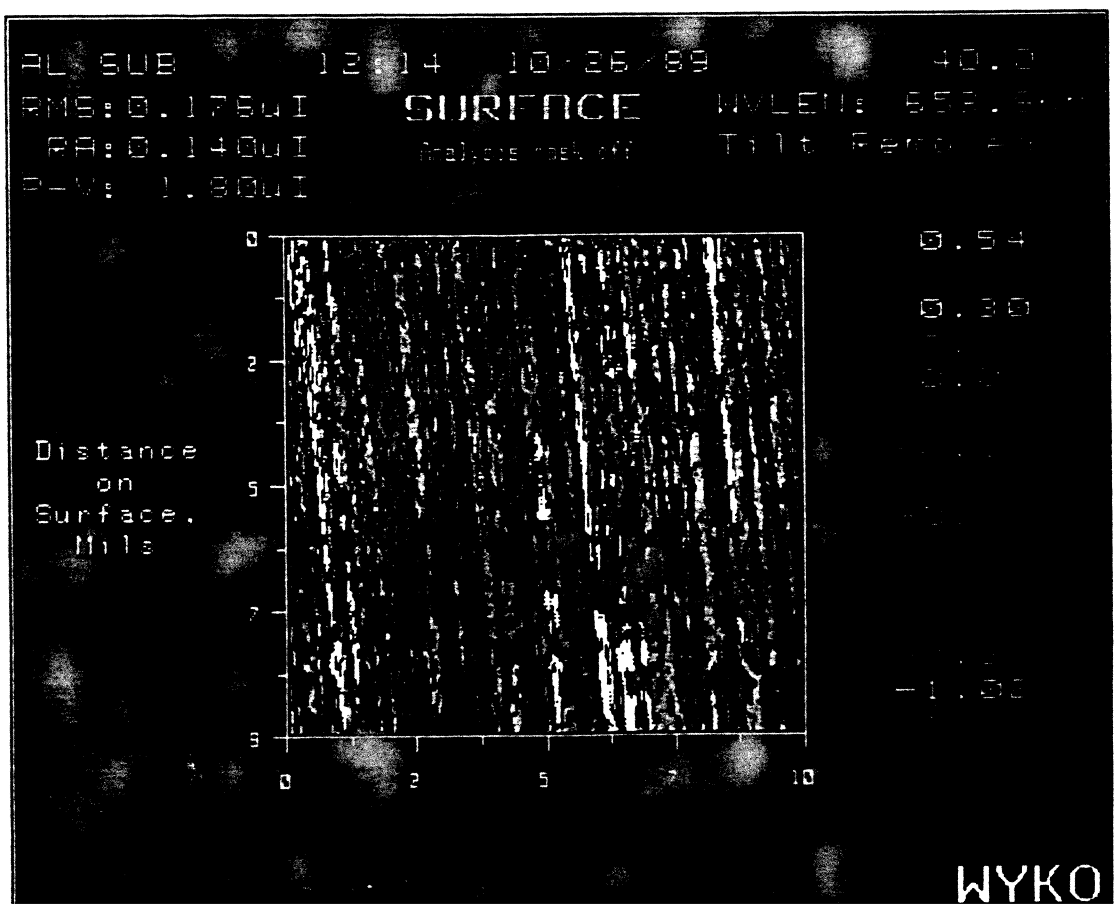
AL SUB 12:14 10-26-89
RMS:0.179uI
RA:0.140uI
P-V: 1.80uI
SURFACE
Analysis mask off
Tilt Removed
Distance on Surface, Mils
0.54
0.30
WYKO

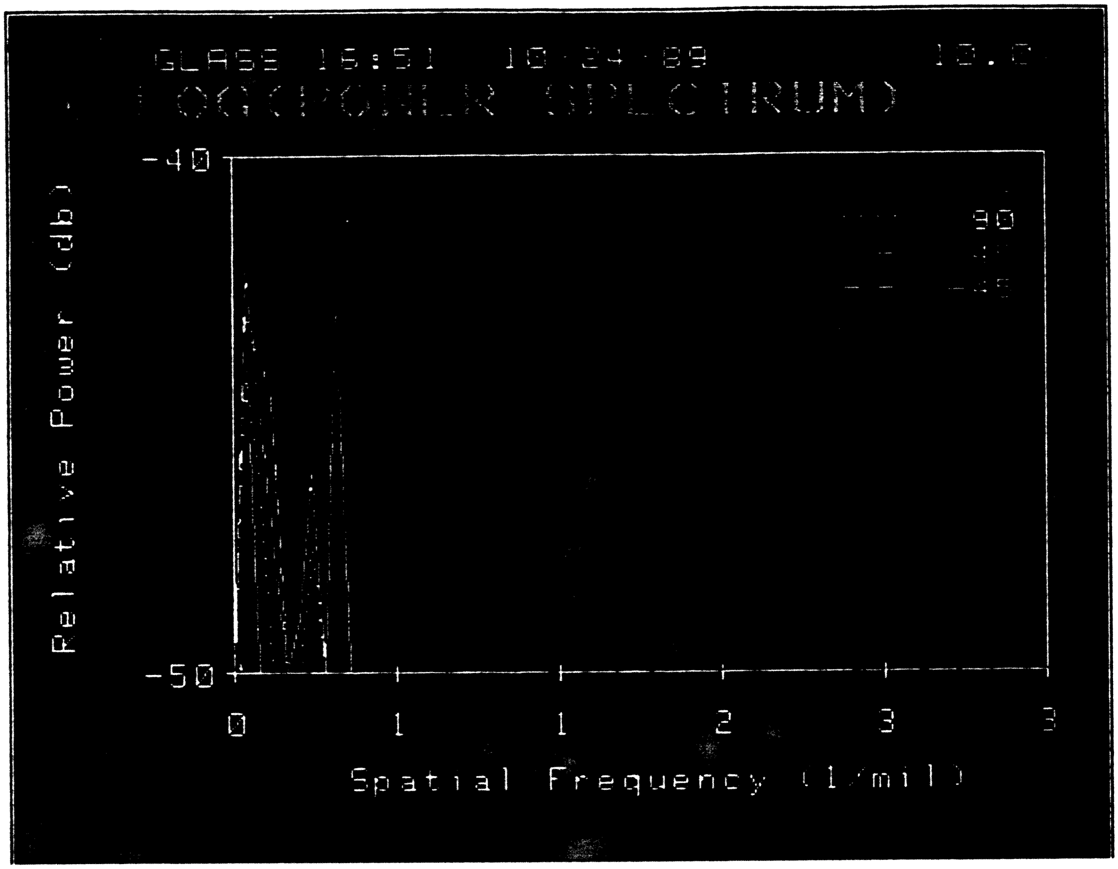

GLASS 16:51 10-24-89
LOG(POWER SPECTRUM)
Relative Power (db)
-40
-50
0
1
1
2
3
3
Spatial Frequency (1/mil)

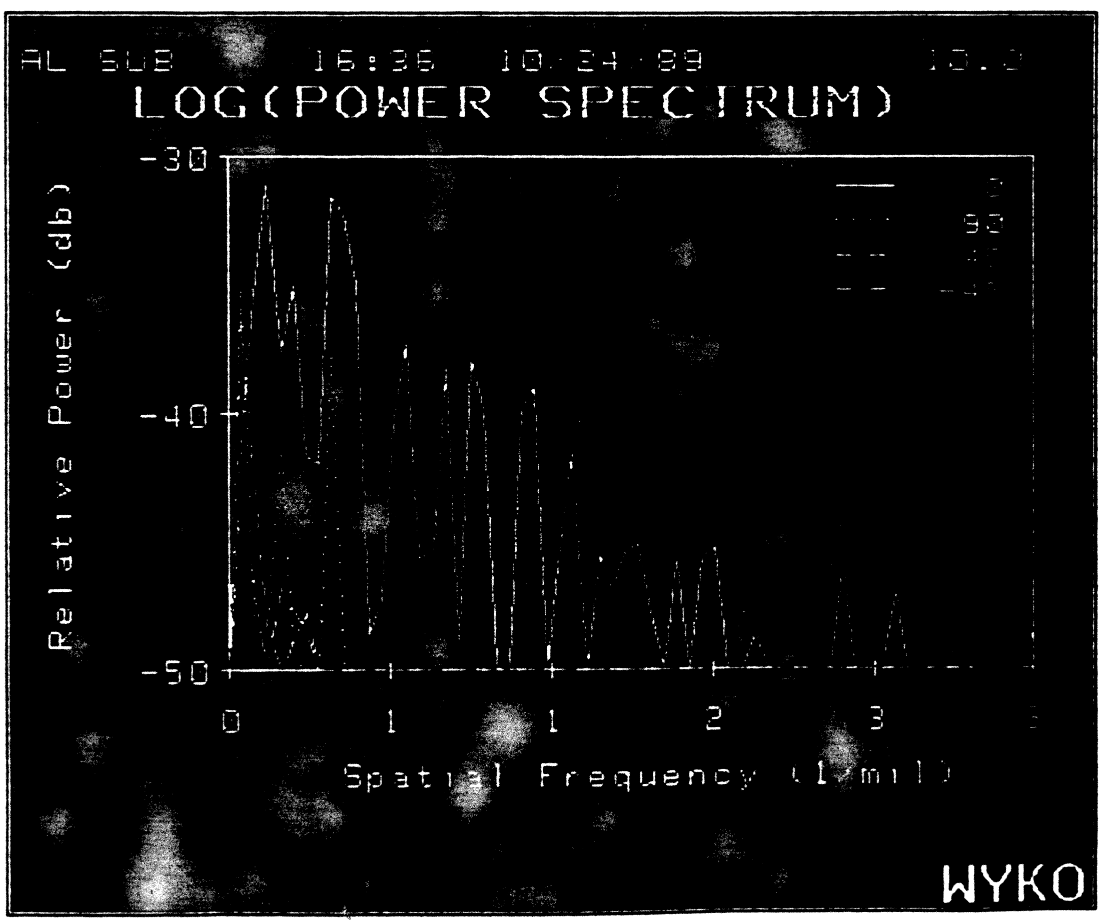

AL SUB 16:36 10-24-89
LOG(POWER SPECTRUM)
Relative Power (db)
-30
-40
-50
90
0
1
1
2
3
Spatial Frequency (1/mil)
WYKO

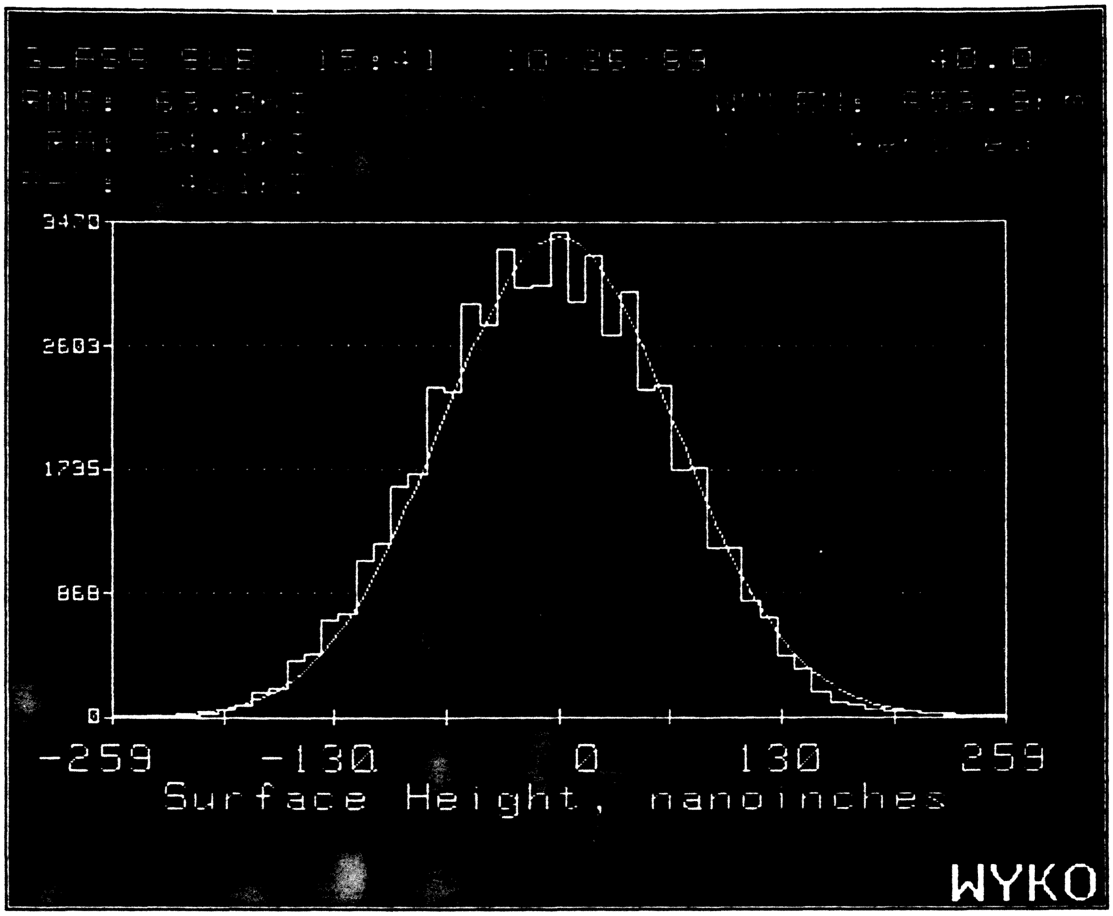

3470
2603
1735
868
0
-259 -130 0 130 259
Surface Height, nanoinches
WYKO

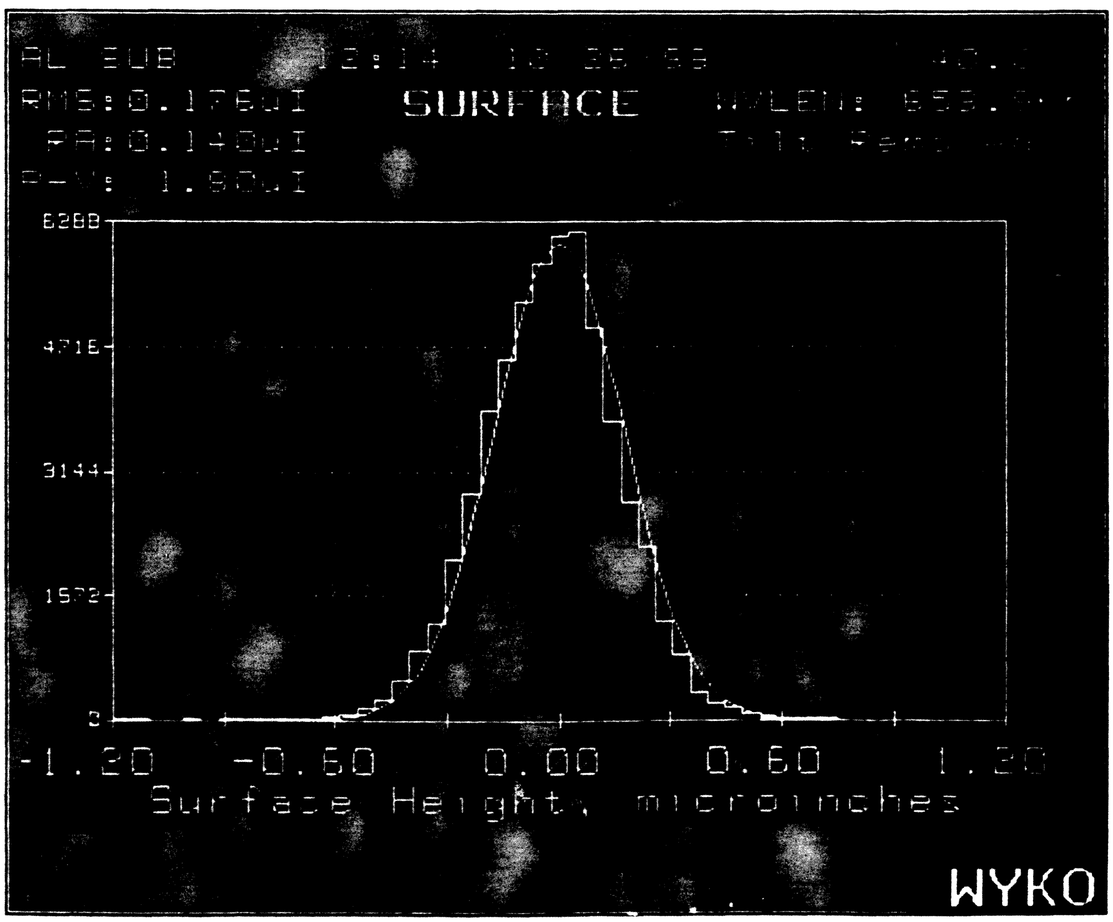

AL SUB 12:14
RMS:0.176uI
SURFACE
RA:0.140uI
P-V: 1.80uI
6288
4716
3144
1572
0
-1.20 -0.60 0.00 0.60 1.20
Surface Height, microinches
WYKO